INTERNATIONAL ENERGY AGENCY
energy conservation in buildings and
community systems programme

12th AIVC Conference

Air Movement and Ventilation Control Within Buildings

Proceedings
Volume 1

University of Warwick Science Park
Barclays Venture Centre
Sir William Lyons Road
Coventry CV4 7EZ
Great Britain

This report is part of the work of the IEA Energy Conservation in Buildings & Community Systems Programme

Annex V Air Infiltration and Ventilation Centre

Document AIC-PROC-12-1991-1
ISBN 0 946075 53 0

Participants in this task:

Belgium, Canada, Denmark, Federal Republic of Germany, Finland, Italy, Netherlands, New Zealand, Norway, Sweden, Switzerland, United Kingdom, and United States of America

Distribution: Unrestricted
Additional copies of this report may be obtained from:

The Air Infiltration and Ventilation Centre
University of Warwick Science Park
Barclays Venture Centre
Sir William Lyons Road
Coventry CV4 7EZ
Great Britain

Luk VANDAELE
BBRI

12th AIVC Conference

Air Movement and Ventilation Control Within Buildings

(held at Château Laurier, Ottawa, Canada
24-27 September 1991)

Proceedings

Volume 1

Co-Sponsors:

IEA Energy Conservation in Buildings and Community Systems
Annex 18 'Demand Controlled Ventilating Systems'
Annex 20 'Air Flow Patterns within Buildings'

CONTENTS (i)

Volume 1

Preface

International Energy Agency

The International Energy Agency (IEA) was established in 1974 within the framework of the Organisation for Economic Co-operation and Development (OECD) to implement an International Energy Programme. A basic aim of the IEA is to foster co-operation among the twenty-one IEA Participating Countries to increase energy security through energy conservation, development of alternative energy sources and energy research development and demonstration (RD&D). This is achieved in part through a programme of collaborative RD&D consisting of forty-two Implementing Agreements, containing a total of over eighty separate energy RD&D projects. This publication forms one element of this programme.

Energy Conservation in Buildings and Community Systems

The IEA sponsors research and development in a number of areas related to energy. In one of these areas, energy conservation in buildings, the IEA is sponsoring various exercises to predict more accurately the energy use of buildings, including comparison of existing computer programs, building monitoring, comparison of calculation methods, as well as air quality and studies of occupancy. Seventeen countries have elected to participate in this area and have designated contracting parties to the Implementing Agreement covering collaborative research in this area. The designation by governments of a number of private organisations, as well as universities and government laboratories, as contracting parties, has provided a broader range of expertise to tackle the projects in the different technology areas than would have been the case if participation was restricted to governments. The importance of associating industry with government sponsored energy research and development is recognized in the IEA, and every effort is made to encourage this trend.

The Executive Committee

Overall control of the programme is maintained by an Executive Committee, which not only monitors existing projects but identifies new areas where collaborative effort may be beneficial. The Executive Committee ensures that all projects fit into a pre-determined strategy, without unnecessary overlap or duplication but with effective liaison and communication. The Executive Committee has initiated the following projects to date (completed projects are identified by *):

I Load Energy Determination of Buildings*
II Ekistics and Advanced Community Energy Systems*
III Energy Conservation in Residential Buildings*

IV Glasgow Commercial Building Monitoring*
V Air Infiltration and Ventilation Centre
VI Energy Systems and Design of Communities*
VII Local Government Energy Planning*
VIII Inhabitant Behaviour with Regard to Ventilation*
IX Minimum Ventilation Rates*
X Building HVAC Systems Simulation*
XI Energy Auditing*
XII Windows and Fenestration*
XIII Energy Management in Hospitals*
XIV Condensation*
XV Energy Efficiency in Schools
XVI BEMS - 1: Energy Management Procedures
XVII BEMS - 2: Evaluation and Emulation Techniques
XVIII Demand Controlled Ventilating Systems
XIX Low Slope Roof Systems
XX Air Flow Patterns within Buildings
XXI Thermal Modelling
XXII Energy Efficient Communities
XXIII Multizone Air Flow Modelling

Annex V Air Infiltration and Ventilation Centre

The IEA Executive Committee (Building and Community Systems) has highlighted areas where the level of knowledge is unsatisfactory and there was unanimous aggreement that infiltration was the area about which least was known. An infiltration group was formed drawing experts from most progressive countries, their long term aim to encourage joint international research and increase the world pool of knowledge on infiltration and ventilation. Much valuable but sporadic and uncoordinated research was already taking place and after some initial groundwork the experts group recommended to their executive the formation of an Air Infiltration and Ventilation Centre. This recommendation was accepted and proposals for its establishment were invited internationally.

The aims of the Centre are the standardisation of techniques, the validation of models, the catalogue and transfer of information, and the encouragement of research. It is intended to be a review body for current world research, to ensure full dissemination of this research and based on a knowledge of work already done to give direction and firm basis for future research in the Participating Countries.

The Participants in this task are Belgium, Canada, Denmark, Germany, Finland, Italy, Netherlands, New Zealand, Norway, Sweden, Switzerland, United Kingdom and the United States of America.

AIR MOVEMENT & VENTILATION CONTROL WITHIN BUILDINGS

12th AIVC Conference, Ottawa, Canada
24-27 September, 1991

PAPER 1

THE MESSAGE OF ANNEX 20:

AIR FLOW PATTERNS WITHIN BUILDINGS

ALFRED MOSER

Swiss Federal Institute of Technology, ETH,
Energy Systems Laboratory, Energietechnik ML,
ETH-Zentrum, CH-8092 Zurich,
Switzerland

SYNOPSIS

The International Energy Agency (IEA) task-sharing project "Air Flow Patterns within Buildings" was initiated in May 1988 for a duration of 3 $^1/_2$ years. Twelve nations contribute work and expertise and "share the task" specified in the project's objectives. This project and the AIVC belong to the same Implementing Agreement: The Energy Conservation in Buildings and Community Systems Program. As "Attachments" to the Implementing Agreement, they are called Annexes.

The general objective of the Annex is to evaluate the performance of single- and multi-zone air and contaminant flow simulation techniques and to establish their viability as design tools. To reach this goal, the work was divided into two parallel subtasks: One on single-room air and contaminant flow, the other on multi-zone air and contaminant flow and measurement techniques.

This survey paper reviews project objectives and approach, both technically and from the point of view of project management. It offers an overview of the work performed and solutions contributed by the participating countries, it discusses problems encountered during the project and how these were solved, and summarizes final results. It shows how the various technical Annex-20 contributions to this conference are related to the overall Annex effort. General conclusions are drawn, consequences for future international projects are examined, and the main message of the multi-national program is formulated.

1. Introduction

"It should become possible to predict air flow patterns within buildings by numerical simulation!"

- This was concluded by a small group of ventilation experts who met in September 1987 in Ittingen, Switzerland. New commercial codes appeared on the market, and research codes were developed at universities and research labs. The workshop participants expected that some expensive laboratory tests could be avoided if air flows in rooms, infiltration between rooms, and exchange with the outside atmosphere could numerically be predicted with a certain degree of confidence. New tools would enable the designer to evaluate different variations of a ventilation concept on a computer. Contaminant transport within buildings or rooms could be modelled and the effectiveness of ventilation assessed in a systematic way.

The idea to start a new "IEA Energy Conservation in Buildings and Community Systems" Annex was born: Many promising simulation models existed and specialists have started to apply them to real buildings [1]. Experienced engineers voiced skepticism, while their younger colleagues looked for the "best" computer programs! It was the right time to survey and evaluate existing methods on an international basis.

Annex 20, *Air Flow Patterns within Buildings*, provided the framework to bring the experts together, to compile information, and to undertake validation exercises. For single- and multi-zone air flow, experimental data sets were required as benchmark cases. Therefore, experiments had to be specified for the project. Soon the scope of the Annex was extended to include the evaluation and documentation of advanced measurement techniques for multi-zone air flow and the development of new algorithms to model special flow mechanisms.

During the past three years, Annex-20 workers have learned quite a lot about air flow simulation. They will present some of their results at this conference, and the knowledge will be made widely available through publications and references in the AIVC bibliographic data bank "AIRBASE".

We have learned how to calculate air movement in buildings and rooms but also encountered and identified problems and found ways to deal with these. The experienced user of air flow codes will appreciate the benefits of numerical simulation:

- Information is available in all points of the flow field (on computational grid).
- Any desired variable of the physical model can be output and plotted: Air velocity and its fluctuations (turbulence), temperature, concentrations of contaminants and humidity, "local age" (an indicator of the "freshness" of the air), and comfort parameters (thermal comfort and "risk of draft"). Also heat transfer to and from window and radiator surfaces.
- Sensitivity tests and parameter variations are easy to do, and computed trends should be even more reliable than absolute values of variables.

The objective of the Annex is expressed in one short sentence (see next section), but its relevance was immediately recognized by all countries of this IEA Implementing Agreement. Thirteen nations decided to participate in Annex 20 (Section 3).

One reason for this wide participation certainly was the strong impact the work has on energy conservation. The trend to air-tight buildings with improved thermal insulation asks for controlled air exchange as already documented by the work of Annex 18, *Demand Controlled Ventilating Systems*, Annex 14, *Condensation*, and Annex 9, *Minimum Ventilation Rates*. The energy required to exchange the air grows with the temperature difference between fresh outside air and supply air to the rooms. In mechanical Systems, a substantial portion of the energy is used to move the air through the ducting and the rest for cooling or heating and other conditioning. The former is a function of the air change rate, the latter of temperatures and heat recovery, if installed.

This energy consumption is of growing significance in relation to the heat loss through the envelope of well insulated buildings. The designer of these new-generation buildings wants to know how the air flows before the house is built!

2. Annex 20 objectives

Formal participation in this task-sharing Annex is based on the legal text [2] that defines project objectives, tasks, and responsibilities. The document states:

> "Research attention has recently been given to the patterns of air circulation within rooms and through buildings, to ensure that fresh air supply and pollutant removal requirements are effectively obtained without undue use of energy resources.
>
> "Recent developments in measurement techniques and computer hardware open new possibilities to study this phenomenon, while several advanced computer-based simulation methods have been produced in an attempt to describe this flow.
>
> "The objectives of this task are to evaluate the performance of single- and multi-zone air and contaminant flow simulation techniques and to establish their viability as design tools. The task is divided into two subtasks:
>
> (a) Subtask 1 - Room air and contaminant flow;
> (b) Subtask 2 - Multi-zone air and contaminant flow, including related measurement techniques."

3. General approach and project organization

Once the main objectives were formulated [2], we had to find the most effective approach to reach them. At the "Kick-off" meeting in May 1988 we decided on the organization and structure of the project.

We tried to keep it as simple as possible and agreed on the following:

(1) Two parallel subtasks for the full project term, because the methods are different for single- and multi-zone air movement.

(2) Each subtask has a subtask leader responsible for the scientific product of the task.

(3) The technical work within each subtask is structured in *Research Items* (RI), each with a RI-*Description* (RID). The RID states objectives, methods, completion date, and the principal investigator (PI).

(4) The project has a preparation phase, main performance, and reporting phases. Observer status is restricted to the preparation phase.

(5) Expert meetings are held twice a year (8 total).

The recommendations in the guidelines [3] of the IEA Energy Conservation in Buildings and Community Systems (ECB) Implementing Agreement have been observed.

Wide publicity for our work was sought by the publication of a news letter and by inviting interested persons of participating countries, - in addition to the active experts, - to the Annex meetings. Early dissemination of information (within Annex-20 countries) was promoted.

As a general policy, the experts were encouraged to publish their own work already during the course of the project as Annex reports, in journals, or at conferences. Reports and publications were advertised in a "List of Annex-Documentation," that was updated periodically. It now holds over 100 titles and abstracts. Records of final publications are also fed into AIRBASE.

This policy also led more than twenty Annex experts to report their own work directly at this AIVC Conference.

Table 1 lists the participating countries along with their subtask commitments and cities where they organized meetings.

Country	Commitment: Subtask 1	2	Expert Meeting: City and date	
Belgium		full	Lommel	Nov. 89
Canada	full	c	Ottawa	Sep. 91
Denmark	full		Aalborg	May 89
Finland	full			
France	full	full	Nice	Oct. 90
Germany	full		Aachen	Apr. 91
Italy	full			
Netherlands	full STL	full	Lommel	Nov. 89
Norway (to April 90)	full		Oslo	June 90
Sweden	full	c		
Switzerland	full	full STL	Winterthur	May 88
United Kingdom	c	full	Warwick	Nov. 88
USA	c	full		
totals 13	10	6	8	

Table 1 Participating countries and meeting sites. The meeting in Lommel, Belgium, was organized jointly by Belgium and the Netherlands. (**full** = full commitment, **c** = contribution, **STL** = subtask leader)

We have cooperated with other ongoing projects: Annex 5 (AIVC), Annex 23 (and COMIS [4]), and the IEA Solar Heating and Cooling Task XII, *Building Energy Analysis and Design Tools for Solar Applications.*

4. Subtask 1: Room Air and Contaminant Flow

Objectives for this subtask are:

- To evaluate the performance of three-dimensional complex and simplified air flow models in predicting flow patterns, energy transport, and indoor air quality,
- to show how to improve air flow models,
- to evaluate applicability as design tools,
- to produce guidelines for selection and use of models,
- to acquire experimental data for evaluation of models.

4.1 Approach

The basic approach was to solve *identical problems* in different participating countries by *different methods* and in different facilities. The results are now collected, analyzed, and compared [5]. This approach not only allows each country to assess the performance of the employed method but will also provide a methodology and experimental data sets to evaluate simulation models of the future.

Special problems encountered during this evaluation process were studied in separate research items: Modifications of turbulence models for low Reynolds numbers and thermal buoyancy [6], [7], [8], simulation of air supply devices [9], [10], or the specification of temperature boundary conditions that account for radiation.

Simplified methods have also been evaluated, and in some cases even developed [11]. These have a particular appeal to the design engineer, because he can apply them with little expenses for resources and specialized training.

Complex and simplified simulation methods have been evaluated by applying them to four different benchmark cases [5], each representative of a particular basic air flow phenomenon, such as forced or natural convection. Measurements and simulations have been carried out simultaneously by different groups. To compare the *numerical* performance of simulation methods, simple two-dimensional flow fields have also been calculated.

Available codes for air flow simulation are listed in [12]. Some general air flow codes used in North America and elsewhere may be found in [13]. And a critical review of computational fluid dynamics procedures was prepared for the ASHRAE by Baker and Kelso [14].

Table 2 shows a partial list of air flow programs. The programs that were used by Annex-20 participants are indicated by country names. "FloVENT" (distributed by FLOMERICS Ltd., UK) is used by IEA Solar Task XII, Project A.3, *Atrium Model Development*. All programs listed use finite-volume discretization (sometimes called finite-difference or finite-domain) with the exception of three, which employ the finite element method (FE). Subtask-1 workers have used eight of the listed algorithms. Denmark has its own research code.

Name	Origin of Code	Type	Annex-20 users	Remarks
ARIA	Abacus, UK	C		
ASTEC	Harwell UK	C		
CALC-BFC	Chalmers S	R	Sweden	own develop.
CHAMPION	TUD NL	R		
EOL-3D	INRS F	R	France	
EXACT3	NIST USA	R	Canada	
FEAT	UK	?		FE
FIDAP	FDI USA	C		FE
FIRE	AVL A	C		
FLOTRAN	Compuflow	C		FE
FloVENT	FLOMERICS UK	C		SHC Task 12
FLOW-3D	Harwell UK	C		
FLUENT	Creare USA	C	Germany	
JASMINE	BRE-FRS UK	R		fire, smoke
KAMELEON	SINTEF N	R	Norway	
PHOENICS	CHAM UK	C	Switzerland	
SIMULAR AIR	AVL A	C	Germany	
STAR-CD	CD UK	C		
TEMPEST	Battelle USA	R		
WISH-3D	TNO NL	R	NL, Finland	

Table 2 Computer codes for air flow simulation. Detailed information may be found in [12]. (**R** = Research algorithms, **C** = commercial algorithms, **FE** = finite element method, **SHC** = IEA Solar Heating and Cooling Implementing Agreement)

The Subtask-1 conclusions are restricted to the methods and programs actually used and are not applicable to others.

4.2 Results and contributions to this AIVC Conference

Table 3 shows an overview of papers/posters contributed by subtask-1 experts to this AIVC Conference. Contributions are identified by the name of the first author and session number.

Problem	*Measurement*	*Simulation*
Air supply device	Ewert 5A	Chen 3A = Ewert Heikkinen 5B Skovgaard 5B
Room flow field - turbulence	Sandberg 3A Zhang 5C	
- concentration	Heiselberg 3A	
- scaling & LRN		Moser 3A Skovgaard 5B
- water scale-model	Biolley 3A	= Biolley
Simplified methods - zonal model		Inard 3A
- jet models		Nielsen 1
Evaluation	Whittle 1	= Whittle

Table 3 Papers and posters presented at this 12th AIVC Conference by Annex-20, Subtask-1 investigators: Name of first author only is shown, along with conference session number. ("**= Ewert**" means, the same paper reports measurements *and* simulations, **LRN** = low-Reynolds-number effects)

The table shows that efforts have concentrated on problem areas (air supply) and on detailed measurements of flow quantities that are important to occupant comfort (turbulence intensity and concentrations of contaminants). Two contributions report the development and verification of simplified methods. The Summary Report by Lemaire [15] covers all work performed by subtask 1, whereas conference contributions, table 3, only report highlights.

4.3 Technical problems with numerical simulations

The major problems encountered during numerical simulation may roughly be grouped into five classes:

(1) Turbulence model at existing range of Reynolds numbers and near walls.

(2) Natural and mixed convection at cold or warm surfaces.

(3) Simulation of air supply device.

(4) Problems with number and size of numerical control volumes (computational grid) and difficulty to reach grid independent solutions.

(5) Numerical procedure to reach solution of system of finite difference equations.

Attempts have been made to handle these problems, as documented in several Annex-20 technical reports. But many approaches still leave plenty of space for improvement, and future research into these areas is badly needed.

Problem (1): We have not tested turbulence models other than the widely-used k-epsilon closure [12]. But experts have agreed that so-called low-Reynolds-number corrections are needed near walls and at low turbulence levels [7].

Problem (2): Three methods of dealing with heat transfer had been tried. The desirable approach is to prescribe wall temperature and have the program compute the heat flux. This works for forced convection (with wall functions) but is difficult for free convection because it requires a fine grid near the surface, low-Reynolds-number corrections in all equations, and careful setting of boundary conditions for computed variables. More work needs to be done on this method.

The second approach is to prescribe wall temperature and an empirical local heat transfer coefficient. This approach works well for window or radiator surfaces.

The third method is to estimate the local heat flux by empirical formulas and apply it in the simulation as a heat source (or sink) over the surface. If the correct heat flux (in W/m^2) is available, the method is reliable and does not require very fine grid, but the surface temperature is not automatically calculated.

Problem (3): A number of approaches are reported at this conference (table 3). It would be helpful if the manufacturers of air diffusers would publish some near field data (e.g., profiles in front of the device) with their technical specifications.

Problem (4): All computations were done with cartesian grids, where grid lines run through the entire flow domain ("tensor grid"). This mesh system has the disadvantage that grid refinements, also, extend from wall to wall, and into regions, where a fine resolution is not needed and cells with undesirable large aspect ratios may appear. Computational meshes with local grid refinement [12] were not tested. We found that grid independence was not reached.

Problem (5): Convergence of computations of flow fields with buoyancy effects in general is slow or inexistent. Monitoring of convergence is assisted by plotting the logarithmic residuals against iteration number (sweep number). Adjustments of relaxation factors during the solution process is normally required.

Experimental and numerical results suggest unsteady air motion under certain conditions at high Rayleigh number. However, this must still be verified. If, in fact, steady solutions do not exist under some circumstances, time-dependent simulation would be appropriate.

Simulations of case **e** (mixed convection, summer cooling) have shown asymmetric flow fields at symmetric boundary conditions and geometry. Two stable solutions (with the jet turning left or right, respectively) and one unstable but symmetric solution were observed. The latter is obtained by just computing one half of the flow field and enforcing symmetry-plane conditions. The asymmetric flow pattern is confirmed by measurements [16].

5. Conclusions from Subtask-1 evaluation of simulation methods

A detailed description of the benchmark exercises and quantitative comparisons of measurements and simulations with a critical evaluation is presented by Whittle [5].

What can we say now about the performance of room air flow simulation techniques and about their applicability as design tools? - It is certainly not our intention to say which computer code is the best!

It is not a question of codes but of *methods* for flow simulation. The available computer codes are only one component of a method. Figure 1 shows a few components or *techniques* that make up a method.

Simulation Method consists of:	Remarks/Examples:
Turbulence model	k-ε two-equation model
Computational grid	non-uniform grid with 30x30x30 cells, finer near walls
Boundary conditions	for velocity and turbulence at supply device for temperature or heat flux at surfaces for concentrations at contaminant sources etc.
Wall functions	appropriate for forced or free convection
Difference scheme	upwind, hybrid, PL, QUICK, etc.
relaxation technique	techniques to accelerate convergence
Computer code	(see table 2 for examples)

Fig. 1 A simulation *method* has many components, seven are shown here. (**PL** = power law, **QUICK** = quadratic upstream interpolation for convective kinematics [17])

Most commercial and some research codes include options to select or influence the features listed in figure 1.

The "best" method then would be the one that combines the "best" techniques. The evaluation [5] and summary [15] reports contain specific discussions of each technique.

The simplified methods must also be included in a general evaluation, of course. To assess performance and viability of methods, performance *criteria* should first be specified. But each potential user has different requirements. Three groups of users are listed in figure 2.

Users of simulation methods	Remarks:
Designers and consultants	1) computing themselves 2) subcontracting air flow simulations
Specialists of a CFD service-organisation	
Scientists and students at research labs	

Fig. 2 Potential users of simulation methods. (**CFD** = computational fluid dynamics)

The engineers who design ventilation will either use the simulation methods themselves or they commission the CFD analysis to an external service. Sometimes, they do an in-house simulation and back it up by a parallel external verification.

The use of advanced flow simulation techniques requires specialized skills. Therefore, private or public service groups are getting established in different countries. These organizations ideally have specialized staff and the right hard- and software to do useful flow field analyses within reasonable cost and time.

The third group are researchers at universities, research institutes, or industrial laboratories. These users spend considerable time with simulation algorithms with the following objectives:

- To develop or improve computer codes,
- to validate CFD-models with experimental data,
- to validate (and calibrate) simplified methods by comparison with CFD-models,
- to document methods, to train new users, and to transfer knowledge to the engineering community.

Each of the three groups of figure 2 has different criteria as illustrated in figure 3.

User: / Criterion:	Design	CFD Service	Research
Cost of resources: staff, training, hard- & software	important		
Cost per case: labor, CPU-time	important		
Speed: response time	crucial	important	
Reliability & expediency: accuracy, detail, questions answered?	important	crucial	crucial
User-friendliness: ease of input, pre-sentation of results	important	important	important
Interaction with other programs: building dynamics, radiation, CAD, etc.	important	important	

Fig.3 Criteria for performance of simulation methods by different user groups. (**CPU** = central processor unit, refers to machine-time and fee for using computer, **CAD** = computer aided design)

The entries in the table of figure 3 reflect the author's opinion as based on discussions during Annex-20 expert meetings. The weight "crucial" means that this user would *not* undertake a numerical simulation if that criterion were not met. The CFD-service has essentially the same criteria as the designer but is in a better position to optimize cost. For instance, the CFD-service can more efficiently maintain a skilled staff.

"Response time" refers to the span of time elapsed between formulation of task and delivery of usable results. "Expediency" expresses whether the computed output answers the questions of the user or client. For instance, have velocities, temperatures, and concentrations been calculated and output for the zones of interest, have local comfort and indoor air quality parameters been determined?

A novel approach to make detailed CFD calculations available in the design office was developed by Chen [18], [19]: He has pre-calculated a large number of typical flow patterns with a CFD code and arranged them in a systematic manner in a catalog called "Air Flow Pattern Atlas." So far, office rooms with different dimensions, loads, and ventilation systems have been modelled. The publication of this part of the Atlas is in preparation. Engineers may consult the Atlas to get a quick idea of air motion, indoor air quality, and draft risk (comfort parameter expressing the human sensation of air current) in a situation that resembles an actual design.

5.1 Technical conclusions

The work of Subtask 1 [15] and the evaluation of benchmark exercises [5] lead to these conclusions:

- CFD-simulations are useful when values of difficult-to-measure variables are needed in all points of the flow field.
- CFD-simulations are useful to study the sensitivity of flow patterns to small changes of conditions (trends).
- CFD-simulations are useful to predict air flow patterns for critical projects, i.e., when neither similar experience nor measured data exist (large spaces, unconventional ventilating systems, strong buoyancy effects).
- Simplified methods are useful to estimate the throw of supply air jet, the maximum velocity in the occupied zone, or the thermal plume in a radiator-window configuration.
- The catalog of pre-calculated cases (Atlas) is useful to get a quick overview of flow patterns that may develop in standard office rooms under various conditions.

In his evaluation report [5], Whittle concludes that CFD codes can predict room air movement with sufficient realism to be of use to design practice. Skill and experience are still required to use these codes. Many problems have been identified during this project, and Whittle [5] mentions three areas where further work is needed (modelling of supply jet, modelling of turbulence, thermal wall functions).

The Subtask-1 work demonstrates that CFD methods and several simplified approaches are now ready to be used as design tools. These powerful techniques, familiar to aerospace, propulsion, and environmental engineers, are still relatively new to building applications. Initial use will be by specialists, but further developments of methods and improvements of the user-interface will lead to a wide acceptance in the not-so-far future.

6. Subtask 2: Multi-zone air and contaminant flow and measurement techniques

Objectives for this subtask are:

- To develop new algorithms for specific problems, as flow through large openings, inhabitant behavior, air-flow-driven contaminants, or multi-room ventilation efficiency,
- to develop new, or improve existing measurement techniques,
- to collect and test input data sets of experimental data (reference cases for code validation),
- to establish a data base of physical parameters for multi-zone modelling in the design process.

6.1 Approach

The goals of this subtask point in two different directions:

- preparations for new multi-zone simulation packages,
- publication of a state-of-the-art measurement techniques handbook.

The subtask experts have developed algorithms for new multi-zone air flow models but have not engaged in developing such programs. The actual development may later be undertaken by individual countries and is also underway in IEA ECB Annex 23, *Multi-zone air flow modelling* [4]. The data bases will be indispensable for validation of these simulation tools.

To acquire the data for the data sets and to verify the algorithms for the planned simulation packages, proven measurement techniques have to be available. The authors of the measurement techniques guide have emphasized that measuring a particular flow parameter involves more than just 'putting in a sensor':

- Clear understanding of the *physics* of the investigated flow (e.g., effects of variable density on volumetric infiltration measurements),

- Clear understanding of the *purpose* of the measurements (e.g., if concentrations are measured to determine "local age of air," the definition and significance of this air quality indicator must be known),

- Selection of *equipment* and sensors and their characteristics,

- *planning* and setting up of experiments in a cost-effective way (e.g., number and locations of measured points should be optimized to get meaningful results in reasonable time),

- Data acquisition, *interpretation*, and presentation,

- *error analysis*, and problems that may be encountered.

The approach in the subtask included a state-of-the-art review of techniques and know-how relevant to the above goals. It turned out that many participants had experience in one or the other of the special fields. The team managed in a perfect way to bring this competence together. Topics to be addressed in depth have been assigned to six task groups, each with a responsible coordinator:

New algorithms:

2.1 Flow through large openings and single-sided ventilation [20],
2.2 Inhabitant behavior, e.g., simulated use of doors and windows [21],
2.5 Air-flow-driven contaminants [22],
2.6 Multi-room ventilation efficiency and ventilation performance index [23].

Measurement methods:
2.7 Multi-zone air flow measurement methods and techniques to measure ventilation efficiency [24].

Data bases and data sets:
2.11 Data bases for planning and validation [25].

The work of these groups is reported in the referenced Annex reports and in several technical reports.

6.2 Results and contributions to this AIVC Conference

Table 4 shows an overview of papers/posters contributed by subtask-2 experts to this AIVC Conference. Contributions are identified by the name of the first author and session number.

Problem RI	*Experiment*	*Modelling*
2.1 Large openings		
- algorithms		Pelletret 1
- single-sided ventilation: effects of wind and wind turbulence	Bienfait 1	= Bienfait Rao 1
2.2 Inhabitant behavior		Roulet 3A
2.5 Air-flow-driven contaminants	Phaff 1	= Phaff
- sources	Gehrig 3A	
- moisture		Jiang 3A
2.6 Multi-room ventilation efficiency		Haghighat 3A
2.7 Measurement techniques	Roulet 3A	

Table 4 Papers and posters presented at this 12th AIVC Conference by Annex-20, Subtask-2 investigators: Name of first author only is shown, along with conference session number. ("**= Phaff**" means, the same paper reports experiments *and* models, **RI** = Research Item number).

The papers listed on the first line of each research item contain an overview of the work of that task group, whereas the remaining contributions report specific results. Full documentation of the work is contained in the Annex reports referenced in section 6.1 above.

6.3 Technical problems with multi-zone modelling

Instead of listing all the problems that had to be solved, one exciting discovery is mentioned here to illustrate the type of questions that were discussed in this subtask.

French researchers made measurements on an experimental house with an opening exposed to turbulent wind [26]. Haghighat et al. [27] have made similar investigations. Both groups found that the air exchange rate through the opening depends on the turbulence intensity of a head-on wind.

It was speculated that air compressibility comes into play. It was argued by some, that compressibility will have vanishing effects at these low velocities (low Mach numbers), by others, that a repeatable experimental result cannot be lightly ignored.

An order-of-magnitude estimate shows for a turbulent wind velocity, $w = W + w'$ (where W is the mean velocity):

Pressure fluctuation: $\delta p \approx \delta\{ \rho/2 \ (W + w')^2 \}$

$$\delta p \approx \delta\{ \rho \ W \ w' \}$$

The *amplitude* of the fluctuation (in *italics*) is approximately

$$dp \approx \rho \ W \ w'$$

and w'/W expresses the turbulent intensity of the wind.

How much does this small pressure difference compress a fixed mass, m, of air? The volume, V, initially occupied by this mass is $V = m / \rho$.

The relative change of volume is $dV/V = - d\rho/\rho$. The air density in the room reacts to the applied pressure, *dp*, in a adiabatic manner [27], and

$$dV/V = - d\rho/\rho = - (\partial\rho/\partial p)_{is}\, dp/\rho \approx \pm W\, w'/\, a^2 ,$$

where the isentropic (is) pressure-dependence has been expressed by the speed of sound, a. Thus, the rough estimate yields:

$$dV / V \approx (W/a)^2 (w'/W),$$

i.e., the relative volume change is proportional to the square of the wind Mach-number multiplied by the turbulence intensity. Example: At W = 10 m/s the Mach number is, W/a = 0.03 ; at 20 % turbulence the volume change becomes 0.0002, or 40 liters for a house of 200 m^3. If this displacement of air is renewed periodically, the exchange rate (liter/s) would be *displacement* **X** *frequency*.

It is interesting to see that the Mach number appears in an infiltration problem. The subtask-2 team has analyzed and documented many surprising phenomena that have an impact on modelling or diagnostics like this compressibility effect.

7. Conclusions from Subtask-2 work

The accomplishments of this subtask extend over many different areas, and on each sub-project experts have discussed and drawn technical conclusions as reported in [20] - [25].

The main conclusions are:

- *Algorithms* of practical realism and manageable complexity have been developed and tested and are ready for integration into multi-zone air flow models.
- *Measurement techniques* relevant to multi-zone air, contaminant, and energy transport have been critically reviewed, updated to current state of knowledge, and presented in a way comprehensible by users.
- A methodology for compiling *validation data* has been developed and demonstrated by storing two measured data sets of existing buildings in a numerical data base.
- *Improvements* to experimental methods have been tried out, new physical effects discovered, and novel algorithmic methods developed.

8. General conclusions and recommendations for future work

It is no exaggeration if I say that work for this project has been done with great enthusiasm! Air flow pattern pioneers came to the meetings, willing to share their best ideas with international colleagues around the table, - always alert to point out flaws of discussed concepts, and open to fair criticism. The atmosphere of efficient teamwork was a good experience by itself. And the commitment of all participants to the common goals made the project a success. The creativity of many has contributed to the joint product of the Annex. As expressed in one of the news letters, - "Air flow research is people."

8.1 General technical conclusions

- The experimental verification of proposed design methods has shown that *validation* is an impossible task: Experiments are never perfect and *all* potential applications of a method cannot be foreseen. Therefore, the performance of a design tool may only be *evaluated* for certain specific uses. Annex experience shows that independent, parallel experiments should be conducted if possible.

- Attention has been focussed on technical *problems*. In both subtasks, these have been described and analyzed. Future progress is only possible by concentrating on these problems and not by ignoring them.

- The technical results are in a form that can be implemented in practice, as well as in future projects.

8.2 General project conclusions

- On the whole, project objectives have been met within the planned 42 project months. In some research items much more has been done than intended, in others emphasis had shifted a little and working objectives been reformulated. This is a consequence of a dynamic approach, where the direction of a new step is based on previous results. In some instances, the availability of staff and facilities had an influence.

- For Annex 20, it is true that the whole collaborative achievement amounts to *more* than the sum of individual national efforts. That means, the international teamwork produced a synergetic effect. Some results would have been impossible without international cooperation, as for instance, the verification of a theory developed in one country by test data from another.

- Cooperation with the IEA Air Infiltration and Ventilation Center, AIVC, was excellent. The assistance by the Center was vital to the success of Annex 20 (e.g., bibliographic searches, data handling and storing, reviewing reports, publishing, and providing the opportunity of this conference).

- In a task-sharing Annex, as this one, project leaders have no financial incentives to control productivity of participants. In spite of this, all participants have felt responsible and were well motivated to deliver promised work of high quality.

8.3 Recommendations for future work

- At special workshops, Annex-20 participants have developed proposals for new IEA Energy-Conservation-in-Buildings-and-Community-Systems projects. Two of these, *Air Flow in Large Enclosures* and *Residential Ventilation Systems*, are now in review by the Executive Committee. In fact, the products of Annex 20 may directly flow into these two projects and into Annex 23.

- International projects should have immediate impact on conservation of energy and environment. Their results should be in a form easily implemented in engineering practice. On the other hand, such projects are ideally suited to study the physics of energy systems. Therefore, objectives should reflect a sound balance between fundamental *and* applied products.

9. Acknowledgments

The project management by the Operating Agent and the direction of Subtask 2 by the Subtask Leader were financially supported by the Swiss Federal Office of Energy, BEW. The Swiss Federal Institute of Technology, ETH, provided the administrative infrastructure.

The support of the Annex-20 work by authorities and agencies of participating countries is gratefully acknowledged. Thanks go to all contributors, task coordinators, and Subtask Leaders. The names of the active experts of the project are recorded in several meeting minutes, their institutions or employers are listed in Annex-20 ExCo Progress Reports. The support by the AIVC, its staff and Director, Dr. Martin W. Liddament, is thankfully appreciated.

10. REFERENCES

1. NIELSEN P. V.
"Air flow simulation techniques, - progress and trends," 10th AIVC Conference, Dipoli, Finland, September 25-28, 1989.

2. INTERNATIONAL ENERGY AGENCY, IEA,
"Air flow patterns within buildings, - Annex XX of the IEA Implementing Agreement on Energy Conservation in Buildings and Community Systems." Legal text with description of project objectives, means, and responsibilities, etc., drafted by the IEA R&D staff, reviewed by the IEA Office of the Legal Counsel, and adopted by the Executive Committee. No.0633R/13.6.89.

3. SMITH J. A.
"Management guidelines for executive committee and operating agents," IEA Energy Conservation in Buildings and Community Systems program, October 1987.

4. FEUSTEL H. E. and RAYNOR-HOOSEN A. (Editors)
"Fundamentals of the multi-zone air flow model - COMIS," COMIS Group at the Lawrence Berkeley Laboratory, USA, and IEA, Air Infiltration and Ventilation Center, Technical Note AIVC TN 29, May 1990.

5. WHITTLE G. E.
"Evaluation of measured and computed test case results from Annex 20, Subtask 1," IEA Annex 20, Subtask 1, Research Item 1.35. 12th AIVC Conference, Ottawa, Canada, September 24-27, 1991.

6. MOSER A.
"Low Reynolds number effects in single room air flow," Annex 20, Subtask 1, Research Item 1.1, Working Report, ETH, Zurich, Switzerland, November 1988.

7. CHEN Q., MOSER A., HUBER A.
"Prediction of buoyant, turbulent flow by a low-Reynolds-number k-epsilon model," ASHRAE *Transactions*, Vol. 96, Part 1, 1990. Paper AT-90-2-2(3366) of ASHRAE Atlanta Winter Meeting, Feb.1990.

8. SKOVGAARD M., NIELSEN P.V.
"Numerical investigation of low Reynolds number effects," IEA Annex 20, Subtask 1, Research Item 1.1. 12th AIVC Conference, Ottawa, Canada, September 24-27, 1991.

9. HEIKKINEN J.
"Modelling of a supply air terminal for room air flow simulation," IEA Annex 20, Subtask 1, Research Item 1.24. 12th AIVC Conference, Ottawa, Canada, September 24-27, 1991.

10. CHEN Q. and MOSER A.
"Simulation of a multiple-nozzle diffuser," IEA Annex 20, Subtask 1, Research Item 1.20. 12th AIVC Conference, Ottawa, Canada, September 24-27, 1991.

11. INARD C., BUTY D.
"Simulation of thermal coupling between a radiator and a room with zonal models," IEA Annex 20, Subtask 1, Research Item 1.26. 12th AIVC Conference, Ottawa, Canada, September 24-27, 1991.

12. LIDDAMENT M. W.
"A review of building air flow simulation," IEA, Air Infiltration and Ventilation Center, Technical Note AIVC TN 33, March 1991.

13. SAID M. N.
"Two- and three-dimensional computer codes developed for applications other than room air flows," Annex 20, Subtask 1, Research Item 1.10, Working Report, IRC-NRC, Ottawa, Canada, November 1988.

14. BAKER A. J., KELSO R. M.
"Computational fluid dynamics procedures applied to prediction of room air motion," Contract Technical Report, ASHRAE TR on 464-RP, Report CFDL/89-2, Dept. Engineering Science and Mechanics, University of Tennessee, Knoxville, June 1989.

15. LEMAIRE A. D.
"Room air and contaminant flow, - a summary report of IEA Annex 20, Subtask 1," Annex 20, Subtask 1, Annex Report, TNO, Delft, Netherlands, September 1991.

16. BLOMQVIST C.
"Measurements of test case e (mixed convection, summer cooling)," Annex 20, Subtask 1, Research Item 1.17, Working Report, The National Swedish Institute for Building Research, Gävle, Sweden, March 1991.

17. VOGL N., RENZ U.
"Simulation of simple test cases b1, b2, b3," Annex 20, Subtask 1, Research Item 1.19, Working Report, RWTH Aachen, Germany, March 1991.

18. CHEN Q., SUTER P., and MOSER A.
"A data base for assessing indoor air flow, air quality, and draft risk," ASHRAE *Transactions*, Vol. 97, Part 2, 1991. (Paper no, 3504 of Indianapolis Annual Meeting, June 1991).

19. CHEN Q., MOSER A., and SUTER P.
"Interpolation theory and influence of boundary conditions on room air diffusion," accepted by *Building and Environment*.

20. VAN DER MAAS J. (Editor)
"Large openings and single-sided ventilation," Annex 20, Subtask 2, Research Item 2.1, Annex Report, LESO-EPFL, Lausanne, Switzerland, September 1991.

21. ROULET C.-A., CRETTON P.
"Inhabitant behavior," Annex 20, Subtask 2, Research Item 2.2, Annex Report, LESO-EPFL, Lausanne, Switzerland, September 1991.

22. PHAFF H., DE GIDS W. F.
"Air-flow-driven contaminants," Annex 20, Subtask 2, Research Item 2.5, Annex Report, TNO, Delft, Netherlands, September 1991.

23. PHAFF H., DE GIDS W. F., BIENFAIT D.
"Multi-zone ventilation efficiency and ventilation performance index," Annex 20, Subtask 2, Research Item 2.6, Annex Report, TNO, Delft, Netherlands, and CSTB, Champs-sur-Marne, France, September 1991.

24. ROULET C.-A. and VANDAELE L.
"Air flow patterns within buildings, measurement techniques," Joint Annex-20 / AIVC Report, Air Infiltration and Ventilation Center, Technical Note, September 1991.

25. HARRJE D. T. and PIGGINS J.M.
"Reporting guidelines for the measurement of air flows and related factors in buildings," IEA, Air Infiltration and Ventilation Center, Technical Note AIVC TN 32, January 1991.

26. RIBERON J., BARNAUD G. and VILLAIN J.
"Wind turbulence and ventilation," IEA Annex 20, Subtask 2, Research Item 2.1, Flow through large openings; Annex Report, CSTB, Champs-sur-Marne & Nantes, France, June 1990.

27. HAGHIGHAT F., RAO J., and FAZIO P.
"The influence of turbulent wind on air change rates, - a modelling approach," submitted to *Building and Environment*, 1990.

AIR MOVEMENT & VENTILATION CONTROL WITHIN BUILDINGS

12th AIVC Conference, Ottawa, Canada
24-27 September, 1991

PAPER 2

EVALUATION OF MEASURED AND COMPUTED TEST CASE RESULTS FROM ANNEX 20, SUBTASK 1

G E Whittle
Arup Research and Development
13 Fitzroy Street
London W1P 6BQ
UK

1. INTRODUCTION

The ability to accurately predict air movement and temperature distribution in spaces offers the potential for design engineers to evaluate and optimise room air distribution systems at an early stage, leading to improved thermal comfort and ventilation effectiveness. The computer models which are used for detailed analyses are based on computational fluid dynamics [1,2] and employ sophisticated numerical algorithms to satisfy the basic laws of physics. The programs are such that they are more complex and more difficult to use than those with which design engineers may be more familiar. Specialised skills are required to get the best from the codes, and, as with most new techniques, a greater confidence is needed before their use can be expected to become more routine. It is the latter point concerning confidence in use which is addressed by IEA Annex 20, Subtask 1.

IEA Annex 20 is a task-sharing project on "Air flow patterns within buildings". The objective is to evaluate the performance of single- and multi-zone air and contaminant flow simulation techniques and to establish their viability as design tools. In subtask 1 of the Annex, which deals with single-zone spaces, laboratory experiments in similar test rooms and computer simulations have been carried out at a number of sites in Europe and North America. The data comprises information on air flow patterns and on point-by-point values of mean velocity, turbulent velocity, temperature and contaminant concentration throughout a space.

This paper outlines an initial evaluation of this data and highlights some of the features which the comparisons of measured and computed room air distribution have yielded. Work is continuing in completing the evaluation for tests and data not reported or discussed here.

Besides giving a unified perspective on data from different sites to quantify the general degree of agreement, the evaluation exercise also has the potential for:

- establishing benchmarks for the validation and evaluation of computer codes for room air movement;
- highlighting advantages/limitations of the methods used;
- assessing overall confidence level in computer simulations;
- indicating accuracy and repeatability of measurements and simulations;
- guiding research on simplified models of air movement and identifying problem areas where attention should be focused.

2. THE TEST CONDITIONS

Four full test configurations and one simulation-only test case have been considered. These comprised forced convection,

isothermal flow (case B) [7]; free convection with a radiator (case D) [8], mixed convection, summer cooling (case E) [9], forced convection with contaminant concentration in an isothermal flow (case F) [10], and a two-dimensional isothermal and summer cooling test case (case 2D) [11].

Figures 1 and 2 show the geometry and basic configuration of the basic test room and conditions. The room is sized 4.2m x 3.6m x 2.5m height, with a single-glazed window of area 3.2m^2 in one of the 3.6m walls and a diffuser and extract in the opposite wall [12]. For test case D, a radiator sized 0.3m x 2.0m and rated at 0.862kW was used sited beneath the window [13]. In reality, because existing test facilities were used, some small differences existed in the dimensions of individual test rooms [12].

The supply air diffuser for test cases B and E was the Hesco type KS (no. KS4W205K370) (Figure 3) and was common between all the test facilities [14]. With its 84 tiny nozzles, this type of diffuser provides a real challenge to simulation codes and practitioners.

The two-dimensional test case (isothermal and summer cooling) is shown in Figure 4. The room is specified by ratios of L/H= 3, h/H= 0.056, t/H= 0.16, where 'L' is the room length, 'h' the inlet slot height, 't' the exhaust height and H the room height (3.0m). Experimental data for a Reynolds number of 5,000 is available. For the non-isothermal case, the critical factor is the influence of Archimedes number on jet penetration.

For the contaminant concentration, tests are based on test case B but with the addition of a passive contaminant released in the centre of the room.

The test cases are summarised below.

Test case B (isothermal flow)

Test case B represents forced convection (at isothermal conditions) at three different air flow rates.

Case: B1 flowrate: 0.0158m^3/s (1.5 ach^{-1}).

Case: B2 flowrate: 0.0315m^3/s (3.0 ach^{-1}).

Case: B3 flowrate: 0.0630m^3/s (6.0 ach^{-1}).

Test case D (radiator)

Test case D represents free convection with a radiator located beneath a cold window, with three corresponding radiator and window surface temperatures.

Case: D1 radiator surface temperature: 46°C,
window surface temperatures: 10°C.

Case: D2 radiator surface temperature: 55°C
window surface temperature: 5°C

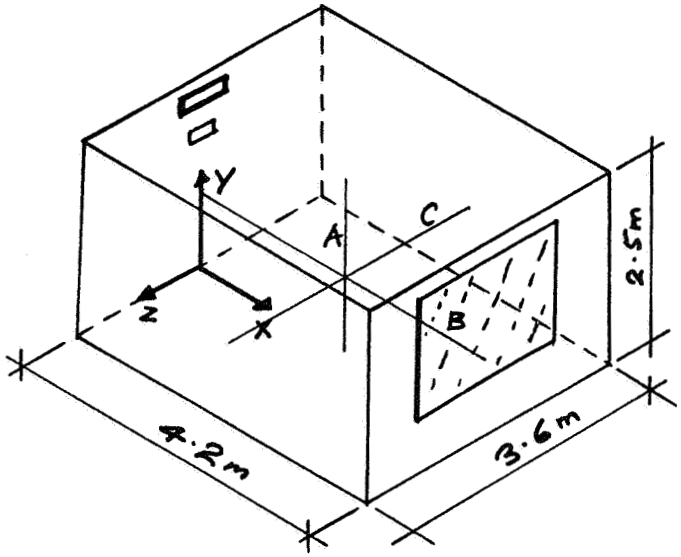

Figure 1. Geometry of test room showing profile locations.

b) Forced convection, isothermal conditions

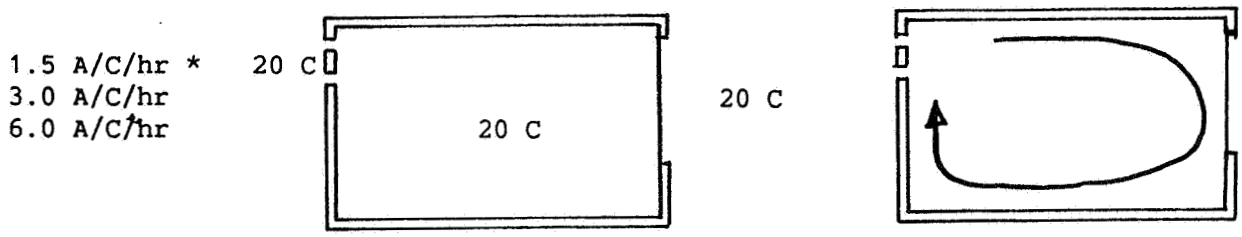

d) Free convection with radiator

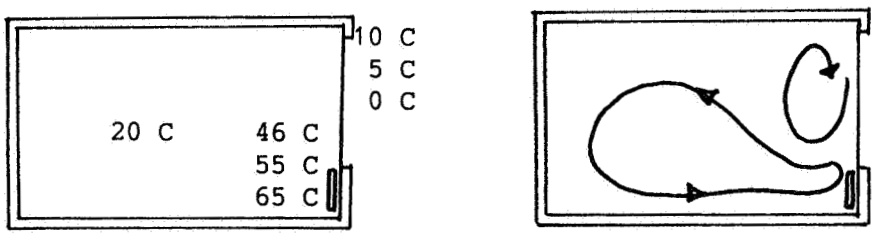

e) Mixed convection, summer cooling

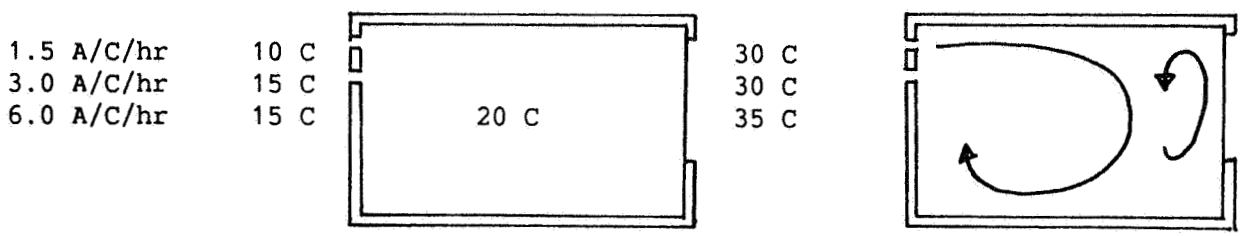

Figure 2 Summary of test case conditions

(* 0.0157, 0.0315, 0.063 m3/s)

Case: D3 radiator surface temperature: 65°C
window surface temperature: 0°C

Test case E (summer cooling)

Test case E represents mixed convection under summer cooling conditions at three different supply air flow rates.

Case: E1 flowrate: 0.0158 m3/s (1.5 ach^{-1}),
supply air temperature: 10°C,
window surface temperature: 30°C.

Case: E2 flowrate: 0.0315 m3/s (3.0 ach^{-1}),
supply air temperature: 15°C,
window surface temperature: 30°C.

Case: E3 flowrate: 0.0630 m3/s (6.0 ach^{-1}),
supply air temperature: 15°C,
window surface temperature: 35°C.)

Test case F (contaminant concentration in isothermal flow)

Test case F represents contaminant concentration in forced convection (at isothermal conditions) at the three different air flow rates indicated above for case B.

Two-dimensional test case 2D (simulation only)

The two-dimensional test case represents both isothermal at a Reynolds number of 5,000, and summer cooling.

3. MEASUREMENTS AND SIMULATIONS

Results were obtained from participants generally according to a prescribed format [15,16]. A full data set for test cases B, D and E comprised 560 points at which mean air speed (Um), turbulent velocity (Ut) and temperature (T) were measured or predicted. In the case of contaminant concentration (case F), then, of course, concentration was also specified. In addition, data on the velocity decay of the supply air jet and the jet penetration length related to Archimedes number were obtained from some participants for test cases B and 2D, and E, respectively.

The specification of 560 points meant that those undertaking simulations were required to limit the data supplied. As expected, simulations were carried out with many thousands of calculation nodes. However, for those undertaking measurements, the requirements of the 560 specified points proved to be demanding. Some contributors concentrated their attention in measuring the detailed flow structure in the jet, whilst others were able to measure throughout the space and mostly, but not universally, at all the agreed positions.

Table 1 identifies the co-ordinates of the standard measuring locations. As a subset of these locations, an occupied zone is defined up to a height of 1.8m and to within 0.6m of walls [3,4].

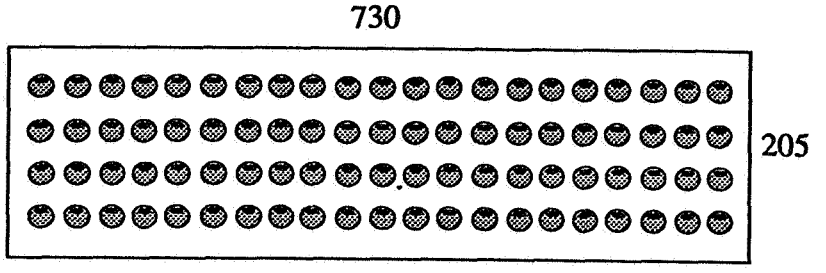

Figure 3 Hesco diffuser (84 nozzles)

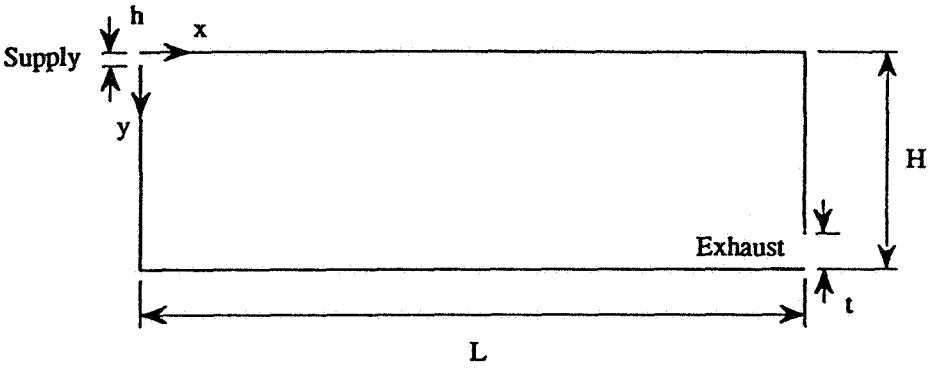

Figure 4 2D Testcase

Table 1 Measurement locations (see Figure 1)

X	Y (height)	Z
0.1	0.05	-1.7
0.6	0.10	-1.2
1.4	0.2	-0.6
2.2	0.5	0.0
3.0	1.0	0.6
3.6	1.5	1.2
4.0	2.0	1.7
4.1	2.3	
	2.4	
	2.45	

Occupied zone data is of interest to designers in assessing thermal comfort and ventilation effectiveness.

The measuring instrumentation was mainly based on thermal anemometry using hot-wire and omnidirectional hot-film probes from Disa-Dantec, TSI and B&K, IMG constant-current hot_wire, and constant-temperature thermistors.

The computer codes used were all of finite volume formulation and all utilised a pressure-correction method [1]. The codes were: CALC-BFC, EOL3D, EXACT3, FLUENT, KAMELEON, PHOENICS, SIMULAR-AIR, WISH3D. A number of zonal models were also used, operated by INSA/CSTB, France.

CFD simulations were carried out with the different codes identified above, with collective guidance given on options for modelling boundary conditions such as the supply terminal [17] and the radiator [18]. For the supply terminal, alternative inlet models were defined. These included a basic model with an opening of 0.180m x 0.062m representing the diffuser, a prescribed velocity model where the velocity is fixed over a surface some distance from the diffuser. The code operators were free to generate meshes which they felt were appropriate, bearing in mind the need to resolve certain features of the flow such as the supply air jet and boundary layers, whilst also recognising practical limitations associated with computing resources, code capabilities and project time-scale. Some contributors investigated different options in specifying boundary conditions, in mesh resolution and alternative differencing schemes. The difference schemes used include Upwind, Hybrid, Power Law and Quick. All CFD simulations were carried out with turbulence represented using the two-equation k - epsilon model. Some turbulence models incorporated the buoyancy-extension to represent the generation or suppression of turbulence energy due to temperature gradient, and some models incorporated a low Reynolds number variant.

Most simulations were carried out in one half of the room, assuming symmetry, although some simulation data was generated for the whole space.

More detailed information on the methods used in these studies can be found in participants' individual reports listed in the References section at the end of this paper.

4. DATA ANALYSIS

The fundamental quantities which are calculated and compared are the mean air speed (Um), turbulent velocity scale (Ut), air temperature (T) and contaminant concentration. However, the mean air speed from measurements using an omni-directional probe is the time-averaged value of velocity, whilst in simulations it is the magnitude of the mean velocity. The turbulent velocity from measurements is the standard deviation of velocity (given by an omnidirectional probe), but in simulations it is $(2k)^{1/2}$ where 'k' is the turbulent kinetic energy per unit mass. These are not identical physical quantities since averaging is performed

differently. To ensure consistency between measurements and simulations [7,19] a modified air speed has been defined, where the modified air speed is,

$$U^* = (Um^2 + Ut^2)^{0.5}$$

This has been presented only for the averaged comfort parameters and for some statistical comparisons. In practice, the modified air speed is very similar to mean air speed, but it relies on two items of data and is more difficult to interpret in a physical sense, and hence has limited value.

Measurement and simulation data are considered in the following ways:

Flow patterns

A comparison of flow patterns provide a first and qualitative indication of whether agreement exists between data sets. Indications are given in the figures of flow patterns and contours of velocity and temperature for selected cases. These are reproduced from participants' reports. In the case of measured data, speed contours are shown rather than vector plots.

Key comfort parameters

The thermal comfort of occupants and air movement in the room can be assessed by consideration of comfort parameters such as average air speed, turbulence, and air temperature, and the maximum and minimum air temperatures in the occupied zone [3,4]. The measured data shown is that for the whole of the occupied zone whilst the simulation data was generated mainly for half the zone (by specifying a symmetry boundary along the middle of the room).

Statistical correlations and RMS differences

Some early analysis was carried out using a statistically-based point-by-point comparison of data using calculations of linear correlation coefficient and RMS error.

The sample linear correlation coefficient (SCC) and root mean square of the difference (RMS) was calculated between each pair of data sets for the modified air speed, the turbulence scale and the air temperature according to the following formulae [5]:

For the SCC between the mean air speeds (Um) predicted by participant A and that of participant B,

$$SCC, Um(A,B) = \frac{n\sum Um_i^{(A)} Um_i^{(B)} - \sum Um_i^{(A)} \sum Um_i^{(B)}}{\sqrt{n\sum Um_i^{(A)^2} - \left(\sum Um_i^{(A)}\right)^2}\sqrt{n\sum Um_i^{(B)^2} - \left(\sum Um_i^{(B)}\right)^2}}$$

where the summation is from i= 1, n over the n (= 560 = 10*8*7)

standard measuring points. e.g. Um_1 is Um for the point X= 0.1, Y= 0.05, Z= 0.0. Similarly the RMS difference between the data sets is given by,

$$RMS, Um(A,B) = \sqrt{\frac{\sum \left(Um_i^{(A)} - Um_i^{(B)}\right)^2}{n}}$$

Thus, the results from participant A are compared with those of participant B for the corresponding measuring points. The SCC must take a value between +1 and -1 with +1 arising if, plotting Um(A) against Um(B), all 560 points lie on a straight line with positive slope. Correspondingly lower values arise when the points show greater scatter about the linear regression line.

RMS values will range upwards from 0 (perfect agreement between all 560 measured and simulated values) and have the units of the variables being compared.

In practice, correlation coefficients and RMS difference were relatively large even comparing measured to measured data. The nature of room air movement, which is characterised by large amplitude and low frequency velocity fluctuations, is such that point-by-point comparisons do not yield meaningful results. Therefore, analyses using this approach has been discontinued.

4.5 Profiles/graphs

Velocity decay with distance from the diffuser, variation of maximum (or mean) velocity in the room and penetration length of the jet in summer cooling have been identified as a critical factors in quantifying agreement. Examples of some of these graphs are shown in this paper.

5. MAIN FINDINGS

Work is continuing from previous analyses [35,36] in comparing and evaluating the data. Some observations are made below.

Test case B (isothermal flow)

Air flow patterns for the isothermal case (B1, B2 and B3) are well predicted by the simulation models. As examples of velocity fields, Figure 5 show air centre-line speed contours for case B2 from measured data from Blomqvist [20] and from Heikkinen [21] compared to simulation data from Skovgaard [22].

Occupied zone data on mean velocity, turbulent velocity, modified velocity and maximum velocity are summarised in Tables 2, 3 and 4.

As seen in Figure 6 the occupied zone velocities increase almost linearly with supply air flow rate, as expected (Tests B1 to B2 to B3). There are, though, simulation results where the predicted

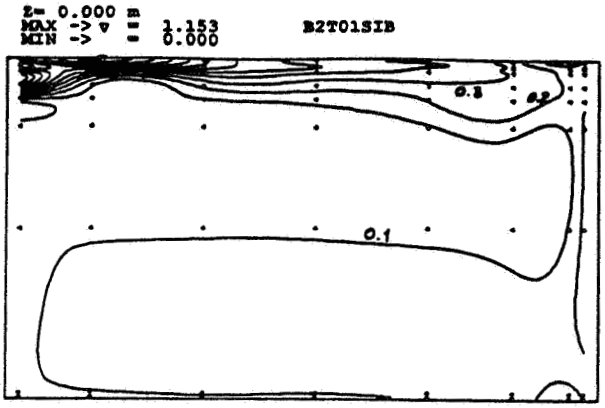

Isovels in plane z= 0.0 m

Measurements from Blomqvist

Case b2, plane 1, measured air speed, m/s

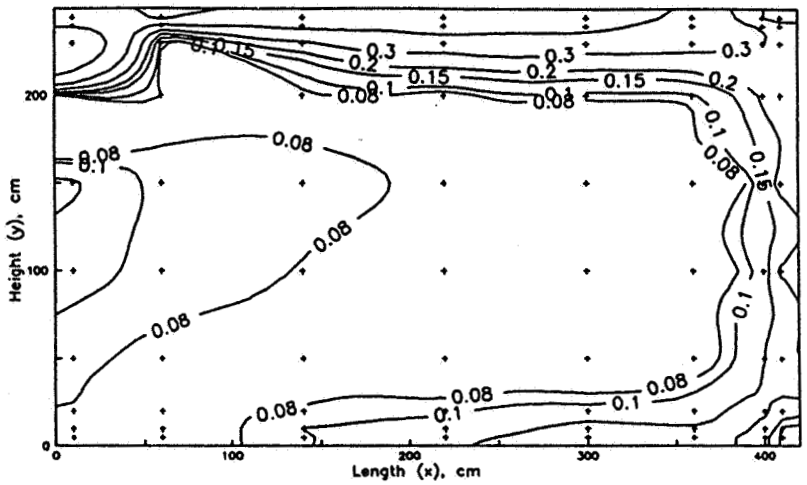

Measurements from Heikkinen

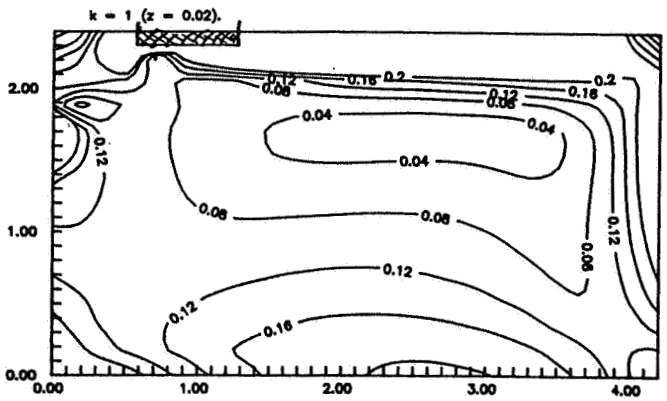

Simulation from Skovgaard

Figure 5 Test case B2

Table 2 Test case B1

Ref.	M or S	Ave. Um	Ave. Ut	Ave. U*	Max Um	Max Temp	Ave. Temp	Min Temp
B1CH	S	0.020	0.007	0.022	0.038	-	-	-
B1_CTH_C	S	0.032	0.010	0.034	0.057	-	-	-
B1C01SF1	S	0.041	0.010	0.043	0.073	-	-	-
B1004DK	S	0.041	0.019	0.046	0.070	-	-	-
B1001DK	S	0.045	0.019	0.051	0.075	-	-	-
B1GER	S	0.049	0.022	0.055	0.090	-	-	-
B1C03SF1	S	0.053	0.014	0.055	0.093	-	-	-
B1M001NL	M	0.059	-	0.059	0.123	-	-	-
B1P001NL	S	0.060	0.016	0.063	0.104	-	-	-
B1FRG	S	0.083	0.036	0.093	0.151	-	-	-

M= measured, S= simulated

Table 3 Test case B2

Ref.	M or S	Ave. Um	Ave. Ut	Ave. U*	Max Um	Max Temp	Ave. Temp	Min Temp
B2CD	S	0.017	0.005	0.020	0.049	-	-	-
B2N2	S	0.027	0.107	0.114	0.073	-	-	-
B2_CTH-C	S	0.033	0.010	0.035	0.060	-	-	-
B2CH	S	0.048	0.019	0.052	0.086	-	-	-
B2T01SIB	M	0.082	0.031	0.089	0.189	22.30	21.08	20.20
B2FRG	S	0.083	0.036	0.093	0.151	-	-	-
B2C01SF1	S	0.092	0.024	0.097	0.161	-	-	-
B2T03SF1	M	0.100	0.023	0.103	0.178	18.40	18.07	17.75
B2C02SF1	S	0.108	0.029	0.113	0.189	-	-	-
B2C03SF1	S	0.108	0.029	0.113	0.189	-	-	-
B2B002NL	S	0.108	0.022	0.112	0.190	-	-	-
B2B001NL	S	0.109	0.019	0.112	0.192	-	-	-
B2GER	S	0.109	0.047	0.122	0.211	-	-	-
B2C04SF1	S	0.119	0.040	0.128	0.205	-	-	-
B2P001NL	S	0.123	0.034	0.129	0.213	-	-	-
B20F	S	0.130	0.055	0.146	0.221	-	-	-
B2004DK	S	0.131	0.054	0.145	0.222	-	-	-
B2P002NL	S	0.135	0.051	0.148	0.234	-	-	-
B2001DK	S	0.151	0.061	0.167	0.252	-	-	-

Table 4 Test case B3

Ref.	M or S	Ave. Um	Ave. Ut	Ave. U*	Max Um	Max Temp	Ave. Temp	Min Temp
B3CH	S	0.033	0.053	0.063	0.070	-	-	-
B3_CTH_C	S	0.034	0.010	0.036	0.061	-	-	-
B3C01SF1	S	0.190	0.052	0.202	0.333	-	-	-
B3T02SF1	M	0.205	0.055	0.213	0.418	18.65	18.40	17.97
B3C03SF1	S	0.218	0.061	0.229	0.381	-	-	-
B3GER	S	0.221	0.095	0.247	0.434	-	-	-
B3FRG	S	0.242	0.092	0.265	0.440	-	-	-
B3P001NL	S	0.251	0.070	0.264	0.436	-	-	-
B3004DK	S	0.253	0.104	0.280	0.428	-	-	-
B3001DK	S	0.314	0.123	0.347	0.527	-	-	-

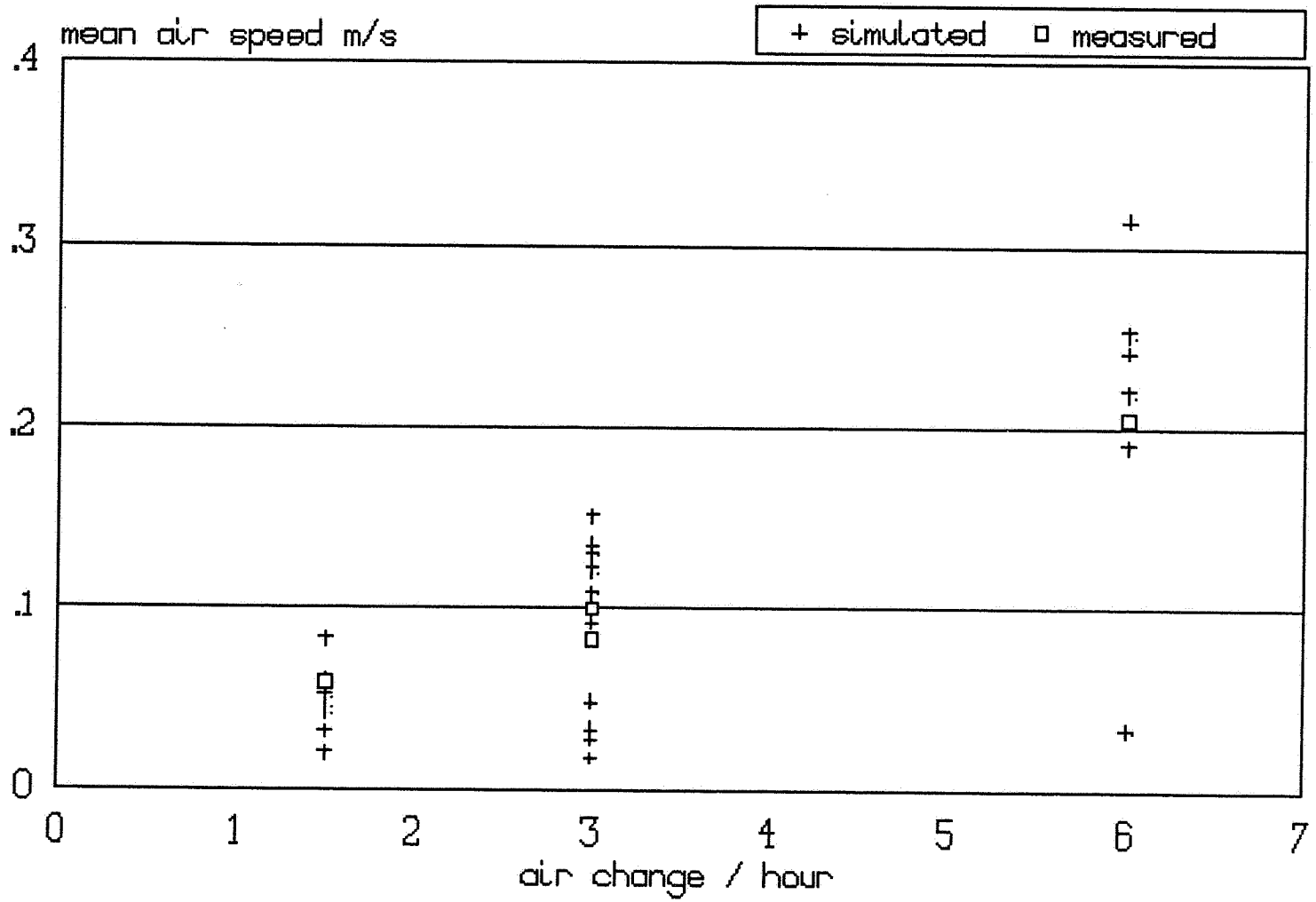

Figure 6 Occupied zone air speed (test cases B)

mean velocity is clearly too low and some which are high. It is unclear as yet whether this is due to the characteristics of the code used or related to assumptions made by the operator. The figures for modified velocity generally follow those for the mean velocity.

It should be noted that certainly for case B1 and possibly case B2 the mean velocities are very low and hence difficult to measure with any reasonable accuracy.

In reality it may be expected that some low Reynolds number effects would be evident at the low flow rate end of the range. However, those who performed simulations using a high Reynolds number turbulence model (the majority) would not expect to predict this. Individual researchers have commented on measurements [6] and have discussed the physical effects and models [23,24].

Regarding numerics, Vogl and Renz [25] indicated that the Quick differencing scheme on a fine grid had the potential for a greater accuracy, although the scheme exhibited poorer numerical stability than the power law scheme.

Test case D (natural convection, radiator)

Figures 7 and 8 show speed and temperature contours from measurements (Lemaire [29]) and simulation (Heikkinen and Piira [30]) of case D2, and Tables 5-7 summarise the occupied zone velocity and temperature data.

The air velocities in the occupied zone are uniformly low, and the average temperature is in almost all cases between 20°C and 21°C. It is unfortunate that measured data is limited, and that the only set indicates an occupied zone air speed higher than the simulation data and a temperature slightly lower.

In simulations, Lemaire [26] found that the flow pattern remained similar for the three cases, with the pattern driven by the buoyant flow from the radiator upwards over the cold window. Prescribed heat fluxes were used for the radiator and the window. Previous simulations had demonstrated that the logarithmic wall functions dramatically under-predict the surface convection coefficients.

Zonal model results have been generated by Inard and Buty [27] for comparison with measurements and CFD simulations. It is found for case D2 and for assumed constant heat transfer coefficients, that a single-zone model yields the same mean air temperature of 20.3°C as a five-zone model. However, a similar two-zone model gives an increase in mean temperature of about 0.6°C, whilst the assumption of variable convection coefficients in a five-zone model reduces the mean air temperature by approximately 0.6°C. The predicted temperature gradients vary from 0.4°C (five-zone, variable convection coefficients) to 1.2°C (two-zone, constant convection coefficients). Similar findings apply for cases D1 and D3.

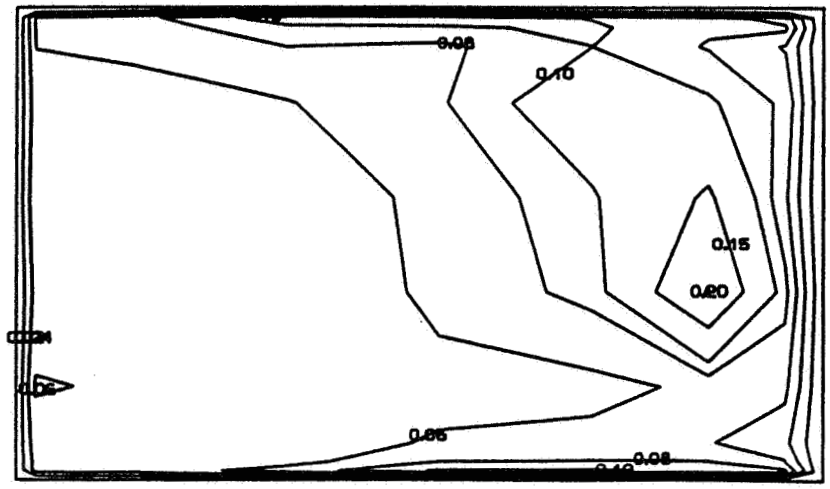

Run: d2M001NL
Iso-vels (m/s)
plane k = 1
(z = 0.00 m)

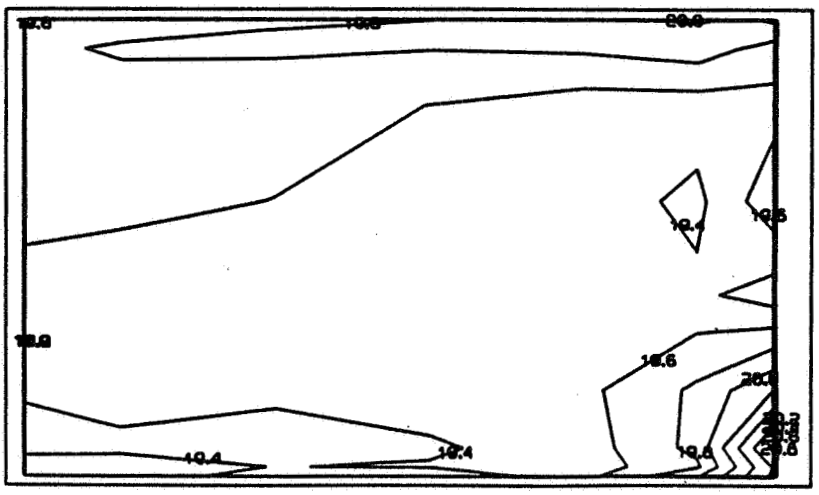

Run: d2M001NL
Isotherms (°C)
plane k = 1
(z = 0.00 m)

Figure 7 Measurement data for test case D2
(from Lemaire)

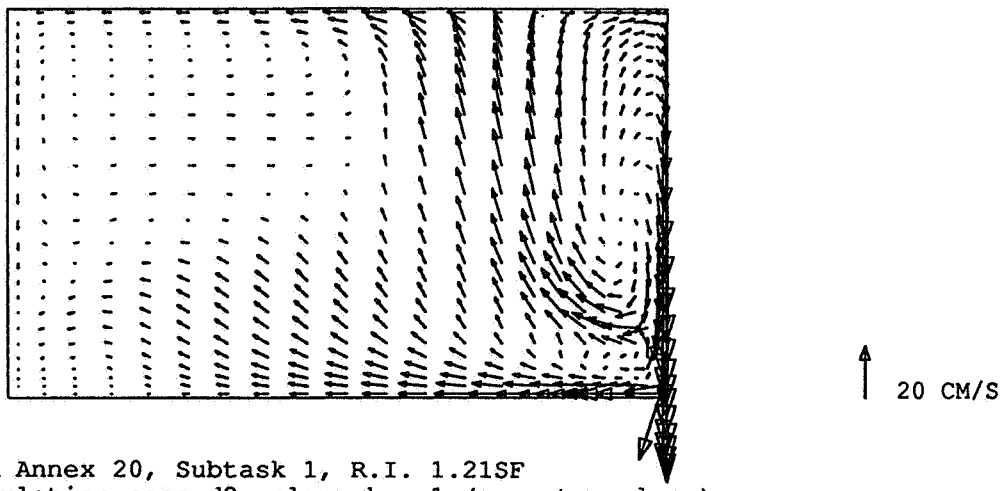

IEA Annex 20, Subtask 1, R.I. 1.21SF
Simulation case d2, plane k = 1 (symmetry plane)
Simulated velocity vectors

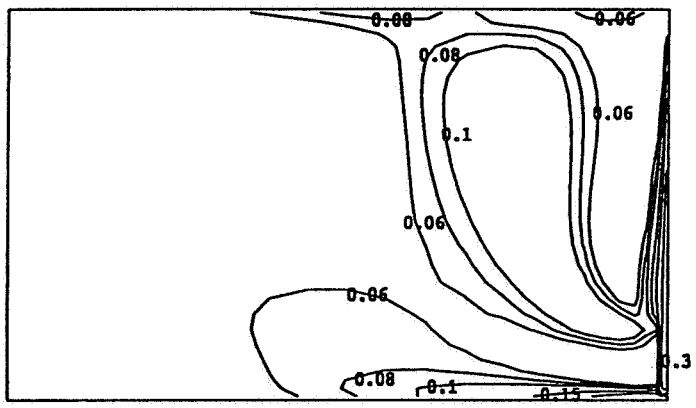

IEA Annex 20, Subtask 1, R.I. 1.21SF
Simulation case d2, plane k = 1 (symmetry plane)
Simulated contours of velocity (m/s)

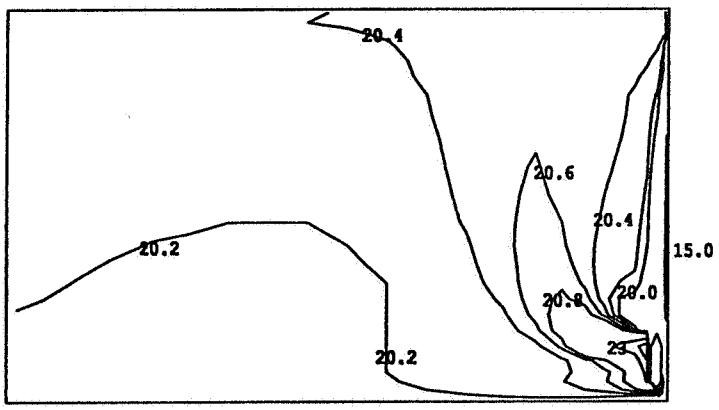

IEA Annex 20, Subtask 1, R.I. 1.21SF
Simulation case d2, plane k = 1 (symmetry plane)
Simulated contours of temperature (^{o}C)

Figure 8 Simulation data for test case D2 (from Heikkinen)

Table 5 Test case D1

Ref.	M or S	Ave. Um	Ave. Ut	Ave. U*	Max Um	Max Temp	Ave. Temp	Min Temp
D1CH	S	0.017	0.009	0.020	0.074	20.54	20.28	20.08
D1Q001NL	S	0.020	0.005	0.021	0.081	20.89	20.40	20.06
D1FRG	S	0.022	0.014	0.028	0.046	21.10	20.52	20.10
D11GER	S	0.028	0.007	0.030	0.085	21.76	20.93	20.23
D1CO2SF1	S	0.036	0.020	0.042	0.127	20.66	20.15	19.89
D1GER	S	0.037	0.019	0.042	0.126	20.38	20.11	20.01

M= measured, S= simulated

Table 6 Test case D2

Ref.	M or S	Ave. Um	Ave. Ut	Ave. U*	Max Um	Max Temp	Ave. Temp	Min Temp
D2CH	S	0.021	0.010	0.025	0.084	20.57	20.29	20.07
D2Q001NL	S	0.022	0.006	0.024	0.087	21.17	20.58	20.11
D2FRG	S	0.024	0.016	0.030	0.049	21.30	20.61	20.10
D2CO1SF1	S	0.026	0.012	0.029	0.154	20.58	20.18	19.98
D21GER	S	0.029	0.008	0.031	0.085	21.56	20.85	20.23
D2CO2SF1	S	0.041	0.022	0.047	0.150	21.06	20.20	19.96
D2GER	S	0.062	0.036	0.074	0.213	20.28	20.10	19.93
D2M001NL	M	0.071	-	0.071	0.203	20.16	19.52	19.23

Table 7 Test case D3

Ref.	M or S	Ave. Um	Ave. Ut	Ave. U*	Max Um	Max Temp	Ave. Temp	Min Temp
D3CH	S	0.019	0.008	0.021	0.085	20.76	20.38	20.09
D3Q001NL	S	0.024	0.006	0.025	0.090	21.57	20.84	20.21
D3FRG	S	0.028	0.018	0.035	0.059	21.60	20.83	20.10
D31GER	S	0.033	0.009	0.035	0.093	21.95	21.12	20.32
D3CO2SF1	S	0.047	0.026	0.055	0.165	20.71	20.23	19.88
D3GER	S	0.058	0.033	0.070	0.227	20.40	20.11	19.91

Test case E (mixed convection, summer cooling)

Figures 9 (Fossdal [32]) and 10 (Blomqvist [33]) show measured speed and temperature contours for case E2. Simulation data from Heikkinen and Piira [34] is shown in Figure 11. The simulation of the jet indicates a slightly earlier and more positive detachment from the ceiling. Table 8-10 summarises the occupied zone velocity and temperature data.

The measured data for the summer cooling case indicates the difficulty in reproducing the test conditions accurately. Figure 12 shows, as expected, a sensitivity of the penetration length of the jet to the Archimedes number for measurement data sets (Blomqvist [28] and Heikkinen [21]) and simulation (Heikkinen [21] and Renz [31]). The measured data from Heikkinen indicates a varying jet penetration length across the room. This test case represents a particularly onerous one to simulate. However, whilst some differences exist between the simulated results and measurement at high Archimedes number the nature of the flow is quite well represented in terms of flow patterns, mean velocities, penetration length and occupied zone temperatures.

Lemaire [37], in simulations with the prescribed velocity inlet model found that for the higher flow rate cases (E2 and E3) the supply air jet dominates the flow pattern, causing a down-flow at the window. However, at the lowest flow rate (E1) the warm air rising from the window deflects the jet down from the ceiling. Flow instabilities were found at this condition which caused difficulties in achieving convergence to a steady-state solution. Simulations with the basic inlet model were easier to converge although some reduction in penetration length were observed.

Test case F (isothermal flow with contaminant)

Comparative data for the contaminant cases will be reported in the final Evaluation Report, to be completed prior to November 1991.

Test case 2D (isothermal flow and summer cooling)

Very detailed computations are possible for this particular test case, and useful data is coming forward. Some examples of the 2D test case results are shown in Figure 13. Generally good agreement is evident for velocities and turbulence quantities in iso-thermal flow. For non-isothermal flows both Chen [] and Lemaire [] have found strong hysteresis effects and difficulties in identifying an intermediate stage of jet projection.

Flow asymmetries

Evidence of flow asymmetries exists from the experimental data. In most simulations, however, a symmetry plane has been assumed, and so by definition no asymmetric flow patterns could be identified. However, some fine grid simulations have, under certain circumstances, been able to demonstrated flow asymmetries. Further analysis is required to identify the importance of this effect.

Case e2 PLANE K1

Air flow rate	: 0,0315 m^3/s	Air supply temperature	: 14,0 °C
Air change rate	: 3,0 1/h	Wall surface temperature	: 21,4 °C
Inlet velocity	: 3,32 m/s	Window surface temperature	: 30,2 °C

VELOCITIES

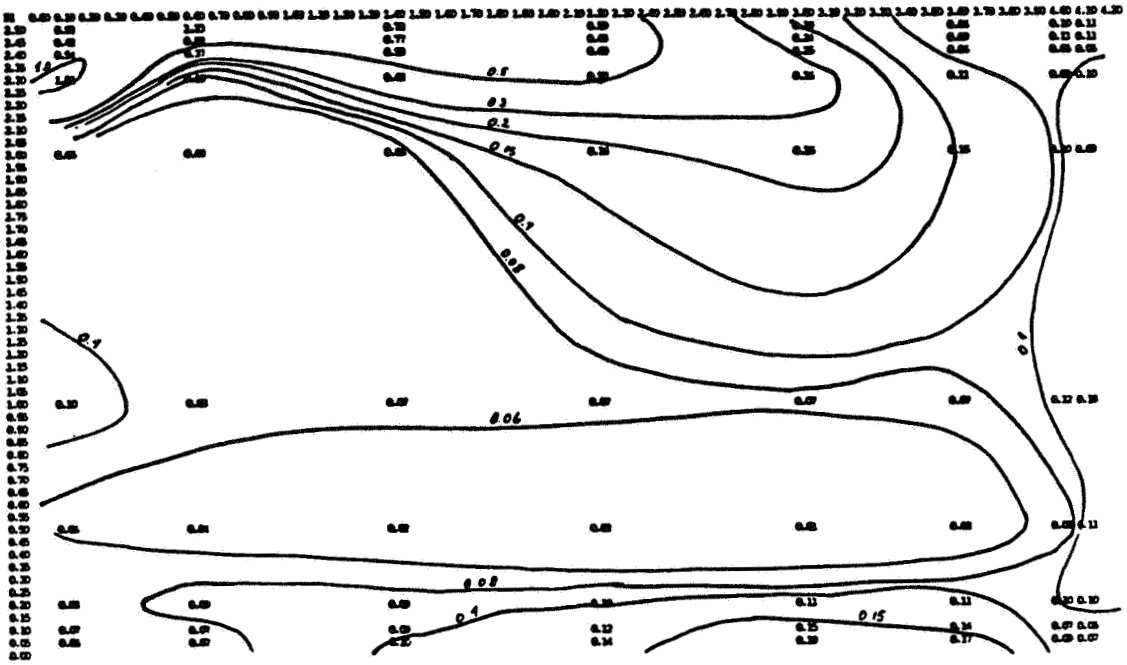

TEMPERATURES

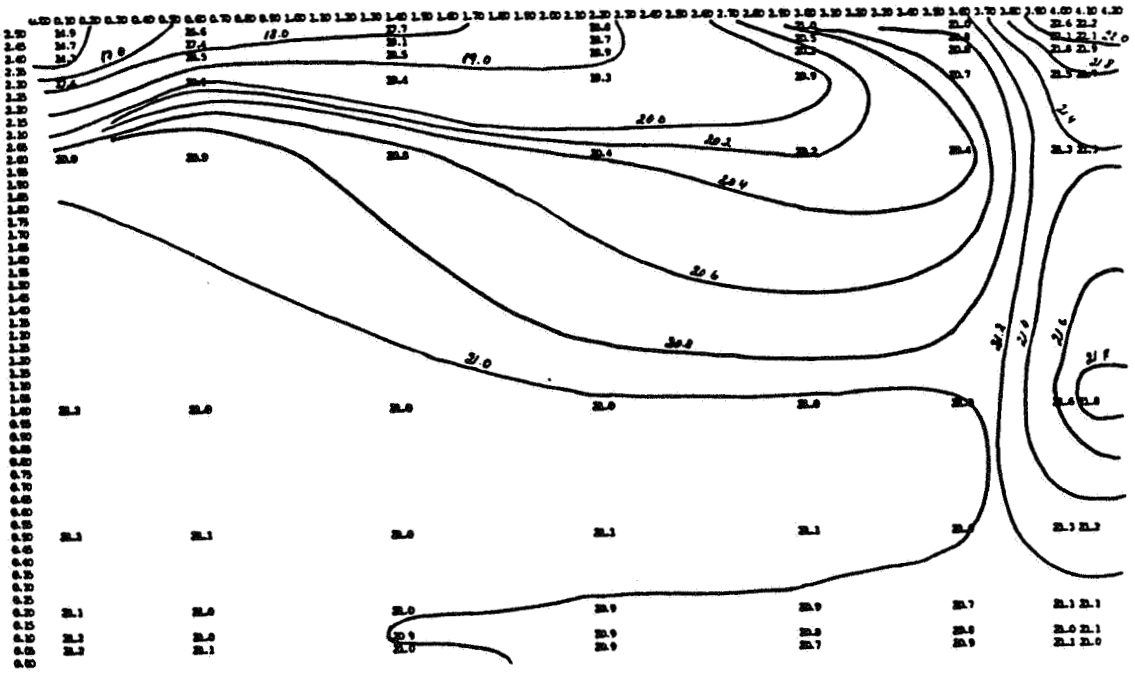

Figure 9 Measurement data for test case E2 (from Fossdal)

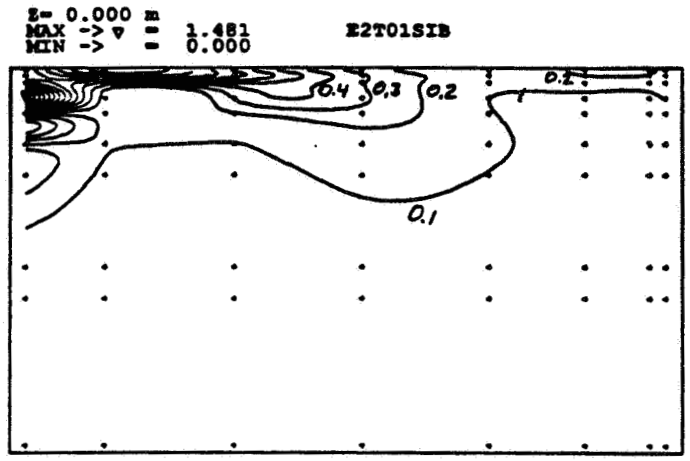

Isovels in plane z= 0.0 m

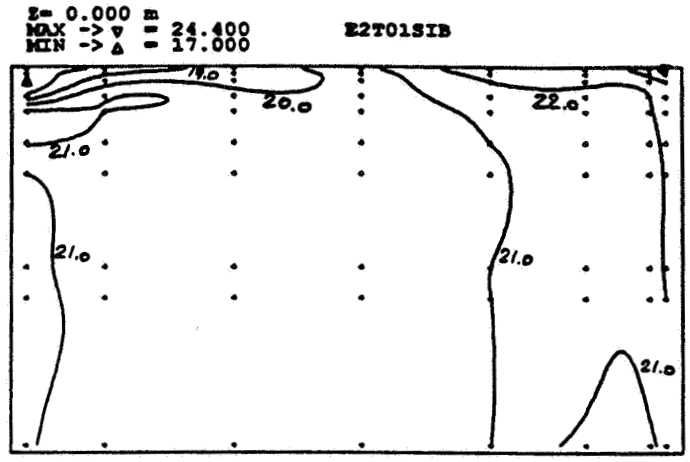

Isothermes in plane z= 0.0 m

Figure 10 Measurement data from test case E2
(from Blomqvist)

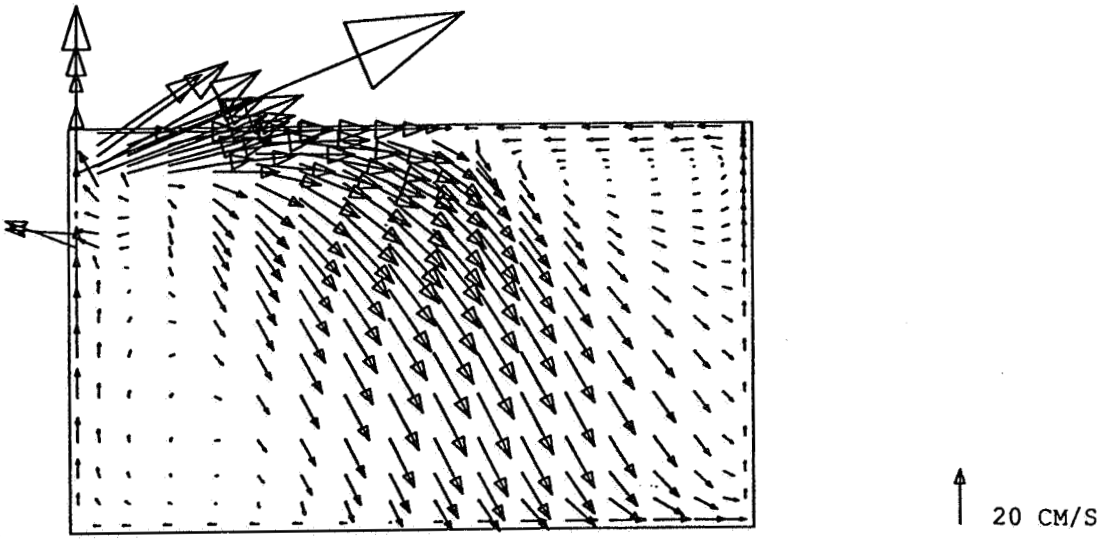

IEA Annex 20, Subtask 1, R.I. 1.20SF
Simulation case e1, plane k = 1 (symmetry plane)
Simulated velocity vectors

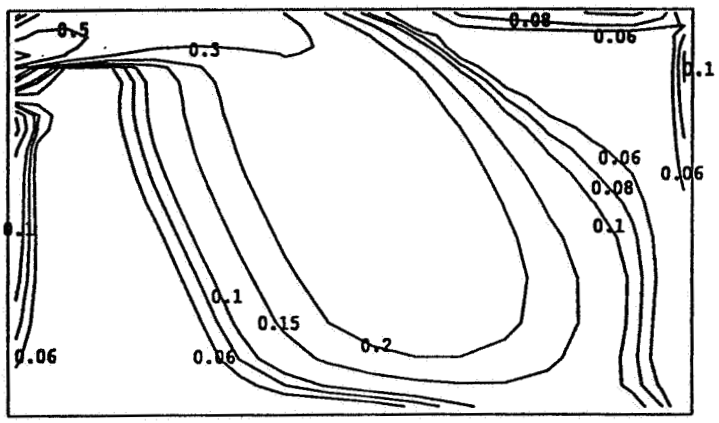

IEA Annex 20, Subtask 1, R.I. 1.20SF
Simulation case e1, plane k = 1 (symmetry plane)
Simulated contours of velocity (m/s)

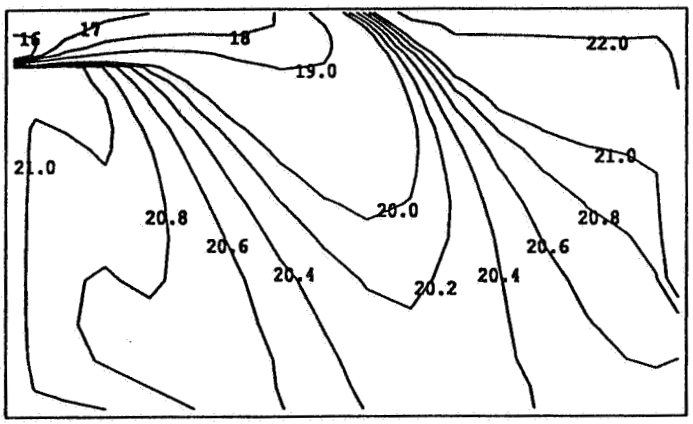

IEA Annex 20, Subtask 1, R.I. 1.20SF
Simulation case e1, plane k = 1 (symmetry plane)
Simulated contours of temperature (^{o}C)

Figure 11 Simulation data from test case E2 (from Heikkinen)

Table 8 Test case E1

Ref.	M or S	Ave. Um	Ave. Ut	Ave. U*	Max Um	Max Temp	Ave. Temp	Min Temp
E1FRG	S	0.029	0.040	0.052	0.112	18.90	18.56	18.10
E1CH	S	0.054	0.023	0.061	0.252	19.11	18.70	17.80
E1N	M	0.060	0.016	0.064	0.230	20.50	19.98	18.90
E1P001NL	S	0.060	0.031	0.069	0.266	20.09	19.81	19.07
E1CO2SF1	S	0.077	0.044	0.090	0.287	21.00	20.65	19.82
E1TO2SIB	M	0.087	0.039	0.096	0.234	21.80	20.85	20.00
E1GER	S	0.089	0.041	0.101	0.269	19.31	19.07	18.48

M= measured, S= simulated

Table 9 Test case E2

Ref.	M or S	Ave. Um	Ave. Ut	Ave. U*	Max Um	Max Temp	Ave. Temp	Min Temp
E2CD	S	0.015	0.005	0.019	0.056	20.00	20.00	19.99
E2FRG	S	0.049	0.052	0.074	0.085	19.40	19.15	19.10
E2FRGXQ	S	0.049	0.057	0.078	0.105	20.10	19.82	19.70
E2TO1SIB	M	0.066	0.034	0.075	0.181	22.00	21.19	20.50
E2N2	S	0.067	0.029	0.075	0.393	20.15	19.98	19.78
E2CH	S	0.068	0.038	0.080	0.279	19.50	19.18	18.50
E2B002NL	S	0.078	0.017	0.081	0.157	19.70	19.54	19.45
E2B001NL	S	0.078	0.019	0.081	0.167	19.46	19.35	19.26
E2N	M	0.083	0.021	0.086	0.260	21.40	20.95	20.20
E2P001NL	S	0.092	0.051	0.107	0.177	20.51	20.39	20.30
E2GER	S	0.096	0.048	0.109	0.181	19.75	19.63	19.46
E2CO1SF1	S	0.103	0.036	0.112	0.173	19.58	19.26	19.17
E2CO2SF1	S	0.108	0.048	0.122	0.194	21.09	20.75	20.60
E2T02SF1	M	0.123	0.036	0.129	0.260	21.35	20.86	20.28

Table 10 Test case E3

Ref.	M or S	Ave. Um	Ave. Ut	Ave. U*	Max Um	Max Temp	Ave. Temp	Min Temp
E3CH	S	0.092	0.051	0.109	0.172	19.50	19.24	19.07
E3FRG	S	0.121	0.100	0.163	0.217	19.40	19.06	18.90
E3N	M	0.152	0.030	0.155	0.350	21.20	20.51	20.10
E3GER	S	0.221	0.100	0.249	0.436	18.88	18.59	18.37
E3CO2SF1	S	0.231	0.065	0.243	0.417	20.21	19.83	19.53
E3P001NL	S	0.249	0.088	0.270	0.434	20.31	20.08	19.83
E3T02SF1	M	0.250	0.065	0.260	0.474	22.07	20.88	20.46

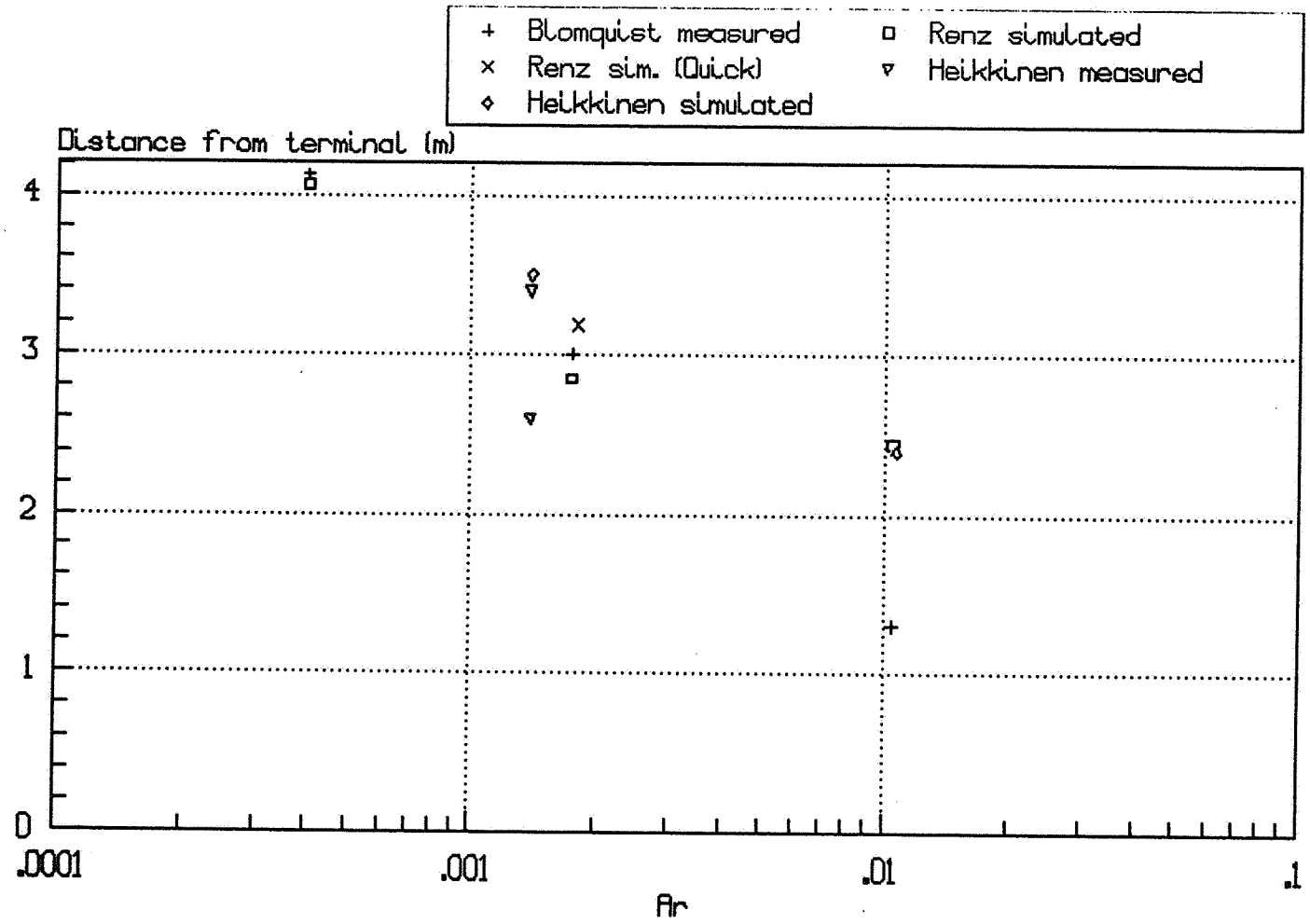

Figure 12 Penetration length of jet, test case E

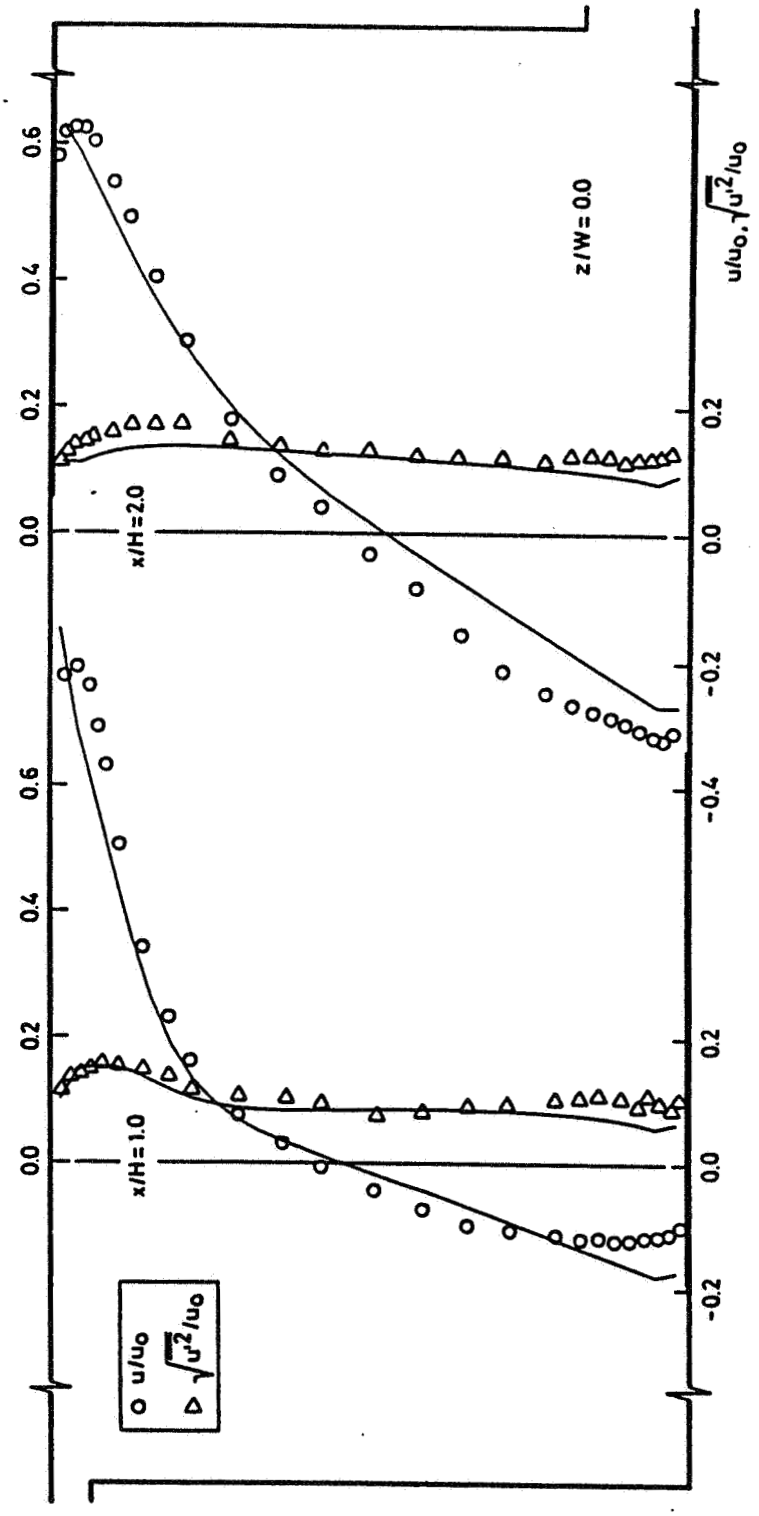

Comparison of measured and computed (solid-lines) mean and rms velocity.

Figure 13 Two dimensional simulation (isothermal) (from Lemaire)

Differencing scheme

The difference schemes used include Upwind, Hybrid, Power Law and Quick. Some indications are that higher order differencing schemes (eq. Quick) can be effective (Renz).

Grid refinement

A number of grid resolutions have been employed. Generally, the finer the grid the more accurate becomes the solution.

6. CONCLUDING REMARKS

The task of comparing and evaluating codes for room air movement prediction is an ambitious one. It is clear from the work already completed that difficulties exist, both associated with the computer predictions and in interpreting and rationalising real measurement data. The codes are difficult to use, time consuming and demanding in computer resources. Skill and experience are required to get the best from them. However, when used with care and, most importantly, with the exercise of sound engineering judgement it is clear that they can make a valuable contribution to understanding air movement in spaces and can predict room air movement with sufficient realism to be of use to design practice.

Some areas where further work is clearly needed, though, are:

- The modelling of the supply jet characteristics (which in these tests proved to be particularly difficult).

- Turbulence modelling. A range of results is found for predictions of turbulent velocity under similar conditions, particularly in buoyant flow. This can have implications for thermal comfort.

- Thermal wall functions. Temperature differences, in the occupied zone, from measurements and simulations are generally quite similar. But some simulations have identified serious shortcomings in predicting surface convection coefficients.

More detailed information on the findings of these studies can be found in participants' individual reports either listed in the References section at the end of this paper or about to be issued.

The project continues until 1 November 1991 and a more detailed written report must await the completion of the work.

8. ACKNOWLEDGEMENTS

The work reported here is based on measurements and computations carried out by many researchers. Table 11 lists those contributors and their organisations. The operating agent for Annex 20 is Dr. Alfred Moser, ETH Zurich, Switzerland, and the subtask 1 leader is Ir. Tony Lemaire, TNO, Delft, The Netherlands.

Table 11 Contributing investigators and organisations

Mr. Claes Blomquist	NSIBR, Gavle	SWEDEN
Mr. Jorma Heikkinen	VTT, Espoo	FINLAND
Dr. Qingyan Chen/ Dr. Alfred Moser	ETH, Zurich	SWITZERLAND
Mr. Michael Skovgaard/ Prof.Dr. Peter Nielsen	Univ. of Aalborg	DENMARK
Dr.-Ing. Johann Furst/ Mr. R Mohr	ROM, Hamburg	GERMANY
Ing. Tony Lemaire	TNO, Delft	NETHERLANDS
Prof.Dr.-Ing. Ulrich Renz/ Prof.Dr. Manfred Zeller/ Dipl.Ing. Markus Ewart	RWTH, Aachen	GERMANY
Dr. Christian Inard/ Dr. Francis Allard	INSA de Lyon	FRANCE
Ing. Didier Buty	CSTB, Marne la Vallee	FRANCE
Dr. Francis Biolley/ Dr. Jean-Raymond Fontaine	INRS, Vandoeuvre	FRANCE
Dr. M Nady Said	NRC, Ottawa	CANADA
Dr.Ing. Sverre Fossdal	NBRI, Oslo	NORWAY
Dr. Per Tjelflaat	SINTEF, Trondheim	NORWAY
Prof. Erik Olsson/ Dr. Lars Davidson	Chalmers Univ. of Tech., Goteborg	SWEDEN
Ing. Paolo Oliaro	Politecnico di Torino	ITALY

Financial support for the evaluation task is provided by the Building Research Establishment, Garston, Watford, UK.

7. REFERENCES

1. Patankar, S V. Numerical heat transfer, Hemisphere Pub., Washington DC, USA, 1980.

2. Baker, A J. Finite element computational fluid mechanics, Hemisphere Pub., Washington DC, USA, 1983.

3. ASHRAE Standard 55-1981. "Thermal Environmental Conditions for Human Occupancy", 1981.

4. ISO Standard 7730. "Moderate thermal environments - determination of the PMV and PPD indices and specification of the conditions for thermal comfort", 1985.

5. Anderson, D R., Sweeney, D J., and Williams, T A. Introduction to statistics - an applications approach. West publishing company. 1981.

6. Skovgaard, M., Hyldgaard, C E. and Nielsen, P V. High and low Reynolds number measurements in a room with an impinging isothermal jet, Proceedings of second international conference, ROOMVENT '90, Oslo, June 1990.

IEA Annex 20 Working Reports:

7. Heikkinen, J. Specification of testcase B (forced convection, isothermal). RID 1.13, April 1989.

8. Lemaire, A D. Specification of testcase D (free convection with radiator). RID 1.15, May 1989.

9. Heikkinen, J. Specification of testcase E (mixed convection, summer cooling). RID 1.14, April 1989.

10. Skaaret, Eimund. Specification of testcase F (forced convection, isothermal with contaminants). RID 1.31, Oct 1989.

11. Nielsen, P V. Specification of a two-dimensional test case. RID 1.45, Nov 1990.

12. Lemaire, A D. Testrooms, Identical testrooms. RID 1.03, May 1989.

13. Lemaire, A D. Selection of radiator. RID 1.04, April 1989.

14. Nielsen, P V. Selection of Air Terminal Device. RID 1.02, Dec. 1988.

15. Ruddick, K. and Whittle, G E. A proposed specification for a common data format. rid 1.22, May 1989.

16. Whittle, G E. and Ruddick, K. Proposal for data processing, evaluation and presentation. RID 1.22, November 1989.

17. Nielsen, P V. Representation of boundary conditions at supply openings. RID 1.11, February 1989.

18. Lemaire, A D. Modelling of boundary conditions near the radiator. RID 1.12, May 1989.

19. Heikkinen, J. Private communication.

20. Blomqvist, C. Measurement of test case B (forced convection, isothermal). AN20.1-S-91-SIB1, March 1991.

21. Heikkinen, J. Measurement results. May 1991.

22. Skovgaard, M. Simulation results. June 1991.

23. Moser, A., "Low Reynolds number effects in single room air flow". November 1988.

24. Chen Qingyan. Simulation of testcase B. January 1990.

25. Vogl, N. and Renz, U. Simulation of simple test cases. March 1991.

26. Lemaire, A D. Simulation of test case D (free convection with radiator), March 1991.

27. Inard, C and Buty, D. Simulation of test case D with zonal models. March 1991.

28. Blomqvist, C. Measurement results. June 1991.

29. Lemaire, A D. Measurement results for test case D2. July 1991.

30. Heikkinen, J. and Piira, K. Simulation of test case D (free convection with radiator) Preliminary Report. December 1990.

31. Renz, U. Simulation results. May 1991.

32. Fossdal, S. Measurement of test case E (mixed convection, summer cooling) Preliminary report. June 1990.

33. Blomqvist, C. Measurement of test case E (mixed convection, summer cooling). AN20.1-S-91-SIB2, March 1991.

34. Heikkinen, J. and Piira, K. Simulation of test case E (mixed convection, summer cooling) Preliminary Report. December 1990.

35. Ruddick, K R. and Whittle, G E. Presentation of Results from Measurements and Simulations of Test Cases B, E, and D, June 1990.

36. Whittle, G E. and Clancy, E. Presentation of Results from Measurements and Simulations of Test Cases B, D, and E, April 1991.

37. Lemaire, A D. Simulation of test case E (mixed convection , summer cooling), March 1991.

38. Chen Qingyan. Simulation of simple test cases. RID 1.46, March 1991.

39. Lemaire, A D. Simulation of simple test cases 2D1, 2D2. May 1991.

AIR MOVEMENT & VENTILATION CONTROL WITHIN BUILDINGS

12th AIVC Conference, Ottawa, Canada
24-27 September, 1991

PAPER 3

MODELS FOR THE PREDICTION OF ROOM AIR DISTRIBUTION

PETER V. NIELSEN

University of Aalborg
Sohngårdsholmsvej 57, DK-9000 Aalborg, Denmark

SYNOPSIS

The paper describes work on simplified design methods made in connection with the International Energy Agency programme "Air Flow Pattern within Buildings", Annex 20, subtask 1.

It is shown that simplified models are able to indicate design values as the maximum velocity in the occupied zone and penetration depth of a non-isothermal jet in a room.

The design according to throw of an isothermal jet is a fully developed method which has a sufficient level of accuracy when it is used in regular rooms. Models for prediction of the maximum velocity in the occupied zone and penetration depth of non-isothermal jets need further development.

The possibility of Computational Fluid Dynamics (CFD) is evaluated and it is compared with simplified models. It is shown that the CFD-method is special useful because it gives the distribution of the variables as well as the design values. The CFD-method can also predict variables which are time consuming to measure by full-scale experiments.

The CFD-method is especially useful for the prediction of air distribution in large enclosures with complicated geometry and different sources for the air movement.

LIST OF SYMBOLS

a_o	Supply area	m^2
Ar	Archimedes' number	
c_p	Specific heat	J/kg°C
g	Gravitational acceleration	m/sec^2
H	Height of room	m
K_a	Constant for diffuser	
K_{sa}	Constant for calculation of penetration depth	
L	Length of room	m
ℓ_{Th}	Throw	m
n	Air change rate	h^{-1}
q_o	Flow rate	m^2/s
T_o	Supply temperature	°C
T_R	Return temperature	°C
u_L	Velocity in wall jet with lenth L	m/s
u_o	Supply velocity	m/s
u_{rm}	Maximum velocity in occupied zone	m/s
u_{Th}	Reference velocity	m/s
u_x	Velocity in wall jet with length x	m/s
W	Width of room	m
x	Length of wall jet	m
x_o	Distance to virtual origin	m
x_s	Penetration depth of wall jet	m

β	Volume expansion coefficient	K^{-1}
ε	Ventilation efficiency	
ρ_o	Density	kg/m^3

1. INTRODUCTION

The International Energy Agency (IEA) has the basic aim to promote co-operation among the twenty-one participating countries, to increase energy security through energy conservation, development of alternative energy sources and energy research development and demonstration. One programme in this activity is "Energy Conservation in Building and Community Systems".

Annex 20, subtask 1, in this programme works with predictions of accurate air flow patterns within rooms in order to obtain maximum energy efficiency, high thermal comfort and optimum indoor air quality.

The purpose of the project is to formulate requirements for design tools and to lay the groundwork for their development. Computational Fluid Dynamics (CFD) is one of the main activities in subtask 1, but experimental work in full-scale rooms does also play an important role.

It is also desirable that some attention should be devoted to simplified design methods. This paper is a part of this decision. It discusses the limitation and possibility of the simplified models in comparison with CFD-codes and shows the necessary boundary conditions needed for the models.

The evaluation of the simplified design models is supported by comparisons with measurements made in test rooms in different countries.

The following models are discussed

- design according to throw of isothermal jet
- maximum velocity in occupied zone
- penetration depth of non-isothermal jet

and for comparisons

- prediction of air distribution with a CFD-code.

The subtask 1 work involves development work on other simplified models as e.g. zonal models and data base models but those activities are not discussed in this paper.

2. DESIGN ACCORDING TO THROW OF ISOTHERMAL JET

The design models described in this paper are all based on the theory of self-similar jet flow. Figure 1 shows an example of this type of flow in a room with sidewall mounted grille. The flow below the ceiling is a self-similar wall jet which is rather independent of the downstream room geometry, which means that it is independent of room height and room length.

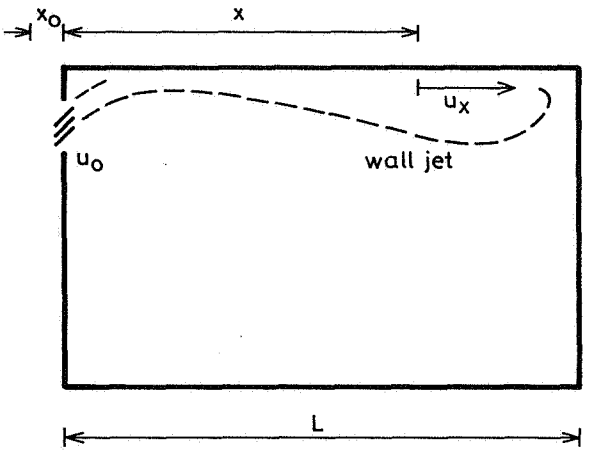

Figure 1. Wall jet in a ventilated room.

The velocity decay in the three-dimensional wall jet below the ceiling is given by:

$$\frac{u_x}{u_o} = K_a \frac{\sqrt{a_o}}{x + x_o} \tag{1}$$

where u_o and u_x are supply velocity and maximum velocity in the wall jet in the distance x from the opening, respectively. a_o is the supply area of the diffuser and x_o is the distance to the virtual origin of the wall jet. K_a is a constant.

K_a takes values from 2 to 10 and x_o is about zero, dependent on the actual diffuser and diffuser location. K_a, a_o and x_o may be dependent on the Reynolds number in the case of low turbulent flow.

A length ℓ_{Th}, called the throw, is defined as distance from the opening to a location where the maximum velocity u_x is equal to a given reference value u_{Th}, see reference [1].

$$\ell_{Th} = \frac{u_o K_a \sqrt{a_o}}{u_{Th}} - x_o \qquad \text{(m)} \tag{2}$$

It is the purpose of the design procedure to control the air distribution in the room in such a way that the maximum velocity in the occupied zone u_{rm} is up to 0.15 m/s. General experience shows that this is achieved when the throw ℓ_{Th} is equal to room length L and the reference velocity u_{Th} is equal to 0.2 m/s or 0.25 m/s.

Producers of Air Terminal Devices are presenting equation (2) as design charts where it is possible to find the flow rate q_o when the diffuser (x_o, a_o and K_a) and the throw ℓ_{Th} are selected. The throw is normally recommended to be the room length in the situation in figure 1. More generally the throw is the half lenght between two diffusers with opposite position or the length between diffuser and wall. Other definitions of ℓ_{Th} may be used to compensate for different diffuser designs and different room geometry. A throw of $L + H$ - 1.8 m is for example used when the room is high and it expresses formally that the maximum velocity in the wall jet is supposed to be equal to u_{Th} when it passes through the occupied zone.

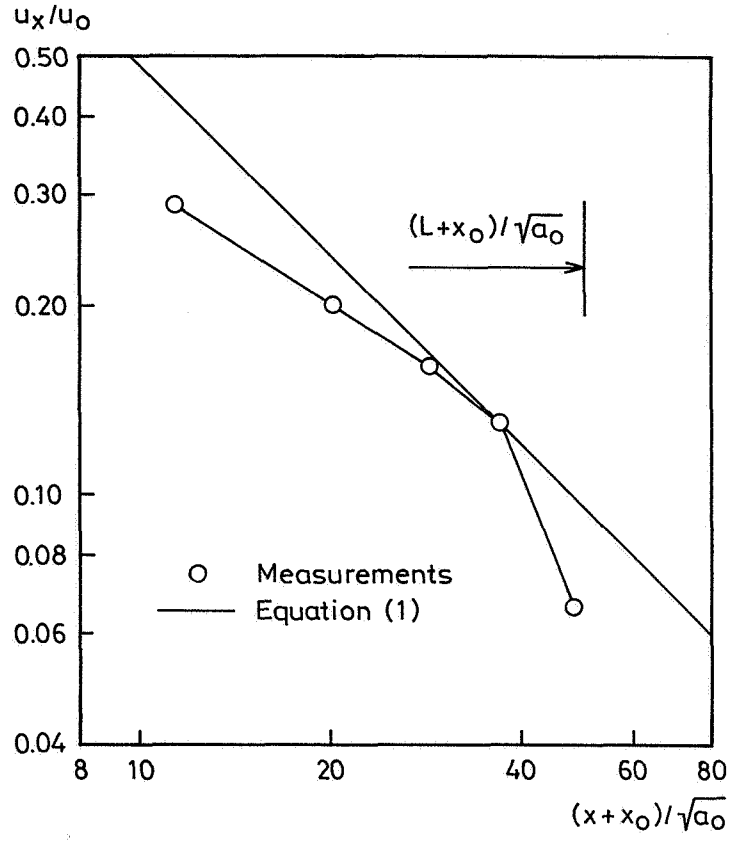

Figure 2. Measurement of maximum velocity in the wall jet as a function of distance, see reference [2]. Air change rate $3h^{-1}$. Room and diffuser are specified according to the requirements in references [3] and [4].

The design of supply conditions in the IEA test room, according to throw of isothermal jet, is based on measurements of the velocity decay shown i figure 2. The line for equation (1) corresponds to a K_a-value equal to 4.8. This is a value which ensures that calculated velocities in the wall jet always are higher or equal

to the measured values, and this is a normally accepted procedure to ensure that too high velocities in the occupied zone are avoided.

Equation (2) shows that the design supply veloicty u_o is equal to 2.09 m/s under the following assumptions

$$a_o = 0.00855 \text{ m}^2, \quad K_a = 4.8 \text{ m}, \quad x_o = 0.45 \text{ m}$$

$$\ell_{Th} = 4.2 \text{ m} \quad \text{and} \quad u_{Th} = 0.2 \text{ m/s}$$

The design supply velocity corresponds to a specific air flow rate of 1.78h^{-1} in the test room.

Figure 3 shows the measured level of maximum velocity in the occupied zone as well as the predicted values with CFD-codes, see reference [5]. The maximum velocity in the occupied zone will have the following values

$\sim$ 0.08 m/s (Design according to throw of isothermal jet)

$\sim$ 0.08 m/s (CFD-code, Basic case)

$\sim$ 0.12 m/s (CFD-code, Prescribed Velocity Method)

which should be compared to an expected value of 0.15 m/s.

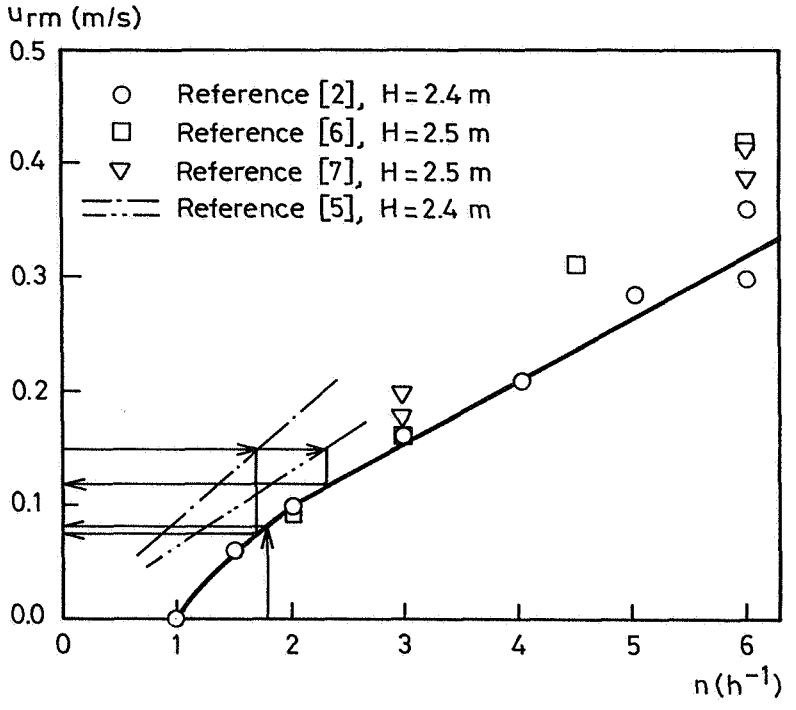

Figure 3. Maximum velocity in the occupied zone. Measurements and predictions from CFD-codes.

There is some deviation in the measurement shown in figure 3 which should be considered when the different design methods are evaluated. This situation is also expressed in figure 4 which shows the measurement of velocity decay in the isothermal wall jet made by the countries, Denmark [2], Sweden [6], Finland [7], and Germany [8].

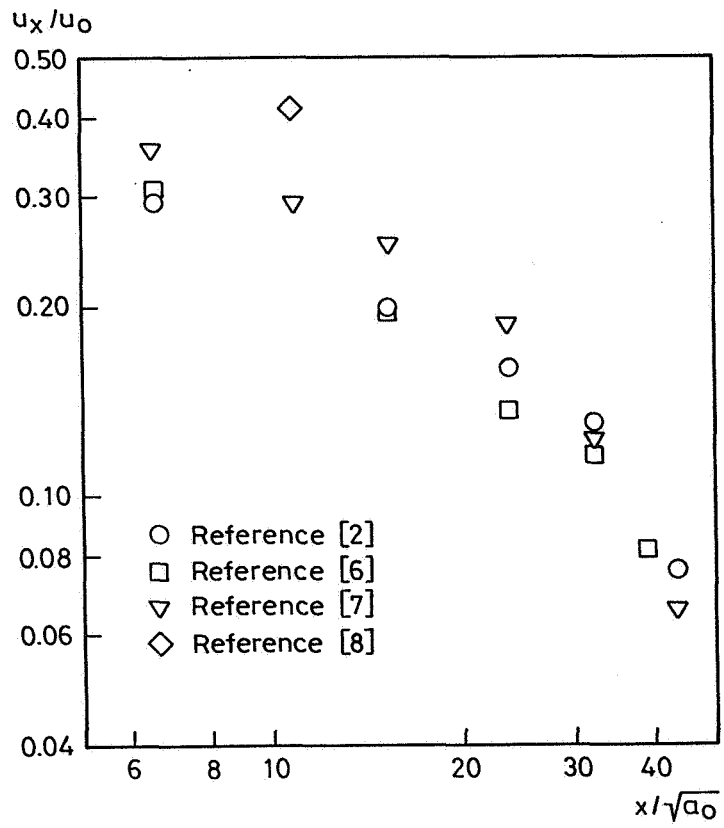

Figure 4. Velocity decay versus distance measured in four different countries. Test case B2.

Furthermore, it should be considered that the actual velocities in the occupied zone may deviate from design velocities because it is difficult to adjust every single diffuser, and because there are small differences in the diffusers. The velocity level is also influenced by individual furnishings in the rooms.

It may be concluded that all the design methods are able to predict a maximum velocity in the occupied zone which is comparable with measured values.

It is possible to make further improvement in both the design, according to throw of isothermal jet, and in the design based on a CFD-method.

3. MAXIMUM VELOCITY IN THE OCCUPIED ZONE

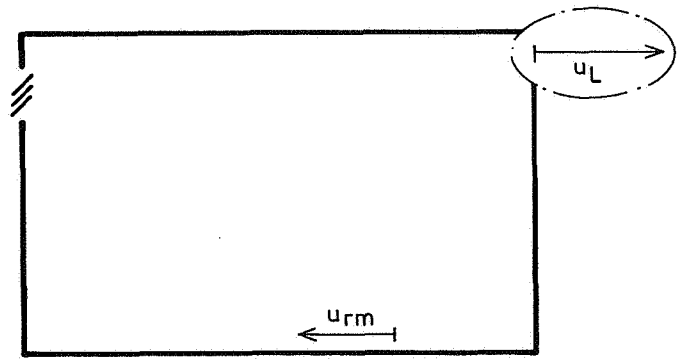

Figure 5. Location of the reference velocity u_L and location of the maximum velocity u_{rm} in the occupied zone.

The maximum velocity in the reverse flow u_{rm} is located close to the floor at a distance of $\sim 2/3\ L$ from the supply opening. This velocity is also the maximum velocity in the occupied zone in cases where the jet below the ceiling and the jet at the end wall are outside the occupied zone. Experiments with isothermal flow show that u_{rm} is a simple function of a reference velocity u_L, which is the velocity in an undisturbed wall jet of the length L from the actual diffuser, see Hestad [9]. The velocity u_L contains information on supply velocity, distance from inlet and geometrical details around the initial flow, such as type of Air Terminal Device, adjustable blades and distance from ceiling. The relation between u_{rm} and u_L, as well as the level of u_L, can therefore be used as elements in a design procedure.

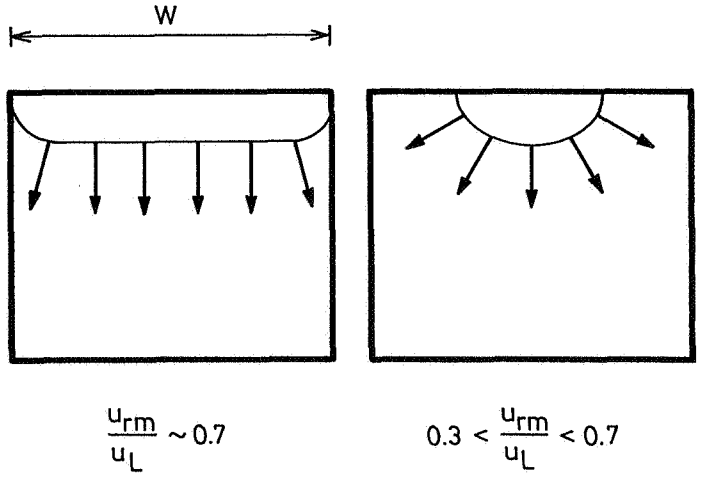

Figure 6. Flow at the end wall opposite the supply opening in case of two-dimensional and three-dimensional air movement.

The sketch in the left side of figure 6 shows the flow at the wall opposite the supply opening in case of a two-dimensional flow. The deflected jet flows vertical down the end wall as a new two-dimensional wall jet, and experiments show that u_{rm}/u_L is egual to 0.7, see reference [10]. A design according to throw of isothermal jet will in this case give a maximum velocity in the occupied zone of $u_{rm} = 0.14$ m/s ($\ell_{Th} = L$, $u_{Th} = 0.2$ m/s).

The sketch in the right side of figure 6 shows the air movement at the end wall in case of a three-dimensional flow. The deflected jet flows down the wall as a semi-radial jet, and experiments show that u_{rm}/u_L varies between 0.3 and 0.7. Hestad [9] shows that u_{rm}/u_L is a function of jet width compared to the widt of the end wall. Large jet width corresponds to two-dimensional flow ($u_{rm}/u_L \sim 0.7$), and a small width of the primary jet corresponds to radial flow at the end wall ($u_{rm}/u_L \sim 0.3$).

The maximum velocity in the occupied zone u_{rm} can be obtained from equation (1) when the variation of u_{rm}/u_L is known

$$u_{rm} = u_o(\frac{u_{rm}}{u_L})K_a\frac{\sqrt{a_o}}{L+x_o} \qquad \text{(m/s)} \tag{3}$$

Experiments in the subtask 1 work do not involve change in jet width or change in room width, and therefore it is not possible to add much new experience to the assumptions. The experiments show that u_{rm}/u_L is equal to 0.45 in the room geometry specified in subtask 1.

4. PENETRATION DEPTH OF NON-ISOTHERMAL JET

An undisturbed wall jet will penetrate the ventilated room in case of isothermal flow, and it will entrain air from the occupied zone to induce recirculating air movement in the room. This picture will change when a thermal load is supplied to the room. The supply temperature will be reduced and the load may reach a level such that the wall jet will separate from the ceiling at a distance x_s from the diffuser and flow down into the occupied zone as shown in figure 7.

Situations with a short penetration depth are undesirable because the jet may have a high velocity and a low temperature when it flows into the occupied zone, and a calculation of the penetration depth is thus a part of the design procedure of the air distribution system.

Grimitlin [11] has shown that the penetration depth for a cold three-dimensional wall jet is proportional to $1/\sqrt{Ar}$, where Ar is the Archimedes number. An analysis of the forces acting on a non-isothermal wall jet leads to the following equation

$$\frac{x_s}{\sqrt{a_o}} = 0.19K_{sa}K_a(\frac{1}{Ar})^{0.5} \tag{4}$$

where K_{sa} is a constant dependent on parameters outside the wall jet, such as room dimensions, location of thermal load, etc.

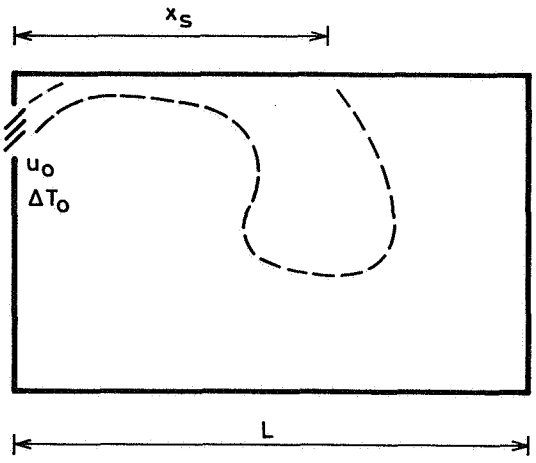

Figure 7. Penetration depth x_s of a thermal jet in a room.

Comparisons between measurements on different Air Terminal Devices and values calculated from equation (4) show a fairly reasonable agreement for $K_{sa} = 1.5$. The measurements are made in a large test area with floor mounted heat sources, see reference [12].

The influence of heat source location must be an important parameter. Some measurements in reference [9] suggest that K_{sa} should be equal to 1.6 for end wall mounted heat sources as used in the IEA test case E.

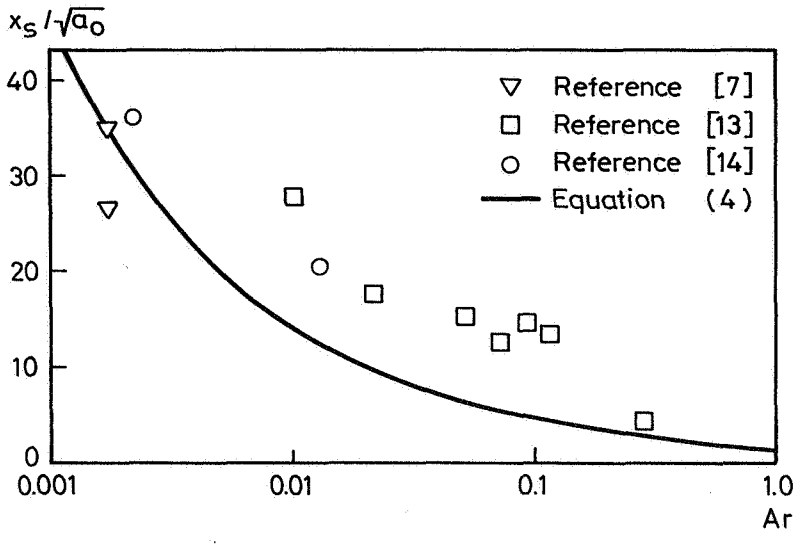

Figure 8. Measurements and predictions of penetration depth for the three-dimensional wall jet in the test case E. Room and diffuser are specified according to the requirements in references [3] and [4].

Figure 8 shows the measurements made by the following countries: Finland [7], Sweden [13] and Norway [14]. The measurements confirm the variation of the type $x_s \sim 1/\sqrt{Ar}$ but it is obvious that the penetration depth calculated according to equation (4) is underpredicted at high Archimedes' numbers.

Experiments in the subtask 1 work do not involve change in heat source location and room dimensions, so it is not possible to get insight into the shortcomings of equation (4). It can be concluded that equation (4) describes the general behaviour of a non-isothermal jet, but further research is needed to use this simplified model as part of a general design procedure.

Equations (3) and (4) can be used to make some general statements on the design of an air distribution system. The specific load in the room is expressed by

$$Q = \rho_o c_p \frac{a_o u_o \Delta T_o}{LW} \qquad (\mathrm{W/m^2}) \tag{5}$$

where ρ_o and c_p are density and specific heat, respectively. Equation (5) is rearranged by substituting u_o from the expression in equation (3) and ΔT_o from the expression in equation (4). x_s/L is restricted to a constant value (e.g. 0.5) due to comfort considerations. The specific heat load of the room will now have the following connection to the design variables

$$Q \sim \frac{u_{rm}^3}{K_a} \tag{6}$$

It is desirable to have an air distribution system which can handle a high heat load. Equation (6) shows that this is possible if a high maximum velocity in the occupied zone is tolerated, and also that the ability to handle heat load is proportional to the third power of this velocity. Therefore it is important that the design procedure is able to lay down a system which gives a velocity u_{rm} close to 0.15 m/s or close to another high design velocity.

The K_a-value is another important design parameter. Equation (6) shows that it is efficient to use an Air Terminal Devise with a low K_a-value. A low K_a value corresponds to a high initial diffusion and it is partly achieved by a semi-radial or radial flow in the wall jet below the ceiling. The Air Terminal Device in the subtask 1 work does have a high initial diffusion, and a semi-radial wall jet is generated in the ceiling regions, see references [2] and [4].

5. PREDICTION OF AIR DISTRIBUTION WITH A CFD-CODE

The aim of this chapter is to evaluate the CFD-method as a design tool in comparison with the simplified models. A general evaluation of CFD-mehods in connection

with the subtask 1 work is given elsewhere, and the trend of the method is also given in reference [15].

Comparison with simplified models shows only a small gain if the design work is a question about obtaining the level of maximum velocity in the occupied zone and penetration depth of a non-isothermal jet in a room of conventional geometry.

Demands on the design work is increasing due to comfort and energy considerations. The CFD-method shows in this connection a number of possibilities compared to simplified models which will be discussed in the following

- the CFD-method gives a general description of the parameters in the room at design conditions as well as at other conditions,
- the CFD-method can predict some parameters which are important in the evaluation of the air distribution system but very time consuming to measure by full-scale experiments,
- the CFD-method may be the only practical design method in case of very large enclosures with complicated geometry and complicated boundary conditions.

Reference [5] shows an example on prediction of comfort level. It is expressed by the percentage of dissatisfied people because of turbulent and draught at foot level. The predictions show that half of the room has a draught risk about 16 - 20%, and the rest of the room has a draught risk which is below 16%. This type of information is general and useful compared to the statement that the maximum velocity in the occupied zone is 0.2 m/s. Furthermore, it is a type of information which reflects the accuracy of the method and an example of the general description of the situation which can be achieved by the CFD-method.

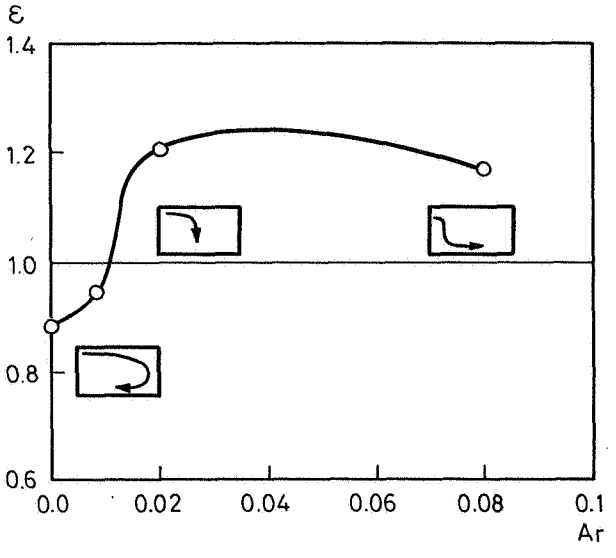

Figure 9. Ventilation efficieny versus Archimedes' number in a room with two-dimensional flow, see reference [15].

The prediction of ventilation efficiency is an example where the CFD-method is used to obtain results which would be very time consuming and expensive to obtain by full-scale experiments. Figure 9 shows the ventilation efficiency as a function of the Archimedes number in a room with a slot and two-dimensional flow. The predictions show that the ventilation efficiency is high in the case when the jet penetrates half of the room length, and this is also the flow pattern which is optimum for thermal comfort, taking into account that the heat load had to be removed from the room by the ventilation system. Computer predictions of this type are useful in the evaluation of an air distribution system and in the work on minimizing the energy consumption.

The most important area for the airflow simulation is undoubtedly the predictions of air movement in large enclosures with complicated geometry and complicated boundary conditions.

Large areas exclude the use of full-scale experiments. It is also difficult to use a simplified design method because the geometry may be complicated and there can be more sources for the air movement as for example diffusers, pressure difference around the building, cold downdraught and thermal plumes.

The glass covered "Hansa" shopping arcade in Turku is a typical example of a large enclosure with a complicated geometry, see figure 10. It is raised between a number of older buildings which include some warehouses, a hotel and the theatre of the town. The arcade may be looked upon as one large room and further research will show if it is possible to make any subdivisions of such a space. Figure 11 shows a part of the arcade or atrium between an old building and some of the new constructions. Is is obvious that the space also has a complicated geometry in the vertical direction.

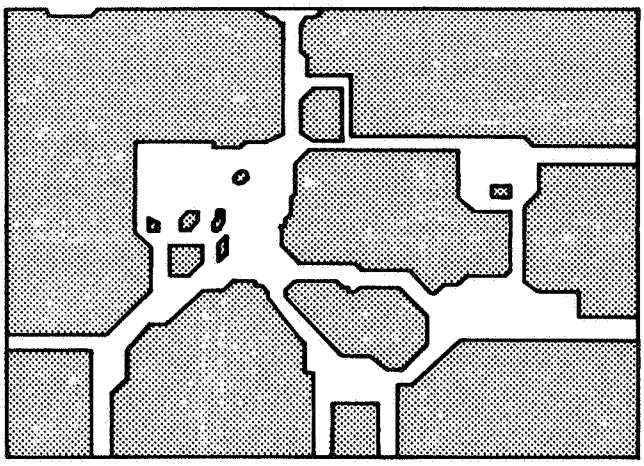

Figure 10. Horizontal section of the glass covered "Hansa" shopping arcade in Turku.

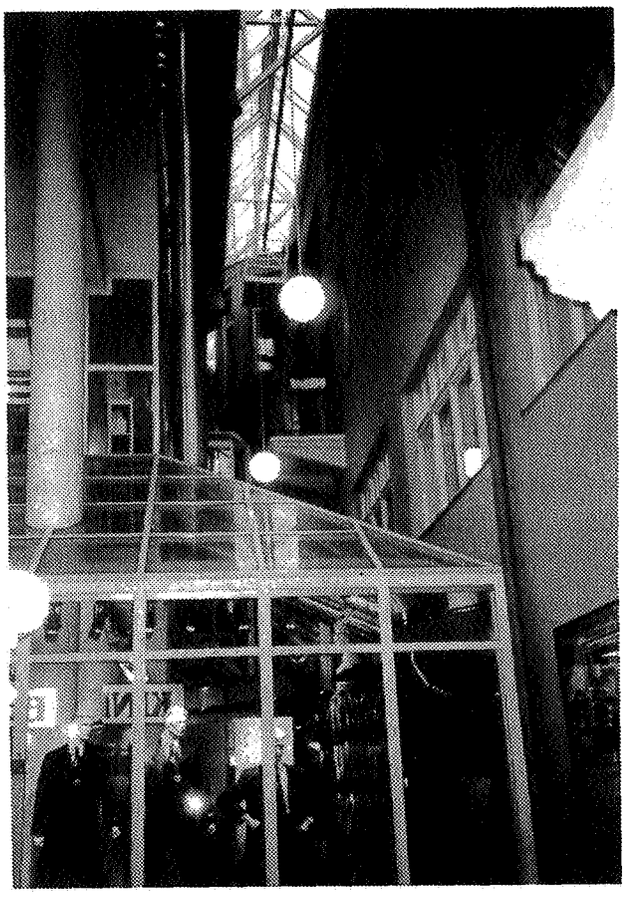

Figure 11. Details in "Hansa" shopping arcade.

The main purpose of the design work in large enclosures is to control the energy flow and temperature level. It is also very important to have a high ventilation efficiency in the occupied areas, and a system which can handle this area without too large air exchange in the rest of the air volume. Smoke movement in case of a fire and necessary escape route is an important subject. It is also necessary to limit the air velocity in the occupied areas because many people will work with restricted activity level in the shops and in open offices.

It is obvious that a CFD-method can be an important tool for the design of air movement in constructions as shown in figures 10 and 11. The CFD-method is able to handle many different sources as diffusers, pressure difference and temperature difference in a single calculation and is therefore able to predict the total effect of all sources.

In special situations when the space can be subdivided into conventional geometry and the flow can be described by parabolic equations it will also be possible to use simplified design models in large enclosures.

CONCLUSION

Simplified models are able to indicate design values as the maximum velocity in the occupied zone and penetration depth of a thermal jet in a room.

The design according to throw of an isothermal jet is a fully developed method which has a sufficient level of accuracy when it is used in a regular room. The producers of Air Terminal Devices can incorporate experience in the method by the selection of constants for the ATD and by the selection of throw and reference velocity.

A simplified model which is able to predict the real value of the maximum velocity in the occupied zone needs further development.

The prediction of penetration depth of a non-isothermal jet seems to be possible but is is necessary to do more experiments on different room geometry and heat source location.

Airflow simulation by a CFD-method is specially useful because the information is extended compared to the information obtained by a simplified model. Airflow simulation shows for example the distribution of velocities in the occupied zone as well as the design velocity. It is also possible to predict parameters which are difficult and time consuming to obtain by other models or by experiments.

The CFD-method is specially important in cases when the air distribution has to be predicted in large enclosures with complicated geometry and different sources for the air movements, as for example in shopping arcades, atria, factories, and theatres.

Generally speaking, simplified design models work well when the space can be subdivided into conventional geometry and the flow can be described by parabolic equations while a CFD-model can handle complex geometry and elliptic equations.

Measurements in different identical test rooms show significant deviation. This deviation seems also to correspond to the deviation between the simplified models and the CFD-method. In real installations, however, there will be larger deviations.

APPENDIX

The experiments in the subtask 1 work are made in test rooms with the dimensions $H \times L \times W$ equal to $2.5 \times 4.2 \times 3.6$ m. Only the Danish test room has a different height of 2.4 m.

The differences in height H will influence the measurements shown in figure 3, partly because they are made in sligthly different rooms and partly because the air exchange rate n is based on different room volumes. The practical importance is small because the difference in volume flow rate is within 4%.

The diffusers in all the test rooms are of the same type (HESCO type KS4W205K 370), and the individual difference between diffusers is small because it consists of

injection moulded plastic parts. There may be differences due to the adjustment of the diffusers.

The diffuser area a_o is either measured as a geometrical area or it is calculated from flow rate and supply velocity, see reference [2]. The area has the following value

$a_o = 0.0095$ m^2, Geometrical area

$a_o = 0.00855$ m^2, Effective area ($n = 3\text{h}^{-1}$)

The effective area is used in figures 2 and 4 and the geometrical area is used in figure 8.

The Archimedes number is defined as

$$Ar = \frac{\beta g \sqrt{a_o}(T_R - T_0)}{u_o^2} \qquad (A1)$$

except in figure 9, where the slot height is used as reference length. β and g are volume expansion coefficient and gravitational acceleration, respectively, and T_R - T_o is the temperature difference between return temperature and supply temperature. The velocity is given as $u_o = q_o/a_o$, where a_o is the geometrical area (figure 8).

REFERENCES

1. "Air distribution and air diffusion - Laboratory aerodynamic testing and rating of Air Terminal Devices"
   Draft for international standard ISO/DIS 5219.

2. SKOVGAARD, M., HYLDGAARD, C.E., and NIELSEN P.V.
   "High and Low Reynolds Number Measurements in a Room with an Impinging Isothermal Jet"
   ROOMVENT '90, International Conference on Engineering Aero- and Thermodynamics of Ventilated rooms, Oslo, 1990.

3. LEMAIRE, A.D.
   "Testrooms, Identical Testrooms"
   Internal report for IEA Annex 20, TNO Institute of Applied Physics, Delft, 1989.

4. NIELSEN P.V.
   "Selection of Air Terminal Device"
   Internal report for IEA Annex 20, University of Aalborg, ISSN 0902-7513 R8838, 1988.

5. SKOVGAARD, M. and NIELSEN P.V.
"Modelling Complex Inlet Geometries in CFD - Applied to Air Flow in Ventilated Rooms"
12th AIVC Conference on Air Movement and Ventilation Control within Buildings, Ottawa, 1991.

6. BLOMQVIST, C.
"Measurements of Testcase B"
Internal report for IEA Annex 20, The National Swedish Institute for Building Research, Gävle, 1991.

7. HEIKKINEN, J.
Private communication, Technical Research Centre of Finland, Espoo, 1991.

8. EWERT, M. and ZELLER, M.
"Turbulence Parameters at Supply Opening (measurements)"
Internal report for IEA Annex 20, Rheinisch-Westfälischen Technischen Hochschule, Aachen, 1991.

9. HESTAD, T.
"A Design Method for Diffusers Based on Theory, Full-Scale Experiments and Practical Experience"
(In Norwegian), Tekniska Meddelanden nr. 83, Institutionen för Uppvärmnings- och Ventilationsteknik, KTH, Stockholm, 1975.

10. NIELSEN, P.V.
"Mathematical Models for Room Air Distribution"
Conference on "System Simulation in Buildings", Liege, 1982.

11. GRIMITLIN, M.
"Zuluftverteilung in Räumen"
Luft- und Kältetechnik, nr. 5, 1970.

12. NIELSEN, P.V. and MÖLLER, Å.T.A.
"Measurements on Buoyant Wall Jet Flows in Air-Conditioned Rooms"
ROOMVENT '87, International Conference on Air Distribution in Ventilated Spaces, Stockholm, 1987.

13. SANDBERG, M.
Private communication, The National Swedish Institute for Building Research, Gävle, 1991.

14. FOSSDAL, S.
"Measurement of Testcase E"
Internal report for IEA Annex 20, Norwegian Building Research Institute, Oslo, 1990.

15. NIELSEN, P.V.
"Airflow Simulation Techniques - Progress and Trends"
10th AIVC Conference, Espoo, 1989.

AIR MOVEMENT & VENTILATION CONTROL WITHIN BUILDINGS

12th AIVC Conference, Ottawa, Canada
24-27 September, 1991

PAPER 4

SINGLE SIDED VENTILATION

Authors: Jacobus van der Maas
LESO-PB (Lab. d'Energie Solaire et de Physique du Bâtiment)
EPFL (Ecole Polytechnique Fédérale de Lausanne)
CH-1015 Lausanne, Switzerland

Dominique Bienfait
CSTB (Centre Scientifique et technique du Bâtiment)
F-77421 Marne-la-Vallée, France

Luk Vandaele
BBRI (Belgian Building Research Institute)
B-1342 Limelette, Belgium

Richard Walker
BRE (Building Research Establishment)
WD2 7JR Garston, United Kingdom

SYNOPSIS

Single sided ventilation was one of the topics of the research project "Air flows through large openings in buildings," which is part of subtask 2 of the IEA/ECB Annex XX (Optimization of Air Flow Patterns Within Buildings). The scope of this project was to test the range of validity of available algorithms to calculate heat and mass flow through large openings, and where possible to develop new ones.

We report on four new full scale experiments that were designed to measure the influence of wind on the ventilation and/or heat loss rates through single large openings: a) test-house with horizontal slit opening, set-up to measure internal pressures and the effect of air-compressibility (CSTB, France), b) attic with window ajar, set-up to measure long term ventilation rates with varying wind and temperatures (BBRI, Belgium), c) fully open window, set-up to measure ventilation rate and cooling as a function of time (BRE, UK) d) fully open window, set up to measure cooling as a function of time (EPFL, Switzerland).

The ventilation rates are measured with a tracer gaz technique. A new method is proposed to determine ventilation energy loss rates, by comparing the time variation of air and wall temperatures with a simplified dynamical thermal model.

New results include (i) the contribution of air compressibility to the single sided ventilation rate can be considerable in particular for relatively small openings to large volumes, (ii) wind induced two-way flow is not only caused by pressure fluctuations but a systematic variation of the pressure coefficient over the opening is observed (iii) long term observation of the ventilation rate scaled with the wind velocity (iv) ventilation heat loss rates after opening a window are described by a simple model allowing a better estimate of the energy consequences of inhabitant behaviour (v) an effect of (steady) wind on the airflow in a large opening is observed. Finally, uncertainties in single-sided ventilation appear to be dominated by uncertainties in the characterization of the local wind at the opening.

LIST OF SYMBOLS

ACH	Air change per hour (1/h)
ACR	Air change rate (m^3/s)
A	opening area (m^2)
b	wall thermal effusivity $b=\sqrt{\lambda\rho c}$
C_1	wind coefficient
C_2	stack coefficient
C_3	turbulent coefficient
C_d:	Discharge coefficient
Cp	heat capacity of air
Cs	area fraction for heat transfer
f	frequency (Hz)
F	non dimensional ventilation
g:	Acceleration of gravity (m/s^2)
H:	Height of the opening (m)
P,p:	Pressure (Pa)
Q:	Volume flow rate (m^3/s)
T:	average absolute air temperature (K)
T_{in}	inside air temperature (C)
T_{out}	inside air temperature (C)

v:	velocity (m/s)
V	Volume (m^3)
W:	Width of the opening (m)
ρ:	Air density (kg/m3)
Φ	Heat flow density (W/m^2)
δp,P	pressure variation (Pa)
ΔT	inside outside air temperature difference (K)

1. INTRODUCTION

The general scope of Subtask 2 of the the Annex XX is to help the development of multizone simulation programs. Part of the work concerned the development of new algorithms and one of the research topics chosen for this international cooperation was the study of flow patterns through large openings. In this paper an overview is given of the obtained results on external openings (i.e. single sided ventilation), and we refer to another paper in this conference for new results on internal openings [1]

The description of airflow through large external openings is basically the same as for internal openings as long as there is no wind. Therefore previous research on large external openings was mainly concentrated on wind effects [2], and a main goal of the new research has been to improve the knowledge of wind effects on ventilation.

A new topic for single sided ventilation is the evaluation of the energy consequences of inhabitant behavior. Inhabitants open windows and doors, and leave them open for some time before closing. The research project inhabitant behaviour for example [3], provides opening time intervals and therefore an algorithm was required for the calculation of both heat and mass flow as a function of time.

Literature reviews [2,4,5] formed a basis for the planning of the experiments. In addition to stack flow, air flows induced by *fluctuating wind pressures* and *eddy circulation* have been observed in single-sided ventilation. Two types of problem have then to be distinguished

(i) the prediction of fluctuating wind pressures at the position of the window from a knowledge of the geometry of the building, its surroundings and the wind characteristics some distance from the building (e.g. meteorological station).

(ii) the relation of these local fluctuating wind pressures to the total air exchange through a single opening.

The emphasis in the present studies is on the second type of problem.We report on four new full scale experiments involving four laboratories in Europe:

- BOUIN test-house with horizontal slit opening, set-up to measure internal pressures and the effect of air-compressibility (CSTB, France),
- GENT-attic with window ajar, set-up to measure long term ventilation rates with varying wind and stack effect (BBRI, Belgium),

- BRE-office with fully open window, set-up to study the effect of wind on ventilation and heat loss rate as a function of time after opening a window (BRE, UK)
- EPFL-offices with open window, set up to study the energy consequences of user behaviour by measuring ventilative cooling as a function of time and for rooms of different mass (LESO-PB, Switzerland).

In the next section, §2, we present the measurement set-ups, in §3 we discuss the models used for the interpretation of the data and in §4 the experimental results are presented and discussed. We conclude with a conclusion and recommendations for future research.

2. EXPERIMENTAL

2.1 SET-UP: CSTB (Marne-la-vallée, F)

The test house at Bouin (Figure 1) is a single zone building on an exposed site near the Atlantic coast. The volume of the test house is 93.6m3. The equivalent air leakage area of the house was measured and is less than 5cm2, which is small compared to the studied ventilation openings of 100 and 200cm^2. A key feature of this site is the mounting of the building on a turntable. This means that it can be rotated during an experiment, keeping the same side to the wind throughout a test.

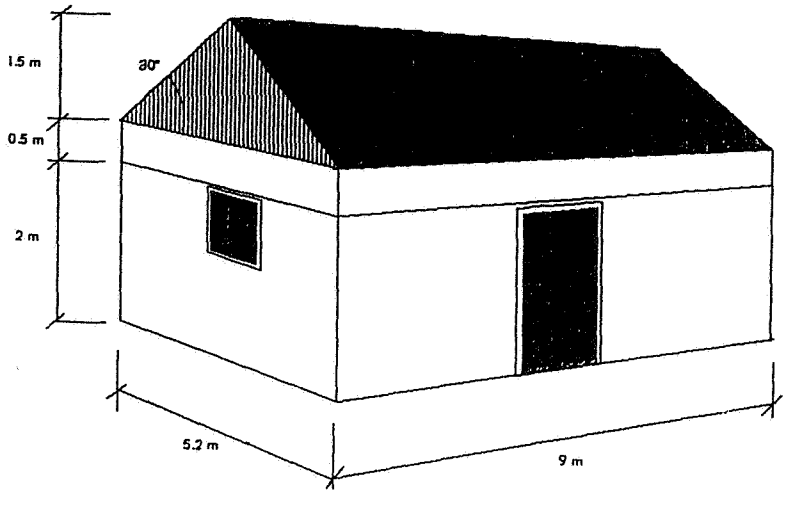

Figure 1. BOUIN test house.

A single opening was introduced into the building envelope and maintained either windward or leeward. Two sharp edged slots of 40cm width (2.5 and 5cm height, 1cm thick) were investigated. The ventilation rate is obtained from the tracer gas concentration decay measured in the room. The wind-induced external pressures,

internal pressures, wind speed and direction and tracer gas concentration are all measured simultaneously, at a rate of 5 Hz. Each test consists of a 10 minute mixing period, with the opening sealed, and then after removing the seal, a 20 minute decay period. The tracer gas concentration is measured from five different sampling points in the room, to ensure the result is representative of the whole room. These points are 1.5m above the floor, and linked through a manifold to the gas analyser. During the mixing period, small fans are used to provide complete mixing of the tracer gas.

The wind pressure is measured close to the opening. This pressure is equal to the difference between the total pressure and the external static pressure. The internal pressure is also measured with respect to this same external static pressure. The pressure was measured at eight points within the opening (Figure 2), both inside and outside the building, allowing the direction of flow to be known locally. Full details of the site and the measuring equipment used can be found in [15].

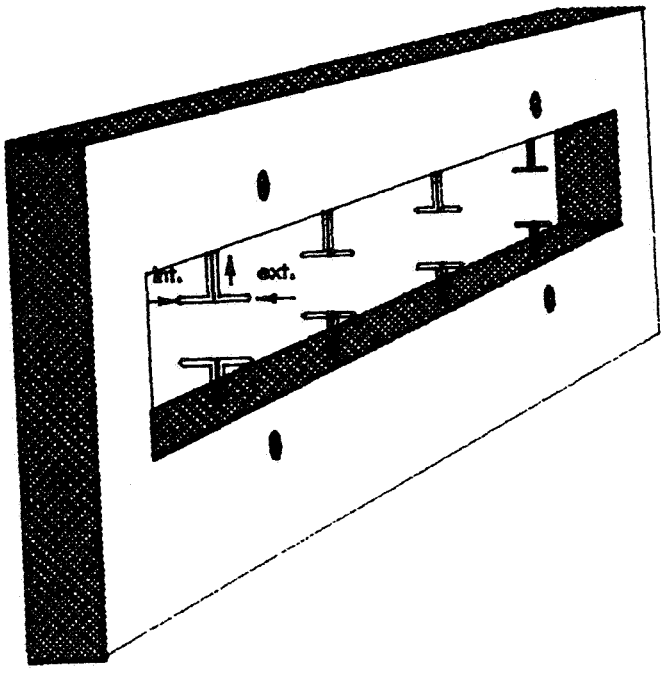

Figure 2. BOUIN: The four tapping points located in the frame are used for the determination of average wind pressure. The eight tapping points in the aperture are used for the investigation of two-way flow

2.2 SET-UP: BBRI (Limelette, B)

A single sided ventilation experiment was set up in an attic space of a 4-storey row house in the city of Gent (volume ca 28 m3). The highly insulated roof contains a 'Velux' roof window in both North and South slopes (width 1.25m. height 0.80m) as shown in Figures 3 and 4. A pressurisation test gave an airtightness level of 20 ACH at 50 Pa. Air change rates were measured with a constant injection tracer gas technique using N_2O as a tracer and an injection rate of 1 ml/s. Air samples were taken at 28 points. The room air temperature is measured at 12 points by means of thermo couples. The outdoor climate was measured through, the outdoor temperature, the windvelocity and the wind direction at ca. 2m above the roof top.

Reported are the results of three single opening experiments: one with the South window (tophinged) opened over 7.5 cm, the second with the North window (mid-

hinged) open over 5.5 cm (both on top and bottom), and a third experiment on a ventilation slit at the top of the North window (120 cm wide, 2 to 3cm high). In the latter slit configuration, pressure tubes were mounted outside and at the left and right part of the opening in order to test the validity of the assumption of a single pressure coefficient for the opening.

As illustrated in Figure 5, pressure differences were measured over both façades (N–S), inside-outside over both windows and outside left-right on both windows. The pressures, windvelocity and direction were measured about every 4 minutes, while the concentration and temperatures were measured every 40 minutes.

Air change rates and climatic parameters were monitored during a three week measuring period.

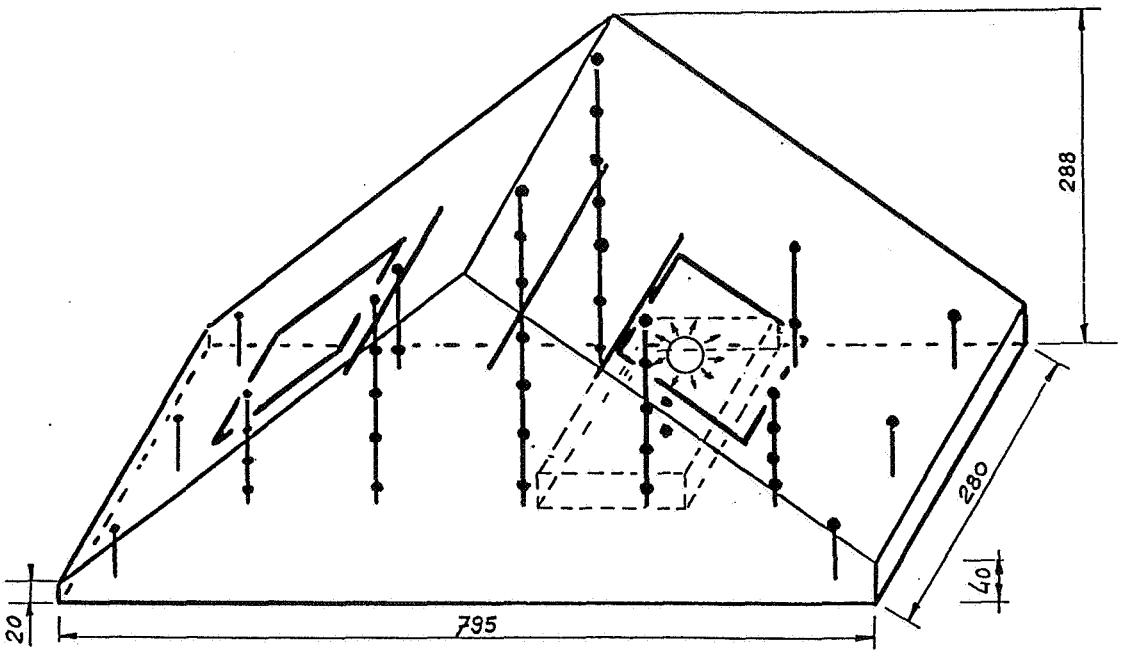

Figure 3. The attic in Gent.

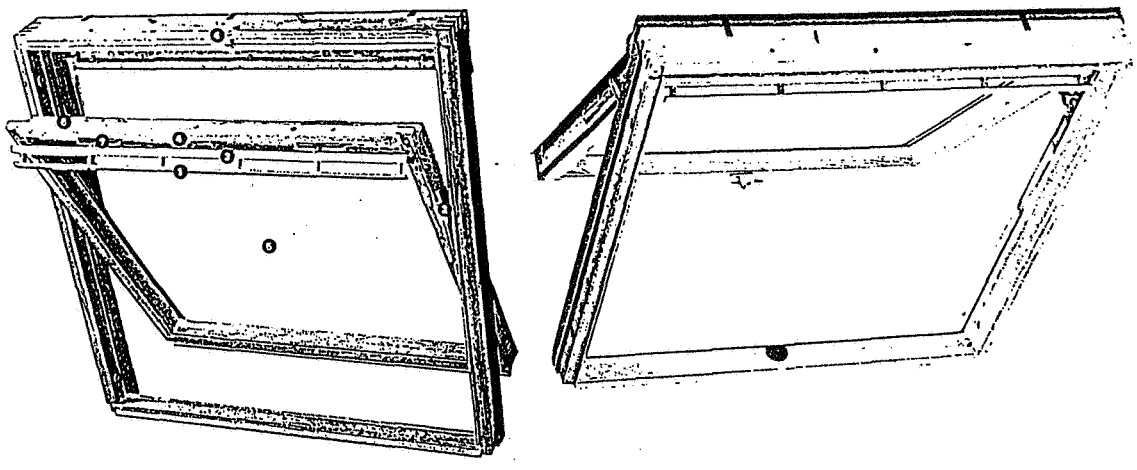

Figure 4. Roof window in north slope is midhinged (left) and the roof window in south slope is tophinged (right).

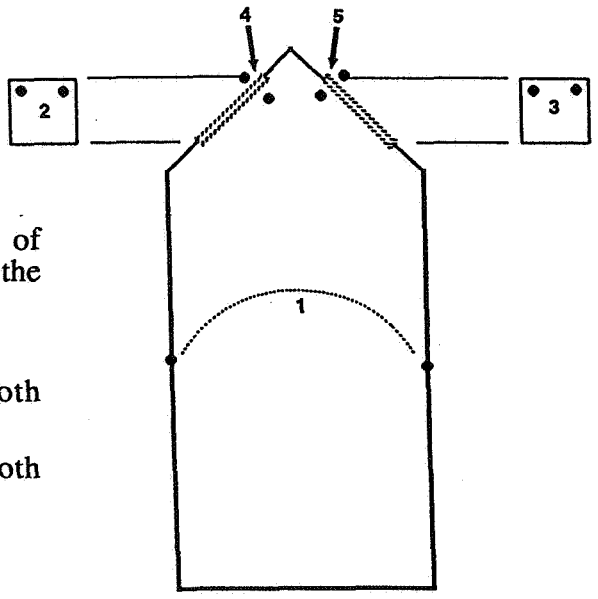

Figure 5. Measurement of the pressure differences in the attic in Gent:

- over both façades (N–S)

-.inside-outside over both windows

- outside left-right on both windows..

2.3 SET-UP: BRE (GARSTON, UK)

A series of experiments have been performed to measure the effect of wind on the time dependent ventilation rates and heat loss rates after the opening of a window. The data have been used to test a new single sided ventilation algorithm that includes both heat and mass transfer. When validated this algorithm would allow to make more realistic estimates of the energy consequences of user behaviour.

Measurements were carried out in an office room located at the corner on the top floor of a four-storey, naturally ventilated building (see Figure 6). The room comprised one internal wall and three external walls with glazing to their full height, and a false ceiling with poorly sealed roof vent above. Two adjacent glazed walls (east- and north-facing), and also the ceiling, were made airtight. This ensured single-sided ventilation via the remaining external wall (south facing) which incorporated five side-mounted casement windows evenly spaced along its width . The room volume is 242m^3 and the total wall surface area is 263m^2.

Ventilation rates were measured using the constant injection method using SF6 as a tracer gas. The precise concentration (parts by volume) is related to the ventilation rate Q m3/s as follows Q = s/C, where s is the injection rate.

Air samples were taken at eight measurement locations (Fig.6) within the room. Air temperature was recorded with thermistor probes at two locations at 1.1 m height, and surface temperatures were also measured using similar probes. Two ultrasonic anemometers were fixed into the aperture of the central window. The window measured 1.4 m high by 0.64 m wide, although the false ceiling partly obscured the upper 0.28 m (see Fig. 6). These anemometers measured three orthogonal velocity components at intervals of 12 ms, which are averaged over intervals of 0.25s and recorded. They were aligned to record one component perpendicular to the plane of the window aperture, and two within the plane.

A weather monitoring mast (ht 10m) located approximately 100m to the south-west provided data on external wind speed, direction and air temperature, averaged over 15 minute intervals. The height of the lower edge of the open window was 12.3 m.

Concerning the measurement procedure, two electric fan heaters (total 5.4 kW) were switched on to preheat the room for a minimum of approximately 24 hours before each test. Initially the windows were firmly closed and the test was immediately preceded by starting the mixing fan and tracer gas delivery and sampling system. The test began by switching off the fan heaters and fully-opening (to 180°) the central window. Tests proceeded for approximately two hours duration in all cases. Tests were carried out over a variety of external conditions.

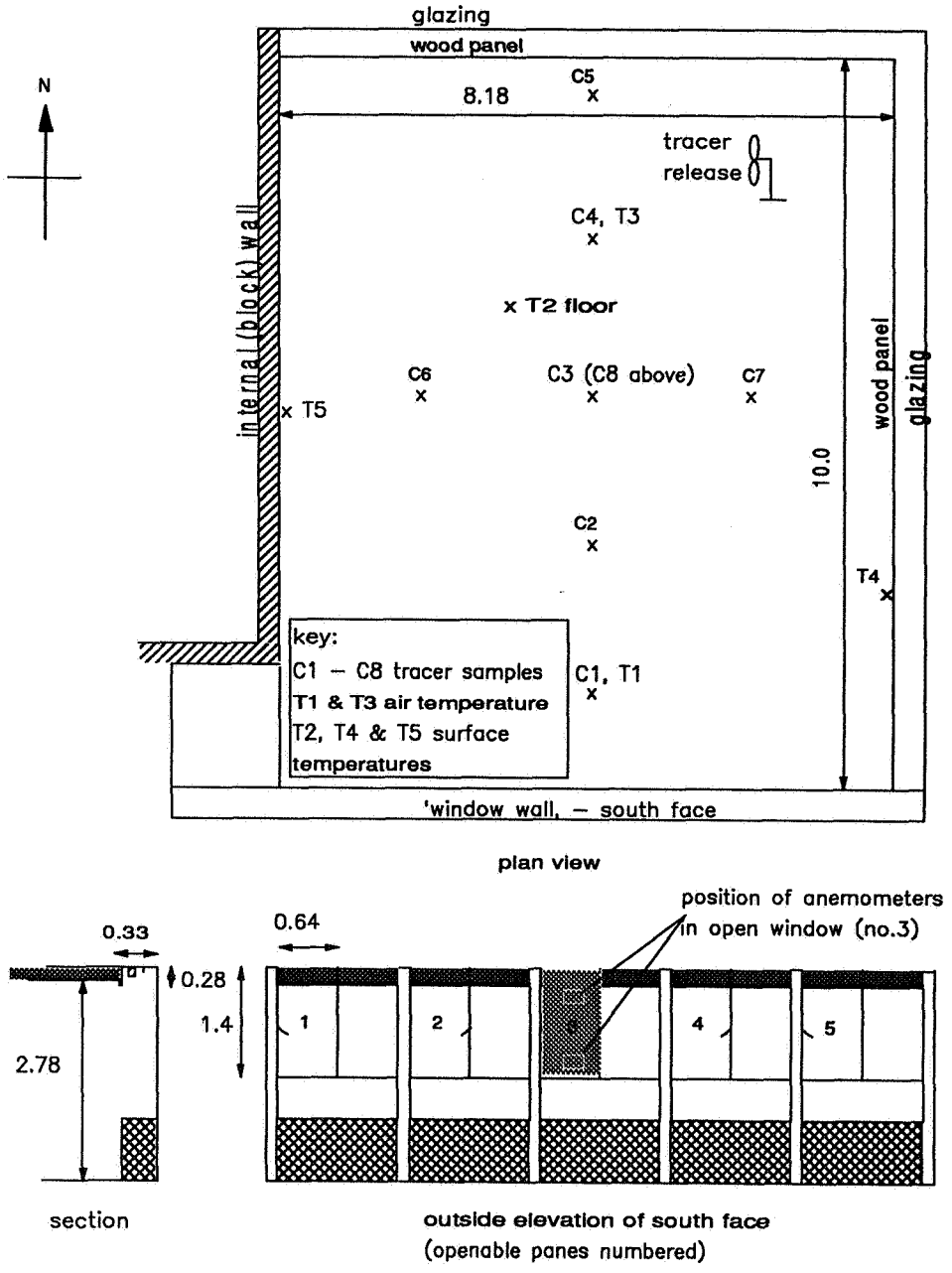

Figure 6. BRE testroom and measurement locations. The average thermal effusivity of the walls b=850 [J/ (m^2 K.$s^{0.5}$)]

2.4 SET-UP: LESO-PB (LAUSANNE, CH)

In a series of experiments performed at the LESO-PB, a newly developed algorithm coupling heat and mass transfer during single sided ventilation is tested on different rooms. The thermal characteristics of each room are determined in a separate heater test with the window closed.

The air velocity is measured with an omni-directional DISA anemometer, with a time constant <0.1s. Wall temperatures variations were detected by scanning the walls with a radiation infrared thermometer and the temperatures were measured with thermocouples. Velocity and temperature profiles were analogue recorded by mounting the probes on a motor-driven trolley moving in the opening.The inflowing cold air temperature was measured at the bottom of the window opening. The heat loss tests were performed at night to avoid solar heat gains through the south window.

Three rooms with vastly different thermal characteristics have been studied. We will consider here only the a room of the LESO building 40m^3 volume and 70m^2 wall surface (see Figure 7). The room is characterized by an average thermal effusivity of the walls of b=1000 [J/ (m^2 K.s$^{0.5}$)] with a 20% uncertainty, determined in a separate heater test with the window closed.

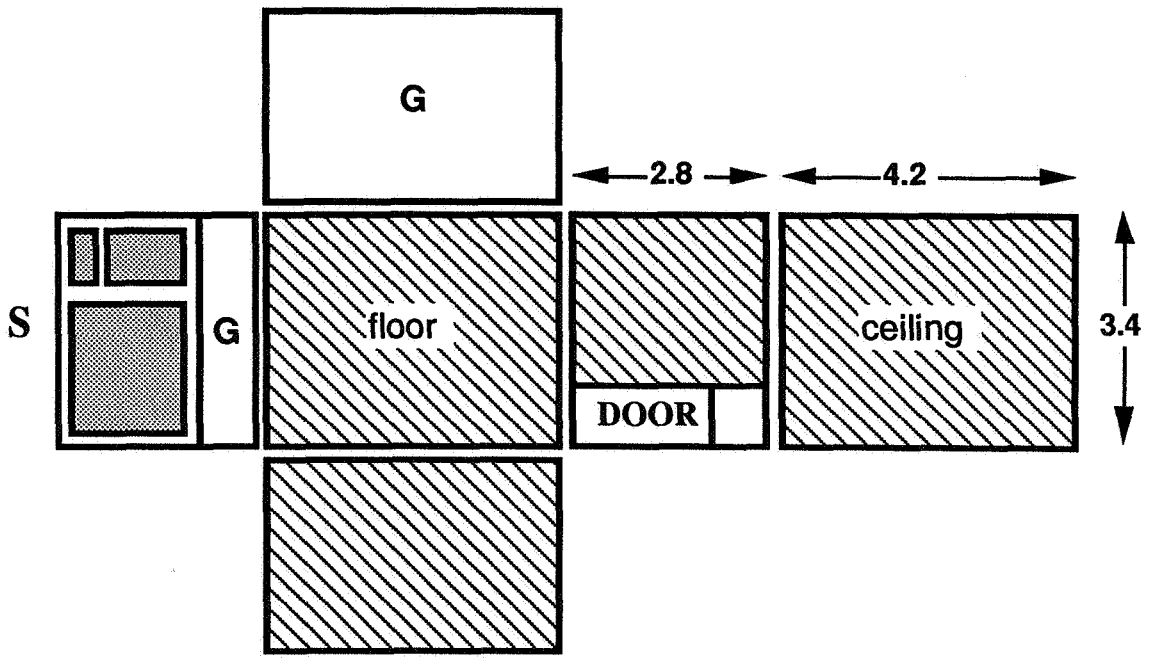

Figure 7. Floorplan of the LESO test room. The walls, floor and ceiling have 10cm glasswool insulation as a second layer. The first layer is 10cm concreet (dashed) and 1cm gypsum (G). The door is of wood. The windows have an U-value of 1.5W/m2-K. The maximum window opening is 0.85 by 1.05m^2 and the distance between the top of the opening and the ceiling is 0.7m. The width of the window could be reduced to 27cm by placing a wood board in the opening.

3. MODELING SINGLE SIDED VENTILATION

3.1 General

The ventilation rate (Q m^3/s) can be measured independently either with a tracer gas decay method or with a constant injection method.

The latter method is more suitable to measure high ventilation rates that vary in time. (Assuming complete mixing and slow variations in the ventilation rate the constant supply rate (s m^3/s) and the measured concentration (parts per volume) are related to the ventilation rate by Q=s/C).

In the case of single sided ventilation through a rectangular opening of area A, the air flowing in through one half of the opening must flow out through the other half at least when assuming mass conservation (no compressibility). This leads to the definition of an effective velocity in the opening v_{eff}

$$v_{eff} = \frac{Q}{(A/2)} \tag{1}$$

3.2 Stack effect

The steady ventilation resulting from natural convection flow caused by air density differences (the stack effect) can be calculated with a simple model based on the Bernoulli theorem [1]. If the two interconnected zones can be considered uniform in temperature (the zone temperature variation over the opening height is relatively small), the stack flow is calculated for an opening (height H and width W) with

$$Q = \frac{1}{3} C_d W H \sqrt{\frac{g}{T} H \Delta T} = \frac{A}{2} v_{eff} \approx \frac{A}{2} \sqrt{0.0052\, H\, \Delta T} \tag{2}$$

where ΔT is the interzone temperature difference. To obtain the numerical value a discharge coefficient C_d=0.6 is used.

It is interesting to note that this discharge coefficient takes two different effects into account :

(i) streamline contraction, which means that the effective opening area is smaller than A=WH

(ii) viscous pressure loss, which means that for a given pressure difference the velocity is lower than would be expected from the Bernoulli equation.

In the interzone experiments of reference (1) it was found that the C_d of equation (2) varies between 0.3 and 0.5. The measured velocities did not follow a parabolic profile, and the velocity calculated from the Bernoulli equation was systematically much larger than measured. For simplicity and for comparison with the existing literature we will yet use the overall discharge value $C_d = 0.6$ in expression (2).

3.3 Empirical description

Because ventilation increases nearly proportionally to the wind velocity and the opening area it is easy, in practice, to define a dimensionless ventilation parameter

$$F = \frac{Q}{A\, v_w} \tag{3}$$

Comparison with expression (1) makes clear that the maximum value of F is 0.5.

From windtunnel experiments of the single sided ventilation induced by turbulent wind, it is concluded that the pressure fluctuations in the plane of the window have a dominant influence [8] and in particular the eddies of the size of the window are important because they can completely penetrate into the space. Reference [8] concludes that for airflow parallel to the façade of the model F can be considered constant having a value of about 0.03, which is close to the windtunnel result found by Warren [9]. For other inflow directions Crommelin and Vrins [8] have found decreased ventilation, with a minimum value for an opening at the leeside.

De Gids and Phaff [6,7] investigating the consequences of opening one window on the internal climate of a number of apartment rooms, proposed an empirical formula

$$Q = \frac{A}{2}\sqrt{C_1\, v_w^2 + C_2\, \Delta T\, H + C_3} \tag{4}$$

and obtained by a least mean square fit the following values for the coefficients $C_1 = 0.001$, $C_2 = 0.0035$, $C_3 = 0.01$. The window heights were about 1m.

From the relatively high value of the turbulence term $C_3 = 0.01$, this fit suggests that for windvelocities smaller than 3m/s, or for a 1m high window temperature differences less than 3K, there is a lowest value for the ventilation parameter $F = 0.05$, caused by turbulent fluctuations.

Without the C_3 term, the value $C_1 = 0.001$, would correspond to a ventilation parameter $F = 0.015$, which is low, also comparing $C_2 = 0.0035$ with expression (2), the fit predicts a relatively weak stack effect.

While the spread in the data around the fit to equation (4) is considerable [6,7], this result is a very useful reference for new ventilation studies.

3.4 Fluctuating wind pressures

Cockroft and Robertson [10] studied ventilation with normal wind incidence, and proposed a theory to take pressure fluctuations into account and more recently, Haghighat [11] proposed a new model approach.

To understand the interpretation of the measurements presented in the next section the models will be qualitatively discussed.

A quick estimate can be made of the air change rate resulting from a fluctuating pressure at a single large opening of a volume V. We assume that the pressure variations are instantaneous, this means that the size of the opening does not limit the flow. For a change in pressure of δp (Pa), the air density changes by $\delta\rho = \rho\, \delta p/p$ and this causes an air flow of $\delta V \cong V\, \delta p/p$. Therefore fluctuations of frequency f(Hz) and amplitude δp would induce an in and outflow of air of

$$Q(\text{fluctuating}) = f\, V\, 2\, \delta p / p \tag{5}$$

This is the maximum value one can expect for a single frequency component of the external wind. As an example, taking a room of $100m^3$ and windpressure fluctuations at 1Hz and 20Pa amplitude, then $0.04m^3/s$ of air flows in and out. Assuming complete mixing this fluctuating windpressure would cause a total influx of fresh air of 1.4ACH.

In general there is a pressure drop over the opening, and for rapid fluctuations the inertial mass of the air will limit the acceleration of the air.

In Figure 8, we show the analogous electrical elements included in the air flow model proposed by Haghighat [11]. The effect of the non-zero air-mass is represented by an impedance L, whose impedance value increases with frequency. R is the non-linear air flow resistance of the opening which increases with the air flow rate, and the amount of air stored in the volume is represented by a capacitance.

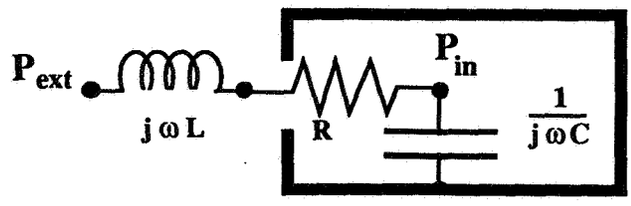

Figure 8. The equivalent circuit for the modelling of ventilation induced by pressure fluctuations

For particular forms of the external pressure, the 2nd order non-linear differential equation corresponding to this model has to be solved numerically to find the internal pressure and the airflow, which both can be compared with experiments.

For a given situation the problem can be simplified by estimating the relative magnitude of the three circuit elements in Figure 1. The non-linear flow resistance and the capacity are forming a low pass filter, and an estimate of the cut-off frequency f_c, will show whether the flow impedance $2\pi f_c L$ can be neglected. The calculation of the internal pressure is now reduced to the solution of a first order non-linear differential equation.

This is the approximation used for the interpretation of the BOUIN measurements. Defining the non-linear flow resistance R by the flow equation

$$Q = C_d A \sqrt{\frac{2\Delta P}{\rho}} \tag{6}$$

and measuting the external pressure directly, the equation to be solved for the internal pressure is of the form

$$\frac{dP_{in}}{dt} = \pm \frac{A}{V} \frac{\gamma R T_{in} C_d}{\sqrt{\rho}} \sqrt{|P_{ext} - P_{in}|} \tag{7}$$

We note that the model presented schematically in Figure 8 does not include two-way flow, neither does it take into account effects related to the finite velocity of pressure (sound) waves.

3.5 Ventilation rate and heat tranfer

The heat loss rate Φ, resulting from a ventilation rate Q is proportional to the temperature difference between the in and out flowing air, and the calculation of the heat loss rate reduces to the problem of calculating the outflowing air temperature.

As a first approximation a single zone thermal model was proposed [12,13] where the inside air temperature is taken uniform, T_{in}. This is reasonable in practice when the outside temperature, T_{out}, is relatively low. The heat loss rate is then written as

$$\Phi = Q\,\rho\,C_p\,(T_{in} - T_{out}) \tag{8}$$

Due to the heat transfer resistance between the air and the walls, T_{in} is situated in between the inside wall surface temperature and the outside air temperature. This is illustrated in Figure 9 where the heat current source 1, represents the ventilation heat loss rate given by equation (8).

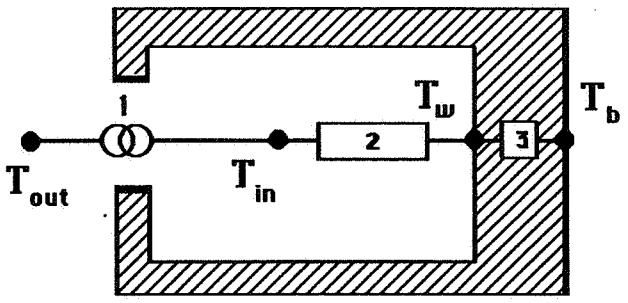

Figure 9. The equivalent circuit for the modelling of ventilation heat loss rate. The ventilation heat loss rate (1), the heat transfer resistance (2) the dynamic wall resistance (3). T_{in} is the inside air temperature and T_w is the wall surface temperature.

As discussed in references [12,13] the wall surface temperature T_w is changing slowly and can be calculated from a solution of the heat equation for a half-infinite homogeneous wall. The difference between the wall surface temperature and the nearby air temperature, $T_w - T_{in}$, is easily measured and is given by

$$T_w - T_{in} = \frac{\Phi}{Cs\ h_c\ S_i} = \frac{Q\,\rho\,C_p\,(T_{in} - T_{out})}{C_2\ h_c\ S_i} \tag{9}$$

The new parameters in equation (9) are the total inside surface area S_i, the convective heat transfer coefficent h_c and the coefficient Cs, the fraction of S_i actif in convective heat transfer. It was found that a constant value of $h_c = 6 W/m^2K$ is consistent with the data (the value is typical for low velocity forced convection). The concept of Cs is illustrated in Figure 10.

From (9) it follows that we can *calculate the ventilation rate indirectly from* $T_w - T_{in}$. Even if Cs is initially unknown variations in $T_w - T_{in}$ with time (or from measurement to measurement) are related to variations in the ventilation rate.

Ventilation rates determined from such heat transfer measurements allow an independent comparison with tracer ventilation rates.

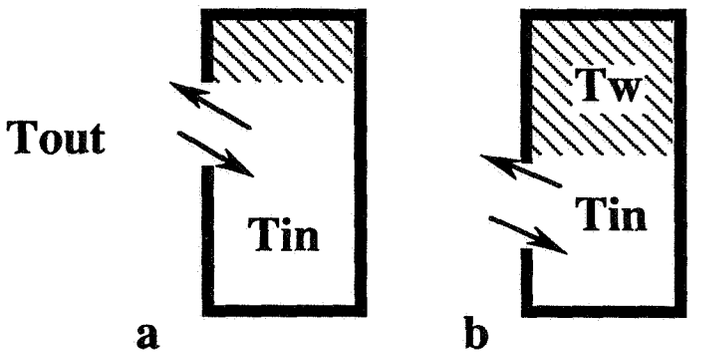

Figure 10. Above the upper level of the window the trapped warm (dashed) is at the same temperature as the wall, the ceiling and wall surface above the top of the window do not cool by convection. The coefficient Cs is about 0.8 in (a) and 0.4 in (b).

4 EXPERIMENTAL RESULTS AND DISCUSSION

4.1 CSTB (BOUIN test house)

Table 1 summarizes the ventilation configurations studied with the test house in BOUIN. Are given the average windvelocity, the wind direction (from normal incidence to the opening) and the ventilation rates calculated from the measured decay of tracer gas concentrations. The standard deviation of the windvelocities and the wind direction is given between parentheses. Test cases 1, 2 and 4 are therefore with the opening to windward and cases 3 and 5 with the opening on the lee side. We note that the stack effect is calculated to be less than 0.01ACH and therfore neglected.

The external windpressure is measured at the orifice and can then be used directly as input for a simulation programme to calculate the internal pressure and the air change rate.

4.1.1 Internal pressures

For the simulations with the air infiltration program SIREN of the CSTB, it was assumed that the only mechanism for air exchange is the compressibility of the air. Therefore the external pressures measured at the opening are averaged, and the internal pressure is calculated by solving the first order differential equation (Equation 7) numerically. In Figure 11a are plotted the measured and calculated internal pressure for the windward test 1. It is seen that the algorithm reproduces the main features of the internal pressure variations. Figure 11b concerns the same plot for leeward test 3, but this time there is a systematic difference between the observed and calculated pressure. This could be due to the simplifying assumption

Test	opening area (cm2)	wind velocity (m/s)	wind incidence angle ϕ	tracer measured (ACH)	compressi-bility calculated (ACH)	F (Eq.3)
1	100	7.7 (1.2)	18 (7)	0.21	-	0.07
2	100	5.1 (0.9)	0 (?)	0.20	0.09	0.10
3	100	10.2 (1.5)	229 (8)	0.58	-	0.15
4	200	5.8 (1.15)	10 (10)	0.35	0.24	0.07
5	200	5.8 (1.1)	191 (10)	0.20	-	0.045
Ref7	230	5	0	0.02	0.06	$<10^{-3}$

Table I

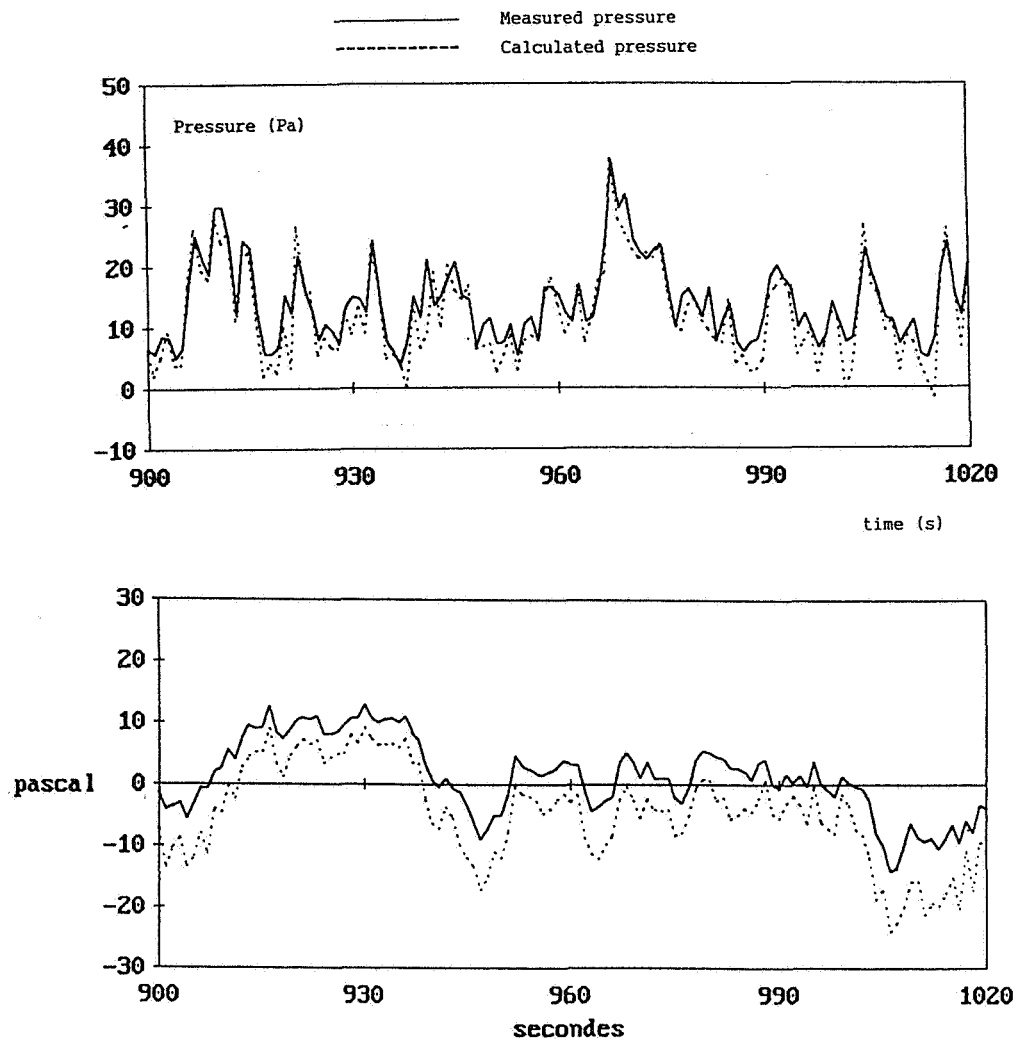

Figure 11. The measured and calculated internal pressure of the BOUIN house for 100cm^2 : windward test 1 (a) and leeward test 3 (b).

that there is no two-way flow. In particular in test 3, the incidence of the wind is not normal but almost at an angle of 45° so that eddy flow can be expected.

The solution of Equation 7, with experimental data points every 0.2sec as input , can become unstable. Indeed there appeared to be a numerical problem with the solution for the larger 200cm^2 opening.

The French group has made his measured data available to other groups in Subtask 2 and the wind pressure and velocity data of test 4 have been received at the LESO-PB in Lausanne. Analysis with a computer code specially written to solve Equation 1 (code TURBUL), the numerical instability and aliasing problems were immediately apparent. Using a NAG FORTRAN library routine, the internal pressure could be correctly calculated from the external pressure data as shown in Figure 12.

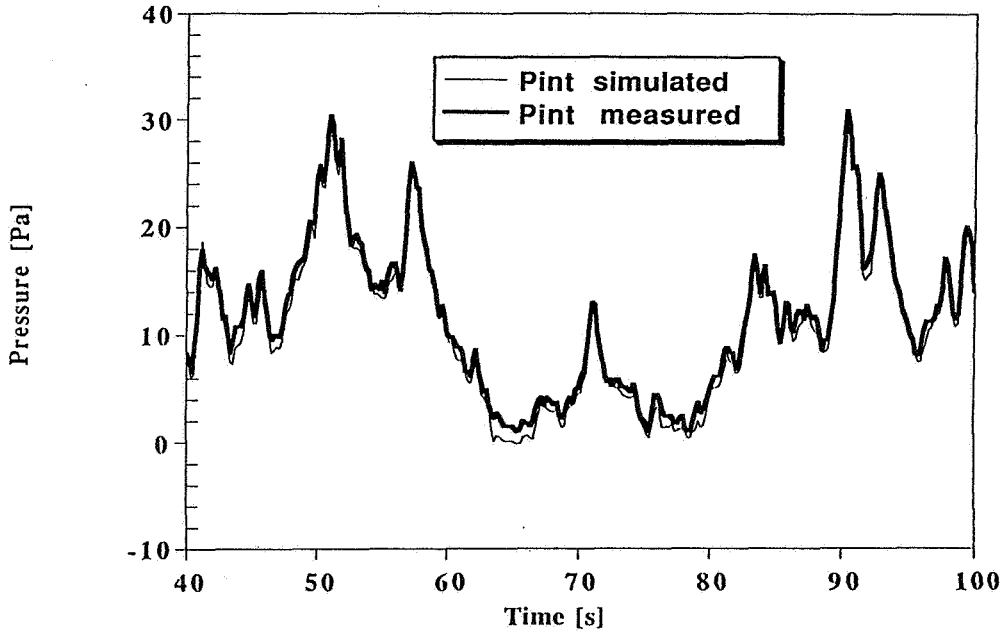

Figure 12. The measured and calculated internal pressure of the BOUIN house for 200cm^2 windward test 4.

4.1.2 Air change rates.

As discussed in §3, to calculate the air change rate resulting from fluctuating pressures one has to know which part of the inflowing fresh air flows out without mixing with the air.

Assuming that the inflowing air mixes completely, the air change rate was calculated with the code SIREN giving 0.09ACH for test 2, about half the measured ACR. Using the same assumption, the code TURBUL gives 0.24 ACH for test 4, which is 70%.of the measured ACR.

This result contrasts with the findings of Cockroft and Robertson [10] who found that only one-third of the fluctuating air flow into the enclosure was finally mixed with the bulk of air in the enclosure. Their set-up was very different though, using a 225 cm^2 opening in a 3.5m^3 isothermal model, and wind simulated with a variable speed fan. The result is included for comparison in Table 1.

With a comparable opening size but with a 30 times larger volume, the BOUIN data do not show evidence for incomplete mixing. A factor that may be important is the 5-10K inside-outside temperature difference in the BOUIN experiments (zero in Ref.7). Indeed the colder air entering the enclosure is likely to fall immediately being automatically replaced by inside air during the backflow. Systematic experiments are necessary to study this mechanism.

For test 2 the importance of two way flow was examined. Instead of just taking the pressure spatially averaged over the whole opening, the pressure was measured at eight points within the opening (see Figure 2). The pressure was measured both inside and outside the building, allowing the direction of flow through each part to be measured. A new estimate of the ventilation rate taking two-way flow into account gave 0.15 ACH, which is still smaller than the observed rate, and detailed further analysis of the data is necessary.

Finally the fact that the measured internal pressure can be simulated in detail means that Equation (7) applies to these particular cases, but it is not known yet what the limits of this model are in particular with respect to ventilation.

Indeed, with increasing opening to volume ratio the time constant (RC in Figure 8) decreases and a much higher measurement frequency is necessary.

Finally for comparison with the empirical models presented in §3, in the last column of Table I are given the ventilation coefficients F (see expression (3)). They appear to be unexpectedly high compared with the scale model measurements showing that for a correct prediction of ventilation rates a detailed knowledge of the ventilation mechanisms is necessary.

4.2. BBRI (attic in Gent)

4.2.1. Ventilation rates

The results of ten days monitoring of the attic in Gent with the south window slightly opened (1500cm^2) are given in Figures 13a,b and c. As seen from Figure 13a the outside temperature peaked around 15°C in the afternoon and reached a minimum of around 8°C in the early morning hours. The well insulated attic was not heated and stayed systematically warmer than the outside air by 6 to 11K. The air change rate due to the stack effect alone is then expected to be less than 0.1ACH.

The wind direction was between south and east as shown by the upper trace in Figure 13b (south is 180°). The lower trace is the wind speed, typically 2m/s but peaking above 4m/s during days 265, 266, 267-268 etc., with a maximum at 6.5m/s in the morning of day 268.

The measured air change rates have been correlated to the windvelocity and the stack effect by a multiple linear regression using equation (4) The best fit gave the values C_1=0.003 and C_2= 0.005 and C_3=0; this expression is plotted with the measured ACR in Figure 13c.

The factor C_1= 0.003 corresponds to a ventilation parameter F=0.027 (expression (3)), in excellent agreement with the results of Crommelin and Vrins [8]. The fitted factor C_2= 0.005 agrees with expression (2) for the stack effect. Putting in the values for ΔT and H it is seen that the stack effect is contributing less than 0.1[1/h] which is insignificant compared to the wind effect. Neglecting then the stack effect, expression (4) reduces for this particular case to $Q \approx 0.5\ v_w$ [1/h]. Indeed the simulated trace in Figure 13c is nearly proportional to the windvelocities in Figure 13b.

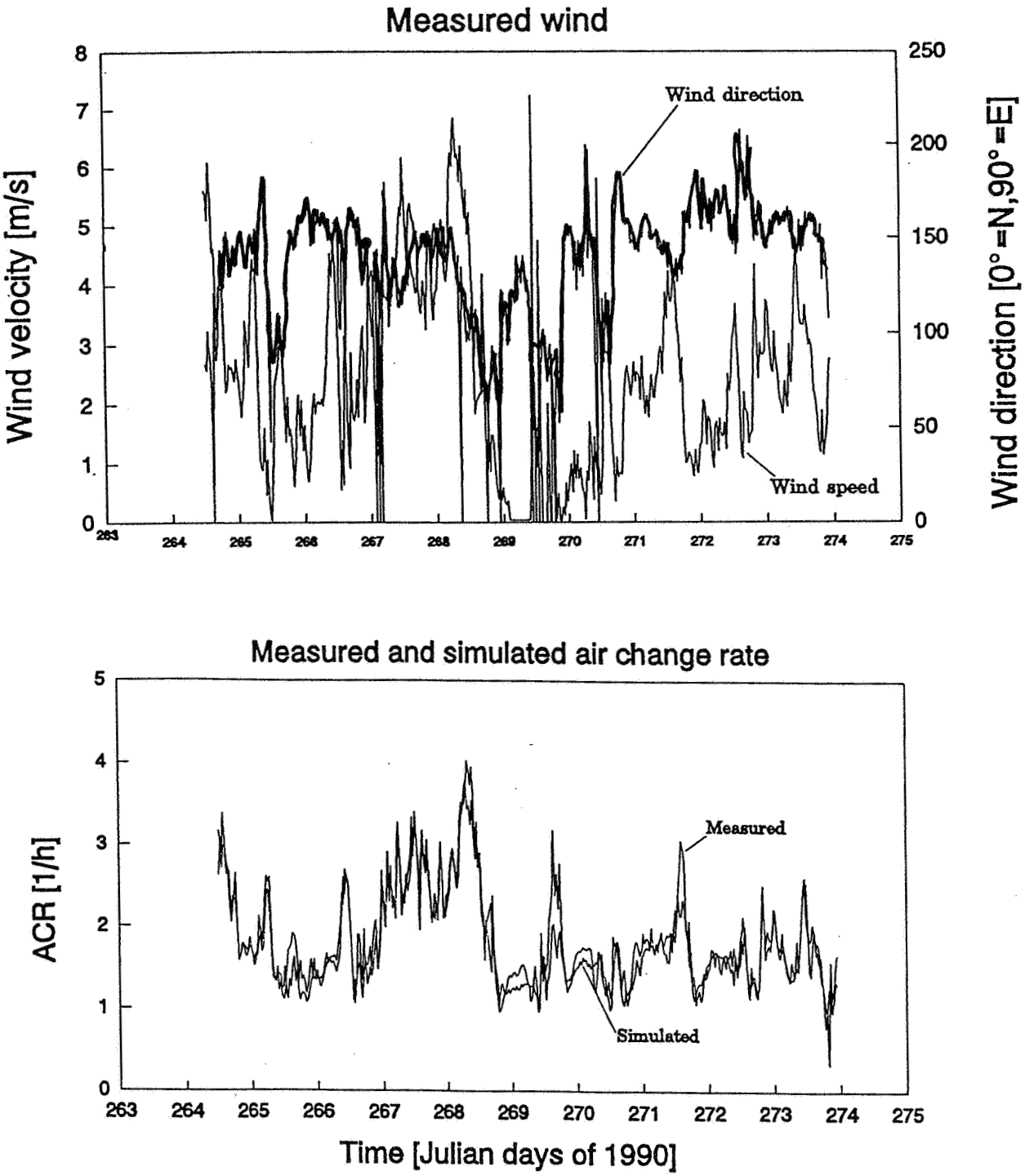

Figure 13. Attic in Gent, south window opened over 7.5cm (A=0.15m^2). (a) measured temperatures; (b) wind velocitiy (lower trace) and wind direction (upper trace); (c) measured and calculated air change rate.

The overall agreement between the simulated and measured ACR is good, showing that for a particular situation the ventilation rate can be characterized by one such a coefficient C_1. The peak ventilation rates are underestimated however and the analysis of the data should be pushed further. By looking closely at the differences it can be found out how the value of C_1 is correlatedwith the measured pressure coefficients and what the relative importance is of two-way flow and compressibility effects.

The same type of measurements and analysis has been performed for the North window that was then on the *lee-side*. It was noted that there was a negative correlation between the wind velocity and the stack effect. For a given wind, an increased inside-outside temperature difference corresponded to a reduced ACR. This is reflected by the correlation coefficients C_1=0.038 and C_2= –0.041. We note that these coefficients are an order of magnitude higher than before for similar ventilation rates. This means that the interpretation of the fit is difficult and uncertain: in calculating Q with expression (4) one subtracts two large numbers.

Unfortunately after the measurements, a pressurization test revealed a leakage in the South wall-roof junction. This means that with the north window open, cross-ventilation may have contributed significantly to the ventilation rate, complicating the interpretation of the data

4.2.2. Pressure coefficients

In general for the modelling of ventilation through openings of small height the airflow is calculated from the pressure difference between the inside and the outside and one single pressure coefficient is assumed for the outside.

A series of measurements have been made on the ventilation slit at the top of the window shown in Figure 4, which is 2-3cm high and 120 cm wide, in order to test the hypothesis that the pressure coefficient does not vary over the opening.

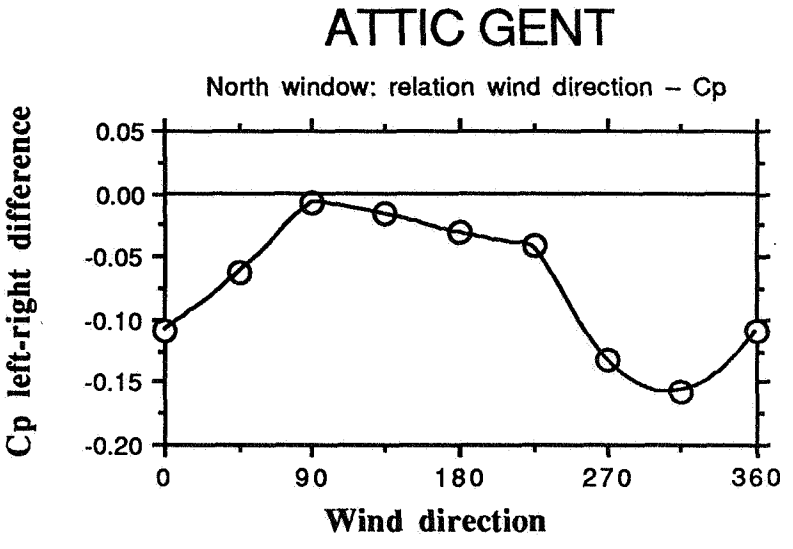

Figure 14. Attic in Gent, ventilation slit. The difference in pressure coefficients measured left and right of the opening as a function of the winddirection (0=North, 90=East). Wind velocities >2m/s. The standard deviation in each plotted value is about 0.03.

Two pressure tubes are mounted one at each side of the opening and connected to a differential manometer. The difference in left-right pressures was recorded and converted in a difference in pressure coefficient by dividing by the dynamic pressure $1/\rho v_w^2$ .Only data corresponding with wind velocities larger than 2m/s have been taken into account. .

In Figure 14 we have condensed the results by plotting average values of the difference in left-right pressure coefficents as a function of the wind orientation. It is seen that the variation is sytematic and that differences in Cp of 0.15 are possible. Surprisingly the situation is not symmetric with respect to normal wind incidence: the pressure coefficient at the right side is always larger than the left side. It is believed that this the influence of the surrounding houses, rather than a problem with the manometer readings.

The result indicates that the assumption of a homogeneous pressure coefficient for the whole width of the ventilation opening is not correct. The assumption may be acceptable when the air flow through the opening is in a single direction, but not when two way flow is taking place as in single sided ventilation.

The two-way flow mechanism could explain the magnitude of the observed air change rates in Figure 13c. Indeed, for the data in Figure 13c to be understood in terms of two-way flow, one can estimate that a difference in pressure coefficient left-right of about 0.05 would be sufficient.

Future measurement campaigns should therefore measure both ventilation rate and pressure distribution over the opening.

4.3 BRE

4.3.1 Heater experiments

Before starting the ventilation experiments, the thermal behaviour of the room was extensively investigated with a number of heater tests. The procedure is explained in references [12,14], and these tests give confidence in the interpretation of changes in wall temperatures in terms of heat flow rates.

In Figure 15b is shown the measured and calculated variation of both air and floor temperature for a thermal effusivity $b=\sqrt{(\lambda\rho c)} = 850$ [J/ (m^2 K.$s^{0.5}$)], and a time constant of 20minutes. The uncertainty in the average b-value of the room is about 20% mainly due to uncertainty in the background drift of the room. It is surprising that such a complex room (see §2.3) can still be described reasonably well by the simplified dynamic thermal model (see ref 12).

4.3.2 Ventilation

We report on eleven ventilation experiments with an identical procedure so that they can be intercompared. As discussed in §2.3, at time t=0, the background heating is put off and the window is opened completely. The air temperature which was much higher than the floor temperature before t=0, drops with a time constant of about 10 minutes. In Figure 16 compares the observed air and floor temperature with the model calculation. The ventilation rate is calculated with expression (2) for the stack expression. There are no free parameters in the model and the agreement is rather good. The calculated curves are slightly above the measured data points.

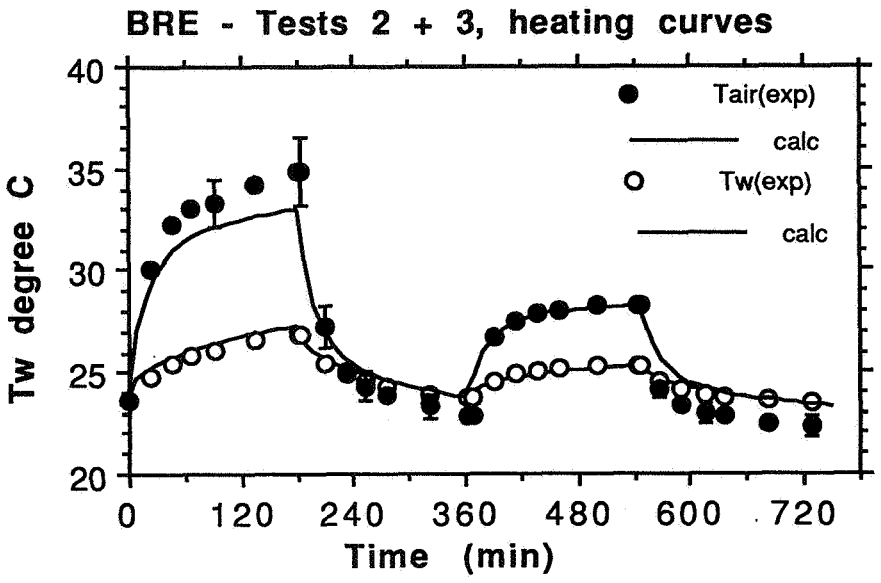

Figure 15. Heater test of the BRE room. A 9kW electrical fan heater is switched on (t=0) and off (t=180min); 5kW is switched on (t=360min) and off (t=540min). The floor surface temperature is used as a reference for the wall temperature. The air (filled symbol) and the floor temperature variation compared with the model calculation (see ref 12) using a thermal effusivity $b=\sqrt{(\lambda\rho c)}$ = 890 SI units, characteristic for the room. Compensation for background drift has been made.

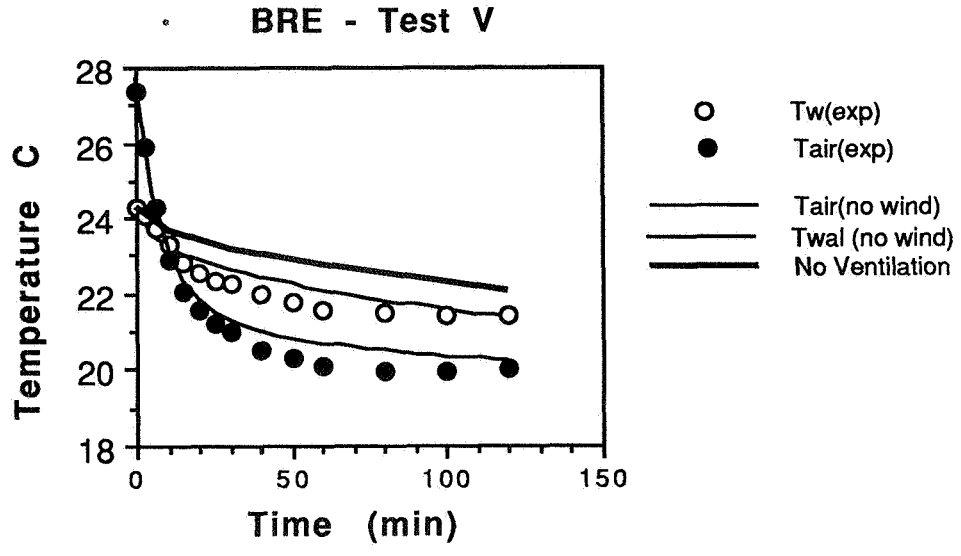

Figure 16. At t = 0 the background heating is switched off and the window is opened. In the calculation only stack ventilation is assumed. The temperature difference, Twall-Tair, measured after one hour (t=60min) depends on the ventilation rate.

After about one hour, the temperature difference between the floor and the air is quite constant and equal to about 1.5K for both the model and the experiment. This is the parameter we will compare in the following for the different ventilation experiments

In Figure 17, we have plotted as a function of meteo wind speed, both the calculated stack velocity (open symbol) and the effective ventilation velocity. The latter has been calculated from the tracer air change rate and expression (1). The inside outside temperature difference is not very different for the various experiments so that the average stack velocity is for all the experiments about 30cm/s.

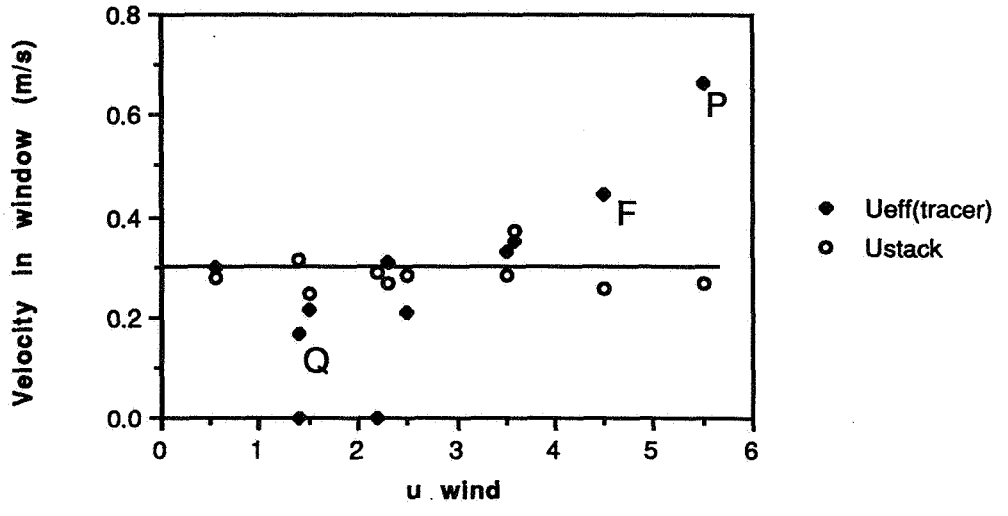

Figure 17. BRE test room. Stack velocity and effective velocity as a function of the windvelocity.

The available data have not yet been analysed in all detail but no clear corelation with wind direction is apparent.

The data point indicated by Q corresponds to the leeside and surprisingly the air change rate is reduced by nearly 50% with respect to the stack effect.

The only measurements where the ventilation rate is significantly increased by the wind are F and P. For the P-case, with normal incident wind, the effective velocity has more than doubled. The ventilation parameter is then F=0.06, not a very exceptional value and it is rather the absence of strong wind effects that is surprising.

For $T_{in}-T_{out}$ nearly the same in all tests, Equation 9 predicts a linear relationship between Q and T_w-T_{in}. Therefore we compare in Figure 18, T_w-T_{in} (at t=60min) with the air change rate. With the exception of the P test, there is apparently a good correlation, and it should be possible to compare systematically ventilation rates with heat loss measurements. This will be found out when all the data have been analysed.

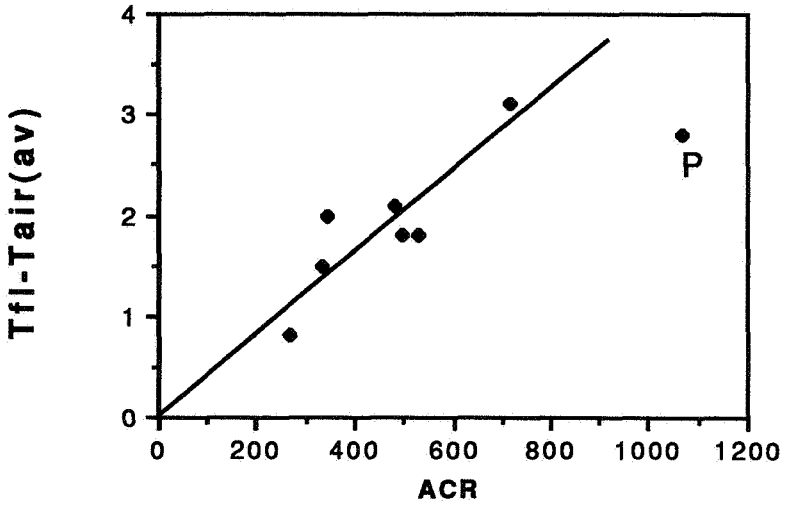

Figure 18. BRE test room. The air change rate in m^3/hr is well correlated with the floor-air temperature difference as predicted by equation 9. The P measurement corresponds to a wind increased ACR.

4.4 LESO-PB

The single sided ventilation algorithm predicting the ventilation energy loss caused by an inhabitant who leaves a window open for a certain period of time (see §3), has already been tested for various cases where the stack effect was dominating (12-14). We present here an experimental result where the ventilation and heat loss rate were increased by wind. The case without wind is used as a reference.

For the test without wind (<1m/s) the 0.85m wide window was left open for 10 hours during a windless night (outside temperature near 5.5°C). The unfurnished office room was initially at 21.5°C for 24 hrs, and the time dependent decrease in air and wall temperature are reasonably well explained by the model illustrated in Figure 9, and calculating the ventilation rate with the stackflow equation (equation (2).

A test with a strong southern wind was conducted for 7 hours at night and with the window opening reduced to one third of the width (W=0.26m; outside temperature near 4.5°C). The room was initially at 19°C for 24 hrs in thermal equilibrium with the building, and the effect of the wind was to increase the average air velocity in the window to 0.6m/s, about two times the expected stackvelocity.

In Figure 19, we compare the cooling rate from stack flow (well known from other experiments see ref 12) with the observed cooling.

The picture is consistent.

(i) There is strongly increased cooling of the walls.

(ii) The temperature drop T_w–T_{in} is more than two times larger than expected from the stack effect (see equation 9).

(iii) The velocity in the window is more than two times higher than the stack velocity.

Comparison with the model (Figure 9) shows that taking not the stack velocity but a window air velocity of 0.65 m/s, the observed cooling can virtually be explained.

We have no data to corelate the external wind velocity and the air flow in the window. The wind at the LESO building is strongly attenuated by surrounding buildings and difficult to characterize from meteo values.

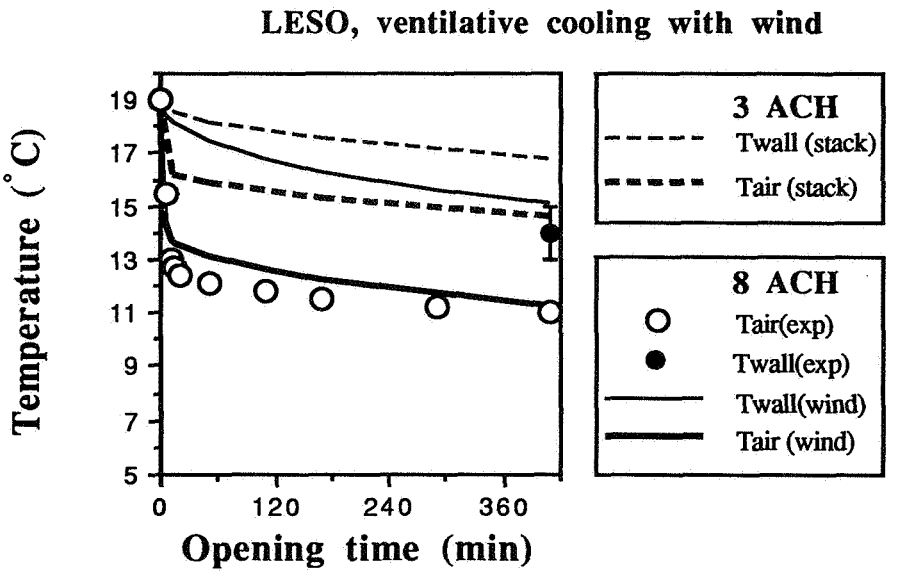

Figure 19 The window width is 0.27cm and the wind increases the ventilation rate and therefore the cooling. The windy case is calculated with an effective velocity of 0.65m/s in the window instead of the stack velocity of 0.21m/s.

The velocity profile suggests that it is possible in single sided ventilation that the stack flow in the opening is continuously accelerated by wind. Usually one assumes that the wind has only a perturbing action creating turbulence and fluctuating flows. The apparent steady outflow of air is remarquable because it is not documented as far as we know.

The velocity profile was continuously measured in the window with a probe mounted on a trolley 1cm in front of the inner window frame (1.1m high) traveling up/down in 30min.

In Figure 20 we show an original analog recorder trace. There are the following interesting features

(i) a neutral level can be distinguished near the center of the opening.

(ii) the top trace is rather smooth and is close to a parabolic profile, while the lower trace is very much effected by the turbulence of the wind.

(iii) the profile is asymmetric

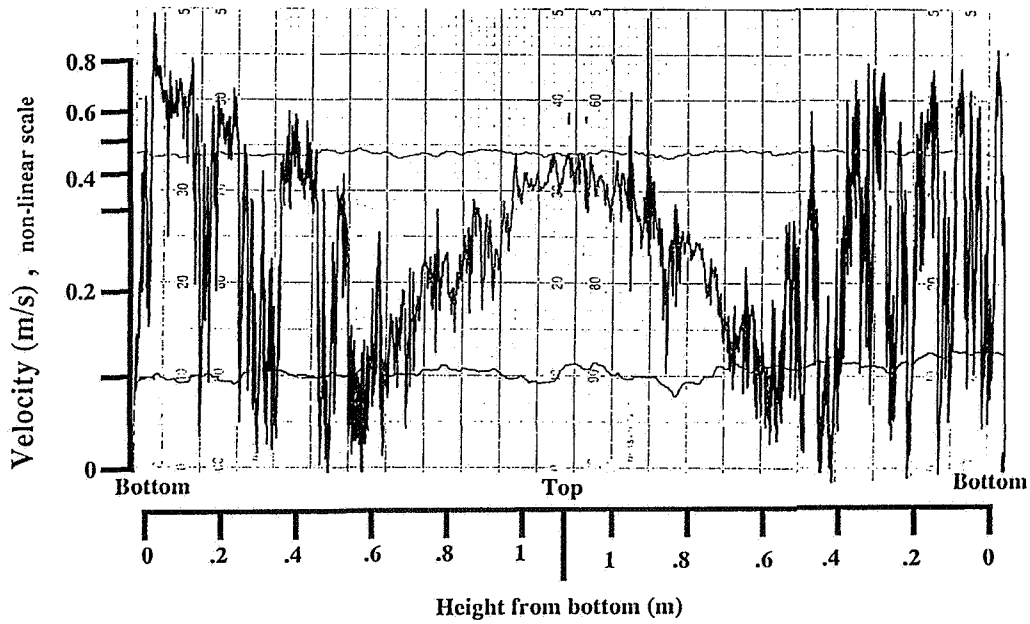

Figure 20. Part of continuous recorder trace of an omni-directional anemometer traveling in the centre line of the window. The window height is 1.1m and the probe velocity is about 3cm per minute. The velocity scale is not linear. The calculated average stack velocity is 21cm/s. A neutral level can be distinguished at the middle of the opening. Below the neutral level the turbulence is systematically much higher than above.

5 CONCLUSIONS

Single sided ventilation experiments have been conducted in the frame work of the Annex 20, and allowed fruitful cooperation between four laboratories in four countries. Experiments have been coordinated, data and types of analysis have been critically discussed. The results include new insights on ventilation caused by wind pressure fluctuations, two-way flow and ventilation energy loss. It has become clear that while the greatest uncertainty resides in lack of knowledge of the local wind, even when the local wind is measured the results on ventilation is not well known

6 ACKNOWLEDGEMENTS

The authors acknowledge research support from the AFME (France), OFEN (Switzerland), BRE (United Kingdom) and BBRI (Belgium). Many people contributed to the measurements and data analysis, thanks to all of them.

REFERENCES

[1] Pelletret R., Allard F., Haghighat F., Liebecq G., and Van der Maas J., 'Modelling of large openings' 12th AIVC Conference 24-27, Ottawa, September 1991.

[2] Warren P R, "Flow through external openings, Draft Extract", Annex 20: Second Expert Meeting in Warwick, UK, Nov. 7-10 1988.

[3] Roulet C. and Scartezzini J, 'Stochastic model of inhabitant behaviour in regard to ventilation' 12th AIVC Conference 24-27, Ottawa, September 1991.

[4] Vandaele L, Wouters P, "Air flows through large openings; an overview of existing approaches", Third Expert Meeting in Aalborg, Denmark, May 30-June 2, 1989

[5] Van der Maas, J., 'Airflow through large internal and external openings' Status Report subtask 2, task 2.1, Fourth Annex 20 Expert Meeting in Lommel, Belgium, November 13-16,1989

[6] Phaff J C , de Gids W F, Ton J A et al Ventilatie van gebouwen. Onderzoek naar de gevolgen van het openen van een raam op het binnenklimaat van een kamer (Investigation of the consequences of opening one window on the internal climate of a room) Delft IMG-TNO rapport C448, March 1980. Airbase #2201 (Data tables and Figures only available in the Dutch version).

[7] De Gids, W., and Phaff, H., 1982. "Ventilation Rates and Energy Consumption due to Open Windows", Air Infiltration Review. Vol. 4 N° 1, pp. 4 - 5.

[8] Crommelin R.D., Vrins E.M.H., "Ventilation through a single opening in a scale model", Publication P 87/048, TNO Delft, 1987-09-01.

[9] Warren, P.R., 1986. The Analysis of Single-Sided Ventilation Measurements, Air Infiltration Review, Vol. 7 N° 2, pp. 3 - 5.

[10] Cockroft J.P. and Robertson P. "Ventilation of an enclosure through a single opening", Building and Environment Vol 11,pp29–35, 1976

[11] Haghighat F., Rao J. and Fazio P. 1991, "The influence of turbulent wind on air change rates–a modelling approach", Building and environment Vol 26, pp. 95-109

[12] Van der Maas J, Roulet C -A, Hertig J -A, "Some aspects of gravity driven airflow through large openings in buildings" ASHRAE Transactions 1989, Vol.95, Part 2, pp. 573-583

[13] Van der Maas J., Roulet C.-A. "Ventilation and Energy loss rates after opening a window", Air infiltration review, Vol 11, No 4,1990, pp 12–15

[14] Van der Maas J., Roulet C.-A.and Hertig J.-A., "Transient single sided ventilation trough large openings in buildings", ROOMVENT '90, Oslo, June 1990, C48

[15] Riberon J., Villain J., 'Etude en vraie grandeur des débits effectifs de renouvellement d'air', CSTB GEC/DAC-90.101R, Champs-Sur-Marne, July 1990

12th AIVC Conference, Ottawa, Canada, 24-27 September, 1991

SINGLE SIDED VENTILATION

by Van der Maas et al

ERRATA

page 11 eq. (5)	drop factor 2 in
page 12 line 3:	$0.02m^3/s$ (not 0.04)
page 12 line 5:	0.7 ACH (not 1.4)
page 12 eq. (7):	multiply by $\sqrt{(2\rho)}$, (not divide by $\sqrt{\rho}$)
page 17 §4.2.1, line 6	"..expected to be about 1.5ACH"
page 17 5th line from bottom	"..is contributing 1.5[1/h] which is significant"
page 17 bottom	drop last two sentences

§5. Conclusions

Single sided ventilation experiments have been conducted in the frame work of the Annex 20, and allowed fruitful cooperation between four laboratories in four countries. Experiments have been coordinated, data and types of analysis have been critically discussed. This paper is an overview of the obtained results that will be published in an Annex 20 report [16].

It has been shown in separate experiments that

(i) the contribution of air compressibility to the single sided ventilation rate can be considerable in particular for relatively small openings to large volumes.

(ii) a systematic variation of the pressure coefficient over the opening has been observed and appears to vary with wind direction; the resulting two-way flow significantly contributes to the airchange rate under conditions of single sided ventilation

(iii) the ventilation rate of the attic in Gent (long term observation under varying conditions of wind speed and direction) is well described by a simple model with a single free parameter.

(iv) ventilation heat loss rates after opening a window are described by a simple model allowing a better estimate of the energy consequences of inhabitant behaviour

(v) an effect of steady wind on the airflow in a single large opening can be measured.

The validation process of more detailed single sided ventilation models has only started. One difficulty in future research will be the simultaneous presence of pressure fluctuations, two way flow and stack effect. To reduce the complexity, one should learn to know the relative importance of each ventilation mechanism under various circumstances.

On the other hand the uncertainty in predicting ventilation is in many cases dominated by a lack of knowledge of the local wind. New research on the transfer of meteo data to local wind values is therefore mandatory if we want to make use of the more detailed models developed for single sided ventilation.

[16] Van der Maas J., Allard F., Haghighat F., Pelletret R., Riberon J., Vandaele L. and Walker R. , "Airflow through large openings in buildings", a Technical Report of subtask 2 of the Annex 20: Optimization of air flow patterns within buildings. To be published: autumn 1991.

AIR MOVEMENT & VENTILATION CONTROL WITHIN BUILDINGS

12th AIVC Conference, Ottawa, Canada
24-27 September, 1991

PAPER 5

MODELLING OF LARGE OPENINGS

Authors : Dr. Roger Pelletret
CSTB (Centre Scientifique et Technique du Bâtiment)
Sophia Antipolis, France

Dr. Francis Allard
INSA (Institut National des Sciences Appliquées)
Lyon, France

Dr. Fariborz Haghighat
Center for Building Studies
Concordia University
Montréal, Canada

Dr. Georges Liebecq
Laboratoire de Thermodynamique
University of Liège
Liège, Belgium

Dr. Jacobus van der Maas
LESO-PB (Lab. d'Energie SOlaire et de Physique du Bâtiment)
EPFL (Ecole Polytechnique Fédérale de Lausanne)
Lausanne, Switzerland

SYNOPSIS.

The subtask 2 of Annex XX (Optimization of Air Flow Patterns Within Buildings) involved a research project called "Air Flows Through Large Openings In Buildings". The scope of this project was to test the range of validity of available algorithms, and where possible to develop new ones. This paper focuses on the new interzonal airflow studies which have been carried out in this frame. The research was based on three test rooms (respectively at the University of Liège, at INSA Lyon and at CSTB Sophia Antipolis) and mainly focused on natural convection ; the aim was to improve the knowledge and the numerical prediction of heat and mass transfer through doorways. This goal was achieved through a joint research effort which was based on the comparison of our experimental results. Moreover, these experimental results have been used to validate a C.F.D (Computational Fluid Dynamics) model developed at Concordia University.

The main result consists of validated models to compute the mass flows in large openings assuming either isothermal air volumes or linear temperature profiles in both rooms ; the discharge coefficient that has been found is about 0.43. Local discharge coefficients have also been determined but this topic needs more studies ; C.F.D models, as those developed at Concordia University, seem well adapted to fulfill this task as long as they are validated.

LIST OF SYMBOLS.

$\dot{m}_h$	Mass flow in the upper part of the opening	(kg/s)
$\dot{m}_c$	Mass flow in the lower part of the opening	(kg/s)
$\dot{m}_{measured}$	Measured mass flow	(kg/s)
$\dot{m}_{computed}$	Computed mass flow	(kg/s)
z_b	Height of the bottom of the opening	(m)
z_n	Height of the neutral plane	(m)
z_t	Height of the top of the opening	(m)
Cd	Discharge coefficient	
W	Width of the opening	(m)
ρ_h	Density of hot air	(kg/m^3)
ρ_c	Density of cold air	(kg/m^3)
ΔP	Pressure difference	(Pa)
g	Acceleration of gravity	(m/s^2)
$V(z)_{measured}$	Measured air velocity	(m/s)
$V(z)_{computed}$	Computed air velocity	(m/s)

1. INTRODUCTION.

Numerous studies have been performed on the subject of "Airflow Through Large Openings" connecting two zones at different temperatures. Literature surveys (Barakat 1985, Sandberg 1989, Vandaele and Wouters 1989) have shown that the developed models, to compute heat and mass transfer through a large opening, generally assume that the flow is one-dimensional and that the interconnected rooms are isothermal ; the only free parameter is the discharge coefficient. The three dimensional nature of the flow and the presence of a vertical temperature gradient are then neglected and the discharge coefficient appears to vary from experiment to experiment (the discharge coefficient reported in the literature varies between 0.3 and 0.8 and it is not clearly understood where the difference comes from).

The scope of subtask 2.1 of Annex XX was to test the range of validity of available algorithms, and where possible to develop new ones. This subtask was coordinated by Dr. van der Maas from LESO-EPFL, Lausanne, Switzerland ; it involves three laboratories in Europe with each a different experimental set-up : the "MINIBât" test cell at INSA Lyon, France, a climatic test cell at University of Liège, Belgium, and the DESYS test cell at CSTB Sophia Antipolis, France. It involves also a laboratory from the Concordia University, Montréal, Canada, which has developed a C.F.D code and wanted to try to validate it by comparison with experimental results.

This paper focuses on the new interzonal airflow studies which have been carried out in this frame. The research was based on the three test rooms above-mentioned and mainly focused on natural convection ; the aim was to improve the knowledge and the numerical prediction of heat and mass transfer through doorways. This goal was achieved through a joint research effort which was based on the comparison and the analysis of the experimental results.

In this paper, we present first the various laboratory set-ups (§ 2), then the typical experimental rough results (measured velocities profiles in the doorways) (§ 3). The experimental results are analyzed in order to validate models based on Bernoulli's equation ; two models have mainly been validated : a model based on the assumption of isothermal air volumes and a model based on the assumption of linear temperature profiles in both rooms (§ 4). An example of the comparison between the Concordia University's C.F.D model with some of our experimental results is detailed in § 5.

2. EXPERIMENTAL SET-UPS.

The three set-ups are described below (see figure 1) ; their main common characteristic is to be real scale experiments. The test rooms at University of Liège and at INSA Lyon are climatic test rooms ; the CSTB's set-up is in natural environment.

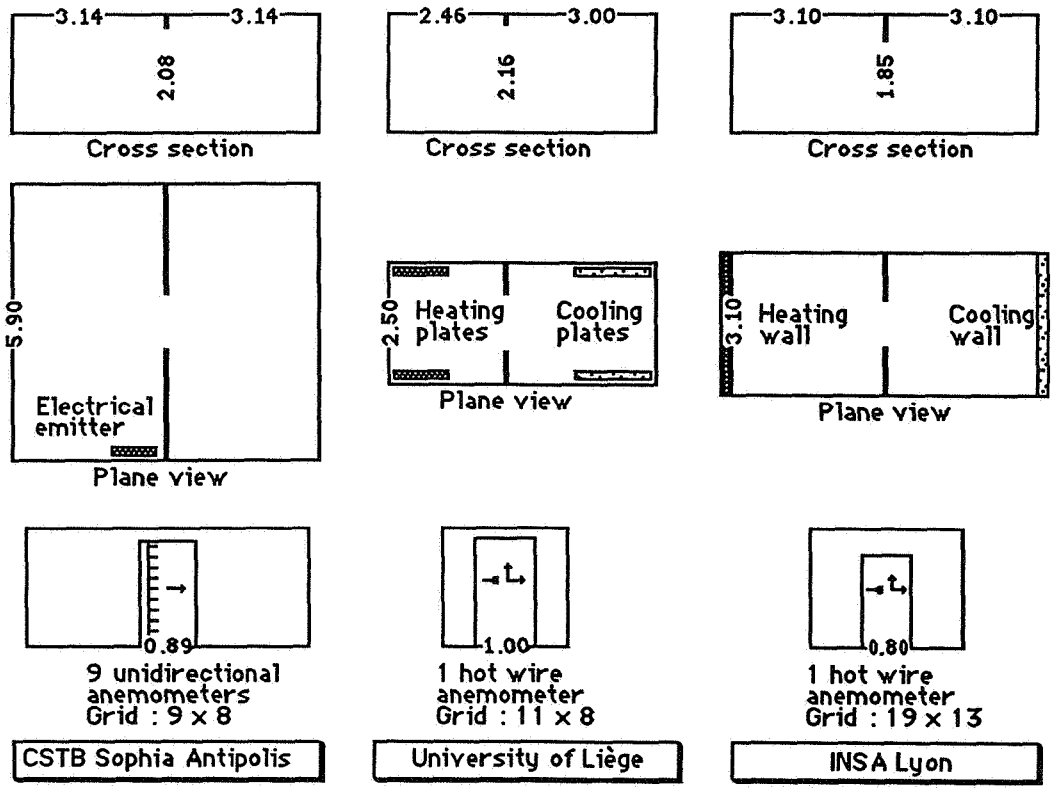

Fig. 1 : The three laboratory set-ups.

The CSTB's test cell is called the DESYS test cell ; the DESYS test cell is a 86 m^2 house built with industrial envelop components and of which the detailed thermal characteristics have been carefully measured (Pelletret 1987). The test cell area is partitioned in three main zones ; the partitions between the zones are very well insulated ; one of these zones is divided into two symmetric rooms connected with a large opening.

The experimental studies, carried out at University of Liege, started with a set of experiments in a calorimetric chamber (Lebrun and Liebecq 1987) ; then a new set of experiments has been performed to better understand the influence of the width of the door on the heat and mass transfer (Baranowsky 1989). The calorimetric chamber is bounded by a double envelope through which the air temperature is controlled. In the hot zone, heating films were mounted to raise the air temperature as well as cooling plates were placed in the cold zone to cool it.

The basis of the experimental facility at INSA Lyon is the MINIBât test cell (Allard 1987) built in a controlled environment (each of the two zone is bounded on five sides by air volumes controlled at a constant temperature, the sixth side is submitted to controlled climatic conditions ; a solar simulator and electrical heating films located along the surfaces on the internal side of the walls of the two rooms complete the set-up and enable to generate a wide range of boundary conditions.

3. VELOCITY PROFILES.

In the CSTB's test cell, about hundred experiments with various heights and positions of the opening have been performed. Some experiments have been made with none of the rooms heated or one heated with an electrical emitter but not the other one or both heated or one heated and the other one cooled with a cooling air system ; but, in general, the experiments were performed with only one room heated as shown in figure 1 ; twenty experiments of this kind have been made with an opening's height of 2.08 m and fifteen experiments with an opening's height of 1.56 m. Figure 2 shows an example of a velocity profile measured with these typical experimental conditions (one room heated but not the other one) and an opening's height of 2.08 m.

In the test cell of the University of Liège, five experiments with an opening's height of 2.16 m have been performed. These experiments aimed to approximate the experimental conditions to fit as well as possible with the hypothesis of the mathematical model (which is based on Bernoulli's equation) : with symmetrical heating and cooling plates, located as shown in figure 1, it was possible to minimize the effect of air movements in the rooms due to the thermal devices. The five measured profiles are very similar and the profile shown in figure 2 is really a typical one.

In the INSA's test cell five experiments with an opening's height of 1.85 m have been performed including two experiments with a cooling wall and a heating wall, two experiments with a single cold active surface and one experiment with a single hot active surface. With two active walls, the neutral plane is close to the mid height of the opening ; this fits very well with the symmetric boundary conditions.The other profile shown on figure 2 was measured when only the cooling wall was active ; this boundary condition leads to a different airflow pattern within the cooled room and the displacement of the neutral plane (which, in this case, is below the mid height of the opening) is only the result of this fact.

Our goal is to facilitate the comparison between the typical velocity profiles measured in the three test cells. To reach this goal, the velocity profiles are plotted in the same way : the velocity profiles are plotted as a function of the ration z/H where H is the opening's height ; then, for all the experiments, the ration z/H varies between 0 and 1 (see figure 2). The velocity profiles are specific for each experimental set-up ; the various heating or cooling devices explain why the shapes are different :

- in the CSTB's experiments, the neutral plane is approximately located at the two thirds of the opening's height ; this is because the electrical emitter creates a specific air movement in the heated room and then a typical vertical temperature profile with a 2 K/m gradient ;

- in the Liège's experiments, the neutral plane is sightly above the mid height of the opening ; this results fits well with the INSA's experiments when the opposite walls are active ;

- in the INSA's experiments with only the cooling wall active the velocity profile is asymmetric and the neutral plane is below the mid height of the opening ; this result is symmetrical of the one of CSTB's experiments and strengthens previous experiments performed in the Liège's test cell with non symmetrical devices : the cooling plates were close to the opening and faced it, then the neutral plane was greatly below the mid height of the opening.

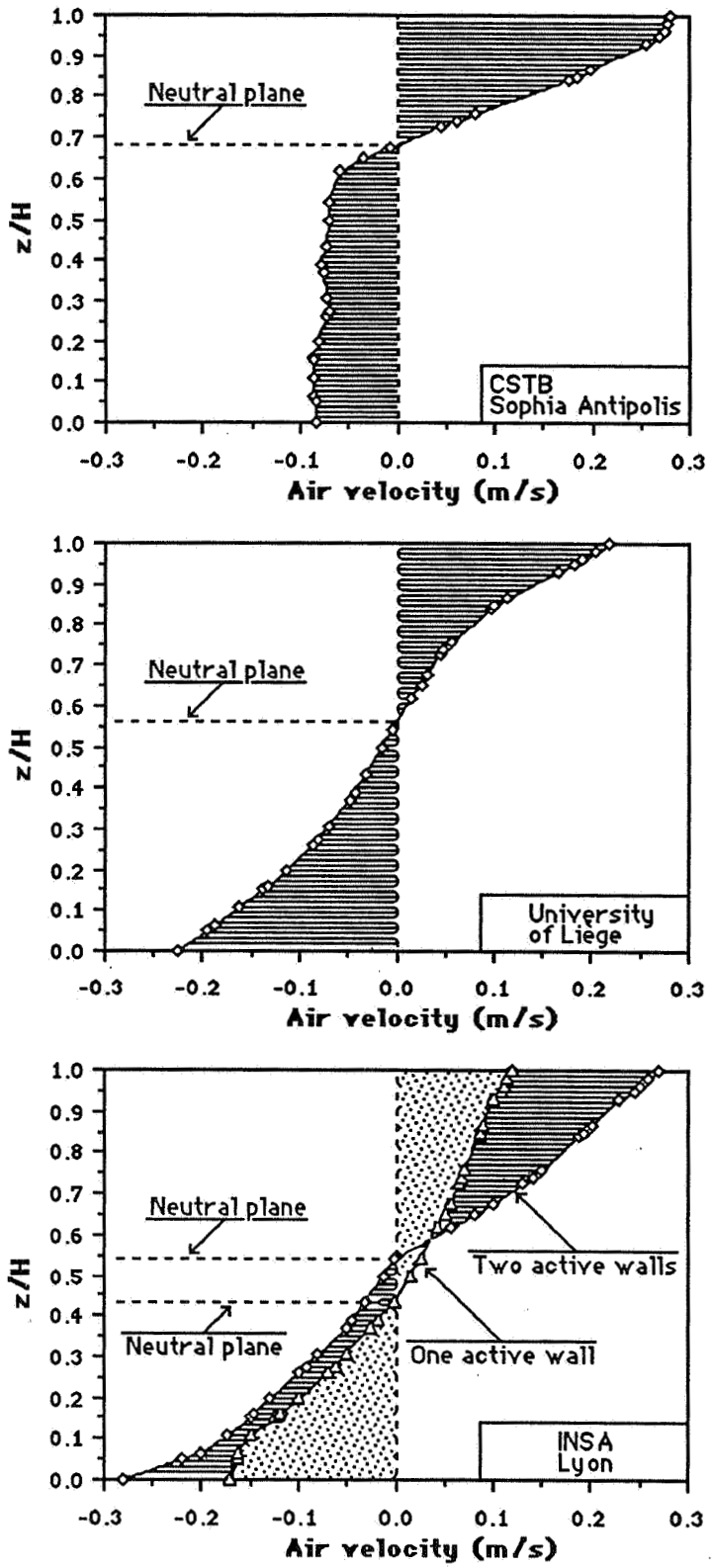

Fig. 2 : Typical velocity profiles (the plot symbols do not indicate the points where the velocities were measured but only the points were the experimental results have been interpolated in order to plot them in the same way).

4. MASS TRANSFER MODELLING.

Both CSTB and INSA calculated the experimental mass flows by integration of the measured velocity profiles. University of Liège calculated the experimental mass flows both integrating the measured velocity profiles and computing it from the heat balance of the test rooms but concluded that to compute them with a heat balance was more accurate in their case.

4.1. Assumption of isothermal air volumes.

With this assumption of isothermal, the theoretical mass flows are computed as :

$$\dot{m}_h = Cd\ (2/3)\ W\ (2\ \rho_h)^{0.5}\ \Delta P(z_t)^{3/2}\ /\ [g\ (\rho_c - \rho_h)] \qquad \text{(Eq. 1)}$$

$$\dot{m}_c = Cd\ (2/3)\ W\ (2\ \rho_b)^{0.5}\ \Delta P(z_b)^{3/2}\ /\ [g\ (\rho_c - \rho_h)] \qquad \text{(Eq. 2)}$$

In natural convection, $\dot{m}_h = \dot{m}_c$. Equations 1 and 2 are equivalent to equations 3 and 4 when replacing the pressure differences by their expressions as a function of the differences between the heights at the top and at the bottom of the opening and the neutral plane :

$$\dot{m}_h = Cd\ (2/3)\ W\ [2\ \rho_h\ g\ (\rho_c - \rho_h)]^{0.5}\ (z_t - z_n)^{3/2} \qquad \text{(Eq. 3)}$$

$$\dot{m}_c = Cd\ (2/3)\ W\ [2\ \rho_b\ g\ (\rho_c - \rho_h)]^{0.5}\ (z_n - z_b)^{3/2} \qquad \text{(Eq. 4)}$$

$$\text{with :}\quad z_n = [\rho_h^{1/3}\ z_t + \rho_c^{1/3}\ z_b]\ /\ [\rho_h^{1/3} + \rho_c^{1/3}] \qquad \text{(Eq. 5)}$$

The Cd coefficient is computed with : $Cd = \dot{m}_{measured} / \dot{m}_{computed}$

To compare our results, the Cd coefficients are plotted versus the difference between the rooms average temperatures but for the INSA's experiments for which it is computed as the difference between the two central air temperatures measured in each room (see Figure 3).

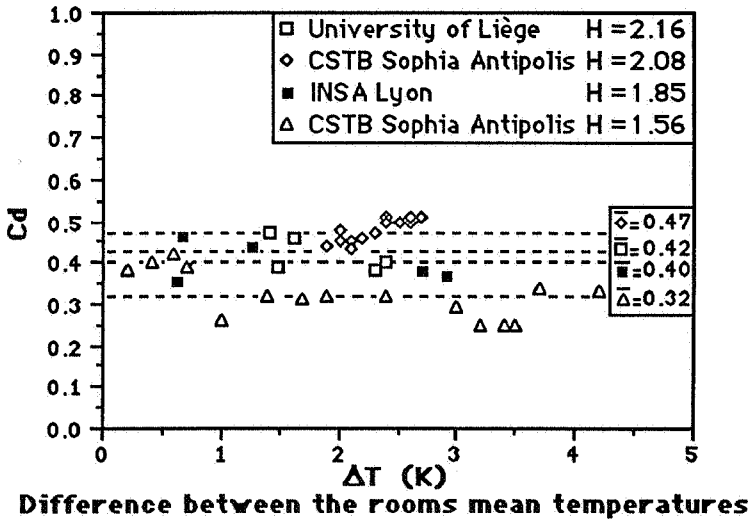

Fig. 3 : Discharge coefficients with an assumption of isothermal air volumes.

As shown on figure 3, the results obtained from the three experiments fit quite well :

- the discharge coefficient decreases with the opening's height
- the Cd mean value computed from the CSTB's experiments is slightly higher than the Cd mean value computed from the Liège's experiments though the openings' heights are similar (2.08 m and 2.16 m) ; of course this can be explained because of problems of uncertainty in the measurements but, presumably, this is also because, in the CSTB's set-up, the air movement in the heated zone (due to the electrical emitter) influences the air movement in the opening. And this assertion is strengthened by the INSA's results : for the asymmetric experiments (with only a cooled wall), the Cd coefficient is about 0.45 (close to the mean value of the CSTB's experiments), this value is 20% higher than the Cd mean value computed with symmetric boundary conditions.

4.2. Assumption of linear temperature profiles.

Similar computations to determine Cd values have been made assuming that the temperature profiles in each room were linear. The new Cd values are very close to the Cd values computed with an assumption of isothermal air volumes for the computation of the theoretical mass flows with an assumption of linear temperature profiles give quite the same results than with an assumption of isothermal air volumes. When there are differences they can be explained because, with a linear approximation of the real temperature profile, the mean value of the temperature can be different from the mean value directly computed from the rough results.

4.3. Local discharge coefficients.

Taking into account the measured temperature profiles in each room and using a model based on Bernoulli's equation, it is possible to compute a theoretical velocity profile in the opening and to compare it to the measured velocity profile ; then one can define local discharge coefficients as : $Cd(z) = V(z)_{measured} / V(z)_{computed}$.

Figure 4 shows the typical Cd(z) profiles found with the INSA's experiments and with the CSTB's experiments ; each profile depends on the boundary conditions. On these figures, we plotted only three Cd(z) profiles for the CSTB's experiments but the seventeen others are very similar to these threes. For the INSA's experiments, one profile is obtained in a symmetric case (two active walls), for the other comparable experiment which has been made at INSA the Cd(z) profile is very close to the one displayed on figure 4 ; in this case, it is very interesting to note how much the Cd(z) profile is symmetric. The other plotted Cd(z) profile is for a single cold active wall, the Cd(z) computed for the two other experiments made with only one active wall are quite different from the example plotted on figure 4 ; in this case, the discrepancy is greater than with the symmetrical cases or with the CSTB's cases.

Nevertheless, these specific studies have demonstrated that it was possible to define Cd(z) profiles, adapted to a specific configuration, and then the models using these Cd(z) profiles enable an accurate calculation of the mass flows and the velocity profiles (including, of course, the height of the neutral plane).

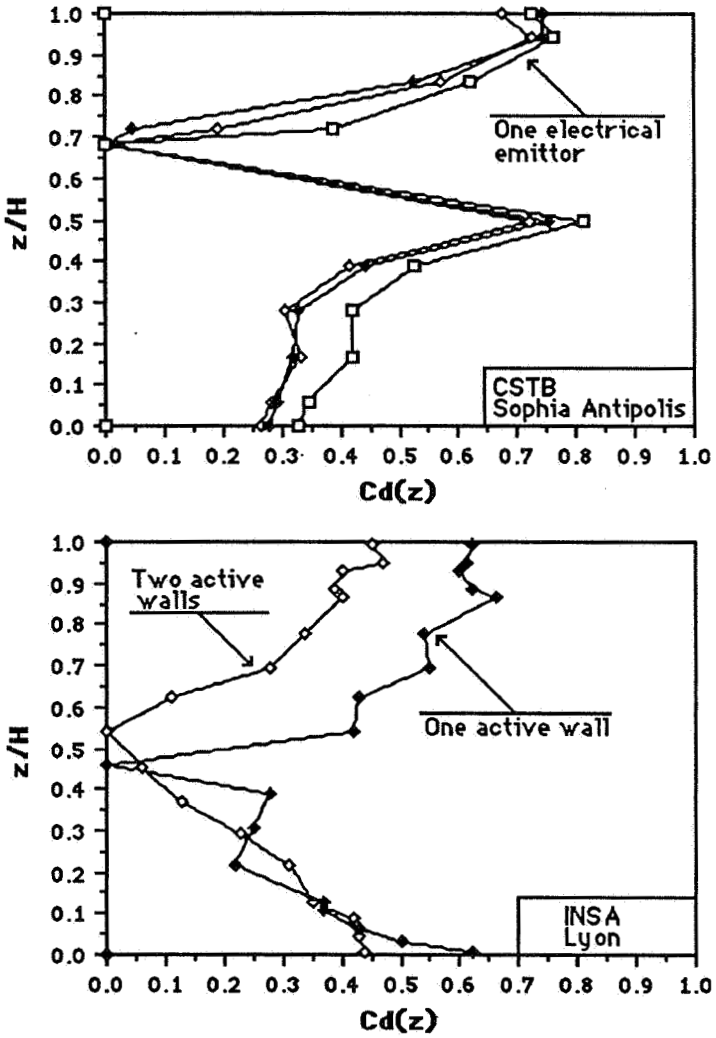

Fig. 4 : Local discharge coefficients.

5. COMPARISON WITH A COMPUTATIONAL FLUID DYNAMICS CODE.

5.1. Brief description of "Concordia" code.

This code employs a finite-difference method and the K-ε two-equation model of turbulence to obtain the approximate solution of governing equations for the three-dimensional turbulent flow in rectangular enclosures. At the region near a solid surface, where the viscosity effects become important, the wall function method is adopted to modify the K-ε two-equation model.

More details are given in the final report of Annex XX and in "Haghighat 1989".

5.2. Validation.

Some comparisons with experimental results from Liège or from INSA have been made. As an example of these comparisons, the measured and the computed velocity profiles are plotted in figure 5 :

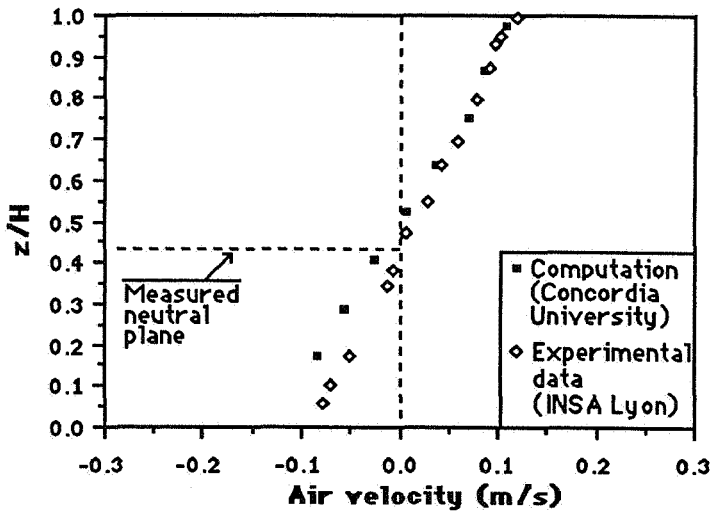

Fig. 5 : Velocity distribution at the center of door opening in comparison with measurements.

Discrepancy is observed in the low region of the door opening. This can be explained because, in this experiment, there was a 0.08 m step on the floor of the door opening and this step is neglected in the computation with the "Concordia" code because it is too small to be considered in a uniform mesh system adopted. In the east part of the door opening, the predicted velocity distribution is in very good agreement with experimental data.

6. CONCLUSIONS.

The joint research effort led to validate models based on the Bernoulli's equation assuming either isothermal air volumes or linear temperature profiles. The discharge coefficients in both case are quite similar ; Cd varies from 0.37 in case of pure natural convection to 0.51 if a (cold or hot) plume exists. An average value of 0.45 seems adequate to correctly model a large variety of configurations such as non heated rooms, or one room heated not the other one or both heated and for an opening's height higher than 2 m. The discharge coefficient decreases with the opening's height ; a very simple relation as Cd = 0.21 H fits well our experimental results in the range $H \in [1.5\ m ; 2\ m]$.

The vertical Cd distribution seems to be strongly related with the boundary conditions. Further studies are necessary to define average Cd distribution corresponding to typical boundary conditions or real flow patterns observed in buildings in case of heating or air conditioning.

More experiments are obviously necessary although experiments are expensive, heavy to carry out , time consuming and , furthermore, in most cases, it is hard to change significantly the design parameters of the experimental set-ups ; that is why airflow modelling using computational fluid dynamics could be useful as long as the code is validated ; we have began to make progress in that direction trying to validate the "Concordia" code ; this task is not yet achieved but this is a promising way for general parametric studies.

REFERENCES

1. ALLARD F. and al.
Thermal experiments of full scale dwellings in artificial conditions.
Energy and Builidings, v.10, pp.49-58, 1987

2. BARAKAT S.A.
Inter-zone convective heat transfer in buildings : a review.
Heat transfer in building and structures - HTD Vol.41, 45-52
ASME-AICHE Conference.
Denver, Colorado, USA, August 1985

3. BARANOWSKY and al.
Experimental studies of convective heat exchange between zones.
Thermodynamics laboratory. Research report for CSTC.
University of Liège. Belgium, October 1989.

4. HAGHIGHAT F. and al.
Natural convection and air flow pattern in a partitioned room with turbulent flow.
ASHRAE Transactions, vol 95, part. 2, pp. 600-610, 1989.

5. LEBRUN J. & LIEBECQ G.
Experimental studies of convective heat exchange between zones.
Thermodynamics laboratory. Research report.
University of Liège. Belgium, 1987.

6. PELLETRET R.
Interzonal heat transfer in builidings.
Research report for AFME.
CSTB DPE/87-500, August 1987.

7. SANDBERG M.
Flow through large internal openings.
IEA, Annex XX, Subtask 2 draft report, 3rd Expert Meeting.
Aalborg, Denmark, May 30 - June 2, 1989

8. VANDAELE L. and WOUTERS P.
Airflow through large openings. An overview of existing approaches.
IEA, Annex XX, Subtask 2 report, 3rd Expert Meeting.
Aalborg, Denmark, May 30 - June 2, 1989

AIR MOVEMENT & VENTILATION CONTROL WITHIN BUILDINGS

12th AIVC Conference, Ottawa, Canada
24-27 September, 1991

PAPER 6

WIND INDUCED FLUCTUATING AIRFLOW IN BUILDINGS

JIWU RAO AND FARIBORZ HAGHIGHAT

CENTRE FOR BUILDING STUDIES
CONCORDIA UNIVERSITY
MONTREAL QUEBEC CANADA

ABSTRACT

Airflow through a building has both mean and fluctuating components due to spatial and temporal variations in wind-induced pressures. Most of the existing investigations consider the average values of wind pressures and predict steady-state solutions for airflow [1]. This paper presents some experimental results for the validation of a proposed fluctuating airflow model [2]. The new model employs spectral analysis and statistical linearization methods to model the pulsating airflow through buildings. Frequency information of wind pressures, spectral and co-spectra, in addition to mean values are used as inputs. The model calculates the frequency characteristics of resultant airflow and estimates the effects of fluctuations on total air exchanges. The fluctuating wind pressures and airflow are simulated in a laboratory experimental setup. The action of varying wind pressure is simulated by a controllable fan-damper unit. The experimentally estimated transfer functions and RMS values of airflow are compared with theoretical ones, good agreements are obtained.

LIST OF SYMBOLS

P^w, P^i, Q, ΔP: total wind-induced pressures, internal pressure, airflow through openings, and pressure differences across openings,

$\bar{P}^w$, $\bar{P}^i$, $\bar{Q}$, $\Delta\bar{P}$: steady-state components of above variables,

p^w, p^i, q, Δp: corresponding fluctuating components,

$P^w(\omega), P^i(\omega), Q(\omega), \Delta P(\omega)$: Fourier transforms,

$S_{p^w}(\omega), S_{p^i}(\omega), S_q(\omega), S^{(c)}_{p_1^w p_2^w}(\omega)$: spectra and co-spectrum,

K_1, K_2, n_1, n_2: flow coefficients and exponents,

A_1, A_2, L_1, L_2: opening cross areas and depths.

1. INTRODUCTION

Wind-induced pressures on building envelopes have both spatial and temporal variations due to the gustiness of the incoming wind and the interaction between wind and buildings. Existing research focuses on calculating the steady-state airflow due to average spatial variations of wind pressures, while increased interests have been drawn on the study of fluctuations in airflow through buildings due to temporal variations in wind pressures.

The fluctuating airflow through openings can be divided into two categories: eddy flow and pulsating flow. The eddy flow represents the

additional air exchange through an opening due to the penetration of eddies. The pulsating flow is the result of bulk flow caused by fluctuations in the pressure difference across the opening.

A method was proposed to use a spectral analysis method to calculate the pulsating airflow due to temporal and spatial variations of wind-induced pressures [2]. The fluctuating airflow is influenced both by the building characteristics, the resistance of the openings to flow, the inertia of the air mass in the openings and the compressibility of the room air, and by the frequency characteristics of wind pressures, their power spectra and the correlations among them. In this method, the mean and fluctuating airflows are calculated separately, and then are combined to predict the total airflow. This paper presents experimental validation results.

2. EXPERIMENTAL SETUP

The actions of varying wind pressures on a building and the resultant fluctuating airflow are simulated in an experimental setup. The setup includes the chamber, damper, tracer gas unit, sensors, and data acquisition system (Fig. 1).

The chamber has dimensions of 7.5'X15.5'X7.7' and a volume of 900 ft^3 (25 m^3). It is built of two 3/4" plywood boards and filled with vertical wood stud frames and fibre glass insulation. Two laminated doors and two small single-glazing peep-windows are located on the same facade of the chamber. The cracks are sealed with caulking compound from inside. A purpose-provided opening is placed through the chamber wall and is filled with straws. Parameters of flow equations for the opening and the chamber porosity are measured by fan pressurization tests. When the opening is sealed, the chamber has approximately 1/20 ach (air changes per hour) in 50 Pascal pressurization tests.

The fluctuating wind-induced pressure is simulated by the damper unit. It consists of a proportional controller, a servo motor and a rotary position sensor, a damper, a venturi tube and a flow meter, blower fans and some ϕ3" plastic tubes. This unit is connected to the opening on the outside end. The analog output signal of the data acquisition system to the controller turns the damper to a designated angle, so that only a certain amount of airflow is allowed to pass and a required pressure level is generated at the opening.

The tracer gas set consists of tracer gas cylinders, injection mass flow controller, sampling tubes and pumps, and a GC analyzer. SF_6 is used as the tracer gas. The gas chromatograph analyzer is programmed, with the assistance of a digital relay switch, to sample at 20 second intervals. Calibrations have

been carried out, and the relationship between GC reading and the SF_6 concentration derived. A 12 channel sampler, with auto switching capability, pumps sampling air to the GC analyzer.

Pressures are measured with digital micromanometers with build-in auto-zero facility. Pressure taps are placed near two ends of the opening and inside the chamber.

The data collection and damper control are performed by a data acquisition system. The system has a capability of measuring up to 96 thermalcouple input channels, 16 range-adjustable analog input channels with 12 bit accuracy, 16 digital 1-bit input channels, and providing four 0-10V analog output channels of 12 bit accuracy. The system has built-in programmable timers and software/hardware interrupts, and run BASIC-like programs.

3. THEORETICAL CALCULATIONS

The chamber is modelled as a single-zone building with two openings. Opening 1 is the purpose-provided opening, and opening 2 represents the total porosity of the chamber envelope. In the steady-state calculation, the mass balance for this building is governed by:

$$K_1\left(\bar{P}_1^w - \bar{P}^i\right)^{n_1} + K_2\left(\bar{P}_2^w - \bar{P}^i\right)^{n_2} = 0 \tag{1}$$

For the analysis of fluctuating components in the pressures and airflows, the pressure/force balances for both openings result in two nonlinear governing equations:

$$\frac{\rho L_i}{A_i}\frac{dq_i}{dt} + \left(\frac{1}{K_i}\right)^{\frac{1}{n_i}}\left[\left(\bar{Q}_i + q_i\right)^{\frac{1}{n_i}} - \left(\bar{Q}_i\right)^{\frac{1}{n_i}}\right] = p_i^w - \frac{\gamma P_a}{V}\int_0^t (q_1 + q_2)dt, \tag{2}$$

where i=1, 2, same for the following equations.

The nonlinear terms in the above equations are approximated to linear relations through a statistical linearization method [3] as:

$$f_i = \left(\frac{1}{K_i}\right)^{\frac{1}{n_i}}\left[\left(\bar{Q}_i + q_i\right)^{\frac{1}{n_i}} - \left(\bar{Q}_i\right)^{\frac{1}{n_i}}\right] \sim \lambda_i q_i \tag{3}$$

Therefore, a set of linear governing equations can be obtained:

$$M_i \frac{dq_i}{dt} + \lambda_i q_i - p_i^w - B \int_0^t (q_1 + q_2) dt \tag{4}$$

where $B = \gamma P_d / V$ and $M_i = \rho L_i / A_i$. The coefficients of λ_i have values such that the variances of f_i and $\lambda_i q_i$ in both sets of equations (2 & 4) are the same. Assuming normal distributions for airflow rates q_i, the λ_i values can be expressed as:

$$\lambda_i = \frac{1}{\sigma_{q_i}} \int_{-\infty}^{\infty} \left\{ \left(\frac{1}{K_i} \right)^{\frac{1}{n_i}} \left[\left(\bar{Q}_i + q_i \right)^{\frac{1}{n_i}} - \left(\bar{Q}_i \right)^{\frac{1}{n_i}} \right] \right\}^2 \frac{e^{-\frac{q_i^2}{2\sigma_{q_i}}}}{\sqrt{2\pi}\,\sigma_{q_i}} dq_i \tag{5}$$

The linear equations (4) are Fourier transformed into the frequency domain, and converted in matrix form as:

$$\begin{bmatrix} K_1\lambda_1 + j\omega M_1 + \dfrac{B}{j\omega} & \dfrac{B}{j\omega} \\ \dfrac{B}{j\omega} & K_2\lambda_2 + j\omega M_2 + \dfrac{B}{j\omega} \end{bmatrix} \begin{bmatrix} Q_1(\omega) \\ Q_2(\omega) \end{bmatrix} = \begin{bmatrix} P_1^w(\omega) \\ P_2^w(\omega) \end{bmatrix} \tag{6}$$

The transfer function matrix can be obtained as:

$$H(\omega) = \begin{bmatrix} H_{11}(\omega) & H_{12}(\omega) \\ H_{21}(\omega) & H_{22}(\omega) \end{bmatrix} = \begin{bmatrix} K_1\lambda_1 + j\omega M_1 + \dfrac{B}{j\omega} & \dfrac{B}{j\omega} \\ \dfrac{B}{j\omega} & K_2\lambda_2 + j\omega M_2 + \dfrac{B}{j\omega} \end{bmatrix}^{-1} \tag{7}$$

When the spectra of wind pressures and the co-spectrum between them are known, the spectra for the fluctuating airflows can be expressed as:

$$S_{q_i}(\omega) = |H_{i1}(\omega)|^2 S_{p_1^w}(\omega) + |H_{i2}(\omega)|^2 S_{p_2^w}(\omega) - 2|H_{i1}(\omega)||H_{i2}(\omega)| S^{(c)}_{p_1^w p_2^w} \tag{8}$$

The RMS values of the fluctuating airflow are obtained through integration of corresponding spectra over frequency, i.e.:

$$\sigma_{q_i}^2 = \int_0^{\infty} S_{q_i}(\omega)\, d\omega \tag{9}$$

Equations (5 & 9) show that λ_i and σ_{q_i} are functions of each other. Iterative procedures are employed to adjust λ_i and σ_{q_i} gradually, until both equations hold for one set of λ_i and σ_{q_i}.

The procedure for the theoretical calculation is as follows: first, the steady-state solution for the given building situation is obtained, and the initial set of σ_{q_i} is assumed; second, λ_i values are calculated for the current σ_{q_i} values; third, the transfer functions are calculated, spectra and RMS values are obtained; finally, the new σ_{q_i} are compared with the old values, and repeated from the second step if necessary.

4. EXPERIMENTAL PROCEDURE AND COMPARISON OF RESULTS

The experiment is conducted in the following manner: (1) A measured amount of tracer gas SF_6 is injected into the chamber and mixed for 10 minutes with a mixing fan. (2) During the mixing, a pressurization test is performed. The damper angle is increased or decreased step by step with a time lag between two steps to allow the flow to reach steady-state condition. The pressures and flow rate are monitored and data is used to calculate the flow relations of the opening and chamber porosity. This test is repeated several times during the experiment. (3) A program that generates a temporal fluctuating signal to the damper is executed, and data is collected at 5 Hz for about 45 minutes. (4) The damper is set at a constant angle to conduct a steady-flow decay test for around 30 minutes.

The fluctuating airflow data comes from step (3) of the test. The damper control signal is generated according to a certain spectrum. The collected data of external pressure, internal pressure, airflow rate and the control signal varys with time (Fig. 2). In the analysis, the data are examined in pairs of two such as external pressure ($p^w{}_1$) and airflow (q_1), external pressure and internal pressure (p^i), and, external pressure and pressure difference (Δp_1). The emphasis of validation is to compare the relationship within these pairs in the frequency domain.

For the external pressure ($p^w{}_1$) and airflow (q_1) pair, the spectra and transfer function are estimated using a smoothed Fourier transform spectral estimator with a sample length of 1024 data points and Hanning windows. The magnitude of the transfer function (Fig. 3c) shows a peak between 0.1 to 1 Hz, which is due to the inertia of air in the opening and the compressibility of room air. The fluctuating airflow model is implemented, on a case bases, in MATLAB [4] programs. In the theoretical calculation, the estimated external pressure spectrum, as well as the building characteristics and measured flow relations, are used as input. The calculation converges in four iterations to a precision of 10^{-7} when the experimental RMS values are used for initialization. The transfer function between $p^w{}_1$ and q_1 corresponds to $H_{11}(\omega)$ in the equation (7). If the calculated transfer function confirms with the measured one, the theoretical model will correctly predict the resultant airflow.

In Fig. 3c, the theoretical transfer function magnitude is plotted against the experimental results. It agrees well with the measured one for frequencies less than 0.3 Hz. At higher frequencies (>0.5 Hz), the measured curve shows very low values instead of reaching the peak as the theoretical results. This is probably due to the data quality. The coherence between p^w_1 and q_1 are low at higher frequencies (Fig. 4), thus, the estimated transfer function is inaccurate. A second possible explanation is that the assumption of inertia of air in the theoretical model is invalid for higher frequencies. Nevertheless, the power density of wind pressure is mainly concentrated at the low frequency range away from where the low coherence occurs. The resultant airflow at the high frequency range generally contributed very little to the total value. Therefore, the poor agreement between the experimental and theoretical transfer functions would not cause great inconsistency in the prediction.

The theoretical and experimental phase plots of the transfer function between p^w_1 and q_1 (Fig. 3d) are in good agreement. At low frequencies, the lag between q_1 and p^w_1 is negligible. The q_1 is ahead of p^w_1 in frequency 0.02 to 1.0 Hz due to the inertia of air in the opening. At high frequencies greater than 2 Hz, the inertia makes q_1 lag behind p^w_1.

Above calculations are also performed on the other pairs of data. In Fig. 5, the magnitude and phase plots of both estimated and calculated transfer functions for p^w_1 and p^i ,and, p^w_1 and Δp show very good agreements.

The theoretically calculated mean and RMS (root-mean-square) values of q_1, p_i, and Δp_1 are listed in Table 1. The calculated mean values match those of measured ones well as expected, since experimentally measured flow equations of the opening and porosity of the chamber are used as input. The calculated RMS values of fluctuating components also match within a 7% relative error range with the test results.

Figure 6 shows the results of the tracer gas decay conducted during the test step 3. The fitting result indicates an effective mean air infiltration of 6.5 l/s, or 85% of the mean airflow rate through the opening.

5. Discussions

Experiments are performed to validate a fluctuating airflow model which considers the pulsating airflow due to the temporal variations in wind pressures. The comparison of transfer functions and RMS values between experimental estimations and theoretical calculations show good agreement, especially in the low frequency range (<0.5 Hz). At the high frequency range, discrepancies exist between experimental and theoretical results, but the effect on predictions is minimized.

The theoretical model has not considered eddy flows whose effects on airflow are significant especially for large openings or single-sided ventilation. The argument for the omission is that the eddy flow is a more isolated phenomena, it depends mainly on the local flow field near the openings. A generalized analysis is more difficult than for the pulsating flow. In the experiment, the airflow is limited to pulsating by using straws in the opening.

ACKNOWLEDGEMENTS

Financial support through research grants from the Department of Energy, Mines and Resources of Canada and from the Natural Sciences and Engineering Research Council of Canada is acknowledged with thanks.

REFERENCES

1. F. Haghighat, "Air Infiltration and Indoor Air Quality Models - A Review", *The International J. of Ambient Energy*, Vol. 10, No. 3, pp 115-122.
2. F. Haghighat, J. Rao, and P. Fazio, "The Influence of Turbulent Wind on Air Change Rates - a Modelling Approach", *Building and Environment*, Vol. 26, No.3, pp 95-105, 1991.
3. V. V. Bolotin, *Random Vibration of Elastic Systems*, Translated by I. Shenkman, and H. Leipholz, Martinus Nijhoff Publishers, Boston, 1984.
4. C. Moler, J. Little and S. Bangert, *PRO-MATLAB for VAX/VMS Computers, Version 3.1-VMS*, The MathWorks, Inc., 1987.

Table 1. Experimental and Theoretical Results

	Experimental		Theoretical	
	Mean	RMS	Mean	RMS
Opening	$0.7467\ \Delta p^{0.80} \times 10^{-3}$ m^3/s		input	
Porosity	$0.3264\ \Delta p^{0.80} \times 10^{-3}$ m^3/s		input	
p^w_1 (Pascal)	64.6613	17.7177	input	
p^i (Pascal)	47.0775	12.6139	47.0716	12.3003
Δp_1 (Pascal)	17.5938	6.6735	17.5900	6.4239
q_1 ($\times 10^{-3}$ m^3/s)	7.6763	2.1314	7.6755	2.2732
q_2 ($\times 10^{-3}$ m^3/s)	7.6763	*	7.7655	1.6396
(q_1+q_2) ($\times 10^{-3}$ m^3/s)	*	*	0.0	2.2346
Decay Test	0.9235 ach 6.537×10^{-3} m^3/s		*	

* Not measured or calculated.

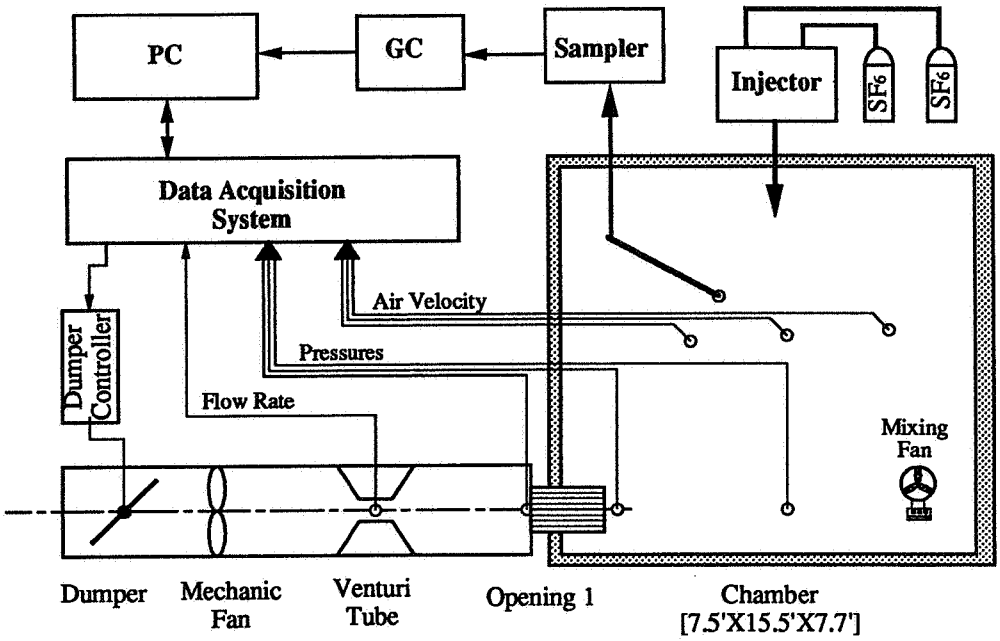

Figure 1. Experimental Setup

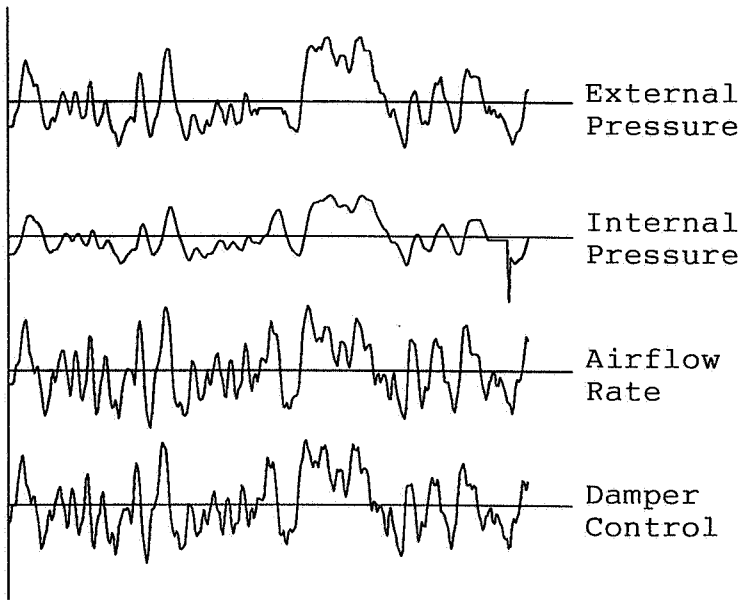

Figure 2. Experimental Data in the First Minute

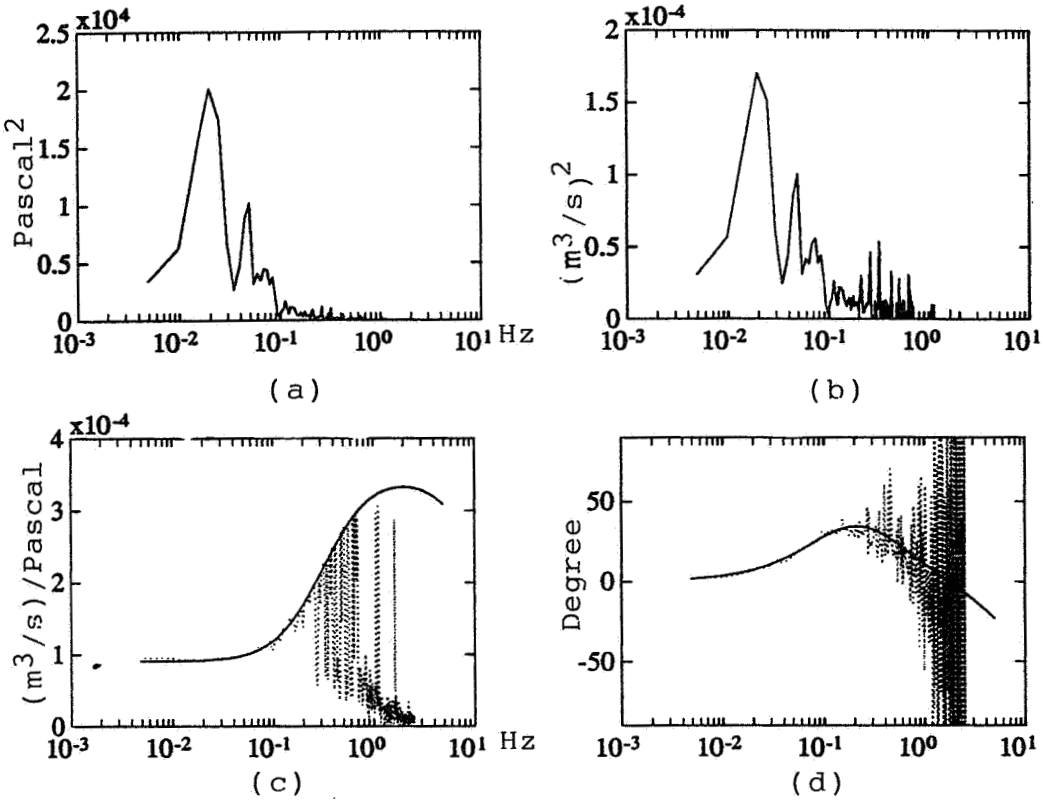

Figure 3. Frequency Results of External Pressure and Airflow: (a) External Pressure Spectrum, (b) Airflow Rate Spectrum, (c) & (d) Transfer Function

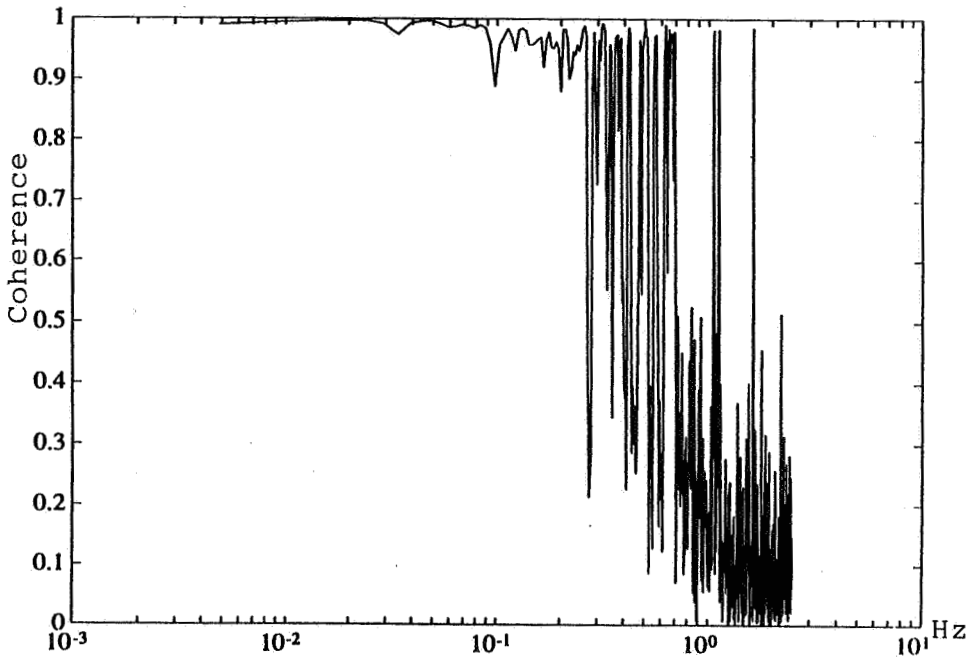

Figure 4. Coherence Between External Pressure and Airflow

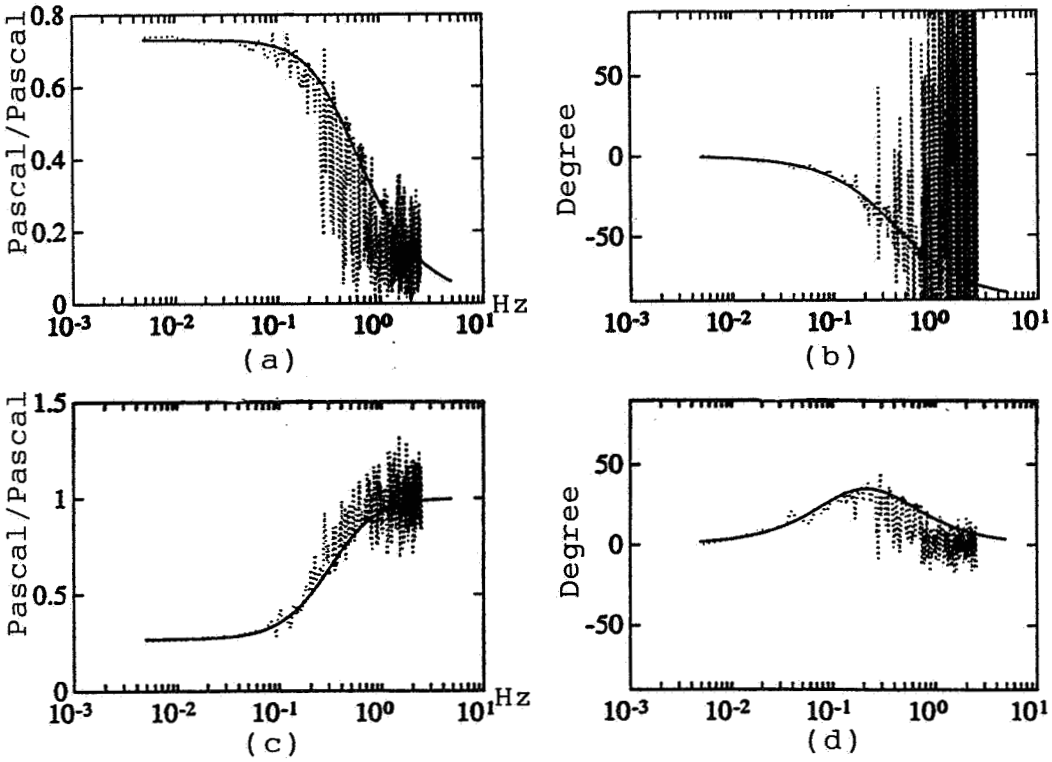

Figure 5. Magnitude and Phase Plots of Transfer Functions:
(a) & (b) External Pressure and Internal Pressure,
(c) & (d) External Pressure and Pressure Difference

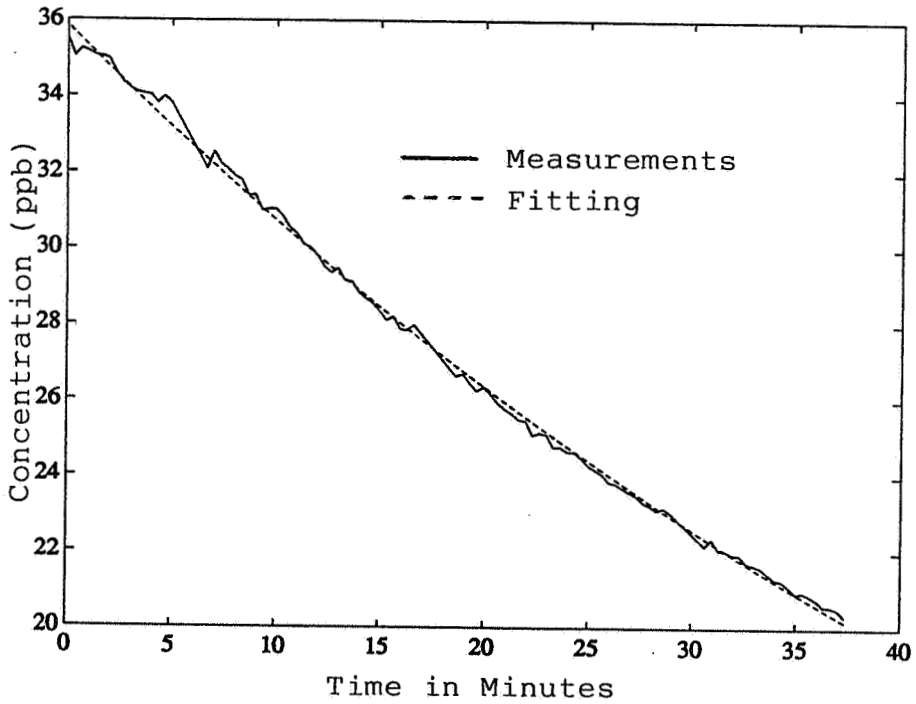

Figure 6. Tracer Gas Decay Test Results

AIR MOVEMENT & VENTILATION CONTROL WITHIN BUILDINGS

12th AIVC Conference, Ottawa, Canada
24-27 September, 1991

PAPER 7

Airflow Driven Contaminants. Transport through Buildings.
ANNEX 20 Subtask 2.5.

J.C. Phaff, W.F. de Gids

TNO Building and Construction Research. Department of Indoor Environment, Building Physics and Systems.
PB 29, NL 2600 AA Delft, Netherland.

AIR MOVEMENT & VENTILATION CONTROL WITHIN BUILDINGS

12th AIVC Conference, Ottawa, Canada
24-27 September, 1991

PAPER 7

Airflow Driven Contaminants. Transport through Buildings.
ANNEX 20 Subtask 2.5.

J.C. Phaff, W.F. de Gids

TNO Building and Construction Research. Department of Indoor Environment, Building Physics and Systems.
PB 29, NL 2600 AA Delft, Netherland.

Synopsis

Air is the main transport medium for contaminants in buildings. Minimizing source strengths has first priority, second is to control air flow rates, supply and exhaust, and directions between zones in buildings.
Computer simulation models for ventilation and pollutant spread in buildings have been proven to give useful predictions. Large measurement campaigns for optimizing ventilation and pollutant problems are complex and expensive. They are often jammed by too many vague parameters influencing the result. The computer models are an alternative and form a supplement to measurements. New ventilation systems or control strategies can be tested to some extent with the models. Measurements for checks and determination of source and sink coefficients for different materials are needed to tune the simulation models.

List of symbols

α	=HCHO emission rate at zero concentration	$\mu g/s/m^2$
β	=reduction coefficient	$\mu g/s/m^2/ppb$
λ	=filter efficiency	-
ρ	=the density of air	kg/m^3
τ	=time constant	s
A	=the deposition surface	m^2
C_{in}	=concentration in the supply air	kg/kg
C_n	=concentration in zone or room	kg/kg
i	=index for individual incoming flows	
j	=index for different surfaces per zone	
k	=reactivity of contaminant	kg/s
k_r	=Radon soil source strength constant	
N_{ach}	=air change rate of the building	h^{-1}
N_{achv}	=air change rate of the subfloor void	h^{-1}
p_{in}	=vapour pressure in the room	Pa
p_{out}	=outside vapour pressure	Pa
p_{sat}	=saturation pressure at inside temperature	Pa
p_{win}	=saturation pressure at cold window	Pa
q_f	=flow rate through the floor	m^3/s
q_{in}	=mass flow rate supplied	kg/s
q_{out}	=mass flow rate extracted	kg/s
RP	=the BRE Radon Parameter	-
ser	=HCHO emission rate	$\mu g/m^2/s$
S_n	=source of pollutant	kg/s
t	=time	s
V	=volume of the zone or room	m^3
Vd	=deposition velocity	m/s
X_{sat}	=moisture content of saturated air	kg/kg

1. Introduction.

IAQ

During the last years indoor air quality (IAQ) has become a very important issue, mostly health related. Reasons for this might be :

* increasing awareness that indoor air pollution affects health,
* a high proportion of time is spent indoors,
* growing capability to measure and simulate pollutant concentrations in and around buildings,
* change in (synthetic)building materials,
* decreasing ventilation rates to save energy.

A description of the term, acceptable IAQ, is : The air should be sufficiently free from biological, physical and chemical contaminants to ensure that there is a negligible risk to the health and safety of occupants.
To improve IAQ, source strengths have to be minimized and an optimization is needed for : supply and exhaust flow rates, flow directions between zones, sink strengths and filter efficiencies.
To sketch the steak for supply optimization, it is nice to keep in mind that less than 3% of the normal ventilation flow rate in buildings (about 0.007 m^3/s per person) is inhaled (about 0.0002 m^3/s), the other 97% is used to dilute pollutants, like odour and CO_2 .

It is expected that analysis of indoor air quality will become more and more important as a part of the design process of healthy indoor air environments and control strategies. Analysis both by measurements and computer simulation.

Process

The main process is the generation of pollutants and dilution by ventilation. Ventilation plays a double role, it dilutes but also spreads the contaminants over the building. Transport by air, entrainment, is the most important mechanism for a pollutant to be spread over a building. This means that controlling the flow directions in a building one can control the spread of pollutants. In many cases however ventilation is not the only loss term. Filtering, deposition to surfaces, chemical reactions and radioactive decays can be more important.
In most investigations pollutant levels are presented. Less attention is paid tot the spread of contaminants within a building, ventilation flow rates and directions.
Single room ventilation efficiency does have an influence on the concentration levels, but in general it is thought that flows from room to room have a larger range of impact on the concentration picture of a building. In this last case, calculations can be done with the assumption of total mixing per room. In the case of local sources with a local exhaust(hood) the source strength must be reduced with the removal efficiency to get a reasonable simulation. An other way would be the use of extra zones around the local source to simulate the removal effectiveness, or to use computer fluid dynamics (CFD).
Flow through large openings has been considered as blind spot. Now a few mechanisms are available that can be used in simulation models (Feustel, 1989). The effect of the large opening flow on the ventilation efficiency end hence the transport of contaminants from zone to zone is yet another vague factor.

Pollutants

The number of pollutants that plays a role, is increasing, partly because of the development of sensitive measurement techniques, simulation techniques and results of research that show the importance to health.
Because of the many pollutants and the many combinations pollutants-materials that serve as an absorber, it will never be possible to create a complete data base with source and sink terms and their relations with other conditions. However it is thought that classes of sources and sinks may be defined that allow for useful handling of measurement results and simulations.
Most investigated pollutants are: H_2O, CO_2 , CO, NO_x , SO_2 , O_3 , HCHO, VOC's, cigarette smoke, Radon , dust, fibres, Pb, micro biological contaminants and odours .

Zone

In measurements and simulation models the term 'zone' is used. A zone can be a small volume element of a room for which concentration, flow rates and other state variables are described. A zone can also be just one room, a set of rooms, or a complete floor or set of floors in a building. Here the word building is used but applications can be any enclosure like cars, planes, cupboards, housing of apparatus.
The choice of the spatial zone dimensions can be given by the limitations during measurements and the capabilities of the simulation model. On the other hand the choice can be based on knowledge about the distribution of concentrations in the building. If an area, which can consist of one ore more rooms, is supposed to have an uniform concentration and ventilation, it can form one zone. If significant spatial variations of concentration occur in a zone it must be split up to give a proper simulation. For measurements this means that in this zone a single sampling point will not be sufficient to depict the whole zone.

Losses

Several mechanisms change the level of a pollutant during the transport from outside to inside, as well as inside from one room to another. These losses may give a greater reduction of the pollutant level than ventilation only. Some mechanisms and coefficients can be found in literature on deposition to surfaces and radioactive decay, nothing has been found on filtering or the penetration efficiency in cracks.
Air cleaning devices and filters can have a predominant effect for instance in clean rooms and operation theatres.

Occupants, exposure

Occupants play a key role. They can influence ventilation and some sources. If the pollutant can impose a health hazard the occupant is important because he is exposed to the (indoor) air.
Therefore a simulation tool must take into account in which room occupants stay, indoor or outdoor, and how long, to calculate average exposures.
For all health related problems the presentation of human exposure is preferable over the concentration histories in the different zones.
Occupants may have a direct influence on pollutant levels, for instance CO_2, therefore scheduled occupants in the different rooms are needed.

It is thought that calculation of the exposure for different groups of occupants for a building with

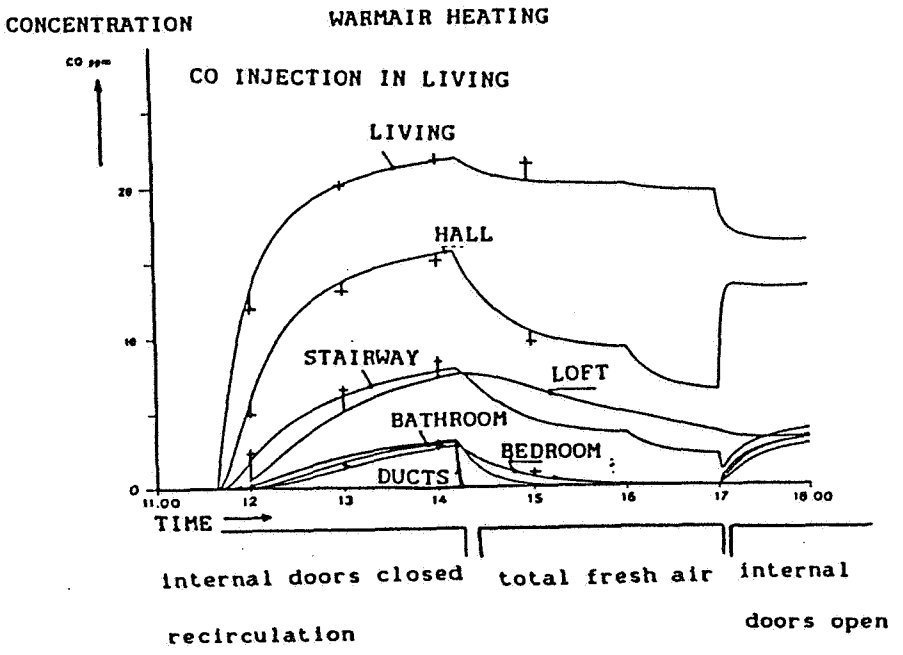

Figure 1. Comparison of model results and measured result for a non absorbing gas.

computer simulation models can be a very efficient way to interpret the IAQ. In this way comparisons with other buildings or variations in same the building are possible.
The exposure can be normalised by demanded limits from standards, and then summed for different chemical substances. Care must be taken for threshold values and non linear steps in the standards like 24 hour limits and 8 hour limits or percentile values.
There are a few cases in which health aspects are not of primary importance, for instance :

* condensation with the risk of building damage,
* pollutants that influence the quality of products in industry,
* dust in clean rooms

In those cases it is not useful to present the exposure of occupants, although it might be possible to present an estimated rate of product failure in stead of concentration histories.

2. Review.

A lot of information can be found on indoor pollutant levels (MCMurry, 1985) (ASHRAE 1989) . Most papers already give a review on existing pollutant levels for the most important pollutants. A lack of information exist on measured losses and sink terms especially in cracks. Some more information is available on sources and source strength of pollutants. Computer models exist which take into account pollutant transport by airflow, based on a mass conservation principle (Axley, 1988 a,b). Some models describe the reduction of a single pollutant under several conditions, for formaldehyde (Grot, 1985) and (Godfish, 1988).
As long as source strengths and ventilation flow rates are properly simulated, excellent agreement between measurements and simulations is found in the case of non absorbed gasses. Some results of air and pollutant transport models are given in figure 1 (Gids 1988) and 2 (Axley, 1988 a).

Spread of contaminants in a single zone has been studied for instance by (Vandaele, 1989). Measurements were performed on 50 points in an attic room of about 38 m^3 with an air tightness of N_{50} =8 . With closed windows and an air change rate of 0.3 +/- 0.1(std) per hour a line source resulted in a ratio between maximum and minimum of the 50 spatial concentrations of 1.2 . A point source gave a spatial concentration ratio of 1.5 . With a window open the air change rate has been 0.75 +/- 0.5(std) per hour. Spatial ratios of the concentration for the line source were 1.2 to 1.3 and for the point source 1.5 to 1.7 .
These single zone concentration ratio's are thought to be much smaller than room-to-room concentration ratio's.
A possibility to include odour in pollutant transport models has been introduced by Fanger (Fanger, 1987).

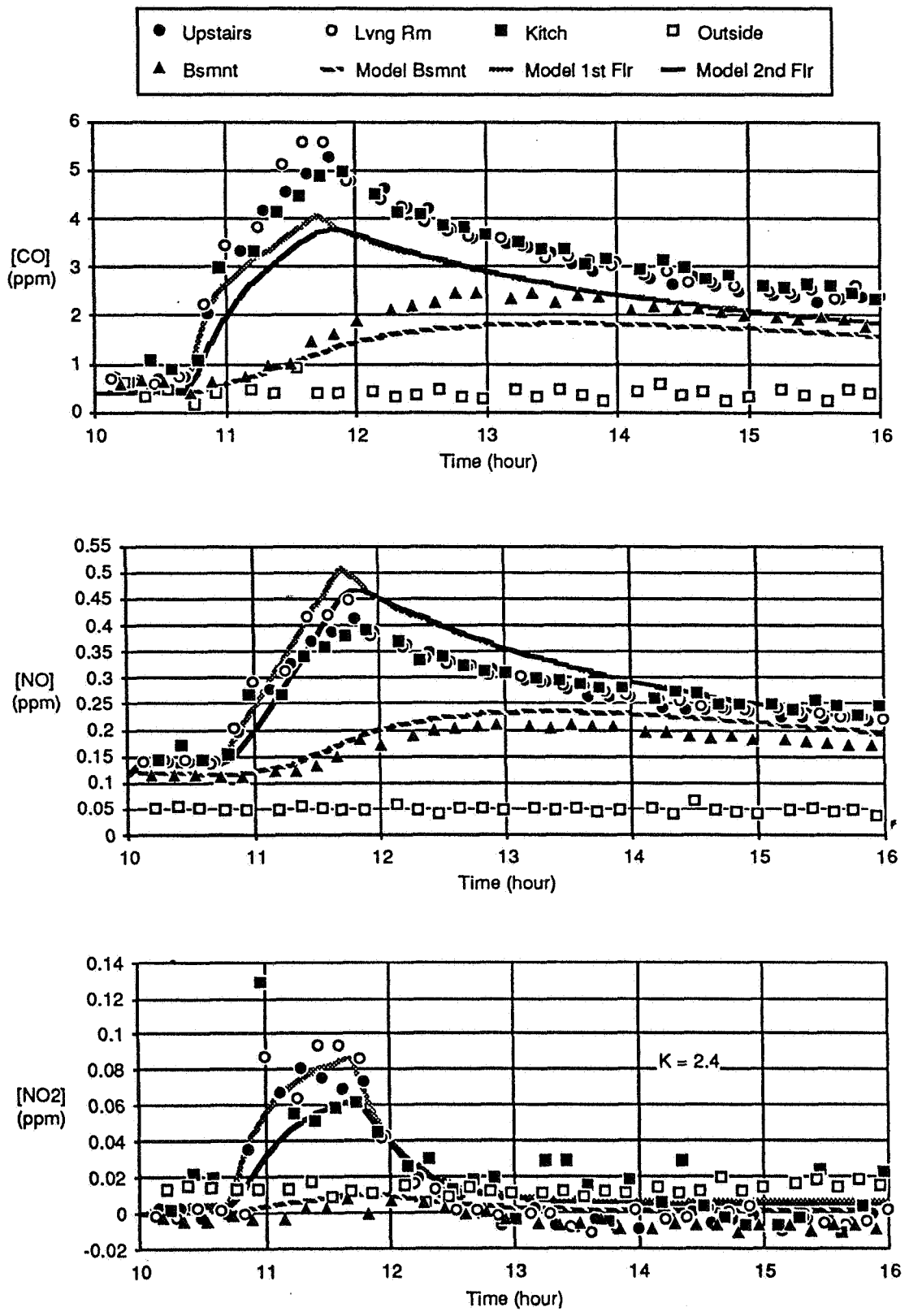

Figure 2. Comparison of a model predicted and measured response for several gasses as pollutants

3. Mechanisms.

3.1 General

The mechanisms can be subdivided into : source-, sink-, dilution-, transport-, exposure- mechanisms.

Assumed is a mass conservation for each zone, while the air is well mixed within the zone, the equation which describes the mass balance can be given (Feustel, 1989);

$$\frac{d(\rho V C_n)}{dt} = \sum_{i=1}(q_{ini}(1-\lambda_i)C_{ini}) - (q_{out} + k)C_n + S_n \quad ...(1)$$

The unit of equation (1) is (kg[contaminant]/s). The summation is for all the incoming flows i.
in which:
With the ventilation time constant :

$$\tau = (\rho V)/q_{in} \qquad (s^{-1}) \qquad ...(2)$$

and with :

$$dt/\tau = (1-e^{-\Delta t/\tau}) \qquad (\Delta t << \tau) \qquad ...(3)$$

This leads to the form that can be used directly in numerical pollutant transport models in which t and t+1 are two successive timesteps:

$$C_{n|t+1} = C_{n|t} + (1-e^{-\Delta t/\tau}) / q_{in} * \left[\sum_{i=1}((1-\lambda_i)C_{ini} * q_{ini})/q_{in} - (q_{out} + k)C_n + S_n\right] \quad ...(4)$$

Equation (4) can be used if the air density remains constant and if the incoming flow is not zero. The substitution of (3) avoids overshoot of the concentration for timesteps as big as the ventilation timeconstant of the zone, but some accuracy is lost. Small zones, like a duct section with large flows, can have very small timeconstants and would otherwise have led to unpractical small time steps in the case of a linear equation.

Filter efficiencies (4) for dust can be found for filter units but unfortunately not for cracks.

The reactivity term k in (4) can be expressed as a deposition velocity to a surface:

$$k = \rho \sum_{j=1}(V_d * A)_j \quad (kg/s) \qquad ...(5)$$

This means that the amount of pollutant in the volume $V_d * A$ disappears per unit of time into the surface A . For low concentrations, say in the 1 ppm range, saturation of the surface doesn't occur. The process has not been found to end in time. Cleaning, renovations or repainting is likely to occur before a saturation would be noticeable.

In experiments the deposition can be determined as a decay rate :

$$1/\tau_{con} = V_d * (A/V) \qquad (s^{-1}) \qquad ...(6)$$

The experimental concentration decay in a closed room without ventilation and deposition only is :

$$\frac{C_t}{C_0} = e^{-t/\tau_{con}} \qquad ...(7)$$

Source terms S_n in (4) are often given as mass flows per time unit and need only scaling into the proper units.

3.2 Air paths

The air from outside passes on its way to inside either a mechanical ventilation system or the building fabric in which losses of a pollutant take place.
In the room some mixing followed by the transport from one room to another room will occur, via a mechanical ventilation system or via cracks, openings around the doors, grids and/or through the construction of the internal walls.
During the transport of air by a mechanical system there can be losses in terms of uncontrolled deposition and/or filtering in the purpose provided filtersection.
The air will leave the building by exfiltration through the building envelope and/or by the mechanical extract system. During this transport a certain amount of the pollutant will be left behind and hence give a decrease of the emission.
The air flow over large openings is mainly not one directional. Due to local turbulence, flow in both directions i.e. inward and outward flow is possible and can occur simultaneously in one opening. In the case of large openings the chance to have total mixing in the room decreases. The flow in the opening and the ventilation efficiency to the bulk air of the room determine the transport of pollutant in both directions via the large opening. Therefore the contaminant transport due to this flow mechanism is not quite well known. In simulation models two estimates are necessary:

case 1. The concentration in a zone has to be kept low by means of large opening ventilation,
case 2. A zone has to be protected against polluted air infiltrating via a large opening.
In the first case the best average air flow exchange over the large opening is needed. In case 2 a higher estimated large opening flow is necessary in order to be sure that the protection pressure hierarchy will be sufficient to keep the contaminant out.
In clean rooms laboratories and hospitals large openings are a thread to the pressure hierarchy. This is an important application of ventilation-pollutant transport models.

3.3 Source mechanisms

As source mechanisms for contaminants can be mentioned: emission or release of mass, evaporation, desorption, resuspension, growth of micro-organisms, radio activity.

Examples of emission or release of mass are for instance: human CO_2 production, combustion products from a furnace, heaters, formaldehyde from particle board and plywood. Grot (Grot 1985) has performed many measurements of the surface emission rate of formaldehyde from wood materials and found in many cases a good agreement with the equation:

$$ser=\alpha - \beta C \qquad ...(8)$$

A useful value has been the surface emission rate at a concentration of 120 $\mu g/m^3$ or 100 ppb and the cutoff concentration where the emission rate becomes 0, defined as:

$$cutoff=\alpha/\beta \qquad ...(9)$$

Correction terms for on α and β for temperature and relative humidity have been determined by (Matthews , 1986).
Degradation of resins increases at increasing temperature and relative humidity, resulting in a higher formaldehyde generation on the average of about 23% per K temperature increase and 5.5% per %RH increase.

Examples of evaporation are: Watervapour in homes, solvents, VOC's from paint, carpet and furniture materials.
Several controlled test chambers have been constructed in Europe to determine the source strength of several furniture materials. These test chambers are based on guide lines of the EC COST working group (Project 613, WG8).

Desorption and resuspension can occur for instance with odours absorbed by furniture materials, gas molecules that are physically bound to the surface and dust particles larger than 1 μm, due to mechanical vibrations or high local air velocities. Vacuum cleaning and walking can temporarily increase the amount of aerosol dust.

Growth of micro-organisms like fungi, house dust mites and allergens from domestic animals are harder to be modelled as besides growth conditions, elapsed time is important. The different stadia of the life cycle of the organisms have different production rates of allergens or fungus spores. Most of these sources are related to moisture, and especially the moisture in the boundary layer near the surface. There is a feeling that instead of measuring and simulating these kinds of sources in buildings in order to show the current status and relations, it would be better to focus on solutions directly: To build buildings that will not be moist, not to use building materials that are a breeding ground, to use beds that can be periodically electrically heated or frozen to kill mites.

Radiation from Radon is commonly investigated (Dijkum, 1986) (Collé, 1980). Geological composition of the soil has a large influence on the Radon generation levels. Uranium rich soil is known to result in higher Rn levels, both directly from the soil and from building materials which originate from such soil. ^{222} Radon has a half life time of about 3.8 days and its daughters to ^{210} Pb all shorter than that. As this half life time is generally much longer than the ventilation time constant of a building, the main loss term is ventilation. This may not be true for spaces with stale air like closed wells, where high concentrations can build up (Meyer, 1983).
Soil generated Rn cannot be looked at separate from its mechanism to infiltrate in a building.
By diffusion Rn enters cracks in the bedrock. Moved by ground water levels, wind pressures on the field around the building, in the soil under the building and in the subfloor void Rn infiltrates in the building. Large local variations and variations in time have been observed. Some of the pressures are related to the shape of the building and the ventilation parameters of the building. Therefore the building and its ventilation parameters have an influence on the amount of Rn that is transported. This can be studied effectively with multizone ventilation- pollutant transport models. BRE has derived a simplified way to handle this process and calls it the Radon Parameter (Hartless, 1990).
For positive pressures between soil gas and subfloor void the equation is:

$$RP=(q_f * \Delta P_f / N_{ach} * N_{achv}) \qquad ...(10)$$

and the radon concentration in the building :

$$Rn_i = Rn_o + k_r * RP \qquad ...(11)$$

The constant k_r includes many different, unpredictable factors such as soil type and Radon generation. The Radon Parameter can be seen as a sense for a buildings sensitivity for Radon infiltration if it would be placed on a Radon generating soil.

Other Radon sources are building materials, domestic and ground water, natural gas and industrial aerosol dust. Attached to aerosol dust or directly, and subsequent respiration it can be deposited on the lung tissue. This leads to an increased tumour risk.
The effect of radioactivity from outdoor air infiltrated in dwellings on the dose has been investigated by (Roed, 1990).

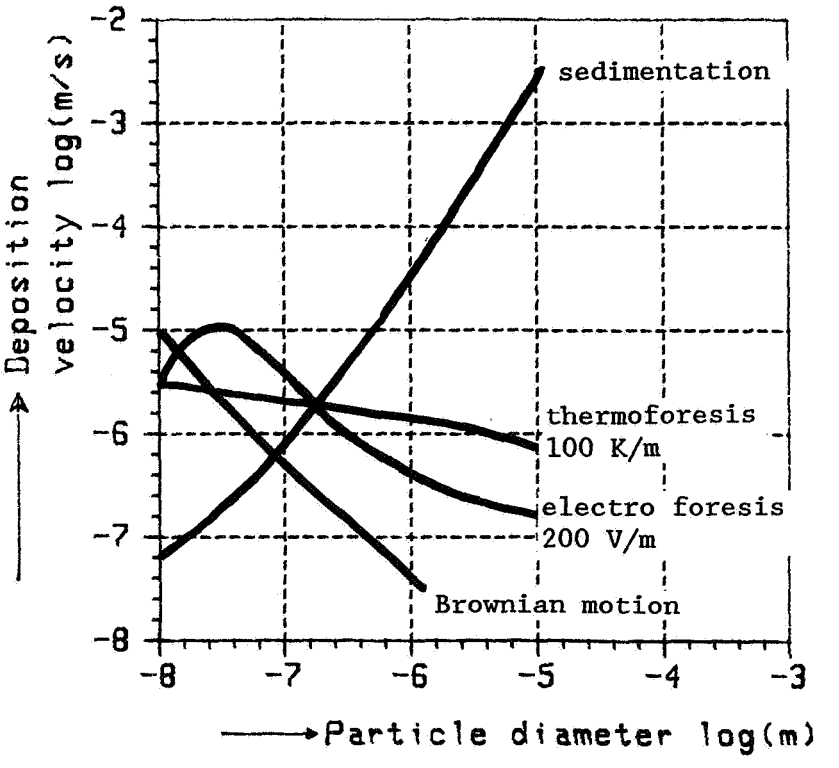

Figure 3. Deposition velocity of particles

3.4 Sink mechanisms

The most important sink mechanisms are: deposition (absorption and adsorption) sedimentation, plate out, filtering, condensation, chemical reaction, radio active decay.

The deposition process has two steps (Lanting, 1991). First there is a pollutant mass transport through the undisturbed boundary layer to the surface. The second step implies chemical or physical interaction with the surface. For gasses the second step is the limiting factor and for particles the first step. With full absorption on the surface the theoretical deposition velocity for gasses should be 1E-5 m/s in stale air, with natural convection and laminar flow along the surface 7E-4 m/s and in turbulent air 1.8E-3 m/s. The real deposition velocity will be lower if not all molecules interact with the surface and can be higher if the surface is rough (for instance carpet) and if the humidity is high for water soluble gasses. Temperature has minor influence on the process.
More processes play a role at the deposition of particles on a surface.
Small particles (cigarette smoke) bind irreversibly to a surface.
The processes that move particles to a wall are:

* Brownian motion (particles <0.5 μm show a gas like diffusion that is bigger than the sedimentation velocity in stale air),
* Thermoforesis (particles >0.05 μm move through a temperature gradient to a 1K colder surface 10 times faster than if the surface is 1K warmer),
* Electroforesis (Computer and TV screens),
* Sedimentation (Stokes, dominant for particles >1 μm).

The particle size is the most important parameter. The effect of the different mechanisms is shown in figure 3.

A summary for the deposition velocity in m/s of gasses is:

Situation	SO_2	NO_2	O_3	HCHO	VOC
Rooms with much absorbing material	6E-4	3E-4	9E-4	1E-4	2E-5
Rooms with little absorbing material	1E-4	3E-5	4E-4	5E-5	2E-6

For turbulent conditions the values are typically 3 times higher.

Data for filter efficiency for particulate matter can be directly applied in pollutant transport models provided that the particle size is known. The effect of aircleaners on other pollutants is not generally known. Some air cleaners for domestic use have been found to have no effect at all on dust concentrations while ionization filters have been found that produce high concentrations of O_3 . Performance of several air-cleaners has been reported by (Daisey, 1988). Most air-cleaners have a lower flow rate than those indicated by the manufacturers. Removal efficiencies for NO_2 and VOC's have been found in the range of 0% to 40% for the various cleaners.

Condensation occurs if for instance a surface is below the dewpoint of the water vapour in the zone. The condensation heat produced, heats up the surface. A detailed simulation is possible only with combined heat flow-ventilation models. Condensation rates can be up to 1E-4 kg/s/m² in bathrooms during a shower.

Chemical reactions in air are for instance SO_2 with H_2O. Most reactions play a negligible role as the concentrations of both contaminants are relatively small.

Radio active decay for Radon can be a significant loss term in spaces with full mixing and a very low air change rate (N_{ach} < 0.01) but also when a relatively high concentration of the heavy Rn formes a stagnant, stratified layer on the floor. Radon is 9 times heavier than air.

3.5 Exposure

If the concentrations in the zones are simulated in time with a computer model, and if those concentrations are good estimates for the concentration inhaled by the occupants, then it is a relative easy step to calculate the exposure to air pollutants.
In fact it is a way of presenting the vast amounts of results from multizone concentration histories into a few daily, weekly or for instance annually averaged exposures for a defined set of occupants.
Exposure does not deal with the problem of health risks, dose-effect relations. It is only meant here as a sense for a better IAQ in a building.
In literature the term exposure is also used for intake of contaminants via food and skin (EPA, 1989). The here mentioned 'exposure to air pollutants' does not deal with that.

If the occupant does not influence the sources and sinks and ventilation then with a record of the concentrations from a single simulation run, the exposure for many occupant patterns (in which room they stay) can be calculated without recalculating the concentrations.
If the occupant does influence the parameters, for instance with CO_2 as a gas, then the complete concentration simulation run has to be repeated for every occupant schedule.
In most cases the ventilation flow rates will not be driven by the contaminant levels in buildings as the concentrations will be low enough to neglect their influence on the air density and thus on the buoyancy or stackeffect pressures. This means that with a fixed record of ventilation flow rates many concentration histories can be produced.
An exception might be H_2O vapour as a contaminant, which does have a small influence on stack effect. The effect of water vapour 0.001kg/kg dry air is about the same as the effect of 0.17 K temperature difference.
Air flows within one room can be influenced by concentration differences but in most cases heat that is co-generated (cooking) or air movements by the generation activities (vacuum cleaning) have a larger influence on air movements than concentration only.

4. Standard contaminant levels.

Many standards exist for acceptable levels of indoor contaminants. Overviews can be found in (ASHRAE 1989) and (Canadian EHD, 1987). Values differ between countries. A selection is made here. Contaminant levels should be as low as possible. Within pollutant transport models these values can be used to normalise predicted levels, and to signal if threshold values are exceeded.

Source	short term		long term	
	µg/m³	ppm	µg/m³	ppm
moisture			<80% RH at surfaces	
formaldehyde	120	0.1	60	
CO	1E4	9		
CO_2		10,000		1000 (comfort)
SO_2			80	0.03
O_3	240	0.12		
dust			40	
NO_x			100	0.055
Pb			0.5 to 1.5	
VOC's			component dependent typical several 10.000 µg/m³ unless carcinogen	
radiation			25mrem/y 28nSv/h	

A ranking of agens for health risk assessment has been performed by (Lanting, 1990 a) based on:

* MAC values and WHO guidelines or odour
* existence of sources
* emission/exposure profile in time
* concentration levels of exposure.

Sources with the highest priority for which exposure or measures to be taken, are known are: Combustion appliances, tobacco smoke, formaldehyde from particle board.

Sources with high priority and insufficient knowledge about exposure and measures to be taken, are:

* pesticides, wood conservation, additives to textile
* aldehydes and carbon acids in wood, floor covering, textile or in combination with odour
* phthalate-esters in plastics, paints and glues
* isocyanates in paint, insulation foam, glues
* water based paints and cleaning products with glycol-ethers, -esters, alcohols, conservatives, fungicides
* floor covering vinyl linoleum and textile with suspect carcinogenic compounds, softeners or in combination with odour.
* cleaning and maintenance products with suspect carcinogenic compounds or in combination with odour.
* mercury from broken thermometers and barometers.
* terpenes in floor and furniture wax, cosmetics, wood products, paint.

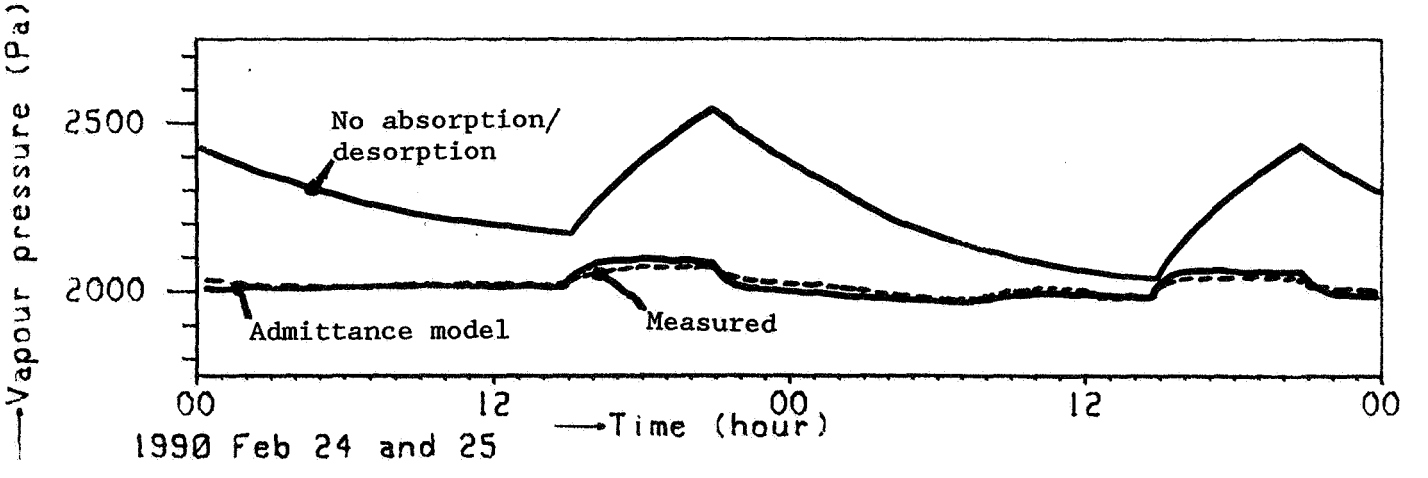

Figure 4. Moisture admittance model of Jones, BRE

5. Contaminants from indoor

moisture, formaldehyde, CO, CO_2 , O_3 , dust, NO_x , VOC's, radiation.

Moisture generation rates in homes generally are about 7 to 14 kg/day. Moisture is of importance as one of the growth conditions of microorganisms. It is thought that ANNEX 24 will yield specialized models to predict moisture transport through building components, like for instance the Danish model Match.
A promising simplified dynamic model, called moisture admittance model, has been produced by BRE (Jones, 1990).
Its coefficients have been experimentally fitted with results from 2 experimental rooms and need work to be generally applicable in buildings and with non uniform surface temperatures. The equation looks like:

$$\frac{d(p_{in})}{dt} = \{N_{ach}(p_{in} - p_{out}) - 2.5p_{in} + (1.4 \text{ to } 1.8)p_{sat} - 0.3p_{win}\}/3600 + S_n * p_{sat} / X_{sat} \quad ...(12)$$

The coefficients are valid for the specific test chamber. In figures 4 a comparison of the model with measurements at a changing vapour input is shown.

A recent overview of existing concentrations of formaldehyde in European countries has been given by (COST , 1990). The outdoor background concentration is about 1 $\mu g/m^3$ with peaks up to 100 $\mu g/m^3$ due to traffic.
Formaldehyde from building materials has been shown to be a non constant source (Grot, 1985) (Godfish, 1988). Moisture, temperature and the Formaldehyde concentration itself influence the generation process. Source strengths of particle board and plywood have been found in the range of 0.003 to 0.5 $\mu g/m^2/s$ at a formaldehyde concentration of 0.1 ppm. Cutoff concentrations, where the emission becomes 0, have been found to be in the range of 0.2 to 0.4 ppm (240 to 480 $\mu g/m^3$) with some medium density fibre boards up to 1.8 ppm (1800 $\mu g/m^3$). An excellent agreement between the measured formaldehyde concentrations and a mass balance indoor air quality model has been obtained.
Other sources of formaldehyde are UF-insulation foams, tobacco smoke, combustion gasses from gas appliances, traffic, industry (production of resins). Formaldehyde source strengths of 0.4 to 4 $\mu g/kJ$ were measured by (Traynor, 1985) at unvented heaters.

Carbon monoxide is produced by incomplete combustion, cooking, traffic.
The number of fatal CO poisonings per year in Holland normalised for a 1000.000 population:

0.4	kitchen unvented geysers
0.14	geysers with a flue
0.29	central and decentral heaters
0	cookers and other appliances

In 17 % of kitchens (Brunekreef, 1981) CO concentrations were measured above 50 ppm after using the unvented geyser for 15 minutes . CO source strengths of 13 to 165 $\mu g/kJ$ have been found for unvented gas heaters under poor ventilation conditions by (Traynor, 1985).

The current trend is to use closed gas-appliances, with a fan for supply and exhaust gas and separate flues. The amount of supply air for gas burning is usually negligible, 1 to 3% of the ventilation flow rate of the house. Closed appliances have a better efficiency due to the lower, controlled excess supply air flow rate.
Malfunctioning natural gas exhaust flues in airtight houses with mechanical extract ventilation are a known problem (Steel, 1982).
Unintended transport from parking garages to buildings has been reported by (Hodgson, 1989) and can impose a CO and VOC source. CO levels of 10 ppm have been measured in the building above the garage.

CO_2 is produced by combustion. The human CO_2 production is about 5.6E-6 m^3/s, mainly dependent on the skin area(Dubois area) and the metabolic rate.

NOx is also produced by combustion from gas appliances and traffic. Traynor (Traynor 1985) measured source strengths for unvented gas heaters to be from 10 to 20 $\mu g/kJ$ both for NO and NO_2 .
Average indoor levels of more than 200 $\mu g/m^3$ (0.1 ppm) with 1-minute peaks of 4000 $\mu g/m^3$ (2 ppm) have been found in homes with unvented gas appliances (COST 1989 NO_2). Negative health effects are reported at concentrations as low as 200 $\mu g/m^3$. The trend is to use cooking ranges with special low NO_2 burners.

VOC's have been shown to be originating form solvents in liquid-process copiers in an office building at rates of 2 kg solvent/day total for 26 copiers (Hodgson, 1989). Other sources of VOC's are finishing, furniture materials. An unexpected source might be the evaporating benzene from gasoline from cars in parking garages attached to a building.

To determine material source strengths a series of european test cells has been made within COST 613 TG 8. It is expected that many results will soon be available from this. In principle these test rooms allow for determination of sink rates as well. Two floor covering carpet tiles with PVC back emitted 4600 $\mu g/m^2/h$ total VOC on the first day and 2700 on the 7th day, the second tile 1160 and 370 $\mu g/m^2/h$ (Wal, 1991).

Ozone is generated by photochemical processes like in laser printers. Measurements in a test chamber with some adsorption on walls showed source strengths of 10 $\mu g/s$ or about 100 μg per copy without any

filter on the printer. Filter efficiencies have been reported from 70 to 99% .
Some air cleaners for domestic use with an ionisation filter section produce up to 1 $\mu g/s$ O_3 .

6. Contaminants from outdoor.

In most cases outdoor levels will be used as an input to pollutant transport models.
Outdoor levels are mainly influenced by industry, traffic and agriculture. Below are given some figures from various guide lines just to give some idea.

Sources	target average annual levels $\mu g/m^3$
SO_2	30
Dust	30
NO_x	25
Ozone	120
lead	0.5

Measured levels can have very large peaks if measured in the vicinity of the source. For NO_2 levels in the range of 100 $\mu g/m^3$(year) have been reported in urban area's with hourly values up to 1000 $\mu g/m^3$ due to traffic. Some simplified and limited calculation models exist for levels as a function of traffic intensity (Jansen, 1987).

7. Control Strategies.

An overview of strategies has been given by (Levin, 1992).

7.1 Indoor sources.

The general strategy is to minimize source strengths. As ventilation in cold climates or cold periods increases energy consumption, the preference is to keep the ventilation rates close to minimum rates (IEA ANNEX 9, 1987) (Trepte, 1989).
During warm periods ventilation may be higher, due to open windows, and pollution levels may be non important with respect of the cold period.
At outdoor temperatures higher than acceptable, cooling by air conditioning will lead to the same preferable minimum ventilation as in cold periods.
To increase the effect of ventilation, air flow rates must be at the proper locations and controlled in time. This means local exhaust near sources and local supply near occupants, displacement ventilation.
Increased ventilation during cooking is common. But the local exhaust above the cooker is usually not very effective compared with a fume cupboard. Local exhaust near showers in bathrooms, WC , on printers and copiers is rarely seen. In Industry too local exhaust is often not applied because of (supposed) draw backs to the accessability of processes.
Demand controlled ventilation (IEA ANNEX 18) is the (near) future to optimize IAQ versus the used ventilation flow rates.
In many cases the control of flow directions prevents contaminated air to reach occupants or to enter into sensitive areas. Unfortunately in most buildings the natural flow direction spreads the contaminant through the building, like Radon from the crawlspace and vehicle exhaust gasses from the basement parking garage.
Evaporation of gasoline from cars in the garage is effectively reduced by the Californian canisters, a carbon filter in the car. This is an environmental measure but it also reduces benzene exposure from parkings into buildings.
A special case of flow direction control is the operation theatre in hospitals and clean rooms. Large openings (doors) and temperature differences can spoil the desired pressure hierarchy. Large bypass flows through grilles besides such doorways can minimize the disturbance, and maintain sufficient air velocity in the open door way to avoid a two-way flow.

7.2 Outdoor sources.

If outdoor sources have a constant too high level, filters or cleaners must be used to get an acceptable IAQ. Some contaminants can be removed very efficiently or disappear already in the HVAC or humidifier like SO_2.
Care must be taken at the position of the air inlets, not on the side of busy traffic or the exhaust on the roof.
If outdoor concentrations fluctuate and the duration of peaks are shorter than the building ventilation time constant then a time control of the amount of outdoor air may be possible. A good example for this is the control of ventilation in vehicles in dense traffic. The problem here is that the ventilation time constant in vehicles is usually in the range of some 100 s and a quick response of the sensor and control is needed. The reduction of the concentration level in the intake air can be large as outside levels in traffic usually fluctuate with a ratio of 1:100. Switching off the outdoor air supply

increases indoor source effects. An optimum has to be found, a perfect field of application for 'intelligent' controllers. An example in a simulated bus of 48m³ with measured outside NO_x concentrations as input, is given in figure 5. To account for some internal pollutant generation 34 µg/s is added as source. Two runs have been made : one with fixed ventilation flow rate 0.5 m³/s, the second with the same integral flowrate but switched on and off (30% on, with 3 times the nominal flow rate) if the outside concentration is lower than inside (no sensor-control delay).
Average outside concentration is 688 µg/m³, inside 748 at constant ventilation and 283 at controlled ventilation. The effect is dependent on the amount of internal pollutant load, which is about 10% of the outside pollutant load in figure 5.

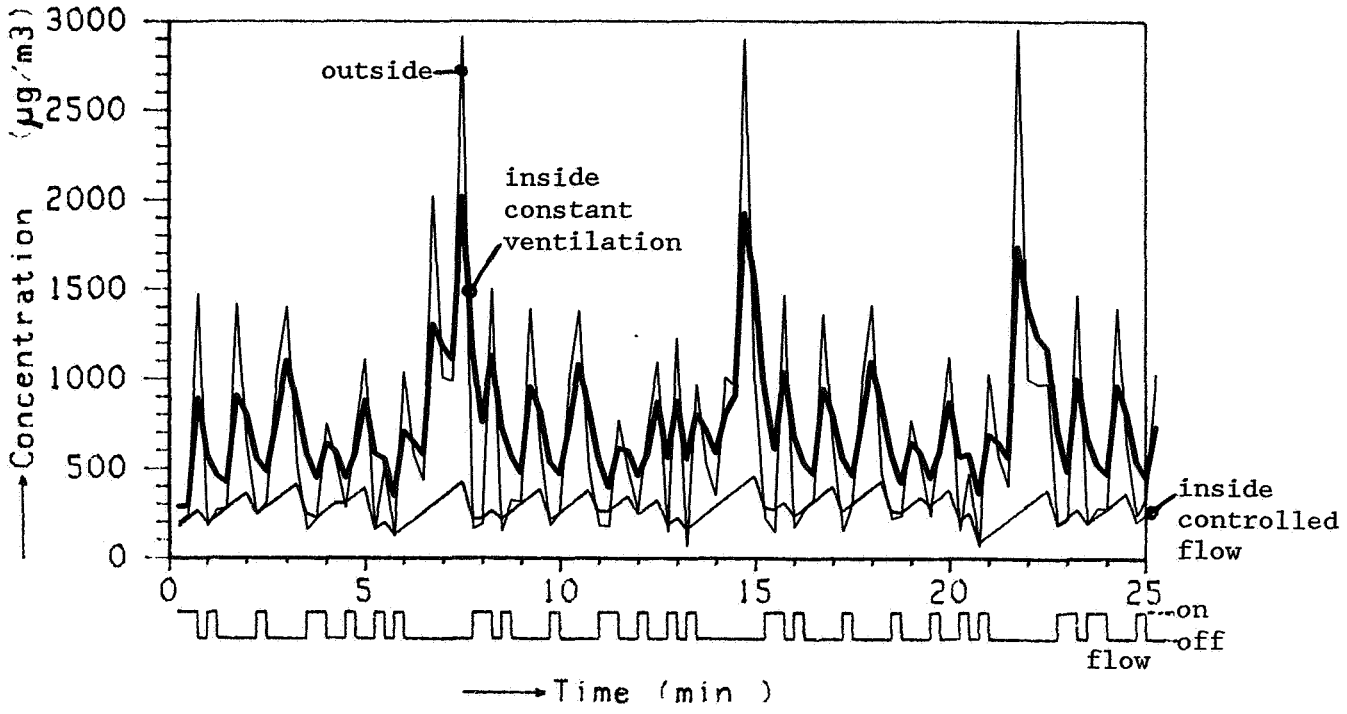

Figure 5. Simulated NO_x concentrations in a bus, constant and controlled ventilation.

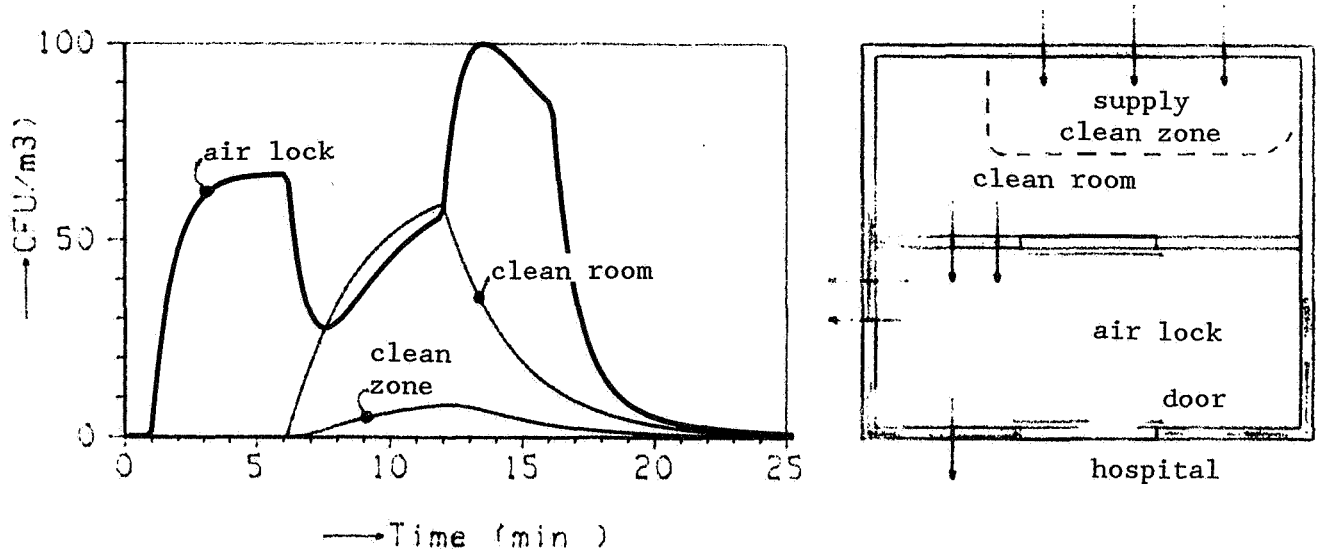

Figure 6. CFU concentration in an isolation chamber and floor plan.

7. Examples

7.1 NL Archives and museums

In museums and archives IAQ is not health related but meant to prevent deterioration of paper and cultural inheritage. SO_2 , NO_2 and O_3 have been measured in 6 buildings by (Lanting, 1990 b). A significant part of the outdoor pollution is introduced via the HVAC system, from which the recirculation ratio has been varied. SO_2 is absorbed by the humidifier of the HVAC system. Low levels of the contaminants indoors have been explained by the rapid absorption by the large quantities of archival material. Outside the working hours 100% recirculation has been advised.

7.2 Hospitals

Pollutant transport models can be used for prediction of the number of dust particles that contains germs that could cause infection. This is called CFU, Colony Forming Units, expressed in CFU/m³ . In this example the source strength of a person is 20 CFU/s . Levels of CFU's are simulated in a protected room and its air lock to the corridor, when a person enters from the air lock into the protected room. The limit is 10 CFU/m³ in the clean zone in the protected room. Figure 6 shows the concentrations.

At minute 1 a person enters the air lock, at 6 the protected room is entered and the door is open for 10 seconds. At 12 the person returns to the air lock, which is left at minute 16. No CFU generation is taken into account for a patient staying in the protected room .

7.3 NL Leidschendam

Airborne moisture transport has been investigated by (Oldengarm , 1990) (Elkhuizen, 1990). In a dwelling three moisture generation types have been considered:

* cooking
* shower
* laundry drying

Moisture storage and release from walls and furniture could be seen as simultaneous measurements of different tracers were used. In figure 7 the moisture content from 12:00 to 14:00 is below that of a non absorbed tracer, indicating absorption of moisture. After 14:00 moisture is released from the surface and the moisture content is higher than the equally scaled non absorbed tracer gas.

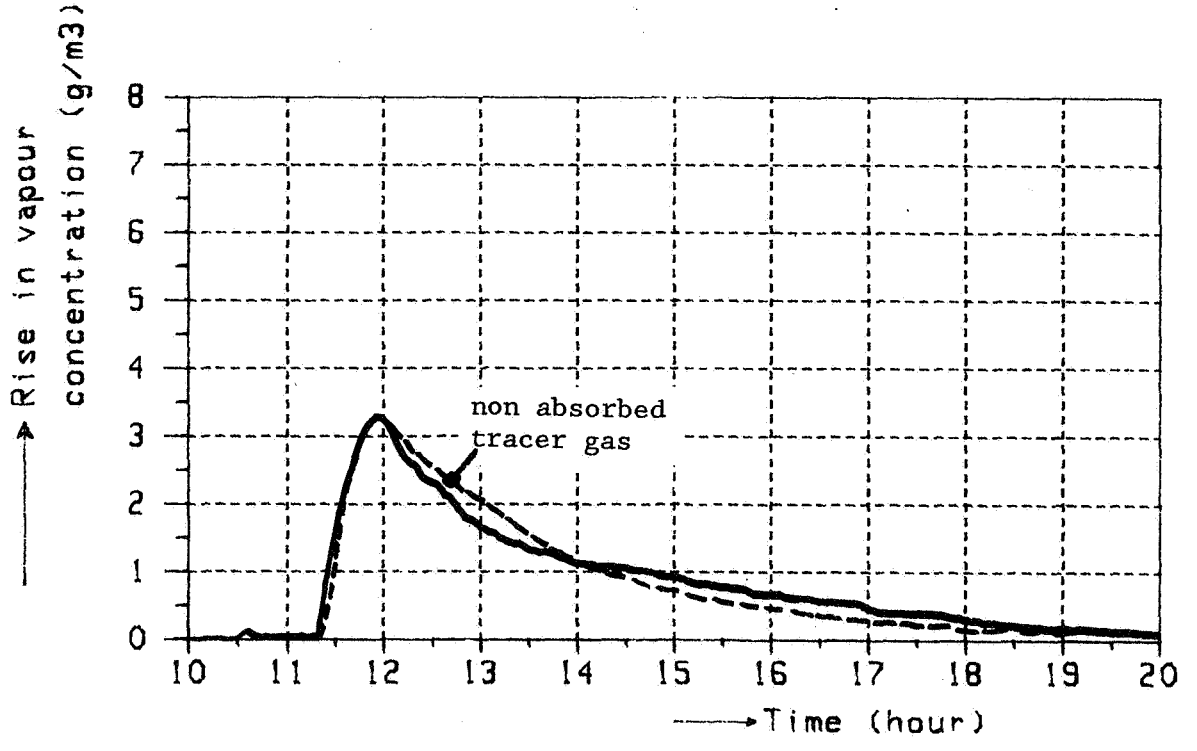

Figure 7. Vapour concentration in a house after a 30 minute moisture input, compared to a similar scaled non absorbed tracer.

7.4. NL Almere Schools

Schools have a high demanded ventilation rate, N_{ach} >2.5 h^{-1} , which is generally not met with natural ventilation, because windows are not sufficiently opened. As a result CO_2 concentrations over 3400 ppm were measured in a period with switched off mechanical ventilation (Knoll, 1984).
Perceived odour, based on questionnaires, however did not differ much for the period the system has been on, with less than 1200 ppm CO_2 . Conclusion is that occupants in schools are not capable of controlling their windows in order to get an acceptable IAQ.

7.5. NL Lelystad.

The aim of the Lelystad project has been to compare houses with warm air heating and recirculation of air with houses with warm water heating and no recirculation of air. Recirculation of air from living room to bedrooms has not been allowed by the Dutch standard NEN 1087. It is said that in houses with warm air heating and recirculation there are more problems with allergic reactions and respiratory diseases. No investigation exists that proves this. The thought is that the forced air movement in the heating system and high velocities at the grilles keep the dust moving. This has been proven to be not true, grille velocities are too low to resuspend dust.
The air tightness of both houses meets the demanded value in the Dutch standard (NEN 2686), with N_{50} =1.3 (air heating) and 3.1 (water heating) per hour.
Three tracer gasses have been injected in the living rooms under various conditions. Figure 1 warm air heating and figure 8 warm water heating.

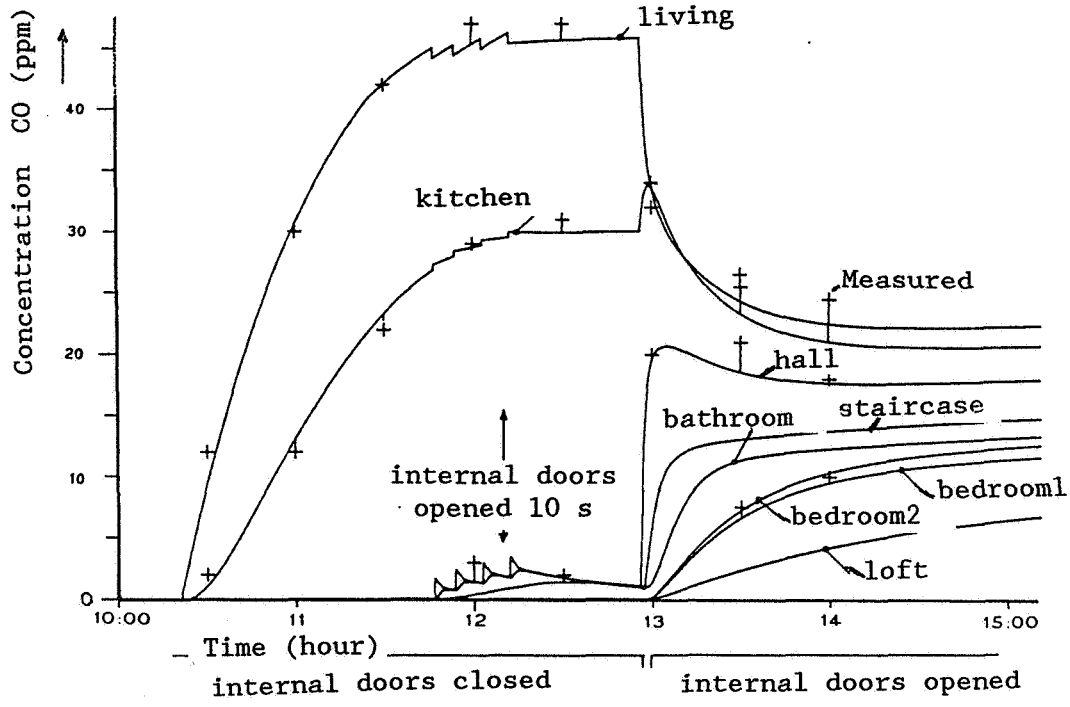

Figure 8. Measured and simulated concentrations. Warm water heating.

The gasses were :

gas	target concentration in the living room.	
Carbon monoxide	25	ppm
Nitrous dioxide	0.2	ppm
Paraffine oil aerosol and cigarette smoke	1000	µg/m³

Carbon monoxide is not absorbed and served as a tracer to see the spread of air and dilution from living room to the other rooms.
NO_2 is absorbed by building materials and is used to show the effect of absorption.
Paraffine oil smoke has been used to simulate cigarette smoke. The oil drops show a plate out effect and are adsorbed when the air hits a surface or filter. Spread of cigarette smoke is considered to be one of the important draw backs of recirculation.
In figure 9 and 10 the ratios between the concentrations of the different gasses are drawn by

normalising them to the same value in the living room.
The deposition velocity to the floor area for NO_2 are about 0.5mm/s.

Ratio of NO_2 and smoke to CO in the livingroom. Internal doors closed.

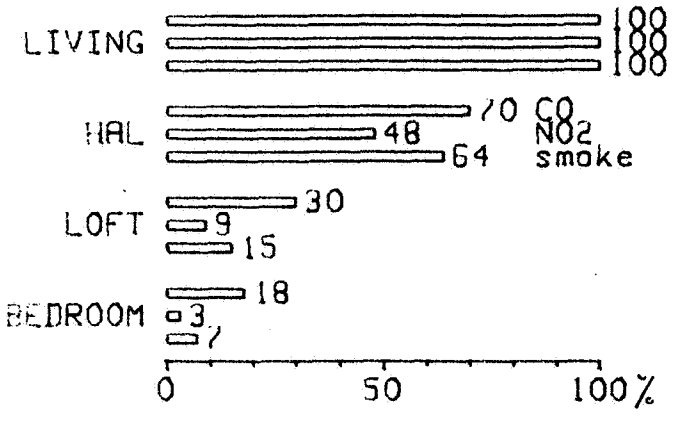

Figure 9. Warm air heating

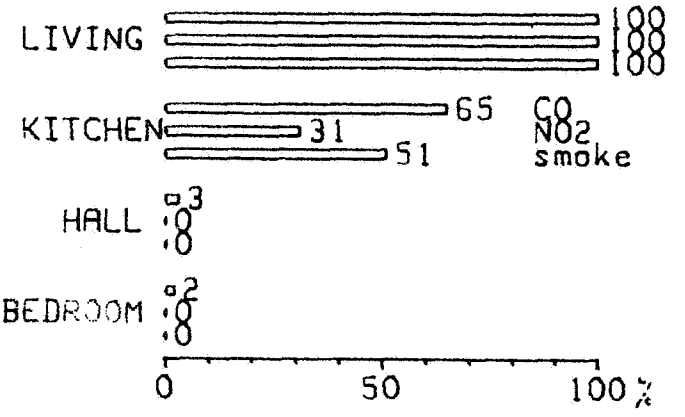

Figure 10. Warm water heating.

A second set of measurements has been held (Kornaat, 1990). Thereby Al_2O_3(97%) and TiO_2(2%) dust particles of 2 tot 14 μm (90%) have been injected into all rooms. The decay has been monitored with Tyndallometers which have their peak sensitivity between 2 to 5 μm. The theoretical velocity at which these particles will fall to the ground is about 2 mm/s.
Dust concentrations have been simulated for different conditions, as shown for the living room in Figure 11.

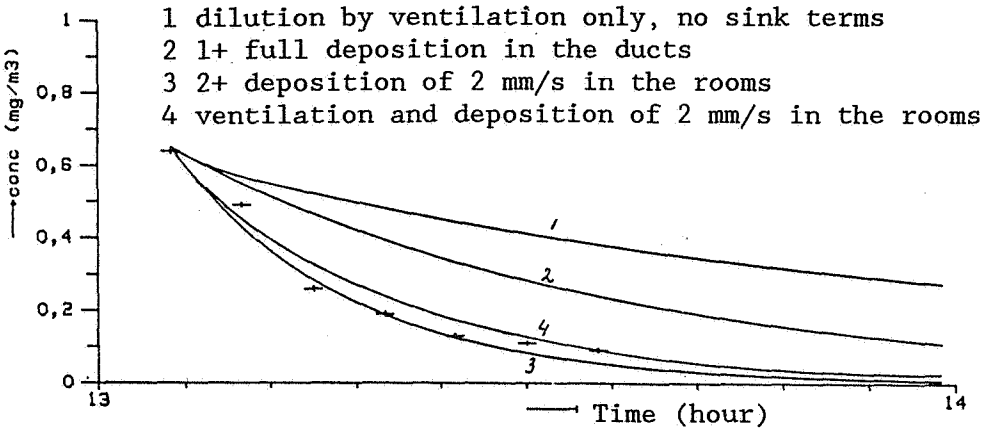

Figure 11. Measured and simulated decay of dust.

For the combination of "ventilation and full deposition in the ducts and a certain deposition velocity in the rooms" the influence of the deposition velocity in the simulations has been investigated. The deposition velocity has been set to: 1,2 and 4 mm/s, see figure 12.

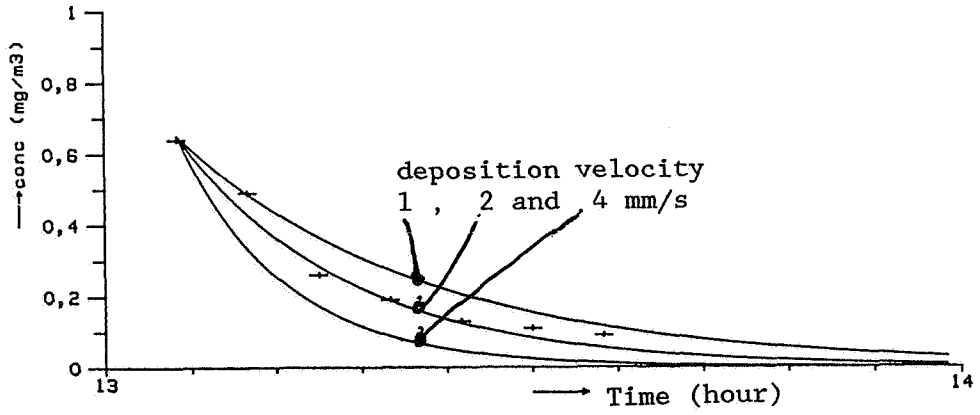

Figure 12. Measured and simulated decay of dust, varied deposition.

8. References

ASHRAE. 1989. Ventilation for Acceptable Indoor Quality. ASHRAE standard 62-1989. Atlanta, GA, USA.

Axley, J, 1988 a. Indoor air quality modelling. U.S. department of Commerce, NBS. Washington, USA. July 1988

Axley, J. 1988 b. Progress toward a general analytical method for predicting indoor air pollution in buildings. Indoor air quality modelling. Phase 3 report NBSIR 88-3814. NIST, Gaithersburg, MD, USA.

Brunekreef, B. and others 1982. Indoor carbon monoxide pollution in the Netherlands. Environment International, 8 (1982), 193-196.

Canadian Environmental Health Directorate, 1987. Exposure Guidelines for Residential Indoor Air Quality. Ottawa, Canada.

Collé, R. and McNall, P. E., Jr 1980. Radon in Buildings. NBS Special Publication 581. Washington, D.C. USA.

COST, 1989, NO_2 . Indoor pollution by NO_2 in European countries. COST project 613 Report 3. EC, Luxembourg.

COST, 1990. Indoor Air Pollution by Formaldehyde in European Countries. COST project 613, Report 7. EC, Luxembourg.

Daisey, J.M. and others, 1988. Efficiencies of portable air cleaners for removal of nitrogen dioxide and volatile organic compounds: Final report. LBL, Berkeley, USA.

Dijkum, P.H. Van, and others, 1986. Straling in het Leefmilieu. (report in Dutch. Radiation in the environment). Utrecht, NL: PEO

Elkhuizen. P.A. and others, 1990. Measurements of air borne moisture transport in a single family dwelling at Leidschendam. IBBC-TNO, B90-128. Delft, NL.

EPA, 1989 . Exposure Factors Handbook. EPA 600.8-89.043. Washington, D.C. USA.

Fanger, P.O., 1987. Introduction of the olf and the decipol units to quantify air pollution perceived by humans indoors and outdoors. Energy and Buildings, 12(1988) 1-6.

Feustel, H. 1990. Fundamentals of the multizone air flow model- COMIS. AIVC, Technote 29. Warwick, UK.

Gids, W.F. de and others 1988. Recirculation of air in dwellings. 9th AIVC Conference, paper 17. AIVC, Warwick, UK.

Godfish, 1988. Residential Formaldehyde Control by Mechanical Ventilation. Muncie, Indiana, USA: Applied Industrial Hygiene, Vol3, No. 3, March 1988.

Grot, R.A. and others, 1985. Validation of models for predicting formaldehyde concentrations in residences due to pressed wood products. U.S Department of Commerce, NBS. Washington, D.C. USA.

Hartless, R.P. 1990. BREVENT - a Ventilation Model. Building Research Establishment. UK.

Hodgson, A.T, and others 1989. Source strengths and sources of volatile organic compounds in a new office building. Air and Waste Managenment Association. 82 meeting. Paper 89-80.7. June 1989, Anaheim, CA, USA.

IEA ANNEX 9, 1987. Minimum Ventilation Rates. Uhldingen, Germany :Stephanus Druck.

IEA ANNEX 14, 1990. Condensation and Energy. Volume 2 . Guidelines & Practice. Leuven (B): ACCO.

IEA ANNEX 18, 1990. Demand Controlled Ventilating System. State of the Art Review. Stockholm, Sweden: Swedish Council for Building Research.

Jones,R. , 1990. Modelling water vapour pressure conditions in an enclosed space. BRE, CIB conference, Rotterdam, NL

Knoll, B. , 1984. Energiezuinige scholen in Almere. (report in Dutch. Energy efficient schools in Almere). IMG-Rapport C553, TNO, Delft, NL

Kornaat, W. 1990. Invloed van luchtverwarming op stofconcentraties in de binnenlucht. (report in Dutch. Influence of air heating on particle concentrations in the indoor air.) MT-TNO, R 89/298. Delft, NL

Lanting, R. , 1990 a. Selectie van chemische agentia in het binnenmilieu t.b.v kwantitatieve risicoschatting (report in Dutch. Selection of chemical agens in the indoor environment for quantitative risk estimation.) Gabimil: Deelprojekt1. MT-TNO, Delft NL.

Lanting, R.W. 1990 b . Air pollution in archives and museums, its pathways and control. MT-TNO, P90/015. Delft, NL

Lanting, R. , 1991 . Depositie snelheden van gassen en deeltjes in het binnenmilieu. (report in Dutch. Deposition velocities of gasses and particles in the indoor environment). TNO-Bouw, Delft, NL.

Levin, H, 1992. Critical building design factors for indoor air quality and climate: current status and predicted trends. Indoor Air,Vol 1, No 1, March 1991, Copenhagen, Denmark.

MCMurry, P.H. and others, 1985. Air and aerosol infiltration in homes. ASHRAE transactions, part 1, 1985

Meyer, B. 1983. Indoor Air Quality. Massachusetts, USA: Addison-Wesley.

Oldengarm, J. and others, 1990. Field experiments on airborne moisture transport. Paper I-22. CIB, Rotterdam, NL

Jansen, J. and others, 1987. Onderzoek naar de invloed van files op de emissie van NO_x , NO_2 en CO en de luchtkwaliteit op en rond de weg.(report in Dutch. Influence of traffic jams on the emission of ... on and near the road) R87/235 MT-TNO, Delft, NL

Roed, J. and A.J.H. Goddard, 1990. Ingress of radioactive material into dwellings. Seminar on Methods and Codes for Assessing Offsite Consequences of Nuclear Incidents. CEC, Athens, Greece. May 7-11, 1990.

Steel, F. 1982. Airtight Houses and Carbon Monoxide Poisoning. Canadian Building Digest. Ottawa Canada.

Traynor, G.W and others, 1985.Indoor air pollution due to emissions from unvented gas-fired space heaters. Air Pollution Control Association Volume 35 No.3 . USA.

Trepte, L and F. Haberda, 1989. Minimum ventilation rates and measures for controlling indoor air quality. AIVC, Technote 26. Warwick, UK.

Vandaele, L. 1989. Air change rate and pollutant distribution in an attic space. Results of summer time measurements. First draft. BBRI Brussels, Belgium.

Wal, J.F. van der, 1991. Onderzoek naar de emissie van vluchtige organische verbindingen uit materialen. (report in Dutch. Investigation of the emission of VOC's from materials). TNO-Bouw, Delft, NL.

AIR MOVEMENT & VENTILATION CONTROL WITHIN BUILDINGS

12th AIVC Conference, Ottawa, Canada
24-27 September, 1991

PAPER 8

Source Book Presentation of Annex 18 - Demand Controlled Ventilating System

Lars Goran Mansson* and Sven A. Svennberg**

* LGM Consult AB
Adler Salvius vag 87
S-146 00 Tullinge

**RAMAS Teknik AB
Solkraftsvagen 25
S-135 70 Stockholm
Sweden

ABSTRACT

An overall presentation will be given of the final report from Annex 18 - DCV systems. Based on state of the art review and test cases the experts are proposing DCV-systems in various building types.

The presentation will be focused on strategies and pre-requisites and on DCV-systems in the building types not presented separately.

AIR MOVEMENT & VENTILATION CONTROL WITHIN BUILDINGS

12th AIVC Conference, Ottawa, Canada
24-27 September, 1991

PAPER 9

DEMAND CONTROLLED VENTILATION - AN APPLICATION TO AUDITORIA

M. Zamboni, O. Berchtold, Ch. Filleux, J. Fehlmann*),
F. Drangsholt**)

Basler & Hofmann, Consulting Engineers, Forchstrasse 395,
8029 Zürich (CH)

*) Dept. of Hygiene and Applied Physiology, Fed. Institute of Technology, Zürich (CH)

**) SINTEF, VVS Divisjion, Trondheim (N)

1. SYNOPSIS

This paper is based on field measurements in auditoria which were carried out in Norway and in Switzerland. In both cases carbon dioxide (CO_2) was chosen as the relevant indicator to establish ventilation demand.

Investigations in Norway focus on the aspects of air flow patterns, ventilation efficiency and air quality. Intensive monitoring and numerical calculations with the computer code KAMELEON were performed.

The Swiss project puts more emphasis on impacts of demand control on energy consumtion and occupant response. The results of the field measurements, of the questioning of occupants as well as of simulations which were carried out with the simulation code TRNSYS are presented.

Results show that demand control with CO_2 as indicator for ventilating demand can maintain an acceptable indoor climate while allowing substantial energy savings.

These investigations were conducted as part of the IEA research programme "Annex 18: Demand Controlled Ventilating Systems".

2. INTRODUCTION

The principle aim of demand control of ventilating systems is to achieve energy savings by reducing operation time und air flow rate of the ventilating system without indangering an acceptable indoor climate. Ventilation demand can be caused by heat sources (e.g. persons, sun) or different pollutant sources within or outside the room.

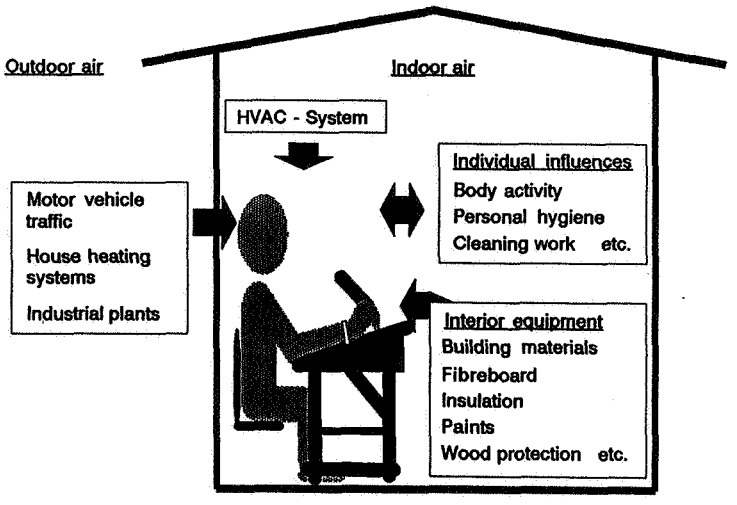

Fig. 1: Different sources of pollutants in auditoria

In auditoria, like in any other building, it is very important to eliminate or at least reduce pollutants caused by the interior equipment or the ventilating system.
Auditoria differ from other rooms in the way that all the remaining main influences on indoor climate are directly caused by the number of occupants. Usually auditoria are non-smoking areas.

Therefore only "pollutants" that are directly caused by the presence of people and correlate well with the perceived indoor climate can be used for demand control in auditoria.

The concentration of carbon dioxide (CO_2) in the room air is a good indicator for ventilation demand in auditoria since the CO_2 concentration in the room air correlates well with perceived indoor air quality and the occupants are the only relevant source of CO_2 ($C_{outside}$ = 360 ppm; C_{breath} = 40'000 ppm).

Other indicators could also be used to establish ventilation demand but have serious disadvantages:

- *presence, motion*: does not indicate the number of occupants, therefore the needed air flow can not be established; could be used to cut off superfluous operating time
- *humidity*: wide range of comfort inside which only a weak correlation with perceived indoor climate can be observed
- *temperature*: important to be held within certain limits; dynamic behavior (and thus correlation with perceived air quality) is strongly dependent on building construction; can be combined with CO_2 control
- *volatile organic compounds*: still uncertainties about which substances can/should be measured; poorly defined comfort range; better suited for smoking areas

3. CASE STUDY IN TRONDHEIM

3.1 Object description

The auditorium EL5 is located at the University of Trondheim, NTH. It has a floor area of 340 m^2 and a seating capacity of 320 persons. The room volume is about 1'600 m^3. The height-difference between the seats in front of the room and those at the back is about 3 m.

Back and side walls are made of light concrete. Front wall, floor and intermediate ceiling are made of wood. Since the auditorium is placed within the building and doesn't have any direct contact to the outside it has no transmission losses.

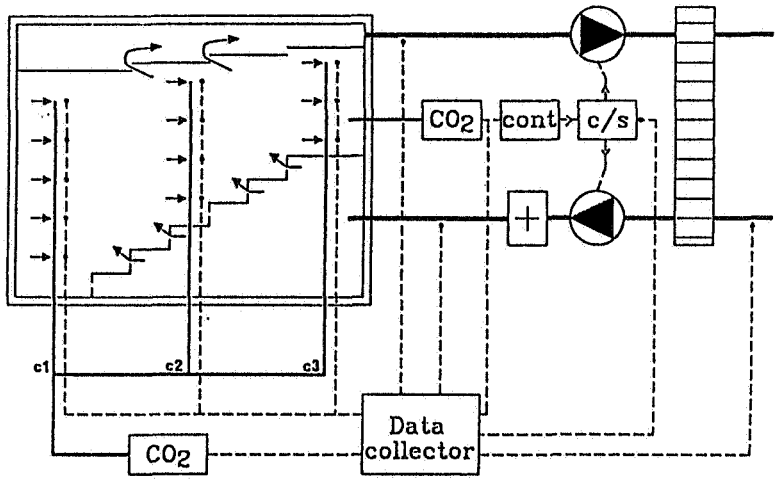

Fig. 2: Sketch of the ventilating system with placement of sensors (column 1 - column 3) and data aquisition

The auditorium is ventilated by displacement ventilation with inlets under the seats and outlets in the ceiling. For this field study rpm controlled fans were installed. The air flow may vary between 0 and 10'000 m^3/h. The air flow can be adjusted manually or controlled with a sensor.

3.2 Monitoring programme

Investigated control strategies

a) Time control
Before activating the demand control CO_2 measurements were carried out with constant air flow. The air flow was set to 10'000 m^3/h which is equivalent to an air change rate of 6.25 h^{-1} or 30 m^3/h and person.

b) Demand control according to CO_2 concentration
During operation with demand control a basic ventilation rate of about 2'600 m^3/h was adopted. Dependant on CO_2 production due to occupancy the air flow could be raised to a maximum of 10'000 m^3/h. The set point for CO_2 concentration was set to 1'000 ppm and the controlling CO_2 sensor was placed on column 2 (mid-height of the room) at 1.1 m from the floor level.

Monitoring periods

Monitoring and tests have been carried out at different person loads during selected periods through 1990 and winter 1990/91.

Monitored parameters

The data aquisition system was built around a micro computer which handles a mechanical multiplexer with 30 channels for gas samples, 30 analog inputs for humidity, temperature and gas sensors, 30 channels for thermocouples and 16 channels for sensors with pulse output (velocity).

Inside the auditorium the sensors were placed on three measuring columns which were situated on three different levels (see also Fig. 2). Three measuring spots located at the side walls cover the boundary conditions. Every measuring spot includes sensors for CO_2, temperature and relative humidity.

column	channel	location in cm above floor level
column 1	1-8	10, 60, 110, 170, 250, 350, 450, 550
column 2	9-15	10, 60, 110, 170, 250, 350, 450
column 3	16-19	10, 60, 110, 170
	20-22	left wall
	24	outside conditions
	25	supply air
	26	exhaust air

Tab. 1: Location of sensors

With this set up of the measuring equipment temperature, relative humidity and CO_2 concentration cannot be measured simultaneously.

3.3 Results

Performance of the ventilating system

The capability to bring fresh air to and to remove contaminants from the occupied zone is of great importance when evaluating the performance of the ventilating system. Tracer gas technique was used to establish ventilation effectiveness ($<\varepsilon_v>$), local ventilation indexes (ε_v), air change efficiency ($<\varepsilon_a>$) and local air change indexes (ε_i).
Ventilation efficiency and local ventilation index were measured using CO_2 dissipation from the occupants as tracer gas. Air change efficiency and local air change indexes were measured by step injection of tracer gas (N_2O) into the supply air duct.

Ventilation rate	5'000 m³/h			12'000 m³/h		
Nr. of occupants	0	130	220	0	150	240
$<\varepsilon_a>$	0.63	0.65	0.63	0.62	0.57	0.59
ε_i at column 1/1.1m	1.77	0.83	1.01	1.18	0.96	0.88
ε_i at column 1/1.7m	0.86	0.69	0.84	1.13	1.00	0.85
ε_i at column 2/1.1m	1.61	1.00	1.41	1.65	1.54	1.28
ε_i at column 2/1.7m	1.47	0.85	1.09	1.64	1.22	1.29
ε_i at column 3/1.1m	0.63	0.67	0.94	0.74	1.02	0.85
ε_i at column 3/1.7m	0.69	0.91	1.06	0.92	1.42	1.01

Tab. 2: Air change efficiency $<\varepsilon_a>$ and local air change indexes (ε_i) at 1.1 m and 1.7 m from floor level

The results for the air change efficiency show that the air distribution is better than the ideal value for complete mixing ($<\varepsilon_a>=0.5$). It is difficult to get a trend from the measurements of local air change indexes since these results are influenced by by the seats chosen by the occupants even if the number of persons is the same.

Indoor climate

As expected for a displacement ventilation system the highest CO_2 concentrations were registered at the top of the auditorium (column 3). Figure 3 shows that while the system was operated based on demand control CO_2 concentrations between 1'000 and 1'500 ppm were registered in the middle of the auditorium (column 2).

The comparison of the values for temperature, relative humidity and CO_2 which were monitored under similar operating conditions shows that also temperature and humidity can be used as an indicator for occupancy. But since changes are quite small compared to the comfort range these parameters are not equally suited for demand control as CO_2.

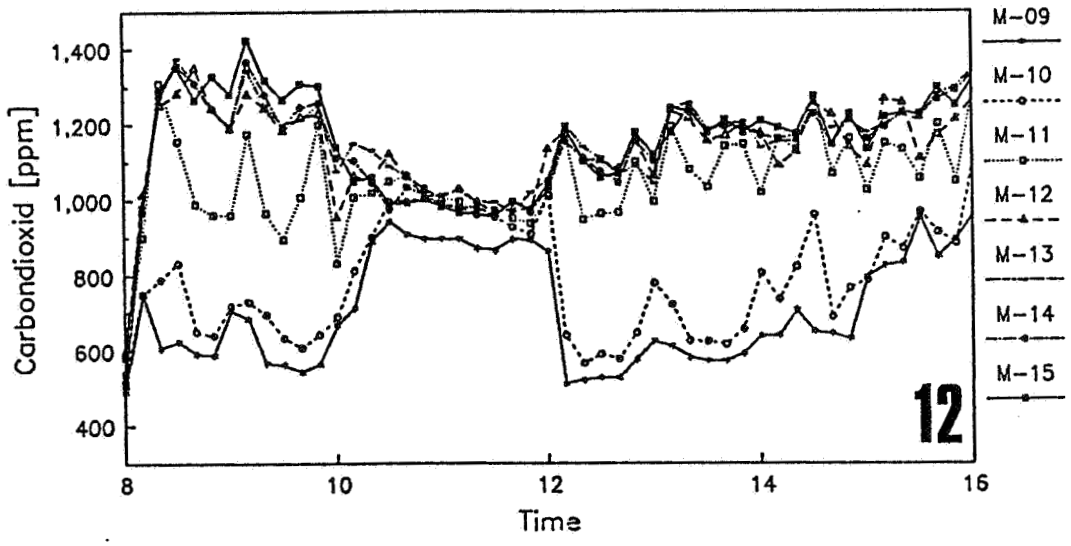

Fig. 3: CO_2 concentrations under CO_2 control (column 2 in the middle of the auditorium)

Measurements of dust concentration in the exhaust air showed that it is the movement of the arriving and leaving students that raises the dust.

Computer simulations

Temperature, velocity and mass fraction fields were calculated using the computer code KAMELEON which was developed at SINTEF. Figure 4 shows the mass fraction field for CO_2 in a vertical section.

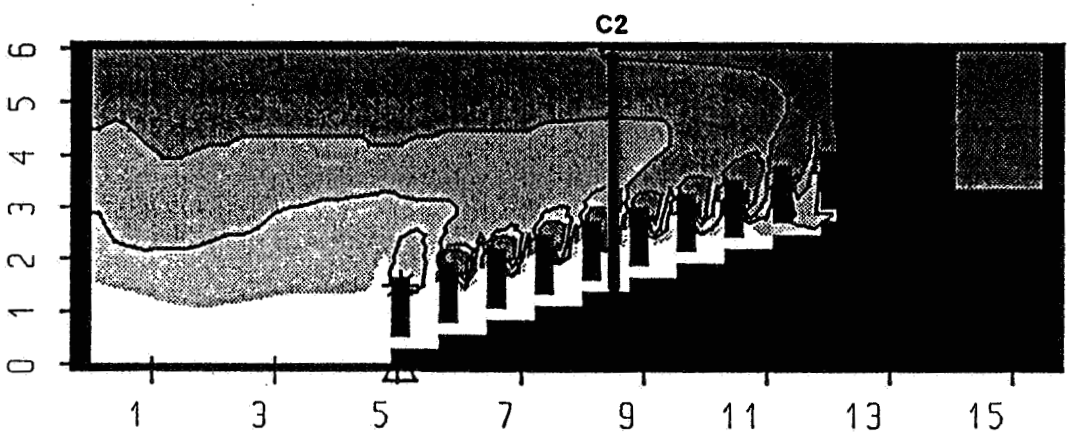

Fig. 4: Mass fraction field for CO_2 including column 2 (room fully occupied)

Measurements and numerical fluid dynamics techniques show that the air flow pattern in the auditorium is very complex. Due to this fact air quality and thermal comfort in the occupied zone are not uniform. Depending on occupancy and distribution some zones have stratification of pollutants and temperature while others are mixed.

4. CASE STUDY IN ZÜRICH

4.1 Object description

The investigated room is one of the smaller auditoria at the Swiss Federal Institute of Technology in Zürich. It has an area of about 120 m^2 and a capacity of 80 persons. The auditorium is situated in a corner of the main building and has windows on one side and at the rear. Because of the near traffic these windows have to be kept closed at all times.

The occupancy of the auditorium is subject to large fluctuations. The room is often used but usually not more than 20 persons are present.

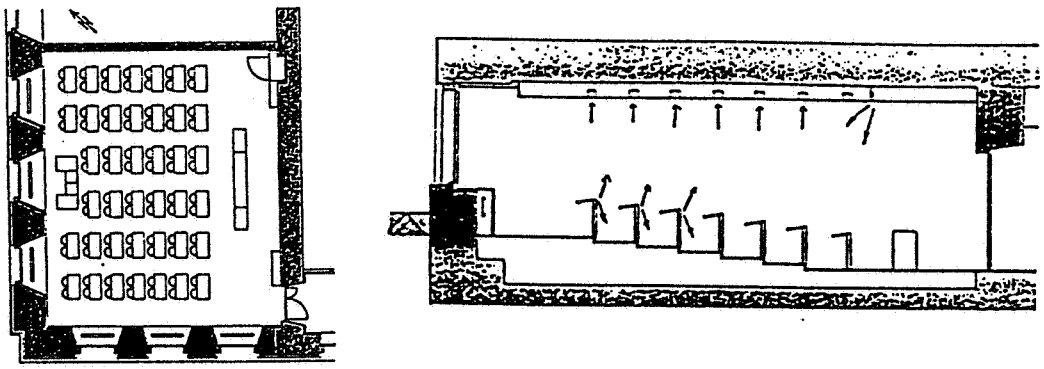

Fig. 5: Ground-plan and sectional view of the auditorium HG D 16.2

The walls of the auditorium are heavily built but poorly insulated. Floor and ceiling consist of lightweight constructions. The floor of the auditorium rises towards the back of the room but the elevation is not significant (1 m).

The auditorium is equipped with a balanced ventilating system with heat recovery (wheel). The ventilating system supplies air only to this room. The supply air can be heated or cooled and enters the room at the desks (85%) and through ceiling diffusers over the catheder (15%). The exhaust air is removed through ceiling slots.

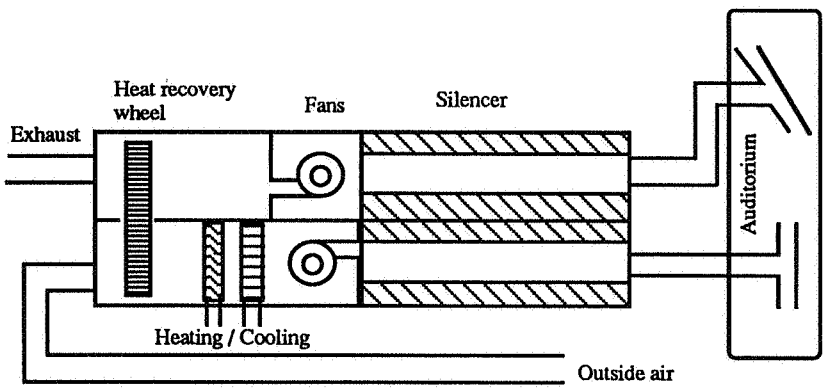

Fig. 6: Sketch of the ventilating system

Both fans have two steps but since no adequate control parameter was available the system was always operated on step 2.

Convectors with thermostatic valves are placed below every window and keep the room temperature at an almost constant level.

4.2 Monitoring programme

Investigated control strategies

a) Time clock control
All the heating and ventilating systems of the main building are connected to a centralized control and monitoring system. In the investigated room this system controls room und supply air temperature and running time. Room and supply air temperature are controlled according to the outside temperature. The running time can be programmed according to the expected occupancy of the room but usually the ventilating system is running on step 2 from 7:00 until 19:00.

b) Demand control according to CO_2 concentration
The temperature control of room und supply air was left unchanged. Only running time and step choice are now controlled by a CO_2 sensor.
Every morning before people arrive the auditorium is ventilated for half an hour at maximum air flow (time clock control: 7:30 - 8:00). At 8:00 CO_2 sensor control takes over until 22:00 when the whole system is turned off.
For comfort reasons the ventilating system would also be turned on if the room air temperature rises above a certain level (27°C).

During demand controlled operation the fans are turned on / off according to the following values for CO_2 concentration or room air temperature:

CO_2 concentration	room air temperature	operation
> 750 ppm	> 27 °C	step 1 on
< 600 ppm	< 26 °C	step 1 off
> 1'300 ppm	> 28 °C	step 2 on
> 1'100 ppm	< 27 °C	step 2 off

Tab. 3: Treshold values for step control

Monitoring periods

The system was monitored during two short periods of about one month in summer and one month in winter. During both monitoring periods the system was operated alternatively with one of the control strategies mentioned above. The evaluation of the aquired data is based on the period of one week during summer/winter and time control/CO_2 control respectively.

Monitored parameters

The monitoring focused on the parameters which are relevant for the assessment of:
- energy consumption of the system
- indoor climate in the auditorium

During the monitoring periods all users of the auditorium were questioned about their perception of indoor climate. The questions focused on perceived temperatures, air quality and draft. The room occupants were asked to answer the questions both when entering and before leaving the room.

The first aspect (energy) concentrated on measurements within the ventilating system: air and water temperatures, mass flow in heating and cooling coils, etc..
The second aspect (indoor climate) lead to the monitoring of the following parameters inside the auditorium: air temperatures, CO_2, air quality, humidity. The sensors were placed near the front desk, near the projection desk at the back of the auditorium and on one seat in the middle of the room.

Used sensors

Parameter	Sensor	Application	Measuring range / Output signal
CO_2	Leybold, BINOS 100 NDIR	room air	0 - 5'000 ppm
	Sauter, EGQ 10 F001	room air	0 - 2'000 ppm
	Sauter, EGQ 10 F003	exhaust and supply air	0 - 2'000 ppm
	Aritron, AROX 425A	room air	0 - 2'000 ppm
IAQ	Stäfa control systems, FRA-Q1	room air	10 - 0 V
	Sauter, EGQ 1	room air	0 - 10 V
Motion	Stäfa Control systems, FRA-B2	room	0 / 10 V
Humidity	Rotronic, YA-100	room air	0 - 1 V
Temperatures	Resistance thermometers, PT 100		

Tab.4: Used sensors

To avoid problems of accuracy caused by commercial CO_2 sensors the BINOS 100 NDIR gas-analyzer was used for system control. The values of the commercial CO_2 sensors were monitored for comparison.

4.3 Results

Preliminary measurements

No recirculation of exhaust air was planned. Tracer gas measurements [1] showed a recirculation through the heat exchanger of almost 40 %.

This serious recirculation is caused by the position of the fans in respect to the recovery-wheel. Since the space in the installation room is very restricted the correct positioning of the fans (both fans on the suction side) was not possible.

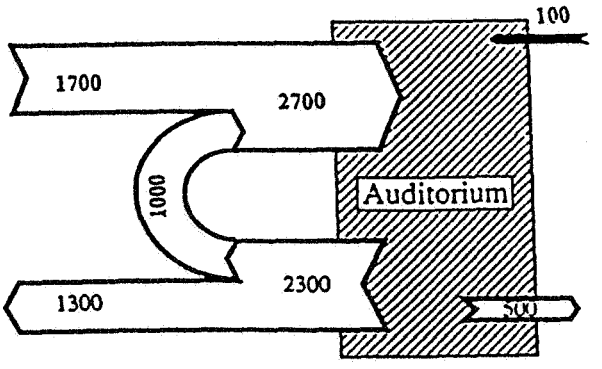

Fig. 7: Air flows during system operation on step 2 [kg/h]

Energy consumption

In both monitoring periods (summer and winter) the consumption of electricity could be reduced by 70 - 80 % due to demand control. These large energy savings are due to the fact that the room was poorly occupied and therefore the operation time of the system could be remarkably reduced. Step 2 was never used during demand control operation.
Even in summer the room air temperature never rose above the treshold value of 27 °C, which means that in practice the operation of the ventilating system was only controlled by the CO_2 sensor.
Cooling energy consumption in summer could be reduced by 75%.
Heating energy consumption was reduced by 15% although during the week with CO_2 control the average outside temperature was 6 K lower.

The following diagram shows the different operation times for two days with similar occupancy but different control strategies.

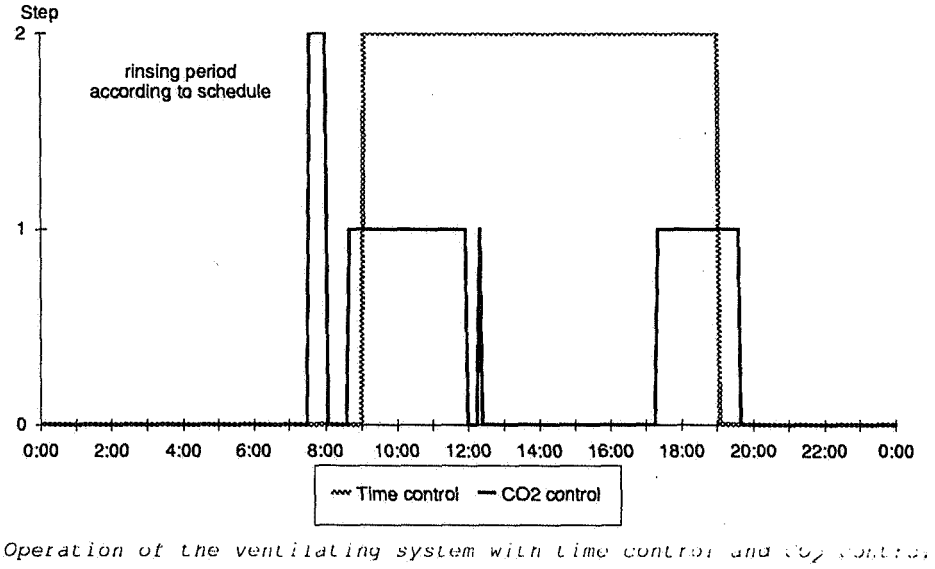

Fig. 8: Operation of the ventilating system with time control and CO_2 control (same weekday)

Indoor climate

The perception of draft and the acceptance of air temperature is directly connected with the operation time of the system. Since the operation time and the air change rate was much lower with CO_2 control (less draft) the perceived thermal comfort was definitely higher with CO_2 control.

On the other hand during the first monitoring period in summer air quality was considered to be slightly worse for system operation with CO_2 control. Figure 9a shows a clear tendency towards greater annoyance by odours.
Further questionning of the occupants showed that the source of odours were not the occupants themselves but bad smelling cleaning fluids which were used for the cleaning of the blackboard. The evaluation of the winter period when these cleaning fluids were avoided shows much better results for odour perception (Figure 9b).

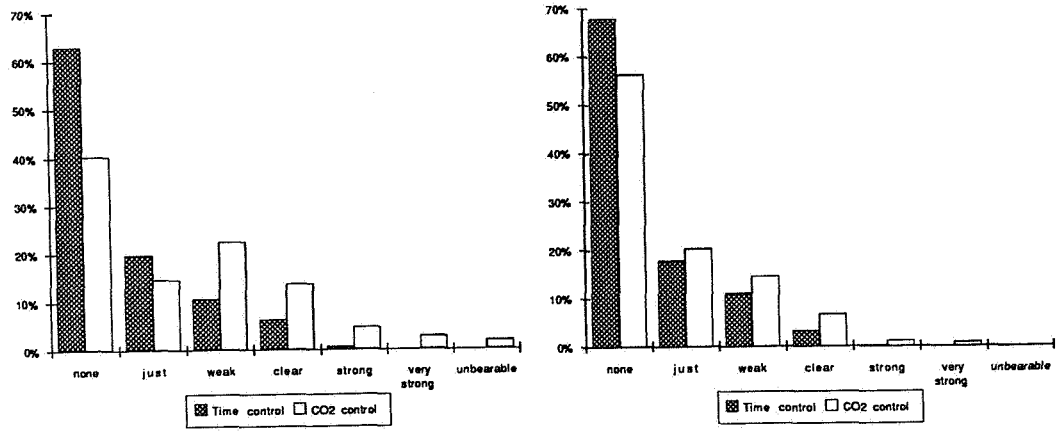

Fig. 9: Perceived odours during system operation with time control and CO_2 control (left: summer; right: winter)

Computer simulations

The short monitoring periods lead to a comparison of energy consumption based on one week's operation in summer and one week's operation in winter. This comparison strongly depends on the choice of the single week and and on the actual occupancy of the auditorium. Computer simulations can provide results both for
- annual performance comparisons (Fig. 10) and for
- different conditions of operation.(Fig. 11)

The computer simulations were performed with the simulation code TRNSYS. Thanks to the modular structure of TRNSYS a new module for the calculation of CO_2 concentration was easily integrated. This module is based on mass balance and dilution. The effect of imperfect mixing of supply air with room air is expressed by the introduction of a mixing factor γ (γ = 1 implies perfect mixing).

Operating conditions as monitored (treshold values, occupancy) were simulated on a yearly basis and showed important energy savings.

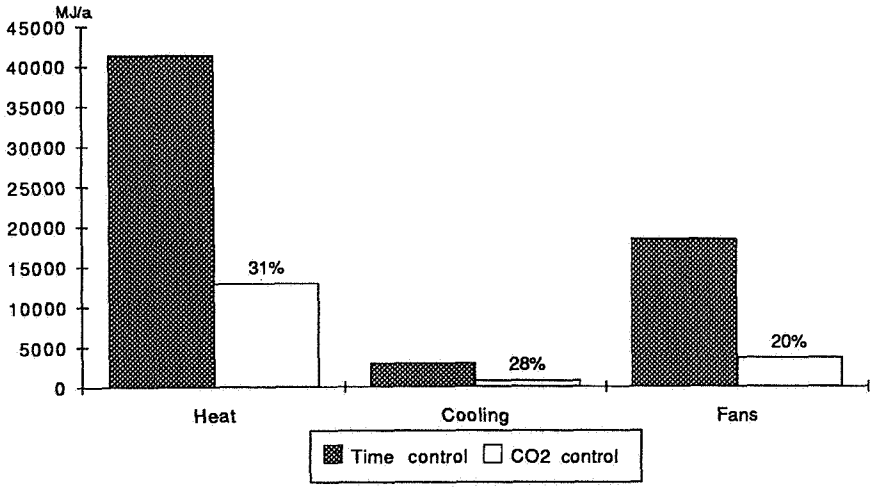

Fig.10: Calculated energy consumption for monitored operating conditions

Since energy consumption is strongly influenced by the choice of treshold values for step control and occupancy of the room these two parameters have been varied. Figure 11 shows the results of this parameters study.

- 100% occupancy corresponds to the presence of 80 persons between 8:00-12:00 and 13:00-18:00 (720 person hours / day)
- 100% treshold values means that step 1 is activated at 1'000 ppm, step 2 is activated at 1'500 ppm
- 100% energy consumption is equal to the energy consumption with time control, the same occupancy and the same max. air flow

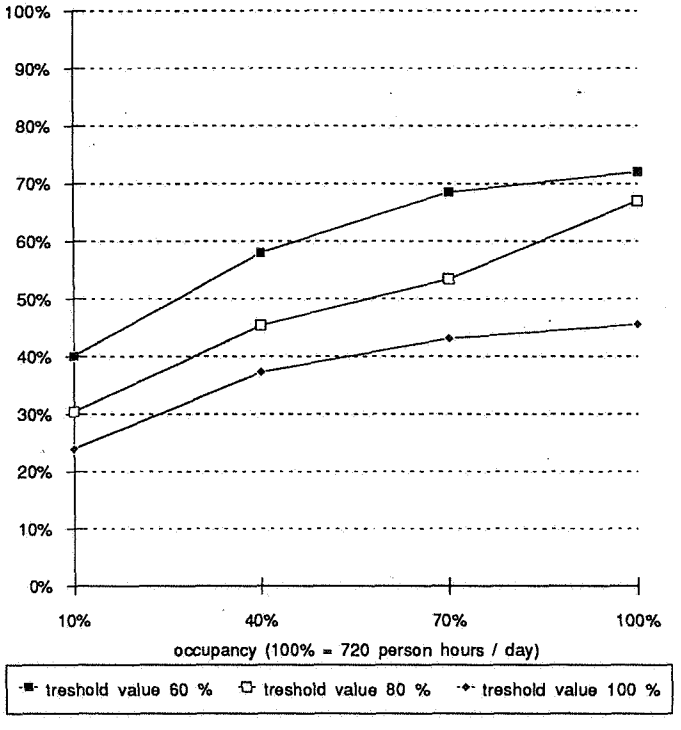

Fig.11: Annual heat energy demand for different control strategies and different occupancy

Similar savings were also achieved for cooling energy and electricity. The choice of treshold values is of great importance for

the achieved energy savings and has to be adapted according to the comfort needs of the occupants. High comfort standards lead to lower energy savings.
The energy savings for monitored conditions as shown in Fig. 10 correspond to an occupancy of 10% and chosen treshold values of approximatively 80%.

5. CONCLUSIONS

The results of the field measurements and simulations lead to the following conclusions:

- The experience from the case studies shows that CO_2 is very well suited for demand control of ventilating systems in auditoria.
- Important energy savings are possible without serious drawbacks for indoor climate.
- The effective energy savings depend strongly on occupancy and chosen comfort level but are very often in the range of at least 50 %. The highest energy savings were observed for heating energy.
- A combination of CO_2 control and temperature control is recommended for comfort reasons but doesn't have a strong impact on energy consumption
- The elimination of other pollutant sources (e.g. cleaning fluids) is very important for the concept of demand control
- Today's quality of commercially available CO_2 sensors is sufficient for a widespread application. A small security margin is recommended when choosing the treshold values. This margin has only a small influence on energy consumption.
- The choice of control strategy has to be in accordance with the planned ventilating system:

a) *Displacement ventilation with variable air volume*: a minimum ventilation rate should be guaranteed to remove the remaining pollution from building materials etc.; the ventilation rate can then be raised according to the presence of people (measured CO_2 concentration); the CO_2 sensor can be placed in the exhaust duct.

b) *Mixing ventilation with steps*: a periodical rinsing of the room (e.g. every morning) should be adopted to remove the remaining pollution from building materials etc.; the step control of the system is based on the measured CO_2 concentration; CO_2 sensor should be placed in the room.

6. ACKNOLEDGEMENTS

The Norwegian contribution was supported by the Royal Norwegian Council for Scientific and Industrial Research (NTNF).
The Swiss contribution was supported by the Swiss Federal Office of Energy (BEW).

7. REFERENCES

1. ROULET C.-A., COMPAGNON R., JAKOB M.
"Planning of experiments to measure ventilation efficiencies";
Laboratoire d'énergie solaire et physique du bâtiment;
Lausanne; 1990

Ref #NO 5251 Demand controlled ventilation systems in office buildings.

Author AUTHOR Davidge B, Vaculik F

Bibinf BIBINF UK, AIVC 12th Conference, "Air Movement and Ventilation Control within Buildings", held 24-27 September 1991, Ottawa, Canada, proceedings published September 1991, Volume 1, pp 157-172. #DATE 00:09:1991 in English

Abstract ABSTRACT This paper illustrates the principles of demand controlled ventilation systems (DCV) as applied to office buildings. Appropriate ventilation approaches and control strategies are demonstrated in this paper for small area control (ieboardrooms) and for office buildings as a whole. Findings are illustrated by the results of field experiments. Impacts on energy consumption, indoor air quality and occupant response are examined. General conclusions and recommendations applicable to similar building types are also presented. The principles presented are applicable only to spaces where the dominant pollutants are generated by the occupants. In many instances the potential energy savings resulting from active DCV systems willnot be large although the technique of monitoring and recording CO2 levels may lead to very significant benefits.

Keywords KEYWORDS demand controlled ventilation, office building, occupant reaction

AIR MOVEMENT & VENTILATION CONTROL WITHIN BUILDINGS

12th AIVC Conference, Ottawa, Canada
24-27 September, 1991

PAPER 10

Demand Controlled Ventilation Systems in Office Buildings

Bob Davidge

Public Works Canada

Synopsis: This paper illustrates the principles of demand controlled ventilation (DCV) systems as applied to office buildings. For the purposes of this paper, DCV systems are defined as ventilation systems where the fresh air flow rate is governed by a control system measuring air borne pollutants, keeping the level of concentration below a preset value. These principles were developed during the conduct of IEA Annex 18, Demand Controlled Ventilating Systems.

Appropriate ventilation approaches and control strategies are demonstrated in this paper for small area control (ie boardrooms) and for office buildings as a whole. Findings are illustrated by the results of field experiments.

Impacts on energy consumption, indoor air quality and occupant response are examined. General conclusions and recommendations applicable to similar building types are also presented.

The principles presented are applicable only to spaces where the dominant pollutants are generated by the occupants. In many instances the potential energy savings resulting from active DCV systems will not be large although the technique of monitoring and recording CO2 levels may lead to very significant benefits.

Primary Goals: The primary goals of DCV systems on office buildings are to:

a) guarantee a higher quality of interior environment,

b) save energy or

c) a combination of both.

It is often easy to add extra fresh air to a building, but at an extra energy penalty. The intent of this Annex was to ensure that energy expenditures were more effective by only adding fresh air when needed. It was hoped that overall fresh air ventilation rates could be reduced since a DCV system would reduce fresh air rates when it was not required. Alternatively, it was hoped that instead of ventilating at a constant rate even when not needed, the ventilation rate could be shaved during periods when not required and then this "saved" fresh air could be added back into the system when the need was large, improving the quality of the environment.

Applicability of DCV systems to Office Buildings: In order for DCV related energy savings to be significant in any building, it was found that several conditions must exist:

a) the fresh air rates must be variable,
b) the occupancy must be unpredictably variable,
c) the building must spend a very significant proportion of the year in a mode where fresh air is either heated or cooled or otherwise conditioned and
d) the density of occupancy in the areas controlled must be high and the emissions from other sources must be low.

The reasoning follows.

a) If the fresh (outdoor) rates are not variable, then control is not possible.

b) If the occupancy is not variable, then alternate technologies such as a constant ventilation rate controlled by a programmable controller (ie a time clock) would be simpler, cheaper and equally effective. If the variations in occupancy are predictable, then the control strategy need only be modified to include alternate levels of ventilation.

c) This point is self explanatory. If the air is not conditioned, then the savings will be low since we are only talking about fan energy.

d) Control of ventilation in office buildings will normally be according to CO2 levels which may be considered a surrogate measure of occupancy and occupant generated pollutants. If other pollutants predominate (ie outgassing from materials in a new building), then CO2 measurements no longer reflect the building's ventilation needs. Also the CO2 related ventilation rates may only be a very small portion of the total and in the case of a very strong pollution source, it may never be possible to add enough fresh air to create occupant satisfaction, even if very few people are present.

Appropriate DCV Strategies: DCV system strategies are driven by the same forces as normal ventilation strategies. In order to understand how a DCV strategy should be tailored to any specific building, the other factors influencing ventilation must be examined. These are code requirements, thermal control of the building and control of pollutants that the DCV ventilation system is not capable of sensing. To this end, two components of ventilation must be considered which are defined here as:

a) the base rate (ventilation that not controlled by the DCV system) and

b) the portion of the ventilation that is controlled according to measured demand.

The ventilation rate controlled by demand should be seen as a wave riding on top of the base rate.

Impact of "Free Cooling" Cycles: Figure 2 illustrates how the "free cooling" in many buildings will vary over the year.

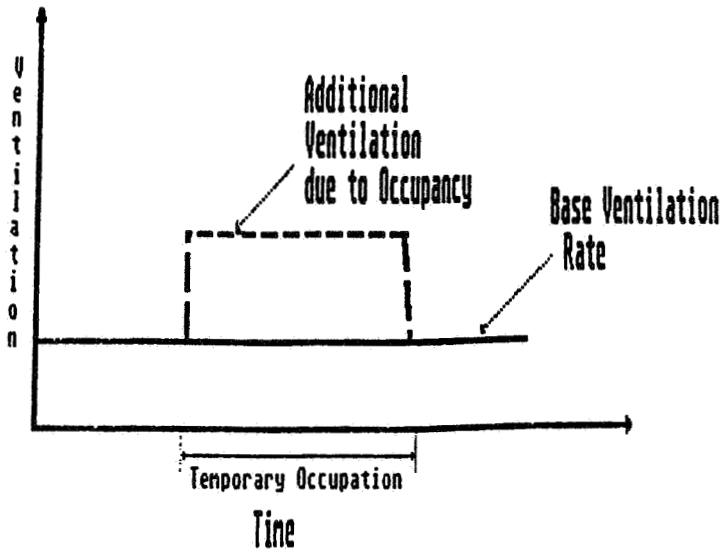

Figure 1

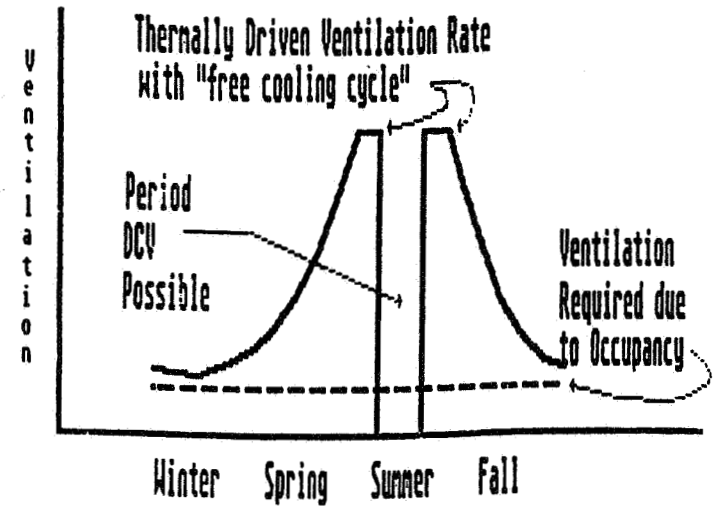

Figure 2

In order for DCV to be possible, the ventilation required for control of occupant generated pollutants must be larger than that required to cool the building. As the above diagram illustrates, this is not always the case. In the majority of large office buildings, free cooling ventilation requirements will negate any potential energy benefits from DCV systems during most of the year.

The appropriate design strategy for dealing with "free cooling" ventilation requirements is to give them precedence. When the building requires more outside air in order to save energy, it makes no sense except to receive it regardless of whether it is required to satisfy pollution purging requirements.

Impact of Air Leakage: At first glance, it might seem that in a leaky building, DCV is not possible and would not result in any benefits. This is not the case. Often in a leaky building, the mechanical ventilation strategy is based on the assumption that little or no leakage is present. Even under weather conditions where considerable leakage is present, the fresh air ventilation normally continues to function in its normal manner. If the CO2 levels are measured, then at times it may even be possible to turn the fresh air component off entirely.

The strategy illustrated in figure 3 for dealing with air leakage is to use the DCV system to monitor total effective ventilation rates and to reduce the controlled portion of ventilation as the leakage increases.

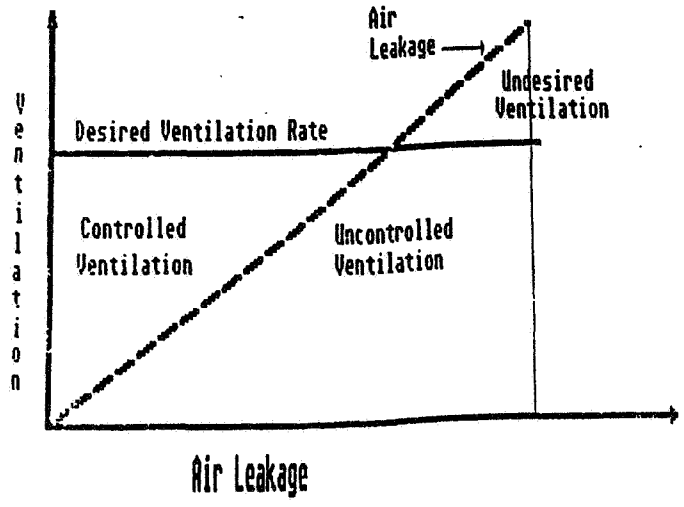

Figure 3

Of course, there is an even better strategy for dealing with air leakage: seal the building and then ventilate it properly. Uncontrolled air leakage often results in thermal control and comfort problems, building degradation due to condensation and may create air quality problems due to mould growth.

Impact of Other Pollutants: For the purposes of this paper, it is assumed that there are three basic categories of pollution sources:

a) building materials,
b) ventilation systems, and
c) people and their direct activities.

As will be seen, these three behave quite differently with respect to time. Their impact on any ventilation strategy must therefore be considered separately.

In the absence of other information, it has also been assumed that the requirements for ventilation resulting from various pollutants sources will be additive. It is acknowledged that the most effective means of dealing with pollutants is not by ventilation but by reducing source strengths. However, this will never be completely possible and significant pollutant sources of each category will always remain.

Building Materials: Building materials tend to emit pollutants at all times. They emit more when new and may sometimes work as a sponge, absorbing pollutants and odours during the day and releasing them at other times.

Often to save energy, building systems are turned off at night. Pollutants from building materials will build up. These must be at least partially cleared out before occupancy or the impression of the occupants will be that of a poorly ventilated building with stale air.

Unfortunately, these pollutants are generally difficult to measure and their source strengths are also difficult to predict. They must still be considered in any ventilation strategy whether related to a DCV system or not. In the case of a DCV system, the base ventilation rate must purge these contaminants.

The most usual strategy for dealing with these pollutants is to preventilate, flushing the building out just before occupancy. The amount of preventilation required will depend on the outgassing characteristics of the materials and the time that the pollutants have been left to build up. In general, new materials will require more preventilation as will longer unventilated periods such as weekends, especially if they are long or hot. Of course, some post ventilation after occupancy will also help.

Figure 4 illustrates the general concepts of how these pollutants will respond to a constant ventilation rate over a portion of the day. As you can see, the pollution levels will build overnight, perhaps eventually reaching a steady state level but will decay quickly once fresh air is introduced, perhaps eventually reaching

a much lower steady state level.

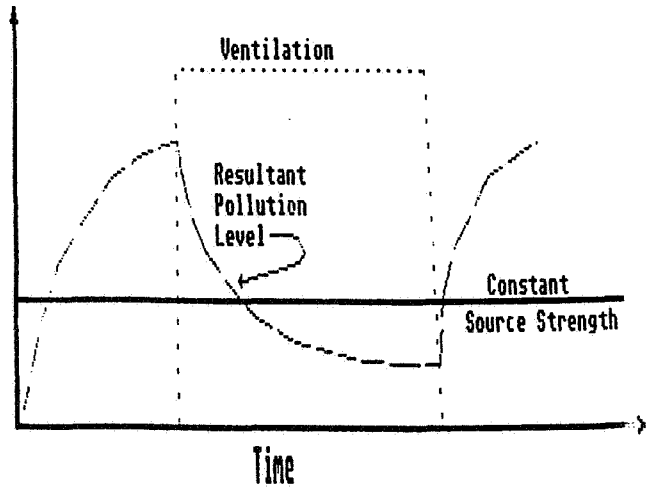

Figure 4

If the hours of occupancy are limited to certain general periods but are not precisely predictable, an alternate ventilation strategy exists. In this case, it is most effective to flush the area of concern quickly to rid it of accumulated pollutants and to then use a low base rate of ventilation to maintain these pollutants at a low level so that when occupancy does occur, the air quality will be judged as acceptable. An example of where this would be an appropriate strategy is a boardroom. It will generally be used only during working hours, but will tend to be occupied by different numbers of people at different times in an unpredictable manner.

Figures 5 and 6 illustrate the ventilation profile and resultant pollution concentrations with and without people present. In the second case, if the pollution concentrations rose too high, the ventilation rate could be stepped to the high level or perhaps to some intermediate setting. Where CO2 were used as a controlling contaminant in a boardroom, the whole building would be flushed early in the morning. A constant low rate of ventilation into the boardroom would serve to keep it as "fresh" as the rest of the building. A CO2 controller could cause extra ventilation in the room to come into play at some preset level such as 800 ppm. In this manner, the boardroom would always receive an acceptable rate of ventilation whether few or many people were present.

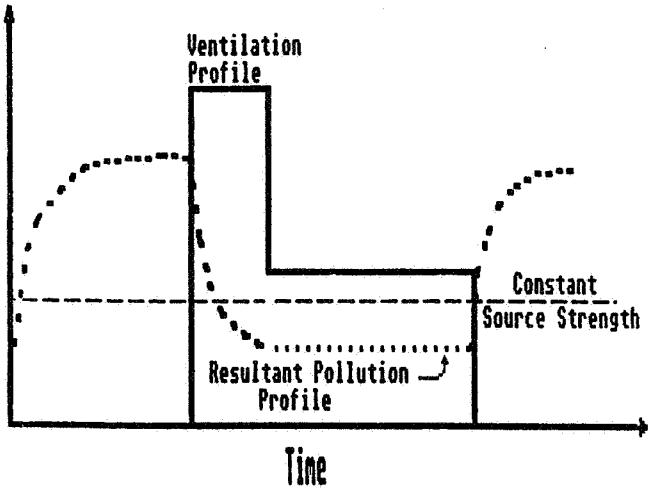

Figure 5

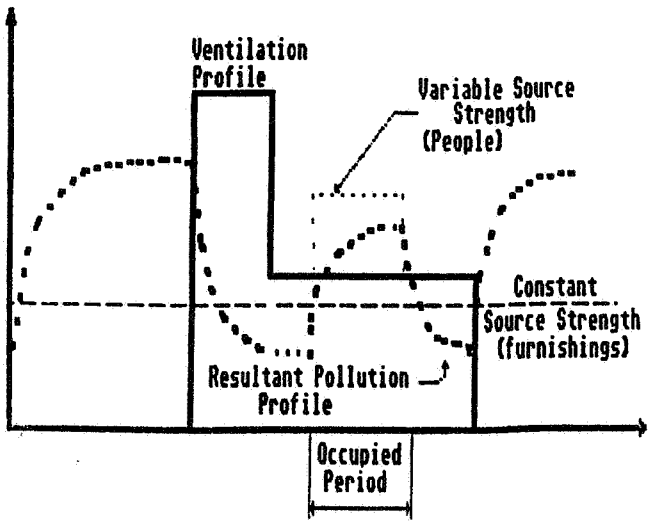

Figure 6

Of course, if the hours of occupancy are completely unpredictable, then it will be necessary to maintain a base rate of ventilation at all times if good IAQ is desired at all times. There are very few office buildings which fall into this category.

Ventilation system: The ventilation system itself may very often be a major source of building pollutants. It is assumed that the pollutants generated in the system itself should not enter the building except when the system is in operation. Like building materials related pollutants, these are very difficult to measure or to predict in terms of impact. They must be accounted for, however, in the base rate of ventilation.

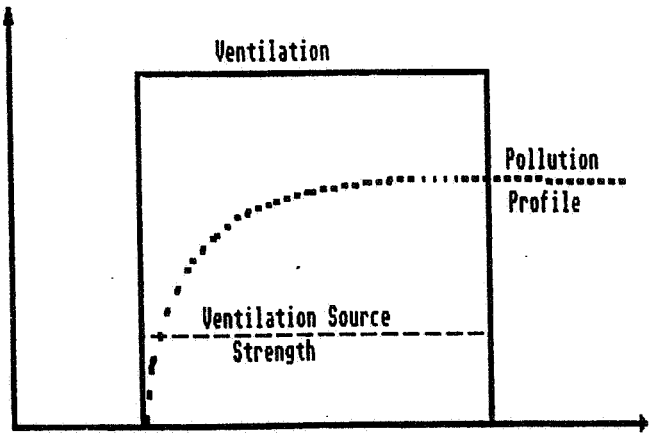

Figure 7

As illustrated in figure 7, the general strategy for dealing with these pollutants must be to eliminate or to reduce them or to increase the outdoor ventilation rate accordingly. Since a dirty ventilation system may produce biological contaminants, elimination as effectively as possible is the strongly preferred option.

Occupants and their Activities: By monitoring for the presence of people, we have a good chance of controlling occupant generated pollutants. Unfortunately, we have no guarantee that we will likewise control activity generated pollutants (ie photocopier effluents).

The most often used means of detecting occupants is to measure CO2. If we can assume their level of activity, we can get an idea of not

only when people are present, but how many there are. In addition, other pollutants and odours produced directly by the occupants themselves will tend to increase and decrease directly in proportion to the CO2 levels.

An alternate for measuring CO2 levels is to use motion detectors. Although these are readily available, reliable and inexpensive, they are limited since they do not detect the number of people present, nor do they sense presence if people are inactive for long periods.

If a constant fresh air ventilation rate is present, CO2 build-up will follow a curve similar in nature to that of the ventilation system pollutants. It will not start to increase until the occupants are present. In the building as a whole, it will rise over several hours, usually hitting a peak just before noon. If the area of concern is smaller (ie a boardroom or a classroom), then it will take much less time for a peak to be reached.

Ideally, a CO2 driven controller might take into consideration both the absolute level and the rate of rise of CO2 to calculate occupancy. In a small area where the peak level is attained quickly, control to shave peak levels only is often considered acceptable.

If we were concerned about controlling CO2 levels only, then we would not turn ventilation systems on until the building had been occupied for some period of time and the levels had risen to some preset value. Figure 8 illustrates this principle.

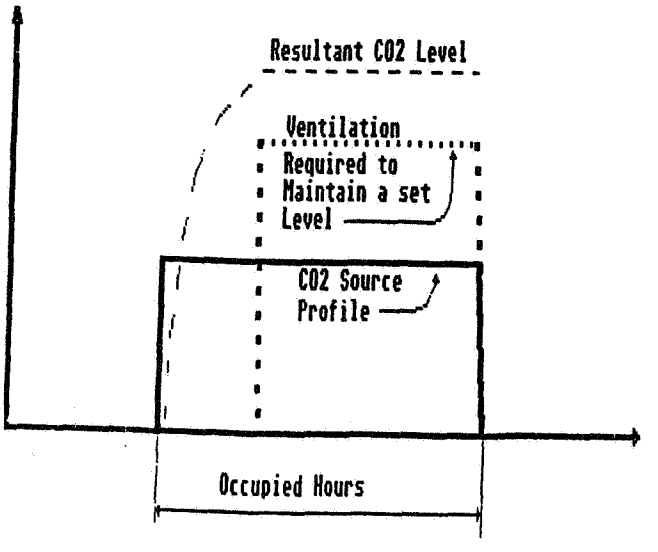

Figure 8

Of course, if we followed such a ventilation strategy in isolation, we would create great problems. We would be ignoring the predominant pollution and odour sources. High levels of complaint would be sure to follow. The design of a proper ventilation strategy must take all pollution sources and other ventilation requirements such as code and thermal control into consideration.

Combinations of Strategies: Taking the above into consideration, how do we arrive at an appropriate DCV strategy for any particular building?

a) DCV will not be possible most large office buildings during much of the year in cool climates. We must use this information when calculating possible benefits. During those portions of the year when "free cooling" is called for, its requirements must be given precedence.

b) A pre and post occupancy ventilation strategy must be chosen to purge building materials generated pollutants. In some cases, this will also require a steady ventilation rate even when no one is present just to ensure that the controlled are is reasonably "fresh" when occupants do arrive. This must be included in the base ventilation rate.

c) Ventilation systems generated pollutants must also be acknowledged in the choice of a base ventilation rate.

d) The DCV system may now be used to control additional ventilation according to occupancy.

Figure 9 shows how pollutants might build up and decay in a building with no people present. The ventilation rate is constant but is turned off at the beginning of time. As can be seen, the pollution levels initially build to a level higher than the desired pollution level. Once the building's ventilation system starts, contaminants drop to below the predetermined critical level.

In this case, some of the ventilation energy might be considered to be wasted since the environment is better than desired. It might be possible to reduce ventilation rates once the desired pollution levels have been attained, thereby saving energy. The following diagram shows how pollution levels might follow such a strategy. In the paragraphs which follow, the ventilation profile in this diagram is the base rate since it is the ventilation rate necessary to adequately control pollutants which are not monitored.

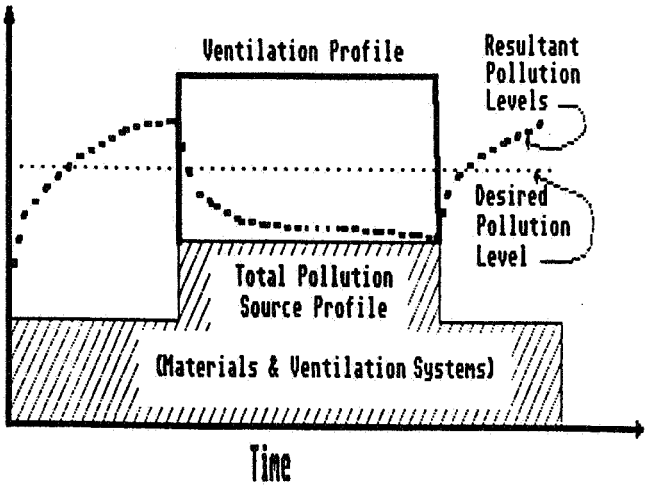

Figure 9

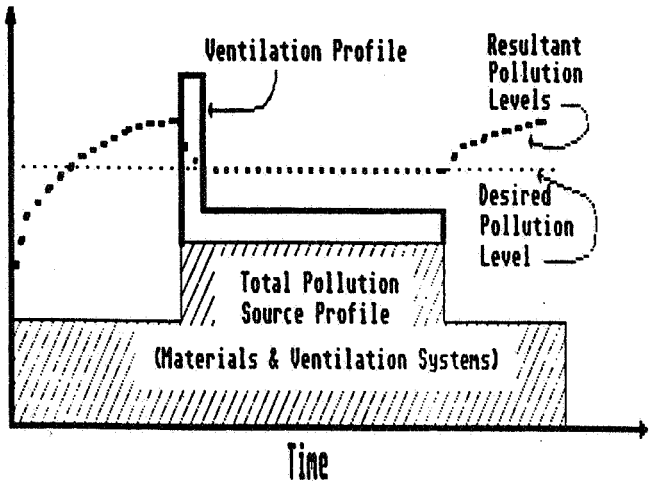

Figure 10

Of course, the building in this illustration is a good one. If the building is not clean or if it is new, the pollution levels may never drop to the desired pollution level depending on how it is defined. In this case, it will never be possible to reduce ventilation rates - in fact, if possible, they should be increased still further.

What happens to our example if we now add people? Figure 11 illustrates such an example. In this case, we have sufficient ventilation before occupancy that the occupants will think their building is fresh before they enter. The ventilation rate then drops to another level in this example at about the same time as the occupants arrive. This second level is higher than the base ventilation rate developed in figure 10. As a result, the materials and systems related pollutants will continue to drop as the occupant generated pollutants start to rise. If we could choose our ventilation rates perfectly, the two effects would counterbalance and the resultant total pollution level would remain exactly as desired. The building would be neither over nor under ventilated. In figure 11, ventilation continues after occupancy in order to help flush out remaining contaminants.

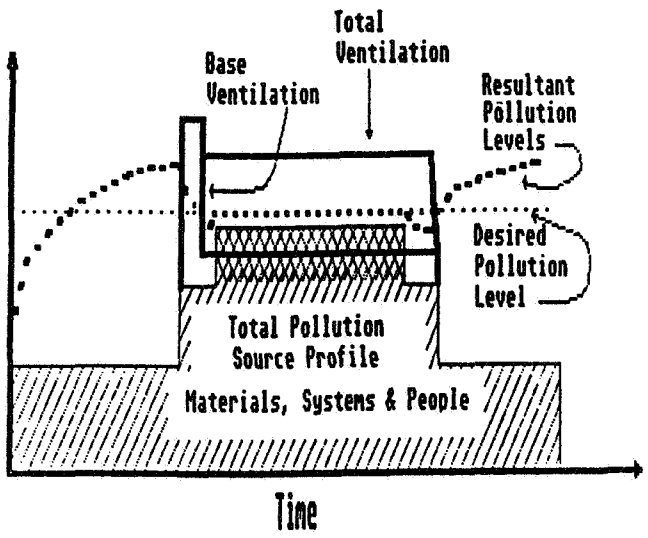

Figure 11

The above arguments have been presented without the inclusion of numbers in order to convey the general principles of DCV in office buildings. What happens when we look at "real life" examples? How significant are the pollutants generated by materials, ventilation

systems and the occupants? Unfortunately little is known about their relative values except from an odour point of view. Work by Fanger and Clausen has shown that in office buildings, the occupant generated portion of the odour load may normally be less than one third of the total.

Taking these factors into consideration, an analysis of many buildings will show that the DCV system may only control a relatively small portion of the ventilation for a relatively short period in the year.

Field Study - Whole Building Control: A CO2 driven DCV system was installed in a Canadian Office Building of about 30,000 m2 floor area in order to test the practicality of the DCV approach. The system was carefully commissioned and was verified to be fully capable of ensuring the building achieved desired ventilation rates (10 liters per second per person).

In fact, the system never controlled the building's ventilation rate. More air than 10 liters per second per person were supplied all year round. Outdoor temperatures were never low enough in the winter for the building to go off its "free cooling" cycle. In the summer, it was found that leakage past the fresh air dampers was more than sufficient to control CO2 levels. Since the warm months tend to coincide with summer holidays this may have been partially due to fewer people being present than expected. The net result was that CO2 based control was not possible. No energy savings could be achieved.

An analysis of CO2 data from other office buildings showed that this is normally the case in buildings with variable fresh air rates. It also shows that there is much more fresh air going into most buildings than is recognized. Simple measurement of CO2 levels and careful adjustment of dampers may lead to significant energy savings - with or without a CO2 driven DCV system. The monitoring of the CO2 levels may be very useful, however, as a means of proving that required ventilation levels were maintained. In the event of a dispute, this data could be very valuable.

Field Study - Board Room: A board room in a large Canadian office building was equipped with supplemental ventilation controlled alternately by a light switch, a motion sensor and a CO2 driven controller.

In all cases, the whole building was preventilated before occupancy to purge odours and a base ventilation rate existed even when no one was in the boardroom. Sometimes the light switch controlled the extra ventilation fan, sometimes the fan ran all the time regardless of the switch position and sometimes the fan was disconnected. In the case of the CO2 sensor, the fan was energized at 800 ppm CO2 and shut off at 600 ppm CO2. The occupants were not informed which mode of control was in operation.

A questionnaire was used to determine occupant response.

The findings indicated that in terms of air quality, the occupants could not distinguish if the fan was connected or not or if it was controlled by the motion sensor. They rated the CO2 driven system very highly - even better than when the extra ventilation was running continuously. It is hypothesized that this may be because they could sense the change whereas if the air quality only slowly got worse or remained the same, they could not tell and gave the system a medium rating. Interestingly, they were able to tell the difference in terms of thermal control.

Although the CO2 driven DCV system was rated highest, the air quality would have not been as good as when the fan ran all the time. At the current costs of controls, the CO2 driven DCV system would not pay for itself. An inexpensive and humane approach was to let the occupants turn the extra ventilation on themselves if they felt they needed it. It was found in practice that they did not turn the fan on unless a large number of people were present.

A disadvantage of the motion sensor system was that once people a meeting started, the sensor was no longer capable of detecting presence. Also, if even one person entered the room for a very short period of time, the fan would start up.

The manual and sensor driven DCV systems in this case resulted in energy savings since the fan was not energized when not needed. Since it exhausted into the return air plenum and did not bring extra fresh air into the building as a whole, the energy savings were not large.

Conclusions:

- CO2 driven DCV systems are technically feasible.
- In many buildings, they will not be cost effective.
- They provide no guarantee of good indoor air quality, since that is more dependant of other factors.
- In buildings with an existing computerized energy monitoring and control system, the addition of such a system may not be costly and, at the least, will serve as a warning when under or over ventilation exists and will provide a proof that code requirements were met.
- In boardrooms, CO2 driven systems worked and were well received by the occupants.
- In boardrooms, a manually controlled fan giving supplemental ventilation was responsibly used by the occupants, resulting in excellent environmental control for a low cost investment.

AIR MOVEMENT & VENTILATION CONTROL WITHIN BUILDINGS

12th AIVC Conference, Ottawa, Canada
24-27 September, 1991

PAPER 11

Dispersion pattern of contaminants in a displacement ventilated room - implications for demand control

H. Stymne, M. Sandberg, M. Mattsson

The National Swedish Institute for Building Research
P.O Box 785
S-801 29 GÄVLE
Sweden

Synopsis

A passive tracer gas technique has been used in an experimental study of the distribution of contaminants in a room with displacement ventilation. Humans are simulated by heated metallic bodies and the tracer concentration in the breathing zone (exposure) is shown to be greatly influenced by both the position of the tracer source and the air convection current around the bodies. It is shown that pollutants emitted close to a body are completely and directly transported to the upper mixed zone and not mixed into the lower zone. Pollutants emitted at a small heat source or close to a wall in the lower zone are transported to, but do not directly penetrate the boundary between the two zones, thus accumulating below the interface. By natural convection currents, occupants will draw uncontaminated air from the lower zone, and experience a better air quality at the breathing level than that of the surrounding air - even if the interface is below the head.

It is concluded that air quality demand control of the supply air flow rate is a suitable means of securing the excellent air quality possible in a displacement ventilated room. A carbon dioxide sensor should preferably be positioned, so that the interface height can be maintained at a level slightly above the head of the occupants.

1 Background

1.1 Demand controlled ventilation

Demand control of the ventilation rate can be used advantageously in rooms and buildings where there are large variations in the pollutant emission strength with time. The aim is to save energy by minimizing the ventilation flow rate. The principle is to adjust the ventilation flow rate to the minimum required to attain an acceptable air quality, irrespectively of the pollutant source strength. Automatic control requires the use of an air quality indicator as a feedback to the regulation system.

The energy savings which can be attained by demand control, come from reduced power for ventilation fans and reduced need for cooling or heating of un-necessary outdoor air. The indicator should reflect the variation in the total contaminant level, otherwise demand control may affect the air quality negatively. Demand control is especially well suited when people are the predominant pollution sources. The carbon dioxide concentration being a suitable indicator of air quality in this case.

In an ideal fully mixing ventilation system, all locations in a room have the same pollutant concentration. Therefore, there would be no problem of where to locate an air quality sensor. However, the mixing in real systems can be very non-uniform. (Stymne *et al* 1990). A room ventilated by displacement constitutes an extreme case of incomplete mixing. It is not therefore self-evident where to place the sensor in this case. The aim of this work is to gain information on how pollutants are distributed in a room ventilated by displacement, and to draw conclusions on the most appropriate location of a carbon dioxide sensor for demand control.

1.2 Principles for ventilation by displacement

Ventilation by displacement is a type of ventilation where the buoyancy forces (induced by heat sources) govern the air flow. Because the air flow is thermally driven, this type of ventilation functions satisfactorily only, when excess heat is to be removed. Low temperature ventilation air is supplied at the floor level, while the warmed air is extracted at the ceiling level. By this arrangement one obtains two zones in the room, one lower zone with uni-directional flow and one upper recirculation zone. With regard to the air quality the aim of this ventilation principle is to create supply air conditions in the occupied zone. This is in contrast to traditional mixing type ventilation, where the aim is to achieve extract air conditions in the whole space. In order to avoid comfort problems, the cool air is supplied to the occupied zone by low velocity diffusers. Thus, the air enters the room as a gravity current in contrast to the high velocity jet streams usually used in traditional mixing ventilation. Some general features of the displacement type of ventilation are summarized in fig. 1.

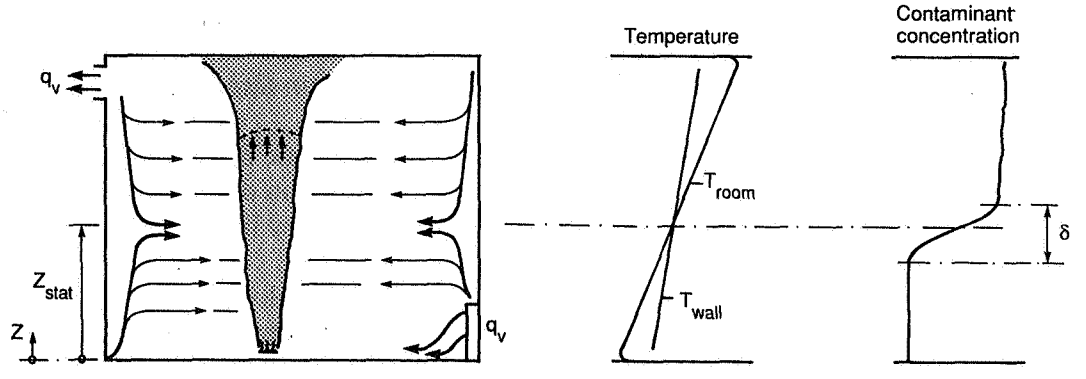

***Figure 1** Principle of ventilation by displacement*

It is shown in fig. 1 that although heat and pollutant have the same source in the lower part of the room, the temperature (density) stratification is continuous and nearly linear, whereas the vertical pollutant concentration profile shows a pronounced leap at a certain level. This difference in the distribution pattern is due to the fact that heat and contaminants are *not* transported by the same physical processes. Both are transported by a velocity field and by molecular diffusion. Heat, however, is also transported by radiation from warmer to colder room surfaces.

The velocity field in the room is set up by the vertical plume flow generated by the heat source. Surrounding air is entrained in the plume, and consequently the plume flow increases with height.

It is illustrative to write down the continuity equation, integrated over a horizontal plane. We make the assumption that the flow field at an arbitrary level in the room can be separated into two parts. The first is the primary air stream - the plume flow q_p. This primary air stream drives, by entrainment, a secondary air stream outside the plume. The horizontal velocity of the entrained air is inversely proportional to the distance from the plume. At each level the total vertical net flow rate must be equal to the ventilation flow rate, q_v. The equation of continuity becomes:

$$q_v = U(z)A + q_p(z) \qquad \text{eq. 1}$$

Where

A = room floor area

U = Average vertical transport velocity in the ambient outside the plume

In writing down the equation of continuity we have assumed that the area of the plume may be neglected when compared to the room area. The average vertical velocity outside the plume will be

$$U(z) = \frac{q_v - q_p(z)}{A} \qquad \text{eq. 2}$$

Because the plume flow starts from zero and increases with height, it follows that the vertical flow changes sign, i.e. direction, when the flow rate in the plume becomes greater than the supply air flow rate. We obtain three regions.

- *Uni-directional flow*, which occurs where the plume flow rate is less than the ventilation flow rate. When this occurs the direction of the flow in the ambient is concordant with the direction of the flow in the plume.

- *Horizontal ambient flow*, which occurs at the height where the flow rate in the plume is equal to the ventilation flow rate. At this height, Z_{stat}, the vertical component of the flow in the ambient is zero, so the only vertical transport occurs within the plume

- *Recirculating region*, which occurs where the flowrate in the plume is greater than the ventilation flow rate. Within this region the direction of the flow in the plume is upwards, whereas the direction in the ambient is downwards.

Centered at the level where only horizontal flow occurs outside the plume, there is an interface between the region with unidirectional flow and the recirculating region. At this interface the vertical velocities are so low that molecular diffusion becomes important. The thickness of the interface is controlled by a balance between convection and diffusion (Sandberg & Lindström 1990).

The net effect of the pure horizontal flow at the interface and the density stratification caused by the increasing temperature with height is that the transport of contaminants from the upper zone to the lower zone is hindered.

2 Experimental

2.1 Description of test room

The test space used for this investigation is a 4m x 3.45m (L x W) full scale office model, with 2.5 m height, built in the laboratory hall of the ventilation laboratory. The four walls are insulated with 5 cm styro-foam, while the floor, which is elevated above the concrete floor of the laboratory hall consists of a 2.5 cm hard particle board covered with a 1.5 cm plywood sheet. The ceiling consists of un-insulated glass panels.

The room is equipped with a conventional low velocity air supply unit with a face area of 0.15 m^2 (22% perforation degree) at the floor level. The extract terminal is situated on the same wall as the supply unit 0.2 m below the ceiling.

The experiment is carried out with nearly balanced flows, leaving a slight overpressure in the room. The supply air flow rate is appr. 80 m^3/h (2.3 room volumes per hour) and its temperature is kept at appr. 17°C.

Sitting persons are simulated by dummies constructed from metallic air duct tubes (20 cm diameter). The dummies which are of 135 cm height are heated from the inside with two bulbs (60 + 40 W). One or two dummies are used in the experiments. They are positioned in the measurement plane which divides the room into two equal halves. The ventilation air is entering from the supply unit at the center of a wall parallel to the measuring plane.

2.2 Measurement technique

150-200 passive sampling tubes for tracer gas made up a grid of measurement points in the measuring plane. The sampling tubes were positioned closer to each other in interesting regions. Two different tracer gases in permeation tubes were used to simulate pollutants. One tracer source (perfluorbenzene or PB for short) was positioned close to the ceiling (away from the measuring plane) in all experiments. The other tracer source (perfluormethylbenzene, PMB) was positioned in the measuring plane in the lower part of the room to simulate pollutants emitted in this region. The integrating sampling was allowed to continue for 1-3 weeks under steady conditions. After an experiment, the passive samplers were analysed for the amount of adsorbed tracer gases with a gas chromatograph (GC) equipped with an electron capture detector (ECD). The analysis technique is described in another paper at this conference (Stymne & Eliasson 1991). During an experiment both the vertical air temperature and wall temperature distributions were intermittently monitored.

Three different experiments with displacement ventilation are reported here:

a Two heated dummies - one tracer source close to the ceiling and one tracer source close to one body.

b Two heated dummies - tracer source above an extra 4 W heat source between the bodies.

c One heated dummy - both tracer gas sources located close to a wall in the measuring plane - one in the upper part of the room and the other in the lower part of the room.

For comparison an experiment with mixing ventilation was carried out with the same tracer positions as in a above.

3 Results

The results of the measurements are displayed in graphic form in figures 2-6. The figures show the two-dimensional interpolated iso-concentration lines in the measuring plane. All concentrations are given relative to that found in the extracted air. Also displayed are the positions of the dummies and the tracer gas sources. In figure 2, the vertical temperature gradients in the air and at the wall are also shown.

Below are the main findings from the tracer gas distribution measurements.

3.1 Two heated dummies - tracer close to one body

Fig 2 shows how a tracer emitted in the upper zone is spread when there are two heated dummies in the room. The interface is at a height lower than the "breathing level" - at 0.85 m above the floor. Evidently, the ventilation flow rate (11 l/s, person) is too low to raise the interface above the head of sitting people. However, it is also obvious that there are regions above the heat sources that are depleted of tracer gas due to the dilution from the plume flows. This behaviour has also been observed by Holmberg *et al* (1990). The interface between the lower clean air zone and the upper contaminated zone is locally displaced appr. 0.2 m upwards around the heated bodies. In the upper zone, the tracer is otherwise relatively well mixed. The thickness of the interface is less than 0.2 m.

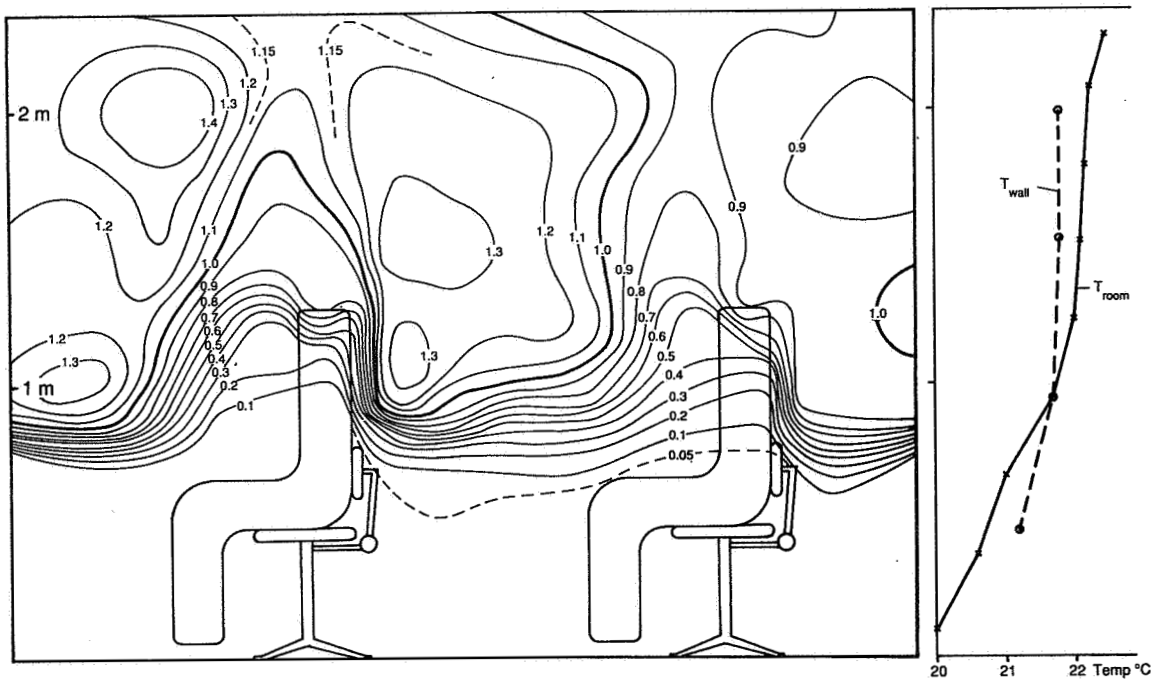

Figure 2 Iso-concentration map showing the dispersion pattern of a tracer gas emitted close to the ceiling. The concentration figures are given relative to the concentration in the extract. The dummies are situated in the measuring plane and are heated with 100 W power. Also shown are the vertical temperature profiles at the wall and in the room air.

Fig 3 shows the dispersion pattern of a tracer emitted close to one heated dummy. The tracer is directly and completely transported into the upper mixed zone. Moreover, it is apparent, that, although the "heads" of the dummies are above the transition zone, a person at that level is exposed to pollutants emitted from the other person to only a limited extent. This is due to the fact that the contaminants are transported directly to the upper zone and that each person is fed by fresh air from the lower zone.

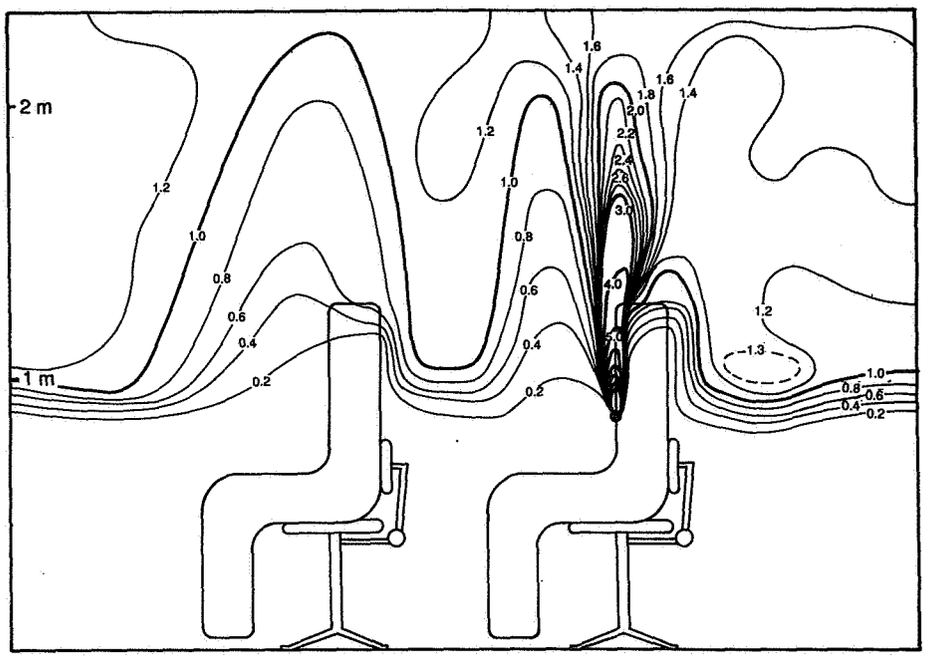

Figure 3 *Iso-concentration map showing the dispersion pattern of a tracer gas emitted close to one of the two heated dummies. Concentrations are given relative to that in the extract*

3.2 Two heated dummies - tracer at a low power heat source

Fig 4 shows how pollutants emitted from a low power heat source (4 W) do not penetrate directly through the interface. On the contrary they accumulate just below the interface and are transported into the upper zone only at the "holes" generated by the heated bodies. There is, however, only limited mixing within the lower zone. This type of accumulation of contaminants below the interface has been observed earlier (Sandberg & Blomqvist 1989).

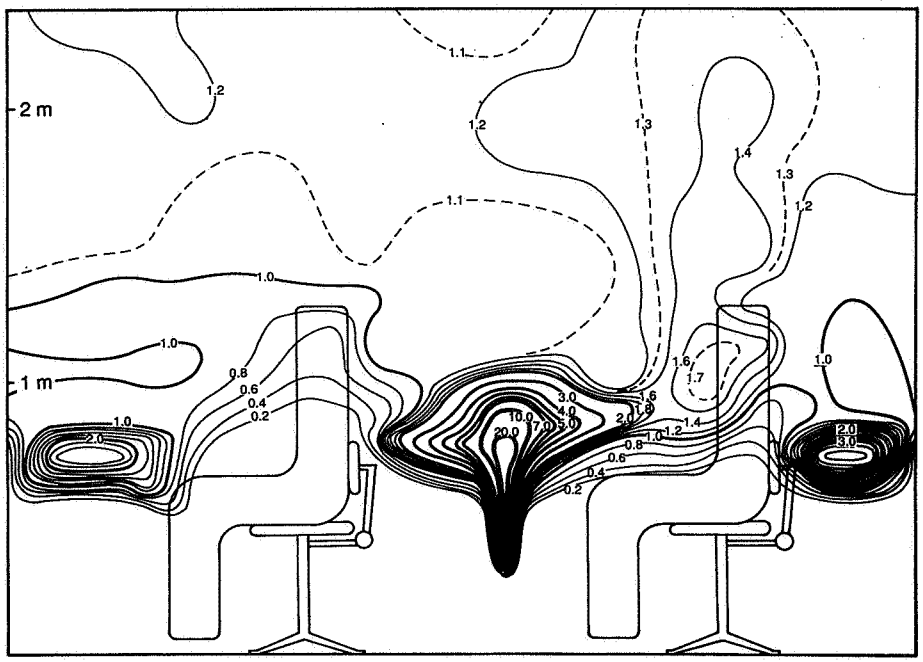

Figure 4 Iso-concentration map showing the dispersion pattern of a tracer gas emitted directly above a 4 W heat source in the lower zone. Concentrations are given relative to that in the extract

3.3 One heated dummy - tracer close to a wall

Fig 5 and **Fig 6** illustrate how a contaminant emitted close to a wall is transported in a room. In this case only one heated dummy was used, but the ventilation flow rate (22 l/s) was kept the same. Consequently the interface now appears at a considerably higher level (1.8 m). Fig. 5 shows how the tracer released close to the wall in the lower zone, follows the wall upwards. When it reaches the interface it is deflected and transported along the interface to the plume, where it is entrained and transported upwards. Fig 6 shows how the tracer released close to the wall in the upper zone flows downwards along the wall until it reaches the interface, before mixing into the upper zone. No evidence of the tracer emitted in the upper zone is found in the lower zone.

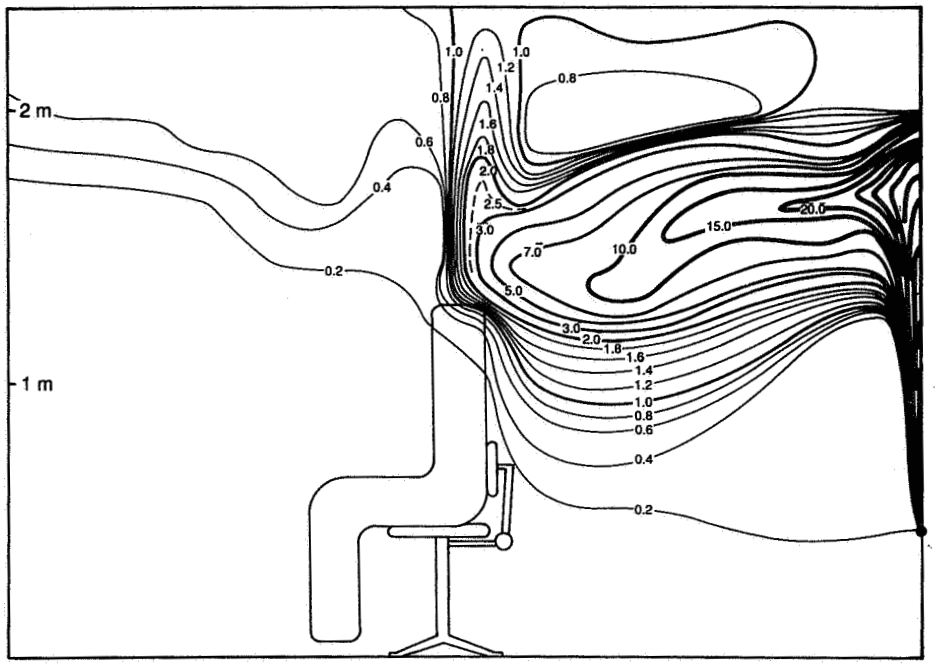

Figure 5 *Iso-concentration map showing the dispersion pattern of a tracer emitted close to the wall in the lower zone. One heated dummy is present.Concentrations are given relative to that in the extract.*

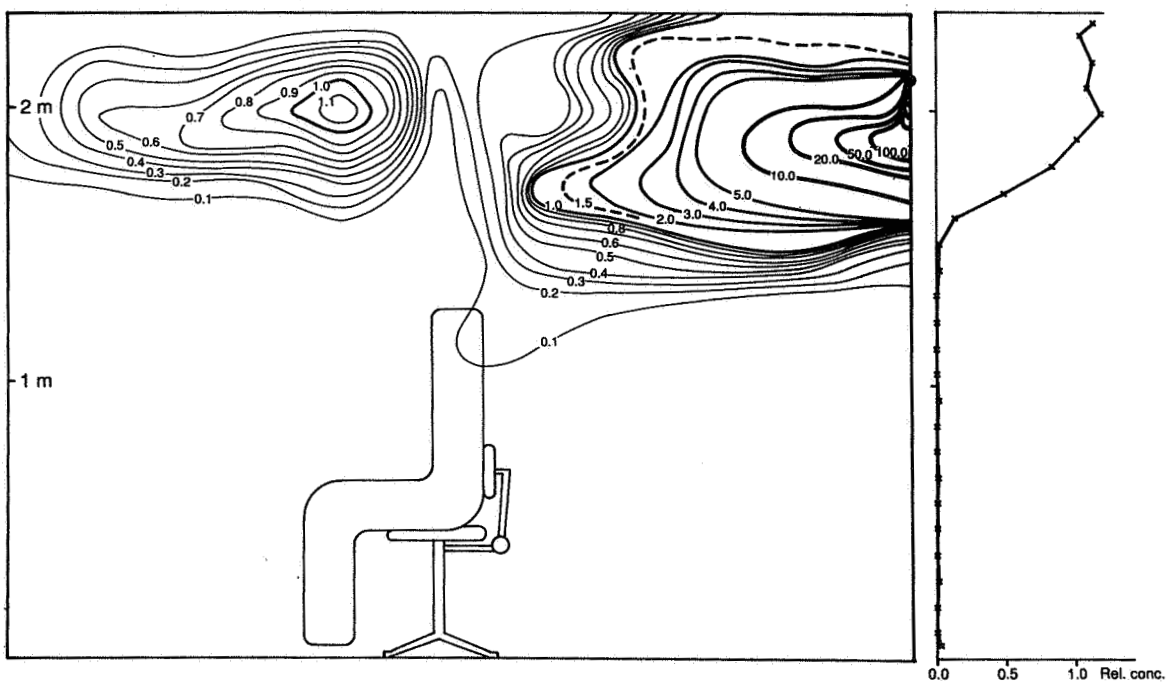

Figure 6 *Iso-concentration map showing the dispersion pattern of a tracer gas emitted close to the wall in the upper zone. Concentrations are given relative to that in the extract. Also shown (to the right) is the vertical concentration profile of a tracer released close to the ceiling.*

The observed behaviour can be explained by considering the heat balance in the room. In the lower zone, the wall temperature is higher than the room air temperature, whilst the conditions in the upper zone are the opposite. On the whole, the vertical temperature gradient of the walls is less steep than in the room air. This behaviour is illustrated from measurements displayed in fig 2. The levelling out of temperature differences at the walls is due to the radiative heat transfer between

the surfaces in the room. The center of the interface is found at a "neutral point where the wall temperature is equal to the room air temperature. The created temperature differences between the walls and the room air will cause natural convection flows downwards above the neutral point and upwards below the neutral point. The observed kind of flow pattern has been noticed earlier in water model experiments (Sandberg & Lindström 1990).

3.4 Mixing ventilation

One experiment with mixing ventilation, utilizing a high velocity supply device close to the ceiling was also carried out. The plume flows above the dummies were not affected. This was evident from the locally high tracer concentrations above the tracer gas source located close to one dummy. The concentration profile over the dummy showed that the plume extends nearly unaffected to the ceiling level similarly as shown in fig 3. Outside the plume, however, the tracer concentration was uniform in the whole room and close to the concentration found in the extract. This indicates a complete mixing of contaminants in the supply air.

4 Discussion

4.1 Main findings

It should be noted that this laboratory experiment has a number of limitations, which make conclusions uncertain for behaviour in a real case. The main limitations are the absence of normal disturbances such as:

- Body movements
- Breathing
- Heat sources other than people
- Lighting
- Solar heat gain

The disturbances mentioned contribute to a more or less increased mixing, and consequently a lowering of the interface level. In the extreme case, there will be a complete disappearance of temperature and pollutant stratification.

For the time being it is not possible to estimate the effect of such disturbances. The following discussion is mainly valid for the extreme case of no such disturbances.

It has been shown that pollutants emitted from (simulated) people in a room ventilated by displacement are transported directly into the mixed upper zone and do not contribute to the contamination level in the lower zone. Pollutants emitted from the walls and small heat sources in the lower zone will flow directly towards the interface, where they accumulate and will be transported into the upper zone only by entrainment into the plumes generated by the stronger heat sources. Only limited mixing within the lower zone will occur.

Since people act as heat sources they will set up natural convection currents around their bodies, which draw uncontaminated air upwards, toward the heads. Thus, even if the supply air flow rate is not high enough to raise the interface above the head of people, they will breathe air of a better quality than that achieved by a mixing ventilation system, run at the same flow rate.

A ventilation system based on the displacement principle, therefore, inherently requires a lower ventilation air flow rate to give the same air quality as a mixing ventilation system.

This is in accordance with the aim of a demand controlled ventilation system - that is reduction of the ventilation flow rate in order to save energy.

4.2 Possibilities of demand control

A crucial question is whether it is an advantage to control the flow in a displacement ventilation system with an air quality indicator.

In this respect mixing ventilation systems and displacement ventilation systems have quite different characteristics. Both systems have their advantages and disadvantages when controlled by demand.

4.2.1 Mixing ventilation

Advantages

A mixing ventilation system can take care of both highly varying heating and cooling demands. The ventilation air temperature can be supplied either with a high over-temperature or a high under-temperature. Heating or cooling demand can also be satisfied by other means, like radiators, convectors, cooling panels etc., without affecting the performance of the ventilation system.

Thus the ventilation system and the system for maintaining good thermal comfort can be separated to a high degree. The supply rate of air can be solely determined by ventilation demand. Thermal comfort can be achieved by other means than with supply air.

Disadvantages

Usually, the mixing is achieved by supplying the ventilation air as a high velocity jet. If the air flow rate is decreased much below the design level, there is a risk of bad mixing. Warm air may short-circuit from the inlet to the outlet, while supply air with an under-temperature may fall down into the occupied zone - causing thermal discomfort. The ventilation efficiency might be low when demand is low.

4.2.2 Displacement ventilation

Advantages

In a room ventilated by displacement, the air quality in the breathing zone is usually better than in a mixing system operated vith the same air flow. This is due to the fact that people act as heat sources, drawing uncontaminated air from the lower zone along their bodies.

The ventilation efficiency is not adversely affected by decreasing ventilation flow rate at low demand.

Disadvantages

The flow pattern in a displacement ventilation system is set up by heat sources. Thus, there is a very strong coupling between thermal load, ventilation air rate and ventilation efficiency.

A ventilation efficiency, which is significantly better than with mixing ventilation can only be expected when the supply air flow rate matches the heat load. Thus, all heat sources require supply air, whether they are polluting the air or not. In a sense there is a short-circuiting of ventilation air between the clean lower zone and the contaminated upper zone at each heat source in the lower zone.

Controlling the supply air flow rate entirely by an air quality indicator in the exhaust will not ensure that people are surrounded by air of a better air quality than with a mixing ventilation system.

Displacement ventilation requires that the supply air has a lower temperature than the room air. Therefore, it is not possible to heat the room with the supply air.

There are more severe restrictions due to thermal discomfort in a displacement system than in a mixing system. This is especially the case whith high cooling demands. The thermal comfort aspect is discussed in a subsequent paragraph.

4.3 Ventilation demand contra cooling demand

In rooms ventilated by displacement the demand of air flow rate necessary for cooling, frequently dominates over that necessary for keeping the air quality acceptable according to current standards. This is because too low supply air temperatures can not be tolerated. This would lead to discomfort due to both the low temperature at the floor level and a steep vertical temperature gradient. An acceptable under-temperature of the supply air is 5-7 K. A special air diffuser equipped with an induction chamber which allows a ΔT of 10K has, however, been suggested (Holmberg *et al.* 1990)

One person dissipates approximately 100 W. To cool away that amount of heat with air ($\Delta T = 5K$) requires 15 l/s. This is more than that, normally assumed to be necessary from an air quality point of view. This amount of outside air per person would yield a carbon dioxide level of approximately 700 ppm in the extract.

Additional heat sources will call for even more supply air per person. This is often the case in offices. Thus, cooling requirements, combined with the requirements of thermal comfort often determine how much supply air is needed in a displacement ventilated system. An air quality indicator with a set point of 700-800 ppm carbon dioxide (which is usually recommended) would seldom take over the control, even if positioned in the extract.

A displacement ventilation system, however, offers the opportunity to achieve appreciably better air quality in the breathing zone than that which is normally assumed to be acceptable. This is reached without substantially increasing the supply air flow rate and energy consumption over the level needed to yield an acceptable thermal comfort.

Displacement ventilation can also advantageously be used in rooms where unusually polluting activities, such as smoking, are present. An acceptable breathing zone air quality can be achieved even in this extreme case, without increased demand for ventilation air, because the interface level is determined only by the strength of the heat sources - not the pollutant emission rate.

4.4 Concentration setting and location of an air quality sensor

The leading principle for controlling a displacement ventilation system by demand should be to establish the interface as low as possible, whilst at the same time allowing people to breathe air from the lower zone. This would secure the lowest possible flow rate from an air quality point of view.

To ensure the excellent air quality achievable with displacement ventilation, it is important to adjust the supply air flow rate, so that the interface level appears above the breathing zone of the occupants.

Demand control of supply air governed by an air quality sensor seems to be an excellent means of controlling the level of the interface. Carbon dioxide is a suitable indicator, both because it is emitted from heat sources (people) and because it indicates the presence or absence of people, requiring air quality control.

To ensure that the interface is at a sufficiently high level, the sensor should be located at the same height as the normal breathing zone. For sitting people this is at appr. 1.1 m above the floor.

The set point for the carbon dioxide concentration at the sensor position should be appreciably lower than that normally suggested for mixing ventilation (700-1000 ppm, ΔCO_2 = 350-650 ppm). A reasonable value might be 500 ppm (ΔCO_2 = 150 ppm). This value is low enough to ensure that the mixed zone is above the height of the sensor, but not so low that the interface is far above the sensor.

To monitor a typical concentration at this level the sensor should not be positioned in the vicinity of people or heat sources. Nor should it be positioned very close to a wall, because of the natural convection currents occuring along the walls mentioned earlier.

At a set ΔCO_2-value of 150 ppm a demand controlled system will respond quickly even for one person present in a room of normal size.

4.5 Thermal comfort considerations

As in the case of a mixing ventilation system, there must be some indicator and feed back system for temperature and thermal comfort. While, in a mixing system the thermal comfort can be regulated with radiators, convectors etc., the thermal comfort in a displacement system has to be regulated by means of the temperature of the supply air.

The criteria for thermal comfort in displacement system, not only refers to the average room temperature, but also to the vertical temperature gradient and the supply air temperature. The temperature difference between 0.1 m and 1.1 m should not exceed 3K according to ISO/DIS 7730 (1984). An even lower difference (e.g. 2K) might be necessary in connection with displacement systems. The supply air temperature should not be lower than 17°C and the difference in temperature between extract and supply air should not exceed 7K.

The regulation interval for the supply air temperature (17°C-21°C) is rather limited. Internal heat loads of more than 30 W/m^2 can hardly be taken care of without thermal discomfort (Wyon & Sandberg 1990).

4.6 Disturbances occurring in real systems

There are few detailed measurements reported for real occupied rooms with displacement ventilation. There are, however, indications that the interface is lowered, and the thickness of the transition zone increased, by mixing actions created by human movement. The local displacement of the interface around heat sources are probably especially influenced by such movement (Holmberg *et al* 1990).

There are probably large local fluctuations of the carbon dioxide concentration. Such fluctuations can severely influence the behaviour of a demand controlled system governed by the carbon dioxide concentration close to the interface. The amplitudes and frequencies of such fluctuations caused by human movement, must be investigated further, before any firm conclusions can be drawn on the set point and location of the air quality sensor.

For selection of a suitable sensor location it is also important to identify the natural concentration fluctuations that occur. The most rapid fluctuations are due to the turbulent velocity field. The turbulent fluctuations are so rapid (fractions of a second) that no normal sensor respond to them. There are, however, slower natural fluctuations due to internal gravity waves, supported by a stratified environment. The magnitude of the frequency (f) of such waves is given by the Brunt-Väisäla angular frequency (N) (Turner 1973).

$$f = \frac{N}{2\pi} = \frac{1}{2\pi}\sqrt{g \cdot \frac{1}{T} \cdot \frac{\delta T}{\delta z}} \qquad [Hz] \qquad \text{eq. 3}$$

where T is the room temperature in Kelvin

In our tests the maximum vertical temperature gradient amounted to 2°C/m which gives rise to an oscillation period of 25 seconds (0.04 Hz) according to eq. 3. We can conclude that there will be natural fluctuations with a period of about 1 minute. Experience shows that such fluctuations have their largest amplitude at the level of the interface (Mellin & Sandberg 1990).

5 Conclusions

The following conclusions refer to a ventilated space of simple geometry, where the air flow pattern is not disturbed by the mixing action of human movement.

It has been shown from tracer gas distribution experiments, that pollutants emitted from a (simulated) person are transported directly to the upper mixed zone in a space ventilated by a displacement system. Pollutants emitted close to a wall or a low power heat source in the lower zone flow vertically towards the interface between the zones, but do not directly penetrate to the upper zone. The pollutants accumulate below the interface and are transported to the upper zone only at the "holes" generated in the interface by the natural convection plumes from the heated bodies.

The interface is locally displaced upwards approximately 0.2 m around the heated bodies, thus ensuring the occupants a better air quality than the surrounding air, even if their heads are above the interface level. Pollutants, which are emitted in the upper mixed zone or transported to that zone from the lower zone do not appear in the lower zone.

It is also shown that the plume above a heated dummy is similar in a mixing ventilation system to the plume created in a displacement ventilation system. In the case of mixing ventilation, however, there is no sign of any vertical concentration stratification outside the plume.

It is concluded that demand control of the supply air flow rate in a room ventilated by displacement is a suitable means of controlling the level of the interface between uncontaminated air in the lower zone and the polluted air in the mixed upper zone. The location of an air quality sensor for demand control should preferably be positioned at the height of the heads of the occupants, thereby ensuring an excellent air quality in the breathing zone at the lowest possible air flow rate. The concentration set point for the sensor should be at an appreciably lower value than that (e.g. 800 ppm CO_2) normally considered to be appropriate for the air quality. Otherwise, the sensor would seldom take the control.

Acknowledgements

This work was initiated by the IEA annex 18 - Demand Controlled Ventilation. It has been partly financed with grant BFR-880614-8 from the Swedish Council for Building Research, which is here gratefully acknowledged.

References

ISO/DIS 7730 1984.
"Moderate thermal environments. Determination of the PMV and PPD indices and specification of the conditions for thermal comfort"
Int. Standardization Organization, Geneva 1984

HOLMBERG, R. B., ELIASSON, L., FOLKESSON, K. and STRINDEHAG, O.
"Inhalation-zone Air Quality Provided by Displacement Ventilation"
Proceedings of ROOMVENT '90, 2nd International Conference, Oslo, Norway June 1990, Paper B2-32

MELLIN, A. and SANDBERG, M.
"Prov av rökrum" ("Test of room for smokers")
National Swedish Institute for Building Research, Internal report 1990 (in Swedish)

SANDBERG, M. and BLOMQVIST, C.
"Displacement Ventilation Systems in Office Rooms"
ASHRAE Transactions **95,** 1041, 1989.

SANDBERG, M. and LINDSTRÖM, S."
Stratified Flow in Ventilated Rooms - a Model Study"
Proceedings of ROOMVENT '90, 2nd International Conference, Oslo, Norway June 1990, Paper D1-56

STYMNE, H. and ELIASSON, A.
"A New Passive Tracer Gas Technique for Ventilation Measurements"
Proceedings of the 12th AIVC Conference, Ottawa Canada 1991

STYMNE, H., MELLIN, A. and SANDBERG, M.
"Dispersion pattern of carbon dioxide from human sources - A factor to consider in demand controlled ventilation systems"
Proceedings of the 5th International Conference on Indoor Air 90, Toronto, July 1990, Vol **4**, p 317

TURNER, J.S.
"Boyancy effects in fluids"
Cambridge University Press 1973

WYON, D.P. and SANDBERG, M.
"Thermal Manikin Prediction of Discomfort due to Displacement Ventilation"
ASHRAE Transactions **96**, 3307, 1990

AIR MOVEMENT & VENTILATION CONTROL WITHIN BUILDINGS

12th AIVC Conference, Ottawa, Canada
24-27 September, 1991

PAPER 12

Performance Evaluation of Humidity Controlled Natural Ventilation in Apartments.

P.Wouters, D.L'Heureux, B.Geerinckx, L.Vandaele

Belgian Building Research Institute
Aarlenstraat 53/10
B-1040 Brussels
Belgium

12th AIVC CONFERENCE

AIR MOVEMENT AND VENTILATION CONTROL
WITHIN BUILDINGS

TITLE : Performance evaluation of humidity controlled natural ventilation in apartments

AUTHORS : P. Wouters, D. L'Heureux, B. Geerinckx, L. Vandaele
ADDRESS : Belgian Building Research Institute
Aarlenstraat 53/10 B-1040 Brussels
tel : +32.2.653.88.01 fax : +32.2.653.07.29

Abstract

A commercially available humidity controlled natural ventilation system (Aereco)has been installed in the framework of a CEC demonstration project in 3 apartment buildings in France, the Netherlands and in Belgium. An extensive monitoring campaign in reference apartments and humidity controlled apartments during the 2 previous winters allowed a detailed analysis of various ventilation related parameters. Special attention is given to the evaluation of the humidity control on the performances.

The majority of the analysis will be finished before the summer of 1991 so that rather complete conclusions will be available for the AIVC conference.

Specific trends will be shown by means of snap shots. However, the majority of the efforts went to a statistically treatment of all the data in order to come not only to impressions of certain tendencies but also to scientifically supported conclusions of these tendencies.

AIR MOVEMENT & VENTILATION CONTROL WITHIN BUILDINGS

12th AIVC Conference, Ottawa, Canada
24-27 September 1991

PAPER 13

CONTROLLED NATURAL VENTILATION

Authors: B. Knoll B.Sc.
W. Kornaat B.Sc.

Department of Indoor Environment,
Building Physics and Systems;
TNO Building and Construction Research;
Delft, The Netherlands.

SUMMARY

Natural ventilation of dwellings is commonly applied, especially in mild and moderate climates.The disadvantage of natural ventilation is the poor control of both flow directions and flow rates within the ventilated building. To improve control, the use of mechanical exhaust is often recommended.Though this may improve total ventilation, the ventilation of separate rooms often is insufficient still.

Our approach was to try and find a highly controlled natural ventilation system, whose control is highly independent of weather changes and dwelling properties, just like in thermostatic temperature control. Therefore a study has been carried out, using a ventilation calculation model.

The results show that controlled natural ventilation is possible and very advantageous. What's more, the principle is also applicable to improve mechanical exhaust systems.
In both cases, for a good controllability and maximum energy saving, a high air-tightness is recommended, though the control in the mechanical exhaust option is more sensitive to air-tightness.
The main conditions for controllability appear to be over dimensioned vertical exhaust ducts to the pitch of the roof and special, self-regulating supply provisions in habitable rooms.
With this system, ventilation flow rates of separate rooms may be kept constant, without occurrence of flow reversion, during over 90 % of time. Hence, the air quality will be highly improved to almost optimum. On the other hand, the occurrence of draughts, due to unheated air supply, will be highly reduced. Also, total ventilation energy consumption will reduce up to about 20 %, compared to a good manual control.

CONTENTS

1. INTRODUCTION

To get both an acceptable indoor air quality and a reduction of energy consumption in dwellings the control of ventilation flows per room is necessary. The present natural ventilation systems do not allow a proper control. This is illustrated by figure 1, showing the results of in-situ ventilation measurements for an airtight dwelling with natural exhaust duct, when ventilated respectively by cracks-only and by opening vent-lights [ref. 1].

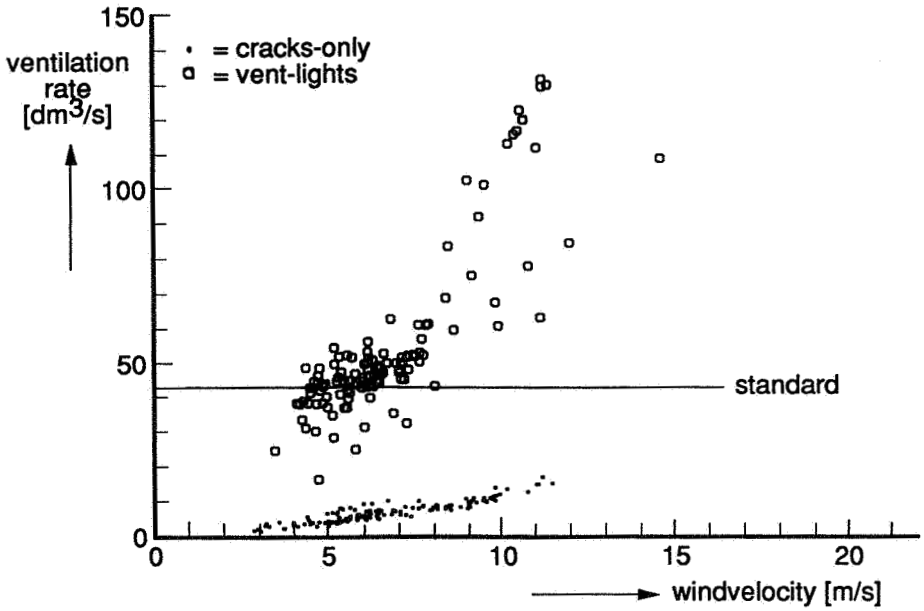

Figure 1: Measured natural ventilation rates in an air-tight dwelling by cracks only and by vent lights

The reason for the variation of ventilation flows is obvious; the setting of natural ventilation openings by the inhabitants has to depend on :

- -the wind-velocity and -direction,
- -the shape of the building,
- -surrounding obstacles,
- -temperature-differences between in- and outside,
- -the building lay-out,
- -the air-tightness of the building,
- -the use of internal doors,
- -location and size of ventilation ducts,
- -the use of ventilation provisions in other rooms.

The complexity of the ventilation process, combined with the lack of accurate signals to sense the ventilation level or even the ventilation effect, is obstructing a good manual control of natural ventilation devices.

As a solution for this problem the use of mechanical exhaust systems is often suggested. Though research has shown an improvement of the total ventilation control by the use of mechanical exhaust (see figure 2), still the control of separate rooms ventilation appears to be insufficient (see figure 3) [ref. 1].

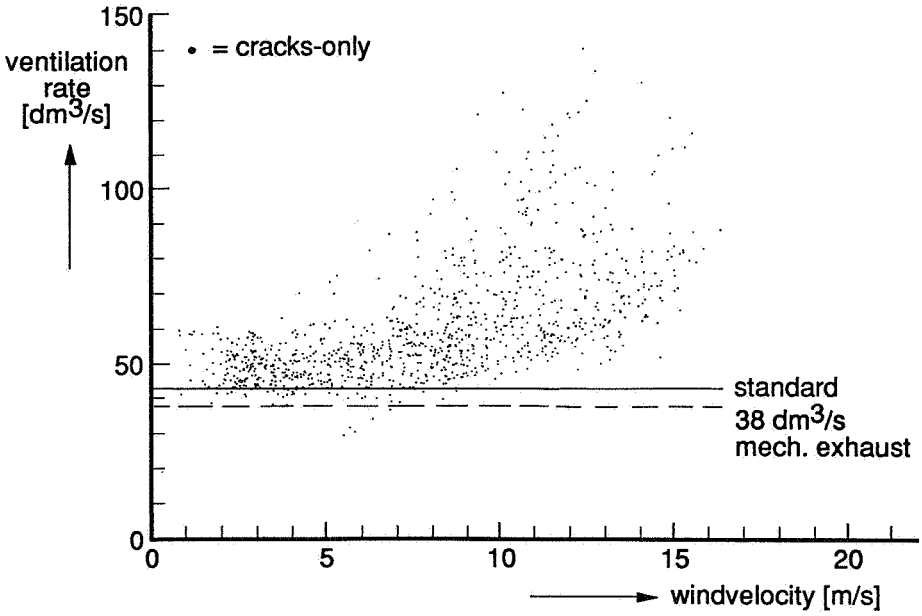

Figure 2: Measured ventilation rates in an air tight dwelling with mechanical exhaust

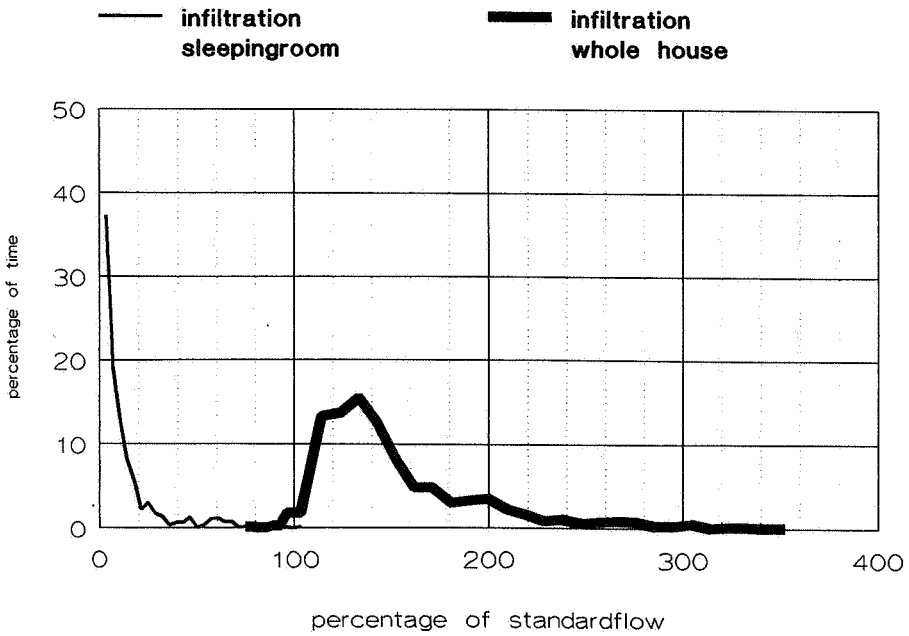

Figure 3: Ventilation distributions related to the standard flows for the whole house and a separate bed room of the air-tight dwelling with mechanical exhaust

This may be solved by the use of mechanical supply and exhaust systems. However, this type of system needs a high air-tightness of the building, to prevent extra ventilation losses by infiltration. Moreover, the costs of these systems are high, especially when installed within existing buildings.

To deal with the disadvantages mentioned before, our approach was to try and find an improved, low-cost control of natural ventilation systems or mechanical exhaust ventilation systems. A parallel may be made with thermostatic temperature control. In this system the temperature has been kept constant to a set level, independent of weather changes, dwelling properties (e.g. insulation level) or fluctuations of the internal heat load.
The aim was to develop a comparable ventilation control, which automatically compensates the effects of weather changes in combination with the air-tightness and the use of internal doors within a high range, thus maintaining a pre-set ventilation level.

This publication deals with the generation of the new control principle, the determination of important system dimensions and control features by model calculations and the advantages compared to other systems. Finally, the requirements for the development of system components are summarized.

2.PRINCIPLE

Natural ventilation is mainly generated by wind forces and thermal buoyancy. These forces create pressure differences over all kinds of openings and leakages, thus causing ventilation flows through these openings. Both, the pressure differences and ventilation flows are depending on the distribution of openings over and within the building and on the parameters mentioned in chapter 1.

The main flow directions through dwellings, due to wind and thermal buoyancy, are shown in figure 4. Also shown are simplified, related pressure distributions [Note: in fact, due to thermal buoyancy, not the outside pressure but the inside pressure is varying with the height]. The actual flow directions and pressure differences under different circumstances may be all kinds of combinations of these shown in figure 4. Hence, the flow rates may differ accordingly. An often occurring pressure distribution, with related flow directions and flow rates, is presented in figure 5. The often almost zero pressure difference on the leeward side explains the under ventilation of the bed room presented in figure 3.

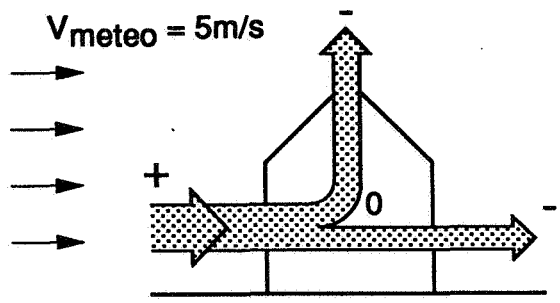

due to wind

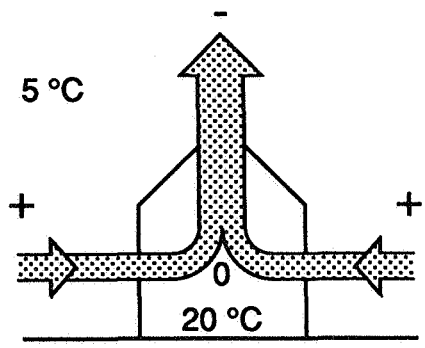

due to thermal buoyancy

Figure 4: Pressure distribution over a dwelling and related flow directions and flow rates

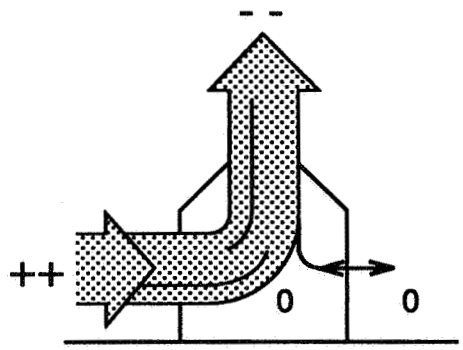

Figure 5: Often occurring pressure distribution and related flows

<u>The first step in controlling natural ventilation is to control the flow directions.</u>
It may be noticed from figures 4 and 5 that, during heating season conditions, near the pitch or the middle of the roof always extraction of air will occur. This general occurrence of exhaust in the pitch or the middle of the roof plays a significant part in controlling the flow directions. It means within this zone the lowest pressure levels will occur. By installing over dimensioned, vertical exhaust ducts into the dwelling, with outflow within this zone, the dwelling will be depressurized. This allows supply of air onto each facade, even on the leeward side (figure 6). These flow conditions will especially occur at:

-general occurring wind velocities,
-outdoor temperatures below inside temperatures.

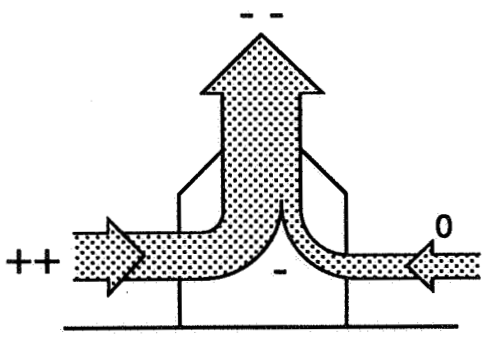

Figure 6: Depressurizing the dwelling by over dimensioned vertical exhaust ducts will improve control of flow directions.

The second step is to control the supply flow rates through the openings into the facade.
Without this control high differences between the flow rates of the windward and the leeward side may occur, or even flow reversion at leeward side will occur at high wind velocities, due to cross ventilation. This means ventilation openings into the facades have to be reduced with increasing positive pressure differences. While the pressure differences may differ on varying locations, decentral control of the various ventilation openings is recommended. Because of the difficulties in manually controlling ventilation openings properly, as mentioned before, automatic flow rate control is considered to be necessary. This may be fulfilled by self-regulating vents. The principle of a self-regulating vent is illustrated by figure 7.

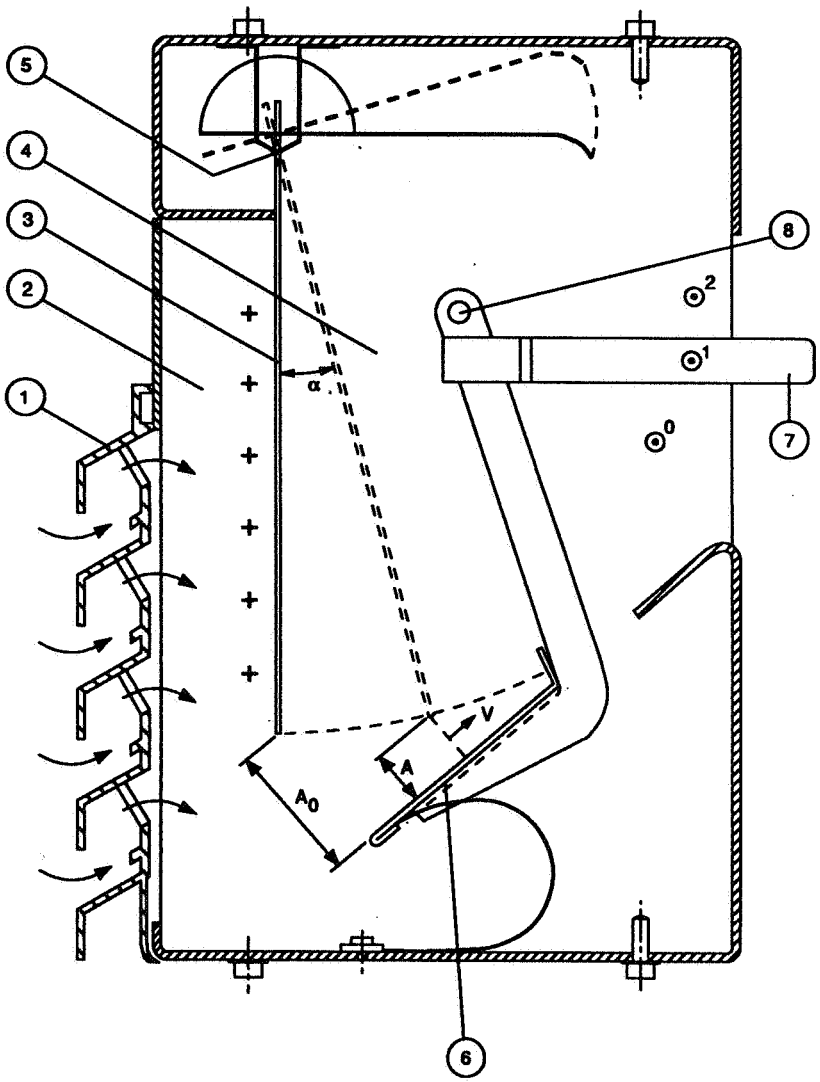

Figure 7: Example of a self-regulating vent

Influenced by over-pressure on the facade, ventilation air enters through the outside grid (1) into the front chamber (2)

of the self-regulating vent. By this, pressure is built up on the entrance side of the valve (3), compared to the chamber (4) behind the valve. The pressure difference between chambers (2) and (4) causes a deflection (α) of valve (3), which is suspended from blade hinges. The flow-through area between valve (3) and bottom plate (6) hereby contracts from A_0 to A. Also the pressure difference causes a flow velocity (v) in the area (A). As the pressure difference over the grid and thus over the valve increases, the flow-through area (A) decreases and the flow velocity (v) increases. The product A*v, multiplied by a contraction factor, depending on its design, is the flow rate (q_v). The aim is to create a relation between the deflection of the valve and the pressure difference, which results in a set, constant ventilation flow at all pressure differences.
To set the required flow level, the bottom plate (6) can be adjusted, using the adjustment arm (7), hinging at point (8). This will cause a proportional increase or decrease of the flow-through area (A) at every position of the valve.

A proper control may be impaired by the presence of non-controllable leakage openings into the building shell. Their contribution to the ventilation will increase at increasing pressure difference. This may be compensated by reducing the flow rate, let through by the self-regulating vent, at increasing pressure difference. While this possibility is restricted, also certain demands are expected on the air-tightness of the dwelling.

3. CALCULATION MODELS

To find out wether the principle of controlled natural ventilation can be worked out within realistic system-dimensions, calculations have been made using the TNO ventilation model [ref.2].
The second aim of the model calculations was to establish the requirements for optimal self-regulating vents.
Finally, the ventilation properties compared to other systems are established.

The calculations have been performed on a typical dutch dwelling. The lay-out of this dwelling is shown in figure 8.

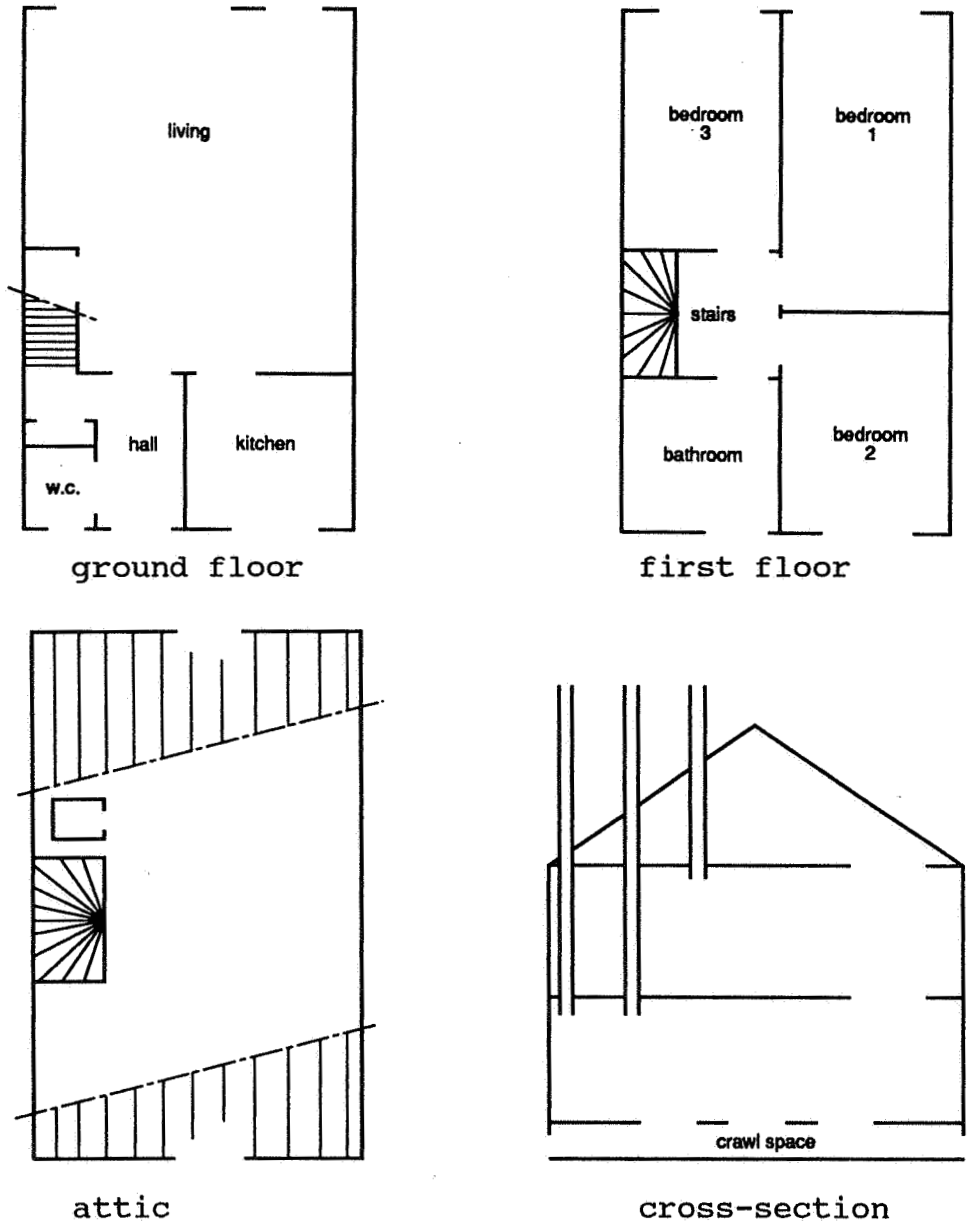

Figure 8: Lay-out of the dwelling, used for model calculations.

The calculations have been made for three levels of air-tightness:

1. Average dutch dwelling, air-leakage 9 ach at 50 Pa, distribution: roof 73%, facades 22% and ground floor 5%.
2. Dwelling with standard air-leakage of 6 ach at 50 Pa, distribution: roof 71%, facades 21% and ground floor 8%.
3. Airtight dwelling, air-leakage 2 ach at 50 Pa, distribution: roof 62%, facades 30% and ground floor 8%.

The inner doors are closed, however, each door has a leakage-opening of 160 cm^2 (2 cm gap beneath it).
The vertical exhaust ducts are situated in the service rooms (kitchen, bathroom and W.C.). The self-regulating vents are situated in the facades of the bed rooms only. This is because dutch standards demand fresh air supply within these rooms, but they allow air to overflow to the living room, to be exhausted from the service rooms, thus creating an optimum use of the ventilation air.
The dimensions of the vertical exhaust ducts are:

- -kitchen 84 cm^2,
- -bathroom 60 cm^2,
- -W.C. 30 cm^2.

Originally the self-regulating vents are dimensioned to supply standard flows at a wind velocity of 2 m/s, which means 39 cm^2 and 77 cm^2 net opening area for respectively 7 dm^3/s and 14 dm^3/s flow rate. Later on, the opening areas are enlarged to 80 cm^2 and 155 cm^2, allowing standard flows even at a very low wind velocity of 0.5 m/s. Correspondingly, each self-regulating vent is tuned to supply the standard flow minus the actual crack flow of the particular room at each pressure difference above 0.5 Pa. Under 0.5 Pa the vent is fully opened.

The dwelling is situated in a low-rise urban area, which is representative for most dutch dwellings. The corresponding wind pressure coefficients (C_p-values) are drawn from a data-base. All calculations are made at an outside temperature of 5°C , representative for average heating season conditions.

To enable a comparison, apart from the controllable natural ventilation system, calculations have been made on a mechanical exhaust system with the next options for supply:

- -cracks only,
- -manual controlled vent-lights or -windows,
- -self-regulating vents.

In these cases the mechanical exhaust flows are:

- -kitchen 21 dm^3/s,
- -bathroom 14 dm^3/s,
- -W.C. 7 dm^3/s.

For supply through manual controlled vent-lights or -windows the next control behaviour for the bed rooms is suggested, depending on the wind conditions:

wind velocity	0	2	5	10	15 m/s
leeward side	300	300	150	65	65 cm^2
windward side	300	300	150	65	0 cm^2

The windows in the other rooms are closed, just as in the option with the self-regulating vents.
The control behaviour mentioned is proved to be one of the best possible types of manual control. In practice bed room windows often are opened much wider during about 4 to 8 hours a day.

4. CALCULATION RESULTS

The results of the model calculations are given in ref. 2 and 3. The most important results will be dealt with in this publication.

Figure 9 presents the ventilation levels in different rooms of the air-tight dwelling (2 ach at 50 Pa), in case of the mechanical exhaust system, for three types of supply:

- -cracks only,
- -self-regulating vents,
- -optimum use of window-vents.

The ventilation is an average over all wind velocities for wind directed to the front facade.
To enable a check of the ventilation levels the standard values are also given in figure 9.

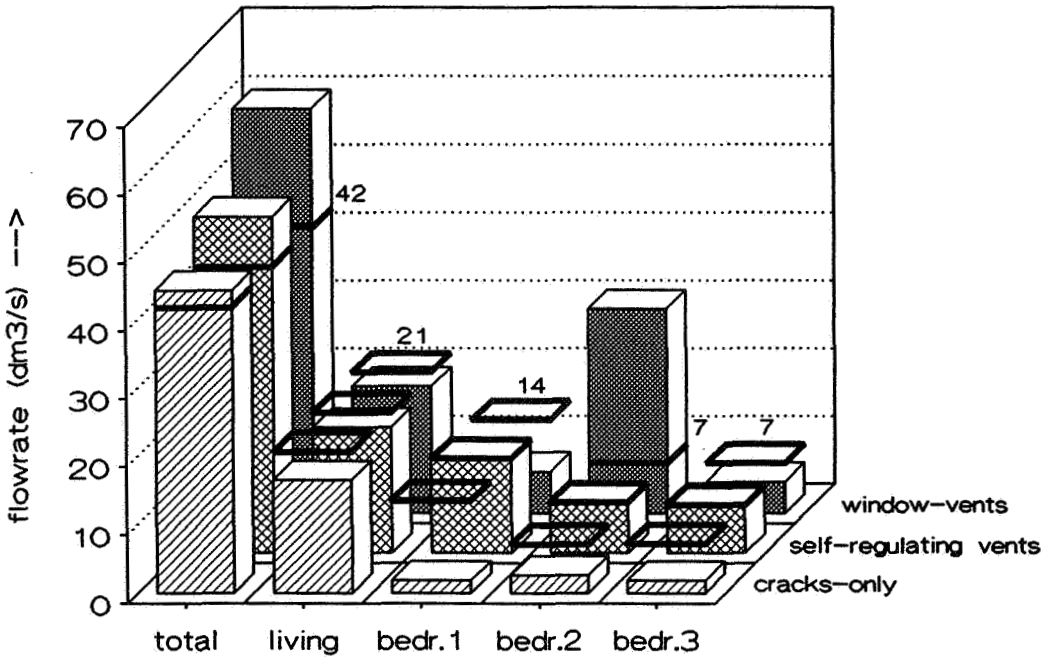

Figure 9: Ventilation for an air-tight dwelling (2 ach at 50 Pa) with mechanical exhaust (42 dm³/s) and different types of supply, related to standard flow rates. Average of all wind velocities. Wind directed to the front facade.

Figure 9 shows the effect already mentioned in chapter 1, concerning sufficient total ventilation, but very insufficient bed room ventilation, in case of mechanical exhaust and supply through cracks. The average bed room ventilation on the leeward side is just 26 % of standard value and on the windward side 37 %
By opening window-vents or vent-lights the ventilation of leeward side bed rooms is still insufficient (66 % of standard value), while the windward side bed room is over ventilated (430 % of standard value), with a high risk of draughts. Also,

the total ventilation shows an overshoot of 42 %, resulting in comparable ventilation energy losses.
The application of self-regulating vents for air supply appears to be a good solution. The flows of all rooms are controlled very well, diminishing draught risks (average bed room ventilation 94 and 100 % of standard value, respectively on leeward and windward side). The overshoot of total ventilation is reduced from 42 to 18 %.

From figure 9 one could suggest that the proper supply through cracks to the bed rooms is impaired by the high level of air-tightness of the dwelling. However, the results in figure 10, referring to a dwelling with standard air-leakage (6 ach at 50 Pa), show this assumption is not right.
Mechanical exhaust, with supply through cracks only, still leads to insufficient ventilation of bed rooms (average ventilation 17 % of standard value on the leeward side and 56 % on the windward side). On the other hand, the increase of air-permeability with a factor 3 does create a 40 % overshoot of total ventilation, resulting in a comparable increase of ventilation energy consumption.
Despite the increase of air-permeability, leading to less authority of the controllable openings, still the standard ventilation rates of separate rooms are approached, using self-regulating vents (average bed room ventilation on the leeward side 76 % of standard value and on the windward side 100 %). Just like in the air-tight dwelling a slight increase of total ventilation occurs, compared to supply through cracks only (total ventilation increased from 140 to 154 %).

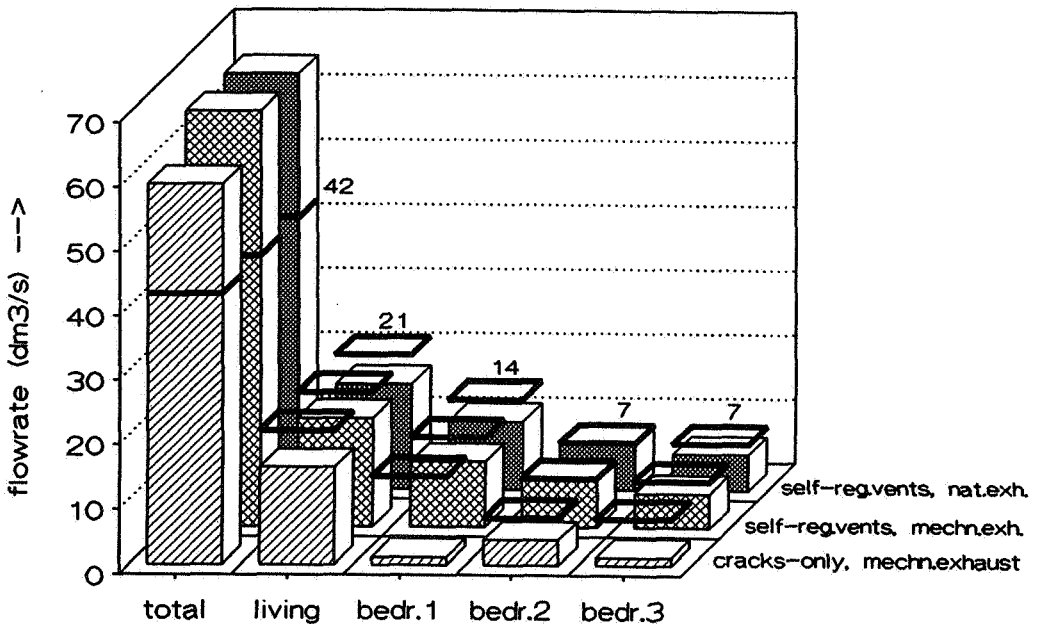

Figure 10: Ventilation of a dwelling with standard air-leakage (6 ach at 50 Pa) and different types of supply and exhaust, related to standard flow rates.
Average of all wind velocities.
Wind directed to the front facade.

Figure 10 also shows the ventilation in case of self-regulating supply vents combined with natural exhaust ducts. There appears to be hardly any difference with mechanical exhaust.
One should notice that average ventilation rates over all wind velocities are concerned. A differentiation to wind velocities for bed room 2 (windward side) and 3 (leeward side) is presented in figure 11.

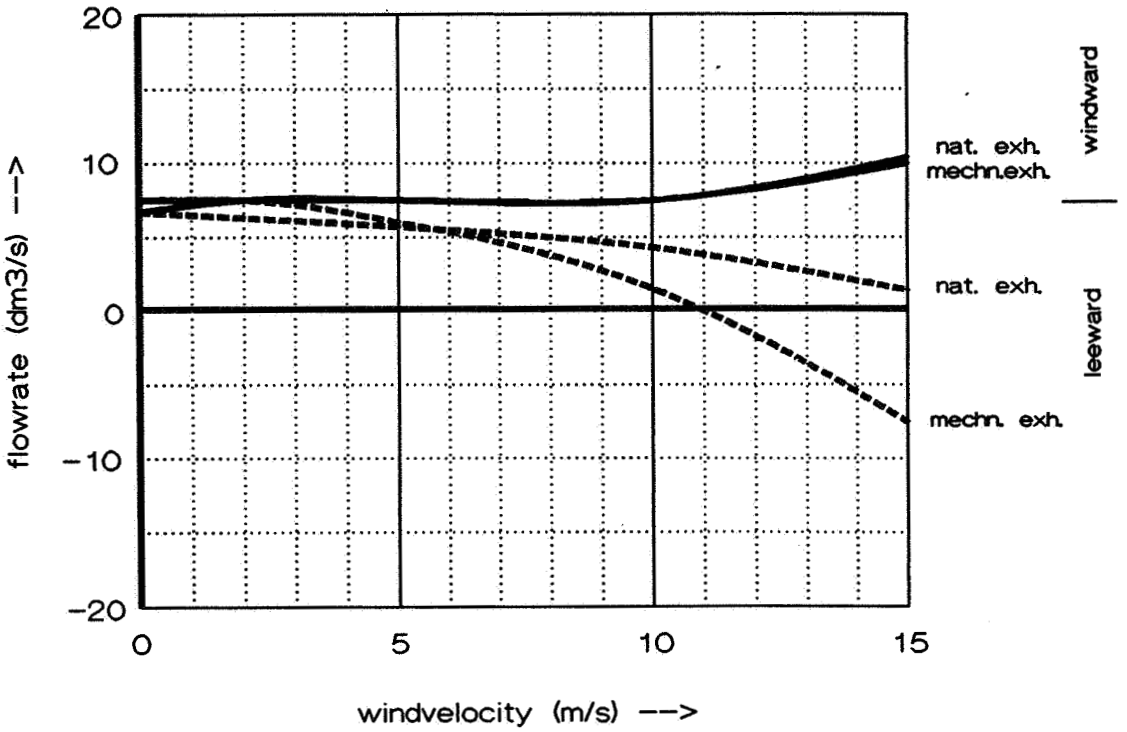

Figure 11: Ventilation flow related to wind velocity for a leeward and a windward bed room. Comparison between self-regulating vents with natural or mechanical exhaust.

Figure 11 still shows no difference between self-regulating vents with natural or mechanical exhaust, as far as the windward room is concerned. In both cases some increase of ventilation occurs at rare wind velocities above 10 m/s. However, the leeward room ventilation shows some remarkable differences. The ventilation with natural exhaust appears to be less variable than with mechanical exhaust. Also, flow reversion does not occur with natural exhaust, contrariness to mechanical exhaust. This could be explained by the pressure stabilizing effect of an exhaust fan, which does not allow the inside pressure to lower with increasing wind velocity, as much as it does with natural exhaust. Consequently, the pressure difference over the leeward facade will decrease more rapidly in case of mechanical exhaust. This effect is confirmed by figure 12, presenting the calculated pressure differences over the leeward facade.
The surprising conclusion may be that the application of self-

regulating vents is preferred in combination with natural ventilation, rather than with mechanical exhaust.
Apart from the improvement on ventilation of separate rooms, this will save installation costs of the exhaust fan, as well as auxiliary energy of about 500 kWh a year [ref. 4].
An exception to this conclusion have to be made for sheltered houses with exceptional wind pressure distributions.

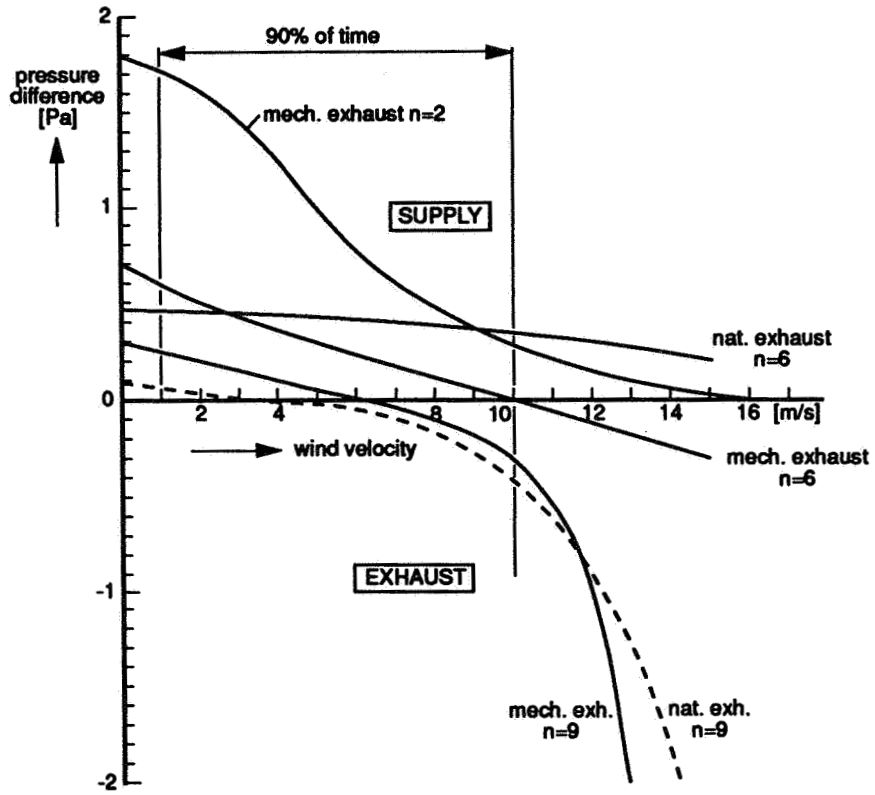

Figure 12: Calculated pressure differences over the leeward facades of dwellings with self-regulating supply vents.
Natural or mechanical exhaust.
Air-leakage n=2, 6 or 9 ach at 50 Pa.

Figure 12 shows that leeward pressure differences are relatively small, compared to the windward pressure differences, as presented in figure 13. Nevertheless, due to the self-regulating vents, leeward pressure differences are positive over 90 % of time, if the air-leakage is not over the standard value. This means supply will occur under this conditions. The importance of the air-tightness is evident.

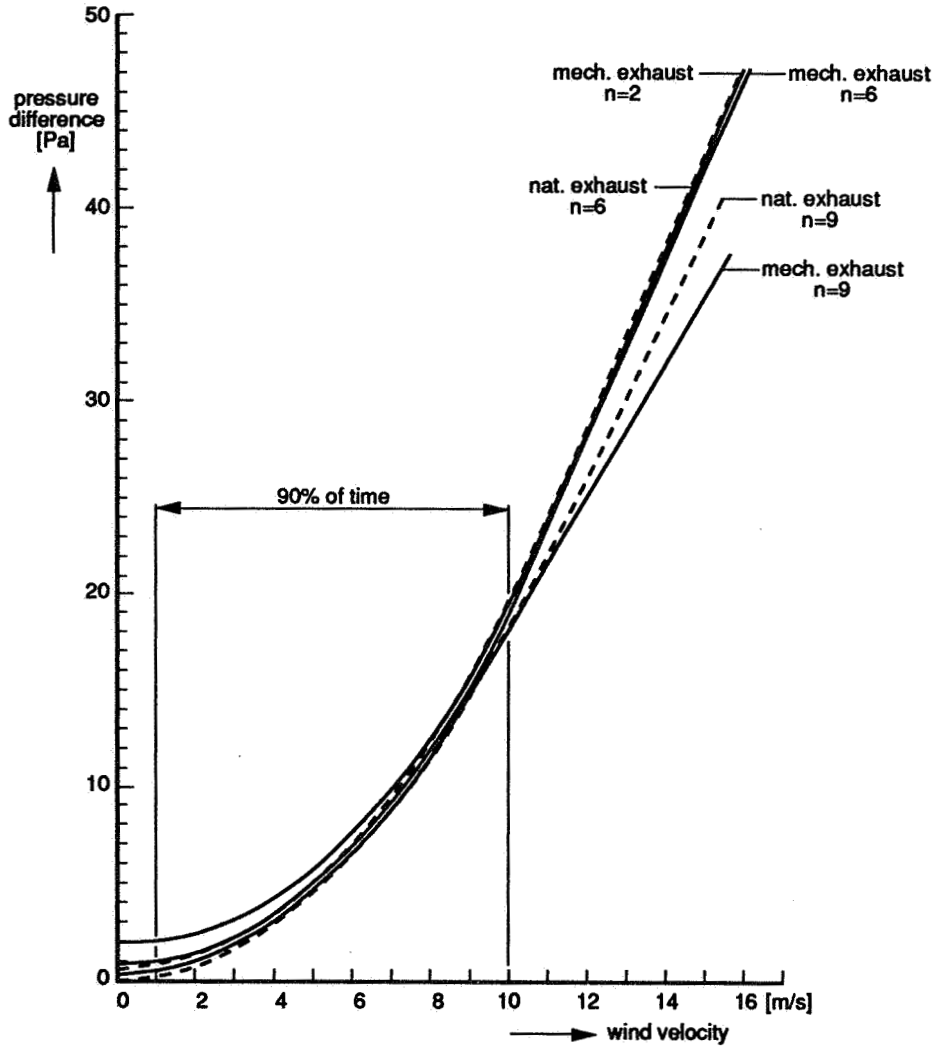

Figure 13: Calculated pressure differences over the windward facades of dwellings with self-regulating supply vents.
Natural or mechanical exhaust.
Air-leakage n=2, 6 or 9 ach at 50 Pa.

To enable the self-regulating vents to control on standard flows for about 90 % of time, control have to start at about 0.5 Pa and the air-tightness have to be at least 6 ach at 50 Pa in case of natural exhaust and 2 ach at 50 Pa for mechanical exhaust.
This is another advantage of the natural ventilation option over the mechanical exhaust option.
The total control range have to be from 0.5 to about 20 Pa, as can be derived from figure 13. Only control of supply flows is considered to be necessary.
This range of pressure differences is considered to be realistic, compared to on-site measurements [ref. 5].

The control requirements of the self-regulating vents are high. Especially control at 0.5 Pa may be hard to fulfil technically. One could wonder if a compromise is possible. Some self-regulating vents, already for sale, are intended to peak shave at high wind velocities, thus reducing draught risks. In this case control starts at about 20 Pa. Another option may be control starting at about 5 Pa, being the windward pressure difference under average conditions. The effect of both options on ventilation control of a windward and a leeward bed room is presented in figure 14. The options "control starting at 0.5 Pa" and "no control" (not even a manual control) are presented too, to enable a comparison. The 5 Pa and 20 Pa control option, as well as the no control option are dimensioned to enable standard flows at a wind velocity of 2 m/s and 5 °C temperature difference, according to the dutch standard.

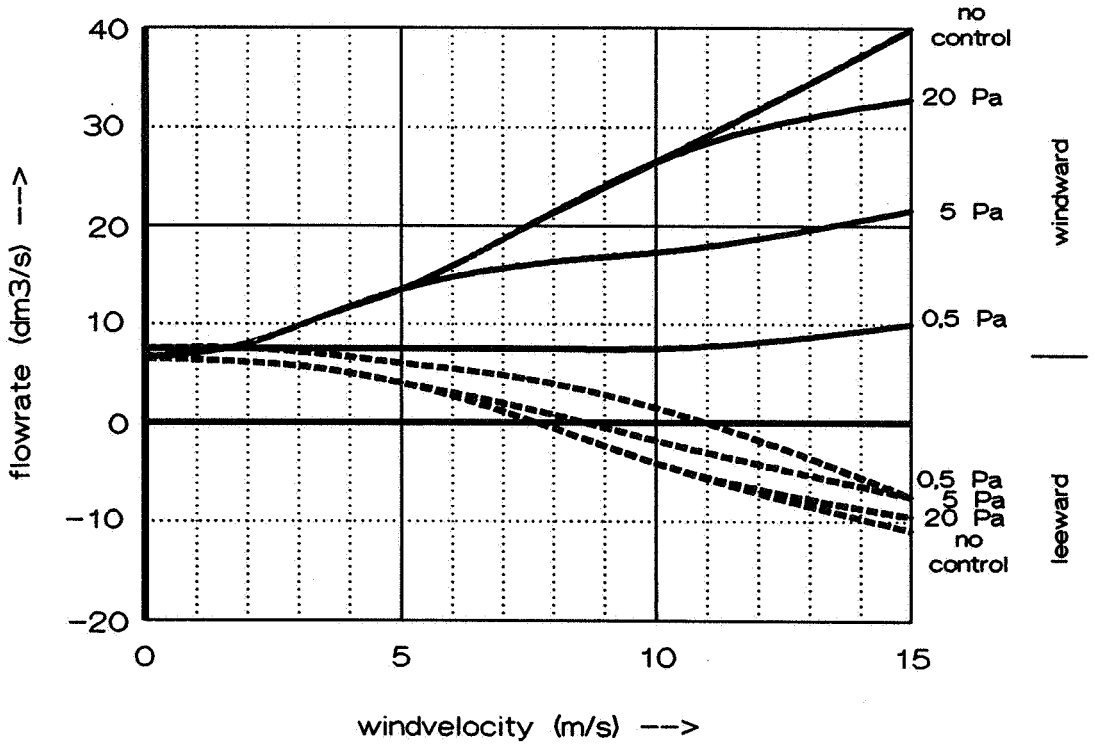

Figure 14: Windward and leeward bed room ventilation in an air-tight dwelling (2 ach at 50 Pa) with mechanical exhaust and self-regulating supply vents with:
-control starting at 0.5 Pa,
-control starting at 5 Pa,
-control starting at 20 Pa,
-no control.

Figure 14 shows that the 20 Pa control option only has a difference to the no control option at wind velocities above 11 m/s. These wind velocities will occur just 3.4 % of time. Hence, the effect of 20 Pa control on ventilation is negligible. The mean total ventilation and ventilation energy

consumption shows an overshoot of 60 % in stat of the 18 % with 0.5 Pa control (percentages related to an ideal standard ventilation). The leeward rooms remain under ventilated. The main aim, draught reduction, is not reached, while windward flows get up to 450 % of standard flows.
The image of the 5 Pa control option is just slightly better. Total ventilation and ventilation energy consumption still have an overshoot of 56 %. The average leeward bed room ventilation is about 47 % of standard values, which still means considerable under ventilation. Draughts at windward side are very likely, while flows get up to 300 % of standard value. Research in our climatic test chamber showed that a draught-less supply to a room, up to the standard flow of 2 persons, is possible, down to an outside temperature of -10°C, without pre-heating the air [ref. 6].

Another feature of the self-regulating vents, to be discussed, is the compensation of air leakage through the facades. The idea is to reduce the controlled flow with increasing pressure difference in the same amount the leakage flow of the same room is increased.

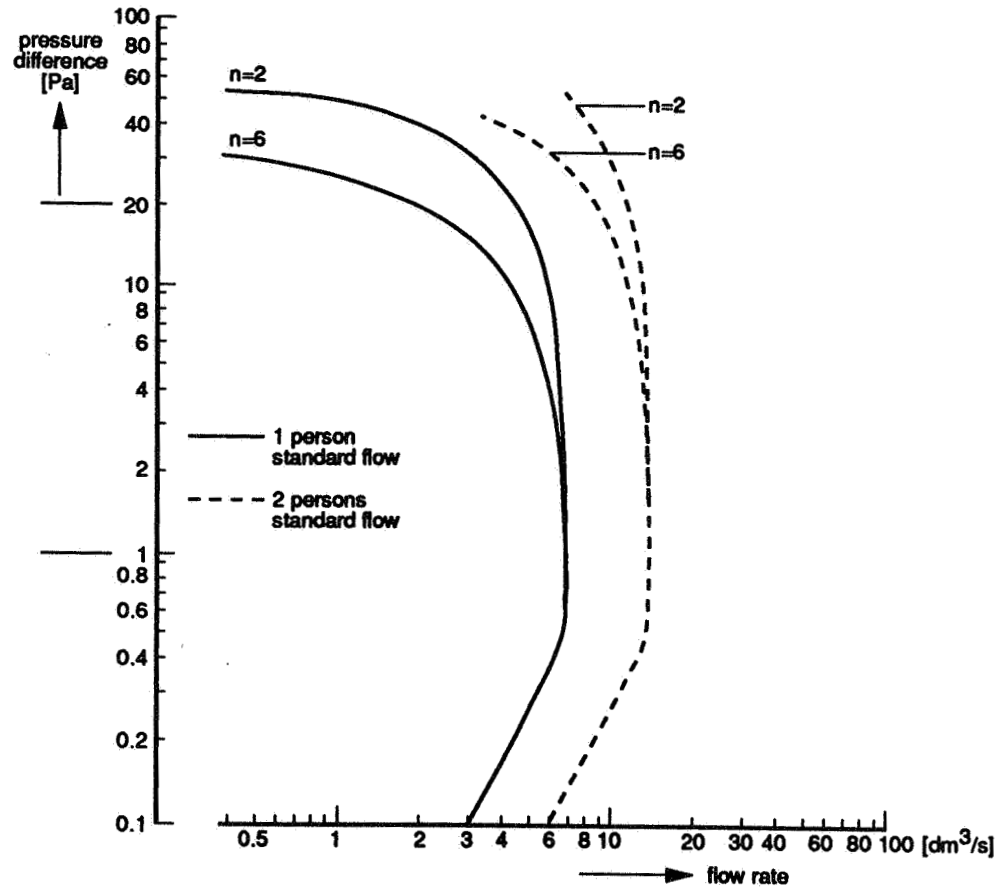

Figure 15: Ideal control characteristics of self-regulating vents with leakage compensation for two levels of air-tightness (n=2 and n=6 ach at 50 Pa).

For the case of leakage compensation the resulting control characteristics of the self-regulating vents are presented in figure 15, both, for 1 and 2 person(s) standard flows and air-tight and standard air leakage dwellings.
Calculations with and without leakage compensation show a minor effect on total ventilation, due to the minor contribution of the facades to total air leakage.
Nevertheless leakage compensation is recommended, because of its positive effect on leeward pressure differences, improving leeward rooms ventilation. It is also recommended because its reduction of draught risks. At increased pressure differences, namely, despite the flow rate control, the entrance velocity through a self-regulating vent is likely to increase. Hence, the impulse increases and with it the draught risk. Reducing the flow rate, because of leakage compensation, however, reduces the impulse and the draught risk again.

5. SUMMARIZED REQUIREMENTS

The calculation results show that controllable natural ventilation or controllable mechanical exhaust ventilation is possible.
The requirements to get an optimum control are mentioned in ref. 7. The main requirements are summarized here.

DWELLING REQUIREMENTS

* Preferred air leakage for optimum control:
  - 2 ach at 50 Pa in case of mechanical exhaust,
  - 6 ach at 50 Pa in case of natural exhaust.

However, to reduce energy consumption the highest air-tightness possible is recommended. Especially air tightening of the ground floor and other lower parts (supply openings) will improve control features.
* Overflow openings in internal walls of at least 10 cm^2 per dm^3/s, to allow the supply into bed rooms to overflow via hall and living room to service rooms, to be exhausted (in special cases silencers on these openings may be preferred).
The ventilation of the living room may be improved by creating an overflow preference to e.g. the kitchen via the living room in the dwelling lay-out.
* The vertical exhaust ducts of the ventilation system have to discharge in or near the pitch of the roof.
Self-regulating vents at least have to be installed into the facades of the bed rooms. Additional installation in the living room may be considered.

VENTILATION SYSTEM REQUIREMENTS

* Minimum dimensions of natural vertical exhaust ducts:
  - kitchen net 84 cm^2 (diameter approximately 16 cm),
  - bath room net 60 cm^2 (diameter approximately 14 cm),
  - W.C. net 30 cm^2 (diameter approximately 10 cm).
* Requirements for self-regulating vents:
  - control ratio 0.5 to 20 Pa, only functioning as supply control;
  - set point equals the standard flow for the number of inhabitants of the particular bed room (usually 1 or 2 persons = 7 or 14 dm^3/s);
  - supplied flow decreased at increasing pressure difference, to compensate air leakage of the facade;
  - set point manual adjustable by inhabitants to their individual ventilation needs, in an easy way and in steps of at least a one person ventilation need;
  - possibility to totally close each vent;
  - good dynamic behaviour at pressure fluctuations up to 60 % of the dynamic wind pressure, within frequencies of 0.3 to 7 Hz (to prevent effects like noise- generation, accelerated wearing and draught aggravation, due to fluctuations of incoming air).
    A time constance of 0.3 s is recommended;

- good design of the inside grid, to get a quick mixing of incoming air (to minimize the draught risk);
- durable, long life construction, insensitive for improper use and disturbances;
- operation preferably without auxiliary energy;
- to be built-in in common facade types;
- rain, insect and burglary protected on the outside;
- insensitive for pollution, combined with good cleaning possibilities;
- insensitive for temperature and humidity variations of the outside climate;
- preferably also available in a noise reducing variety;
- competitive sales price.

6. CONCLUSIONS AND RECOMMENDATIONS

CONCLUSIONS

A highly controllable natural ventilation system for permanent ventilation of dwellings appears to be possible. The main conditions for controllability are:

- over dimensioned vertical exhaust ducts with outflow near the pitch of the roof;
- self-regulating supply vents in the facades of habitable rooms.

The principle of controllable natural ventilation is also applicable on mechanical exhaust systems.
In that case, a higher air-tightness of the dwelling is recommended.
Also, the ventilation of separate rooms shows a slightly stronger relation to wind velocity.

The controllable natural ventilation system allows almost optimal air quality levels in all rooms.
The distribution of ventilation air to separate rooms is highly improved, preventing:

-under ventilation of especially leeward bed rooms (which is about 20 % of room ventilation standards for crack-supply and 65 % for supply through vent-lights),
-over ventilation of windward rooms (up to 400 % of ventilation standards in traditional natural and mechanical exhaust systems).

The ventilation energy consumption in an air-tight dwelling (2 ach at 50 Pa) with mechanical exhaust reduces from 142 % in case of good manual control, to 118 % in case of self-regulating vents (100 % is ideal standard ventilation).
With supply through cracks-only total ventilation is 106. %, however, as mentioned, air quality in bed rooms becomes very poor.
In the natural ventilation option, even an additional yearly reduction of about 500 kWh on auxiliary energy will occur, due to the absence of an exhaust fan.

In moderate climates, the occurrence of draughts, due to supply of unheated ventilation air, will be highly reduced by using self-regulating vents.
Consequently, the features of the highly controllable system will not be impaired by the interaction of the users.

RECOMMENDATIONS

The self-regulating vent is a vital component in the control system. A further product development is recommended.

The model calculations show some clear benefits of the proposed control system. An evaluation in practice is recommended.

7. REFERENCES

[1] Knoll, B.
The part of ventilation in humidity problems of low-energy houses.
Delft(NL), 1987, MT-TNO, publication P87/002 (in dutch).

[2] Kornaat, W.
Model calculations on self-regulating vents.
Delft(NL), 1988, MT-TNO, report R 88/034 (in dutch).

[3] Kornaat, W.
Additional model calculations on self-regulating vents.
Delft(NL), 1991, TNO-Building research, internal report.

[4] Hoeke, P. and P.J. Jansen
Saving on electricity. Still many possibilities.
(NL), 1990, Woningraad nr. 24, p. 53-56 (in dutch).

[5] Gids, W.F. de
Natural ventilation and energy consumption of dwellings.
Delft(NL), 1981, IMG-TNO, report C 482.

[6] Crommelin, R.D. et all
Tests on different types of air supply in dwellings and a climatic chamber.
Delft(NL), 1983, IMG-TNO, report C 513 (in dutch).

[7] Knoll, B.
Requirements on self-regulating vents in dwellings.
Delft(NL), 1988, MT-TNO, report R 88/049 (in dutch).

AIR MOVEMENT & VENTILATION CONTROL WITHIN BUILDINGS

12th AIVC Conference, Ottawa, Canada
24-27 September, 1991

PAPER 14

Design Guidelines for Thermal Envelope Integrity in Office Buildings.

Andrew Persily

National Institute of Standards & Technology
Building & Fire Research Laboratory
Building 226, Room A313
Gaithersburg MD
USA

ABSTRACT

Office building envelopes are generally successful in meeting a range of structural, aesthetic and thermal requirements. However, poor thermal envelope performance does occur due to the existence of discontinuity in the envelope insulation and air barrier systems, such as thermal bridges and air leakage sites. These discontinuity result from designs that do not adequately account for heat, air and moisture transmission, with many thermal defects being associated with inappropriate or inadequate detailing of the connections of envelope components. Despite the existence of these thermal envelope performance problems, information is available to design and construct envelopes that do perform well. In order to bridge the gap between available knowledge and current practice, NIST is developed thermal envelope design guidelines for federal office buildings for the General Services Administration. The goal of this project is to transfer the knowledge on thermal envelope design and performance from the building research, design and construction communities into a form that will be used by building design professionals.

This paper describes the guidelines prepared by NIST for GSA. These guidelines are organised by envelope construction system and contain practical information on the avoidance of thermal performance problems such as thermal bridging, insulating system defects, moisture migration problems, and excessive envelope air leakage. For each envelope system, both good and bad practice are discussed with an emphasis on the graphical presentation of envelope design details.

AIR MOVEMENT & VENTILATION CONTROL WITHIN BUILDINGS

12th AIVC Conference, Ottawa, Canada
24-27 September, 1991

PAPER 15

Buildings, health and energy

Johnny Kronvall

Department of Building Science
Lund University
P.O. Box 118
S-221 00 LUND
Sweden

Buildings, health and energy

A building must be capable of protecting us from cold, rain, wind, noise and air pollution. We should be able to stay in it and carry out various activities in it without suffering from ill-health or discomfort. The indoor climate should contribute to congeniality and wellbeing.

In point of fact, however, many people experience some form of ill-health - allergies, irritation of mucous membranes etc. - when spending time indoors. Some problems of this kind have been found to be attributable to the indoor climate of the buildings. In many cases the troubles are difficult to explain. It is problems of this kind that lie behind the concept of "sick buildings".

Shortcomings in the indoor climate thus constitute a problem in both dwellings and working premises. It is particularly disquieting to note that the problems are experienced mainly in environments in which we spend the major share of our lives: in dwellings, schools, day nurseries and care premises. In all probability, persons suffering from allergies or other types of hypersensitivity are affected to a greater extent than others by shortcomings in the indoor climate. The frequency of hypersensitivity is alarmingly high and seems to be rising, by no means least among children.

This speech comprises a summary of two publications from the Swedish Council for Building Research (BFR); the knowledge survey "Buildings and Health" (BFR T4:90) and "Indoor climate and energy husbandry" (BFR G5:90).

One central conclusion presented in both these publications is that the hygienic and climatic requirements are frequently neglected and that they must reassume a central position in the building and building management process.

This means that the requirements must be stepped up so that greater demands are made on the quality of the materials, on responsibility and competence in the building process and on the overall strategy for energy conservation in conjunction with both new construction and modernization.

Unless such requirements can be satisfied in practical building, the price will have to be paid in the form of more energy.

Climate and air quality

Noise

Noise disturbances depend not only on the level and pitch of the sound but also on the activity which is disturbed and the attitudes of the individual to the sound and its source.

In order for sleep disturbances to be completely avoided the continuous sound level should not exceed 30-35 dBA. The maximum level for individual noise occurrences should not exceed 45 dBA. Most fan and ventilation noise has a frequency which is considered to be underestimated by the dBA unit.

The National Board of Health and Welfare proposes a 35 dBA daytime and 30 dBA night-time limit for sanitary inconvenience due to momentaneous sounds in rooms in dwellings. For noise with elements of very low-frequency sound, equivalent sound levels of 28 dBA daytime and 23 dBA night-time are proposed.

Light and lighting

The amount of light must suffice for the activity engaged in and, moreover, the light must be correctly distributed in the room in the right direction. It is vital to avoid dazzling and unsuitable shadowing. Colours must be reproduced as naturally as possible.

Poor work lighting is hard on the eyes and often leads to unsuitable working postures and accident hazards. Most people do not need work lighting in excess of 300 lux. For precision work, several thousand lux may occasionally be desirable. Daylight and provisions for looking out should be provided in all rooms where people spend any appreciable length of time.

Temperature

Chills and draughts can cause rheumatic troubles. Impaired muscular function, which is more common, can result in clumsiness, thus increasing the risk of accidents. Too high a temperature gives a feeling of dryness and a lower level of wakefulness. It is also believed to cause fatigue and headaches. Owing to individual differences it is impossible to specify a thermal surrounding that satisfies everybody at the same time, even if all the people are similarly dressed. As a rule, it is not possible to get further than to conditions in which 80 per cent of the individuals feel satisfied. Elderly persons and others who spend a great deal of their time sitting still or who suffer from circulation troubles need a higher temperature than younger and healthier individuals.

Draughts are experienced as more troublesome the higher the air velocity is and the colder the air is, but variations in air velocity also give rise to a greater feeling of draught. A certain amount of air motion is obviously necessary in order to produce the requisite air circulation in a room.

The National Board of Health and Welfare recommends the following values:

* The operating temperature in premises should be between 20 °C and 24 °C.

* The difference in air temperature at the head and feet of a seated individual (1.1-0.1 metres above the floor) should not exceed 3 °C.

* The radiation temperature asymmetry due to the influence of, for instance, a cold window or a cold wall, should not exceed 10 °C.

* The radiation temperature asymmetry due to the influence of ceiling heat should not exceed 5 °C at a height of 1.1 metres above the floor for standing persons and 0.6 metres for seated persons.

* The average air velocity at an operating temperature of 20-24 °C should not exceed 0.15 m/s. In this context, it should be noted that rapid variations in air velocity can lead to draughts, even if the average velocity is low.

Air humidity

The ability of the human being to objectively assess relative humidity is relatively poorly developed. Air humidity is therefore primarily of indirect importance for the manner in which the climate is experienced. At low relative humidity, human beings and materials become statically charged and the generation of dust increases. High air humidity, in contrast, increases the risk of condensation on parts of the building and is conducive to the growth of mites and algae. The emission of gas from materials, fixtures and fittings is also facilitated at high humidity.

The water content in the room air in dwellings should be kept below 7 grammes of water per kg of dry air (corresponding to a relative humidity of 40 per cent at 20 °C) for at least 1-3 months of the year in order to prevent growth of dust mites. General humidification of the air is not to be recommended from the standpoint of hygiene, since the risks of side effects are considerable. Discomfort attributable to "dry air" can usually be remedied by lowering the air temperature one or a few degrees.

Air quality

The air change in a room is not utilized only to ensure that the content of oxygen is sufficient and that the content of carbon dioxide is not too high. It is also utilized for cooling, to regulate the air humidity and to lead away different types of pollutants generated in the room. The most important sources of pollution are the following:

* Building and fitting materials, furniture.

* Radon from building materials and foundations.

* People and animals.

* Tobacco smoke.

* Microbiological growth (mould, mites, algae etc.).

* Cooking.

* Cleansers and pesticides.

* Cosmetics.

* Playing and hobby activities.

* Open combustion (e.g. gas stoves).

* Traffic exhaust (e.g. from garages).

* Refuse incineration and industrial plants in the surroundings.

Building materials

Pollutants from building materials and from materials used in fixtures, fittings and furniture can -- either individually or in combination - cause discomfort of various kinds: irritation of the eyes, nose and throat, a feeling of dryness in mucous membranes and skin, skin rashes and unpleasant smells. The development of new materials has made the situation difficult to master, since on many occasions the exact composition of the materials is unknown when they are first introduced on the market, so that there is a lack of knowledge of the substances emitted by the materials and of how these substances behave.

One particular problem is that the ventilation ducts collect impurities that can emit harmful or troublesome substances.

Mineral fibres can accompany the air we breathe and coarse fibres, if touched, can cause skin and mucous membrane irritations. The mineral fibre that has attracted most attention is asbestos, the use of which has been prohibited in Sweden ever since 1976. This material is nevertheless present in built-in form in many different places and the risks thus remain. What is particularly problematical is the circumstance that so many ventilation ducts contain asbestos.

Fibres of mineral wool have been associated with irritation of the skin and of the mucous membranes.

Formaldehyde can give rise to discomfort. The World Health Organization (WHO) recommends a maximum guide value of 100 $\mu g/m^3$. The National Board of Health and Welfare has stipulated 250 $\mu g/m^3$ as a limit for sanitary inconvenience.

Some self-levelling screeds can give rise to hypersensitivity troubles and unpleasant smells.

Radon

The risk of lung cancer being caused by radon is difficult to assess and estimates vary between 100 and 3,000 deaths per annum in Sweden. One of the factors influencing the assessment is the relationship between exposure to radon and smoking.

In the New Building Rules promulgated by the National Board of Housing it is prescribed that the annual mean value of the radon daughter content may not exceed 70 Bq/m^3 in rooms constantly occupied by persons. According to the rules laid down by the National Board of Health and Welfare the limit value for the radon daughter content in existing buildings is 200 Bq/m^3.

Carbon dioxide and carbon monoxide

The content of carbon dioxide in the air exhaled by individuals is frequently used as an indicator of the pollution content from human beings. The outdoor air contains 300-400 ppm carbon dioxide. Inadequate ventilation in combination with a high person load can generate contents in excess of 1,000 ppm indoors.

The occupational hygiene limit value for carbon dioxide is 5,000 ppm, based on the inherent harmful effects of this substance. The National Board of Health and Welfare has proposed that the limit for sanitary inconvenience be set at a total of 1,000 ppm carbon dioxide.

The primary sources of carbon monoxide (CO) indoors are combustion gases from vehicles and tobacco smoke. Open fires indoors can generate high contents. Carbon monoxide is also spread from garages.

Normal, fresh outdoor air contains about 1 ppm of carbon monoxide. In busy streets the content is 10-20 ppm. Smoking in a room increases the content by 5-10 ppm. If the source is known, carbon monoxide can be used as an indicator of several pollutants in particulate and gaseous form from this source.

Environmental tobacco smoke (passive smoking)

The most commonly occurring and rapidly experienced health effects of tobacco smoke are irritation in the mucous membranes of the eyes, nose and throat, and an unpleasant smell. Children of smokers suffer more often than others from diseases of the lower respiratory passages, bronchitis and asthma.

Tobacco smoke resulting in CO contents in excess of 2 ppm in the room air lead to severe irritation of the eyes or other discomfort among about 20 per cent of those exposed.

Outdoor air

An air pollutant is seldom present in outdoor air on its own and normally the air contains a mixture of several pollutants. The composition varies according to the prerequisites. It has not yet been determined how the various substances affect human beings when they interact. The effects of air pollutants also depend on factors such as temperature and humidity and probably also on the presence of pollen and mould, etc. This means that limit values for individual substances are relatively inadequate means.

Guide values have been stipulated for the maximum concentrations of certain substances in the outdoor air:

Substance	$\mu g/m^3$	source
Sulphur dioxide, diurnal mean value	100	SNV
Sulphur dioxide, hourly value	200	SNV
	350	WHO
Sulphur dioxide, 10-minute value	500	WHO
Particle concentration, annual mean value	75	SNV
	50	WHO
Particle concentration, diurnal mean value	260	SNV
	125	WHO
Nitrogen dioxide, diurnal mean value	75	SNV
	150	WHO
Nitrogen dioxide, hourly value	110	SNV
	400	WHO
Ozone, hourly value	150-200	WHO
Ozone, 8-hour value	100-120	WHO

SNV = National Environment Protection Board
WHO = World Health Organization

Hypersensitivity

The number of hypersensitive or allergic individuals appears to have increased substantially in recent years. The substances which are the prime causers of allergies are pollen, animal hair, dust mites and mould.

Dust mites are tiny spiderlike animals only about one-tenth of a millimetre in size. They need both heat and high air humidity in order to propagate. Growth of mites is prevented if the air humidity is kept at a low level for a few months of the year.

As a rule, the mould contents in buildings are not so high that they constitute a risk of allergy among normally healthy individuals. In persons who are already allergic to mould, the contents in a dwelling with a "normal" content of mould can nevertheless suffice to trigger symptoms such as asthma, hay fever, hives or eczema.

The most common problem is that the mould fungi are capable of forming substances emitting a powerful odour of long duration. Sensitive individuals are also likely to suffer from irritation of the respiratory passages, skin and eyes.

Mould fungi thrive on surfaces on which there is nourishment and a suitable humidity, for instance damp water pipes, windows and walls in kitchens and bathrooms or inside damp structures. Mould is also counteracted by low humidity.

Building design and construction

The orientation of buildings and their locations in relation to one another influence the outdoor climate in the immediate surroundings. The outdoor climate, in turn, is one of the prerequisites for the indoor climate. Those parts of the architectonic configuration that probably have the greatest influence are the manner in which light and solar radiation are exploited and how wind protection and local environment are created.

Location of the building

The very location of a building can cause problems with the indoor climate. Waterlogged land or land with difficult runoff conditions should not be built on without a special foundation. Land with a high content of radon also imposes exacting demands in this respect.

Cold spots and areas in which streaks of fog are common should be avoided, as should locations exposed to keen winds. The relative locations of buildings can have a considerable influence on local wind conditions. Other external circumstances that can give rise to problems are noise, smell, smoke, vehicle exhaust and other pollutants.

Sunlight is of major importance for congeniality and comfort. Properly utilized, solar irradiation can also afford a substantial contribution to the heating of buildings. Allowance must nevertheless be made for the risk of uncomfortably high indoor temperatures during the summer months. Large window areas increase the risk of radiation draughts during the winter.

Shape and configuration

Both the configuration of the building and the shape of the rooms and their locations in the building influence air circulation and ventilation requirements. The layout can also be used as an active means of providing protection against noise, good lighting conditions etc. The interplay between form, light and colour is also of considerable importance for climatic experience and wellbeing.

Another important aspect of the layout is the need for sufficient and readily accessible spaces for building services, care and maintenance.

Materials and structures

The choice of the right materials in the building structures, fixtures and fittings may be of decisive importance for how healthy the building will be.

Structures should be consistently tested from the standpoint of building physics (e.g. moisture dimensioning) and with due regard to the long-term permanence. It is also important for the structures to be understandable enough to be executable in practice on the building site.

The rapid development in the area of materials renders the task of both planners and designers more difficult. Mandatory testing and a mandatory statement of the contents of materials are therefore desirable and should also cover furniture, fixtures, fittings and machinery. Many problems can nevertheless be avoided with relatively simple means:

* Use only materials with a statement of contents and which are low-emitting.

* Never use materials with a known or suspected toxic effect on human beings.

* Find out what climate the material will be exposed to in the built-in condition, and never build in a material that perhaps cannot withstand this climate.

* Check the long-term durability of the material and insist upon test certificate of this.

* Make sure that understandable care and maintenance instructions are provided.

Moisture protection

Moisture is one of the most severe stresses to which our buildings are exposed. Rain, snow and ground moisture give water which may have negative effects both on the building (mould, rot and corrosion) and on the indoor climate (growth of fungi and mites). The energy balance also deteriorates, since heat is used when water evaporates.

The following points should be observed in conjunction with the structural work:

* Prevent moisture from reaching sensitive materials in the various parts of the building.

* Locate moisture-sensitive structural parts as warm as possible.

* Make provisions for ventilation of structural parts which are liable to get damp despite everything.

* Elaborate the design so that unwanted water is easily detected.

* Specify how much drying out of different parts of the building is required.

When working on the construction site, good moisture conditions are created, for instance by

* Using prescribed materials.

* Protecting materials against moisture and not building in damp materials.

* Complying with the drawings as regards the location of damp-proof courses, thickness and application method.

* Preventing mechanical damage in damp-proof courses.

* Clearing rubbish and residual materials from all spaces.

* Providing time for drying out.

During the user phase, moisture problems are avoided by:

* Limiting the amount of water vapour generated by showers and laundering.

* Making sure that the air passages in wet spaces are not blocked.

Building ventilation

The task of the ventilation is to supply air of good quality and to contribute to a sound room climate. The ventilation requirements are dimensioned by numerous factors: the balance between oxygen and carbon dioxide in the air, smell, temperature, moisture and the occurrence of unwanted substances. Over and above a certain basic level, emissions from materials, tobacco smoking and the presence of moisture are normally the factors that decide the need of ventilation.

Air change requirements

In the New Building Rules promulgated by the National Board of Housing it is specified that the flow of outdoor air to rooms with a normal room height occupied by human beings more than temporarily shall be at least 0.35 l/s per square metre of floor area. In bedrooms, however, the air change rate must be at least 4 l/s per sleeping place. In offices the minimum requirement is 5-7 l/s and person. From kitchens, bathrooms and toilets in dwellings at least 10 l/s must be extracted, which will be the dimensioning figure in small apartments.

This air change rate is the result of numerous considerations: an acceptable indoor climate, good energy husbandry, no moisture damage to the building structure and so on.

The requirements are valid provided that the strains on the air quality are moderate. In offices where smoking is permitted the outdoor air flow rate must be at least 10 l/s per person.

Design of ventilation systems

A well-designed ventilation system must be easy to install, easy to adjust and easy to look after.

The work on the construction site is facilitated if the various tasks to be performed are uncomplicated and safe. Joints and couplings that are simple to apply should be chosen. Adjustment of the system, which is very important indeed, requires sufficient dampers and measuring devices of good quality.

The operation and maintenance of the building services and systems must be at the focal point of the planning work. The alternatives are sufficient simplicity for practical care or sufficient complexity to eliminate the need of care. Simple and logically arranged systems, by all means divided into smaller units, simplifies operation and increases the possibilities of individual adjustment of the air flow rates.

From the standpoint of operation, apparatus should be placed where it is easy to reach and so that it is easy to carry out service on or replace components. Ducting shall be arranged so that it is easy to clean. Only components with good performance and long service life should be selected.

Effective ventilation

It is of very great importance from both economic and comfort standpoints that air distribution and air flows in the rooms are as effective as possible. This effectiveness is nevertheless fundamentally dependent on limitation of the pollutants and their dispersion.

The ventilation, moreover, must retain its function with the passage of time. Measurements in buildings have proved that the factual outdoor flow is often far below that specified in regulations and procurement documents.

Return air recycling

The New Building Rules promulgated by the National Board of Housing accept ventilation systems with return air under certain conditions. Problems with spreading of tobacco smoke and other pollutants, however, indicate that return air recycling should be avoided. When such systems are required, special requirements must be imposed on fine adjustment, regular functional checking and cleaning of ducting systems and filters.

Responsibility and co-operation

The elaboration of the building process and the conditions under which it is performed afford a necessary background to any and every discussion of the final products of building. Studies of "sick buildings", by no means least, have focussed on the overall building and management process, since the causes of the problems cannot be attributed to any specific phase but appear as an interactive effect of planning, designing, construction, fine adjustment, handing over, operation and maintenance.

Cost rises and obvious shortcomings have rekindled the discussion of quality assurance of building in recent years. Among the obvious problems in this respect are the numerous decisions and deliberations between various interests and areas of competence embraced by building.

Formulating the quality requirements is in itself a difficult task. Following them up and evaluating them is even more complicated. The building process is largely unidirectional, in that earlier stages give instructions, rules and restrictions governing how subsequent stages are to handle the technique. The space available for complete quality loops (planning - execution - follow-up) is extremely limited.

Co-operation in the building process

The programme work is the task during which the fundamental requirements are to be formulated. The forms for this important task are still inadequately developed. This is particularly true of knowledge of how to express demands on the indoor climate.

The ability of the client to place the order is highly decisive for the results. In the dialogue with the designer it is a matter of translating general wishes into quantitative data. The knowledge necessary for this dialogue is frequently lacking. Relatively few clients, moreover, have a really clear idea of the importance of qualified planning and designing. The result may easily be that certain qualities are overemphasized at the expense of others and that cuts are made at the expense of quality and longtermness.

Co-operation problems are also encountered between the different designers. The building services, for example, are not designed sufficient co-ordinated with the design of the building.

One particularly critical point is when the building passes from production to management. Handing over to the management seldom takes place in a systematic manner and with the requisite documentation for operation and maintenance.

Building documentation

The building documents of today are marred by considerable deficiencies. They serve mainly as documentation of the designing and as directions about what is to be done. More seldom do they specify how this is to be done and virtually never why. Consequently, risks are incurred for faulty execution and faulty handling.

Instructions for operation and maintenance are essential with the complicated buildings of today. To the extent that such instructions are provided they are frequently inadequate. A minimum requirement is for the instructions to describe the stipulated functional requirements and how they are satisfied, to give a correct description of the final execution of the building and of how care and maintenance are to be performed.

Division of responsibilities

Purposeful quality work presupposes as a rule that those involved have tangible incentives. The relationship between producer and consumer in the building sector is, however, far too unclear on account of the numerous parties involved.

The system of responsibility must become clearer, for instance in that the client and the manager are given direct responsibility for observance of the demands made by the users on a healthy building. Similarly it is essential for feedback of experience to be improved so that unsuitable technique can quickly be eliminated.

Healthy buildings require a combination of proven experience and scientifically founded knowledge. It is therefore a matter of responsibility that all parties must endeavour to keep themselves informed of and to apply both known and new knowledge.

Operation and maintenance of the building

To the same extent as other technical products, the building and its building services require skilled care and continuous maintenance. Deficiencies in care and maintenance of the building services systems are, however, by no means uncommon. Obviously these deficiencies and shortcomings have an adverse effect on the quality of the air.

Systematic care and maintenance

Experience indicates that not even large facilities, where the manager normally has professional personnel at his disposal, are looked after satisfactorily in practice. Operating personnel often lack the necessary knowledge and the climatic issues are neglected by comparison with energy conservation and structural engineering measures.

For many of the technical subsystems in the building there are clear signals of functional shortcomings. This, however, does not apply to air treatment. The air pollutants are not easy to detect and the costs often decrease with poor function. The conclusion must be that the ventilation requires systematic control and attendance in order to be kept in good condition. Regular functional checks must be combined with cleaning and filter changes at regular intervals.

In order to save energy, air flow rates in working premises are often set at a lower level during nights and weekends. The result is likely to be that the ventilation does not suffice to remove pollutants from building materials, fixtures and fittings. This is particularly unfortunate in new buildings.

Expedient management includes regular and frequent tidying and cleaning -- by no means least of the ventilation ducts. It is nevertheless important for the tidying and cleaning to be done with cleansing agents which in themselves do not cause negative effects on health.

Increased managerial responsibility

Increasingly exacting demands on competent property management are imposed in pace with the increasing complexity of the building services. Obviously, the technique must be chosen in view of the level of knowledge within the management organization, but knowledge within the management must nevertheless be maintained in respect of the selected equipment.
The rules and regulations concerning building impose all too limited demands on function in the operating stage and on the responsibility of the management for healthy conditions.

Energy conservation in buildings

Energy conservation is one of the prerequisites for a good indoor climate in that most forms of energy production and use have negative effects on the outdoor air supplied to the building. Moreover, in our climate a well insulated building that is free of draughts comprises the building engineering base for a sound indoor climate. The thermal comfort will be good in that radiation draughts towards cold surfaces, draughts on account of leaks in the climate screen, etc., are reduced.

Thermal insulation

In the same way as in new buildings, improved thermal insulation normally contributes to a better thermal indoor climate, particularly in the parts situated close to exterior walls and windows. During the spring and autumn, in certain cases, there is a risk of uncomfortably high indoor temperatures in buildings with large window areas facing south and with effective thermal insulation.

Since the amount of heating needed by the building will change in conjunction with supplementary insulation, it is important for the heating system to be readjusted after the measure.

Tightness

Properly functioning and controlled air change in a building presupposes that the building is airtight. On the other hand, an airtight building requires a properly functioning ventilation system with correctly located supply air registers.

Tightening old buildings with the aim of saving energy must be done with great care. As a rule, it will be necessary to make new openings for controlled outdoor air supply.

Air change and energy

Practical experience shows that problems with the indoor climate often arise in the intersection between energy husbandry and changes in materials or technique. This does not mean that indoor climate and energy conservation are in a state of opposition, but increased air change rates inevitably mean that larger volumes of air have to be heated up.

To keep the necessary outdoor air flow down every effort should be made in the first instance to reduce pollution. In those cases when problems with air quality or thermal comfort cannot be remedied except with increased air flow rates or higher air temperatures this is justified despite the fact that the use of energy can increase. The costs for investments in energy conservation or higher use of energy should be considered in relation to the costs incurred by society for production losses, care of the sick and wear on the environ etc.

All outdoor air supply to a building must normally be heated for reasons of comfort. If the air flow rates are increased, more energy is required. The difference

may be considerable. The following table gives a summary of ventilation levels for a room with a floor area of 12 m^2 per person.

Ventilation levels deseribed in different ways for a room with a floor area of 12 m^2 per person. The originally used measure is shown in bold type.

	l/s and person	air changes/h	l/s and m^2 floor area	energy kWh/year	cost, SEK/year
New Building Rules (dwellings, general)	4.2	0.53	**0.35**	554	222
New Building Rules (bedroom for two persons) and ASHRAE Ventilation Rate Procedure, base level	**4**	1	0.67	1,045	418
New Building Rules (offices)	**5**	0.63	0.42	657	264
Buildings and Health, functional margin	**7**	0.88	0.58	920	368
Buildings and Health, high emission	**20**	2.5	1.67	2614	1046
Allergy Commission, low emissions and the NKB proposal	**10**	1,25	0.83	1,307	523
Allergy Commission, safety level	**15**	1,88	1,25	1,965	780
Allergy Commission, high emissions	**30**	3,75	2,5	3,920	1,568

For a detached house with an area of 144 m^2, occupied by six persons, the annual energy requirement to heat the ventilation air may vary between about 6,600 kWh (general requirement of the New Building Rules) and 23,500 kWh (requirement of the Allergy Commission at high emission levels).

Systems for heat recovery are, however, becoming increasingly common. As a rule, up to a good 50 per cent of the heat in the ventilation air can be recovered. With a heat pump which collects the heat in the exhaust air through a heating battery the recovery factor is normally even higher.

The requirements imposed in the New Building Rules for dwellings give a significant safety margin for households that are now overcrowded. (This is particularly true of single-family detached houses.) The true air flows, however,

are often smaller than those specified in the norm, and consequently a satisfactory ventilation standard requires some increase in energy use.

Strategy for energy conservation

Buildings and the built environment account for more than one-third of the total amount of energy used in Sweden. Bearing this in mind, the technique used for heating buildings and hot water is of central importance for the change-over of the energy system necessitated by the phasing-out of nuclear power.

Since the first energy conservation plan of 1978 the building stock in existence at that time has reduced its energy use for heating and hot water by about 25 per cent, from 120 to 90 TWh. The phasing-out of nuclear power is now displacing interest towards more efficient use of electricity and against energy and power husbandry that can limit such electricity use as cannot be avoided.

The possibilities of conserving even more energy are good partly with more efficient insulation, heat recovery, increased quality control and meticulous fine tuning, and partly with developed techniques such as solar heating, heat storage and heat pumps.

The aspiration must be to reduce energy use in buildings in the long term by exploiting the potential offered by modern building and climate techniques. It is important to carry out energy conservation measures in conjunction with modernization and refurbishing of existing buildings in appropriately composed action packages. In existing buildings, this also normally results in improved climatic and functional quality.

The indoor climate must nevertheless be the guiding factor for energy conservation. This implies stricter demands on the quality of the materials, on responsibility and competence in the building process and on the entire strategy for the energy conservation work. Over and above energy-efficient properties, materials, constructions and components must obviously have long durability and give low operating and maintenance costs, both when constructing new buildings and when improving old ones.

A broader view of resource husbandry calls for more than the best possible use of energy in view of kind of energy, time distribution and application areas. In building, also, the approach must be extended to an overall husbandry with resources, involving balances between, for instance, public health, dwelling standard, energy use and nature conservation. Unless such requirements can be satisfied, the aspirations with regard to energy conservation will have to be lowered.

Each individual building is a part of a local/regional ecological system and of several energy systems with a local, regional or national span. There are enormous differences between southern and northern Sweden, between the major conurbations, medium-sized towns, semi-large or small population centres and purely rural areas. Consequently, it cannot be taken for granted that a national uniform view of the configuration of the built environment as a climate system will result in the most efficient husbandry.

Important new components such as natural gas and wind power will be able to be established only in limited parts of the country. Some types of places will have ample access to waste heat from the production of electricity in combined power and heating systems. Other places have biofuels within easy reach and a sparseness

in the built environment that facilitates the use of bulky fuels, establishment of compost/digestion gas production etc. In the built environment that is not heated with power or waste heat, solar heating in combination with other environment-friendly energy systems appears to be interesting.

In this perspective, more stringent demands are imposed on municipal and regional planning with accompanying supply and use of energy. At the same time a prerequisite for successful energy husbandry is for there to be a long-term national strategy with clear goals for the environment and energy policy.

AIR MOVEMENT & VENTILATION CONTROL WITHIN BUILDINGS

12th AIVC Conference, Ottawa, Canada
24-27 September, 1991

PAPER 16

ASHRAE Standard 62-1989
Energy, Cost, and Program Implications

Timothy Steele and Marilyn Brown

Bonneville Power Administration
P.O. Box 3621- RMC
Portland, OR 97208
USA

SYNOPSIS

ASHRAE Standard 62-1989, "Ventilation for Acceptable Indoor Air Quality", increases ventilation rates from 5 to 15 CFM. This study evaluated implications for commercial buildings conservation and demand side management programs adopting Standard 62-89, including potential increases in energy use and cost, and problems with interpretation and verification.

Commercial buildings prototypical of construction in the Pacific Northwest were analyzed by modeling energy use on the DOE-2.1D energy simulation computer program. Standard 62-89 specifies ventilation rates per person with estimated occupancy densities. Use of its occupancy density is at the user's option. This study analyzed the new ventilation rates, by (1) Standard 62-89 occupancy densities, and (2) alternative occupancy densities. For Standard 62-89 densities, energy use and cost increases varied less than 1% up to 43% depending on building type. For densities based on assumed actual occupancies, increases varied less than 1% to 15%. Standard 62-89's occupancy densities created ventilation requirements exceeding system capacity in high density building types.

The study recommends adoption of the new higher ventilation rates, but with the use of alternative occupancy densities. To verify compliance with Standard 62-89, the study recommends the method of taking a ratio of temperatures to determine percent outdoor air with a total supply air measurement to determine supplied outside air for each air handler serving the building.

1.0 BACKGROUND

ASHRAE Standard 62-1989 (Standard 62-89) "Ventilation for Acceptable Indoor Air Quality" is the new heating, ventilating, and air-conditioning (HVAC) industry consensus for ventilation air in commercial buildings. Bonneville Power Administration (Bonneville) references ASHRAE Standard 62-81 (the predecessor to Standard 62-89) in their current environmental documents for required ventilation rates. In terms of Bonneville-sponsored commercial building energy conservation programs, the two most important revisions for the new Standard are (1) the deletion of the distinction between smoking-permitted and non-smoking spaces and (2) an increase in the minimum outside air requirement for most spaces from 5 cfm/person to 15 cfm/person.[1]

Before incorporating Standard 62-89 into Bonneville's energy conservation programs for both new and existing commercial buildings, it was important to review the revised standard to determine the need for interpretation and evaluate its enforceability. Minimum ventilation rates have been tripled by Standard 62-89 (for non-smoking spaces). With almost all buildings, increasing the amount of outdoor ventilation air will increase energy consumption. Therefore, it is important to understand the significance of outdoor ventilation air in terms of energy and cost. Bonneville also experienced problems in interpretation and compliance when Standard 62-81 was simply referenced as the ventilation requirement in commercial building energy conservation programs.

This study was performed with the specific objectives of evaluating the energy and cost implications of Standard 62-89 and providing an interpretation and a verification procedure for use in Bonneville's commercial building programs. To evaluate the energy and cost impacts of Standard 62-89, we performed hourly energy simulations on ten building types in two climates using the DOE-2.1D energy simulation program. Results from these simulations estimate the energy and cost impacts associated with Standard 62-89. To interpret Standard 62-89 we considered only one path of compliance: The Ventilation Rate Procedure. Within that procedure are several provisions, each of which is discussed and interpreted. The costs of verifying compliance with Standard 62-89 are outlined and a verification procedure is given.

2.0 ENERGY USE AND COST IMPLICATIONS

A paper published in the ASHRAE Journal investigated the issue of increased ventilation air on building energy use.[2] The authors performed a study which found annual energy operating costs increase by less than 5 percent as a result of Standard 62-89. Bonneville supported further similar study for the following reasons:

1. No Pacific Northwest climates were considered.
2. Only one building, a large office, was included in the paper.
3. The building had a gas heating system, which would underestimate any impacts on electric demand.

2.1 STUDY OVERVIEW

Bonneville's study estimated the energy and cost implications of ASHRAE Standard 62-89 using simulations based on DOE-2.1D, a computer simulation program which estimates building use hourly as a function of building characteristics and climactic location. Ten types of prototypical commercial buildings used by Bonneville for load forecasting purposes were examined: Large and Small Office, Large and Small Retail, Restaurant, Warehouse, Hospital, Hotel, School, and Grocery. These building characterizations are based on survey and energy metering data and represent average or typical construction and operation practices and mechanical system types.

For each building type, there is an existing building model and a new building model, totaling 20 building models. Each of the prototypes are all-electric, and exist as files on the DOE-2.1D simulation program.

Prototypical building ventilation rates were varied in five steps to estimate the impacts of outside air on building energy use. Input to DOE-2.1D for ventilation air is accomplished in the SYSTEMS portion of the program. Ventilation air can be specified as either a fraction of total supply air, outside air per person, or cfm. For this study, ventilation air was specified as outside air per person. The calculated rate is the minimum outside air rate when the HVAC system supply fans are on and with no economizer control.

2.1.1 Occupancy

Occupancy levels appeared significant when Standard 62-89 Estimated Maximum Occupancy values were compared to the assumed values used in the prototypes. Table 2.1 shows the result of this comparison. For all building prototypes, the Standard 62-89 values for suggested occupancy were significantly higher than those assumed in the prototypes. To interpret the relevancy of these higher occupancy values, we compared Standard 62-89 to two other industry standards: 1988 Uniform Building Code (UBC) occupant load factors for building egress and ASHRAE Standard 90.1P Occupancy Density for use in energy calculations.

Standard 62-89 Estimated Maximum Occupancy values were comparable to UBC occupant load factors. The prototype-assumed levels of occupancy were comparable to ASHRAE Standard 90.1P Occupancy Density. Thus, we concluded that Standard 62-89 Estimated Maximum Occupancy values are specified for sizing the ventilation system and the heating and cooling equipment, since the UBC occupant load factors are meant to represent maximum (not average) peak occupancies while the Standard 90.1P Occupancy Density values represent average conditions.

Although an interpretation of Standard 62-89 was not available at the time of this writing, assuming that occupancy values specified by Standard 62-89 are for sizing building ventilation systems implies that Standard 62-89 requires building ventilation systems to be capable of providing outside air at a rate equivalent to the Estimated Maximum Occupancy values. However, the actual operating outside air rate would be equivalent to the operating maximum number of people. To assess the

significance of this assumption, we evaluated both of these occupancy levels (Standard 62-89 Estimated Maximum Occupancy values and assumed prototype values) in estimates of energy use and cost.

2.1.2 Utility Rate Structures

In order to estimate the cost to building owners of meeting Standard 62-89, utility rates were applied to estimated energy use. Two utility rate structures were chosen as representative of the climate zones east and west of the Cascades: City of Richland General Service Electric Rate and Seattle City Light Schedule 34 . The weather files used in conjunction with these utility rate structures were Typical Meteorological Year (TMY) hourly weather files for Sea-Tac and Yakima, which are the closest available hourly weather sites.

2.1.3 Energy Simulation Method

DOE-2.1D accounts for occupant density in building areas with two inputs: (1) occupancy schedules and (2) peak occupancy value or Number Of People (NOP). Occupancy schedules are hourly ratios of the specified NOP, as in the following example of the large office prototype:

DAYS	HOURS	HOURLY FRACTION
(WEEKDAYS)	(1-6)	(0.0)
	(7)	(0.1)
	(8-17)	(1.0)
	(18)	(0.1)
	(19-24)	(0.02)
(SATURDAY)	(1-8)	(0.0)
	(9-12)	(1.0)
	(13-24)	(0.0)
(SUNDAYS, HOLIDAYS)	(1-24)	(0.0)

Most of the prototype buildings have more than one occupancy schedule to account for different areas. NOP is input as a single number; for example, "58" in the Lobby Zone of the Large Office. The hourly occupant density is then this peak occupancy value times the hourly fraction. The SYSTEMS portion of DOE-2.1D, with outside air specified as OA-CFM/PER (cfm/person), sets the minimum outside air rate equal to the NOP multiplied by the OA-CFM/PER. For prototype buildings with economizer control, the minimum outside air rate is exceeded during pre-specified outside air temperature conditions.

We considered peak occupancy a variable since it isn't clear whether Standard 62-89 is specifying a value or not. This led to two sets of DOE-2.1D simulation runs.

For the first set of simulation runs, we modeled each prototype building, both new and existing, utilizing the assumed prototype peak occupancy densities for sizing the equipment. DOE-2.1D has an autosizing feature which sizes equipment to accommodate the building load. By removing the hard inputs for system equipment in the

prototype input files, we enabled DOE-2.1D to size the equipment for the prototype occupancy densities using the Standard 62-89 ventilation rates per person.

Then we varied the specified cfm/person from 5 to 25 in steps of 5. Next, the files were simulated using the two utility rate structures for the corresponding weather files for a total of 20 files/building.

For the second set of simulation runs, we modeled each prototype building, both new and existing, by first creating an "ASHRAE occupancy" equivalent. This was accomplished by increasing the peak occupancy value NOP to the Standard 62-89 specified value and decreasing the hourly fractions so that the hourly number of people would correspond to the prototype assumed values. We used the DOE-2.1D equipment autosizing feature to simultaneously accomplish two effects: (1) keeping the building's heating and cooling loads constant while (2) simultaneously increasing the minimum outside air rates.

We again varied the specified cfm/person from 5 to 25 in steps of 5, and simulated these using the two utility rate structures for the corresponding weather files for an additional 20 files/building.

Within building types, occupancies are further delineated in Standard 62-89 (see Table 2.2). This delineation was included in the simulations by adjusting the specified cfm/person within different occupancies so that both the entire building and each of the different occupancies met Standard 62-89 at the same time. For instance, in the Large Retail building the basement and street level retail areas were specified as respectively having outside air rates at a ratio of .30/.20 times higher than the upper retail areas.

Since Standard 62-89 gives the Estimated Maximum Occupancy in sq. ft./person for retail areas, we assumed that an equivalent cfm/person could be derived by multiplying the Standard 62-89 specified values for cfm/sq. ft. and sq. ft./person. This resulted in an equivalent ventilation rate in retail areas of 10 cfm/person.

From each of the 40 energy simulations per building, five numbers were extracted: annual electric energy consumption, peak demand, annual energy cost, total cfm, and outside air cfm. Based on these numbers, we estimate regional energy impacts of Standard 62-89 and assess the expected costs to individual building owners of implementing Standard 62-89.

Table 2.1

Comparison of Occupant Densities

Number of People/1000 ft.^{2}

Occupancy	Prototype	Standard 62-89	UBC	Standard 90.1P
Grocery	4.3	8.0	10.0	3.3
Large Office	4.5	7.0	33.3	3.6
Small Office	4.1	7.0	33.3	3.6
Large Retail				
Sales, Lower	2.9	30.0	33.3	3.3
Sales, Upper	2.8	20.0	16.7	3.3
Storage	0.6	15.0	10.0	3.3
Small Retail				
Sales	3.9	30.0	33.3	3.3
Storage	3.0	15.0	10.0	3.3
Restaurant				
Fast Food	30.5	100.0	66.7	10.0
Kitchen	7.6	20.0	5.0	10.0
Warehouse				
Office	2.6	7.0	33.3	3.6
Warehouse	0.5	5.0	2.0	0.07
Hospital				
Rooms	5.9	10.0	n/a	n/a
Surgery	7.1	20.0	n/a	n/a
Admin.	4.4	7.0	33.3	5.0
Other	4.2	20.0	12.5	5.0
Hotel				
Rooms	5.1	20.0	n/a	n/a
Lobby	2.0	30.0	5.0	4.0
Conf. Rooms	13.5	50.0	66.7	n/a
School				
Classroom	19.8	50.0	50.0	13.3
Auditorium	7.2	150.0	142.9	20.0
Office	4.3	7.0	33.3	3.6
Cafeteria	32.4	100.0	142.9	10.0

Table 2.2

ASHRAE STANDARD 62 VENTILATION AIR REQUIREMENTS

BUILDING TYPE		VENTILATION AIR REQUIREMENTS	UNITS
Grocery/Supermarket		15	CFM/PERSON
Hospital			
	Patient Rooms	25	CFM/PERSON
	Med. Procedures	30	CFM/PERSON
	Other	15	CFM/PERSON
Hotel			
	Rooms	30	CFM/ROOM
	Lobby	15	CFM/PERSON
	Conf. Rms	20	CFM/PERSON
Office		20	CFM/PERSON
Restaurant			
	Dining Rooms	20	CFM/PERSON
	Kitchens	15	CFM/PERSON
Retail			
	Basement & Street	0.30	CFM/FT^2
	Upper	0.20	CFM/FT^2
	Storage	0.15	CFM/FT^2
School			
	Classroom	15	CFM/PERSON
	Library	15	CFM/PERSON
	Auditorium	15	CFM/PERSON
Warehouse		0.05	CFM/FT^2

2.2 Simulation Test Results

Simulation test results, shown in Tables 2.3 through 2.10, are as labeled. The following sections, which discuss the test results, are divided into categories for Prototype number of people and Standard 62-89 number of people because of the significance of this parameter to the results.

2.2.1 Prototype Number of People

2.2.1.1 Required Outside Air

As shown in Table 2.3, assuming daily maximum amounts of people (prototype assumptions), Standard 62-89 resulted in outside air rates of from 0.7% to 41.0% of total building supply air (excluding areas requiring 100% outside air). With the exception of the School, these rates should not be considered excessive. In fact, minimum outside air rates of 10% are equivalent to current practice. The School prototype had exceptionally high occupancy density (second only to Restaurant dining areas) which resulted in relatively high outside air requirements.

2.2.1.2 Energy Use Increase

Increasing the outside air from 5 cfm/person to Standard 62-89-required cfm/person resulted in annual energy increases as shown in Tables 2.4 and 2.5. Whether a building is located in Seattle, Washington, or Richland, Washington, the annual energy increase was less than 13%. For prototype buildings, other than the School, the increase was less than 6%. For the Hospital -- the building with the smallest percent increase -- the increase was less than 0.1% in Seattle.

The increase in energy on a kWh/yr basis (see Table 2.5) showed more variability between prototype buildings than when taken as a percent increase. The Large Office prototype building, because of the dominant cooling load, actually saved energy by increasing the minimum outside air. The other prototype buildings all showed the expected increase in annual energy consumption. The largest increase was the Hotel prototype in Richland, Washington, at 307,950 KWh/yr. (Yakima, Washington, TMY weather).

2.2.1.3 Energy Cost Increase

The equivalent increase in annual energy cost, as a percent of total energy cost, is shown in Table 2.6. As with energy use, the average increase in energy cost was less than 5%. The largest increase was the School prototype annual energy cost in Richland, Washington, at 14.6%. The Hospital and Large Office prototypes showed the smallest increases, less than 0.1%.

2.2.1.4 Regional Impacts

The regional increase in energy use (aMW, where aMW is equivalent to the annual energy savings (kWh/yr) divided by 8,760 hrs/yr) is shown in Table 2.7. For all buildings the estimated increase was 115.2 aMW .

The building types and floor area estimates were derived from the Bonneville Load Forecast for new commercial buildings built between 1992 and 2010.

2.2.2 Standard 62-89 Number of People

2.2.2.1 Required Outside Air

Assuming the Standard 62-89 occupancy density resulted in outside air rates from 6.0% to 94.2% of total building supply air (excluding areas requiring 100% outside air). Considering any outside air rate in excess of 20% to be excessive, 6 of the 10 prototypes exhibited excessive outside air rates.

2.2.2.2 Energy Use Increase

Increasing the outside air from 5 cfm/person to the Standard 62-89 required cfm/person resulted in prototype building annual energy increases as shown in Tables 2.7 and 2.8. The increases in energy use assuming the Standard 62-89 number of people were substantially more significant for some of the prototype buildings. For prototype buildings like Grocery and Hospital, the impact of ventilation air was masked on a percentage basis due to high energy use in areas other than HVAC . The Large Office had such a small heating energy use that the increase in ventilation air did not cause a significant increase in total energy use.

The increase in energy on a kWh/yr basis (see Table 2.5) showed more variability between prototype buildings then when taken as a percent increase. The Large Office prototype building, because of the dominant cooling load, showed only a small increase in energy use. The other prototype buildings all showed the expected increase in annual energy consumption. The Hospital prototype building showed an increase of 497,200 kWh/yr in Richland, Washington. The largest increase was 2,416,600 kWh/yr for the Hotel prototype building in Richland, Washington (Yakima, Washington, TMY weather).

2.2.2.3 Energy Cost Increase

The equivalent increase in annual energy cost, as a percent of total energy cost, is shown in Table 2.6. As with energy use, the average increase in energy cost was significant with some of the prototype buildings. The School showed the largest increase in energy cost with an increase of 42.2% in Seattle. The Hotel was close behind with an increase of 39.6% in Richland, Washington.

2.2.2.4 Regional Impacts

The regional increase in energy use (aMW) is shown on Table 2.8. The estimated increase in annual energy use is 687.1 aMW. The regional increase in energy use is 3 times greater for Standard 62-89 than when prototype number of people was assumed.

2.2.3 Adequacy of Ventilation Systems Design

Design of new buildings tends to include less oversizing of equipment than existing construction. The prototype building constructions reflect current design practice. Tables 2.9 and 2.10 show the outside air as per cent of supply air for the most extreme case: new construction with the higher Standard 62-89 occupancy densities. Where outside air reached 100% the building required higher total supply air rates than the system would provide to accommodate the quantity of outside air necessary. The results show that for the ASHRAE occupancy densities, ventilation at the higher rates, although excessive for more than half the buildings, was within the normal system capacity for all buildings except the Restaurant. Here again, the Restaurant and School were at or exceeding the system capacity because of their exceptionally high occupancy densities.

For the Prototype occupancy densities, the Standard 62-89 rates never exceeded the normal capacity of the ventilation systems.

Table 2.3

Number of People/Required Outside Air

Building Type	Number of People		Required Outside Air (cfm)		(% of supply air)	
	Prototype	Std 62	Prototype	Std 62	Prototype	Std 62
Grocery	111	208	1,670	3,130	10.2	17.1
Hospital	1,115	3,685	21,800	65,880	9.8	27.3
Hotel	532	4,845	9,610	58,890	5.5	37.0
Small Office	20	34	400	680	7.7	14.3
Large Office	1,824	2,856	36,480	57,120	0.7	6.0
Restaurant	50	157	800	2,490	30.6	94.2
Small Retail	50	365	500	3,650	4.1	33.9
Large Retail	300	2,730	3,000	27,300	4.3	40.2
School	970	3,603	16,700	34,590	41.0	87.0
Warehouse	14	96	210	1,150	1.7	4.0

Note: Percent outside air column excludes outside air used for process loads, such as kitchen ventilation air, medical procedures ventilation air, etc.

Table 2.4

Average Energy Increase
(Percent of Total Energy)

Building Type	Assumed Number of People			
	Seattle		Richland	
	Proto	Std 62	Proto	Std 62
Grocery	1.5	3.2	1.6	3.5
Hospital	0.0	0.9	0.1	1.4
Hotel	3.9	31.9	4.7	33.6
Small Office	5.5	10.3	5.6	10.5
Large Office	- 0.1	0.0	0.1	0.4
Restaurant	2.5	10.4	2.8	10.7
Small Retail	1.6	11.8	1.5	10.9
Large Retail	0.7	16.5	0.9	15.4
School	12.8	42.3	13.0	40.8
Warehouse	0.4	1.1	0.4	1.1

Note: Percent energy increases are averages between new and existing building configurations and are based on the difference between annual energy consumption at Standard 62-cfm/person and the annual energy consumption at 5 cfm/person.

Table 2.5

Average Energy Increase
(kWh/yr)

Building Type	Assumed Number of People			
	Seattle		Richland	
	Proto	Std 62	Proto	Std 62
Grocery	13,700	53,300	14,600	58,800
Hospital	5,000	335,000	10,600	497,200
Hotel	241,500	2,149,000	307,950	2,416,600
Small Office	5,700	11,000	6,600	12,400
Large Office	-3,100	2,000	9,200	38,700
Restaurant	8,500	35,900	9,900	39,200
Small Retail	8,900	28,200	3,900	31,400
Large Retail	14,600	386,700	22,200	399,400
School	127,000	483,900	135,000	489,400
Warehouse	1,000	2,800	1,200	3,300

Note: Average energy increases are averages between new and existing building configurations and are based on the difference between the energy consumption at Standard 62-required cfm/person and the energy consumption at 5 cfm/person.

Table 2.6

Average Energy Cost Increase
(Percent of Total Energy Cost)

Building Type	Assumed Number of People			
	Seattle		Richland	
	Proto	Std 62	Proto	Std 62
Grocery	1.7	3.9	2.2	4.6
Hospital	0.0	2.7	0.1	3.5
Hotel	4.7	35.8	6.1	39.6
Small Office	5.8	10.7	8.0	14.5
Large Office	0.1	0.1	0.1	0.6
Restaurant	3.1	11.8	3.5	12.4
Small Retail	1.8	13.2	1.7	12.2
Large Retail	0.9	19.8	1.2	18.0
School	13.8	42.2	14.6	38.2
Warehouse	0.5	1.3	0.5	1.9

Note: Percent energy cost increases are averages between new and existing building configurations and are based on the difference between the energy cost at Standard 62-required cfm/person and the energy cost at 5 cfm/person.

Table 2.7

Regional Increase in Energy Use
Assuming Prototype Number of People
(MW)

Building Type	Regional Floor Area (Million Sq Ft)	Prototype Floor Area (Sq Ft)	Base Energy Use (kWh/yr)	Base EUI (kWh/Sq Ft-yr)	Percent Increase (%)	Energy Increase (MW)
Large Office	117.7169	408,000	8,115,521	19.9	-0.05	-0.1
Small Office	85.2433	4,880	97,012	19.9	5.4	10.4
Large Retail	85.3179	120,000	2,069,755	17.2	0.65	1.1
Small Retail	116.3793	13,125	221,314	16.9	1.5	3.4
Restaurant	84.6534	2,624	276,161	105.2	2.1	21.4
Grocery	31.7115	26,050	1,696,155	65.1	1.5	3.5
Hotel/Motel	101.1193	198,500	6,445,550	32.5	3.8	14.2
School	138.2092	62,614	768,725	12.3	15.7	30.4
Warehouse	99.3555	18,025	238,754	13.2	0.4	0.6
Hospital	0	236,620	14,351,413	60.7	0.05	0.0
College	57.6664	N/A				15.8
Health	121.1435	N/A				6.0
Miscellaneous	226.7427	N/A				8.5
	TOTAL					115.2

Notes:

1. Regional floor area is for all buildings built between 1992 and 2010 and is derived from the Bonneville load forecast.

2. Base EUI is the New prototype building energy use at 5 cfm/person for Seattle, Washington, divided by the prototype total square footage.

3. Percent increase in energy consumption is the average prototype value using the assumed value for number of people when ventilating at Standard 62-89 for the new prototype in Seattle, Washington.

4. Energy increase = percent increase (%) x energy intensity (kWh/sq. ft./yr) x regional floor area (sq. ft.) / 8760 hrs/yr.

5. College, Health, and Miscellaneous building categories are derived from combinations of the other prototypes.

Table 2.8

Regional Increase in Energy Use
Assuming Standard 62-89 Number of People
(MW)

Building Type	Regional Floor Area (Million Sq Ft)	Prototype Floor Area (Sq Ft)	Base Energy Use (kWh/yr)	Base EUI (kWh/Sq Ft-yr)	Percent Increase (%)	Energy Increase (MW)
Large Office	117.7169	408,000	8,452,790	20.7	0.0	0.0
Small Office	85.2433	4,880	98,461	20.2	10.3	20.2
Large Retail	85.3179	120,000	2,188,533	18.2	39.8	70.7
Small Retail	116.3793	13,125	240,994	18.4	24.2	59.0
Restaurant	84.6534	2,624	346,544	132.1	10.3	131.5
Grocery	31.7115	26,050	1,697,227	65.2	3.1	7.3
Hotel/Motel	101.1193	198,500	6,382,278	32.2	32.9	122.1
School	138.2092	62,614	919,095	14.7	52.0	120.4
Warehouse	99.3555	18,025	239,579	13.3	1.1	1.7
Hospital	0	236,620	13,463,012	56.9	1.6	0.0
College	57.6664	N/A				82.4
Health	121.1435	N/A				27.6
Miscellaneous	226.7427	N/A				44.2
TOTAL						687.1

Notes:

1. Regional floor area is for all buildings built between 1992 and 2010 and is derived from the Bonneville load forecast.

2. Base EUI is the New prototype building energy use at 5 cfm/person for Seattle, Washington, divided by the prototype total square footage.

3. Percent increase in energy consumption is the average prototype value using the Standard 62-89 Estimated Maximum Occupancy value for number of people when ventilating at Standard 62-89 for the new prototype in Seattle, Washington.

4. Energy increase = percent increase (%) x energy intensity (kWh/sq. ft./yr) x regional floor area (Sq. Ft.) / 8760 hrs/yr.

5. College, Health, and Miscellaneous building categories are derived from combinations of the other prototypes.

Table 2.9

Adequacy of Ventilation System
(outside air as per cent of supply air)

Building Type	Seattle New Construction (outside air cfm/person)				
	5	10	15	20	25
Restaurant	37.7	74.9	100.0	100.0	100.0
School	53.5	87.2	92.4	94.9	96.4
Large Retail	28.7	57.4	86.2	100.0	100.0
Small Retail	22.6	45.0	67.6	90.1	100.0
Hotel	12.4	24.8	37.3	49.7	62.3
Hospital	11.0	17.7	24.4	31.0	37.7
Grocery	8.1	16.3	24.4	32.6	40.7
Large Office	5.0	9.6	14.4	19.1	23.8
Small Office	4.2	7.7	11.1	15.0	18.4
Warehouse	1.7	3.2	4.8	6.4	8.0

Note: Outside air is based on Standard 62-89 occupancy densities and cfm/person. At 100%, outside air requirements forced increase in total supply air.

Table 2.10

Adequacy of Ventilation System
(outside air as per cent of supply air)

Building Type	Richland New Construction (outside air cfm/person)				
	5	10	15	20	25
Restaurant	32.0	63.6	95.6	100.0	100.0
School	53.5	83.8	91.0	93.8	95.5
Large Retail	24.9	49.7	74.6	99.4	100.0
Small Retail	18.5	36.8	55.3	73.6	92.1
Hotel	11.5	23.0	34.5	46.0	57.6
Hospital	10.6	17.0	23.4	29.9	36.3
Grocery	6.8	13.7	20.5	27.3	34.2
Large Office	4.5	8.8	13.1	17.3	21.6
Small Office	3.5	6.4	9.2	12.5	15.3
Warehouse	1.0	2.0	3.0	4.0	5.0

Note: Outside air is based on Standard 62-89 occupancy densities and cfm/person. At 100%, outside air requirements forced increase in total supply air.

2.3 Conclusions

From the results presented in this chapter we conclude the following:

1. Standard 62-89 has a minimum impact on energy use and energy cost, regardless of building type or location when assuming prototype number of people.

2. Interpreting Standard 62-89 as specifying the occupancy density results in significant energy use and energy cost impacts.

3. Two high density occupancy types, Restaurant and School, account for 45% of the expected regional increase in energy use, though these two types total less than 20% of the regional floor area.

4. No prototype building ventilation system was undersized at Standard 62-89 required ventilation rates; all prototype ventilation systems were able to meet Standard 62-89 ventilation requirements easily at the prototype occupancy densities.

2.4 Recommendations

Based on our investigation, we recommend that Bonneville incorporate Standard 62-89 into its programs as follows:

1. Adopt the new ASHRAE Standard 62-89 Outdoor Air Requirements for cfm per person rates.

2. Continue to design equipment based on assumed occupancy or ASHRAE Standard 90.1 Occupancy Density.

In program design or evaluation, the estimated potential energy savings should be adjusted to account for the slight increase in energy use.

Further study should look at ways to minimize impacts of Standard 62-89 on high density building types, e.g., schools and restaurants.

3.0 ASHRAE STANDARD 62-1989 PROBLEMS

Standard 62-89 allows two paths for compliance: Indoor Air Quality (IAQ) Procedure and Ventilation Rate Procedure. In the first path, compliance is reached when 80 percent of a building's occupants don't complain about air quality. Therefore, no designed ventilation system can completely assure compliance simply based on its design. The second path prescribes ventilation rates, which should assure adequate indoor air quality.

It is assumed that only the Ventilation Rate Procedure will apply to Bonneville's commercial sector energy conservation programs. The remainder of this section discusses problems and confusion with the Ventilation Rate Procedure.

3.1 Number of People

Using the Ventilation Rate Procedure of Standard 62-89 requires that the minimum outside air rate be established. As defined by Standard 62-89, this requires the use of Table 2, contained in the Standard. For most occupancies, Table 2 lists required outdoor air in cfm/person and "where appropriate, the table lists the estimated density of people for design purposes."[1] Further, Standard 62-89 states: "Where occupant density differs from that in Table 2, use the per occupant ventilation rate for the anticipated occupancy load." These two statements appear to be in conflict with one another. On the one hand, it says the Table 2 values for occupant density should be used for design purposes; and on the other hand, it says, better estimates of occupant density should be used (although it isn't specified what they should be used for).

As noted earlier, Standard 62-89 Estimated Maximum Occupancy values are excessive when compared to building average peak occupancy. It would therefore seem logical that they are meant exclusively for design purposes. However, Standard 62-89 does not explicitly state what "design purposes" means.

Our interpretation is that the ventilation system has to be capable of providing the design amount of outside air (cfm/person x Estimated Maximum Occupancy); the building supply air (outside air + return air) should be equal to or greater than cfm/person x Estimated Maximum Occupancy. In operation, however, the ventilation system only need provide outside air at the specified rate to the actual number of people.

3.2 Occupancy Categories

Standard 62-89 provides ventilation air requirements which vary by occupancy category. Within buildings it can be difficult to distinguish between different occupancy categories or where one category begins and another ends. It therefore becomes difficult to meet and consequently to enforce Standard 62-89 in practice.

3.3 Infiltration

Standard 62-89 requires ventilation systems to be either mechanical or natural. With natural ventilation systems the ventilation rates must be demonstrable. Infiltration of outside air into commercial buildings is considered to be natural ventilation. Mechanical ventilation is fan-forced air supplied into a building.

Commercial buildings with mechanical ventilation systems still experience infiltration. It has been found that envelope infiltration rates are often the same order of magnitude as the rates of intentional outdoor air intake.[8,11] One study[8] also found that building ventilation rates (including infiltration) are variable depending on outdoor air intake controls, envelope air tightness, and HVAC system operation schedules. Not recognizing infiltration as a source of outside air for mechanically ventilated buildings results in Standard 62 over-specifying required ventilation rates. Combining this with the

Number of People specified by Standard 62 results in over-designing the system by several factors of safety in the required mechanical ventilation rates.

3.4 Energy Code vs Building Code Requirements

The 1989 Model Conservation Standards Code (MCS) is the basis for most energy codes in the Pacific Northwest. The MCS is based on ASHRAE Standard 90.1. As jurisdictions adopt the new MCS, they will likely incorporate it as amendments to the Uniform Building Code (UBC). UBC provides "minimum standards to safeguard life or limb, health, property, and public welfare by regulating and controlling the design, construction, quality of materials, use and occupancy,..."[6]

The 1989 MCS references ASHRAE Standard 62-89 for ventilation rates and occupancy densities, in lieu of Standard 90.1. The 1988 Uniform Building Code specifies mechanical ventilation rates for health and safety based on ASHRAE Standard 62-73. Therefore, within one jurisdiction's code, two ventilation rates could be specified. UBC ventilation rates are typically specified as a total circulated air flow of 15 cfm/person of which at least 5 cfm/person is outdoor air. Standard 62-89 ventilation rates are higher than UBC's rates. Because of this, one might assume that a ventilation rate falling between the two rates "met code".

Having the energy code specify higher ventilation rates than the building code causes confusion. Higher ventilation rates usually relate to higher energy usage. Therefore, one could assume that the lower UBC ventilation rates meet the MCS's limits to energy use. However, the MCS specifies ventilation rates as a minimum to assure adequate indoor air quality, since higher ventilation rates are usually associated with better air quality. Therefore, the building which falls between the two rates actually does not meet code.

3.5 Indoor Air Quality Procedure

Compliance with Standard 62 can be shown by using the Indoor Air Quality Procedure. In addition to specifying acceptable contaminant levels and exposure times, this procedure requires that at least 80 percent of a panel of at least 20 untrained observers find the indoor air to be not objectionable under representative conditions of use and occupancy. The procedure does not provide a method of measuring specified indoor contaminants.

For existing buildings, using this procedure would require that pollutants be measured and that occupant exposure times be established. It is referenced in the Ventilation Rate Procedure as the means for providing cleaned, recirculated air in lieu of outside air. This procedure would be both more difficult and more costly to enforce than the Ventilation Rate Procedure.

For new construction, compliance would require obtaining detailed information on finshes, floor and wall coverings, partitions and other materials to be installed. Using manufacturer's data on contaminant outgassing rates, the designer could calculate necessary rates to meet

IAQ limits. In practice, many of these materials are selected long after mechanical design is complete. This is especially true for speculative construction, where the building shell is completed, but the interior is built to suit a tenant at a later date. Therefore, this procedure is unworkable for new construction.

3.6 Outdoor Air Quality

Standard 62 requires outdoor air to be treated or reduced when certain contaminants exceed air quality standards. Reducing outdoor air requires compliance with the Indoor Air Quality procedure. This requirement for using only clean outdoor air was in ASHRAE Standard 62-81, but compliance was rare.[9]. We doubt if this requirement will be enforceable or met with compliance in Standard 62-89 either.

3.7 Ventilation Effectiveness

Standard 62 states that a ventilation effectiveness approaching 100 percent is assumed for the required rates. The Standard defines ventilation effectiveness as the fraction of outdoor air delivered to the space that reaches the occupied zone. Therefore, if only 50 percent of the outdoor air mechanically introduced into a building reaches the occupied zone the ventilation effectiveness would be 0.5 and the required ventilation rates would be doubled. Given that a method to measure effectiveness does not exist, 100 percent will be the value assumed in the field.

3.8 Multiple Spaces

Standard 62 adjusts ventilation air requirements for multiple spaces with the following provision: "Where more than one space is served by a common supply system, the ratio of outdoor to supply air required to satisfy the ventilation and thermal control requirements may differ from space to space. The system outdoor air quantity shall then be determined using $y = x/(1+x-z)$, where y is the corrected fraction of outdoor air in the supply system, x is the uncorrected fraction of outdoor air in the supply system, and z is the fraction of outdoor air in the space with the greatest required fraction of outdoor air in its supply."[4] With this provision, compliance with Standard 62-89 should be easier to verify. For each set of multiple spaces served by a common supply fan, the percentage of outdoor air need only be established once.

This provision "makes sense for applications where supply air for bathrooms or kitchens might come from adjacent spaces. However, many other situations exist where applications of the reduction allowance results in some unreasonable results."[1]

Percent outdoor air is a design value which is fixed for all occupancies served by a given air supply system. It is reasonable to adjust percent outdoor air so that occupancies requiring more or less outdoor air are not penalized by other occupancies.

4.0 ASHRAE STANDARD 62-89 VERIFICATION METHODS

4.1 New Buildings

4.1.1 Plan Review

Building code enforcement officials review design documents for new buildings at the time of code review. Within the design documents, designers specify the amount of outside air to be delivered at each outside air intake. Actual measurements of outside air are not performed.

4.1.2 Test and Balance Report

A qualified company tests the building HVAC system and equipment, usually linked to a system start-up procedure. The company then develops a report which documents measured airflow, pump and fan performance data, and temperature. On smaller buildings, testing and balancing is usually not performed because of cost. Testing and balancing to determine the amount of outside air could conceivably be done by either zonal air flows or whole building outside air flows.

4.1.2.1 Zonal Air Flow Measurementss

For each independent fan system which supplies outside air, the amount of outside air (on a percentage basis) is determined by the following formula: $\%\ OA = (T_S - T_R) / (T_O - T_R)$, where T_S = supply air temperature, T_R = return air temperature, and T_O = outside air temperature. The system has to be set to deliver minimum air (e.g., for a VAV system to deliver minimum air the thermostat has to call for full heating).

4.1.2.2 Whole Building Outside Air Flow Measurements

To reduce time, effort, and costs, another less conclusive method would be to measure the total outside air being introduced at the fan system inlet. This could be done by the following procedures: (1) measuring total supply air and total return air (outside air equals supply air minus return air); (2) measuring percent outside air as above assuming supply air is equivalent to manufacturer's data; or (3) measuring the outside air at the intake. Each of these procedures assumes that the outside air ultimately reaches the building occupants.

4.1.2.3 Tracer Gas Measurements

This procedure is not commonly performed in commercial buildings, due to high cost. "In this procedure, a harmless and non-reactive tracer gas is released into the building and mixed thoroughly with the interior air. Once the tracer gas concentration within the building is uniform, one monitors the decay in tracer gas concentration over time. The rate of decay of the logarithm of concentration is equal to the air exchange rate of the building during the time of the test."[8] This procedure includes the measurement of infiltration air which makes it somewhat incomparable with the previously described methods. It results, however, in time-averaged overall building air-exchange

rates. Using this procedure, it has been demonstrated that natural ventilation is an important component in overall building ventilation.

4.1.2.4 Carbon Dioxide Measurement

Standard 62-89 ventilation rates are based on an assumption of 1,000 ppm of Carbon Dioxide (CO_2). The measurement of CO_2 is a relatively easy and simple procedure. It is valuable for buildings which are amenable to a one-time spot measurement of CO_2. The technique requires an assumption of CO_2 generation rates per person and measurements of CO_2 concentration in outside and return air. If the calculated outdoor air flow rate, in cfm per person, is above the required rate the ventilation system meets the Standard. (NOTE: This "method" is contained in Appendix D of the Standard and as such is not a part of the Standard. It was suggested that Bonneville consider this approach due to its low cost and because it seemingly meets the Standard's intent.)

4.2 Existing Buildings

4.2.1 System Test

Outside air in existing buildings is not routinely measured, except at times when the HVAC system undergoes a major renovation or remodel. Then the outside air is measured as a commissioning requirement, in similar fashion to that previously described, using zonal air flows and/or whole building outside air flows.

4.2.2 Tracer Gas Measurements

This procedure is identical to that described above for new buildings. Due to high cost (both equipment and personnel) this procedure is not employed by any firm or individual on a regular basis.

4.3 Standard 62-89 Verification Costs

4.3.1 Costs of Zonal Air Flow Measurements

The cost of performing a total HVAC system test and balance in addition to the cost of establishing design air flows, can include the cost of balancing HVAC water flows and pressures. Considering only the cost of testing and balancing air flows, the costs can vary from as little as $1,000 for a small single zone HVAC system to over $25,000 for complex multi-system buildings. These costs are representative of what could be expected when attempting to establish outside air delivered to a particular zone or occupancy category within a building. When delivery of outside air on a percentage basis for each HVAC system is measured, and air delivered from each diffuser is measured, outside air is equal to percent outside air times diffuser cfm. Using the building definitions considered in Chapter 2, the study on energy costs, the costs to perform detailed estimates of outside air following the zonal air flow measurement procedure are summarized in Table 4.1.

Table 4.1: Zonal Outside Air Testing Costs

Building type	Air Testing Cost
Grocery	$ 1,200
Hospital	$27,600
Hotel	$22,600
Large Office	$18,450
Large Retail	$ 7,600
Restaurant	$ 1,280
School	$10,800
Small Office	$ 1,600
Small Retail	$ 2,000
Warehouse	$ 800

These estimates are based on R.S. Means Cost Data.[10] They are specific to the building type considered. The costs are based on $40.00/diffuser and $400.00/system; VAV systems are estimated to cost $800.00. For all buildings except the Grocery, it is assumed that there are 400 cfm/diffuser; for the Grocery, it is assumed that there are 1000 cfm/diffuser. The air flow (cfm) assigned to each building is based on design data.

4.3.2 Costs of Whole Building Outside Air Flow Measurements

If less costly methods were used, such as measuring outside air at the HVAC system inlet and assigning that outside air to the entire building, then air flow would not be measured at diffusers; costs would be a function of number of HVAC systems/outside air inlets and would be approximately that shown in Table 4.2.

Table 4.2: Simplified Outside Air Testing Costs

Building Type	Air Testing Cost
Grocery	$ 500
Hospital	$ 4,500
Hotel	$ 8,000
Large Office	$ 1,000
Large Retail	$ 1,500
Restaurant	$ 1,000
School	$ 4,000
Small Office	$ 1,000
Small Retail	$ 1,000
Warehouse	$ 500

Only the outside air method is referenced in standard testing and balancing manuals.[7] Historically, the determination of outside air has not been a primary purpose of testing and balancing. The absolute accuracy of either the zonal or whole building method has not been established. Companies which specialize in testing and balancing of HVAC systems will quote an accuracy of +/- 10%. This is based on experience rather than empirical data. Fluctuating outside environmental conditions make the measurement of mechanical ventilation difficult.

4.4 Equivalent Energy Savings

For costs of either zonal or whole building verification of Standard 62-89 to be acceptable, the equivalent energy savings of a retrofit conservation measure would have to be on the order of 2.5 times the air testing cost (assuming a program overhead rate of 40%, a fifteen year measure life and a cost-effective limit of 50 mills/kWh). Depending on the method used to establish outside air rates and whether whole building rates are acceptable, the required energy savings would be as shown in Table 4.3. Any increase in energy savings beyond that shown or further decrease in outside air would be cost-effective, in general.

As shown in Table 4.3 at least two of these building types would not likely find a cost-effective retrofit: Hospital and Large Office. The assumptions used for HVAC system(s) are the reason. The Hospital would require a reduction in outside air equivalent to 260 cfm/person if the HVAC systems were tested on a zonal basis; the Large Office would require a reduction of 160 cfm/person. If the whole building approach were used instead, the Hospital would require a reduction of 42 cfm/person the Large Office would require 8.6 cfm/person.

The remainder of the building types could realistically absorb the cost of testing for minimum outside air regardless of the methods considered. Using the whole building approach results in minimal outside air reductions for all other building types.

Table 4.3: Cost-Effective Limits

Building Type	Zonal Testing		Whole Building Testing	
	kWh/yr Savings	cfm/Person Reduction	kWh/yr Savings	cfm/Person Reduction
Grocery	3,000	1.2	1,300	0.52
Hospital	69,000	260.	11,300	42.
Hotel	56,500	2.2	20,000	0.77
Large Office	46,100	160.	2,500	8.6
Large Retail	19,000	7.8	3,750	1.5
Restaurant	3,200	3.7	2,500	2.9
School	27,000	2.1	10,000	0.78
Small Office	4,000	11.	2,500	6.6
Small Retail	5,000	7.3	2,500	3.6
Warehouse	2,000	20.	1,300	13.

5.0 RECOMMENDATIONS

5.1 Interpretations of Standard 62-1989

5.1.1 Number of People

Standard 62-89 Estimated Maximum Occupancy values should only be used as a sizing criteria for design of ventilation systems, if at all. In operation, the average peak number of people encountered in the building should be used. When this value is not available or difficult to determine, ASHRAE Standard 90.1 provides a number that should be used.

5.1.2 Indoor Air Quality Procedure

This procedure is valuable when building air quality problems are of concern. It is not viable for use with new buildings not yet occupied or for major retrofit projects where post-conditions have not yet been established. In evaluating air quality problems in operating buildings, this procedure should be used as part of the regulatory functions of OSHA, UBC, or other regulatory agencies that evaluate building air quality problems.

5.1.3 Outdoor Air Quality

This provision is not enforceable because it requires that pollutants be measured at the outdoor air intake for compliance. This provision should not be included in the interpretation.

5.1.4 Ventilation Effectiveness

Ventilation effectiveness cannot be measured and therefore should not be a part of our adopted interpretation. Its reference in the Standard should be considered a design constraint: Design the system so that the outdoor air is delivered to occupied zones.

5.1.5 Ventilation Standards

UBC is written for public health and safety. It should be the source for minimum indoor air quality/ventilation standards. The energy code (MCS) should limit maximum ventilation rates for energy reasons but should not take precedence over UBC. The purpose of MCS ventilation requirements should be clarified and the differences between MCS and UBC ventilation rates should be resolved.

5.1.6 Multiple Spaces

The allowance for the adjustment of outside air based on varying occupancies served by the same HVAC system should be adopted. This would allow easy verification of multiple spaces, such as conference rooms and lobbies, for compliance.

5.1.7 Energy Codes and Building Codes

The energy codes should prescribe the maximum ventilation rate. The minimum ventilation rates would be more appropriate in the health and safety codes, because the minimum is for the purpose of ensuring adequate indoor air quality.

5.2 Preferred Method for Determining Outside Air Rates

The following conditions have been shown: (1) Building ventilation systems are affected by ambient temperature and wind conditions and (2) Infiltration is a non-neglible contributor to overall building air-exchange. These facts, coupled with the problem of identifying peak numbers of people, make the usefulness of a detailed measurement of outside air suspect. Therefore, a high value should not be placed on particular mechanical ventilation rate numbers. Instead, the intake and distribution of outside air should be verified, either visually or through measurement techniques. The quantification of air quality in the building should be established through subjective measurements or visually identifiable problems.

Considering the cost and accuracy of the two general methods for determining outside air rates, the preferred method is the "Whole Building" method. This method at least assures that an appropriate amount of outside air is being introduced into the building and is not so difficult that its use would be restricted to testing and balancing companies; utility auditors should be able to use it to adequately determine outside air rates. In summary, this Orocedure requires the following steps:

A. Minimum Outside Air Requirements Calculation

1. Determine peak number of occupants

   i. This should be the highest number of people usually encountered during the average workday. If the peak number of occupants is difficult to determine, use Standard 90.1 occupancy values.

   ii. Where requirements are in cfm/sq ft or cfm/room, calculate the square feet or rooms served by the mechanical ventilation system, as appropriate.

2. Calculate amount of outside air to be provided each occupancy served by each mechanical ventilation system. (Multiply peak number of occupants by the required outside air rate (cfm/person)).

3. Adjust outside air rate to account for different occupancies served by the same ventilation system using equation IAQ-1.

   i. Calculate the uncorrected outdoor air fraction (X) by dividing the sum of all the branch outdoor air requirements (V_{ot}) by the sum of all the branch supply flow rates (V_{on}).

ii. Calculate the critical space outdoor air fraction (Z) by dividing the critical space outdoor air requirement (V_{oc}) by the critical space flow rate (V_{sc}).

iii. Use equation IAQ-1 to find the corrected fraction of outdoor air (Y) to be provided in the system supply.

Equation IAQ-1

$$Y = X / [1 + X - Z]$$

Where,

$Y = V_{ot}/V_{st}$ = corrected fraction of outdoor air in system supply
$X = V_{on}/V_{st}$ = uncorrected fraction of outdoor air in system supply
$Z = V_{oc}/V_{sc}$ = fraction of outdoor air in critical space[1]
V_{ot} = corrected total outdoor air flow rate
V_{st} = the sum of all supply air quantities for all branches of the system
V_{on} = sum of outdoor air flow rates for all branches on system
V_{oc} = outdoor air flow rate required in critical spaces
V_{sc} = supply flow rate in critical space

B. Ventilation System Inspection (not applicable to new buildings)

Prior to ECM installation visually inspect the ventilation system to determine that outside air is reaching building occupants, that harmful or irritating contaminant sources are isolated from the main ventilation system, and that there are no known building ventilation problems which could be compounded or exacerbated by a ventilation reduction. If problems exist they must be corrected prior to ECM installation. A short report documenting the inspection shall be prepared and be available in the Energy Analysis Report or other site visit documentation

C. Ventilation Rate Measurement

Determine outside air rate (cfm) using one of the two following methods. For the measurement, the outside air supply shall be set to the minimum amount for systems which supply varying amounts (e.g. variable air volume, economizer control).

Documentation of ventilation rate measurement results shall be contained in the Energy Analysis Report or other site visit documentation.

1. Percent outside air method

   a. Measure outside, return, and mixed air temperatures. Calculate percent outside air using equation IAQ-2.

   b. Measure total supply air (cfm), either by a pitot tube traverse of main supply duct or by measure of supply air at diffusers.

---

1 The critical space is that space with the greatest required fraction of outdoor air in the supply.

Equation IAQ-2

$$\% \text{ OA} = (T_S - T_r) / (T_O - T_r)$$

Where,

T_S = mixed air temperature
T_r = return air temperature
T_O = outdoor air temperature

c. Calculate outside air = (% outside air) x (cfm)

d. Determine total outside air for all mechanical ventilation systems serving building.

e. Determine peak number of occupants

   i. This should be the highest number of people usually encountered during the average workday. If the peak number of occupants is difficult to determine, use Standard 90.1 occupancy values.

   ii. Where requirements are in cfm/sq ft or cfm/room, determine the square feet or number of rooms served by the mechanical ventilation system.

f. Calculate mechanical ventilation rate = outside air (cfm) / peak number of occupants, or cfm/sq ft, or cfm/room as appropriate.

g. Adjust the ventilation rate in accordance with the procedure given for New Buildings.

2. Carbon Dioxide method

Alternatively, where a mechanical ventilation system serves a space(s) where the activities are well known and constant from day-to-day a simplified procedure can be used. This method will show whether indoor carbon dioxide concentrations are below ASHRAE Standard 62-89 recommended levels of 1000 ppm. If the indoor carbon dioxide concentrations are above 1000 ppm, then the building or space does not comply with these requirements.

a. For each mechanical ventilation system measure carbon dioxide concentration in return air and in outside air.

b. Determine if required cfm/person ventilation rate (OA) is being met by solving equation IAQ-3 for indoor carbon dioxide concentration:

Equation IAQ-3

$OA = \text{Gen. Rate} / (C_i - C_o)$

Where,

Gen. Rate = occupant generation rate (cfm/person) of carbon dioxide (refer to Standard 62-89).

C_i = return air (indoor air) carbon dioxide concentration

C_o = outdoor air carbon dioxide concentration

6.0 REFERENCES

1. Cutter Information Corp., "Indoor Air Quality Update", October 1989.

2. Eto, J. and Meyer, C. 1988. "The HVAC Costs of Fresh Air Ventilation." ASHRAE Journal, September 1988.

3. United Industries Corporation, Inc. "DOE-2 Commercial Building Prototype Review and Revision", 1988.

4. ASHRAE 1987. "Proposed revisions to ASHRAE standard 62-81: Ventilation for acceptable indoor air quality, public review draft." Atlanta: American Society of Heating, Refrigerating, and Air-Conditioning Engineers, Inc.

5. ASHRAE 1987. "Standard 90.1P, Energy Efficient Design of New Buildings Except Low-Rise Residential Buildings." Atlanta: American Society of Heating, Refrigerating, and Air-Conditioning Engineers, Inc.

6. International Conference of Building Officials 1988. Uniform Building Code.

7. Associated Air Balance Council 1987. National Standards for Field Measurements and Instrumentation.

8. Persily, A. K., "Ventilation Rates In Office Buildings." ASHRAE Journal, July 1989.

9. Cutter Information Corp., "Indoor Air Quality Update", September 1989.

10. R. S. Means Co., 1988, Means Mechanical Cost Data; 1988

11. ASHRAE 1989, 1989 ASHRAE Handbook: Fundamentals

AIR MOVEMENT & VENTILATION CONTROL WITHIN BUILDINGS

12th AIVC Conference, Ottawa, Canada
24-27 September, 1991

PAPER 17

The Simulation Of Infiltration Rates And Air Movement In A Naturally Ventilated Industrial Building.

P.J. Jones, D.K. Alexander and G. Powell.

The Welsh School Of Architecture,
University Of Wales College Of Cardiff,
PO Box 25,
Cardiff.
CF1 3XE.

SYNOPSIS

This paper describes the application of numerical models to predict the ventilation rate and internal air movement patterns for a naturally ventilated industrial building and compares the results with measured data.

Two modelling techniques have been employed. Firstly, a zonal network model (HTBVent), using leakage area data derived from fan pressurisation measurements, was used to predict the time varying ventilation rate in response to variations in wind velocity and internal-external air temperature difference. The results compare well with measurement data (obtained using constant concentration tracer gas techniques) over a wide range of ventilation rates. The results demonstrate the use of zonal models to estimate the thermal benefits of applying sealing measures to building components.

Secondly, a computational fluid dynamics (CFD) model (DFS-AIR) was used to predict the ventilation rates and also the internal air movement resulting from natural ventilation, for selected external conditions. The predicted ventilation rates again agree well with measurement data. The resulting air movement patterns can be used to indicate the effectiveness of natural ventilation and the implications for comfort throughout the occupied space.

The general conclusion was that these modelling techniques, having been successfully tested against measurement data, can be used in the design of naturally ventilated buildings.

1.0 INTRODUCTION

This paper describes the use of computer models to predict firstly the overall air infiltration rate of the building (using a zonal model called HTBVent) and secondly the internal air movement paths resulting from natural ventilation (using a CFD model DFS-AIR).

The ventilation performance of a factory was extensively monitored over the summer of 1988 and reported on at the 10th AIVC conference [1]. Air infiltration rate data was collected by a continuous constant concentration technique over a wide range of climatic conditions and building sealing levels, whilst air leakage data was obtained by fan-pressurisation and reductive sealing techniques.

The results from the air leakage experiments were used to quantify and locate major sources of air leakage over the building envelope. This information was then used as input data for the ventilation models. The zonal model was used to predict the variation of ventilation rate of the building over time using recorded values of wind speed and direction, internal and external air temperatures, together with suitable wind pressure coefficients for each wind direction. The predicted air infiltration rate was then compared with measurement data over a period of time.

The air leakage data was also used as input data for the CFD model which was used to predict the air infiltration rate and internal patterns of air movement under selected wind and stack conditions.

2.0 TEST BUILDING

The test building was a detached factory with a production space floor area of 466 m^2 and a production space volume of 3050 m^3. Figure 1 contains a floor plan and section of the factory.

The factory walls had an inner skin of masonry and an external skin of profiled metal cladding. The roof had the same external metal cladding with an inner skin of fibreboard. Both constructions incorporated glass fibre quilt insulation to give a U-value of 0.6 $W.m^{-2}.K^{-1}$. The factory was built on a concrete slab base. There was an internal office space which was partitioned off from the production area.

Double glazed windows occupied 7.5% of the total wall area. There was approximately 10% rooflighting. There were also 4 louvered roof vents fitted, each of area 1.56 m^2.

The factory was fitted with a single standard roller shutter loading door of approximate area 16 m^2. The loading bay door faced north, the factory being orientated on an east-west axis.

3.0 MEASUREMENTS

3.1 Air Leakage

Air leakage tests were performed using the fan pressurisation technique. The pressurisation unit was a modular system based on two fan and duct units that were fitted into one of the fire doors. This allowed component testing of the main loading door to take place. The volume flow rate through the ducts were measured using Wilson Flow Grids. The volume flow rate could be varied by means of speed controllers fitted to each fan; the maximum flow rate achievable, with both units at full speed, was 8.4 m^3s^{-1}.

3.2 Air Infiltration Rate

Air infiltration rate tests were performed using constant concentration tracer gas techniques employing the Autovent System developed and marketed by British Gas plc [2].

The constant concentration tests were performed using pure nitrous oxide (N_2O) as the tracer gas. A target concentration of 50 ppm was used. The building was divided into 5 controlled zones for these measurements. A cycle time of 6 minutes was used, and the raw results were amalgamated to provide 30 minute data records.

3.3 Experimental Programme

The air leakage (fan pressurisation) and air infiltration (constant concentration) experiments were carried out during July and August 1988.

Three pressurisation measurements were undertaken; the factory "as-built" (test P03), with the loading door sealed (P01), and with the loading door and roof vents sealed (P02).

Eight constant concentration tests (designated CC01 to CC08) were performed. Tests CC01 through CC06 were carried out on the factory "as-built". Test CC07 was carried out with the loading door sealed. Test CC08 was carried out with both the loading door and ventilators sealed.

The results have been reported in detail in an earlier paper [1]. Air leakage tests P01,P02 and P03, and constant concentration tests CC01 to CC06 have been used in this investigation.

The "as-built" data sets CC01 to CC06 comprised 374 half hourly records of internal and external temperature, wind speed and dominant wind direction, and the measured air infiltration rate. These encompassed a wide range of conditions of stack effect (1.6°C to 15.7°C temperature difference), wind speed (0.3 ms^{-1} to 7.6 ms^{-1}), and resulting air infiltration rates (0.2 $Ac.h^{-1}$ to 1.0 $Ac.h^{-1}$). The wind directions were predominantly southerly, but included some cases from all quadrants.

4.0 MODELLING

4.1 Zonal Model

The infiltration model used for this work was HTBVent, a multi-zone, nodal network model based on that described by Etheridge and Alexander [3].

This model calculates the airflow across the cracks or openings in the building fabric according to their geometry, position and external pressure forces. It differs from other similar models [4,5] through the use of "crack-flow" equations [6], rather than the more typical exponential best fit method. The "crack-flow" equations are based on a quadratic relationship between airflow and pressure difference :-

$\Delta P = \alpha Q^2 + \beta Q$, where, Q is the flow in m^3s^{-1},
ΔP is the pressure difference in Pa.

This form of relationship allows the transition of flow though small openings, from laminar to turbulent, to be handled correctly, whilst also allowing large orifice-type openings to be specified.

The parameters α and β are determined from the physical dimensions and the geometry of the opening :-

$$\alpha = \frac{C\rho}{2A^2} \qquad \beta = \frac{B\rho\nu DL^2}{8A^3}$$

where,
ρ is the air density, Kgm^{-3},
ν is the air viscosity, Nsm^{-2},
A is the crack open area, m^2,
L is the crack length, m,
D is the crack depth, m,
B and C are empirical constants.

The constants B and C are determined by the form of the crack, for instance an "L" shaped opening provides the values 91.36 and 2.20 respectively [6].

In HTBVent, the non-linear network of such crackflow relationships, which describes the building, is solved for pressure and flow by a simple Newton-Raphson scheme. Each solution described in this paper required less than 0.2 second on a 80386/80387 MSDOS PC.

4.2 CFD Model

A 3-dimensional Computational Fluid Dynamics (CFD) model, DFS-AIR, was used to simulate the air infiltration and internal air movement resulting from the effects of a single wind direction on the external fabric of the building with air leakages comparable to those used in the zonal model, only located in 3-dimensional space.

The model is based on the SIMPLE method [7] for solving numerically the equations for the conservation of momentum (ie. Navier Stokes equations), the conservation of mass and the conservation of energy. In this case a simple 'fixed viscosity' turbulence model was used. An internal/external air temperature difference corresponding to the experimental data was achieved by specifying an appropriate fixed amount of heat flux input to the bottom layer of the solution domain. Pressure boundaries at air leakage sites were modelled using the same effective areas as determined by the crack flow equations that were used in the zonal model. The CFD model used a linearised form of the power law equation :-

$Q = \rho KA(\Delta P)^n$ where, ρ is the density of air, Kgm^{-3},
A is the crack area, m^2,
K is an empirical flow coefficient calculated from the above crack flow equations for each leakage area modelled.

The model used a grid of 30x30x35 cells to describe the solution domain. Air leakages were prescribed to occur over a whole cell face at the leakage locations.

The model was run on a 33MHz "i860 Number Smasher" microprocessor based on an 80486 MSDOS PC, which achieved a run time speed of 30 s per iteration

5.0 DERIVATION OF CRACK PARAMETERS

5.1 Data Requirements

In order to run both the zonal and CFD models two sets of information needed to be established.

(i) Crack Characteristics
The physical description of the openings in the building fabric must be determined, in terms of their area, length, depth and type (i.e. straight, kinked, or complex), and then each such opening must be "placed" on the building envelope.

In this work this data was derived from air leakage measurements.

(ii) External Wind Pressure
Surface wind pressures may be determined by site measurement, wind-tunnel measurement, numerical modelling, or simplified algorithms.

In this work the latter were used. Wind pressure coefficients were calculated from the algorithm developed by Swami and Chandra [8]. This algorithm provides generalised surface average coefficients solely from wind direction.

5.2 Crack Flow Characteristics

The data required for the description of the openings of the building was produced by analysis of pressurisation test results. In the case discussed here, the pressurisation data available was;
Test P01- the envelope with the loading door sealed,
Test P02- the envelope with the loading door and roof vents sealed.
Test P03- the whole building envelope "as built",

This data was used in the following way;

A log-log best fit model was produced for these 3 pressurisation tests, as shown in figure 2.

These empirical models were then used to produce, by subtraction, the estimated leakage characteristics for,

- the total background, (Test P02),
- the loading door (Test P03 - Test P01), and
- the roof vents (Test P01 - Test P02).

Each of these characteristic curves (figure 3) were then fit to the quadratic "crack-flow" relationship, to produce the α and β parameters described above. These parameters in themselves are sufficient to proceed, but given logical constraints (i.e. the background leakage is likely to be of a complex type with a length comparable to the dimensions of the envelope) a reasonable set of values for crack area and length may be estimated.

The final disaggregation was checked by calculating, for known pressures, the total flow predicted and comparing this to the measured envelope leakage. This comparison is shown in figure 4. The agreement was considered to be good.

5.3 Crack Locations

The above procedure produced lumped open areas, however it did not identify the location or composition of those openings. For both the zonal and CFD models to be used, the open areas identified must be assigned to appropriate facades and attributed a physical location.

In this case the locations of both the loading doors and the roof vents could be easily identified. There were four vents, located high on the north and south facing roofs and a large loading door on the north facade.

The background leakage is by definition the leakage which is not attributable to a single component. A logical distribution of that leakage area was assumed, in relation to the simple construction of the building. In particular, there was no indication that the facades would be unduly asymmetric; and so is one quarter of the total background was applied to each of the north, south, east, and west faces of the building. Further, the construction type used could be assumed to be have continuous crackage near the location of the main constructional details, i.e. the eaves.

6.0 RESULTS

6.1 Zonal Model

The zonal model was subjected to the full "as-built" data set: CC01 through to CC06.

A number of leakage distributions were considered, each making different assumptions as to the location of the background leakage. Overall, most distributions which were thought reasonable (i.e. those which were not unduly asymmetric between the wall and roof leakage areas) produced an agreement range, over the entire data set, of approximately - 0.05 + 0.25 $Ac.h^{-1}$. There was some tendency to over-predict infiltration for the higher wind speeds.

The best agreement was achieved with a distribution based on the assumption that the majority of the background area would be found near the eaves. This is illustrated in figure 5. The agreement, as in figure 6, was very good; 90% of the

values are within ± 0.10 $Ac.h^{-1}$ of the measurements. There was no correlation between the error and any of the data parameters; wind speed, direction, or temperature difference. The agreement was felt to be approaching the measurement accuracy of the system.

The agreement between prediction and measurement for dynamic time-series data is illustrated in Figure 7, for this final distribution. This figure shows the measured and predicted infiltration rates over a continuous three day period (test CC05). The model appeared to adequately follow the rapid changes of the building air infiltration rate.

The utility of such a model lies in the ease of determining the impact of changes to the building fabric. For example, the effect of sealing the loading door may be assessed. By removing the doors leakage definition from the data file and then recalculating, it was estimated that the infiltration rate would drop on average by 0.12 to 0.14 $ac.h^{-1}$, over the total period of the measurements. This was in good agreement with the decrease actually observed during the measurement project in test CC07 [1].

6.2 CFD Model

The CFD used the same crack specifications as determined for the zonal model.

The CFD model was run for a single point in time, when the wind speed was 2.1 ms^{-1} from the south. The internal air temperature was 21.7°C while the air temperature outside was 20.1°C.

The first simulation was carried out assuming no internal/external air temperature difference. Figure 8 shows a north-south section centre to the factory. The overall air change rate was calculated as 0.218 $Ac.h^{-1}$, which compared well to the measurement value of 0.22 $Ac.h^{-1}$. The air flow paths can be seen with the main inflow of air at the windward facing eaves and the main outflow through the relatively leaky 'closed' roof vent. There is a small airflow through the windward facing roofvent even though there is a slight negative external pressure at this point. It should be emphasised that the predicted air velocities are very low for this simulation.

The second simulation included the effects of the 1.6°C internal/external air temperature difference. The results are shown in Figure 9. The overall air change rate was calculated as 0.217 $Ac.h^{-1}$, which is not significantly different from the first case. However, it can be seen that the air movement set up by wind driven air leakage is now completely masked by the internal air movement due to the buoyancy effects (which are relatively small), and the predicted air velocities are typically an order of magnetude higher than for the isothermal case above.

7.0 CONCLUSIONS

The calculation of infiltration rates, made with a zonal air infiltration model, have been found to be in good agreement with measured values, even though only a generalised wind pressure coefficient algorithm and a simple series of envelope leakage measurements were used as input data. Fine tuning of the assumed background leakage locations, in the light of the measured infiltration rates, produced a model that was able to predict to within ±0.1 $Ac.h^{-1}$ over 90% of test cases, encompassing a range of 0.2 to 1.0 $Ac.h^{-1}$.

The model was successful in estimating the impact of altering the building fabric, i.e. sealing the loading door.

After a wider validation, such a technique could be useful in assessing the ventilation performance of factory or similar buildings, from a simple set of air leakage measurements.

Comparisons with the CFD model indicated that the CFD model could be used to predict air infiltration rates using crack flow equations. Such a model also enabled the air flows inside the space to be visualised. This could be used to predict ventilation effectiveness and comfort conditions. It appeared, for the conditions simulated, that although wind effects dominated the determination of the air infiltration rate, relatively small buoyancy effects could determine the overall internal air movement pattern.

ACKNOWLEDGEMENTS

The authors would like to acknowledge the support of the Welsh School of Architecture during the course of this investigation.

The measurement data on which this paper is based was a result of a BRE funded programme of work investigating the ventilation performance of large single-celled buildings. The views expressed in the paper are those of the authors and not necessarily those of BRE.

REFERENCES

1) Jones, P.J. and Powell, G., "Comparison Of Air Infiltration Rate And Air Leakage Tests Under Reductive Sealing For An Industrial Building". 10th AIVC Conference, Finland, Proceedings Volume 2, 1989.

2) Etheridge, D.W., "Watson House 'Autovent'- A System for Measuring Air Infiltration Rates". Air Infiltration Review, Vol. 4 No. 4 August 1983.

3) Etheridge, D.W. and Alexander, D.K., "The British Gas Multi-Cell Model For Calculating Ventilation". ASHRAE Transactions, volume 86 part 2, 1980.

4) Liddament M. and Allen, C., "The Validation And Comparison Of Mathematical Models Of Air Infiltration". AIVC Technical Note #11, 1983.

5) Feustel, H.E., "Mathematical Modelling Of Infiltration and Ventilation". 10th AIVC Conference, Finland, Proceedings Volume 1, 1989.

6) Etheridge, D.W., "Crack Flow Equations and Scale Effect". Building And Environment, 12, 1977.

7) Patankar, S.V., "Numerical Heat Transfer and Fluid Flow". McGraw-Hill, 1980.

8) Swami, M.V. and Chandra, S., "Correlations For Pressure Distribution On Buildings And Calculation Of Natural Ventilation Airflow". ASHRAE Transactions, Volume 94, Part 1, 1988.

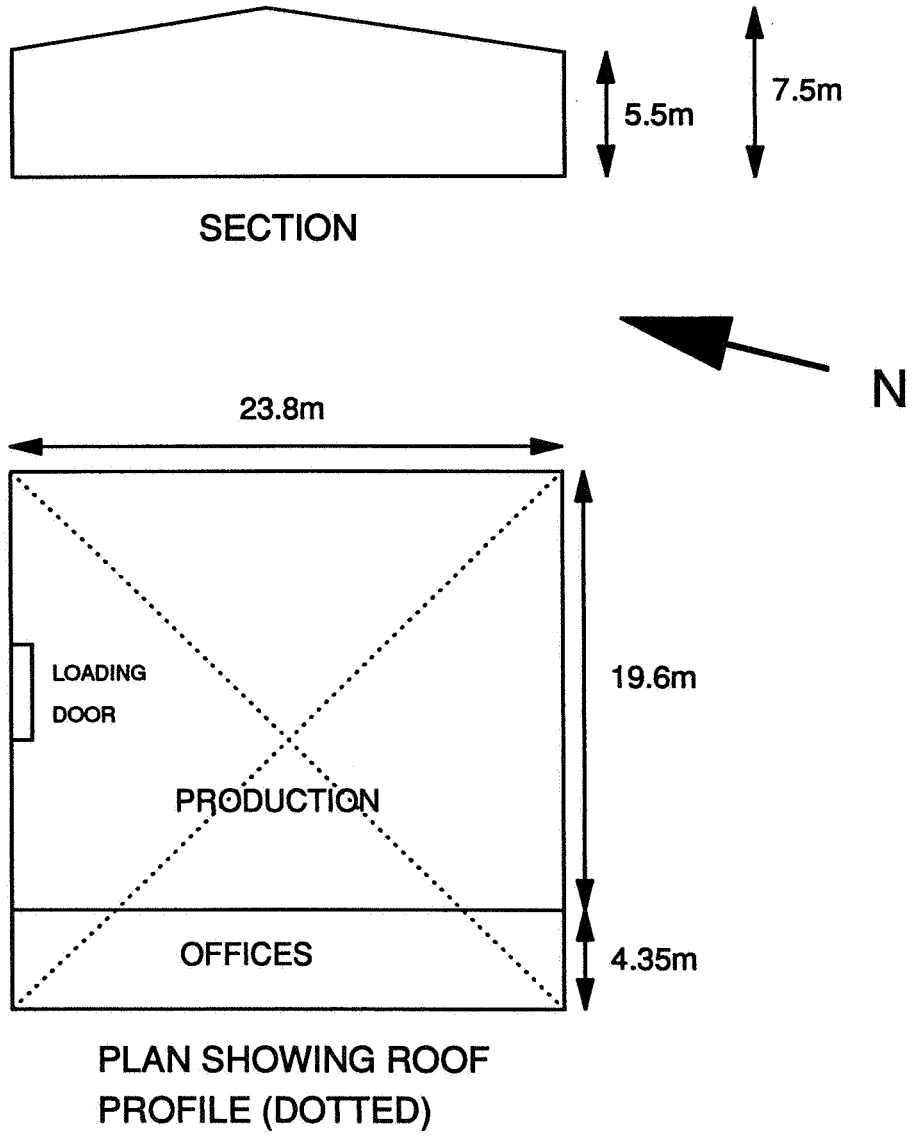

Figure 1: Plan And Section Of Test Factory.

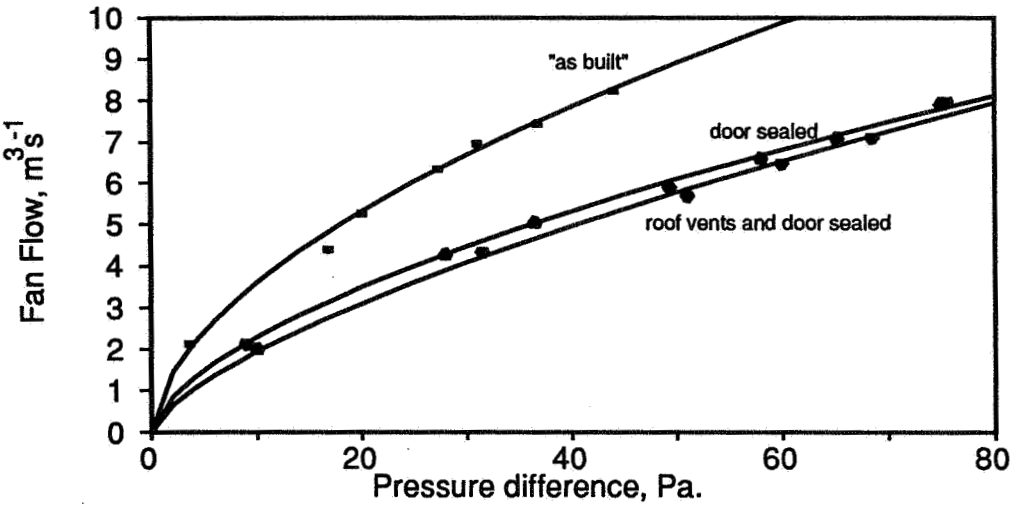

Figure 2: Pressurisation Test Results, Log-Log Regression.

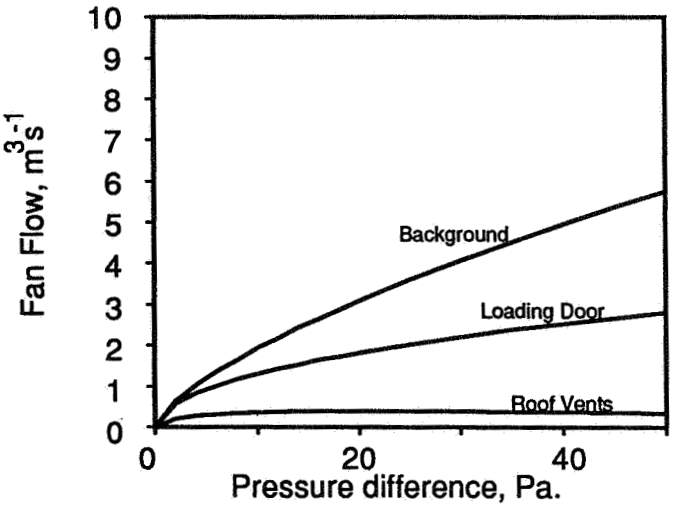

Figure 3: Component Leakages Estimated by Subtraction.

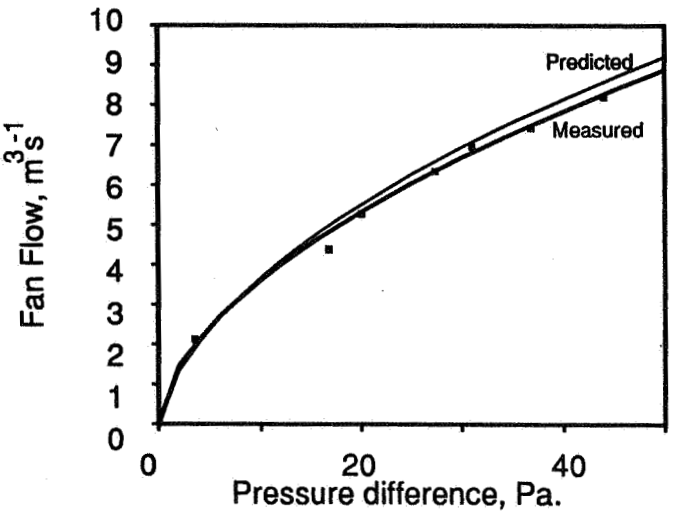

Figure 4: Comparison of Measured and Modelled Leakage.

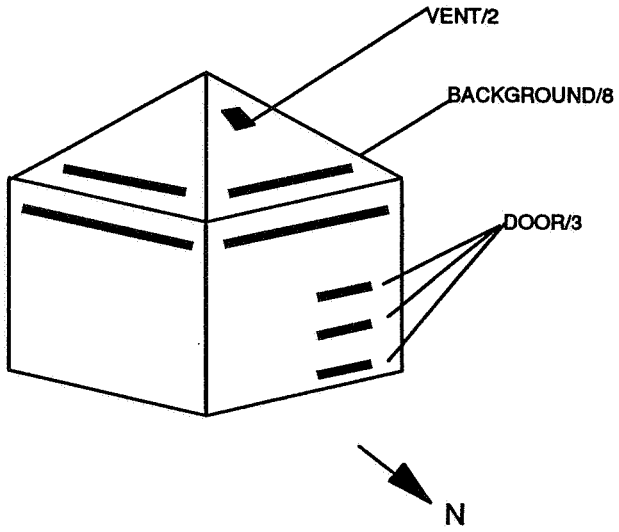

Figure 5: Schematic Of Leakage Areas For 'Best' Distribution.

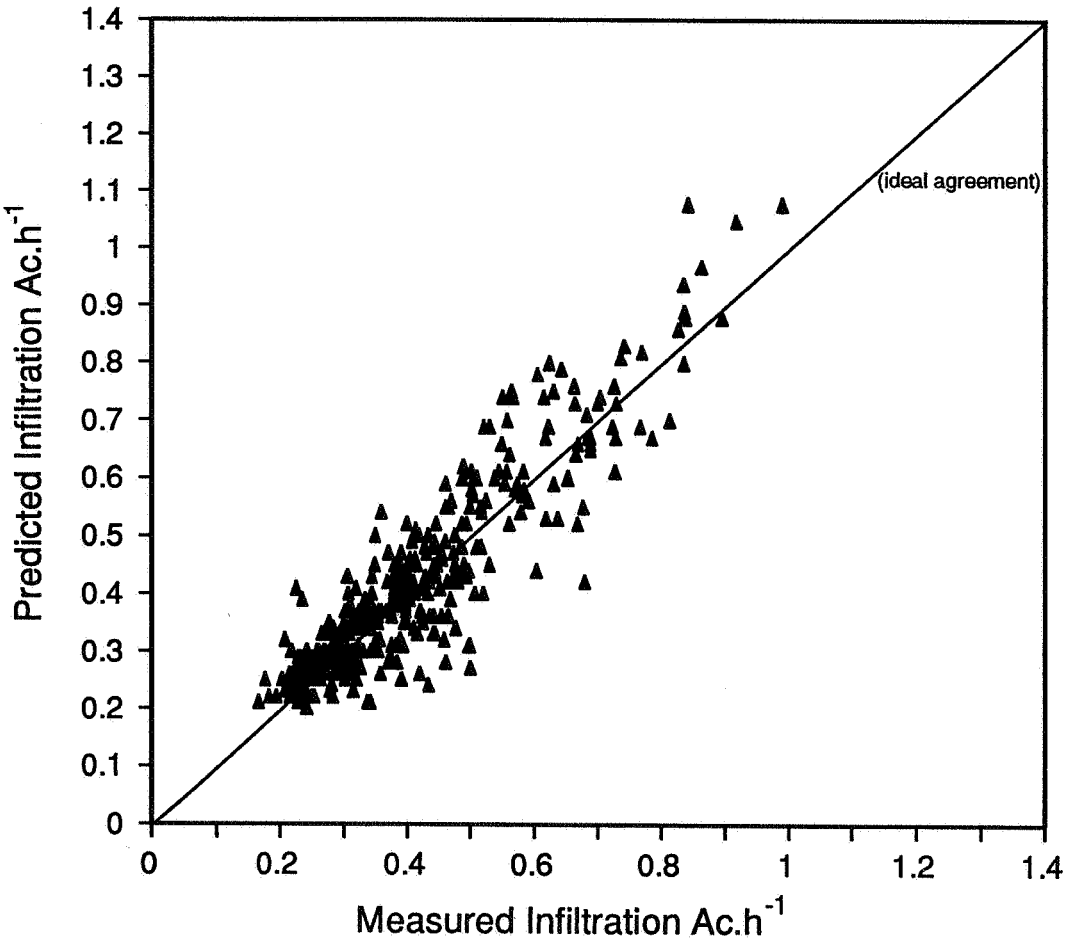

Figure 6: Comparison of Modelled and Measured Infiltration.

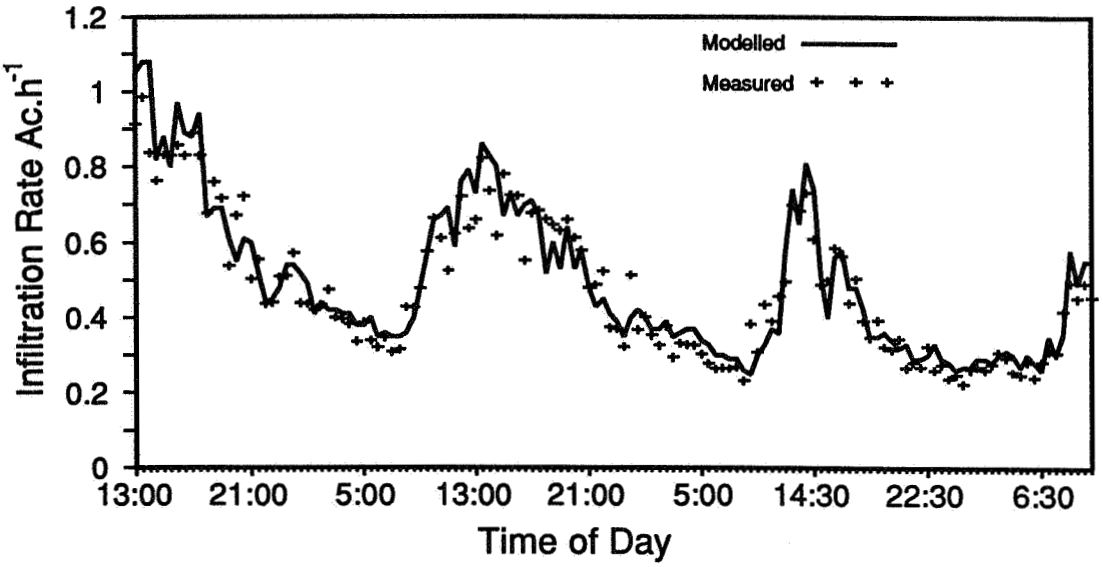

Figure 7: Time Series Comparison for Test CC05.

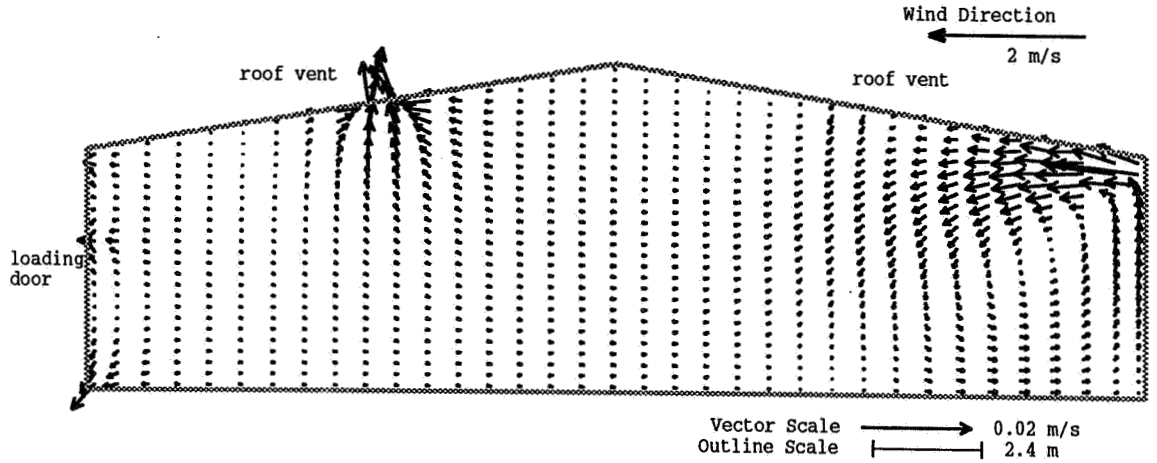

Figure 8: Internal Airflow Modelled with No Stack Effect.

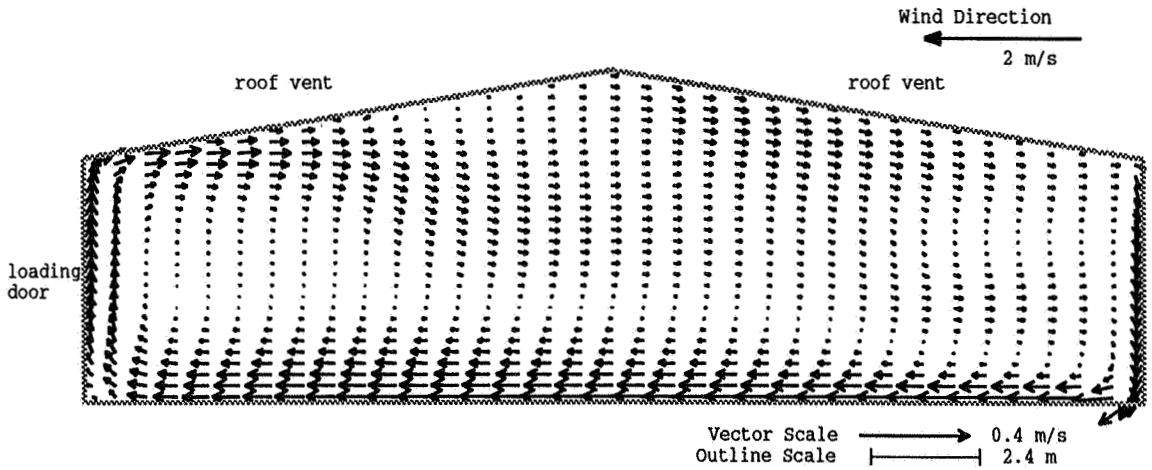

Figure 9: Internal Airflow Modelled with Stack Effect.

AIR MOVEMENT & VENTILATION CONTROL WITHIN BUILDINGS

12th AIVC Conference, Ottawa, Canada
24-27 September, 1991

PAPER 18

INTERACTION OF MECHANICAL SYSTEMS AND NATURAL INFILTRATION

Larry Palmiter and Tami Bond

Ecotope, Inc.
2812 E. Madison St.
Seattle, Washington 98112
USA

SYNOPSIS

Mechanical devices such as exhaust fans and air handlers interact strongly with natural infiltration. In the past, the effects of mechanical systems have either been treated separately from those of natural infiltration or have been combined using simple models.

This paper extends the theory of the interaction of unbalanced mechanical systems with stack-driven infiltration. The effects of leakage distribution and the flow exponent on fan efficiency are discussed.

A simple model for combining the two effects is presented and compared with two previously proposed models. The induced infiltration is one-half of the unbalanced fan flow if the unbalanced flow is less than twice the natural infiltration rate. Otherwise, the induced flow is the difference between the fan flow and the natural infiltration.

The model is supported by detailed flow and pressure measurements made on a home in the Pacific Northwest during winter conditions. The home had a whole-house multiport exhaust ventilation system as well as several other exhaust fans. The measured flow through the multiport exhaust system was 35 L/s. When running, this system induced 17 L/s, in good agreement with the fan-model predictions.

LIST OF SYMBOLS

β	Dimensionless neutral level
β_0	Dimensionless neutral level under conditions of stack only
C	Coefficient from blower door test (L/(s Pa^n))
$\Delta\rho$	Density difference between indoor and outdoor air (kg/m^3)
ε	Fan efficiency (flow added divided by fan flow)
ε_0	Efficiency of an infinitesimally small fan
ε_{crit}	Fan efficiency at the critical point (β=1)
F_s	Stack factor from infiltration model
g	Acceleration due to gravity (9.80665 m/s^2)
h	Height of building (m)
n	Exponent from blower door test
P_s	Stack pressure $P_s = \lvert \Delta\rho \rvert g h$ (Pa)
Q_{add}	Additional flow induced by the fan (L/s)
Q_{crit}	Critical flow (β=1) (L/s)
Q_{fan}	Flow through fan (L/s)
Q_{in}	Flow in through envelope, excluding fan (infiltration) (L/s)
Q_{nat}	Flow under "natural" conditions (fan flow of zero) (L/s)
Q_{out}	Flow out through envelope, excluding fan (L/s)
R	Fraction of leakage in ceiling and floor
X	Leakage difference between ceiling and floor as fraction of total

1. INTRODUCTION AND BACKGROUND

Although it has been traditionally assumed that natural infiltration would provide adequate ventilation in homes, the mandates of energy efficiency combined with new construction materials and techniques have resulted in newer homes being significantly tighter. In many cases, the natural infiltration is no longer adequate. This has led to increasing use of various types of mechanical ventilation systems and growing interest in understanding their performance.

The interaction of mechanical ventilation systems with natural infiltration has been addressed in a number of recent studies. This paper extends the theory of the interaction of unbalanced mechanical systems with stack-driven natural infiltration. The nature of the dependence of the stack-fan interaction on leakage distribution and the power-law exponent are discussed. Based on this discussion, we propose a simple fan interaction model.

The new model is compared with two previously proposed models and is then applied to real-time field infiltration measurements. The chosen home was measured under late winter conditions with stack-dominated natural infiltration and a wide variation in exhaust fan flow rates.

2. THE INTERACTION EFFECT

The interactions of mechanical systems with natural infiltration are quite complex. These interactions include not only the incidental or planned use of exhaust fans or balanced-flow heat recovery ventilation systems, but also the effects which arise from forced air distribution systems used for space heating and cooling. The latter effects can be quite large (Palmiter and Bond 1991; Palmiter et al. 1991) and are largely unintended. In this paper, we will focus on systems which are intended to provide additional ventilation.

Balanced flow systems are those which have two fans, one pumping air into the home and a second pumping air out of the home. These systems are the easiest to understand. If the two flows are equal, there is theoretically no effect on the neutral pressure level and no interaction with natural infiltration. The resultant total infiltration is simply the sum of the natural infiltration and the inward flow through the balanced system.

The most common type of ventilation system installed in the Pacific Northwest is the exhaust or extract system. Because this system changes the neutral pressure level, the added flow is less than the flow through the fan. In extreme cases, a fan flow of 100 L/s might result in only 10 L/s of added ventilation. It should be noted, however, that the total infiltration is never less than the flow through the fan.

Wind-induced infiltration is poorly understood, as is the interaction of wind and stack effects. The manner in which mechanical systems interact with natural infiltration may depend significantly on the relative mix of wind and stack effects.

Various infiltration studies in the Pacific Northwest have shown that natural infiltration in homes in this region is primarily stack-dominated. Palmiter et. al. (1991) give a summary of these studies. A more detailed discussion of the stack effect and its predominance is given in Palmiter and Brown (1989). We will use the stack effect to illustrate the interaction of mechanical devices with natural infiltration.

After examining the interaction of exhaust systems with stack-driven infiltration, we propose a very simple model in which it is assumed that the total natural infiltration interacts with the exhaust fan in the same manner as the stack effect.

3. THEORY FOR FAN-STACK INTERACTION

For the case where unbalanced fan flow interacts with stack-induced infiltration, explicit equations can be given which, in special cases, can be solved in closed form. The primary benefit of analytic solutions is to provide understanding of how the various parameters influence the total flow.

For simplicity, it is convenient to make several assumptions. The relationship between volumetric flow and pressure difference is assumed to have the form of a power law, in which the same exponent applies for all leakage areas and the overall flow coefficient is derived from a blower door test. Field experience has shown that the exponent is typically 0.65 ± 0.05. It is assumed that the building is a simple rectangular box with leakage in the floor, ceiling and walls, and that the wall leakage density is constant with height.

We follow Sherman (1980) and Wilson (1990) in introducing the dimensionless leakage distribution parameters X and R. The parameter R ($0 \le R \le 1$) is the fraction of the total leakage which is in the floor and the ceiling. The parameter X ($-R \le X \le R$) is the fraction of leakage in the ceiling minus the fraction of leakage in the floor. With this terminology, the fraction of leakage in the ceiling is $(R+X)/2$, that in the floor is $(R-X)/2$, and that in the walls is $(1-R)$. It is generally assumed that $R=0.5$ and $X=0$ are reasonable default values.

We assume that the pressure due to stack effect is given by the hydrostatic equation, which leads to a linear relationship between stack pressure and height. The height at which the indoor and outdoor pressure lines cross is the neutral pressure height. It is convenient to use the concept of a dimensionless neutral level, β, which is the ratio of the neutral pressure height to the height of the building. Under stack-only conditions, the neutral level is between 0 and 1; the operation of an exhaust fan shifts the indoor pressure line, resulting in an increase in neutral level, perhaps much above the ceiling.

The flows above and below the neutral level can be found by integrating the power law over the linear pressure gradient. A flow balance then results in a nonlinear equation for the neutral level. As a further simplification, we use a volume flow balance. The results are generally rather close to those obtained from a mass flow balance, and the equations are easier to understand.

The interaction of stack effect with unbalanced fan flow depends on the direction of fan flow (i.e., supply or exhaust) and also on whether the indoor temperature is above or below outdoor temperature (i.e., winter or summer conditions). For brevity, we present only the case of an exhaust fan under winter conditions. A rule for translating the results to all other cases is given later in this section.

The fan-stack interaction results in the added flow due to the fan being less than the flow through the fan. It is therefore convenient to define a fan efficiency, ε, as the added flow induced by the fan divided by the fan flow. The interaction can then be expressed in dimensionless form, giving ε as a function of the ratio Q_{nat}/Q_{fan}. The fan efficiency is defined as

$$\varepsilon = \frac{Q_{in} - Q_{nat}}{Q_{fan}} \tag{1}$$

For a balanced flow system, as noted above, the flow added is the flow through the supply fan, but the total fan flow also includes the flow through the exhaust fan. If we consider the efficiency definition to mean added flow divided by total air pumped, the efficiency of the balanced system is always equal to 0.5.

The volumetric flow due to stack effect can be written

$$Q_{nat} = CF_s P_s^n \quad \text{where} \quad 1/2 \le n \le 1 \tag{2}$$

where the stack factor, F_s, accounts for the effects of leakage distribution.

If there is sufficient flow through the fan, the neutral level can be raised to the ceiling (β=1). After this point, the flow through the ceiling reverses. All flow comes in through the walls, floor, and ceiling, and all flow exits through the fan; therefore, the total flow is known. We refer to this point as the "critical" point and the fan flow at this point as the "critical" flow.

When the neutral level is below or at the ceiling (β≤1), flow in and out are given by

$$Q_{in} = CP_s^n \left(\frac{1-R}{n+1} \beta^{n+1} + \frac{R-X}{2} \beta^n \right) \tag{3}$$

$$Q_{out} = CP_s^n \left(\frac{1-R}{n+1} (1-\beta)^{n+1} + \frac{R+X}{2} (1-\beta)^n \right) \tag{4}$$

For an exhaust fan, a flow balance yields the basic equation

$$Q_{fan} = Q_{in} - Q_{out} \tag{5}$$

By setting β=1 in (3), we obtain the critical flow

$$Q_{crit} = Q_{in} = CP_s^n \left(\frac{1-R}{n+1} + \frac{R-X}{2} \right) \tag{6}$$

The efficiency at the critical point is

$$\varepsilon_{crit} = 1 - \frac{Q_{nat}}{Q_{crit}} = 1 - \frac{F_s}{(1-R)/(n+1) + (R-X)/2} \tag{7}$$

For $Q_{fan} > Q_{crit}$, the total flow in is equal to the flow through the fan, and the efficiency can be expressed as

$$\varepsilon = 1 - \frac{Q_{nat}}{Q_{fan}} \tag{8}$$

The dimensionless neutral level for a fan flow smaller than Q_{crit} can be obtained by solving (5) for β. The flows Q_{in} and Q_{out} can then be calculated from (3) and (4). In particular, the stack neutral level, β_0, is found by solving (5) with Q_{fan}=0 (that is, setting Q_{in} equal to Q_{out}). The resulting flow Q_{nat} is obtained by substituting β_0 into (3) so that, in this case, the term in brackets is the stack factor F_s.

Because (5) is nonlinear in β, its solution generally requires an iterative technique. However, in the context of doing simulations or modeling, it should be noted that β_0 is a constant and the nonlinear equation for β_0, which yields the stack factor, need be solved only once.

Closed form solutions can be found for the above equations in certain special cases. For a flow exponent of n=1 or n=0.5, there is a full solution for all values of fan flow. In the case of an exponent of n=0.5, the solution for β_0 involves the root of a cubic equation; it is quite long and complex and has therefore been omitted. Solutions for the stack-only and critical-point values for general exponents are given below for certain special cases.

Sherman (1990) has derived a partial solution for the efficiency, ε_0, of an infinitesimally small fan. By a limiting argument, it is possible to derive an explicit expression for ε_0 as a function of β_0. This extends Sherman's result to all values of n, R, and X. The equation is

$$\varepsilon_0 = \frac{\frac{1-R}{n}\beta_0^n + \frac{R-X}{2}\beta_0^{n-1}}{\frac{1-R}{n}\beta_0^n + \frac{R-X}{2}\beta_0^{n-1} + \frac{1-R}{n}(1-\beta_0)^n + \frac{R+X}{2}(1-\beta_0)^{n-1}} \tag{9}$$

This is a good approximation to the actual efficiency when $Q_{nat} > 4\,Q_{fan}$. When X=R=1, we define ε_0=1.

We now summarize the solutions for stack-only and critical-point flows and fan efficiencies. The efficiencies are expressed both in terms of n, R, and X and in terms of β_0.

3.1 The case n=1

If the flow exponent n is equal to 1, the equations for natural and critical flow reduce to

$$\beta_0 = (1+X)/2 \qquad \varepsilon_0 = \frac{1-RX}{2} = \frac{1+R}{2} - R\beta_0 \tag{10),(11}$$

$$Q_{nat} = CP_s\frac{(1+R)(1-X^2)}{8} \qquad Q_{crit} = CP_s\frac{1-X}{2} \tag{12),(13}$$

$$\frac{Q_{nat}}{Q_{crit}} = \frac{(1+R)(1+X)}{4} = \frac{1+R}{2}\beta_0 \qquad \varepsilon_{crit} = 1 - \frac{(1+R)(1+X)}{4} = 1 - \frac{1+R}{2}\beta_0 \tag{14),(15}$$

3.2 The case R=1

If all of the leakage is in the floor and the ceiling, the equations reduce to

$$\beta_0 = \frac{(1+X)^{1/n}}{(1+X)^{1/n}+(1-X)^{1/n}} \qquad \varepsilon_0 = \frac{(1-X)^{1/n}}{(1-X)^{1/n}+(1+X)^{1/n}} = 1-\beta_0 \tag{16),(17}$$

$$Q_{nat} = CP_s^n \frac{1-X}{2}\beta_0^n \qquad Q_{crit} = CP_s^n \frac{1-X}{2} \tag{18),(19}$$

$$\frac{Q_{nat}}{Q_{crit}} = \beta_0^n \qquad \varepsilon_{crit} = 1-\beta_0^n \tag{20),(21}$$

3.3 The case X=0

If the leakage in the floor and ceiling are equal, the equations are

$$\beta_0 = 1/2 \qquad \varepsilon_0 = 1/2 \tag{22),(23}$$

$$Q_{nat} = CP_s^n\left(\frac{1}{2}\right)^{n+1}\frac{1+nR}{n+1} \qquad Q_{crit} = CP_s^n\left(\frac{2-R+nR}{2(n+1)}\right) \tag{24),(25}$$

$$\frac{Q_{nat}}{Q_{crit}} = \left(\frac{1}{2}\right)^n \frac{1+nR}{2+R(n-1)} \qquad \varepsilon_{crit} = 1-\left(\frac{1}{2}\right)^n \frac{1+nR}{2+R(n-1)} \tag{26),(27}$$

3.4 Extension to summer conditions and supply fans

As mentioned above, the fan efficiency depends on the direction of fan flow (i.e., supply or exhaust) as well as on whether the indoor temperature is above or below outdoor temperature (i.e., winter or summer conditions).

Equations for either an exhaust fan under summer conditions or a supply fan under winter conditions may be obtained by replacing the parameter X in the equations with $-X$. For a supply fan under summer conditions, there are two sign changes in X, so the resulting equations are identical to those given above for an exhaust fan under winter conditions.

3.5 Simple fan interaction models

Chapter 23 of the *ASHRAE Handbook of Fundamentals* (1989) proposes use of addition in quadrature for predicting the effect of unbalanced flow systems. In this method, the total flow is given by

$$Q_{tot} = \sqrt{Q_{nat}^2 + Q_{fan}^2} \tag{28}$$

Wilson and Walker (1987) proposed another model in which half the fan flow is combined using an exponent rule and the other half is added linearly.

$$Q_{tot} = Q_{fan}/2 + ((Q_{fan}/2)^{1/n} + Q_{nat}^{1/n})^n \tag{29}$$

The authors have proposed a very simple model (Palmiter and Bond 1991) which we will refer to as the 0.5 rule. However, no justification or derivation of the model was given. In this model, the added flow is one-half the fan flow up to a critical point of twice the natural infiltration rate.

$$Q_{tot} = 0.5\,Q_{fan} + Q_{nat} \quad \text{for} \quad Q_{fan} \le 2Q_{nat} \tag{30}$$

$$Q_{tot} = Q_{fan} \quad \text{for} \quad Q_{fan} \ge 2Q_{nat} \tag{31}$$

This is equivalent to asserting that the fan efficiency ε is 0.5 up to the critical point, at which $Q_{fan} = 2\ Q_{nat}$. Above that point, the efficiency is given by (8). This model was also extended to include the effects of balanced and unbalanced duct leakage in a forced air distribution system.

4. DISCUSSION

Many of the general features of the fan-stack interaction are easily predicted using the equations given above. In order to explore the interaction in more detail, we solved the nonlinear equations for a number of cases. Some typical results are illustrated in Figure 1. Each panel shows fan efficiency plotted versus the ratio of natural infiltration to flow through the exhaust fan. In all cases, we used the typical exponent of 0.65.

In each panel, the straight line sloping down from the top left corner has a slope of unity and represents the cases where all flow out is through the fan. The curved portions intersect with the straight line at the critical point. Toward the right side, the curves asymptotically approach ε_o. It is clear that convergence is nearly complete at a natural infiltration to fan flow ratio of about 4-to-1.

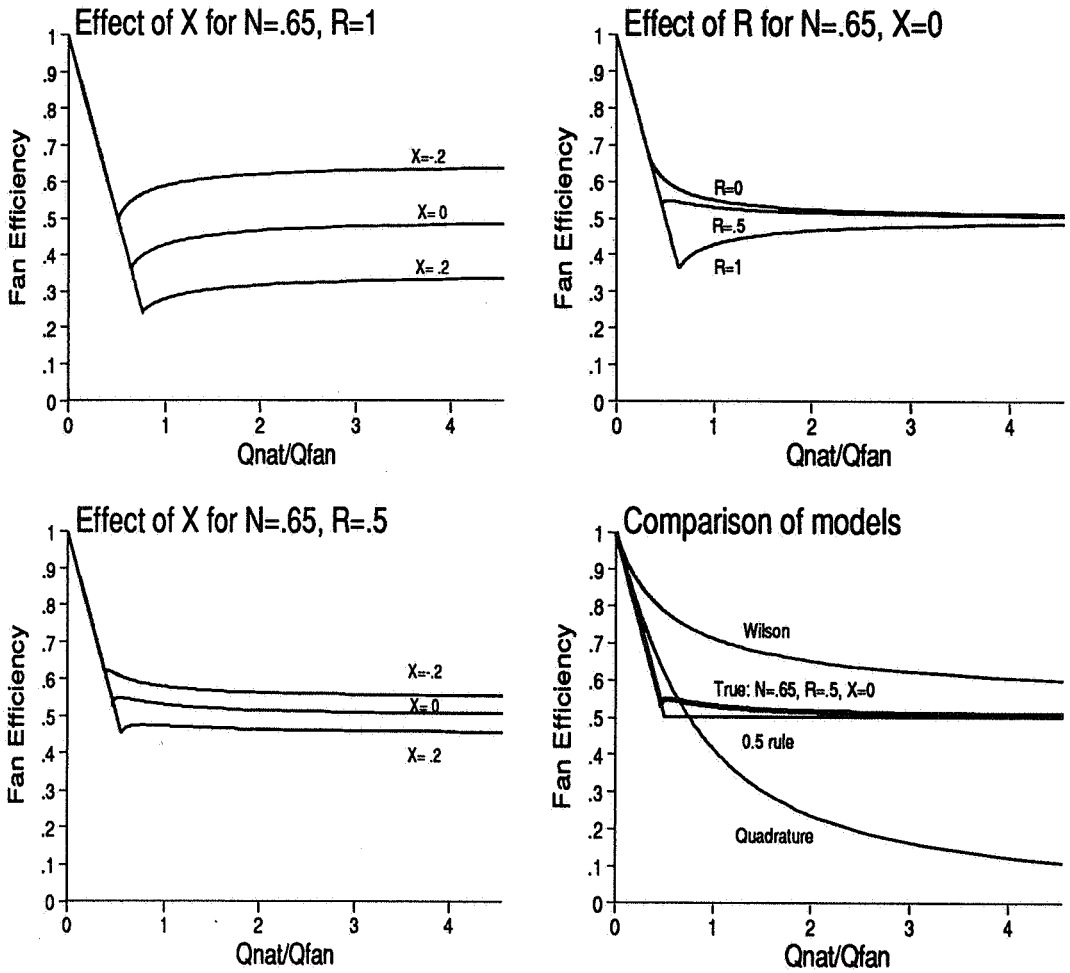

Figure 1. Fan efficiencies. Each panel shows fan efficiency versus the ratio of natural flow to fan flow for n=0.65. The left panels show the effect of varying X; R=1 for the upper left panel and R=0.5 for the lower left panel. The upper right shows the effect of varying R with X=0. The lower right panel compares three simple fan models; the 0.5 rule is the model proposed in this paper.

The efficiency is most strongly influenced by the parameter X when R=1 (i.e., all leakage is in the floor and ceiling). This is shown in the upper left panel. The upper and lower curves are for X of −0.2 and 0.2, respectively. These represent a 60-40 distribution of leakage between the floor and the ceiling. Note that efficiency is lowest at the critical point. These cusps are due to the combination of a power law flow model with a concentration of leakage at a single height. It is clear that more extreme values of X will result in considerable enhancement or reduction of fan efficiency, indicating the undesirability of placing inlet vents high on the walls.

The effect of X when R has the more typical value of 0.5 (i.e., half the leakage is in the walls) is shown in the lower left panel. Notice that the effect of varying X is greatly reduced. The curves are all reasonably close together.

The upper right panel shows the effect of varying R when X=0. Notice that there is relatively little difference between R=0.5 and R=0. A decrease in R tends to increase the efficiency near the critical point; for R=0.5 the cusp effect due to the exponent is almost exactly balanced.

The lower right panel compares the simple models for fan-stack interaction given in the theory section. For comparison, we also show the standard case of X=0, R=0.5 and n=0.65. The quadrature rule tends to underpredict the added fan flow except near the critical point, where there is significant overprediction. The Wilson model overpredicts in all cases. The 0.5 rule is very close to the true value. A comparison with the other panels shows that it gives reasonable predictions for fan efficiency and total flow whenever X does not assume extreme values.

Although it would be easy to model the fan-stack interaction more accurately for more extreme values of X and R, the model would be sensitive to supply versus exhaust flow and summer versus winter conditions. Since the model has to be used for the wind component as well, the improved accuracy would be largely illusory until more is known about the wind component. For the present, we propose to simply apply the 0.5 rule and its extensions to the total natural infiltration.

5. COMPARISON WITH FIELD DATA

In the winter of 1990, detailed real-time measurements were made on a recently constructed, two-story home in Snohomish County, Washington which had been built under a local energy-efficiency program (Palmiter and Bond 1991). Based on a survey of 49 homes located in Snohomish County (Palmiter et. al. 1990), this home was typical in its size, ventilation system, tightness, and measured infiltration rate. The home was all-electric; the heating system consisted of electric resistance wall units with fans. Characteristics of the home are listed in Table 1.

Table 1. Home and environmental characteristics of test home.

Floor area	144 m^2
Volume	350 m^3
Full height	4.95 m
Average stack height	4.18 m
Blower door leakage function	Q (L/s) = 60.1 $\Delta P^{0.629}$ (ΔP in Pa)
Effective leakage area @ 4 Pa	560 cm^2
ACH at 50 Pa	7.24
Specific leakage area (SLA)	3.88
Average ΔT	11.6 C
Average wind speed	0.53 m/s
Average infiltration	37 L/s (0.383 ACH)
Average natural infiltration	28 L/s (0.289 ACH)
Induced by multiport exhaust	17 L/s (0.177 ACH)

The data taken included tracer gas measurements made with a multitracer measurement system (Sherman and Dickerhoff 1989), pressure measurements across each face and the ceiling and floor of the home, and indoor and outdoor temperature measurement. One-time measurements of fan flow were also made using tracer gases and a flow hood.

The whole-house ventilation system consisted of a multiport exhaust system, which drew air from five ports on the second floor, and a single through-wall inlet port with a pressure-regulated damper on the first floor. During the tracer test, the exhaust system was operated by a timer, set to run four hours on and eight hours off.

In addition to the multiport exhaust system, the home had six exhaust fans. The fans and their measured flows, including the whole-house ventilation system, are listed in Table 2. Some of the measured flows are quite low due to poor installation of the fans. The occupants logged their use of the exhaust fans.

The home was well sheltered, so wind-induced infiltration was small and the stack-only infiltration model should be a reasonable approximation to the natural infiltration. We predicted the stack infiltration using the LBL infiltration model (Sherman 1980) and the AIM-2 infiltration model (Walker and Wilson 1990) with the indoor and outdoor temperatures measured at the site. During periods of no fan operation and low wind speed, the LBL model was about 10% too high and the AIM-2 model about 10% too low.

We adjusted the results of the AIM-2 model by 10% so that it generally agreed with the measured natural infiltration. The total fan flow at any given time was the sum of the measured flows through all fans operating. The adjusted natural infiltration and total fan flow were used with the fan combination rule to predict a total flow.

Pressure differences across the floor and ceiling, measured as indoor minus outdoor pressure, are shown in the top graph of Figure 2. The periods of exhaust fan operation, resulting in depressurization of the home and an increase in neutral level, are clearly visible. The pressure across the ceiling is normally positive due to stack effect. When it drops below zero, the flow across the ceiling has been reversed. The pressure datalogger failed on the evening of day 79 and there are no pressure data after that time.

The stack pressure is obtained by subtracting the measured pressures across the floor and ceiling. The effects of fans do not appear in the result. Assuming that the pressure gradient is linear with height, the dimensionless neutral level β is obtained by dividing the pressure across the floor by the measured stack pressure. This neutral level is shown in the second graph of Figure 2. The periods where $\beta>1$ correspond to the periods where the ceiling pressure has been reversed.

The measured and predicted infiltration are shown in the lower two graphs of Figure 2; the top graph shows stack-only predictions and the lower graph shows fan model predictions. The lower graph also includes the signal of the multiport ventilation system.

On the whole, the predictions of the fan model are fairly good. The two spikes in the measured data on day 77 are due to door openings, which show clearly in the temperature and pressure data. We attribute the other discrepancies to errors in the occupant log and uncertainties about flows through some of the fans. All in all, the 0.5 rule gives very reasonable predictions. We note that additional comparisons, not given here, yielded comparable results (Palmiter and Bond 1991).

Table 2. Exhaust fans at test home.

Fan Location	Measured Flow (L/s)	Fan Location	Measured Flow (L/s)
Multiport exhaust	35	Master bathroom	6
Dryer	31	First floor bathroom	14
Laundry	15	Second floor bathroom	29
Kitchen (range hood)	47		

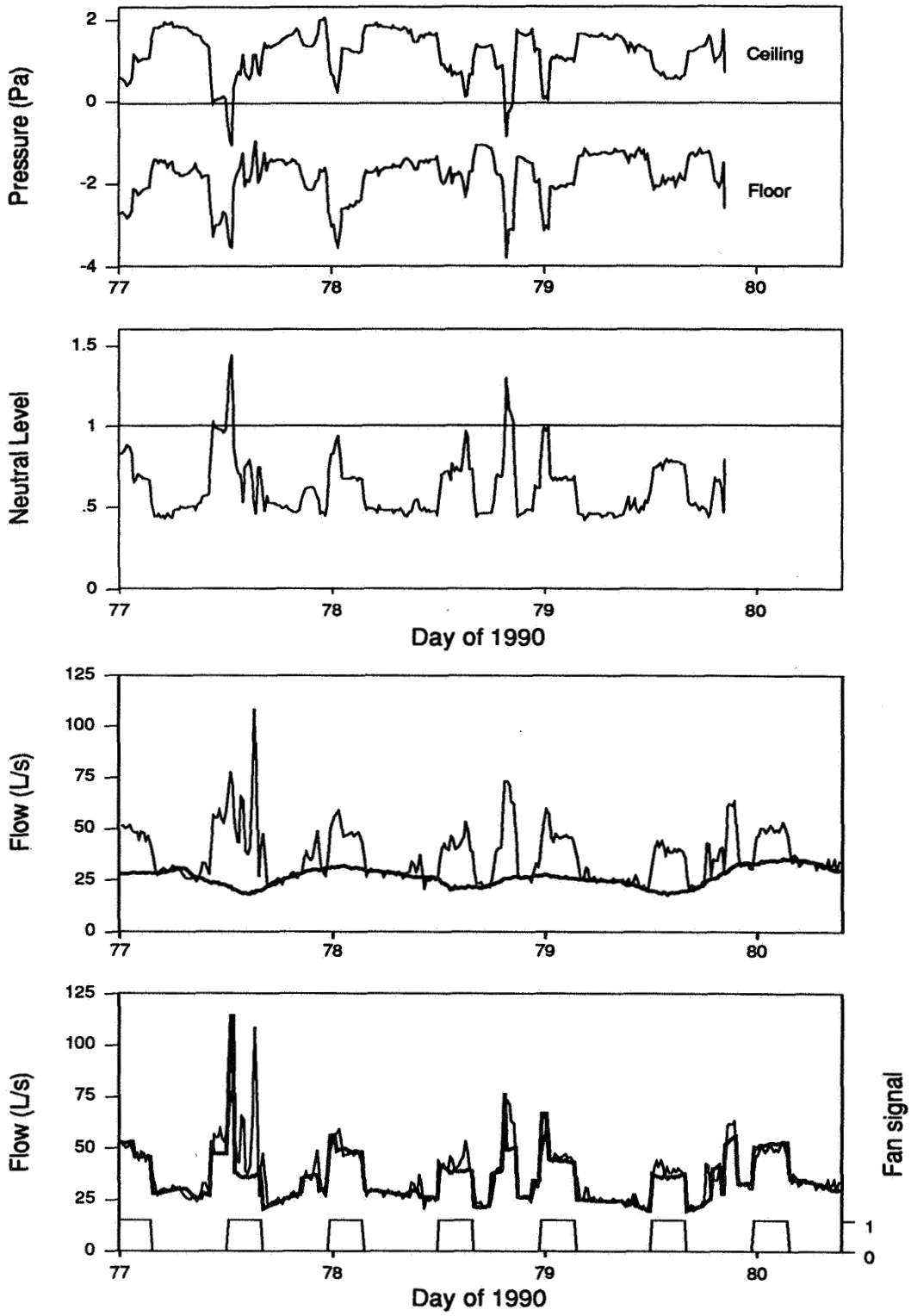

Figure 2. Pressures and infiltration at test home. The top graph shows measured pressures across the ceiling and floor; the second graph shows the dimensionless neutral level. The third graph compares the adjusted AIM-2 stack prediction (bold) with measured infiltration and the fourth shows the fan model predictions (bold), again compared with measured infiltration.

6. CONCLUSIONS

The theoretical development shows that the 0.5 rule for combining unbalanced mechanical flow with natural infiltration works well for stack-dominated infiltration, except in the case where R=1 (all leakage in the floor and ceiling). In particular, it is very good for the typical case of n=0.65, R=0.5, X=0. It is a considerable improvement over the quadrature and Wilson models, both of which have the wrong functional form.

A comparison with detailed field data shows the model to be reasonably good. Although the fan-stack interaction model could be easily improved, the necessity of using it with wind effect and combined wind and stack effects tends to negate the apparent increase in accuracy. Further investigation of the effect of wind is required.

7. REFERENCES

ASHRAE. 1989. *1989 ASHRAE Handbook: Fundamentals.* American Society of Heating, Refrigerating and Air Conditioning Engineers, Inc., Atlanta, Georgia.

Palmiter, L.S.; I.A. Brown; and T.C. Bond. 1990. *Northwest Infiltration Survey Cycle II: Infiltration and Ventilation in New All-Electric Homes in Snohomish County.* Prepared for the Washington State Energy Office under Contract No. 88-04-21.

Palmiter, L.S.; I.A. Brown; and T.C. Bond. 1991. "Measured Infiltration and Ventilation in 472 All-Electric Homes." To be published in *ASHRAE Transactions*, 1991.

Palmiter, L.; and T. Bond. 1991. *Measured and Modeled Infiltration: A Detailed Case Study of Four Electrically Heated Homes.* Electric Power Research Institute, Palo Alto, California, Report # CU-7327.

Palmiter, L.S.; and I.A. Brown. 1989. *Northwest Residential Infiltration Survey: Analysis and Results.* Bonneville Power Administration, Portland, Oregon, Report # DOE/BP-34625-1.

Sherman, M. 1990. "Superposition in Infiltration Modeling." Lawrence Berkeley Laboratory, Informal Report 29116.

Sherman, M.H.; and D.J. Dickerhoff. 1989. "A Multigas Tracer System for Multizone Air Flow Measurement." Proceedings of the ASHRAE/DOE/BTECC/CIBSE Thermal Performance of the Exterior Envelopes of Buildings Conference.

Sherman, M.H.; and D.T. Grimsrud. 1980. *Measurement of Infiltration Using Fan Pressurization and Weather Data.* Lawrence Berkeley Laboratory, Report LBL-10852.

Walker, I.S.; and D.J. Wilson. 1990. *The Alberta Air Infiltration Model: AIM-2.* University of Alberta, Technical Report 71.

Wilson, D.J.; and Walker, I.S. 1987. "Combining Air Infiltration and Exhaust Ventilation." University of Alberta.

AIR MOVEMENT & VENTILATION CONTROL WITHIN BUILDINGS

12th AIVC Conference, Ottawa, Canada
24-27 September, 1991

PAPER 19

SINGLE-ZONE STACK-DOMINATED INFILTRATION MODELING

Max Sherman

Energy Performance of Buildings Group, Indoor Environment Program

Applied Science Division, Lawrence Berkeley Laboratory,

University of California, Berkeley, California 94720

ABSTRACT

Simplified, physical models for calculating infiltration in a single zone, usually calculate the air flows from the natural driving forces separately and then combine them. For most purposes—especially minimum ventilation or energy considerations—the stack effect dominates and total ventilation can be calculated by treating other effects (i.e. wind and small fans) as perturbations, using superposition techniques. The stack effect is caused by differences in density between indoor and outdoor air, normally attributable to the indoor-outdoor temperature difference. This report derives an exact, but practical, expression for calculating the stack effect from the air densities and leakage distribution using the power law formulation of envelope leakage. The neutral height—the height at which there is no stack-related indoor-outdoor pressure difference—is a key intermediate in stack modeling. This report defines a computable parameter called *stack height*, which contains all of the leakage distribution information necessary for estimating stack flows, thus freeing the model from specific assumptions (e.g. that the leakage is separable into evenly distributed floor, wall, and ceiling components). Example calculations including comparisons with other models, as well as validations using measured data from dwellings, are also presented. The dimensionless *neutral level*, which is related to the neutral height, is often used as an indicator of leakage distribution and in superposition. Its definition and role in these regards are discussed in detail. The more exact formulation is then used to analyze the simple box cases normally assumed in infiltration modeling and other approximations. Measured ventilation data will be used to infer leakage distributions and neutral levels as well as for example calculations.

Keywords: Infiltration, Ventilation, Stack Effect, Validation, Dwellings, Indoor Air Quality, Single-zone, Modeling, Superposition.

This work was sponsored by the Electric Power Research Institute.

This work was supported by the Assistant Secretary for Conservation and Renewable Energy, Office of Buildings and Community Systems Building Systems Division of the U.S. Department of Energy under Contract No. DE-AC03-76SF00098.

NOMENCLATURE

β_s	Neutral level [-]
ELA	Effective leakage area [m^2]
f_{β_s}	Neutral level factor [-]
g	Acceleration of gravity [m/s^2]
h	Height [m]
H	Box height [m]
h_n	Neutral height (stack only) [m]
H_s	Stack height [m]
K	Leakage coefficient
$k[h]$	Leakage coefficient per meter at height h
$\dot{m}$	Stack-induced mass flow rate of air [kg/s]
n	Leakage exponent [-]
P	(Air) pressure [Pa]
ΔP	Representative pressure drop across the envelope [Pa]
R	Box ratio [-]
ρ	Density (of air) kg/m^3
Q	Stack-induced air flow [m^3/hr]
X	Vertical leakage asymmetry[-]

Subscripts indicate values associated with:

+	*in*filtration
−	*ex*filtration
↑	lighter air (i.e. leakage through upper part of building)
↓	denser air (i.e. leakage through lower part of building)
o	reference
i	individual leak

INTRODUCTION

The calculation of infiltration-dominated ventilation usually requires the combination of wind-induced, temperature-induced, and mechanically-induced air flows. Complex models solve the problem by finding the pressure at each point on the envelope and then solving for the flow—modifying the internal pressure in order to satisfy the continuity equation.[1] Such an approach is very powerful, but may require inputs and computational requirements that may make it impractical. For many applications simpler models are desirable, even if less accurate. Each of these three mechanisms induces pressures across the envelope to drive the flow, but the spatial distribution of the pressure is different for each one of them. The focus of this report will be to develop appropriate expressions for the descriptions of the *stack effect* for use in single-zone modeling.

Stack Effect

The stack effect is the flow resulting from hydrostatic pressure differences caused by density differences in two fluid columns. For buildings, the fluid is air and the density difference is caused by bulk temperature differences. Although humidity and other variations in constituents of air can cause density differences, they are usually minor compared with normal temperature differences and will be ignored.

The physics of the stack effect is straightforward and has been understood for a long time. In 1926 Emswiler[2] defined the *neutral level* as the height at which there was no pressure difference and thus no flow, and related the flow through large openings in the building to the square-root of the vertical distance from the neutral height.

When there is internal resistance (i.e. airtight partitions or floors) the neutral level may not be unique and the pressure gradient complex. Such has been demonstrated for multistory buildings.[3] By definition a single-zone building has no significant internal resistances and so we will ignore such complexities. The stack effect, however, can cause large pressure differences even in single zones which can adversely affect mechanical ventilation systems.[4]

In tall structures or when the density difference is small, density gradients can play a significant role. We will, however, assume in this report that they are not important.

MOTIVATION

Many infiltration models are currently in use;[5] but the most widely used single-zone model is the LBL infiltration model,[6,7] which is included in the ASHRAE Handbook of Fundamentals.[8] A recent model, AIM-2, by Walker and Wilson[9] builds upon the LBL model and makes some generalizations. All of the single-zone models share the characteristic of treating the zone as a rectangular box, having a fixed floor and ceiling height. Thus all of the *vertical* leakage is concentrated at two heights. As the assumption is usually made that leakage in the walls is evenly distributed, the leakage distribution can be described by three parameters. In the case of the LBL model (and AIM-2), these three parameters are the total effective leakage area, *ELA*, the fraction of leakage in the vertical surfaces, R, and the fractional difference in the ceiling-floor leakage, X[‡].

Real buildings, of course, are not usually simple boxes; there are split level, multiple story, and partially bermed buildings having vertical stacks and uneven surfaces. Palmiter and Brown[10] were the first to quantify the size of the errors caused by this assumption. They compared the definition of lowest leak to highest leak discussed in the ASHRAE Standard on air leakage[11] with an area weighted column of air and found that the former produced an average value 32% higher for their example houses. The two definitions should produce the same result for a simple box.

It is not necessary to determine which of the two definitions is superior to realize that the simple box model may be inappropriate for a large class of real buildings. The size of the error suggested by Palmiter and Brown provides a motivation to develop a stack model which does not rely on the box assumption and then to develop a more general derivation based on a simple box.

‡ Many box models use the parameters, R, X, β_s, etc. The definitions used in this report may be somewhat different, but will, in general, be similar in nature.

ENVELOPE LEAKAGE

The stack effect is buoyancy-caused, pressure-driven air flow through the envelope of the building. It is, therefore, important to understand the leakage properties of the envelope in order to understand the stack effect. Envelope leakage is conventionally treated as a power law.[12] The measurement of leakage is usually performed with a technique called fan pressurization[13] wherein the fan flow induces a shift in the internal pressure:

$$Q = \mathrm{K}\Delta P^n \tag{1}$$

where the exponent $\frac{1}{2} \leq n \leq 1$ depending on the hydrodynamics of the leaks.

In addition to being measured from a fan pressurization test, the leakage parameters can be found from more advanced techniques[14,15]

The exponent is a particularly important characteristic of the flow for both understanding the behavior and modeling it. If the exponent were unity, the modeling would be linear and relatively simple. For most buildings, however, the exponent is in the range $0.55 \leq n \leq 0.75$ with $n=2/3$ being a typical value.[16]

The whole-building leakage is clearly made up of many parallel leakage paths. Although these leakage paths will not, in general, have the same exponent, it is commonly assumed that all macroscopic areas of the building can be treated as having the same exponent. Similarly, it is assumed that K is temperature independent; reference 12 demonstrates this independence only for the specific value of $n=2/3$

For the purposes of this report we will make these same assumptions. Thus, we will treat all leakage sites as though they are described by a single exponent and a temperature-independent leakage coefficient. It is clear, however, that a better understanding of the leakage process is needed.

Rather than describing leakage with a coefficient of mixed dimensions, leakage is often discussed in terms of an effective leakage area, **ELA** defined by

$$ELA \equiv \mathrm{K}\sqrt{\frac{\rho_o}{2}}P_o^{n-\frac{1}{2}} \tag{2}$$

where the reference pressure is usually taken to be 4 Pa. Many of the models also use *ELA* directly, rather than K.

STACK EFFECT

The stack effect is caused by the hydrostatic pressure difference of two columns of fluid at different density. To be specific since indoor air and outdoor air are at different temperatures their densities are different and there is a stack effect. The pressure difference will be a function of the density difference and height:

$$\left|\Delta P\right| = \Delta\rho g \left|h - h_n\right| \tag{3}$$

where

$$\Delta\rho \equiv \rho_{\downarrow} - \rho_{\uparrow} \tag{4}$$

is the density difference between the two columns of air and the neutral height, h_n, is the height at which the pressure in the two columns is equal[1]. Since we are ignoring density gradients, the density inside and out can each be represented by a single (average) value.

To calculate the air flow it is necessary to apply eq. 1 by integrating the leakage at each height.

$$Q_{\downarrow} = \int_{-\infty}^{h_n} k[h] \left(\Delta\rho\, g(h_n - h)\right)^n dh \tag{5.1}$$

$$Q_{\uparrow} = \int_{h_n}^{\infty} k[h] \left(\Delta\rho\, g(h - h_n)\right)^n dh \tag{5.2}$$

Note that we have separated the infiltration (positive pressures) from the exfiltration (negative pressures).

The neutral height is fixed by the requirement that the *mass* balance between infiltration and exfiltration be maintained.

$$\rho_{\downarrow} Q_{\downarrow} = \rho_{\uparrow} Q_{\uparrow} = \dot{m} \tag{6.1}$$

$$\int_0^{\infty} \left(\rho_{\uparrow} k[h_n+h] - \rho_{\downarrow} k[h_n-h]\right) h^n dh \; = 0 \tag{6.2}$$

It is conventional to use volumetric rather than mass flows to describe infiltration so we will seek a form for the stack flow as follows:

$$\rho_o\, Q = \dot{m} \tag{7}$$

which means we must use a reference density. Since eq. 1 is a volumetric flow equation, we can select the density in such a way as to have the stack flow be analogously defined:

$$Q = \mathrm{K} \int_{-\infty}^{\infty} \frac{k[h]}{2\mathrm{K}} \left|\Delta\rho\, g(h - h_n)\right|^n dh \tag{8}$$

The density must then be as follows:

$$\rho_o \equiv \frac{\int_0^{\infty} \left(\rho_{\uparrow} k[h_n+h] + \rho_{\downarrow} k[h_n-h]\right) h^n \, dh}{\int_{-\infty}^{\infty} k[h] \left|h_n - h\right|^n dh} \tag{9.1}$$

↓ Note that the definition for neutral height in this report is specifically for the case in which only the stack effect operates. The actual height at which the indoor and outdoor pressures are equal can be affected by other factors (e.g. fans or wind).

Equivalent Stack

To gain some insight into these formidable integrals, we consider the case of a simple stack in which there is a leak, $K_\downarrow$, at the bottom ($h=H_\downarrow$) and another, $K_\uparrow$, at the top ($h=H_\uparrow$). This situation is exactly analogous to the stack effect in a building in which there are leaks only in the floor and ceiling.

Using the relationships from the previous section, the neutral height is

$$h_n - H_\downarrow = \frac{H_\uparrow - H_\downarrow}{1 + \left(\frac{\rho_\downarrow K_\downarrow}{\rho_\uparrow K_\uparrow}\right)^{1/n}} \tag{10}$$

and the mass flow through the stack is

$$\dot{m} = K \frac{\rho_\downarrow \rho_\uparrow \beta_s^n (1-\beta_s)^n}{\rho_\downarrow \beta_s^n + \rho_\uparrow (1-\beta_s)^n} \left(\Delta\rho\, g (H_\uparrow - H_\downarrow)\right)^n \tag{11}$$

where the neutral level is defined as

$$\beta_s \equiv \frac{h_n - H_\downarrow}{H_\uparrow - H_\downarrow} \tag{12.1}$$

$$= \frac{1}{1 + \left(\frac{\rho_\downarrow K_\downarrow}{\rho_\uparrow K_\uparrow}\right)^{1/n}} \tag{12.2}$$

and K is the total leakage

$$K = K_\downarrow + K_\uparrow = K_+ + K_- \tag{13}$$

We can rewrite the mass flow as follows:

$$Q = \frac{K}{2} f_{\beta_s} \left(P_s\right)^n \tag{14}$$

where the stack pressure, P_s, is the effective pressure drop across the leakage sites:

$$P_s = \Delta\rho\, g \frac{H_\uparrow - H_\downarrow}{2} \tag{15}$$

and the neutral level factor, f_{β_s}, is defined as follows:

$$f_{\beta_s} \equiv \left\{\frac{2^{1+n} \beta_s^n (1-\beta_s)^n}{\beta_s^n + (1-\beta_s)^n}\right\} \tag{16}$$

The reference density reduces to

$$\rho_o = \frac{\rho_\downarrow (\beta_s^n + (1-\beta_s)^n) \rho_\uparrow}{\rho_\downarrow \beta_s^n + (1-\beta_s)^n \rho_\uparrow} \tag{17}$$

We define a parameter, X, to describe the asymmetry in the leakage:

$$X \equiv \frac{\rho_\uparrow K_\uparrow - \rho_\downarrow K_\downarrow}{\rho_\uparrow K_\uparrow + \rho_\downarrow K_\downarrow} \approx \frac{K_\uparrow - K_\downarrow}{K} \tag{18}$$

or, equivalently,

$$X = \frac{\beta_s^n - (1-\beta_s)^n}{\beta_s^n + (1-\beta_s)^n} \approx n(2\beta_s - 1) \tag{19}$$

If we do this we can rewrite some of the previous expressions:

$$\beta_s = \frac{1}{1+\left(\frac{1-X}{1+X}\right)^{1/n}} \approx \frac{1}{2}(1+X)^{1/n} \tag{20.1}$$

$$f_{\beta_s} = 2^n \frac{1-X^2}{\left[(1-X)^{1/n}+(1+X)^{1/n}\right]^n} \approx (1-X^2)^{(1+n)/2n} \tag{20.2}$$

$$\rho_o = \frac{\rho_\downarrow \rho_\uparrow}{\rho_\downarrow + \rho_\uparrow + X\Delta\rho} \approx \frac{\rho_\downarrow \rho_\uparrow}{\rho_\downarrow + \rho_\uparrow} \tag{20.3}$$

The approximations in eqs. 18 and 20.3 are true if the the density difference is small ($\Delta\rho \ll \rho$); the approximations in eqs. 19 and 20 are true if the leakage asymmetry is small ($X \ll 1$); and the approximations in eqs. 19, 20.1, 20.2 are also true if the exponent approaches unity ($n \to 1$). Although the exponent is normally closer to 2/3, the other two conditions are usually true.

This description is complete for a system with exactly two, localized leaks, but it cannot be used in the general case without further refinement. First we must interpret the two leakage sites to be the total leakage area below and above the neutral level respectively:

$$\mathrm{K}_\downarrow \equiv \int_{-\infty}^{h_n} k[h]\,dh \approx \mathrm{K}\,\frac{1-X}{2} \tag{21.1}$$

$$\mathrm{K}_\uparrow \equiv \int_{h_n}^{\infty} k[h]\,dh \approx \mathrm{K}\frac{1+X}{2} \tag{21.2}$$

We define the equivalent stack bottom ($H_\downarrow$) and stack top ($H_\uparrow$) so that the mass flow is correct:

$$\mathrm{K}_\downarrow \rho_\downarrow \left(\Delta\rho\, g(h_n - H_\downarrow)\right)^n = \dot{\mathrm{m}} = \mathrm{K}_\uparrow \rho_\uparrow \left(\Delta\rho\, g(H_\uparrow - h_n)\right)^n \tag{22}$$

$$H_\uparrow \equiv h_n + \left(\frac{\int_{h_n}^{\infty} k[h](h-h_n)^n dh}{\mathrm{K}_\uparrow}\right)^{1/n} \tag{23.1}$$

$$H_\downarrow \equiv h_n - \left(\frac{\int_{-\infty}^{h_n} k[h](h_n-h)^n dh}{\mathrm{K}_\downarrow}\right) \tag{23.2}$$

Thus, as can be directly verified, eqs. 11,12,15 can be used in the general case with these definitions.

Stack Height

We now seek to compress all of the leakage distribution information into a single parameter so as to express the infiltration as follows:

$$Q = \frac{\mathrm{K}}{2}\left(\Delta\rho\, g \frac{H_s}{2}\right)^n \tag{24}$$

where H_s is called the *stack height.*

The general relationship for the stack height can be found by comparing this to eqn 8:

$$H_s = 2\left(\frac{\int_{-\infty}^{\infty} k[h]\ \left|h - h_n\right|^n dh}{\mathrm{K}}\right)^{1/n} \tag{25.1}$$

Equivalently, the stack height can be related to the equivalent stack top and bottom as follows:

$$H_s = f\beta_s^{1/n}\,(H_\uparrow - H_\downarrow) \tag{25.2}$$

Thus all of the information about the leakage distribution (relevant to the stack effect) can be contained in a single parameter, the stack height. Other formulations, such as simple box models, can be converted into this form.

LEAKAGE DISTRIBUTION EXAMPLES

The following examples illustrate the procedure for three houses of differing construction. The procedure calculates the stack height and leakage distribution parameters; specific temperature conditions could be used to calculate the flows. The leakages are quoted in effective leakage area, which is linearly related to K by eq. 2 and can be used in its stead.

For the examples below we will estimate the neutral height by ignoring the density differences, assuming that any unaccounted for leakage is evenly distributed in height, and defining the floor level as the zero in height. Operationally, one can use an exponent of unity in eq. 6.2 to estimate the neutral height, in which case

$$h_n \approx \frac{\sum_i \mathrm{K}_i h_i + (\mathrm{K} - \sum_i \mathrm{K}_i) H/2}{\mathrm{K}} \tag{26.1}$$

or, equivalently

$$h_n \approx \frac{H}{2} + \sum_i \frac{\mathrm{K}_i}{\mathrm{K}}\left(h_i - \frac{H}{2}\right) \tag{26.2}$$

where H is the height of the house and h_i is the height at which leak K_i is located.

Having determined the neutral height, X, β_s, and H_s can then be calculated from eqs. 12,18, and 25.

Default House

Consider a two-story (5m) tall house with a total leakage area of 700cm^2 (with an exponent of 0.65) and 200m^2 of floor area (10m x 10m footprint). If we know nothing else about the leakage distribution, we might reasonably assume that the envelope is uniformly porous in which case there is 175cm^2 of floor leakage, there is 175cm^2 of ceiling leakage, and there is 350cm^2 in the walls. Using the approximate expression for the neutral height,

$$h_n \approx \frac{5}{2} + \frac{175}{700}(5-2.5) + \frac{175}{700}(-2.5) = 2.5m \tag{27}$$

(This result is, in fact, that from the exact neutral height expression, eq. 6.2)

$$\left(\frac{H_s}{2}\right)^{.65} = \frac{\frac{350}{2.5*1.65}\,|-2.5|^{1.65} + \frac{350}{2.5*1.65}\,|2.5|^{1.65} + 175\,|-2.5|^{.65} + 175\,|2.5|^{.65}}{700} \tag{28}$$

The values of the parameters are

$$H_s = 3.57 \qquad X = 0 \qquad \beta_s = 0.50 \tag{29}$$

Slab-on-Grade House

Consider a single-story (2.5m), slab-on-grade house of 700cm^2 of leakage area (with n=0.65) in which the only leakage is in the walls and at ceiling level. There is 140cm^2 of leakage at the level of the ceiling (2.5m), the remainder is assumed to be spread evenly in the walls. Using the approximate expression for the neutral height we get

$$h_n \approx \frac{1}{700}\left(140*2.5 + \frac{560*2.5}{2}\right) = 1.5m \tag{30}$$

The stack height can now be calculated as follows:

$$\left(\frac{H_s}{2}\right)^{.65} = \frac{\frac{560}{2.5*1.65}*|-1.5|^{1.65} + \frac{560}{2.5*1.65}*|1|^{1.65} + 140*|1|^{.65}}{700} \tag{31.1}$$

$$H_s \approx 1.3 \tag{31.2}$$

More exact values of the parameters are

$$h_n = 1.52m \qquad H_s = 1.34m \qquad X = 0.03 \qquad \beta_s = 0.52 \tag{32}$$

The stack height is significantly less than the floor-to-ceiling height because of the concentration of leakage at ceiling height without any compensating leakage at floor level, even though the net asymmetry is small.

Crawlspace House

Consider a single-story, crawlspace house of 700cm^2 of leakage area (with n=0.65). 210cm^2 of leakage is at floor level, there is a 50cm^2 dryer vent 1m above the floor, 140cm^2 of leakage at the level of the ceiling (2.5m), and a total of 100cm^2 of leakage at the 4m level due to (insulated) flues, vents, and chimneys; the remainder is assumed to be spread evenly in the walls. Using the approximate expression for the neutral height we get

$$h_n \approx \frac{1}{700}\left[50 + \frac{200*2.5}{2} + 140*2.5 + 100*4\right] = 1.5m \tag{33}$$

The stack height can now be calculated as follows:

$$\left(\frac{H_s}{2}\right)^{.65} = \frac{210*1.5^{.65} + \frac{200}{2.5*1.65}*1.5^{1.65} + \frac{200}{2.5*1.65} + 50*.5^{.65} + 140 + 100*2.5^{.65}}{700} \tag{34.1}$$

$$H_s \approx 2.3 \tag{34.2}$$

More exact values of the parameters are

$$h_n = 1.44m \quad H_s = 2.30 \quad X = -0.07 \quad \beta_s = 0.45 \tag{35}$$

This house has the same total leakage as the first example, but a significantly larger stack height (and therefore, stack effect), because the leakage sites are vertically separated. The stack flow for this example will be about 70% larger than the first one because of the different leakage distributions. Thus, the stack height is similar to the floor-to-ceiling height.

Daylight Basement

Consider a two-story house in which the bottom level is partially bermed and half of it is taken up by a garage. Again the total leakage is 700cm^2 (n=0.65). There is floor level leakage of 150cm^2; there are 100 cm^2 of leakage between the two stories (2.5m); there are 100 cm^2 of leakage at the ceiling level (5m) ; there are 50 cm^2 of leakage at 7m above the floor from a chimney. The remainder of the leakage is assumed to be spread evenly in the walls. Thus, the neutral height is as follows:

$$h_n \approx \frac{1}{700}\left[\frac{300*5}{2} + 100*2.5 + 100*5 + 50*7\right] = 2.6m \tag{36}$$

From which we can calculate the stack height:

$$\left(\frac{H_s}{2}\right)^{.65} = \frac{150*2.6^{.65} + \frac{300}{5*1.65}2.6^{1.65} + 100*.1^{.65} + \frac{300}{5*1.65}2^{1.65} + 100*2.4^{.65} + 50*4.4^{.65}}{700} \tag{37.1}$$

$$H_s \approx 3.2 \tag{37.2}$$

More exact values of the parameters are

$$h_n = 2.57m \quad H_s = 3.12m \quad X = -0.15 \quad \beta_s = 0.38 \tag{38}$$

Even though the building is twice as tall as in the second example, the stack height is only somewhat larger, because of the concentration of leakage near the middle of the building. Note that there is significant asymmetry (and an accordingly small neutral level) because there is a significant leak just below the neutral height.

BOX MODELS

As discussed in the introduction many models treat the building as a box. There is leakage in the floor, the ceiling, and the walls (of height H), but in order to define it as a simple box we must make an assumption about how the leakage is distributed in the walls. In the LBL model, it is assumed that all wall leakage is evenly distributed. We assume here that there can be different amounts of leakage in the walls above and below the neutral height, but that the distribution in leakage in the walls mirrors that of the

floor and ceiling:

$$\frac{\mathbf{K}_{floor}}{\mathbf{K}_{\downarrow}} = \frac{\mathbf{K}_{ceiling}}{\mathbf{K}_{\uparrow}} = R = \frac{\mathbf{K}_{ceiling} + \mathbf{K}_{floor}}{\mathbf{K}} \tag{39}$$

Thus the box ratio, R, represents the fraction of the leakage lumped at the floor and ceiling.

The neutral level can still be calculated from eq. 20, but it is conventional (in box models) to define the neutral level based on the height of the box (from the floor):

$$\beta_{box} \equiv \frac{h_n}{H} \tag{40}$$

As can be verified, this definition of neutral level is equivalent to the one used previously—*provided the box assumptions are valid* (i.e. $\beta_{box}=\beta_s$ only if eq. 39 is true).

Following the development of the previous sections, the flow equation for the simple box is very similar to that for the simple stack case:

$$Q = \frac{\mathbf{K}}{2} \frac{1+nR}{1+n} f_{\beta_s} \left[\Delta\rho g \frac{H}{2}\right]^n \tag{41}$$

As expected, this solution reduces to the simple stack case for $R=1$.

The stack height can be calculated from the box model parameters as follows:

$$H_s = \left[\frac{1+nR}{1+n} f_{\beta_s}\right]^{1/n} H \tag{42}$$

Equivalent Box Parameters

Few houses are really simple boxes and follow the assumptions above, but it is possible to find a set of parameters that is equivalent to the actual situation. Some of the parameters can be determined from direct measurement while others must be inferred. If the leakage distribution is known, then $X, h_n, \beta_s, and\ H_s$ can all be directly calculated using eqs. 18-25.

We can calculate values for H and R that must exist for the box assumptions to be true. The equivalent box height inferred from the neutral level and height:

$$H = \frac{h_n}{\beta_s} \tag{43}$$

The assumption that eqs. 38, 39 and 42 are true is the *box assumption*. The box parameter can only be calculated by making these assumptions and is as follows:

$$R = \frac{\frac{1+n}{f_{\beta_s}}\left[\frac{H_s}{H}\right]^n - 1}{n} \tag{44}$$

Eqs. 43 and 44 define the equivalent box height and ratio for the case in which the leakage distribution can be calculated directly. If the box assumptions were valid, then the equivalent box ratio would lie between zero and unity, but in general R can have a larger range. If R is greater than unity it implies that there is significant leakage below the nominal floor or above the nominal ceiling. If R is less than zero, it implies a concentration of leakage near the neutral level.

The equivalent box parameters, H and R, can be calculated for our four examples and are summarized in the discussion.

INTERPRETATION OF FIELD MEASUREMENTS

The above approach assumes detailed knowledge of the leakage distribution. For parametric studies or design purposes it may be possible to define the leakage distribution exactly, but when measuring an existing structure it may not be possible to know where all of the leakage is. It is possible to measure the neutral height directly (from pressure measurements) and the stack height from the whole-building leakage, temperature difference and the infiltration rate (using eq. 24).

If a nominal building height is assumed then a set of *apparent* box parameters can be found. The neutral level can then be determined from eq. 40, the leakage asymmetry can be determined from eq. 19 and then the box ratio can be determined from eq. 44.

In order to demonstrate this stack formulation, it is necessary to have field measurements of both the envelope leakage and ventilation with only the stack effect in operation. Such a case study has recently been done by Palmiter and Bond.[17] The sites were in the Puget Sound area of the state of Washington and were relatively new construction. Information not explicitly contained in this report was required for the calculations below.[18]

In all sites continuous multizone air flow measurements were made using tracer gases[19] and while all mechanical systems as well as weather and surface pressures were monitored. The infiltration data for these examples will only include those periods in which the stack effect dominated and there were no effects from HVAC systems.

Site 1

This site was a two-story crawlspace home with attached garage, built in 1988 to the "Super Good Cents" program specifications; it had tight-fitting windows and electric baseboard heating. The Super Good Cents program requires the presence of mechanical ventilation, which consisted of a central exhaust fan in the attic with five ports in upstairs closets and a through-the-wall 5" diameter inlet port (with damper) located 1.6m above the first-story floor. In addition, there were two ceiling and three mid-level exhaust vents, all of which had back-draft dampers. There was also a dryer vent at floor level. The total leakage area was measured at 560cm^2 with an exponent of 0.63.

The measured neutral height for this site was 7.75 ft., which implies an apparent neutral level of 0.48 based on the 16.25 ft nominal height. The stack-induced air change rate was approximately 0.28 h^{-1} which yields a stack height of 11.5ft from the average temperature difference of 11.3 ^{o}C. The apparent R is 0.50 and the apparent X is -.03.

Site 2

This site is also a two-story crawlspace house with attached garage. Built in 1979, it has been the subject of detailed measurement before[20] There are three ceiling vents, one mid-level vent, one ground level dryer vent, and one fireplace on each floor. While the ceiling in site 1 was flat, this site had a partial cathedral ceiling. The total measured leakage area is 1089 cm^2 with an exponent of 0.66.

The neutral height was measured at 8.45ft which implies an apparent neutral level of 0.52 based on the 16.25ft nominal height. Stack induced ventilation was approximately 0.41 h^{-1}, which yields a stack height of 13.1ft from the average temperature difference of 9.3 ^{o}C. The apparent R is 0.67 and the apparent X is -0.02.

Site 3

This site is a split-level home with an integral garage built in 1984 and has partial slab and partial crawlspace. There are two ceiling vents two mid-level vents, and one dryer vent and fireplace on the the lower floor. The total measured leakage area is 902cm^2 with an exponent of 0.70. (Note: this leakage is based on depressurization only.)

The neutral height was measured at 8.48ft which implies an apparent neutral level of 0.52 based on the 16.25ft nominal height. Stack induced ventilation was approximately 0.32 h^{-1}, which yields a stack height of 13.1ft (for depressurization) from the average temperature difference of 8.3 ^{o}C. The apparent R is 0.76 and the apparent X is 0.02.

Site 4

This site was a new manufactured home build under the BPA Residential Construction Demonstration Program. It was single story, but had a cathedral ceiling section. There was a make-up air system whose exhaust (with a damper near the mid-plane of the house) was sealed for the quoted data and accompanying slot inlets. There are three ceiling vents and one dryer vent; for The total measured leakage area is 286 cm^2 with an exponent of 0.64.

The neutral height was measured at 4.6ft which implies an apparent neutral level of 0.49 based on the 9.33ft nominal height. Stack induced ventilation was approximately 0.16 h^{-1} which yields a stack height of 4.8ft from the average temperature difference of 16.5 ^{o}C The apparent R is 0.11 and the apparent X is -0.01.

DISCUSSION

We have applied our stack formulation to four examples where the leakage distribution is known and to four measured instances where it was not. This dataset is summarized in Table 1 below:

TABLE 1: Summary of Examples and Measurements										
	ACTUAL				EQUIVALENT		APPARENT			
Case	h_n	H_s	X	β_s	H	R	H	R	X	β_{box}
Default	2.5	3.57	0	0.50	5.00	0.50	5.0	0.50	0	0.50
Slab	1.52	1.34	0.03	0.52	2.91	0.00	2.5	0.20	0.14	0.61
Crawlspace	1.44	2.30	-.07	0.45	3.23	0.51	2.5	0.90	0.10	0.58
Basement	2.57	3.12	-.15	0.38	6.72	0.05	5.0	0.33	0.02	0.52
Site 1	2.36	3.51	?	?	*4.7*	*0.57*	4.9	0.50	-.03	0.48
Site 2	2.55	3.99	?	?	*5.1*	*0.63*	4.9	0.67	-.02	0.52
Site 3	2.58	4.27	?	?	*5.2*	*0.72*	4.9	0.76	0.02	0.52
Site 4	1.40	1.46	?	?	*2.8*	*0.11*	2.8	0.11	-.01	0.49
italic values are undetermined from measurements, but calculated assuming X=0, β_s=½.										
APPARENT values are based on the nominal building height.										

The first four columns of data represent the true value of the parameters as determined from direct measurement. In the case of the four measured sites, the leakage distribution (i.e. asymmetry or true neutral level) was not determined. The next two columns represent the values of H and R that would be true for the equivalent box. Since the data were missing from the four measured sites these columns were calculated assuming leakage symmetry. The last four columns represent the apparent distribution parameters based on the nominal height of the structures.

One notes that the apparent neutral level, β_{box} is not always the same as the actual neutral level, β_s, and similarly for X. Although calculations based on the four apparent values will yield the correct stack effect, the superposition of the stack effect with other driving forces requires the actual value of neutral level.[21]

The apparent neutral levels of the four measured sites are all quite close to 1/2 (i.e. $X \approx 0$) and one might be tempted to generalize this result. These four sites, however, are all-electric homes and, therefore, do not have as many flues as fossil-fuel heated homes for which a neutral level in the range of 0.6 to 0.7 (i.e. $X \approx 0.2$) would be more appropriate.

In our formulation the neutral level is not a very sensitive factor for calculating the stack effect, because we take into account both infiltration and exfiltration. Because R indicates the relative distance of leaks from the neutral level (in box models), it is significantly more important. The eight cases show a wide range for the box ratio. Site 1 appears very similar to the Default case in that R=.5. Sites 2 and 3 have high values of R suggesting a large amount of ceiling and floor leaks (including the leaky ductwork noted in the report). Site 4, the manufactured home, has quite a low value of R due undoubtedly to the factory-tight construction of the floor and ceiling assemblies.

The data might suggest that a relatively high value of R is appropriate for stick-built homes, but the sample is too small to be conclusive. The importance of this parameter to the result implies that more field measurements should be made to categorize the value of R for different construction types.

Additional conclusions based on the mechanical systems performance of these sites have been made by Palmiter.[22]

Comparison to LBL Stack Model

The box version of this stack model can be compared with the LBL stack model (which is a box model). If we set n=½, eq. 41 becomes equivalent to the LBL stack model (ref 6,7). Doing so reveals that the two equations are similar in form, but slightly different in interpretation (i.e. the box assumptions used are not identical). Additionally, this model allows the correct calculation of mass flow by including a modified density.

In the LBL model the parameters R and X focused exclusively on the floor and ceiling leakages. In this new model the interpretation of these parameters has been expanded to include more general cases, which is quite useful in interpreting field measurements of infiltration.

Stack-Induced Pollutant Entry

Some pollutants (such as those in soil gas) may be driven into the building by stack-induced pressure differences. This pressure can be easily calculated for any height in the building (eq. 3). Since the competitive effects of pollutant entry and infiltration would be simultaneously affected, it is necessary to solve them simultaneously to find the concentration of the pollutant.

A detailed discussion of this is beyond the scope of this report, but as an example we can solve the problem for the special case in which a pollutant enters the structure through a small leak (of the same exponent as the house) driven by the inside-outside pressure at floor level. (Such a case might be reasonable for radon entry into a slab-on-grade house.) The steady-state concentration of this pollutant would thus be

$$C = C_\infty \frac{\mathbf{K}_{crack}}{\mathbf{K}} \frac{2}{1-\frac{1+nR}{1+n}X} \tag{45}$$

where C_∞ is the concentration of the gas entering through the $\mathbf{K}_{crack}$ leak.

This example serves to demonstrate how the exposure will be a function of the leakage distribution. Specifically, if X approaches unity (i.e. a lot of high leakage) the exposure could be quite large, but once X gets into a more normal range (i.e. below 0.7) the concentration is not a strong function of the distribution; even making X go highly negative cannot make the exposure arbitrarily small.

SUMMARY

The model developed herein can be summarized as follows. The whole-building leakage parameters K and n, combined with the temperature and density differences, interact with the leakage distribution to give the stack-induced ventilation:

$$Q = \frac{\mathbf{K}}{2}\left(\Delta\rho\, g \frac{H_s}{2}\right)^n \tag{46.1}$$

Because of the density differences between inside and outside air this flow is neither the volumetric infiltration nor exfiltration, but rather is at an intermediate density (given by

eq. 17),

$$\rho_o \approx \frac{\rho_+ \rho_-}{\rho_+ + \rho_-} \tag{46.2}$$

which is quite close to the density at the average inside/outside temperature.

If the leakage distribution is assumed known then the stack height can be calculated:

$$H_s = 2 \left(\frac{\int_{-\infty}^{\infty} k[h] \left| h - h_n \right|^n dh}{\mathbf{K}} \right)^{1/n} \tag{47.1}$$

where the integral can be converted to a sum for localized leaks and the neutral height is calculated from eq. 6 or estimated from eq. 26.

The neutral level, β_s, is a useful parameter for quantifying the vertical distribution of the leakage and can be calculated from either the leakage distribution directly or equivalently from the vertical asymmetry parameter, X.

$$\beta_s = \frac{1}{1 + \left(\frac{\rho_\downarrow \mathbf{K}_\downarrow}{\rho_\uparrow \mathbf{K}_\uparrow} \right)^{1/n}} = \frac{1}{1 + \left(\frac{1-X}{1+X} \right)^{1/n}} \tag{47.2}$$

Although the neutral level is not strictly necessary for the calculation of the stack effect, it is necessary for other functions such as the superposition of other driving forces or for the estimation of the entry of some pollutants.

In a real building it may be difficult to know the entire leakage distribution and one can make some estimates by assuming the structure can be treated as a box. From eq. 42 the stack height can be estimated from the height of the box and the parameter, R:

$$H_s \approx \left(\frac{1+nR}{1+n} \right)^{1/n} H \tag{48}$$

The problem still remains to estimate R, which quantifies how well the leakage is spread out. (For example, if the leakage is evenly spread in the walls R is zero, if it is all concentrated at the floor and ceiling R is unity; lumped leakage near the neutral level will decrease R, while lumped leakage outside of the floor and ceiling level will increase it.) Some case studies which would yield R were presented, but sufficient data are lacking to provide guidelines on the estimation of this parameter.

Early field measurements indicated a need for improvements to stack models to handle different construction types and leakage distributions. The model developed in this report is more general and more robust than its predecessors. Current field measurements, combined with the model, have allowed us to infer useful information about the leakage distribution in some typical house styles and have demonstrated both similarities and differences from some of the conventional assumptions. The current dataset of measurements is too small to generalize leakage distribution conclusions, but expansion of this effort could led to useful guidelines in the future. Such guidelines would allow a better understanding of typical leakage distributions and, hence, of residential ventilation.

REFERENCES

1. "COMIS Fundamentals", Air Infiltration and Ventilation Centre, H.E. Feustel, A. Raynor-Hoosen Ed., Coventry, UK (1990). Lawrence Berkeley Laboratory Report No. LBL-28560 (1990)
2. Emswiler J.E., The Neutral Zone in Ventilation, ASHVE Trans.32 p.59-72, (1926).
3. Lee K.H., Lee T., Tanaka H, Thermal effect on pressure distribution in simulated high-rise buildings: experimental and analysis, ASHRAE Trans. 91(HA) p.530-544 (1985).
4. Tamura, G.T., Wilson A.G., Building pressure caused by chimney action and mechanical ventilation, ASHRAE, Trans, 73p 11.2.1-11.2.12(1967).
5. Liddament M., Allen C., Validation and comparison of mathematical models of air infiltration, Tech Note No.11, Air Infiltration and Ventilation Centre, Warwick, UK (1983).
6. Sherman, M.H. "Air Infiltration in Buildings", Ph.D Thesis, University of California, 1980, Lawrence Berkeley Laboratory Report LBL-10712.
7. Sherman, M.M. and Grimsrud, D.T. "Infiltration-Pressurization Correlation: Simplified Physical Modelling". ASHRAE Trans 86 II (1980) pp.778-807, Lawrence Berkeley Laboratory Report, LBL-10163.
8. American Society of Heating, Refrigeration and Air-Conditioning Engineers, Handbook of Fundamentals, ASHRAE, Atlanta, GA, Chapter 23, 1989.
9. Walker I.S., Wilson D.J., AIM 2: The Alberta air infiltration model, University of Alberta, Dept of Mech. Engr Report #71(1990).
10. Palmiter L, Brown I., Northwest Residential Infiltration Study: Analysis and Results Bonneville Power Administration Project Report, WSEO Sub-contract No.88-24-01(1989).
11. Air Leakage Performance for Detached Single-Family Residential Buildings, ANSI/ASHRAE Standard 119-1988, American Society of heating Refrigeration and Air-Conditioning Engineers, ISSN 1041-2336 (1988).
12. Sherman M.H. "A power law formulation of laminar flow in short pipes" J. Fluid Eng. (In Review) Lawrence Berkeley Laboratory Report LBL-28505.
13. "Standard Test Method for Determining Air Leakage Rate by Fan Pressurization, ASTM E779-87, American Society for Testing & Materials (1987).
14. M.H. Sherman, M.P. Modera, "Low-Frequency Measurement of Leakage in Enclosures", Rev.Sci. Instrum, 57(7), pp1427 (1986).
15. M.H. Sherman and M.P. Modera, "Signal Attenuation Due to Cavity Leakage" J.Acous Soc.Amer.84(6), (1988).
16. M.H. Sherman, D.J. Wilson, D.E. Kiel, "Variability in Residential Air Leakage"Measured Air Leakage of Buildings, Trechsel/Lagus Ed., STP 904, American Society for Testing & Materials, Philadelphia, PA, pp348(1986).
17. Palmiter L., Bond T. Modelled and Measured Infiltration: A Detailed Case Study of Four Electrically Heated Homes, Electric Power Research Inst. Contract report RP 2034-40, (EPRI CU-7327) (1991).
18. Additional information and calculations concerning these four sites were helpfully supplied as personal communication from Larry Palmiter to the author.
19. Sherman M.H., A MultiTracer System for Multizone Ventilation Measurements, Rev.Sci., Inst. (1990) Lawrence Berkeley Laboratory Report LBL-26538.
20. Palmiter L., Brown I., "Northwest Residential Infiltration Survey: Analysis and Results" WSEO Contract report No.88-04-21 (1989).
21. Sherman M.H., Superposition in Infiltration Modelling, (In Review at Journal) 1991. Lawrence Berkeley Laboratory Report No. LBL-29116 (1990).
22. Palmiter L., "Field Measurements of Interaction of Mechanical Systems and Natural Infiltration", Proc. 12th AIVC Conference Air Movement and Ventilation Control within Buildings, Air Infiltration and Ventilation Centre (1991).

ACKNOWLEDGEMENTS

The author would like to thank Larry Palmiter of Ecotope, as well as Darryl Dickerhoff of LBL, their suggestions and assistance in the interpretation of the field measurements.

AIR MOVEMENT & VENTILATION CONTROL WITHIN BUILDINGS

12th AIVC Conference, Ottawa, Canada
24-27 September, 1991

PAPER 20

COMPARISON OF AIRTIGHTNESS, INDOOR AIR QUALITY AND POWER CONSUMPTION BEFORE AND AFTER AIR-SEALING OF HIGH-RISE RESIDENTIAL BUILDINGS

Anil Parekh
Ken Ruest
Scanada Consultants Limited
436 MacLaren Street
Ottawa, Ontario K2P 0M8

and

Mike Jacobs
Ontario Hydro
777 Bay Street, C25-E6
Toronto, Ontario M5G 1X6

COMPARISON OF AIRTIGHTNESS, INDOOR AIR QUALITY AND POWER CONSUMPTION BEFORE AND AFTER AIR-SEALING OF HIGH-RISE RESIDENTIAL BUILDINGS

SYNOPSIS

Air infiltration and ventilation has a profound influence on both the internal environment and on the energy needs of buildings. In most electrically heated high-rise residential buildings, in cold climates, during the peak winter conditions (below -18 deg C ambient temperature and above 15 km/hour wind velocity), the air infiltration component contributes to heating load by 10 to 18 W/m^2 - roughly 25 to 35% of peak heating demand. Any reduction in such uncontrolled air infiltration, without sacrificing indoor air quality, will have potential to reduce the peak heating demand. To evaluate the effectiveness of air-sealing measure, the air leakage rates through the building envelope were measured both before and after the air-sealing using the large vane-axial fan. Several air quality measurements (indoor temperatures, relative humidity, CO_2, formaldehyde, radon gas) were taken in each building to assess the practical implications of air sealing on the indoor air quality and thermal comfort.

The whole building airtightness tests showed that the air-sealing of the building envelope reduced the air leakage rate by 32% in one building and 38% in other. Energy monitoring for two buildings showed the reduction in heating demand by approximately 6 W/m^2 of floor space -- 12 to 15% due to air leakage control. Indoor air quality tests showed that the air sealing had no negative impact on the general conditions of comfort and air quality in both buildings. The field implementation of air leakage control has helped to remove some of the uncertainties and shown the potentials for conservation are indeed considerable. This paper presents the field tests and results, and suggest a procedure for the use by air-sealing practitioners to evaluate different air-sealing strategies.

1. INTRODUCTION

Concerned especially with reducing peak power demand, Ontario Hydro (the largest electric utility in Canada) is exploring various energy conservation strategies and their potentials. One way to obtain load reduction and energy efficiency is through improvements in the efficiency of electric space heating in high-rise residential buildings.

The energy audit and assessment of four high-rise residential buildings located in Ontario showed that the peak space heating demand varies from 35 to 65 W/m^2 of floor space. During peak winter conditions, the air leakage component contributes to the heating load by 10 to 18 W/m^2 - roughly 25 to 35% of the peak heating demand [Scanada 1991]. Therefore, the control of air leakage in buildings has become recognized as a key element in achieving energy conservation. Clearly, if high-rise buildings could be better air-sealed, the potentials for reductions in peak demand (plant capacity) and energy usage, and the associated costs, should be enormously attractive to building owners and the utility.

Despite the importance of the process of air leakage in high-rise buildings, it is still an aspect of building science about which there is considerable uncertainty. In part, this problem has been made difficult by the diverse range of buildings, each constructed according to widely varying construction practices. The quantification of air leakage flows is difficult due to the complexities of the flow mechanisms. It is this lack of design considerations in the building construction which has frequently resulted in higher heating consumption, and moisture and air quality problems. Clearly, good predictive design methods and demonstrations of air leakage control should assist in formulating programs relating to improve the energy efficiency of high-rise buildings. This paper describes a procedure to assess air leakage and field tests conducted to assess the effects of air-sealing on overall building airtightness, indoor air quality, and power consumption before and after air-sealing of two high-rise residential buildings.

2. PROCEDURE TO DETERMINE AIR LEAKAGE RATE

A simplified air leakage estimation procedure was developed, based primarily on equivalent air leakage area and local net pressure distribution [Scanada-1 1991]. The pressure difference at a given location depends on the infiltration driving forces (stack, wind and mechanical ventilation) and the characteristics of the opening in the building envelope. A simplified network of air-flow paths can be established using the following information: climate and exposure, building types, building form, building dimensions, surface to volume ratios, shafts, and envelope types, windows and doors, envelope crack lengths, openings, and make-up air strategies. The algebraic sum of air-flow through these paths must always be equal to zero. By applying the mass balance equation, the component of air infiltration which would be occurring during the peak winter condition can be determined. This air-flow rate is responsible for the space heating load due to uncontrolled infiltration. Any reduction in this infiltration flow should decrease the heating requirements for the building. The procedure has been simplified and developed into a practical application tool which will be utilized by assessors and air leakage control contractors.

The leakage paths on the exterior building envelope and shafts are classified as following:

- the basement floor plus ground floor [A_G],
- typical floor [A_T], and
- top floor and penthouse [A_R].

Assuming that there is a neutral zone at the m^{th} floor as shown in Figure 1, the infiltration rate Q_i and exfiltration rate Q_o through the exterior wall can be expressed as the following with the inner/outer pressure differential ΔP (Pa) and leakage area A (m^2):

$$Q_i = A_G\sqrt{(2|\Delta P_G|/\rho)} + \sum_{j=2}^{M-1} A_{Tj}\sqrt{2|\Delta P_j|/\rho)} \qquad (1)$$

and

$$Q_o = \sum_{j=M}^{N} A_{Tj}\sqrt{2|\Delta P_j|/\rho)} + A_R\sqrt{(2|\Delta P_R|/\rho)} \qquad (2)$$

The airflow balance is

$$Q_i = Q_o \qquad (3)$$

where, Q = Airflow rate, m^3/s *i* - in-flow, *o* - out-flow
A = leakage area, m^2
ρ = air density, kg/m^3
ΔP = pressure difference across building envelope, Pa

The solution to the above three equations can be obtained using the following steps:

1. Determine the leakage paths at each floor and assign the leakage class (visual inspection, thermography, and simple tests...)
2. Establish the stack pressure, wind pressure and pressure due to mechanical ventilation and determine the net indoor/outdoor pressure difference (ΔP) at each floor.
3. Calculate the air flows at each floor level using the above equations by assuming first that the neutral pressure plane (NPP) occurs at the mid height of the building.
4. Equate the air inflow and outflow ($Q_i = Q_o$). If inflow is greater than outflow, then move the NPP one floor below and repeat the calculations as in Step 3. If the inflow

is lower than the outflow, then assume the NPP one floor above and repeat the calculations. These steps should be repeated until at least three percent difference between inflow (Q_i) and outflow (Q_o) is obtained.

5. The air inflow (Q_i) to the building is the uncontrolled air infiltration. Reduction in this component will result in reducing the peak heating demand and energy consumption.

Based on the above method of determining air leakage rate, a field inspection procedure was developed to assess the potential reductions in peak heating demand [Scanada-2 1991]. The air leakage assessment procedure addresses four concerns: (1) What is the air leakage in the building? (2) How much reduction in peak demand is possible with air leakage control? (3) What will be the air sealing priorities and effectiveness for achieving maximum ratio of reduction in kW to the air sealing costs? and (4) How tight can buildings be and still supply adequate ventilation and maintain indoor air quality? Figure 5 shows the algorithm of the assessment procedure.

3. FIELD DEMONSTRATION AND RESULTS

Two buildings were selected for the demonstration of air leakage control. The following tests were conducted to characterize these buildings before and after the air-sealing work: (i) visual inspection and assessment of air leakage paths, (ii) whole building airtightness tests, (iii) indoor air quality, and (iv) monitoring of energy and power consumption. The buildings are as follows:

Building A: It is a fairly well maintained 21-storey apartment tower located in Ottawa in an open and flat terrain. Its 240 suites are fully occupied. The total heated floor space is 14,290 m^2 and the heated volume is 43,515 m^3. The exposed building envelope area is 7,470 m^2. A detailed energy audit of the building showed that the average annual space heating energy consumption was 105 kWh/m^2/year. The peak space heating demand during the winter months was 42 W/m^2. Ottawa has 4,634 heating degree days and the winter design temperature of -23 °C and wind speed of 12.5 m/s.

Building B: It is a ten-storey apartment building located in a suburban of Toronto. Its 95 suites are fully occupied. The total heated floor space is 9,825 m^2 and volume is 25,455 m^3. A detailed energy audit showed that the average annual space heating energy consumption was 98.6 kWh/m^2/year. The peak space heating demand during the winter months was 46 W/m^2. Toronto has 3646 heating degree days and the winter design temperature is -18 °C and wind speed of 11.5 m/s.

3.1 Estimation of Potential for Air Leakage Control

The air leakage assessment procedure was used to determine the potential for air leakage control in these buildings. The field inspection showed that the total leakage area in the Building A was 2.72 m^2. The air leakage rate at the peak winter conditions was calculated using the above Equations 1, 2 and 3. Figure 2 shows the air leakage rates at the peak winter design condition. The air leakage rate in Building A was 5,990 L/s, resulting in a heating demand of 265 kW - approximately 42% of peak space heating load. By assuming that the air sealing can reduce the uncontrolled air leakage by 32%, the resulting in peak heating demand would be approximately 92 kW. Similar approach was used to assess the Building B. The air leakage control could potentially reduce the peak demand by approximately 33 kW in the Building B.

3.2 Airtightness Tests

A test procedure "*Establishing the Protocols for Measuring Air Leakage and Air Flow Patterns in High-Rise Apartment Buildings*" was used to conduct the whole airtightness tests in both buildings [Magee and Shaw 1990].

Building A: A large axial vane fan with maximum capacity of 23,600 L/s was used to depressurize the building. The fan inlet was connected by 12 m of 0.9 m diameter ducting to a plywood panel temporarily installed in the double doors. Airflow rates were measured upstream of the fan intake using a pair of total averaging tubes. Flow rates are accurate within 5% of the measured values. As shown in Figure 3, this building had a net uncontrolled air leakage rate of 4,740 L/s at 10 Pa pressure difference before air-sealing retrofit. The second test conducted after the air-sealing retrofit showed that the air leakage rate reduced to 3,220 L/s at 10 Pa pressure difference. As shown in Figure 4, the improvement in airtightness was 32% after air-sealing.

Building B: The airtightness results showed that the air leakage rate was 1,885 L/s at 7 Pa pressure difference before air-sealing retrofit. The air-sealing of the building envelope reduced the air leakage rate to 1,165 L/s at 7 Pa pressure difference. The improvement in airtightness was 38% after the air-sealing.

3.3 Indoor Air Quality

Air quality in residential buildings is an area of great concern. With the trend to conserve energy, the effects on air quality should be evaluated to avoid potential health problems which may result from the drastic reduction in air change. Therefore, during this study, air quality tests to monitor the effects of air sealing work were done before and after the air sealing using a test protocol developed by CMHC [CMHC 1990]. The following air quality indicators were chosen for these buildings: formaldehyde, radon, carbon dioxide, relative humidity and indoor temperature. In the Building B, carbon monoxide samples were taken at the ground and underground parking level.

Formaldehyde: The formaldehyde readings did increase slightly in some apartments while remained relatively same in other apartments. However, the upper levels of formaldehyde concentration were well below acceptable limit of 0.1 ppm for residential occupancies.

Radon: Radon samples were taken at the basement, ground and first floor levels. There was not any significant change in the radon level after the air sealing retrofit. The maximum level recorded in these buildings was 20 Bq/m^3 (0.54 pCi/L) which is well below the acceptable level of 148 Bq/m^3 (4 pCi/L).

Carbon Dioxide: The carbon dioxide levels either remained the same or increased in some apartments after the air sealing. However, the upper levels of CO_2 were less than 1000 ppm.

Relative Humidity: The relative humidity levels increased in the lower floor apartments and decreased in the upper storeys. The average RH was at 29% before and 32% after air sealing. The measured data RH readings were within the human comfort zone.

Carbon Monoxide: CO samples were taken at the underground parking and ground floor level at the Building B. Comparison of samples showed no significant difference. The CO levels were well below the accepted limit of 11 ppm.

In both these buildings, it was also observed that the air sealing had reduced the movement of stale odours. In fact, the sealing allowed for more consistent adjustment of air supply to the apartments. The air sealing had no negative impact on the general indoor air quality in the test buildings. Variations and divergent trends observed from apartment to apartment were quite representative of what could be expected due to occupants' lifestyle and habits.

3.4 Comparison of Energy Consumption Before and After Air Sealing

Energy consumption in both the buildings was continuously monitored at every 15 minute interval. The total electric supply to the building and the hot water loads were monitored

from the month of November 1990 to June 1991. Similar weather periods, before and after air sealing, were selected to compare the energy consumption. The analysis was performed using the hourly energy simulation program to develop appropriate correction factors to account for solar gains, weather effects and occupancy using the building description. The results are summarized as follows:

Building A: The comparison of similar weather periods showed that the difference in electric load before and after air-sealing was 64 to 84 kW depending on the ambient conditions. Using the building characteristics, and an assumed weather profile for a peak day (ambient temperature varying from -18 to -21 °C and average wind speed of 12.5 m/s) simulation was performed to predict the potential reductions in heating load. Results showed that the reduction in heating load due to air-sealing would be 85 kW on a peak day -- a reduction of 14% of the peak space heating demand. The space heating energy consumption during the heating season reduced by 12%.

Building B: The comparison of similar weather periods showed that the difference in electric load before and after air-sealing was 24 to 35 kW depending on the ambient conditions. Analyses using the building characteristics and an assumed weather profile for a peak day (ambient temperature varying from -15 to -18 °C and average wind speed of 11.5 m/s) were performed to predict the potential reductions in heating load. The reduction in heating load due to air-sealing was 38 kW on a peak day -- an 18% of the peak space heating demand. This reduction in space heating load represents 10.5% of the total electric load for the building. The energy consumption during the heating season reduced by 15%.

4. CONCLUSIONS

- Based on the successful demonstration of air-sealing work and the use of assessment procedure, it can be concluded that the air leakage control offers a potential to reduce the peak electric demand by 4 to 10 W/m^2 of floor space depending on the location and building characteristics.

- A method has been developed to determine the air leakage rate for high-rise buildings. This assessment procedure has been validated with the field demonstration of air leakage control in two high-rise buildings.

- Indoor air quality tests showed that the air sealing of the building had no negative impact on the general conditions of comfort and air quality in both buildings. In both these buildings, it was also observed that the air sealing had reduced the movement of stale odours. In fact, the sealing allowed for more consistent adjustment of air supply to the apartments.

REFERENCES

1. CMHC 1990: "*Indoor Air Quality Test Protocol for Highrise Residential Buildings*", Canada Mortgage and Housing Corporation, Ottawa, Ontario.
2. Magee R.J. and Shaw C.Y. 1990: "*Establishing the Protocols for Measuring Air Leakage and Air Flow Patterns in High-Rise Apartment Buildings*", Report prepared for Canada Mortgage and Housing Corporation, Ottawa, Ontario.
3. Scanada-1 1991: "*Development of Design Procedures and Guidelines for Reducing Electric Demand by Air Leakage Control in High-Rise Residential Buildings*", Scanada Consultants Limited. Report prepared for Ontario Hydro, Toronto, Ontario.
4. Scanada-2 1991: "*Multi-Storey Residential Buildings Weatherization Project - High-Rise Residential Weatherization: Procedure for Assessing Air Leakage and Potential Control in Electrically Heated Residential Buildings of Eight Storeys and Higher*", Scanada Consultants Limited. Report Prepared for Ontario Hydro, Toronto, Ontario.

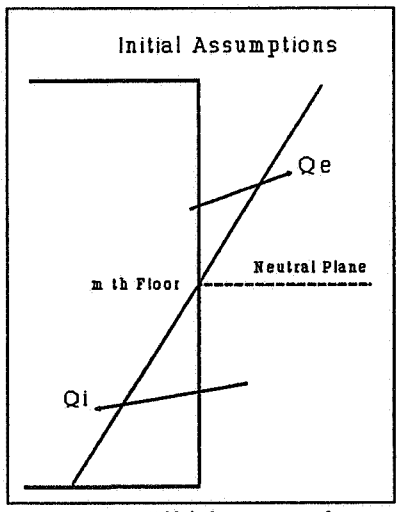

Figure 1: Initial Assumptions.

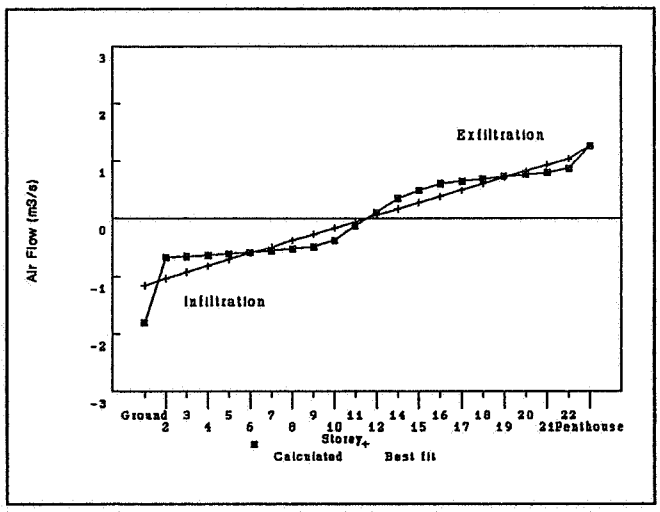

Figure 2: Estimated profile of air in-flow and out-flow at the peak winter conditions for the Building A.

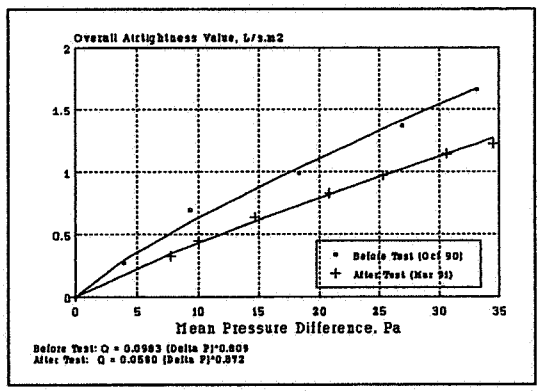

Figure 3: Effect of air-sealing on airtightness of Building A.

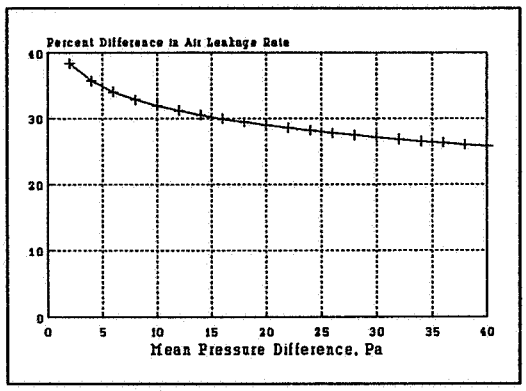

Figure 4: Difference in air leakage rate before and after air sealing of Building A.

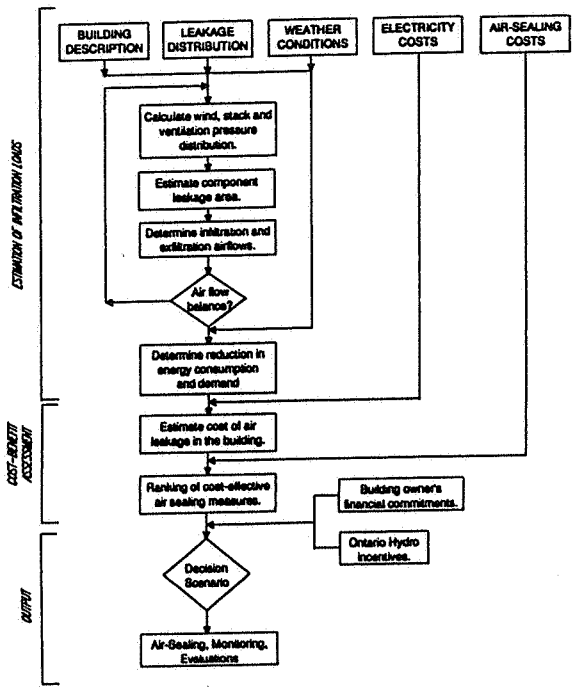

Figure 5: Procedure for Assessing Air Leakage and Potential Control in Electrically Heated Residential Buildings of Eight Storeys and Higher.

AIR MOVEMENT & VENTILATION CONTROL WITHIN BUILDINGS

12th AIVC Conference, Ottawa, Canada
24-27 September, 1991

PAPER 21

Determination of flow direction by a globe-sensor containing thermal anemometers

Prof. Dr.-Ing. F. Steimle, Dr.-Ing. U. Eser, Dipl.-Ing. S. Schädlich

Universität Essen
Angewandte Thermodynamik und Klimatechnik
Universitätsstr.15, W-4300 Essen 1, Federal Republic of Germany

Telephone 49 (0)201/183-2600
Telefax 49 (0)201/183-2584

Determination of flow direction by a globe-sensor containing thermal anemometers

Synopsis

Conventionally used thermal anemometers are able to measure velocity, but cannot determine direction. In the present study, a new kind of thermal anemometer is presented which consists of a 38mm-diameter sphere with 12 NTC resistances on its surface. Each of them is a single Constant Temperature Anemometer which takes measurements of the local heat transfer on the surface depending on the position on the ball. The calibration of this sensor is taken in 325 different directions for 6 velocities by an automatic calibration system which provides curves of the heat transfer depending on the air flow angle.

The simultaneous measurements of the 12 Constant Temperature Anemometers are compared with the data of the calibration and so the value and the angle of the air flow are determined. This sensor allows the measurement of air velocities over a range of 0.05m/s to 6m/s and of the flow angle over the entire room angle of 360^{o}. So it is possible to obtain information on the value as well as the direction of the air velocity. This new measurement method makes a contribution to a better description of indoor air flow. Using this sensor, it is also possible to check the results of computer programs simulating indoor air flow.

1. Introduction

Air temperature, air velocity and air humidity as well as the temperature of the inner room surface have an influence on the human thermal comfort. A comfortable room air conditioning especially requires low air velocities in the occupied zone to prevent complaints about draughts from the occupants. So measurements of air velocity are important for judging indoor air flow and thermal comfort.

2. Measurement technique of indoor air velocity

For measurements of air velocity a Pitot or Prandtl tube is often applied whose principle is based on the kinetic energy of the flow as a determinant of their velocity. This is practicable for higher velocities, but the measurement of indoor air velocity requires a measuring technique able to record strongly fluctuating velocities smaller than 0.3 m/s. Commonly a thermal anemometer is suited for the measurement of fluctuating gas velocities because of its short response time and its sensitivity to low velocities. A thermal anemometer consists of a heated sensor, often a NTC resistance, whose rate of heat loss is dependent on air velocity. The advantage of a thermal anemometer compared with methods based on kinetic energy is shown in Fig. 2.1 in which the heat transfer and the kinetic energy are plotted against the air velocity. It is evident that for low velocities the signal of the heat transfer is to be preferred.

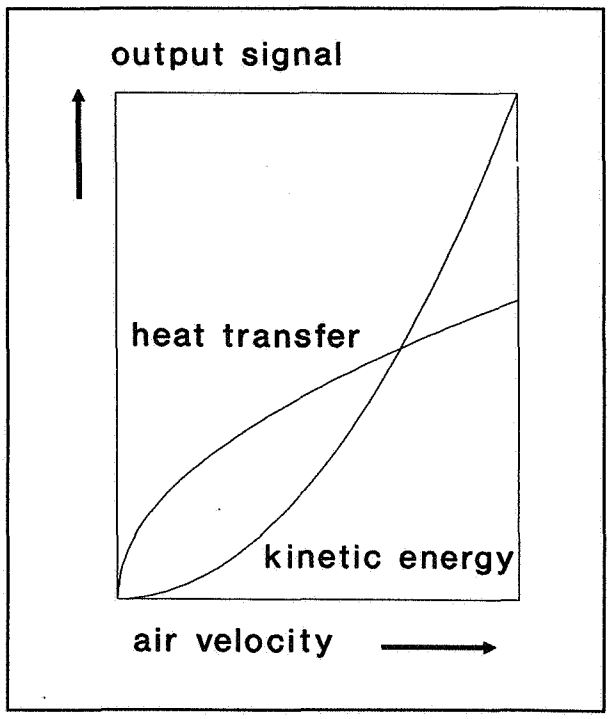

FIG. 2.1: Comparison of the measuring principle of a Prandtl tube and a thermal anemometer

For the present investigation, a Constant Temperature Anemometer is employed. For the description of air velocity, knowledge of the amount and the temporal deviation as well as the direction is essential. To obtain

information about the direction of air velocity, smoke is normally used. But this inexact method allows only a qualitative judgement of the direction.

3. New sensor

Now a new kind of thermal anemometer has been developed which consists in a 38mm diameter sphere with 12 NTC resistances on its surface. Each of them is a single Constant Temperature Anemometer which takes measurements of the local heat transfer on the surface depending on its position on the ball.

3.1. Principle of measurement (Local heat transfer on a sphere)

If a heated sphere is exposed in a flow, the rate of heat loss is strongly dependent on the air flow angle as well as on the air velocity.

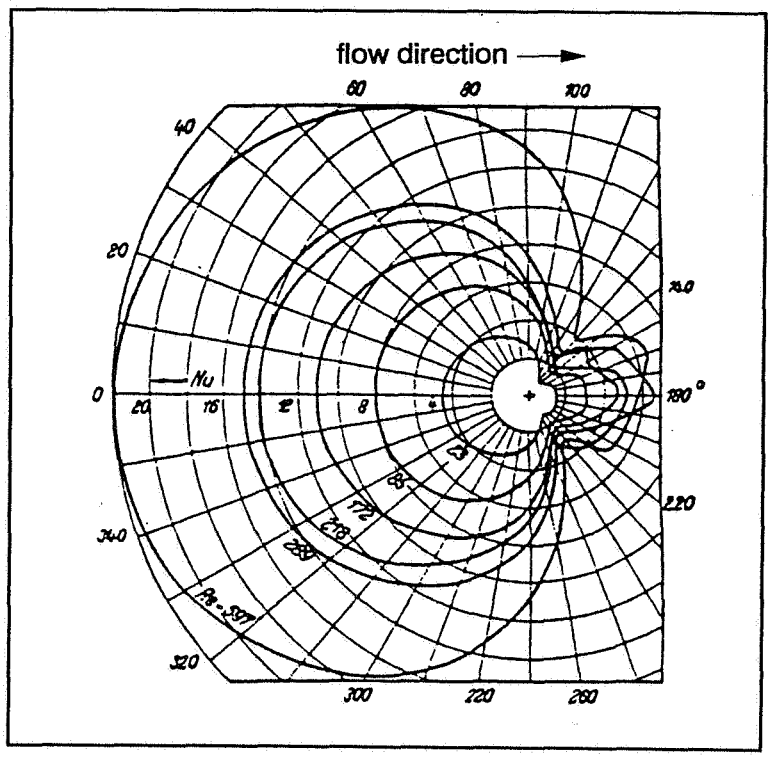

FIG. 3.1: Local heat transfer numbers for Re = 20 - 600 /2/

The heat transfer in an unstable incompressible convection flow over an axisymmetric body (sphere) has been studied by Gröber, Erk and Grigull /2/. For the presentation in Fig. 3.1 polar coordinates are used. The local heat transfer on a sphere (Nusselt number) is presented as a function of the angle between the stagnation point and the point of measurement. The local heat transfer rates are maximum at an angle of 0^{o} to 80^{o} from the stagnation point and they decrease progressively with a continuing increase in the angular position of the stagnation point because of the separation of the boundary layer from the ball. On the rear surface of the sphere, the dead water region, the Nusselt number increases again due to the highly turbulent state of flow. It becomes apparent that the difference between the Nusselt number of streamed and non streamed regions is sufficient to determine the flow direction by measurements of the local heat transfer at several points on the surface.

3.2 Construction of the sensor

The measuring device shown in Fig. 3.2 consists of a 38mm diameter sphere with 12 NTCs attached to the cover. Their electrical connections to the electronic equipment pass through a grip fixed to the ball.

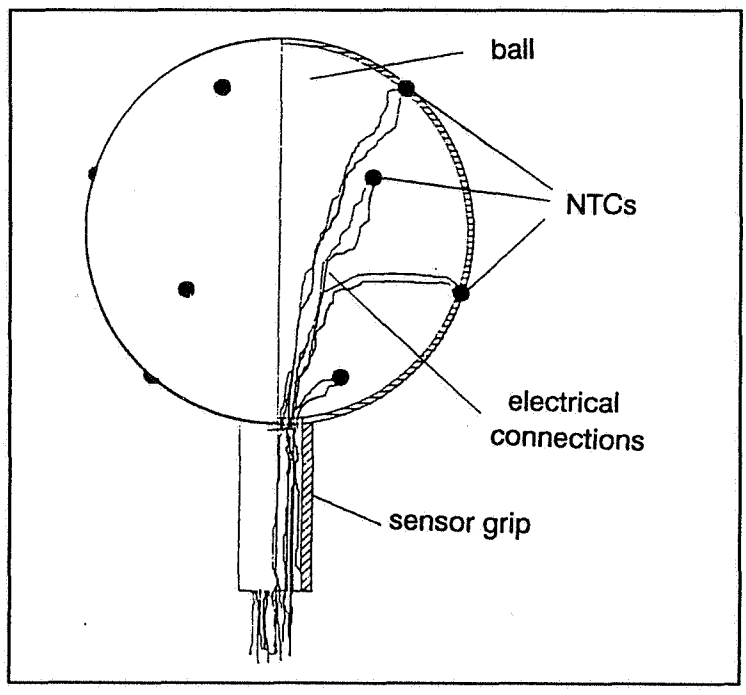

FIG. 3.2: Construction of the sensor

To limit the great influence of thermal buoyancy force especially at low velocities, the heat-up of the whole sphere is avoided. On the surface of the sensor 12 NTC-resistances are arranged at the edges of a regular polyhedron; the chosen geometry is a dodecahedron. In Fig. 3.3 the polar coordinates and the geometry are illustrated.

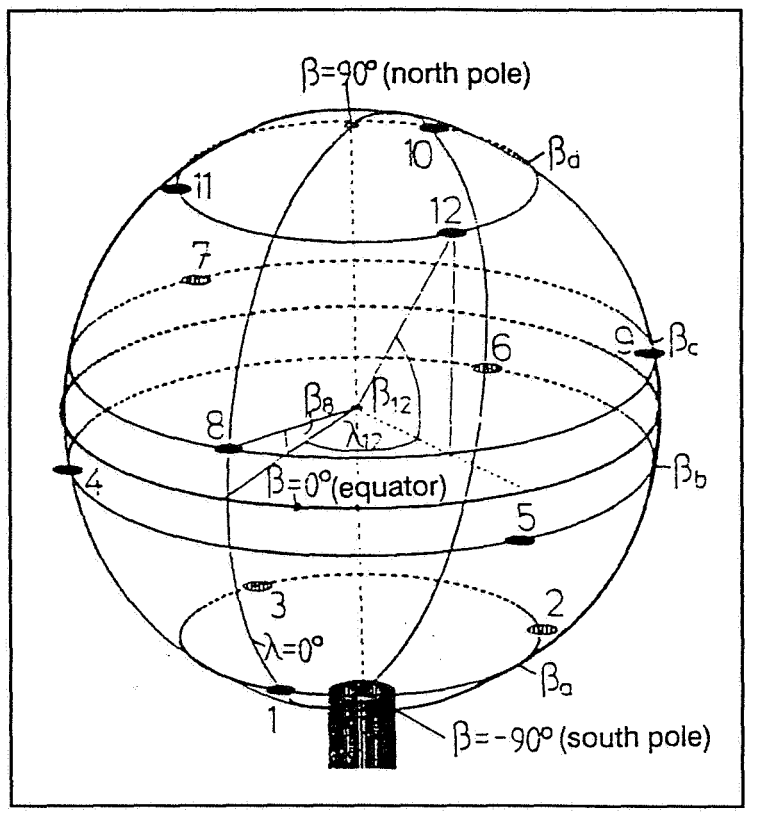

FIG. 3.3: Sensor with 12 measuring points and spatial polar coordinates

4. Calibration

In order to calculate the approach velocity and the initial direction of flow, it is necessary to know the Nusselt number over the whole surface of the sphere as a function of the air flow angle. But the theoretically precise mathematical formulation of the heat transfer problem is exceedingly difficult, so that a calibration has to be carried out.

The calibration of the sensor for the determination of flow direction also requires in addition to the variation in the air velocity, a change in the angle of attack. The air flow angle is the one between the measuring point of the local Nusselt-number and the equator (see Fig. 4.1).

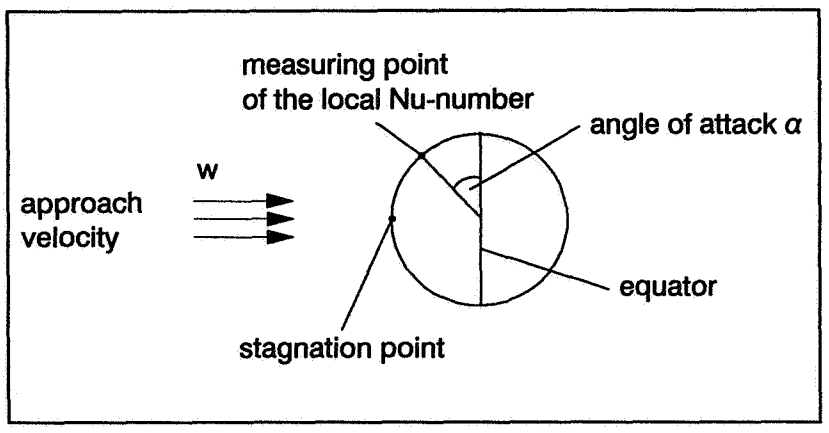

FIG. 4.1: Angle of attack

4.1 Calibration plant

The test apparatus shown in Fig. 4.2 consisted of the sensor mounted in a wooden wheel, subdivided into several chambers equipped with material. The wheel is fixed on the wall and is driven by a stepping motor, controlled by the frequency generator of a computer; this is guaranteeing a constant revolution velocity. The wheel is able to generate different air velocities from 0.05 to 6m/s. It is assumed that after a certain time the enclosed air volume in the wheel is moving with the same velocity as the wheel. The anemometer is attached to a supporting system.

This calibration technique permits in contrast to a tube flow, measurements of low velocities with low turbulence (laminar flow). Furthermore calibrations are taken in a tube flow because of the different heat transfer mechanisms in laminar and turbulent flow.

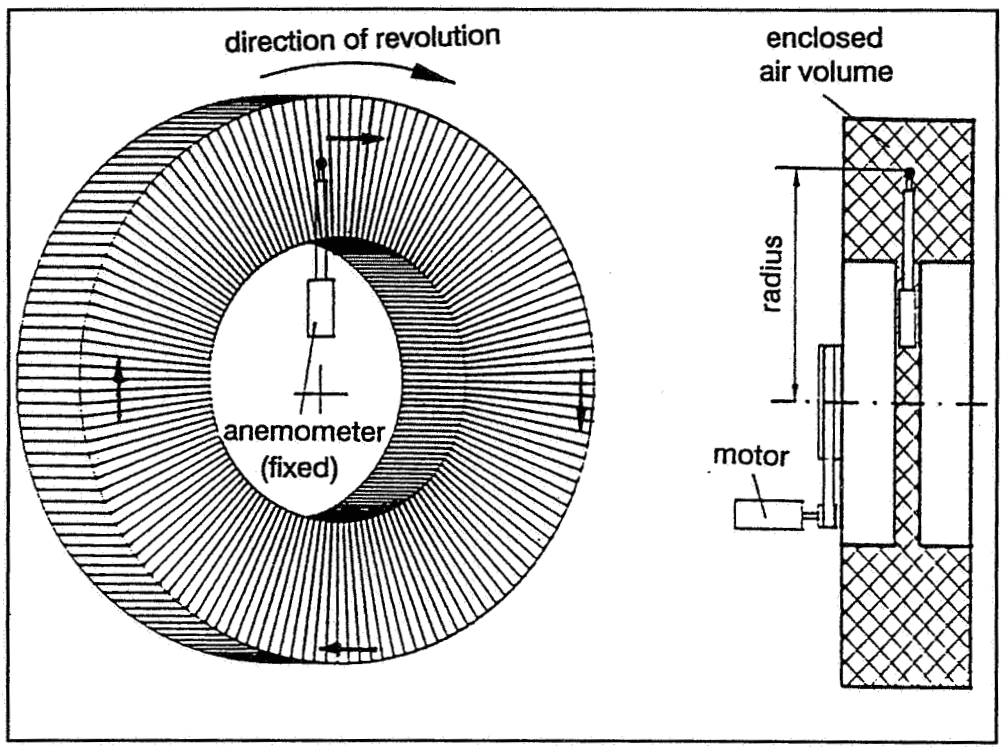

FIG. 4.2: Calibration wheel

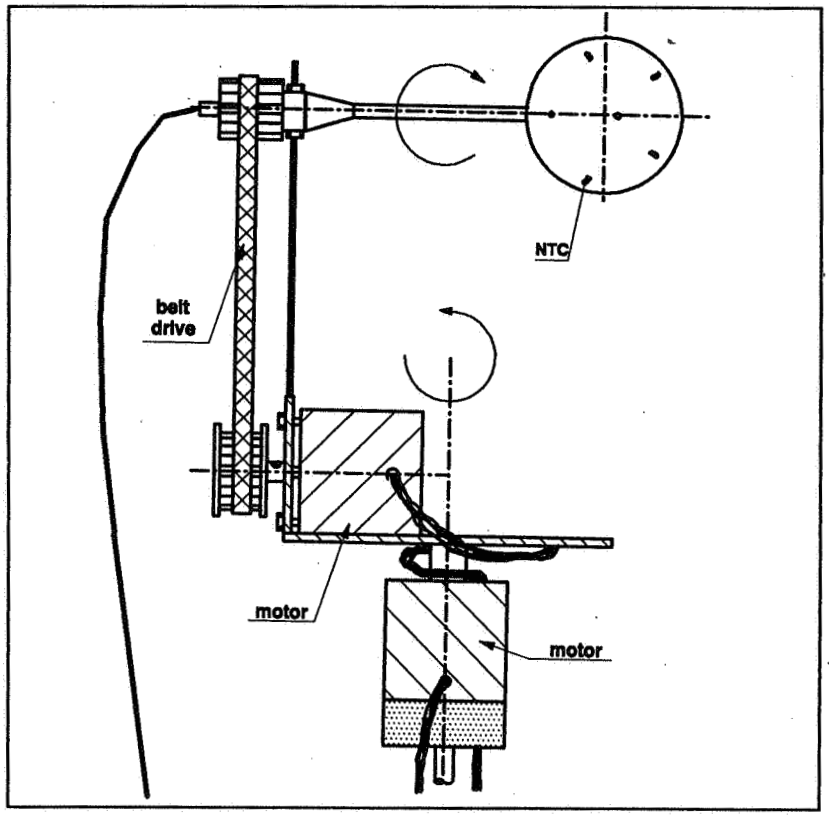

FIG. 4.3: Motion device for the sensor

The motion of the sensor over the whole room angle is carried out by two stepping motors, one for the vertical and one for the horizontal axis, as shown in Fig. 4.3.

4.2 Experimental procedure and results

To permit an exact calibration an investigation of the heat transfer rates of the 12 NTCs depending on the air flow angle and the air velocity is required. The initial conditions such as air pressure and air temperature should be the same as exist in the experimental situation. The impact of air temperature is secondary, because in the field of indoor air flow the air temperature varies only over a small range. The calibration of the sensor is taken for 325 different directions for 6 velocities over a velocity range of 0.08m/s to 5.21m/s by an automatic calibration system which also controls the stepping motors of the motion device and of the wheel. The average of the 10 measurements of air velocity and the polar coordinates are stored.

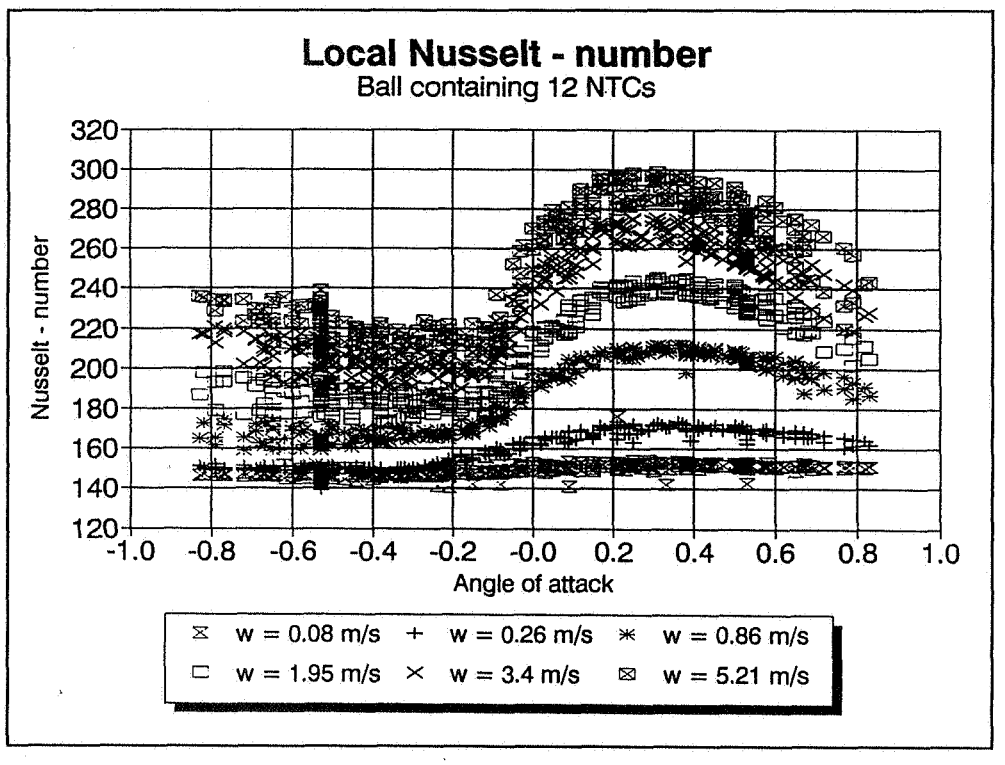

FIG. 4.4: Calibration results of the local Nusselt number for different air velocities (ball containing 12 NTCs)

Based on theoretical knowledge of the heat transfer mechanism, various equations are derived to determine the relation between the Nusselt number and air flow angle. The results obtained from the calibration as well as the curves investigated by using a numerically solved compensation theorem are represented in Fig. 4.4.

It was necessary to subdivide the data into two ranges, below and up to sin alpha = -0.2, in order to give a better agreement between the equation values and the measurements. For velocities above 0.2m/s, the difference in the Nusselt number between the luv and the lee hemisphere is so distinct that the determination of the air flow angle is guaranteed.

For lower velocities, the decay of the Nusselt number in the region of flow separation is insufficient, so that the value of 0.2m/s is taken as the limit of measurement.

5. Measurements

For the determination of the air flow direction, the sensor is placed in an air flow and the simultaneously taken measurements of the 12 Constant Temperature Anemometers are compared with the data of the calibration. Thus the value and the angle of the air flow velocity are determined.

Fig. 5.1 shows shows an illustration of this procedure: First the calibration is taken for different air velocities and air flow angles and the curves of the Nusselt number as a function of the flow angle are investigated. Then measurements in an unknown air flow are taken.

The aim is to achieve agreement by comparative analysis of the calibration and the measurement values so that the required rotation angle is a determinant for the air flow angle.

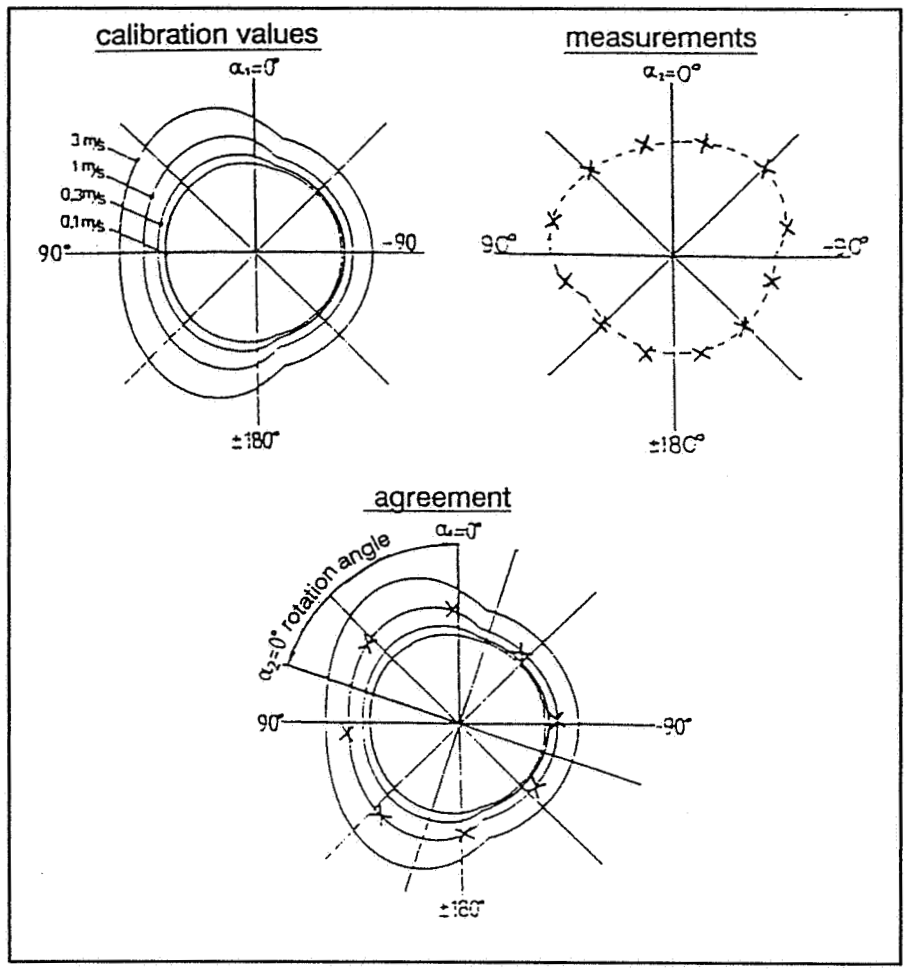

FIG. 5.1: Illustration of the determination of air flow direction

6. Summary

The aim of this investigation was the development of a thermal anemometer able to determine the air velocity over a range of 0.05m/s to 6m/s as well as the air flow angle over the entire room angle of 360^{o}. This sensor was composed of a sphere containing 12 resistances on its surface. The principle of measurement is based on a theoretical treatment and an accurate experimental investigation of the heat transfer mechanisms of a ball.

By calibration, the average Nusselt number for the heat transfer from a sphere was obtained as a function of the air flow angle for different air velocities and air flow angles. In an unknown indoor air flow, the compa-

rative analysis of calibration values and measurements permits the determination of air velocity and flow angle.

This new measurement method makes a contribution to a better description of indoor air flow.

8. References

/1/ ANDREWS, G.E., BRADLEY, D.,HUNDY, G.F.
"Hot wire anemometer calibration for measurements of small gas velocities"
Int.J.Heat Mass Transfer, 15, 1972, pp1765-1786

/2/ GRÖBER, ERK, GRIGULL
"Wärmeübertragung"
Springer Verlag, 1963

/3/ JOHANNESSEN, F.
in: Technical Review No.2, 1985, pp38-52
(Journal of Brüel & Kjaer)

/4/ PADHY, BRAHMA, PRADHAN
"A comparative assessment of fluid flow and heat transfer parameters in laminar flow around a circular cylinder and a sphere"
Wärme- und Stoffübertragung, 22, 1988

/5/ SURMA, DEVI, NATH
"Unsteady mixed convection over two-dimensional axisymmetric bodies"
Wärme- und Stoffübertragung, 22, 1988

AIR MOVEMENT & VENTILATION CONTROL WITHIN BUILDINGS

12th AIVC Conference, Ottawa, Canada
24-27 September, 1991

PAPER 22

Wind Shelter Effects on Air Infiltration for a Row of Houses

D.J. Wilson and I.S. Walker
Department of Mechanical Engineering
University of Alberta
Edmonton, Alberta T6G 2G8

Synopsis

Once the flow-pressurization characteristics of a building are known, the largest uncertainty in predicting air infiltration is the effect of wind shelter from nearby buildings. To study the effects of wind sheltering a large data set of hourly air infiltration and meteorological measurements were made for a row of test houses located on an exposed rural site. This configuration produces strong variations in wind shelter as the wind direction shifts from along the row to perpendicular to it. A simple harmonic function is proposed for interpolating between highly sheltered and unsheltered wind directions for a building. Measurements show that the effect of strong wind shelter can change air infiltration rates by a factor of four, and strongly influence pressures that determine flow rates through passive ventilation intake and exhaust points. Measurements for buildings with varying leakage distributions are correlated to determine appropriate values for wind shelter coefficients.

Introduction

Most air infiltration models average infiltration rates over all wind directions. We have found that wind direction effects are a major source of variability in infiltration rates and are of similar magnitude to the weather effects (both windspeed and temperature difference). This has serious implications for passive ventilation for indoor air quality, making it difficult to provide an adequate minimum ventilation rate without over ventilating the building for some wind directions. Because wind shelter is very difficult to estimate accurately and has a significant effect on infiltration rates, estimates of wind shelter are one of the largest sources of uncertainty in a simple infiltration model.

Some detailed wind tunnel studies of local shielding have been made, notably Wiren (1984), and Lee, Hussian, and Soliman (1979). Only regular patterns of uniform sized obstructions were used in these studies because for more complicated configurations a systematic analysis of the results of the wind tunnel tests would be difficult. In reality, the obstructions around a building are of many sizes. Sherman (1980) produced a table of shielding coefficients to classify shielding effects. The values in Table 1 from Walker and Wilson (1990) are based on those of Sherman and are applied directly to the windspeed.

Test Site Description

The Alberta Home Heating Research Facility is made up of six permanent test houses with poured concrete basements. Their construction is described in Gilpin et al. (1980). The six unoccupied test houses have been continuously monitored since 1980 for building envelope energy losses and air infiltration and ventilation rates.

The flat exposed test site is located on rural agricultural farm land, with fields planted in forage and cereal crops in summer, becoming snow covered stubble in winter. Windbreaks of mixed poplar and spruce trees cross the landscape at intervals of a few kilometres. One of these windbreak rows with 20 meter high trees is located parallel to the line of the houses about 250 m to the north, and another windbreak lies 100m to the northeast. A low tree row with 3 meter height runs perpendicular to the line of the

Table 1. Estimates of Shelter Coefficient S_{wo} for No Flue

Shelter Coefficient	Description
1.00	No obstructions or local shielding
0.90	Light local shielding with few obstructions within two house heights
0.70	Heavy shielding, many large obstructions within two house heights
0.50	Very heavy shielding, many large obstructions within one house height
0.30	Complete shielding

buildings to the southwest. The houses are totally exposed to south and east winds. Wind shelter from man-made structures is dominated by two-storey storage and machinery buildings located about 50 m to the northeast.

The houses are situated in a closely-spaced, east-west line with about 2.6 m separation between their side walls. False end walls, with a height of 3.7 m but without roof gable peaks, were constructed beside the end houses of the line to provide wind shelter and solar shading similar to that experienced by interior houses in the row. Construction dimensions are given in more detail in Wilson and Walker (1991).

In addition to having a smaller floor area, the test modules differ from a standard house in that they have no plumbing or sewer drains, and no interior partition walls except for an entryway with an open interior doorway. The absence of interior walls promotes air mixing, and allows the house to be treated as a single air exchange zone. The houses are heated electrically with a centrifugal fan distributing air through under-floor ducts to the main-floor room. The fan in the electric heater operates continuously, recirculating 4.5 house interior volumes per hour to ensure complete mixing of air infiltration with indoor air tagged with SF_6 tracer gas. Air from the upstairs outlets returns to the basement through the large open stairwell. To avoid basement air stratification, a fan intake is located near the basement floor, and another intake is close to the ceiling.

A thermostat located on the room side of the entryway wall maintained the interior temperature at 22C ± 0.5C during the heating season. In summer, the fan continues to circulate through the house, and room temperature is governed by ventilation and heat gains through the walls and windows. Summer indoor temperature rarely differs by more than ±5C from the outdoor air.

In addition to intentional passive ventilation leakage sites each house had a leakage distribution of small cracks and holes created unintentionally during construction. The major unintentional leakage sites are: the crack between the wall sill plate and the top of the concrete basement wall; vapour barrier penetrations by electrical conduits and

outlet boxes, flue pipes and plumbing vents; and cracks around the frames of windows and doors.

In addition to pressure differences of 10 Pa to 70 Pa required to meet the ASTM (1982) and CGSB (1986) fan pressurization test requirements, the pressure-flow characteristic of the house envelope was measured at low pressures of 1 Pa to 10 Pa that are typical of actual wind and stack effects. The results from over 2500 pressurization tests are summarized in Table 2, where the pressure-flow characteristic of each house has been fitted to the power law

$$Q = C(\Delta P)^n \tag{1}$$

where C is a flow coefficient dependent on leakage flow area and n is an exponent that characterizes the type of leak and ΔP is the pressure difference across the building envelope. The exponent n must lie between n = 0.5 for flow through sharp edged holes to n = 1.0 for laminar flow through long, thin, straight cracks. Because the ensemble of cracks and holes that make up a leakage distribution usually vary widely in their size and shape, the value of n lies between the limits $0.5 \leq n \leq 1.0$. Measurements for short pipes by Kreith and Eisenstadt (1957) suggest n = 0.67 for laminar flow in short cracks typical of envelope construction leakage sites. The values in Table 2 are from tests with windows closed and the flue and passive intake sealed to leave only distributed "background" leakage.

Table 2

Distributed Background Envelope Leakage from Fan Pressurization Tests With Flue and Passive Vent Intake Sealed, Windows Closed
$Q = C(\Delta P)^n$

House	PRESSURIZATION			DEPRESSURIZATION		
	Flow Coefficient C $m^3/(s \cdot Pa^n)$	Flow Exponent n	Leakage Area A_L cm^2 at 4 Pa	Flow Coefficient C $m^3/(s \cdot Pa^n)$	Flow Exponent n	Leakage Area A_L cm^2 at 4 Pa
4	0.00684	0.712	71.0	0.00592	0.742	64.1
5	0.00937	0.625	86.3	0.00970	0.661	93.6

Air Exchange Measurements

The total amount of outside air brought in by combining natural infiltration, passive ventilation, and fan exhaust was measured using a tracer gas system that injected sulphur hexafluoride, SF_6, to maintain a constant concentration in each of the test houses. The total volume of tracer gas, injected eight times each hour, is proportional to the amount of outside air that enters the house and is brought up to the 5.0 ppm setpoint. The gradual decrease of concentration in each of the 7.5 min periods between injections

was accounted for in the data analysis to determine a true hourly average concentration, typically 4.8 ppm. The calibration and operating techniques applied to the gas analyzers is described in more detail in Wilson and Walker (1991).

Measurement uncertainty was much smaller than the hour-to-hour natural variability of the air infiltration rate. An uncertainty analysis of the injection and concentration measuring systems indicated that the standard deviation in measured infiltration rate was ±2.5% of the air exchange rate, added to an absolute error of ± 0.0025 ACH. This corresponds to a measurement uncertainty standard deviation of about ±3% at typical air exchange rate of 0.3 ACH. For random variations this implies a range of about ±6% to encompass 95% of data scatter due to uncertainty.

The wind speed and direction at 10 m height was measured with low-friction cup anemometers and rotating direction vanes. Wind speeds and directions were measured at 2.5 minute intervals and averaged to produce one hour average values. Both the mean and standard deviation of these 24 readings for wind speed and direction were recorded. In addition, east and north vector components of each of the 24 readings were calculated, and stored as mean-squared averages over the hour. These mean-square values were then be used to compute the standard deviation of wind speed, and to calculate a true average wind-run direction.

Data Reduction and Normalization

To minimize stack effects, the data was sorted to include only temperature differences less than 10°C and relatively high windspeeds of 3 to 10 m/s. The ventilation rates are normalized by dividing by U^{2n} to remove the variation due to windspeed, U, (where n is from fan pressurization test results, in Table 2) and then binned every 30° of wind direction (θ). The final normalization is performed by dividing by the average ventilation rate for winds from the south (θ = 180° ± 15°). This is done because the building has no shelter from winds from the south and the shielding factor for southerly winds will be unity. There is a relationship between the shielding factor, S_w, and the normalized air exchange rate, Q_{normal} as follows:

$$Q_{normal} = S_w^{2n} \tag{2}$$

Wind Shelter Effects for a House with Uniform Leakage Distribution

When wind shelter effects on test house #5 with a 0.15 m I.D. flue were examined by Wilson and Dale (1985) they found very little variation of ventilation rate with wind angle. Figure 1 shows data for this house configuration in both unbinned and binned form. The unbinned data shows the large number (975) of data points used, their uneven distribution with wind angle and the scatter present in the data. To reduce these effects and to make for clearer data analysis the binned data is also shown, where the central square is the mean value and the error bars are ± one standard deviation for each bin. Figure 1 shows that the shelter of the row of buildings only changes the ventilation rates by less than 17%. This small effect of changing wind shelter is due mainly to the large flue (about 60% of total leakage) that is unsheltered from wind effects.

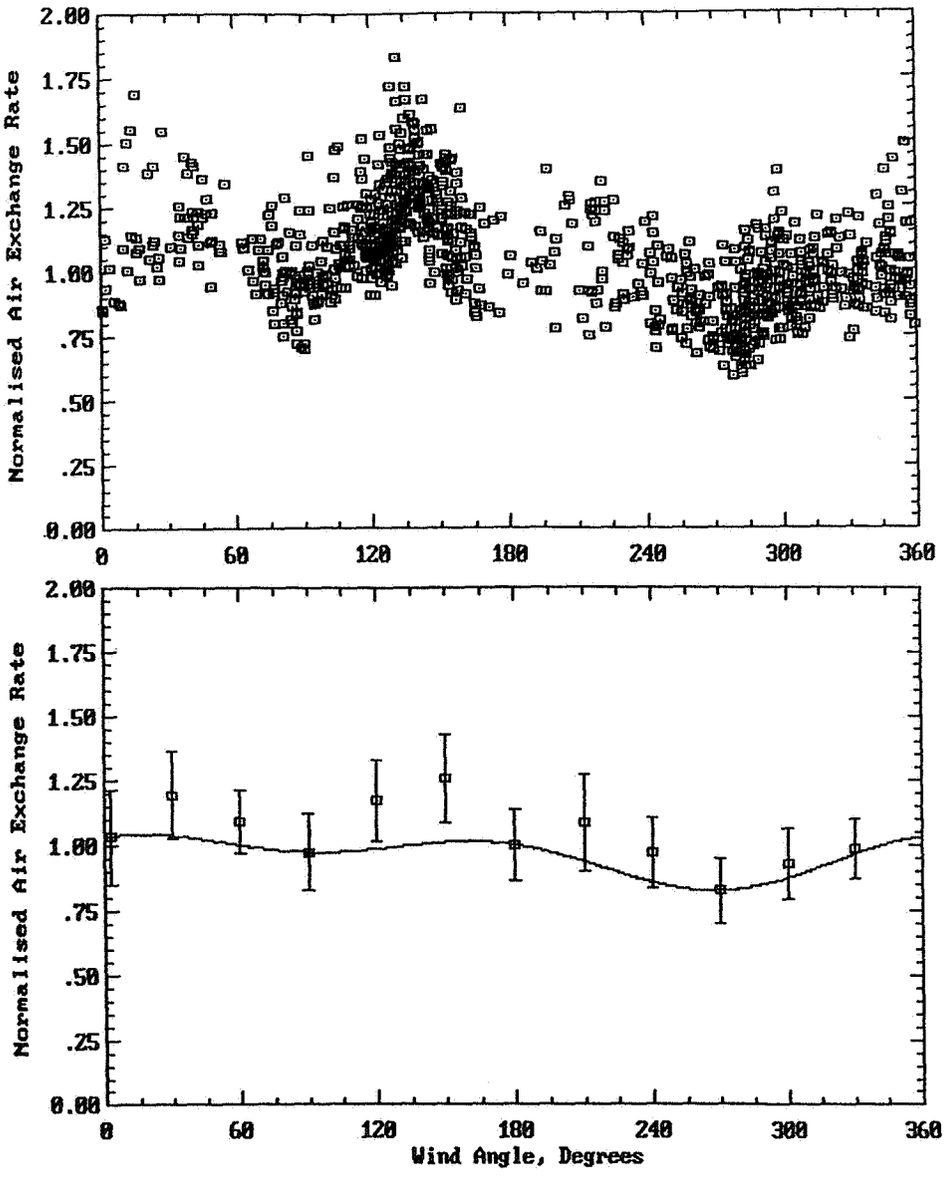

Figure 1. Measured wind shelter for House #5 with an open 0.15 m I.D. flue (975 hours)

The line shown in all the figures is generated by an empirical equation for estimating S_w as a function of wind angle, proposed by Walker (1989), and used in the single zone air infiltration model AIM-2, Walker and Wilson, (1990):

$$S_w = \frac{1}{2}\left[(S_1+S_3)\cos^2\theta + (S_1-S_3)\cos\theta + (S_2+S_4)\sin^2\theta + (S_2-S_4)\sin\theta\right] \qquad (3)$$

where S_1 through S_4 are the S_w values for winds normal to sides 1 through 4 of the building, numbered clockwise from side 1, and θ is the wind angle measured clockwise (looking down) from the normal of side one. The shielding values for S_1, S_2, S_3 and S_4 for the theoretical lines in the figures were calculated from the measured data by averaging the normalized data in the bins at $\theta = 0°$, $\theta = 90°$, $\theta = 180°$, $\theta = 270°$, (North, East, South and West directions).

In Figure 2 the data shown is for house #5 with the flue blocked. As expected this data shows stronger sheltering with air exchange rates reduced by 23% for east winds and 34% for west winds. These correspond to a windspeed reduction factor, S_w, of 0.82 and 0.73 respectively (with n = 0.65). Note that the reduction in effective windspeed is less than the reduction in infiltration rate (see equation 2).

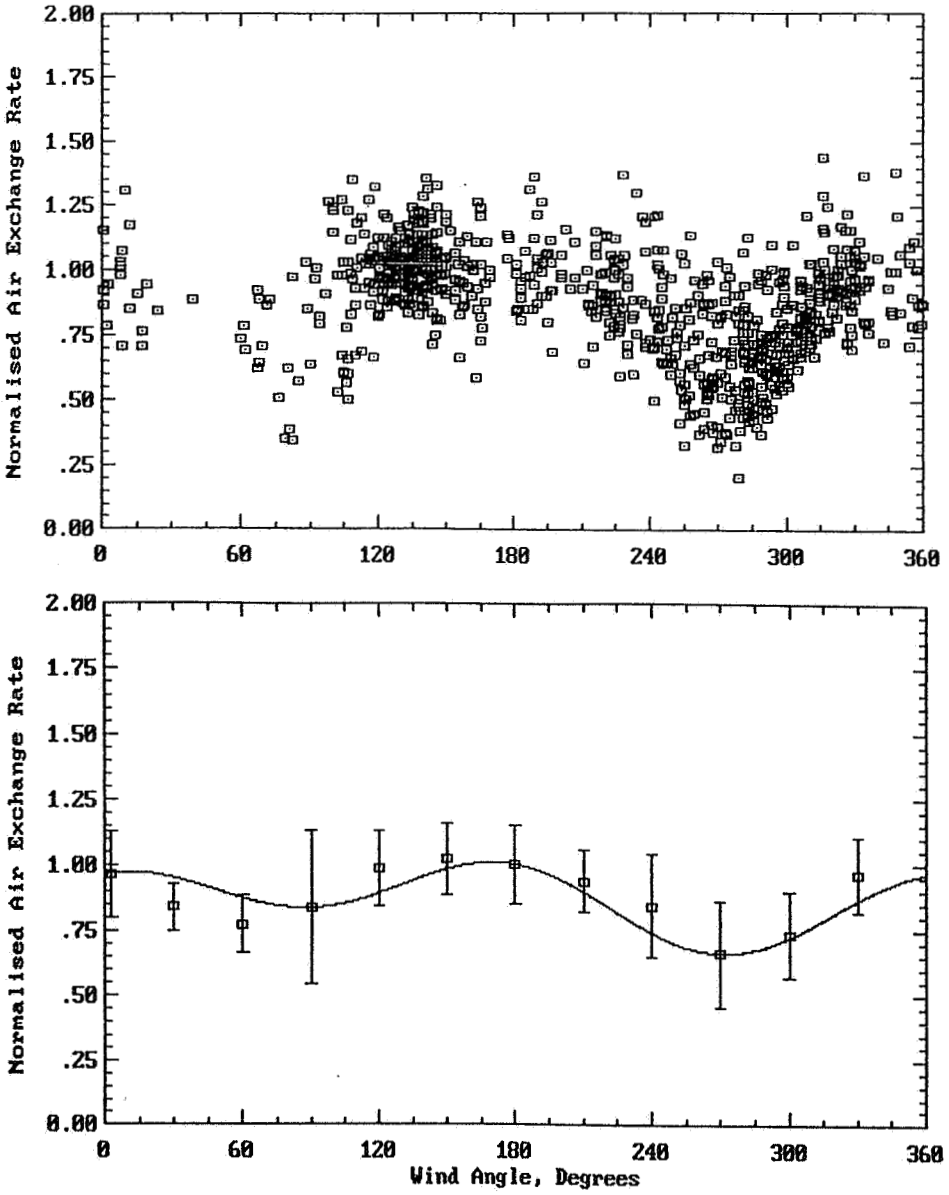

Figure 2. Measured wind shelter for House #5 with no flue (823 hours)

Effect of Varying Leakage Distribution

Most houses in rows have windows and doors concentrated on their exposed sides. House #4 has large south facing windows and is thus more typical of row house construction than house #5 with its evenly distributed leakage. Figure 3 shows how this concentration of leakage in one wall makes the ventilation rate much more sensitive to wind direction. Because most leakage is concentrated in the south-side windows, and the north wall is blank, the infiltration rate when the wind is from the north is only 41% of that for south winds.

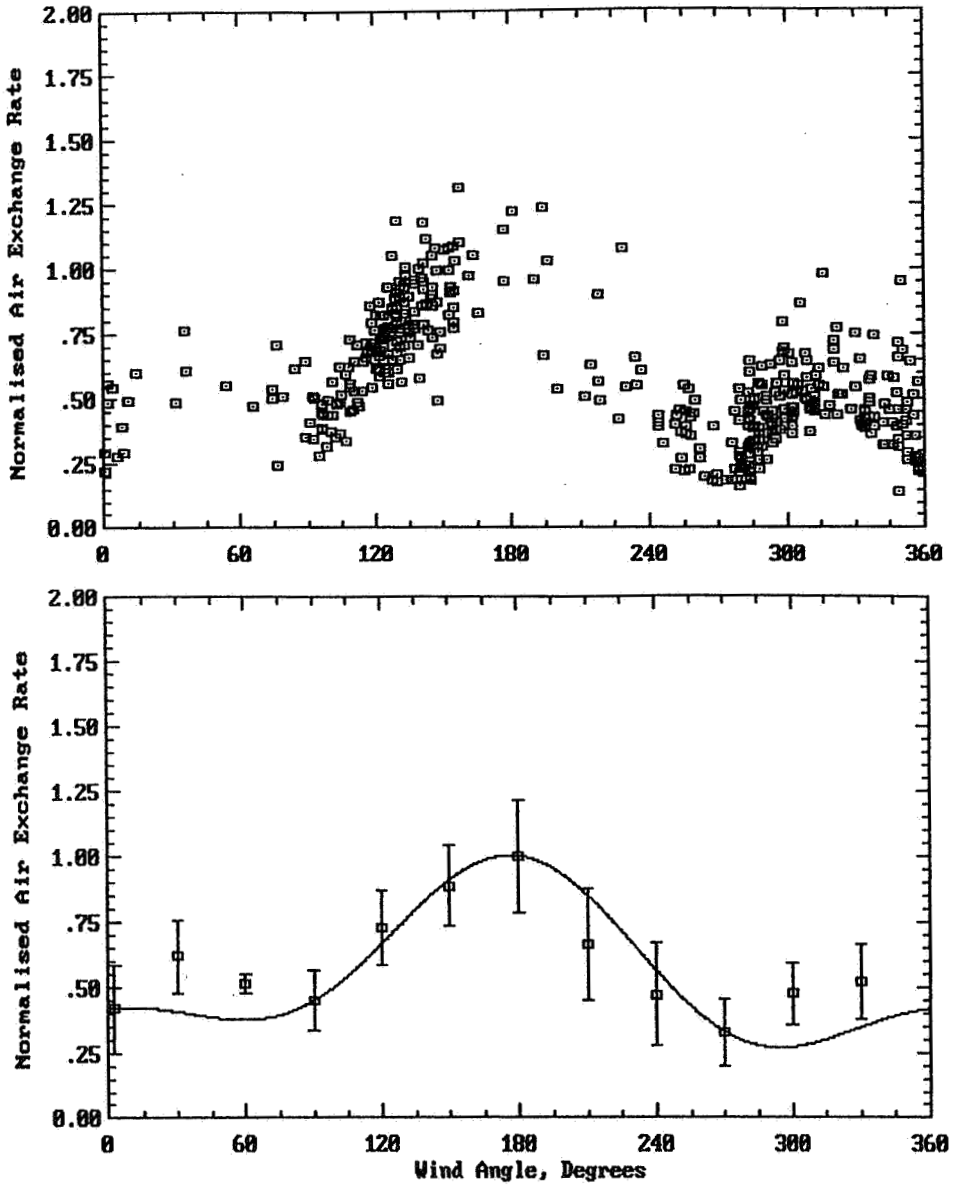

Figure 3. Measured wind shelter for House #4 with no flue (427 hours)

The effects of the row shelter are much greater than in house #5. The air exchange rates are reduced by 55% and 68% for east and west winds respectively. Thus S_w = 0.57 and 0.46, i.e. about a factor of 2 reduction in effective windspeed. A total of 427 points are shown in Figure 3. The individual points and the standard deviation bars in the binned data show that for a narrow wind angle ranges about west (270°) the air exchange rate is reduced by 80% (S_w = 0.32) indicating a factor of 5 difference between shielded and unshielded ventilation rates.

Figure 4 shows that opening a furnace flue that is about one third of the total leakage area of house #4 reduces the variation in ventilation rates to a reduction of 27% and 41% for east and west winds (S_w = 0.79 and 0.67). This is greater variation than in house #5 with the flue blocked which indicates that large influence the asymmetric leakage distribution. Warren and Webb (1980) found a similar variation in shielding effects for a house in the middle of line of common-wall row houses.

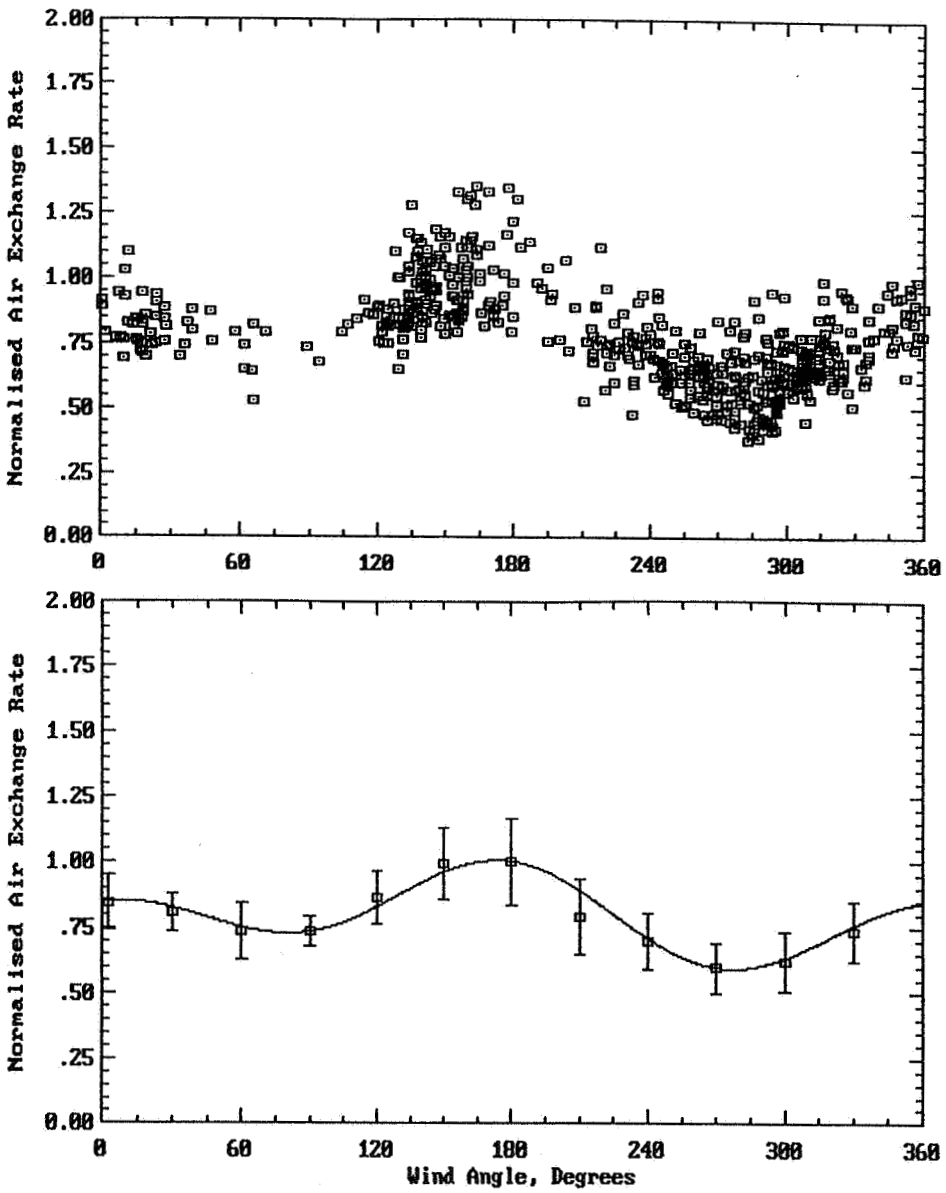

Figure 4. Measured wind shelter for House #4 with 0.075 m restriction orifice in 0.15 m I.D. flue (580 hours)

Accounting for Furnace Flue Contribution to Shelter

To find a shielding factor, S_w, that can be used to correct the windspeed used in simple infiltration models the following simple linear empirical relationship may be used. This relationship allows the flue to experience different shelter effects than the rest of the house (usually the flue is unsheltered and $S_{wf} = 1.0$).

$$S_w = (1-Y)S_{wo} + Y\,S_{wf} \qquad (4)$$

where S_{wo} = wind shielding factor for building
S_{wf} = wind shielding factor for flue
Y = fraction of total building leakage in flue

Measured values of shelter factor for a house with a flue and those calculated using equation (4) are compared in Table 3. This shows that equation (4) is a good rough approximation but does not always give adequate predictions, however it is hard to justify using a more sophisticated method, given the uncertainty in estimating building shelter.

Table 3. Furnace Flue Contribution to Shelter

House #	Wind Direction	S_w		
		No Flue Measured, S_w	With Flue Measured	With Flue Predicted
5	East	0.86	0.98	0.94
	West	0.70	0.85	0.88
4	East	0.57	0.78	0.71
	West	0.46	0.68	0.63
1	East	0.68	0.66	0.87
	West	0.48	0.64	0.79

Summary and Conclusions

A detailed set of air infiltration measurements using a constant concentration tracer gas system in a row of houses have been used to examine the variation in residential building infiltration rate with wind direction. The results of this testing give rise to the following points.

- Wind shelter can change ventilation rates by up to a factor of five for houses in a closely-spaced row.

- Changes in shelter produce changes in ventilation rates that are as important as the wind and stack driving forces.

- A simple harmonic function effectively interpolate between sheltered and unsheltered wind directions.

- Shelter is less effective in buildings with uniformly distributed leakage sites.

- An unsheltered furnace flue reduces wind shelter effects. A simple empirical relationship has been found to account for this effect.

References

ASTM Standard, "Measuring Air Leakage by the Fan Pressurization Method", Annual book of ASTM Standards, Part 18, pp. 1484-1493, 1982.

CGSB Standard 149.10 -M86, "Determination of Airtightness of Building Envelopes by the Fan Pressurization Method", Canadian General Standards Board, 1986.

GILPIN, R.R., DALE, J.D., FOREST, T.W., and ACKERMAN, M.Y., "Construction of the Alberta Home Heating Research Facility and Results from the 1979-80 Heating Season", Dept. of Mechanical Enginering Report 23, University of Alberta, 1980.

KREITH, F., and EISENSTADT, R., "Pressure Drop and Flow Characteristics of Short Capillary Tubes at Low Reynolds Numbers", ASME Trans., pp. 1070-1078, 1957.

LEE, B.E., HUSSIAN, M., and SOLIMAN, B., "A Method for the Assessment of the Wind Induced Natural Ventilation Forces Acting on Low Rise Building Arrays", Report Number BS 50, Department of Building Science, University of Sheffield, 1979.

SHERMAN, M.H., "Air Infiltration in Buildings", Ph.D. Thesis, Energy and Environment Division, Lawrence Berkeley Laboratory, University of California, 1980.

WALKER, I.S., "Single Zone Air Infiltration Modelling", M.Sc. Thesis, Dept. of Mechanical Engineering, University of Alberta, 1989.

WALKER, I.S., and WILSON, D.J., "The Alberta Air Infiltration Model AIM-2", Dept. of Mechanical Engineering Report 71, University of Alberta, 1990.

WARREN, P.R., and WEBB, B.C., "The Relationship Between Tracer Gas and Pressurization Techniques in Dwellings", Proc. First Air Infiltraiton Centre Conference, pp. 245-276, 1980.

WILSON, D.J. and DALE, J.D. "Measurement of Wind Shelter Effects on Air Infiltration", Proc. Thermal Performance of the Exterior Envelopes of Buildings, Florida, 1985.

WILSON, D.J., and WALKER, I.S., "Passive Ventilation to Maintain Indoor Air Quality", Dept. of Mechanical Engineering Report 81, University of Alberta, Edmonton, Alberta, Canada, 1991.

WIREN, B.G., "Wind Pressure Distributions and Ventilation Losses for a Single-Family House as Influenced by Surrounding Buildings - A Wind Tunnel Study", Proc. Air Infiltration Centre Wind Pressure Workshop, Brussels, Belgium, March 1984.

AIR MOVEMENT & VENTILATION CONTROL WITHIN BUILDINGS

12th AIVC Conference, Ottawa, Canada
24-27 September, 1991

PAPER 23

ASSESSING INTAKE CONTAMINATION FROM ATMOSPHERIC DISPERSION OF BUILDING EXHAUST

M D A E S Perera, R G Tull, M K White and R R Walker

Building Research Establishment
Garston, Watford,
HERTS., WD2 7JR, UNITED KINGDOM

SUMMARY

The possibility of unacceptable internal air pollution levels can cause concern at the design stage given the potential for cross contamination between building exhausts and ventilation intakes is there. The complexity of airflows around buildings, however, makes it extremely difficult to predict the contamination levels at the intake locations. This paper reports a wind tunnel technique using a model of a proposed building to determine the pollutant levels expected at various inlet locations due to the re-ingestion of noxious emissions from its two stacks.

Tests were carried out in the BRE environmental wind tunnel on a 1 in 200 scale model of the proposed building with the approach wind simulated to correspond to the flow over a suburban terrain. Two tracer gases, sulphur hexafluoride and nitrous oxide, were injected separately, and at known concentrations, from the stacks at an efflux velocity corresponding directly to that required at full scale. Tests were carried out over a range of wind directions and speeds expected to occur for over 95% of the time. Air samples were taken at various locations on the model surface through brass tubes fitted from the inside. The concentration of the sampled air was measured using infrared gas analysers and the results presented as pollutant fractions in grams of pollutant measured to a kilogram of emitted pollutant.

Comparison of the measured maximum concentration levels with those predicted from an ASHRAE procedure showed in general good agreement. However, the wind tunnel test procedure was able to provide detailed information on the contaminant levels that would be expected at these intake locations for the range of wind speeds and directions anticipated at the site.

INTRODUCTION

The possibility of unacceptable internal air pollution levels can cause concern at the design stage when there is a potential for cross contamination between building exhausts and ventilation intakes. There is a considerable body of work, notably by Wilson [1], and incorporated in the 1989 ASHRAE Fundamentals [2], which provides general guidance to the expected levels of contamination. However, by necessity, this guidance addresses 'isolated' buildings, i.e. where there is no strong and direct airflow interaction with neighbouring buildings. On occasions when interactions are expected, e.g. a building of similar height in close proximity, the complexity of airflows around buildings makes it extremely difficult to predict the levels of contamination. In such instances, wind tunnel studies can provide the nearest approximation to that expected at full scale.

This paper reports a wind tunnel study carried out on a model of a proposed 30 m high research laboratory building (Building A) to be erected in a suburban environment and adjacent (Fig. 1) to an existing laboratory building (Building B) of approximately the same height. A major part of the study was to determine distribution of fume cupboard effluent by two 4 m high stacks (Stacks I and II) on the roof of the proposed building and the resulting levels of contamination at fresh air intakes and windows in both the new and existing adjacent building. Although contamination levels were measured at 14 locations on various facades of the two buildings, measurements made in only three of these locations (Fig. 1) are described in this paper.

This paper describes the wind tunnel modelling arrangements, the testing procedure and the results obtained. The measured contaminant levels, presented as pollutant fractions in grams per kilogram, are compared with those derived from ASHRAE predictions for isolated buildings.

EXPERIMENTAL ARRANGEMENTS

Model

A 1:200 scale model of the proposed building A, the nearby existing building B and some surrounding low-rise buildings was mounted on the 1.75 m diameter turntable of the BRE environmental wind tunnel. Each of the two 4-metre high stacks consisted of 10 individual flues, each modelled by 1.5 mm internal diameter (ID) brass tubing. Apart from the flue outlets, each stack was constructed as an air-tight manifold box with a connector at the base. A 6 mm outer diameter (OD) nylon tube was attached to each of these connectors through which a mixture of air and tracer gas could be supplied (Fig. 2).

At each of the sampling locations, short lengths of 1.5 mm ID brass tubes were fitted from the inside, one end flush with the external building surface. Internally, these were individually connected (Fig. 2) to 300 mm lengths of flexible plastic tubing. These, in turn, were connected (by purpose-built push-fit brass adaptors) to 6 mm OD nylon sampling lines which were then brought together to a multiway valve connected to a sampling system (Fig. 2).

Wind tunnel modelling of the natural wind

The tests were carried out in the BRE environmental wind tunnel with a simulation for the approaching wind corresponding to a suburban terrain at a scale of 1:200. The wind simulation was generated by a bi-planar grid and a 300 mm high saw-tooth wall to start the required boundary layer, followed by a fetch of about 7 metres of 30 mm tall roughness elements (Fig. 3). Fuller details of the simulation are given in Reference 3. Tests were carried out at a 1:1 velocity scale so that air speeds measured in the wind tunnel corresponded to those at full scale.

Ratio of exhaust velocity to mean wind speed

To simulate the atmospheric dispersion of building exhausts, it is also necessary to match (equal in model and full-scale) the ratio V_E/U_H, where V_E is the exhaust velocity and U_H is the mean undisturbed upwind speed at the height of the proposed building A. During the tests, V_E was maintained at a specified full scale speed of 7 m/s.

The mean wind speed, U_H, was measured with a hot-wire anemometer in the free undisturbed flow upstream of the model at 150 mm (30 m in full scale) above the base of the wind tunnel. Tests were conducted at four wind speeds (1, 2, 4 and 8 m/s) to cover a sufficient range of ratios of efflux velocity to wind speed, excluding calm conditions. To relate these speeds to those expected at the site, meteorological wind data were obtained from the UK Meteorological Office for the weather station nearest to the site. Figure 4 summarises the essential features of this data.

For a suburban site, as for the present investigation, Penwarden and Wise [4] have shown that U_H can be related to the open-site meteorological wind speed u_{10} (measured at a height of 10 m) by,

$$U_H = u_{10}\,(0.315\,H^{0.28})$$

$$= 0.82\,u_{10} \qquad \text{for } H = 30 \text{ m}$$

Hence, the wind speed range covered during the tests correspond to a u_{10} range between 1.2 and 9.8 m/s. Figure 4 shows this covers about 95% of the range of expected wind speeds.

TEST PROCEDURE AND CONCENTRATION MEASUREMENTS

The tests involved injecting tracer gas at a known concentration from the two stacks (Fig. 2) and measuring the resulting concentrations at each sampling location. To identify the separate effect of each stack emission, two tracer gases were used. Nitrous oxide (N_2O) was emitted from Stack I located at the south-east end and sulphur hexafluoride (SF_6) from Stack II at the north-west end.

For each stack, an exhaust velocity of 7 m/s meant a flow rate of 7.4 litres/min of the air/tracer gas mixture. The uncontaminated air used in the mix was obtained from compressed air cylinders. The proportion of tracer gas used in this mix was dictated by the need:

(a) to bring its flow rate within the range of the available flow meter, and
(b) to ensure that the maximum concentration sampled at any location is within the range (0 to 200 parts per million by volume) of the infra-red gas analysers used during the tests.

Before each test, these analysers were zeroed and then calibrated using gas/air mixtures of known concentrations.

At each wind speed, contaminant concentration measurements were made at the sampling locations for winds from each of 12 principal wind directions at 30° intervals. Wind directions are given in the conventionally accepted form; 0° is wind <u>from</u> the North, 90° is wind <u>from</u> the East etc..

Taking account of the settling time required from the analysers when switched from one location to another, each measurement took approximately three to four minutes per location for any one wind speed and direction. The resulting analogue signals from the analysers were digitised and processed using an on-line analogue-to-digital convertor linked to an IBM PC. Fluctuations were smoothed out and the average concentration of each of the gases (at that location) evaluated.

Background concentration levels were also monitored throughout the tests to take account of any build-up of tracer gases within the wind tunnel. These levels were, however, found to be negligible. This is possibly because the wind tunnel being an open-jet type has no return circuit and is housed in a building which is well-vented to the outside.

RESULTS AND DISCUSSION

The measurements were noted and the ratio of sample concentration to emitted concentration calculated. This ratio, termed the pollution fraction, is expressed as grams sampled per kilogram emitted. Figure 5 shows the results plotted in a graphical form for each of the three locations.

The concentration measured at these or any other measurement location did not, on any occasion, exceed 3 g/kg (i.e. 0.3% of the emission concentration). In addition, the following salient features were observed at the three locations:

Location 1:

From both Stacks I and II, there is a relatively high level of contamination but is confined to a narrow band of wind directions between 90 and 150°N. This is due to re-entrainment of the stack exhausts to the leeward edge and face of the building. It should be noted, however, that winds from these directions occur only for about 10% of the time (Fig. 4).

Interestingly there is low contamination with a 1 m/s wind, rising to high contamination at the intermediate winds of 2 and 4 m/s and then decreasing to medium contamination at the highest 8 m/s wind. This is because at low wind speeds, the exhaust jet rises well above the building (and the wind region influenced by it) so that concentrations at the building intakes are low. At higher wind speeds, a given amount of exhaust plume is proportionately stretched out by the wind which again results in low concentrations. Between these two extremes, there is a critical wind speed, U_{crit}, at which the highest concentration (C_{max}) occurs. Other locations show similar features.

Location 2:

Emissions from Stack I for wind directions 90 and 120° show low levels at this location - otherwise levels are negligible. Since the sampling point is located approximately mid-way between Stacks I and II (Fig. 1), similar pollutant fractions - but at a higher level - occur (in a symmetrical manner) from Stack II emission for winds from 0 and 330°N. Winds come from these two directions for only about 10% of the time (Fig. 4).

Location 3:

This position (which is on the north-west face of building B) appears to be affected by emissions only for those winds blowing from 330°, i.e. when this location is directly in the lee of the two stacks. Figure 4 shows winds from this direction only for about 5% of the time. Note that pollutant fractions are higher for emissions from Stack II (which is further away from the sampling location) than Stack I and may be a result of the exhaust plume from Stack II being entrained between the two buildings.

COMPARISON WITH ASHRAE PREDICTIONS

ASHRAE [2] provides empirical equations which can be used not only to estimate the expected maximum concentration (C_{max}) levels at intakes affected by emissions from exhaust stacks but also to identify the critical wind speed, U_{crit}, at which this occurs. For an uncapped stack of height h, and which is well clear of local recirculation regions, these equations are given by,

$$C_{max} = \frac{\beta - 3.55\alpha}{[1 + 7B^{0.67}\gamma^{1.33}] \cdot \exp(12.6\alpha^2 + 3.55\alpha\beta)}$$

and

$$U_{crit} = \frac{2.9\ V_e}{B^{0.33}\ \gamma^{0.67}\ (\beta - 3.55\alpha)}$$

where $\alpha = h/S$ in which h (m) is the height of the stack above roof level and S (m) is the 'stretched string' distance between exhaust to intake measured along building surface

$$\beta = (1 + 12.6\alpha^2)^{0.5}$$

and $\gamma = S/A^{0.5}$ in which A (m^2) is the face area of the exhaust outlet.

In the above equations, B is a distance-dilution parameter. ASHRAE [2] recommends values of 0.0625 for flat-roofed buildings in low-rise surroundings when exhaust and intake locations are on the same building wall or on the roof. For roof exhausts with wall intakes, a value of about 0.2 is suggested.

Using values of V_e = 7 m/s, h = 4 m and A = 0.71 m^2, the predicted maximum levels and critical wind speeds have been calculated and tabulated below. For comparison, measured values are shown alongside. Similar comparisons, between measured and predicted, have also been made elsewhere [5].

Emission from Stack I							
Location	**Stretched -string distance**	**Measured**		**Predicted with B=0.0624**		**Predicted with B=0.2**	
	S *m*	**C_{max}** *g/kg*	**U_{crit}** *m/s*	**C_{max}** *g/kg*	**U_{crit}** *m/s*	**C_{max}** *g/kg*	**U_{crit}** *m/s*
1	30	2.3	2	2.4	7	1.1	5
2	14	0.8	all	0.7	19	0.3	13
3	42	0.9	2	2.3	5	1.0	4
Emission from Stack II							
Location	**Stretched -string distance**	**Measured**		**Predicted with B=0.0624**		**Predicted with B=0.2**	
	S *m*	**C_{max}** *g/kg*	**U_{crit}** *m/s*	**C_{max}** *g/kg*	**U_{crit}** *m/s*	**C_{max}** *g/kg*	**U_{crit}** *m/s*
1	13	2.5	> 8	0.6	21	0.3	14
2	20	2.1	> 8	1.8	12	0.8	8
3	58	2.2	2	1.9	4	0.9	3

The above comparison shows acceptable order-of-magnitude agreement between measured and predicted maximum concentration levels. With two exceptions, agreement is particularly good when the distance-dilution parameter is set at B=0.0624, i.e. when there is an implicit assumption of a clear interaction between exhaust and intake. The exceptions, an over-prediction for Location 3

(from Stack I) and an under-prediction for Location 1 (from Stack II), probably result from the airflow interactions between the two buildings.

Comparison between predicted and measured critical wind speed is not good. However, this parameter is only of limited value in any contamination assessment and therefore merits little concern.

GENERAL CONCLUSIONS

The pollutant levels expected at various inlet locations on two adjacent buildings as a result of exhaust-stack emissions was measured in a wind tunnel using a tracer gas technique. Measurements over a range of wind speeds and directions showed the variation of concentration levels with these parameters. These measurements also enabled the identification of the wind parameters that would result in maximum contaminant levels at these locations.

The measured maximum concentration levels were compared with an ASHRAE prediction procedure for the case of isolated buildings. In general there was an acceptable order-of-magnitude agreement but this improved considerably with the choice of the distance-dilution parameter used in the prediction procedure.

To summarise, in the absence of a wind tunnel test, ASHRAE procedures could be used to provide guidance as to expected maximum contaminant levels at intake locations. However, wind tunnel tests provide more detailed and accurate estimates, e.g when there is the possibility of airflow interactions with neighbouring building, or when it is necessary to consider the specific effects of local wind speeds and directions.

ACKNOWLEDGEMENTS

The methodology described in this paper was developed as a result of a specific study carried out under Building Research Establishment's (BRE) technical consultancy work and we are grateful to the Client for permission to present the generic results. The assistance of Alan Penwarden in the experimental work is also gratefully acknowledged. This paper is published by permission of the Chief Executive of BRE.

REFERENCES

1. Wilson, D J, A design procedure for estimating air intake contamination from nearby exhaust vents, ASHRAE Transactions, Vol. 89 (2), pp 136-52, (1983).

2. ASHRAE, Chapter 14: Airflow around buildings, 1989 Fundamentals Handbook (SI), ASHRAE, Atlanta, USA, (1989).

3. Perera, M D A E S, Shelter behind two dimensional solid and porous fences, Journal of Wind Engineering and Industrial Aerodynamics, Vol. 8, pp 89-104, (1981).

4. Penwarden, A D and Wise, A F E, Wind Environment Around Buildings, Building Research Establishment Report, HMSO, (1975).

5. Schuyler, G D, Comparison of wind tunnel test results with empirical exhaust dilution factors, ASHRAE Transactions, Vol 95(2), (1989).

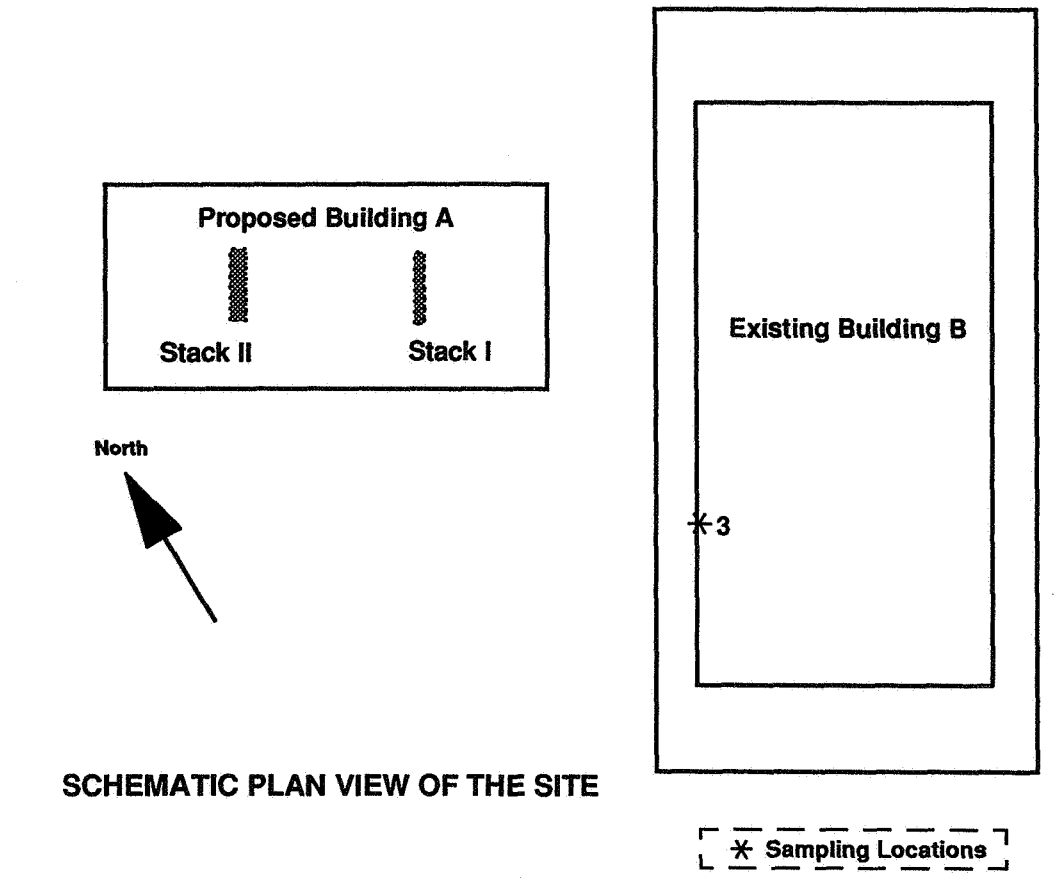

FIGURE 1 - SCHEMATIC OF BUILDINGS

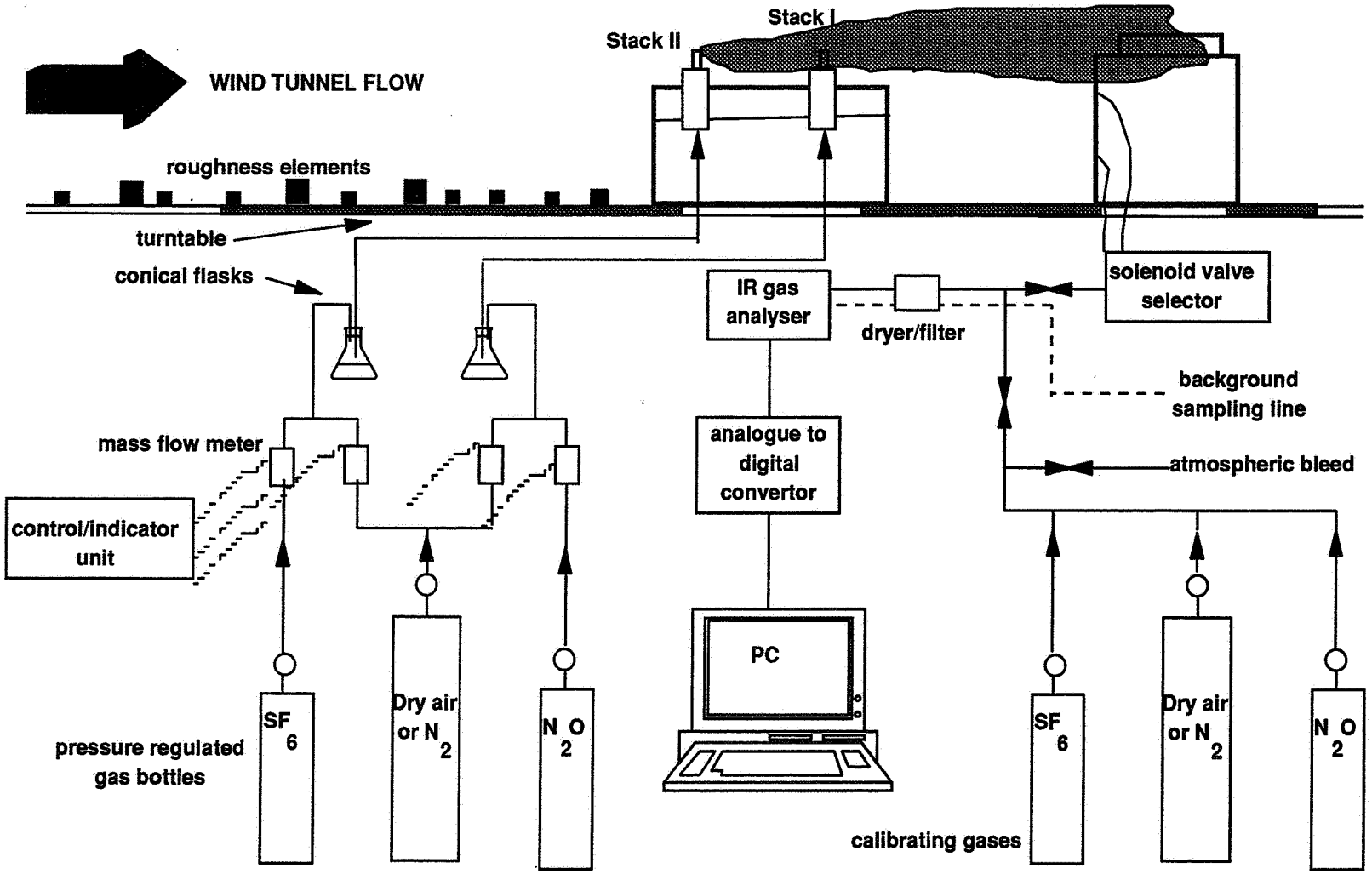

FIGURE 2 - SCHEMATIC OF GAS SUPPLY AND SAMPLING SYSTEM

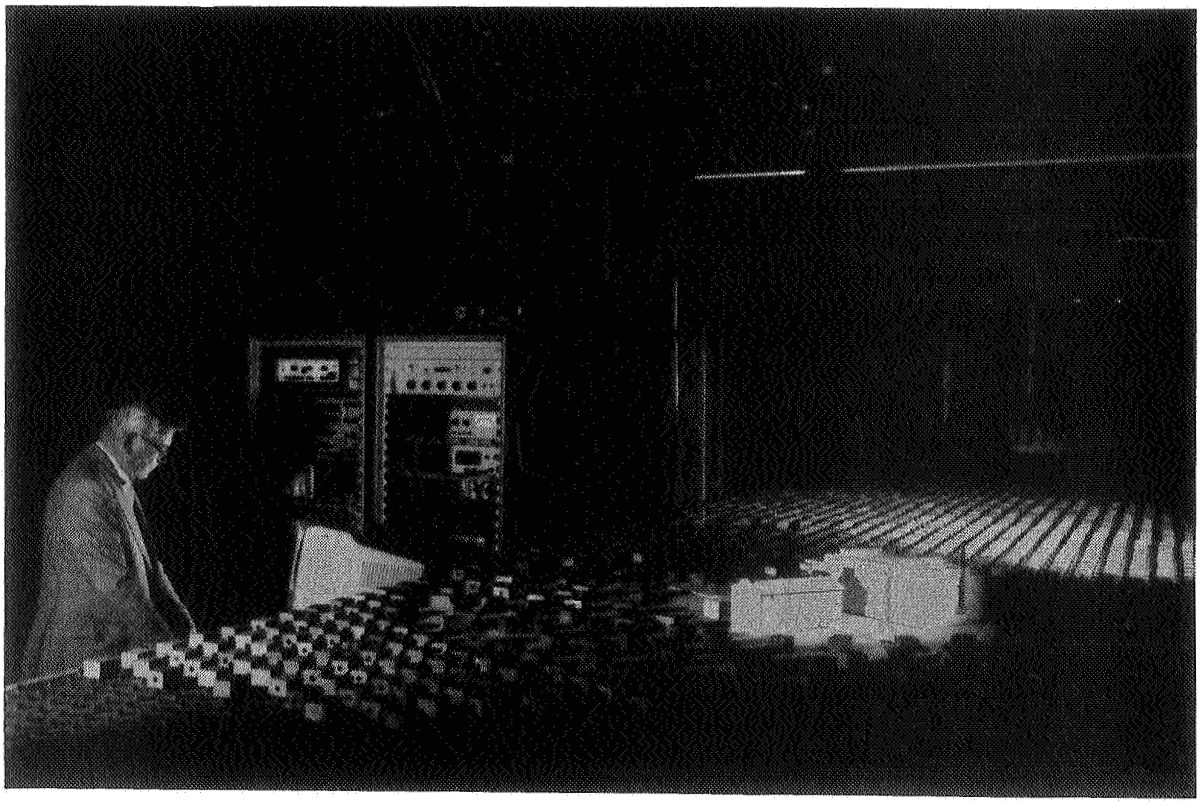

FIGURE 3 - MODEL BUILDINGS IN WIND TUNNEL

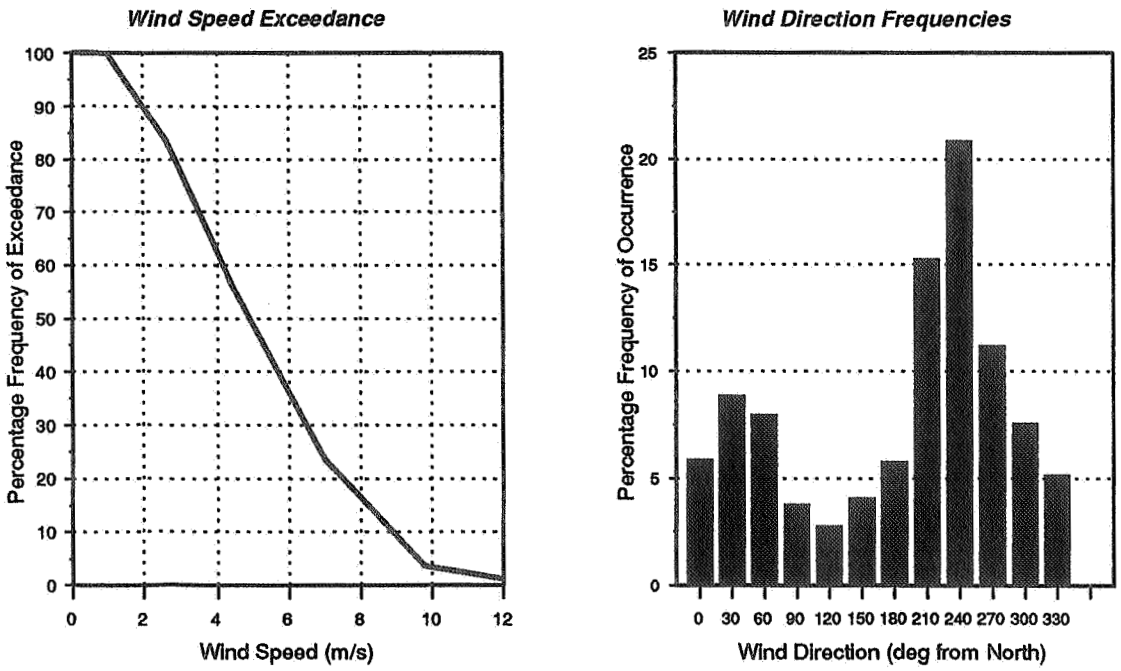

FIGURE 4 - WIND CONDITIONS AT MET. SITE

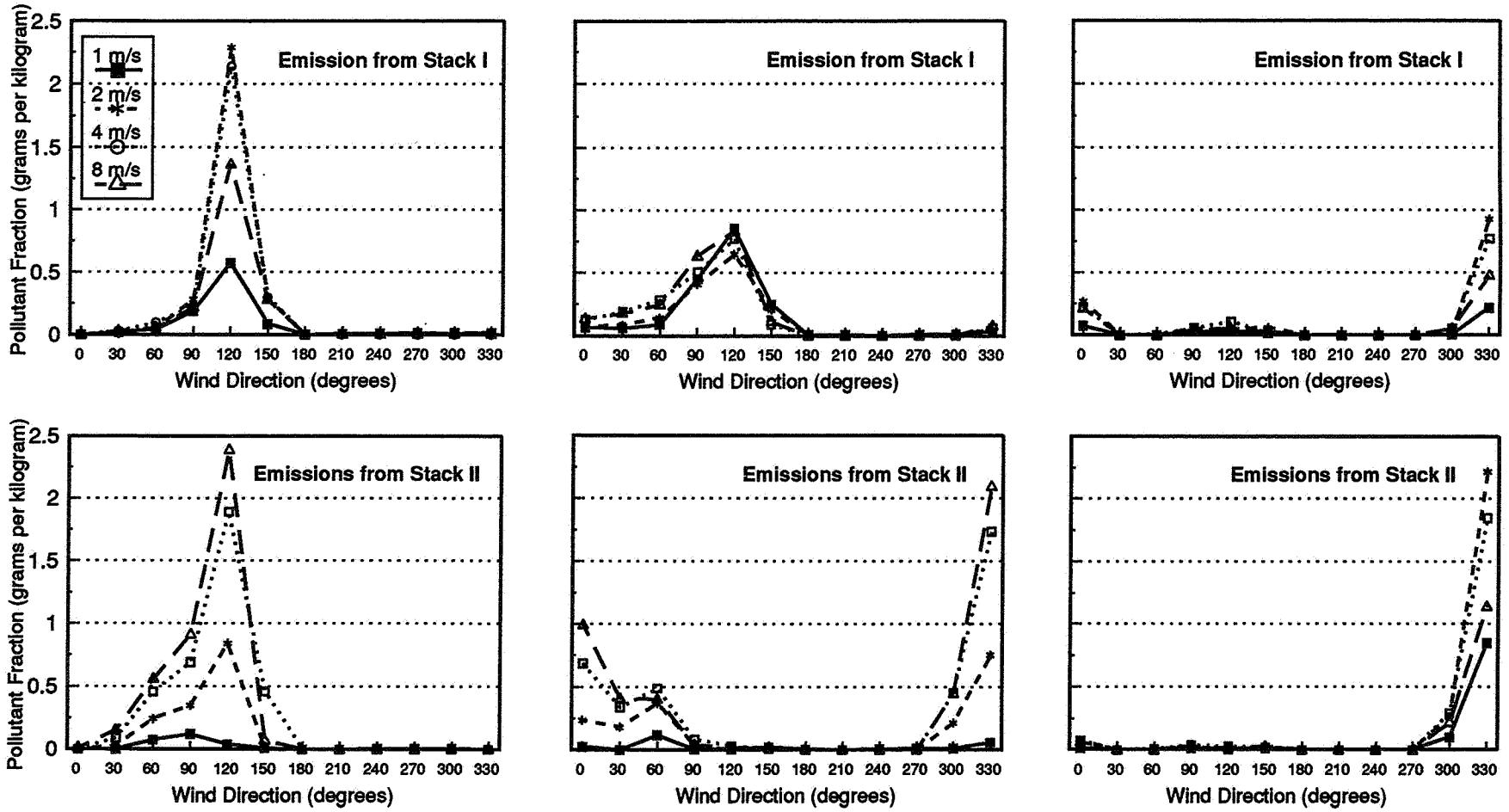

FIGURE 5 - POLLUTION FRACTIONS AT INTAKE LOCATIONS

AIR MOVEMENT & VENTILATION CONTROL WITHIN BUILDINGS

12th AIVC Conference, Ottawa, Canada
24-27 September, 1991

PAPER 24

AIRFLOW PATTERNS IN A FIVE-STOREY APARTMENT BUILDING

C.Y. Shaw, J.T. Reardon, M.N. Said and R.J. Magee

Institute for Research in Construction
National Research Council, Canada

1. SYNOPSIS

Tracer gas tests were conducted on a five-storey apartment building to determine the air and contaminant flow patterns within the building. The test method involves the injection of a small amount of tracer gas, SF_6, into a selected location to create a single source and monitoring the tracer gas concentrations at locations throughout the building. Based on the rates at which the tracer gas concentrations change at various locations, the air and contaminant flow patterns within the building can be determined. Several such tests were conducted. In each test, the tracer gas was injected into one of three locations: a garbage room on the ground floor, a party room in the basement and the supply air duct of the building's heating and ventilating system.

This paper presents the results of the tracer gas tests. It also includes measurements of the overall airtightness of the building envelope, the exterior wall airtightness values of three individual storeys, and the airtightness values of interior partitions, stairwells and floor/ceiling separations.

2. INTRODUCTION

Most high-rise apartment buildings have a central heating and ventilating system to supply outdoor air to the corridors and common areas only. Such a system is designed to pressurize the corridors and common areas of an apartment building which forces the air from the corridors into individual apartments and utility rooms. The intention is to prevent odours or contaminants generated in these areas from migrating to other areas. However, the pressures in the corridors are often inadequate for the system to function as designed. As a result, the air driven by stack action and/or wind can flow from one apartment to another and from one storey to another through corridors and vertical shafts. Non-uniform temperature distributions and odours are two common problems in high-rise apartment buildings caused by such air movement. With a renewed interest in energy conservation and a growing concern for indoor air quality, there is an increased need to understand and control such airflows.

An experimental study has been undertaken to determine the air leakage characteristics and airflow patterns of a 5-storey apartment building. The air leakage characteristics of the building envelope and its interior partitions have been discussed in another paper[1]. This paper presents the results of the airflow measurements. The objectives were to determine (a) the contaminant migration patterns from a source to other locations and (b) the outdoor air distribution through

the central heating and ventilating system. In addition, the measured airtightness values of this building's exterior envelope and interior partitions are also included, so that the data can be used to check various airflow models which have been developed for predicting such air movement[2].

3. TEST BUILDING

The five-storey masonry building was constructed in 1981 (Figure 1 and Table 1). The building has a basement, a ground floor, and four typical storeys. The basement houses a party room, a laundry room, storage areas, a transformer vault, and a mechanical room. Approximately half the ground floor is occupied by commercial tenants and is separated from the rest of the building. The garbage room is also located on the ground floor. Each typical storey (second through fifth floors) has 12 apartments - six on each side of a corridor (Figure 2). The elevator shaft, enclosed garbage chute, and electrical/service room are located at the center of the corridor. There are two stairwells, one on each end of the building. The south stairwell has a hatchway to the roof.

The building has a central heating and ventilating system that supplies air to the corridor of each storey through two supply air registers. There are no return air ducts, but there is a dampered opening in the outdoor air supply duct of the heating and ventilating system inside the basement mechanical room. Some indoor air can be drawn into the heating and ventilating system through this opening.

Each individual apartment is heated by a fan coil unit equipped with a hot water heating coil. There is no outdoor air supply to the fan coil units or to individual apartments. When the kitchen and/or bathroom exhaust fans are operated, some air is drawn into the apartment from outside and from the corridor as ventilation air.

4. TEST METHODS

Tracer gas tests were conducted to determine the air and contaminant flow patterns within the building. These tests involved the injection of a small amount of tracer gas, SF_6, into a selected location to create a source and monitoring of the tracer gas concentrations at locations throughout the building. For determining the distribution of the ventilation air, the tracer gas was injected into the building's heating and ventilating system. For monitoring the dispersion pattern of a contaminant, the tracer gas was injected into either the garbage room (a known source of

contamination) or the party room (representing an atypical apartment).

Immediately after the injection, the tracer gas concentrations at each storey were measured at 10-minute intervals. The sampling locations, shown in Figure 2, were the centre of the corridor, the south stairwell, and two apartments at each side of the corridor. The measured tracer gas concentrations at each sampling location were plotted against time to indicate the magnitude and rate at which it dispersed to other locations.

5. RESULTS AND DISCUSSION

5.1 Air Leakage Characteristics

Fan pressurization and balanced fan pressurization tests[3,4] were conducted to obtain the air leakage characteristics of the building envelope and interior partitions[1]. The results indicated that the overall airtightness value for the whole building at 50 Pa (0.2 in. of water) was 3.1 L/s·m² (0.6 cfm/ft²). The exterior wall airtightness values for individual storeys at 50 Pa (0.2 in. of water) varied from 4.0 to 5.1 L/s·m² (0.79 to 1.0 cfm/ft²). The measured airtightness values for interior partition walls and floor/ceiling separations at 50 Pa varied from 0.65 to 3.1 L/s·m² (0.13 to 0.61 cfm/ft²) and 0.18 to 0.68 L/s·m² (0.035 to 0.13 cfm/ft²), respectively. Table 2 presents the results in terms of flow coefficient, C and exponent, n as defined by the equation,

$$q = C \cdot A \cdot (\Delta P)^n \qquad (1)$$

where,

- q = airtightness value (air leakage rate), L/s
- C = flow coefficient, $L/(s \cdot m^2 \cdot Pa^n)$
- A = area of test component, m^2
- ΔP = pressure difference across the exterior wall, Pa
- n = flow exponent.

More than thirty interior partitions and floor/ceiling separations were tested; only the minimum, average and maximum airtightness values are reported in Table 2 for each of these two component types. These values were determined from the measurements using Eq.(1) with a typical flow exponent of 0.65.

5.2 Contaminant Dispersion

Figures 3 through 8 show how a contaminant, which was represented by the tracer gas, dispersed from the

ground floor garbage room (located on the east side of the building) to other areas within the building. During the test, the building's heating and ventilating system operated normally, the outdoor air temperature was 11°C, and the wind speed about 17 km/h from the southeast first and then changed to the south shortly after the tracer gas injection. The results indicate that concentrations of the tracer gas in the corridor of every floor increased rapidly, while concentrations in individual apartments increased at a slower rate. The results suggest that the contaminant (tracer gas) in the garbage room moved upwards via the garbage chute mainly due to the action of stack effect. The contaminant then dispersed into the corridors and it was subsequently carried by the airflow from the corridors into individual apartments. The effect of wind on the tracer gas concentrations in individual apartments was minimal because of the wind direction (parallel to the exterior walls of the apartments).

The test was repeated in June to minimize stack effect. During the test, the wind blew from the south at 6 km/h and the outdoor air temperature was 22°C. As an example, Figure 9 shows the concentration profiles for the 3rd floor. Similar to the winter results (Figure 6), the contaminant dispersed rapidly into the corridors and more slowly into individual apartments. However, the concentrations in individual apartments were generally lower than the winter results, suggesting a reduced stack effect. The contaminant movement was probably due to the rise of warm contaminant-laden air from the garbage room up through the chute. The garbage room tends to be much warmer than the rest of the building and outdoors because it is located at the centre of the southwest (sunny) side of the building at ground level and has no windows.

Figure 9 also shows that at certain periods of time, the tracer gas concentration in Apt.311 was greater than that in the corridor. This was probably because the kitchen or bathroom exhaust fan was in operation during this period of time. As the sampling location for this apartment was closer to the garbage chute than that the corridor sampling point, the operation of the exhaust fans could produce such a situation.

Both the winter and summer test results suggest that the capacity of the building's heating and ventilating system is inadequate to pressurize the corridors sufficiently to prevent the air in the garbage chute from entering the corridors. Any contaminant generated in the garbage room will, therefore, migrate into individual apartments via mainly the garbage chute and the corridors. The extent and rate of this migration will depend on stack action and the use of exhaust fans in the apartments.

Another series of tests with the basement party room as the source location were conducted to investigate the contaminant dispersion pattern for a source location with no direct links to other floors (e.g., a garbage chute as in the previous case). The wind blew from the northwest at 24 km/h and the outdoor air temperature was -6°C during the winter test. As shown in Figures 10, 11 and 12, the tracer gas concentration in the basement corridor increased sharply immediately after the tracer gas injection. The concentrations in the corridors of the upper floors also increased, but at a lower rate. As the main return inlet for the building's heating and ventilating system is located in the basement mechanical room, it was likely that the tracer gas migrated into the corridors of the upper floors through the building's heating and ventilating system.

The effects of wind and stack action on the tracer gas (contaminant) concentrations in individual apartments for this case are more visible than for the previous case because of the wind direction and lower outdoor air temperature. For example, the tracer gas concentration was almost zero in Apt.202 where the wind and stack action worked together to prevent the corridor air from entering. On the other hand, the tracer gas concentration in the apartment directly downstream of Apt.202 (i.e., Apt.205, across the hall) was considerably higher, because being on the leeward side the wind and stack action worked against each other. The resultant air pressure in Apt.205 was not strong enough to prevent the corridor air from entering.

5.3 Outdoor air distribution by the ventilation system

Figures 13 and 14, show the outdoor air distribution test results. The tracer gas was injected into the supply air duct of the heating and ventilating system. During the test the wind blew from the west at 24 km/h and the outdoor air temperature was -16°C. As shown, the tracer gas migrated rapidly into the corridors first and then into individual apartments. The results also show that there was a large difference in tracer gas concentration between Apt.202 (2nd floor) and Apt.502 (5th floor, directly above Apt.202). Both apartments are located on the west side of the building. At the second floor, the west wind and stack effect acted together to pressurize the apartment. The air pressure inside the apartment was, therefore, strong enough to prevent the corridor air from entering this apartment. On the other hand, at the fifth floor, the wind and stack effect worked against each other, resulting in the pressure inside the apartment being inadequate to prevent the corridor air from entering,

and causing an increase in the tracer gas concentration inside the apartment.

The results suggest that the building's heating and ventilating system is effective at distributing the outdoor air into the corridor of every floor. However, the capacity may not be adequate to overcome the effect of wind and stack action to force the corridor air into individual apartments as designed. Therefore, under certain weather conditions, the air and hence odour or contaminants in the apartments can leak into the corridor and move to other apartments via stairwells or other vertical shafts. On windy days, the air or contaminants can also move from an apartment on the windward side horizontally across the corridor to the apartments on the leeward side.

6. SUMMARY

Tracer gas tests were conducted in a five-storey apartment building to determine the air and contaminant flow patterns within the building. The results are summarized as follows:

Contaminants generated in the garbage room would migrate into the corridors via the garbage chute and its connections to the corridors. Once in the corridor, the contaminants would be carried by the corridor air to other apartments. Any means to lower the pressure in the garbage chute relative to the corridors would be helpful in preventing the contaminants migrating into individual apartments, such as a dedicated exhaust fan for the garbage room, vented directly outdoors.

The wind and stack effect could force contaminants generated in the party room or individual apartments into the corridor of the same floor. Once in the corridor, those contaminants can then be carried by the corridor air to other apartments.

The building's heating and ventilating system was effective at distributing the outdoor air into the corridor of every floor, but the capacity was inadequate to overcome the effect of wind and stack action and force the corridor air into all apartments. As a result, any contaminant generated in the apartments or utility rooms could get into the corridors. The amount would depend on wind speed and direction, stack action and the use of exhaust fans in the apartments.

7. REFERENCES

1. Shaw, C.Y., Magee, R.J. and Rousseau, J. 1991, "Overall and component airtightness values of a five-storey apartment building", ASHRAE Transactions, Vol.97, Part 2.

2. Said, M.N. 1990, "Air and smoke movement model for tall buildings", Internal Report, Institute for Research in Construction, NRC.

3. Shaw, C.Y., Gasparetto, S. and Reardon, J.T. 1990, "Method for Measuring Air Leakage in High-Rise Apartments", in STP 1067 Air Change Rate and Airtightness in Buildings, ed. M.H. Sherman, American Society for Testing and Materials, pp.222-230.

4. Reardon, J.T., Kim, A.K. and Shaw, C.Y. 1987, "Balanced Fan Depressurization Method for Measuring Component and Overall Air Leakage in Single- and Multifamily Dwellings", ASHRAE Transactions, Vol.93, Part 2, pp.137-152.

8. ACKNOWLEDGEMENTS

This was a joint project of the Canada Mortgage and Housing Corporation (CMHC) and the Institute for Research in Construction. The authors acknowledge the co-operation and financial support of CMHC, the Centretown Citizens (Ottawa) Corporation (CCOC), the tenants of the test building and the members of the CCOC Tenants Committee for their cooperation in making this study possible. Thanks are expressed particularly to Mr. J. Rousseau of CMHC and Mr. Glen Dunning and his staff at CCOC for their assistance during the tests. The authors also wish to acknowledge the contribution of L.P. Chabot and R.G. Evans in the field tests.

TABLE 1

Description of Test Building

Year Constructed:	1981
Year Tested:	1989
Height (storeys):	5
Wall Construction	
Exterior Wall:	80 mm (3 in) Face brick 25 mm (1 in) Air space 200 mm (8 in) Concrete block 38 mm (1.5 in) Rigid glass fiber insulation Metal Studs 38 mm (1.5 in) Semi-rigid glass fiber insulation Vapor Barrier 13 mm (0.5 in) Gypsum board
Internal Wall:	13 mm (0.5 in) Gypsum board 92 mm (3.5 in) Metal studs 38 mm (1.5 in) Insulation blanket 13 mm (0.5 in) Gypsum board

TABLE 2

Airtightness Values

	C $L/s \cdot m^2 \cdot Pa^n$	n
Whole Building		
Building Envelope (Overall)	0.264	0.66
Individual Storeys		
Exterior Wall		
Second Storey	0.277	0.73
Third Storey	0.486	0.61
Fourth Storey	0.506	0.60
Floor/Ceiling Separation		
First/Second Floor	0.036	0.64
Second/Third Floor	0.035	0.54
Third/Fourth Floor	0.013	0.76
Fourth/Fifth Floor	0.02	0.69
Individual Apartments		
Internal Partitions		
Minimum	0.052	0.65
Average	0.147	0.65
Maximum	0.286	0.65
Floor/Ceiling Separation		
Minimum	0.015	0.65
Average	0.032	0.65
Maximum	0.045	0.65
Stairwells		
North	0.492	0.5
South	0.755	0.53

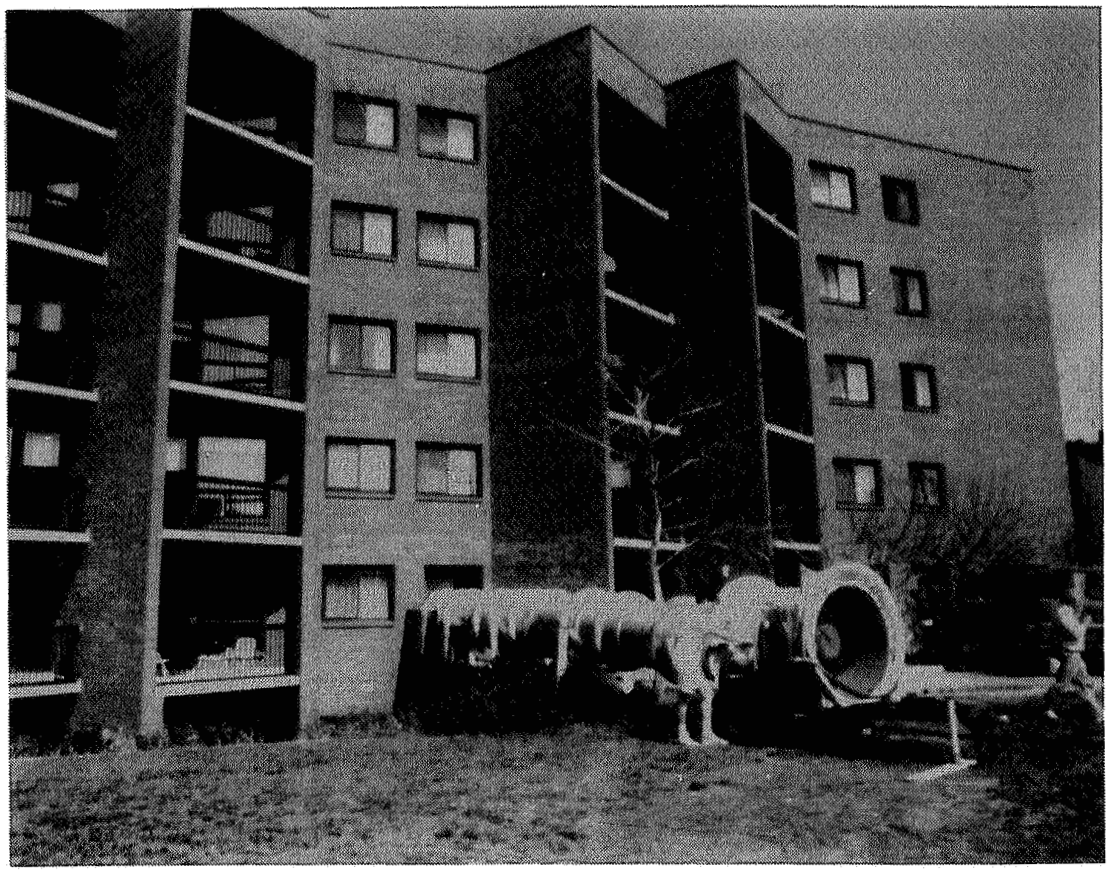

Figure 1 Test Building

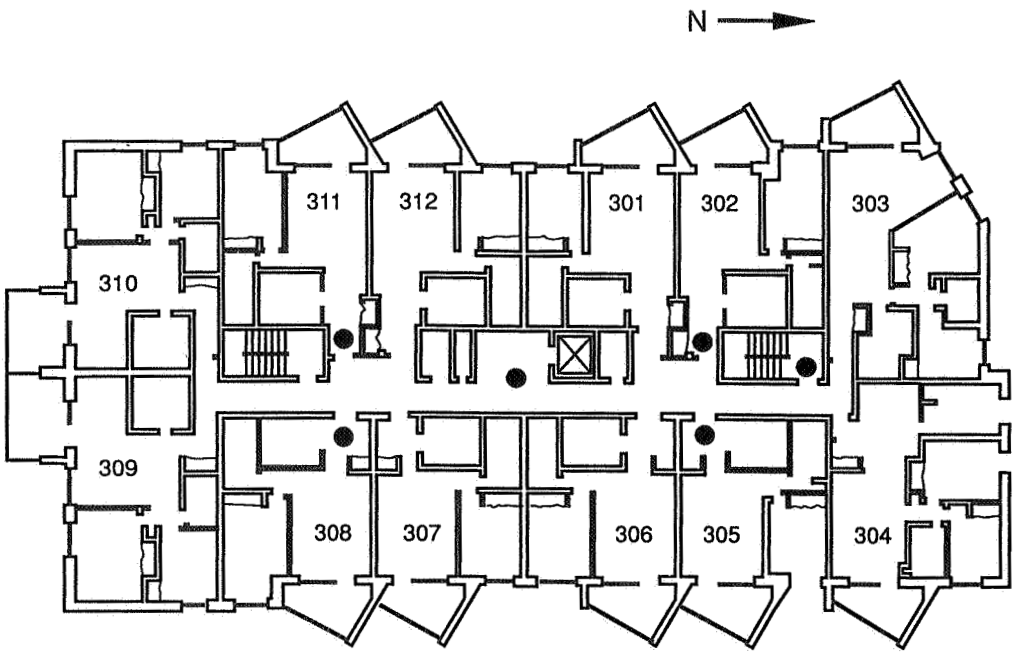

Figure 2

Floor plan of a typical floor showing tracer gas sampling locations.

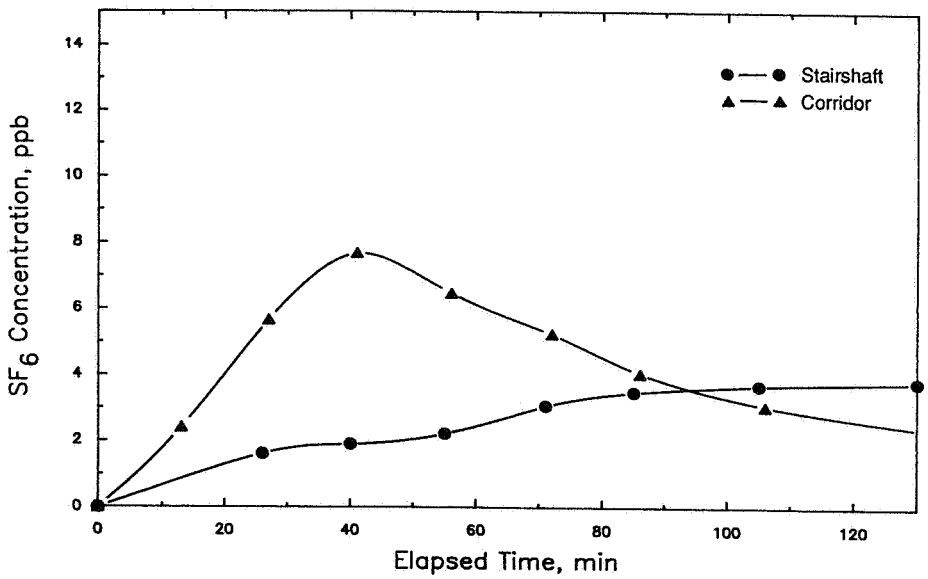

Figure 3

Contaminant dispersion patterns for the basement with the ground floor garbage room as the source location; winter conditions.

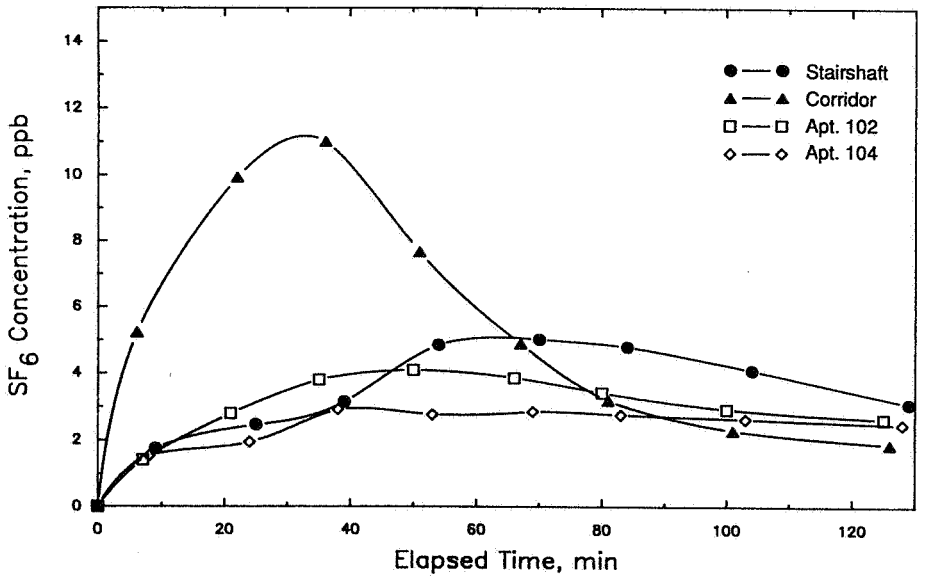

Figure 4

Contaminant dispersion patterns for the first floor with the ground floor garbage room as the source location; winter conditions.

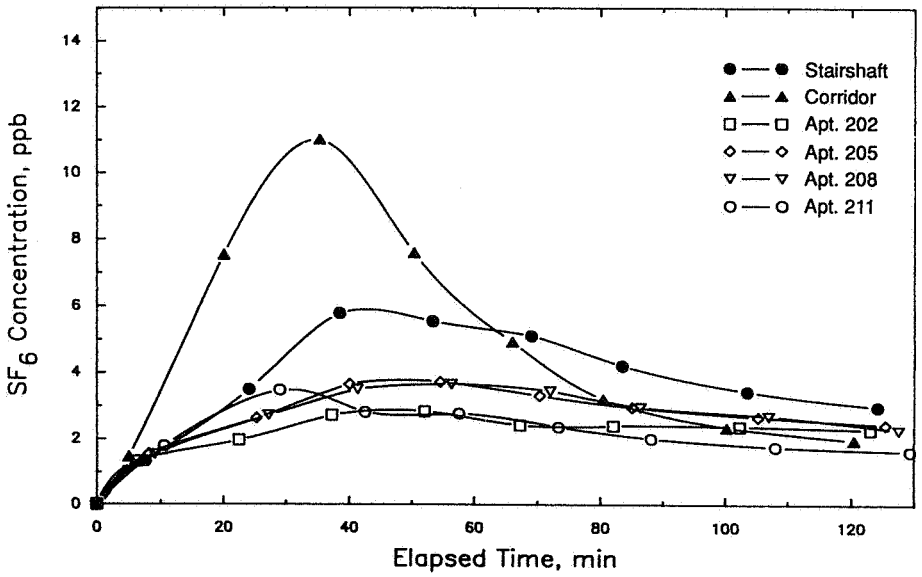

Figure 5

Contaminant dispersion patterns for the second floor with the ground floor garbage room as the source location; winter conditions.

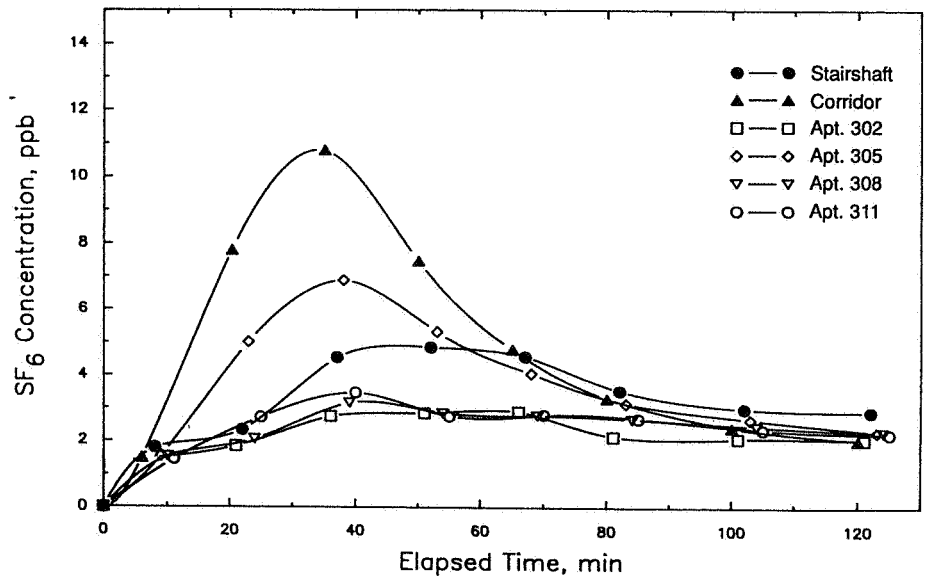

Figure 6

Contaminant dispersion patterns for the third floor with the ground floor garbage room as the source location; winter conditions.

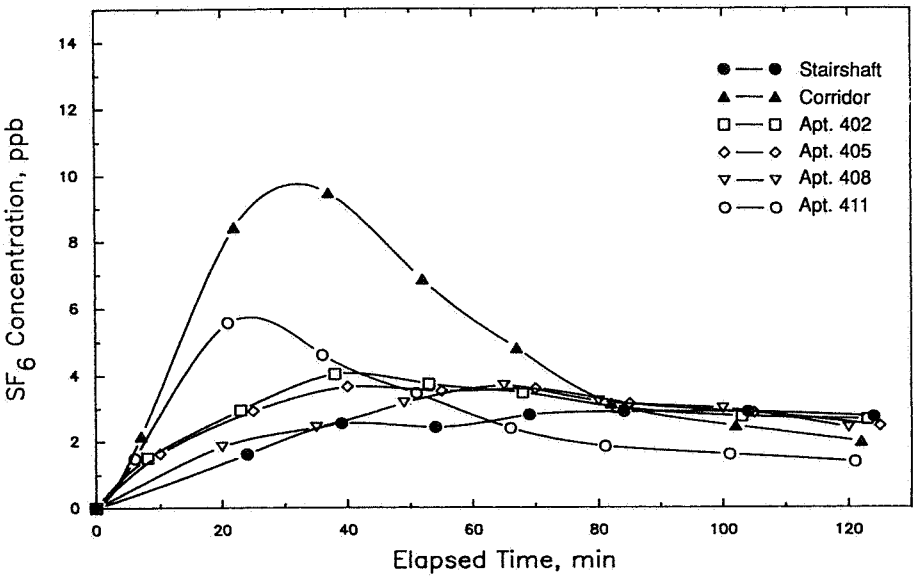

Figure 7

Contaminant dispersion patterns for the fourth floor with the ground floor garbage room as the source location; winter conditions.

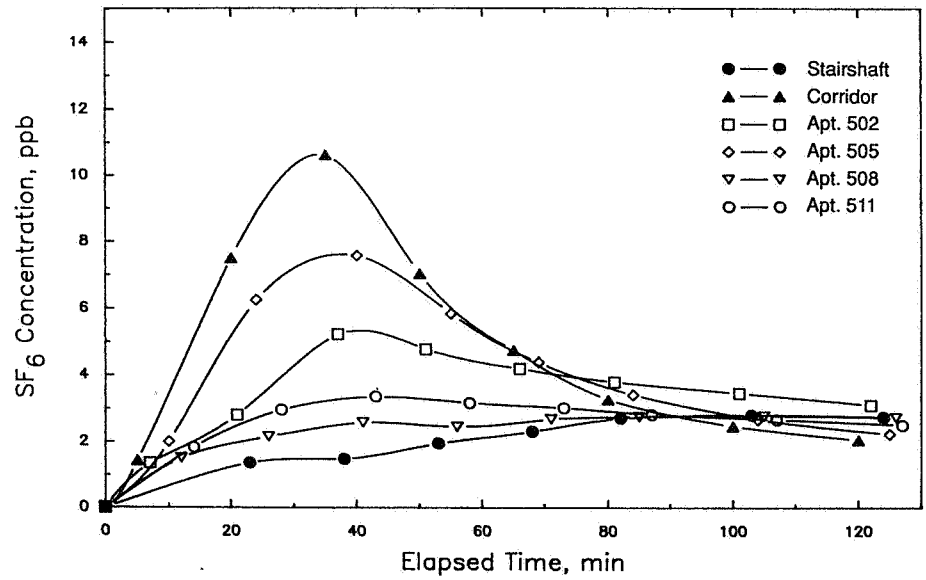

Figure 8

Contaminant dispersion patterns for the fifth floor with the ground floor garbage room as the source location; winter conditions.

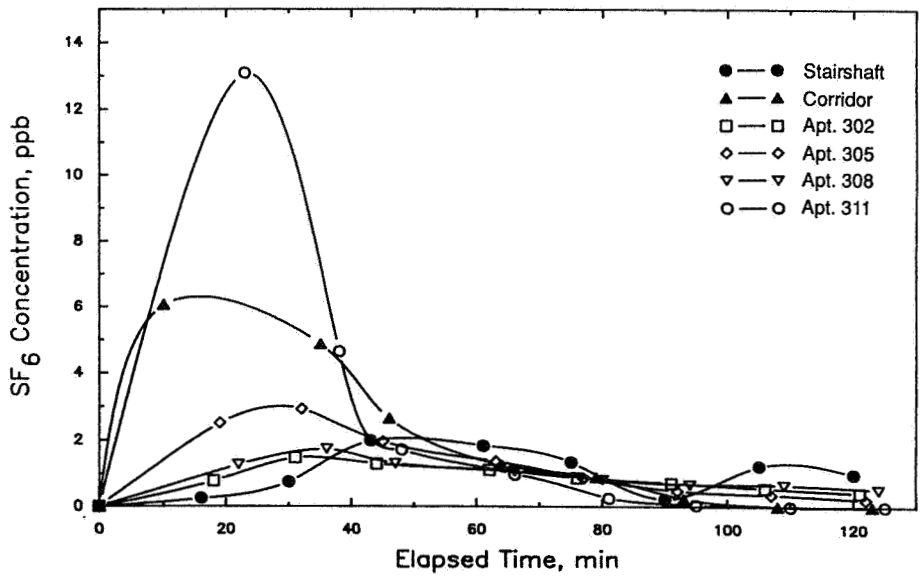

Figure 9

Contaminant dispersion patterns for the third floor with the ground floor garbage room as the source location; summer conditions.

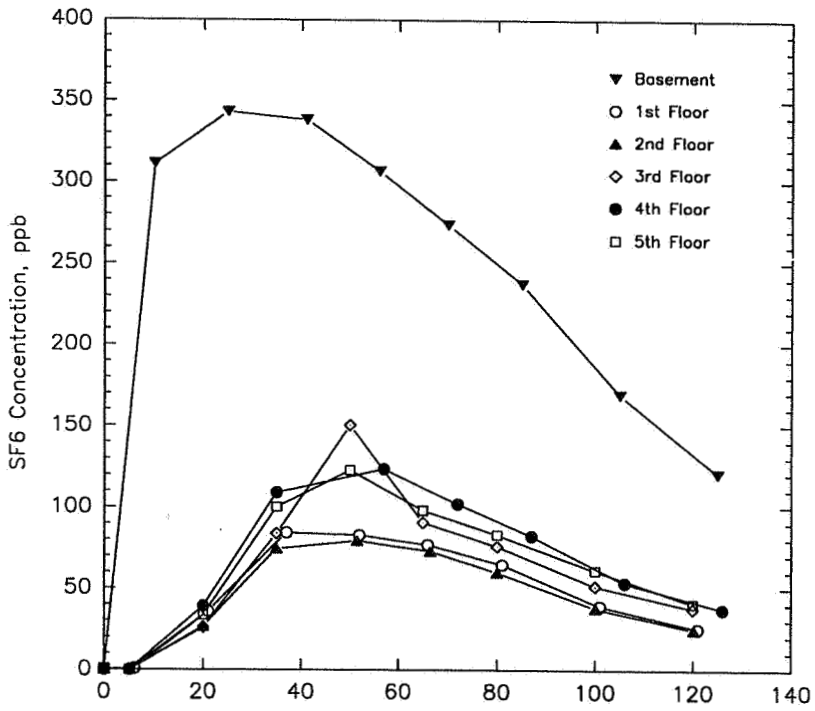

Figure 10

Contaminant dispersion patterns for the corridors with the basement party room as the source location; winter conditions

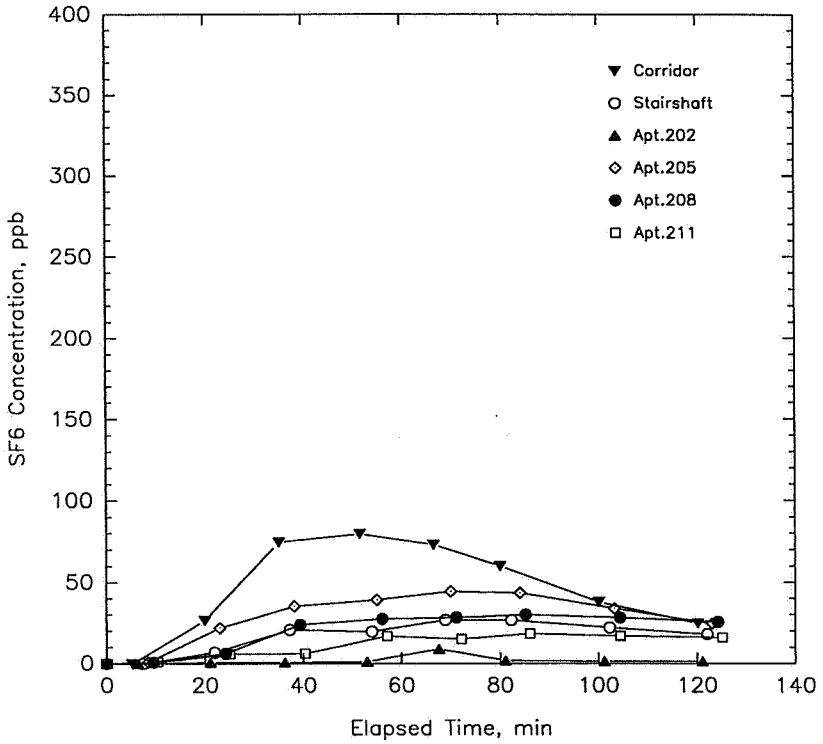

Figure 11

Contaminant dispersion patterns for the second floor with the basement party room as the source location; winter conditions

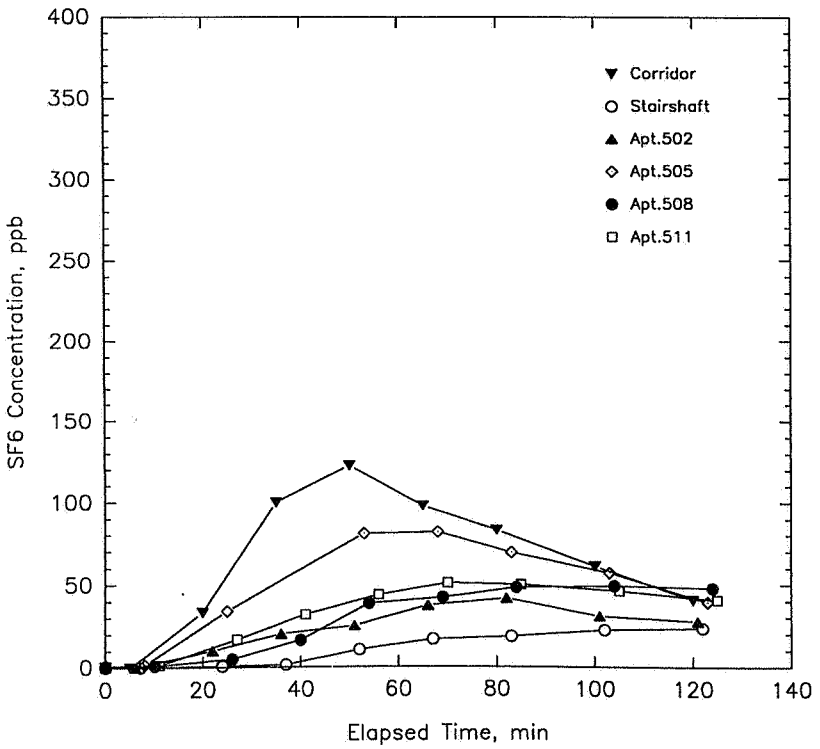

Figure 12

Contaminant dispersion patterns for the fifth floor with the basement party room as the source location; winter conditions

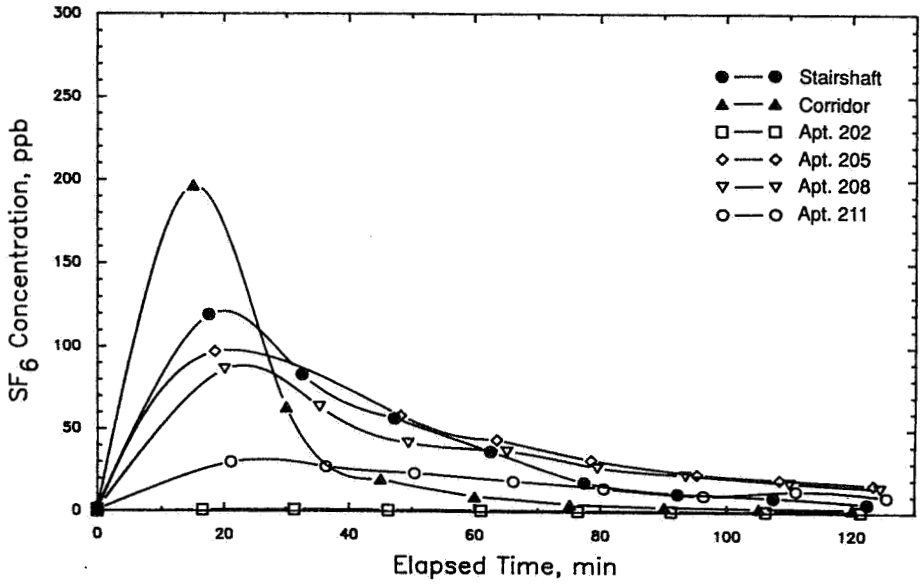

Figure 13

Outdoor air distribution patterns for the second floor; winter conditions.

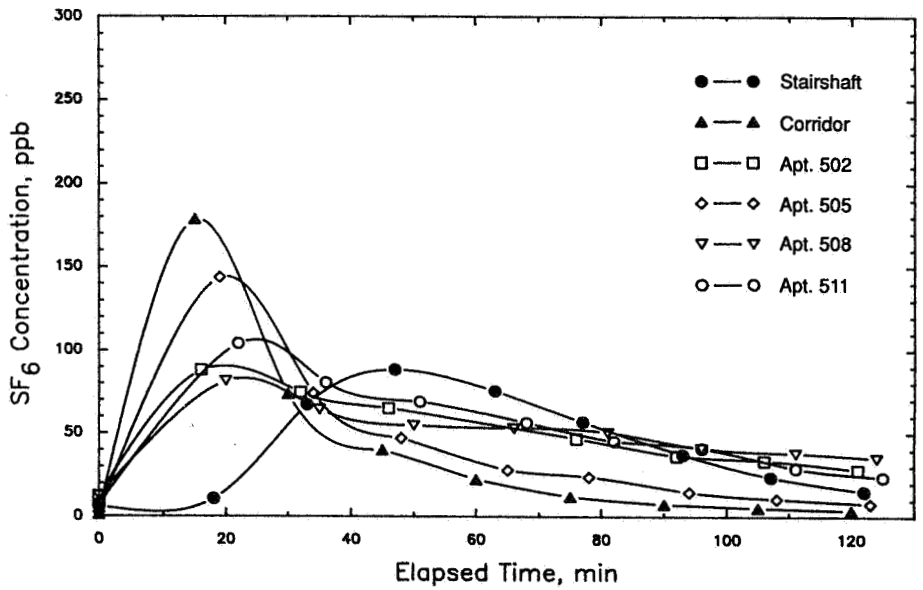

Figure 14

Outdoor air distribution patterns for the fifth floor; winter conditions.

AIR MOVEMENT & VENTILATION CONTROL WITHIN BUILDINGS

12th AIVC Conference, Ottawa, Canada
24-27 September, 1991

PAPER 25

PFT-MEASUREMENTS IN VENTILATION DUCTS

Jorma O. Säteri

Helsinki University of Technology/HVAC-laboratory

Sähkömiehentie 4

SF-02150 ESPOO

FINLAND

SYNOPSIS

The passive perfluorocarbon method (PFT-method) has been successfully applied in ventilation measurements in rooms. The method is, in principle, also applicable to air flow measurements in ventilation ducts. There are, however, several problems in applying a passive sampling technique in a duct. First, the concentration of the tracer may not be uniform through the cross-section of a duct. Second, the velocities in a duct are normally an order of magnitude higher than in a room. Third, the orientation of the sampler in respect to the flow may affect the uptake rate. This study concentrated on the solution of these three problems.

The velocity of the air in a duct had significant effect on the uptake rate of the sampler. The magnitude of the effect was in the order of an 11-16 % increase for each 1 m/s increace in nominal velocity. This indicated that the passive PFT-technique should not be used without correction for uptake rate in duct measurements. More studies are needed in order to establish this correction.

The deviations between samplers were found to be higher in a duct than in a test room. This means that the location of the samplers should be chosen carefully. A good first estimate would be the locations proposed by several standards for air velocity measurements. The orientation of the sampler had only a small effect on the uptake rate. It was found that the samplers should not be placed with their open end against the flow.

1. INTRODUCTION

The passive perfluorocarbon tracer technique introduced by Dietz[1] has been succesfully applied in residential ventilation measurements. The state-of-the-art of this technique in the Nordic countries has been described by several authors in a report published this year[2]. The reliability of the equipment used in this study has been described by Säteri[3].

In principle the method is also applicable to air flow measurements in ventilation ducts. There are, however, several problems in applying a passive sampling technique in a duct. First, the concentration of the tracer may not be uniform through the cross-section of a duct. This may be due to velocity variations within a cross-section. Second, the velocities in a duct are normally an order of magnitude higher than in a room. Increased face velocity and turbulence may have some effect on the uptake rate. Third, the orientation of the sampler in respect to the flow may affect the uptake rate. Tests are needed in order to be able to give recommendations on how to perform a PFT-measurement in a ventilation system. This study concentrated on the solution of these three problems.

2. PASSIVE TRACER GAS MEASUREMENTS IN VENTILATION DUCTS

The PFT-measurement in a ventilation system follows the well known principle of constant emission during which the equilibrium concentration is measured. The air flow is calculated by dividing the emission by the concentration. The PFT-technique measures the average concentration during the sampling time. Thus, the sampling should not be started before the end of the transient tracer step-up period.

With the passive PFT-technique, the measurement period is usually several days. One prerequisite for the use of the passive sampling technique is that the air flows are relatively constant during the measurement period. Should this not be the case, it is preferable to use pumped sampling with short-enough sampling periods.

The application of described measurement method requires that the mixing in the duct at the measuring point be uniform. The problemats are to some extent similar to those of velocity measurements in ducts. However, gravitational forces, for example, can cause the tracer flow pattern to differ from that of the air. This problem can usually be circumvented by increasing the

number of sampling points. Because the number of sampling points is always limited, optimal placement of the samplers should be found. The instructions given for velocity measurements should be used to start with. Indicator smokes could also be used.

In the passive PFT-technique, the sampling is based on diffusion between ambient air and adsorbent. The uptake rate is given theoretically by Fick's law. Dietz[1] has determined the uptake rates for various perfluorocarbons and found that the concentration in the adsorbent can be assumed to be zero. So far, the measurements have usually been carried out in rooms, where the air velocities are low. There is little information available on the effects of increased velocity and turbulence on the uptake rate. It can be assumed, however, that increasing turbulence at the open end of the sampler should also increase the molecule flow between the ambient and the adsorbent. This yields a higher uptake rate if the molecules do not desorb from the adsorbent.

Dietz[1] has also reported that the sampler orientation does not affect the uptake rate. The tests were made in a small test chamber which had a unidirectional air flow. As the test set-up resembled a room more than a duct, it is necessary to check the validity of that assumption as well.

3. EXPERIMENTAL SET-UP

The measurements were made in the HVAC-laboratory during the summertime. Three different set-ups were used. In addition to these tests, two reference tests were made in one room of the test flat. The purpose of these tests was to give reference values for the uptake rate and deviation between samplers in the conditions normally used.

The first two tests were made in the experimental ventilation unit of the laboratory. These tests were made to study the mixing in a duct and the orientation of the samplers. The unit is built of commercially used components. A scheme of the unit is shown in Fig. 1a. The air coming from the unit was traced by 20 PMCP and 20 PMCH sources. The 46 samplers were placed in the D=400 mm circular duct at the distance of 9.0 m from the second 90° bend. The samplers were placed so that 1/4 of them were orientated in each direction: open end against the flow ('A'), open end up ('C'), open end away from the flow ('B') and open end down ('D'). Two different air flows were used. The durations of the tests were 7

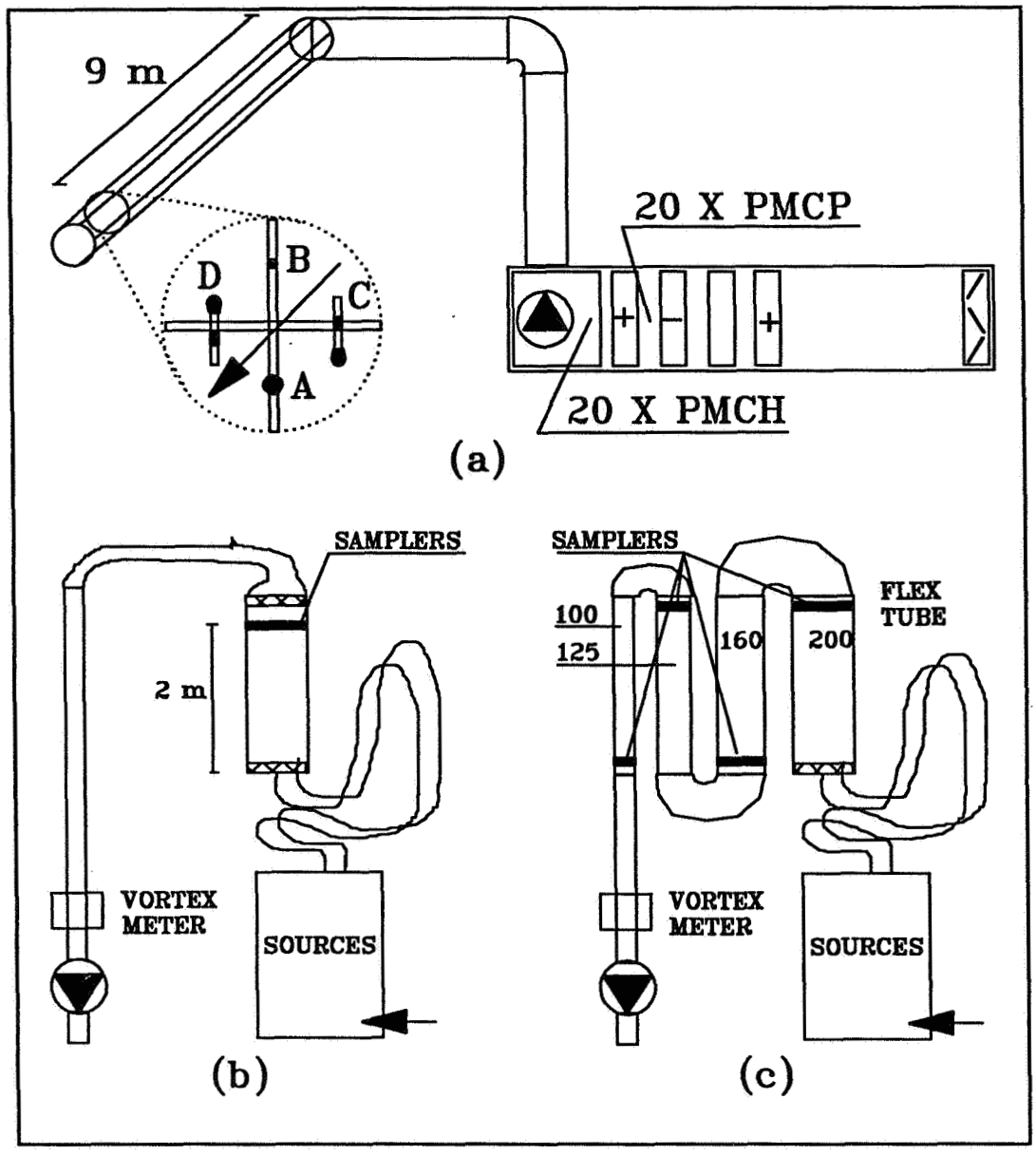

Fig. 1. a) The air-conditioning unit used in tests 1&2
b) The setup in tests 3-6.
c) The setup in testing the effect of velocity

and 11 days.

The next four tests (3 through 6) were made using the set-up in Fig. 1b. These tests were also made to study the effects of the orientation of the samplers. Now, 5 PMCP and PMCH sources and 6 PDCH sources were placed in a mixing chamber. The air was exhausted from the chamber to the measurement duct (D=200 mm) via a flexible tube (D=100 mm). There was a laminar flow stabilizer at both ends of the 200 mm duct in order to minimize the confounding effects of non-uniform mixing. In these tests, 20 samplers were placed similarly to those in

tests 1 and 2. Four tests were made using different air flow rates. The durations of the tests were 7 and 10 (test 3) days.

The third set-up, used to test the effect of air velocity on uptake rate, is shown in Fig. 1c. The principle of the test was to lead the air flow through four consecutive ducts of different diameters. By doing so, four different nominal (flow rate divided by duct area) velocities were achieved in one test. This way the influence of experimental errors could be minimized. The air flow was measured using a vortex meter with an inaccuracy of less than 0.5 %. The tracer sources were the same as in tests 3-6. The duct diameters and numbers of samplers were as follows: D=100 mm, 5 samplers; 125 mm, 8 samplers; 160 mm, 9 samplers; and 200 mm, 11 samplers. Half of the samplers were orientated against the flow ('A') and the rest had their open end pointing up ('C'). Two tests were made using different air flow rates. The duration of the tests was 5 days.

The reference measurements were made in one room of the test flat. The exhaust air flow from the room was measured using an orifice plate tube. The room was depressurized, and the supply air came via the supply duct, but no supply fans were used. The air velocity in the room was measured using an indoor climate analyzer. Two PFT-sources of each type were placed on a chair near the supply plenum. The samplers were placed near each other at the center of the room. Two tests with 8 and 5 samplers were made using the same air flow. The duration of the tests was 7 days.

4. RESULTS AND ANALYSIS

4.1 The mixing of tracer in a duct

The mixing of tracers in a duct was studied in tests 1 and 2. The concentrations were measured at several points on the cross-section. An relative estimate of the concentrations at various points was gained by introducing a sampling index (δ):

$$\delta = C_p / \langle C \rangle \qquad (1)$$

where C_p = concentration at a point,
$\langle C \rangle$ = average concentration of all samplers on a cross-section.

The advantage of a sampling index is being able to compare various measurements and tracer gases. It is

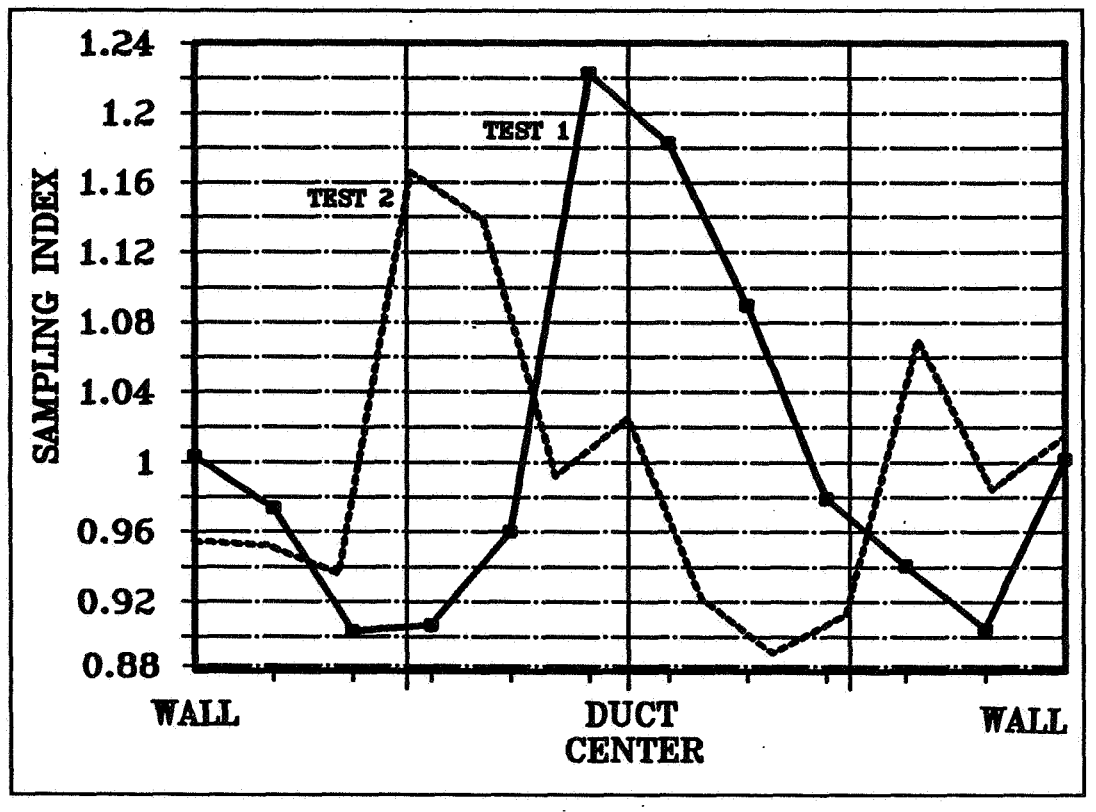

Fig. 2. Sampling indices in tests 1 and 2.

used both in mixing studies as well as orientation studies. Another measure of the mixing on a cross-section is, of course, the relative standard deviation (RSD) of the measured concentrations at various similarly orientated samplers.

The results of tests 1 through 6 are presented in Fig. 2 and tables 1 and 2. From Fig. 2 it can be seen that *on*

Table 1: The relative standard deviations of concentrations measured from similarly orientated samplers.

	A			B			C			D		
test	pmcp	pmch	pdch	pmcp	pmch	pdch	pmcp	pmch	pdch	pmcp	pmch	pdch
1	10.6	8.2	--	20.8	13.1	--	15.3	17.8	--	11.6	12.9	--
2	12.9	9.0	--	8.6	10.4	--	19.1	18.9	--	33.6	18.8	--
3	3.4	4.2	2.8	10.2	17.2	35.2	3.4	5.6	3.3	28.0	21.2	43.5
4	9.7	4.2	10.3	3.7	4.2	6.9	13.8	3.0	10.2	6.5	10.3	13.6
5	13.3	4.2	7.6	3.7	6.2	7.0	4.9	8.7	10.5	10.0	13.1	14.0
6	3.2	4.1	5.1	4.2	4.2	4.3	9.8	6.6	12.0	17.7	47.4	20.2

average the deviation of the measured concentration was within the range of -10 % to +20 % from the average concentration for the whole cross-section. The relative standard deviations (table 1) of similarly orientated samplers varied in tests 1 and 2 between 8.6 % - 33.6 % (PMCP) and 8.2 % - 18.9 % (PMCH). This also includes the deviation due to the orientation of the samplers as well as the uncertainties of the sampling and analysis.

In the reference measurements made in the test flat the relative standard deviations were as follows: test 1; PMCP 9.9 %, PMCH 11.6 % (8 samplers) and test 2; PMCP 9.0 %, PMCH 7.9 % (5 samplers). Another comparison can be made with the relative standard deviations in tests 3 through 6 in which laminar flow stabilizers were used in order to stabilize the flow.

4.2 The effect of sampler orientation

The effect of sampler orientation on the measured concentration was studied in tests 1 through 6. The results are presented in table 2. In table 2, a value of less than unity indicates a lower measured concentration than the average concentration for the whole cross-section (all samplers included), and vice versa for values greater than unity. Theoretically, all tracers should give similar values, but measurement inaccuracies cause some variation in the results. There are not, however, any systematic variations between the three different tracers used. So, the value calculated for each orientation is the average of all used tracers. In tests 1 and 2 the relative standard deviations were higher than in tests 3-6. This may confound the analysis of the effect of orientation. As no systematic

Table 2: The sampling indices of tests 1 through 6.

	A			B			C			D		
test	pmcp	pcmh	pdch	pmcp	pcmh	pdch	pmcp	pcmh	pdch	pmcp	pcmh	pdch
1	0.89	0.87	--	1.15	1.12	--	0.99	1.02	--	0.97	0.99	--
2	0.88	0.88	--	1.05	1.12	--	1.08	1.10	--	0.98	0.90	--
3	0.92	0.85	0.87	1.00	1.10	1.13	0.94	0.88	0.89	1.13	1.17	1.11
4	1.00	1.00	0.98	0.96	0.96	0.99	1.09	1.06	1.01	0.95	0.98	1.02
5	1.02	0.94	0.91	0.99	1.03	1.03	0.99	0.99	0.98	1.00	1.04	1.07
6	0.88	0.93	0.86	0.92	0.97	0.90	1.25	1.33	1.19	0.95	0.77	1.06
avg1	0.93	0.91	0.90	1.01	1.05	1.01	1.06	1.06	1.02	1.00	0.98	1.06
rsd	0.06	0.05	0.05	0.07	0.07	0.08	0.10	0.14	0.11	0.06	0.12	0.03
avg2	0.92			1.03			1.05			1.01		

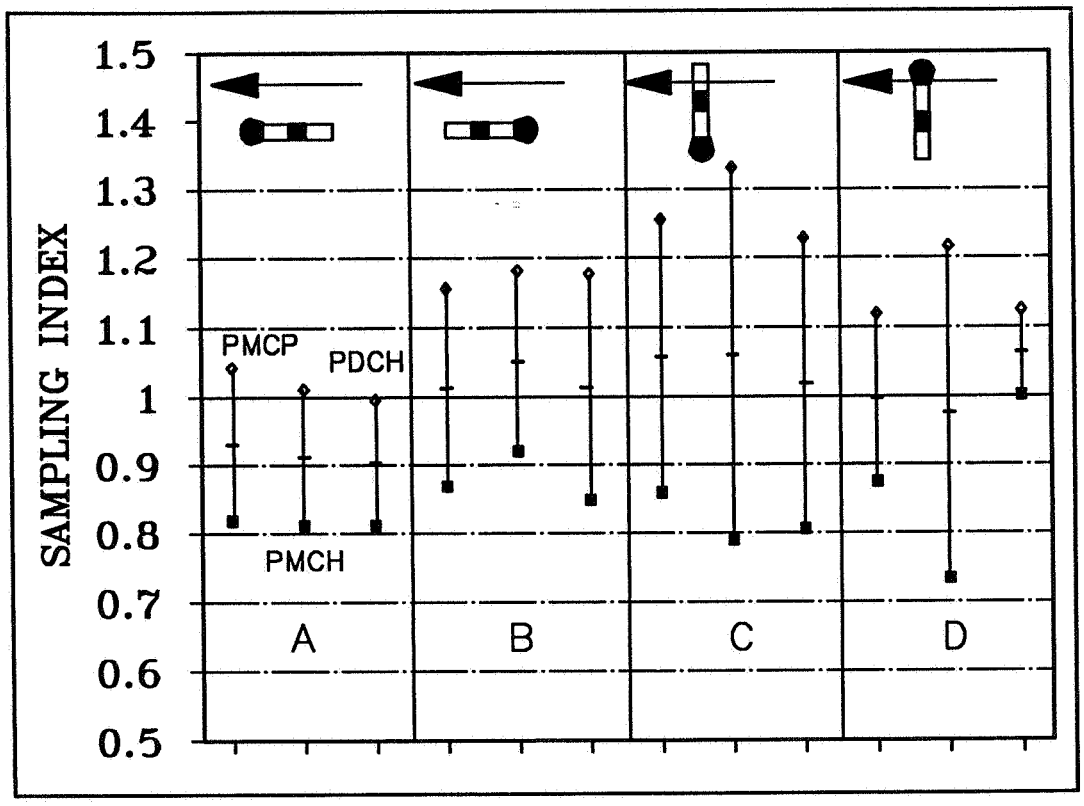

Fig. 3: The 95 % confidence intervals of sampler orientation tests 1 through 6.

difference between tests 1&2 and 3-6 was found, the analysis is based on average values for all six tests.

The sampling index (δ) for samplers orientated against the flow (A) was 0.92. For samplers orientated with their open end up (C), δ=1.05. For samplers orientated with their open end pointing away from the flow (B), δ=1.03. The sampling index for samplers orientated with their open end down (D) was 0.92. The standard deviations of these values varied between 0.03 and 0.14. In cases B, C and D the 95 % confidence intervals included unity (Fig. 3.). This means that the orientation of the sampler did not in these cases have a significant effect on the uptake rate. However, it seems that a sampler should not be placed with its open end directly against the flow (case A).

4.3 The effect of air velocity on uptake rate

The calculated uptake rates are presented in table 3. The plot in Fig. 4 shows the relative increase in the uptake rate compared with the uptake rate measured simultaneously in a room. All samplers (duct and room)

Table 3: The measured uptake rates in the test room and tests A and B. The relative rate is the ratio duct and room rates.

test #	vel. (m/s)	uptake rate (mL/d) pmcp	pmch	pdch	relative rate pmcp	pmch	pdch
room	0.05	186	249	197	1	1	1
A	0.64	219	285	239	1.18	1.14	1.21
A	0.99	230	304	256	1.24	1.22	1.30
A	1.63	225	317	273	1.21	1.27	1.39
A	2.55	245	343	300	1.32	1.37	1.53
B	1.27	266	314	281	1.43	1.26	1.43
B	1.99	241	297	281	1.30	1.19	1.43
B	3.26	275	341	324	1.48	1.37	1.64
B	5.09	305	392	372	1.64	1.57	1.89

were analysed in a random order so that any drift in the analysis would not confound the results. The average air velocities measured in the room were approximately 0.05 m/s. The uptake rates at this velocity were used as references to the rates measured in the duct. Any inaccuracies in the calibration of the analysis system

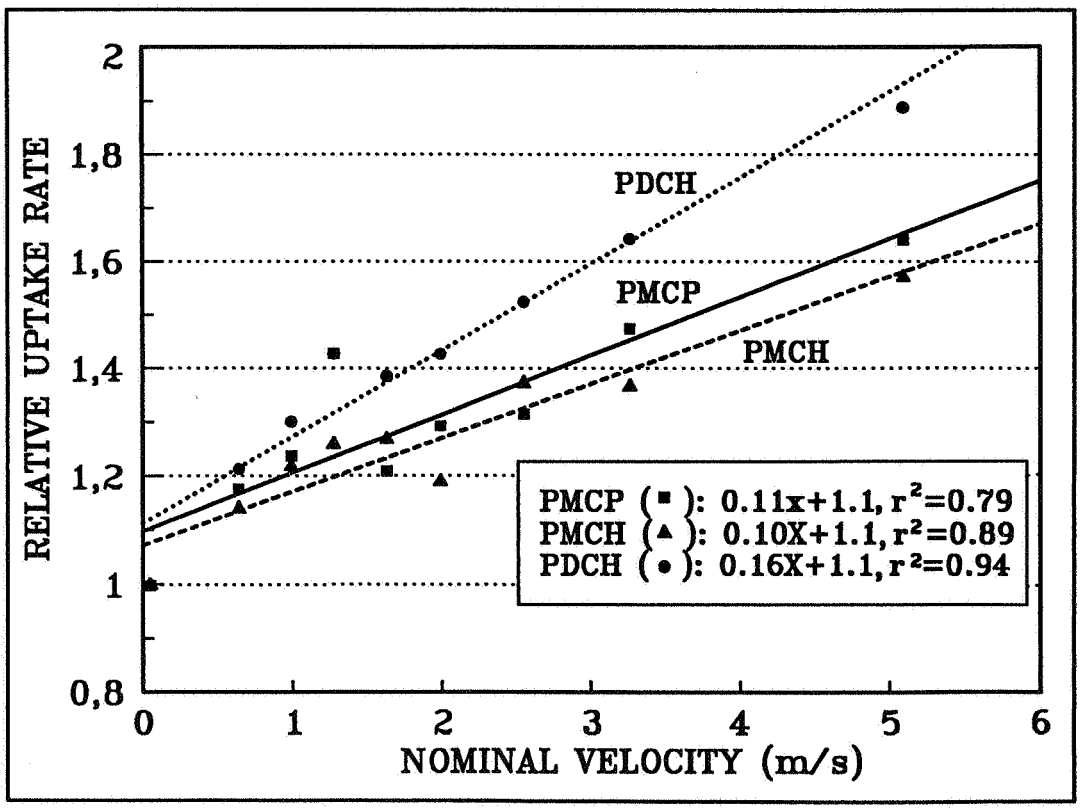

Fig. 4. Uptake rate vs. nominal air velocity in the duct.

and tracer source rates were thus taken into account.

As Fig. 4 reveals, the nominal velocity of air in a duct has a significant effect on the uptake rate. The magnitude of the effect is in the order of an 11% (PMCP), 10 % (PDCH), and 16 % (PDCH) increase for each 1 m/s increase in nominal velocity. This means that passive PFT-sampling should not be used without correction in duct measurements. This effect should be studied more to establish the dependence of uptake rate on velocity and turbulence, which was not measured in this study. Once this correlation has been found, it is possible to iterate the actual uptake and air flow rates from a passive PFT-measurement in a ventilation system. Another possibility could perhaps be the development of shielding techniques, so that the flow field at the end of the tube would be more independent of the flow itself.

5. CONCLUSIONS

The velocity of the air in a duct has a significant effect on the uptake rate of the sampler. The magnitude of the effect is in the order of an 11-16 % increase for each 1 m/s increace in nominal velocity. This indicated that the passive PFT-technique should not be used without correction for uptake rate in duct measurements. More studies are needed in order to establish this correction.

The deviations between samplers were found to be higher in a duct than in a test room. This means that the location of the samplers should be chosen carefully. A good first estimate would be the locations proposed by several standards for air velocity measurements. The orientation of the sampler had only a small effect on the uptake rate. It was found that the samplers should not be placed with their open end against the flow.

The experiences gained from this study yield a conclusion that active (pumped) sampling techniques are preferable to passive techniques in the measurement of air flows in a ventilation system. With active sampling, it is also possible to allow for diurnal operating sequencies of the ventilation systems.

REFERENCES

1. DIETZ, R.N., GOODRICH, R.W., COTE, E.A., and WIESER,R.F.
"Detailed description and performance of a passive perfluorocarbon tracer system for building ventilation and air exchange measurements." In Trechels, H.R. and Lagus, P.L (Ed.) *Measured Air Leakage of Buildings*, ASTM STP 904, Philadelphia, pp. 203-264.

2. SÄTERI, J.O. (Ed.)
"The Development of the PFT-method in the Nordic Countries." Swedish Council for Building Research, Report D9:1991, Stockholm, 1991. 126 p.

3. SÄTERI, J., JYSKE, P., MAJANEN, A. ans SEPPÄNEN, O.
"The Performance of the Passive Perfluorocarbon Method" In *proceedings of the 10th AIVC Conference, Espoo 1989*. pp. 89-107

AKNOWLEDGEMENTS

The author wishes to thank Mr. Jari Paananen and Mr. Jussi Teijonsalo for their assistance in carrying out the measurements.

AIR MOVEMENT & VENTILATION CONTROL WITHIN BUILDINGS

12th AIVC Conference, Ottawa, Canada
24-27 September, 1991

PAPER 26

THE RELIABILITY OF INFILTRATION AND AIR MOVEMENT DATA OBTAINED FROM SINGLE TRACER GAS MEASUREMENTS IN LARGE SPACES

J R WATERS AND H C SUTCLIFFE

Coventry Polytechnic
UK

THE RELIABILITY OF INFILTRATION AND AIR MOVEMENT DATA OBTAINED FROM SINGLE TRACER GAS MEASUREMENTS IN LARGE SPACES

J R Waters and H C Sutcliffe

SYNOPSIS.

The methods available for the measurement of air infiltration and air movement in large industrial halls are restricted by the size of the building and the nature of the operations which take place within it. Single tracer decay measurements are the easiest to perform and this paper examines the possibility of extracting useful information from them. Using a multi-zone representation of the building volume, the properties of tracer decay curves are considered, and the ease of extraction infiltration and air flow data examined by means of simulations. The results show how the error in the derived infiltration rates grow with error in the tracer gas concentration measurements for various methods of treating the results. The simulations are compared to the results of measurements made in a typical industrial hall. Despite the shortcomings of the multi-zone model and the single tracer decay method, it appears possible to obtain reasonable results for the overall air infiltration rates.

1. Introduction.

In recent years there have been many improvements and new developments in the tracer gas methods available for the measurement of infiltration and air movement in buildings. Nevertheless there are some cases in which the choice of method is limited by the characteristics of the building. This is especially true of industrial halls, which are often characterised by large internal volume, continuous operation, unusual contaminants in the atmosphere, and an unwillingness on the part of management to allow interruption of normal activities. Artificial stirring of the air is often

impossible, making it difficult to use constant concentration, constant injection, or any of the pulse methods. In addition the large volume and the presence of other contaminants place restrictions on the choice of tracer. Consequently the single tracer gas decay method is the easiest to use, and a number of reports of its use in large buildings have been published [1, 2, 3]. However, there is little evidence to indicate their reliability, because of the difficulty of validation. Having considered the alternatives, we have returned to the single tracer gas decay method, and attempted to evaluate its reliability and performance in the context of large spaces.

2. Theory.

In the absence of full stirring, there will always be significant spatial variations throughout the air volume of a large building. It is therefore necessary to use some kind of discretisation of the volume into sub-volumes (or zones) in order to model these variations. The greater the number of zones the more closely will the discretisation approach the real case. A system of interconnected zones may be treated by means of the well known multi-zone air movement model. Unfortunately this assumes that the air in each zone is fully mixed, an assumption which is unlikely to hold in the sub-volumes of the real building. Nevertheless, this mismatch may not be serious enough to prevent useful information being obtained, and the agreement between the actual discretisation and its multi-zone representation can always be improved by increasing the number of zones. Assuming that the multi-zone model is acceptable, our problem is the extraction of inter-zone flows from single tracer gas decay experiments in such a model.

The multi-zone model is sufficiently well known to require no special description. Following Sinden [4] and Sandberg [5], the relevant equation (in the absence of a source term) is

$$V\dot{\underline{c}}(t) = F\underline{c}(t) \qquad 1$$

where V is the zone volume matrix, F the flow matrix, and $c(t)$ is the vector

of the contaminant concentrations at time t. The solution for a model of N zones is

$$\underline{c}(t) = \sum_{k=1}^{N} a_k \underline{x}_k e^{\lambda_k t} \qquad 2$$

where λ_k and $\underline{x}_k$ are the eigenvalues and eigenvectors of the matrix F-λV, and a_k are a set of constants determined by the initial distribution of tracer gas. In what follows, it is convenient to define:

F_{ij} the volumetric flow rate from zone i to zone j, where zone 0 represents the outside.

S_i the total inflow/outflow to zone i, $\sum_{j=0}^{N} F_{ji}$ or $\sum_{j=0}^{N} F_{ij}$

f_{ij} flow rate per unit volume, $f_{ij} = \frac{F_{ij}}{V_j}$

r_i total flow per unit volume, $r_i = \frac{S_i}{V_i}$

The most relevant features of multi-zone single tracer decay may be listed as follows:

a) The decay curves are governed primarily by the eigenvalues λ_k and $\underline{x}_k$ their eigenvectors $\underline{x}_k$. There as many eigenvalues as there as zones, the largest is real, and some or all of the remainder may be complex. Repeated eigenvalues occur when some or all of the r_i are equal and some of the internal flows are zero. Physically such cases are likely to occur when at least one zone receives fresh air and supplies air to other zones, but receives no recirculated air, a condition similar to displacement flow. The largest eigenvalue, λ_1, becomes dominant as time progresses, and eventually governs the rate of decay in all zones. If the time constant of the process is taken as the reciprocal of λ_1, then whatever the initial tracer gas distribution, λ_1 is dominant after

approximately two time constants. Thus if the decay is allowed to proceed long enough, λ_1 can always be determined. However, λ_1 is only equivalent to the fresh air infiltration rate when certain conditions are satisfied. There are two types of condition. One occurs when internal flows, f_{ij}, become very large compared to external flows, f_{i0}. This is obvious because it corresponds to full internal mixing. The other occurs when either all f_{i0} are the same or all f_{0i} are the same, which in turn means that,

$$f_{0i} = -\lambda_1 \quad \text{for all } i$$

or

$$f_{i0} = -\lambda_1 \quad \text{for all } i$$

The significance of this is that if either the infiltration or the exfiltration is well distributed between the zones, the dominant eigenvalue will be a good representation of the fresh air infiltration rate.

b) In the region where λ_1 is dominant, the ratios of the zone concentrations approach the components of the dominant eigenvector. Hence, x_1 can be determined. If the concentrations in this region are a_1, a_2, ... then

$$\underline{x}_1 = [a_1, a_2, a_3 \ldots] \qquad 3$$

This must be a solution of the eigenvalue equation, which gives:

$$\begin{aligned} -a_1(r_1 + \lambda_1) + \quad a_2 f_{21} \quad + \quad a_3 f_{31} \quad \ldots &= 0 \\ a_1 f_{12} \quad - a_2(r_2 + \lambda_1) + \quad a_3 f_{32} \quad \ldots &= 0 \\ \vdots & \end{aligned} \qquad 4$$

If the concentrations in all zones are essentially equal at this stage, ie. $x_1 = [1, 1, 1, \ldots]$, then, remembering that $r_i = f_{0i} + f_{1i} + f_{2i} + \ldots$, the eigenvector equation reduces to

$$\begin{aligned} -(f_{01} + \lambda_1) &= 0 \\ -(f_{02} + \lambda_1) &= 0 \\ \vdots & \end{aligned} \qquad 5$$

Again we have the condition

$$f_{0i} = -\lambda_1 \quad \text{for all } i$$

but NOT $$f_{i0} = -\lambda_1$$

If the concentrations are not all equal, then by noting that $r_i = f_{i0} + f_{i1} + f_{i2} + \ldots$, and summing the eigenvalue equations, we get, after some rearrangement, an equation connecting the outflows:

$$a_1 f_{10} + a_2 f_{20} + \ldots = -\lambda_1 \sum a_i \qquad 6$$

c) It has previously been pointed out [6] that it is sometimes possible to derive information from the intersection of the decay curves from two zones. If it is observed that $c_i(t) = c_j(t)$ when $c_i(t) = 0$, and if $c_j(t)$ is the maximum at time t in the subset of zones which have a possible connection to zone j, then it may be inferred that the flows into j, F_{kj}, are all zero except for F_{0j} and F_{ij}.

d) If only one zone, say zone i, contains tracer gas at time zero, the tracer gas balance equations simplify to

$$\begin{aligned} V_i \dot{c}_i(0) &= -c_i(0) S_i \\ V_j \dot{c}_j(0) &= F_{ij} c_i(0) \end{aligned} \qquad 7$$

This would allow determination of S_i and F_{ij}, except that in practice it is difficult to measure concentration gradients near the origin.

The extraction of the flows F_{ij} from the measured decay curves requires the solution of a set of linear equations of the type

$$V_j \dot{c}_j(0) = F_{0j}(c_0(t) - c_j(t)) + F_{ij}(c_1(t) - c_j(t)) + \ldots \qquad 8$$

In a typical experiment there is usually no difficulty in obtaining more equations than is necessary in order to find the N^2 independent unknowns. A least squares method seems appropriate, but has some

drawbacks. Firstly the equations are not truly independent. Secondly the large number of unknowns makes it difficult to achieve satisfactory precision. Thirdly the concentration gradients are difficult to measure with adequate accuracy. The first problem cannot be avoided, the second can be ameliorated by introducing prior knowledge and known constraints, and the third can be dealt with either by smoothing techniques or by integration of the equations.

3. The Solution Procedure and the Scope of the Investigation.

Equation 8 is an over-determined set of linear equations of the form

$$Y = Xb \qquad 9$$

where the vector Y contains the values of $V_j.c_j(t)$, the matrix X is assembled from the concentrations, and the vector b contains the solution for the flows. Three methods of filling Y are:

i) for simulated data, using exact gradients,

ii) using gradients obtained by smoothing,

iii) after integration, using $(c_j(t+n) - c_j(t))$ where n is the integration interval.

In general the solution contains a constant, which is expected to be zero because the concentration gradients and the concentrations all approach zero as time progresses. Nevertheless it is better to retain the constant to allow for an offset in the solution. The simple (or straight) least squares solution is

$$b = (X'X)^{-1} X'Y \qquad 10$$

If some of the flows are known, either individually or in combination, they may be expressed in the form

$$C.b = d \qquad 11$$

where C is an identification matrix and d contains the known values. The

constrained solution is then

$$B = b + (X'X)^{-1} C' \left[C(X'X)^{-1} C' \right]^{-1} (d - Cb) \qquad 12$$

This assumes that the values in the vector d are known precisely. If they are subject to error, and have a variance of σ, we may write (Sherman [7] and Tarantola [8])

$$B = b + (X'X)^{-1} C' \left[C(X'X)^{-1} C' + \sigma \right]^{-1} (d - Cb) \qquad 13$$

Because the flows F_{ij} cannot be negative, a non-negative constraint may also be introduced. The NNLS method of Lawson and Hanson (9) is well known, and may be applied to the simple solution (equation 10) or to the fixed value constrained solution (equation 12). Already we have four possible solutions:

1. Simple (or straight) least squares.
2. Simple least squares with NNLS applied.
3. Constrained least squares.
4. Constrained least squares with NNLS applied.

The quality of the solution may be examined by the usual analysis of variance table. Other indicators are the variance-covariance matrix, and a suitable condition number of the XX' matrix. Where the original data was produced by a simulation, a root mean square error may be formed from the difference between the derived flows and their original values. It is also of interest to compare the fresh air infiltration rate found by summing F_{i0} with the dominant eigenvalue and with the true value.

The main purpose of this study, therefore, was to apply the solution procedures to simulated data sets in order to investigate the error in the solution due to each of the following:

1. Error in the original tracer gas concentrations (0 to 5%).
2. The method of treating the concentration gradient (exact, smoothed or by integration).
3. The time scale of the experiment (one time constant, two time

constants or the full data set).

4. The number of zones (2 to 6).
5. The choice of solution procedure.

4. Results and Discussion.

Table 1 shows the flow matrices used in the simulations. Simulated data for a time period of approximately 2.5 time constants were prepared for each of these flow regimes, and for a range of error levels in the tracer gas concentrations. In most cases, the starting condition corresponded to the seeding of one zone only. The results were analysed by the four LSQ methods listed in section 4, and for each of the three methods of treating the gradient. Table 2 shows the results for the two zone model when analysed by means of the 'straight' LSQ. In the table the codes for the data sets are:

F = analysis using the full data set.

1 = analysis using the first time constant of data only.

2 = analysis using the first two time constants of data.

The codes for the condition numbers refer to the norms on which they are based:

1 = Chebysev

2 = Manhattan

3 = Frobenius

4 = Eigenvalue

The RMS error in the output is given in absolute units of flow, and the fresh air infiltration rate is given in air changes per hour. The results for the data sets with zero input error and analysed using exact gradients confirm the correctness of the procedures. The effect of particular parameters may be highlighted by grouping the results into subsets, and finding the average RMS error in that subset. This has been done for the two zone model in tables 3, 4 and 5. Inspection of these tables leads to some useful conclusions:

1. From tables 3 and 5, using only the first time constant of data creates significantly higher RMS errors than using two time constants. Going beyond two time constants to the full data set produces only

a slight improvement. Thus it is better to use two time constants of tracer concentration data. This agrees with the theoretical prediction that in single zone seeded decay mode, uniform decay is established after approximately two time constants.

2. From tables 3, 4 and 5, the integral treatment of gradient produces substantially lower errors than smoothing.
3. From table 4, increasing the applied error increases the RMS error. However, an increase in the applied error from 0.1% to 1% often produces a proportionally smaller increase in the RMS error.
4. From table 5, the RMS error is significantly lower when zone 1 is seeded. This agrees with the prediction that it is better to seed the zone with the smallest component of the dominant eigenvector. In this case $x_{11} = 1$ and $x_{12} = 2$.
5. Referring again to table 2, it can be seen that there appears to be no correlation between any of the condition numbers and the RMS error.

These conclusions were confirmed by similar analyses of the results for the 3, 4, 5 and 6 zone models. In view of the first two conclusions, the more detailed analyses were restricted to using the first two time constants of data and the integral treatment of gradient.

The two zone model was too simple to explore the effect of constraints. As the number of zones increased, both fixed value and NNLS constraints became more important. Table 6 shows the effect of applying these constraints to the 5 zone model. Both the fixed value constrained solution and the NNLS constrained solution reduce the RMS error substantially compared to the straight solution, with the NNLS constraint being the more effective. Applying both constraints reduces the RMS error even further. The five zone model was used to explore further the effect on RMS error of seeding different zones. In this case the dominant eigenvector is

$$x_1 = [0.309, 0.434, 0.650, 0.416, 0.347]$$

suggesting that best results are obtained when zone 1 is seeded. Table 7

shows that this is not so, and that there is little difference between the five possibilities. However, this is not surprising as the components of x_1 are very nearly equal.

When considering the errors in the output, whether they be RMS errors in the flows or errors in the air change rate, it must be borne in mind that the errors in the input data, that is in the original tracer gas concentrations, were generated by a normally distributed random error generator. Thus each data set at any given error level is unique, and the error in the output is just one value in a normally distributed set of possible errors. This can be explored by repeat runs at the same error level. Table 8 shows the result of repeat runs for the six zone model, using two time constants of data and integration, and table 9 shows the average RMS errors together with the standard deviation of the set and the estimated standard deviation of the population. Clearly, it is the spread of the RMS error that is of particular concern. If this is known it is possible to make an estimate of output errors from an estimate of the measurement error in the original tracer gas concentrations. Because of the small number of repeat runs (only six in each case) the Chi-square test was used to estimate the confidence limits of the population standard deviation, as shown in table 10. It appears from this that the spread in the output error distribution could be quite large. Consequently, where there is only one data set available, as is often the case with field measured experimental data, the error in the result could also be large. On the other hand, the spread in the RMS error does not grow with the applied input error as quickly as may have been expected. This is shown in figure 1. Figure 2 shows the same thing for the percentage difference between air change rate found from the calculated flows and the air change rate found from the exact flows. Finally, the increase in the errors as the number of zones is increased is shown in figure 3, which shows the errors found for the data sets including a 1% applied error level when employing a non-negative least squares and a constrained/non-negative least squares analysis where appropriate.

5. Field measurements.

Analysis of data sets from measurements in real buildings introduce some additional difficulties, especially the identification of zones and zone volumes and the positioning of sampling points. Figure 4 is a typical set of decay curves for an industrial hall, and the results of analysing it are shown in table 11. The solution with fixed value and NNLS constraints gave flows which were plausible in terms of the geometry of the building, and it is interesting to compare the air change rates found by the two methods. In this case it may be presumed that the air change found from the slope of the long term decay is the more reliable, because the decay curves approach each other as time progresses. It often transpires in measured data that the readings from two sample points are essentially equal, suggesting that the zones they represent are indistinguishable. The solution will not be able to separate the flows associated with these two zones, in which case it is better to merge the readings and reduce the number of zones in the model by one. The effect of merging down to a three zone representation is shown in the final column of table 11. Note that it was not possible to merge zones for all the cases.

5. Conclusions.

The single tracer gas decay technique is inherently inaccurate for the measurement of inter-zone flows. Nevertheless it can provide useful information on air change rates and the distribution of air, provided that the analysis includes the points discussed above. In particular, the analysis must include all the prior knowledge that is available, it must take advantage of any of the special properties of the decay curves, and it must use at least non-negative constraints.

References.

1. Potter, I. N., Dewsbury, J. and Jones, T. : The Measurement of Air Infiltration Rates in Large Enclosures and Buildings, 4th AIVC Conference, Switzerland, 26-28 Sept. , 1983.

2. Roussel, C., Garnier, G. and Faivre-Pierret, R. : A Tracer Gas System to Evaluate the Efficiency of Ventilation Systems or Simulate the Consequences of an Accident, Ventilation '85, Ed. by H. D. Goodfellow, pp. 291-295, Elsevier, 1986.

3. Lawrance, G. V. and Waters, J. R. : Measurements of Infiltration and Air Movement in Five Large Single Cell Buildings, 8th AIVC Conference, Germany, 21-24 Sept. , 1987.

4. Sinden, F. W. : Multi-Chamber Theory of Air Infiltration, Building and Environment, Vol. 13, No. 1, pp. 21-28, 1978.

5. Sandberg, M. : The multi-chamber theory reconsidered from the viewpoint of air quality studies, Building and Environment, Vol. 19, No. 4, pp. 221-223, 1984.

6. Waters, J. R. and Simons, M. W. : The evaluation of contaminant concentration and air flows in a multi-zone model of a building, Building and Environment, Vol. 22, No. 4, pp. 305-315, 1987.

7. Sherman, M. H. : On the estimation of multi-zone ventilation rates from tracer gas measurements, Building and Environment, Vol. 24, No. 4, pp. 355-362.

General Case.

$$\begin{matrix} -S_0 & F_{10} & F_{20} & \cdots & F_{n0} \\ F_{01} & -S_1 & F_{21} & & \\ \vdots & & \ddots & & \\ F_{0n} & & & & -S_n \end{matrix}$$

F_{ij} denotes flow from zone i to zone j, (m^3/s).

2 Zone Model.

-6.00	3.00	3.00
5.00	-7.00	2.00
1.00	4.00	-5.00

3 Zone Model.

-6.00	0.00	2.00	4.00
4.00	-7.00	1.00	2.00
1.00	3.00	-4.00	0.00
1.00	4.00	1.00	-6.00

4 Zone Model.

-12.00	3.00	3.00	1.00	5.00
0.00	-4.00	2.00	2.00	0.00
4.00	1.00	-9.00	0.00	4.00
7.00	0.00	0.00	-11.00	4.00
1.00	0.00	4.00	8.00	-13.00

5 Zone Model.

-14.00	1.00	5.00	0.00	5.00	3.00
3.00	-4.00	1.00	0.00	0.00	0.00
4.00	0.00	-11.00	4.00	0.00	3.00
1.00	0.00	2.00	-5.00	0.00	2.00
1.00	3.00	0.00	0.00	-9.00	5.00
5.00	0.00	3.00	1.00	4.00	-13.00

6 Zone Model.

-17.00	1.00	5.00	0.00	5.00	3.00	3.00
3.00	-4.00	1.00	0.00	0.00	0.00	0.00
4.00	0.00	-11.00	4.00	0.00	3.00	0.00
1.00	0.00	2.00	-5.00	0.00	0.00	2.00
1.00	3.00	0.00	0.00	-9.00	5.00	0.00
5.00	0.00	3.00	0.00	4.00	-13.00	1.00
3.00	0.00	0.00	1.00	0.00	2.00	-6.00

Table 1. Flow matrices for simulated models.

Table 2. Results for the simulated two zone model.

Grad Calc Method	Seeded Zone	Error Applied (%)	Data Set	Condition Numbers 1 ($x10^2$)	2 ($x10^2$)	3 ($x10^2$)	4 ($x10^{-1}$)	RMS Error ($x10^{-1}$)	Diff in ACR from Flows (h^{-1})
E	1	0.0	F	2.045	2.045	5.622	0.516	0.000	0.0000
X			1	11.850	11.850	40.960	1.241	0.000	0.0000
A			2	2.839	2.839	8.475	0.745	0.000	0.0000
C		0.1	F	2.043	2.043	5.614	0.517	0.054	0.0009
T			1	11.950	11.950	41.280	1.243	0.205	0.0128
			2	2.829	2.829	8.440	0.746	0.050	-0.0017
		1.0	F	2.108	2.108	5.815	0.511	0.509	0.0133
			1	10.630	10.630	36.650	1.227	1.817	-0.1368
			2	2.857	2.857	8.527	0.736	0.271	-0.0022
	2	0.0	F	10.320	10.320	28.230	0.745	0.000	0.0000
			1	29.310	29.310	119.400	1.703	0.000	0.0000
			2	10.900	10.900	34.480	1.056	0.000	0.0000
		0.1	F	10.390	10.390	28.440	0.754	0.220	-0.0020
			1	29.460	29.460	120.200	1.703	0.280	-0.0037
			2	11.060	11.060	35.040	1.056	0.203	0.0042
		1.0	F	9.298	9.298	25.350	0.755	2.183	-0.0907
			1	25.630	25.630	103.900	1.703	2.423	-0.1769
			2	10.160	10.160	32.100	1.057	1.770	-0.0858
S	1	0.0	F	2.045	2.045	5.622	0.516	0.169	0.0021
M			1	11.850	11.850	40.960	1.241	0.264	0.0067
O			2	2.839	2.839	8.475	0.745	0.178	0.0027
O		0.1	F	2.043	2.043	5.614	0.517	0.475	-0.0086
T			1	11.950	11.950	41.280	1.243	2.176	-0.2026
H			2	2.829	2.829	8.440	0.746	0.683	-0.0338
E		1.0	F	2.108	2.108	5.815	0.511	5.540	-0.1442
D			1	10.630	10.630	36.650	1.227	20.330	-1.3349
			2	2.857	2.857	8.527	0.736	4.361	0.0854
	2	0.0	F	10.320	10.320	28.230	0.754	0.114	0.0037
			1	29.310	29.310	119.400	1.703	0.267	0.0110
			2	10.900	10.900	34.480	1.056	0.131	0.0047
		0.1	F	10.390	10.390	28.440	0.754	3.841	0.2082
			1	29.460	29.460	120.200	1.703	14.650	1.0009
			2	11.060	11.060	35.040	1.056	5.226	0.3064
		1.0	F	9.298	9.298	25.350	0.755	27.730	-1.6772
			1	25.630	25.630	103.900	1.703	61.410	-4.1935
			2	10.160	10.160	32.100	1.057	30.400	-1.8838
I	1	0.0	F	0.121	0.121	0.412	5.337	0.030	-0.0002
N			1	5.886	5.886	9.747	4.291	0.030	-0.0002
T			2	0.346	0.346	0.897	4.982	0.030	-0.0002
E		0.1	F	0.120	0.120	0.412	5.338	0.048	0.0014
G			1	5.828	5.828	9.645	4.291	0.173	0.0126
R			2	0.344	0.344	0.891	4.982	0.525	-0.0006
A		1.0	F	0.127	0.127	0.436	5.365	1.161	0.0054
L			1	5.121	5.121	8.547	4.287	10.700	-0.7984
			2	0.346	0.346	0.907	4.976	1.744	-0.0855
	2	0.0	F	1.428	1.428	3.941	9.806	0.030	-0.0002
			1	17.560	17.560	41.090	9.827	0.030	-0.0002
			2	2.519	2.519	6.511	9.820	0.030	-0.0002
		0.1	F	1.438	1.438	3.968	9.806	0.116	-0.0059
			1	17.940	17.940	41.990	9.827	0.570	0.0399
			2	2.572	2.572	6.658	9.820	0.138	0.0081
		1.0	F	1.364	1.364	3.747	9.808	1.624	0.0908
			1	22.240	22.240	52.220	9.829	17.860	1.2794
			2	2.578	2.578	6.664	9.823	2.088	0.1282

Table 2. Results for the simulated two zone model.

Grad Calc Method	Seeded Zone	Error Applied (%)	Data Set	Condition Numbers 1 ($x10^2$)	2 ($x10^2$)	3 ($x10^2$)	4 ($x10^{-1}$)	RMS Error ($x10^{-1}$)	Diff in ACR from Flows (h^{-1})
E	1	0.0	F	2.045	2.045	5.622	0.516	0.000	0.0000
X			1	11.850	11.850	40.960	1.241	0.000	0.0000
A			2	2.839	2.839	8.475	0.745	0.000	0.0000
C		0.1	F	2.043	2.043	5.614	0.517	0.054	0.0009
T			1	11.950	11.950	41.280	1.243	0.205	0.0128
			2	2.829	2.829	8.440	0.746	0.050	-0.0017
		1.0	F	2.108	2.108	5.815	0.511	0.509	0.0133
			1	10.630	10.630	36.650	1.227	1.817	-0.1368
			2	2.857	2.857	8.527	0.736	0.271	-0.0022
	2	0.0	F	10.320	10.320	28.230	0.745	0.000	0.0000
			1	29.310	29.310	119.400	1.703	0.000	0.0000
			2	10.900	10.900	34.480	1.056	0.000	0.0000
		0.1	F	10.390	10.390	28.440	0.754	0.220	-0.0020
			1	29.460	29.460	120.200	1.703	0.280	-0.0037
			2	11.060	11.060	35.040	1.056	0.203	0.0042
		1.0	F	9.298	9.298	25.350	0.755	2.183	-0.0907
			1	25.630	25.630	103.900	1.703	2.423	-0.1769
			2	10.160	10.160	32.100	1.057	1.770	-0.0858
S	1	0.0	F	2.045	2.045	5.622	0.516	0.169	0.0021
M			1	11.850	11.850	40.960	1.241	0.264	0.0067
O			2	2.839	2.839	8.475	0.745	0.178	0.0027
O		0.1	F	2.043	2.043	5.614	0.517	0.475	-0.0086
T			1	11.950	11.950	41.280	1.243	2.176	-0.2026
H			2	2.829	2.829	8.440	0.746	0.683	-0.0338
E		1.0	F	2.108	2.108	5.815	0.511	5.540	-0.1442
D			1	10.630	10.630	36.650	1.227	20.330	-1.3349
			2	2.857	2.857	8.527	0.736	4.361	0.0854
	2	0.0	F	10.320	10.320	28.230	0.754	0.114	0.0037
			1	29.310	29.310	119.400	1.703	0.267	0.0110
			2	10.900	10.900	34.480	1.056	0.131	0.0047
		0.1	F	10.390	10.390	28.440	0.754	3.841	0.2082
			1	29.460	29.460	120.200	1.703	14.650	1.0009
			2	11.060	11.060	35.040	1.056	5.226	0.3064
		1.0	F	9.298	9.298	25.350	0.755	27.730	-1.6772
			1	25.630	25.630	103.900	1.703	61.410	-4.1935
			2	10.160	10.160	32.100	1.057	30.400	-1.8838
I	1	0.0	F	0.121	0.121	0.412	5.337	0.030	-0.0002
N			1	5.886	5.886	9.747	4.291	0.030	-0.0002
T			2	0.346	0.346	0.897	4.982	0.030	-0.0002
E		0.1	F	0.120	0.120	0.412	5.338	0.048	0.0014
G			1	5.828	5.828	9.645	4.291	0.173	0.0126
R			2	0.344	0.344	0.891	4.982	0.525	-0.0006
A		1.0	F	0.127	0.127	0.436	5.365	1.161	0.0054
L			1	5.121	5.121	8.547	4.287	10.700	-0.7984
			2	0.346	0.346	0.907	4.976	1.744	-0.0855
	2	0.0	F	1.428	1.428	3.941	9.806	0.030	-0.0002
			1	17.560	17.560	41.090	9.827	0.030	-0.0002
			2	2.519	2.519	6.511	9.820	0.030	-0.0002
		0.1	F	1.438	1.438	3.968	9.806	0.116	-0.0059
			1	17.940	17.940	41.990	9.827	0.570	0.0399
			2	2.572	2.572	6.658	9.820	0.138	0.0081
		1.0	F	1.364	1.364	3.747	9.808	1.624	0.0908
			1	22.240	22.240	52.220	9.829	17.860	1.2794
			2	2.578	2.578	6.664	9.823	2.088	0.1282

Table 3. Average RMS errors for each portion of data - two zone model.

Least Squares Technique	Gradient Calculation Method	Average Root Mean Square Error for portion of data set		
		full set	first τ_n	second τ_n
Straight	Exact	0.049	0.079	0.038
	Smoothed	0.631	1.651	0.683
	Integral	0.050	0.490	0.076
Non-negative	Exact	0.048	0.066	0.038
	Smoothed	0.410	1.570	0.450
	Integral	0.050	0.348	0.057

Table 4. Average RMS errors for different applied error levels - two zone model.

Least Squares Technique	Gradient Calculation Method	Average Root Mean Square Error for Applied Error Level		
		0%	0.1%	1.0%
Straight	Exact	0.000	0.017	0.150
	Smoothed	0.019	0.451	2.496
	Integral	0.003	0.018	0.586
Non-negative	Exact	0.000	0.017	0.097
	Smoothed	0.019	0.421	1.154
	Integral	0.003	0.018	0.434

Table 5. Average RMS errors for seeding of each zone - two zone model.

Gradient Calculation Method	Seeded Zone	Average Root Mean Square Error for portion of data set		
		full set	first τ_n	first two τ_n
Exact	1	0.019	0.067	0.011
	2	0.080	0.090	0.066
Smoothed	1	0.206	0.759	0.174
	2	1.056	2.544	1.192
Integral	1	0.041	0.363	0.061
	2	0.059	0.615	0.075

Table 6. Average RMS errors for each analysis technique - five zone model.

Least Squares Technique	Average Root Mean Square Error for applied error level		
	0%	0.1%	1.0%
Straight	0.008	5.842	6.048
Non-negative	0.009	1.357	1.760
Constrained	0.959	2.934	3.993
Const/NNLS	0.232	1.101	1.667

Table 7. Average RMS errors for each zone seeded - five zone model.

Analysis Method	Average RMS error levels for each zone				
	Zone 1	Zone 2	Zone 3	Zone 4	Zone 5
LSQ	4.338	3.669	4.530	4.225	3.018
NNLS	1.007	1.050	1.006	1.307	0.841

Table 9. Statistical analysis of average RMS errors - six zone model.

Applied Error Level (%)		Analysis Technique	
		LSQ	CONST/NNLS
0.1	$\bar{x}$	7.836	0.734
	σ_n	2.545	0.448
	σ_{n-1}	2.788	0.491
1.0	$\bar{x}$	8.836	1.897
	σ_n	1.305	0.493
	σ_{n-1}	1.429	0.481
2.0	$\bar{x}$	7.795	1.507
	σ_n	1.004	0.387
	σ_{n-1}	1.100	0.424
5.0	$\bar{x}$	11.126	2.047
	σ_n	2.421	0.422
	σ_{n-1}	2.652	0.462

Table 8. RMS Errors for each data set - six zone model.

Applied Error Level (%)	Data Set	Root Mean Square Error for analysis techniques	
		LSQ	CONST/NNLS
0.0	1	0.007	0.016
0.1	1	9.718	0.374
	2	5.343	0.600
	3	3.571	1.018
	4	8.048	0.749
	5	10.251	0.139
	6	10.083	1.523
	Average	7.863	0.734
1.0	1	9.824	2.283
	2	8.330	2.039
	3	7.650	2.259
	4	10.838	2.230
	5	9.356	1.259
	6	7.020	1.314
	Average	8.836	1.897
2.0	1	8.164	1.356
	2	6.447	1.256
	3	7.640	1.937
	4	6.903	1.312
	5	9.590	1.053
	6	8.026	2.126
	Average	7.795	1.507
5.0	1	13.288	1.681
	2	10.478	2.264
	3	10.655	1.987
	4	11.278	1.429
	5	6.714	2.121
	6	14.343	2.801
	Average	11.126	2.047

Table 10. Estimates of population standard deviation for RMS errors.

Applied Error Level (%)	Confidence Limit	Estimates of Population Standard Deviation	
		LSQ	CONST/NNLS
0.1	95	1.743<2.788<6.838	0.307<0.491<1.204
	80	2.051<2.788<4.912	0.361<0.491<0.865
	50	2.420<2.788<3.815	0.426<0.491<0.672
1.0	95	0.894<1.429<3.507	0.301<0.481<1.180
	80	1.052<1.429<2.519	0.354<0.481<0.847
	50	1.241<1.429<1.956	0.417<0.481<0.658
2.0	95	0.756<1.100<2.966	0.265<0.424<1.040
	80	0.890<1.100<2.131	0.312<0.424<0.747
	50	1.050<1.100<1.655	0.368<0.424<0.580
5.0	95	1.658<2.652<6.505	0.289<0.462<1.134
	80	1.951<2.652<4.673	0.340<0.462<0.814
	50	2.302<2.652<3.629	0.401<0.462<0.633

Table 11. Air Change Rates for experimental test runs.

Building	Seeded Zone	Data Set	Openings	ACR from Time Constant (h^{-1})	ACR from calculated flows (h^{-1})	
					6 Zone	3 Zone
Structures Lab	6	1	0	0.496	0.995	1.080
		2	0	0.670	1.496	0.884
		3	0	0.158	1.517	-
	1	4	0	0.390	1.624	1.597
		5	0	0.492	1.325	1.133
		6	0	0.467	1.134	1.658
	6	11	7	1.402	4.125	3.005
		12	7	1.705	2.785	2.275
	1	13	7	2.734	4.135	4.786
		14	7	1.657	1.885	-

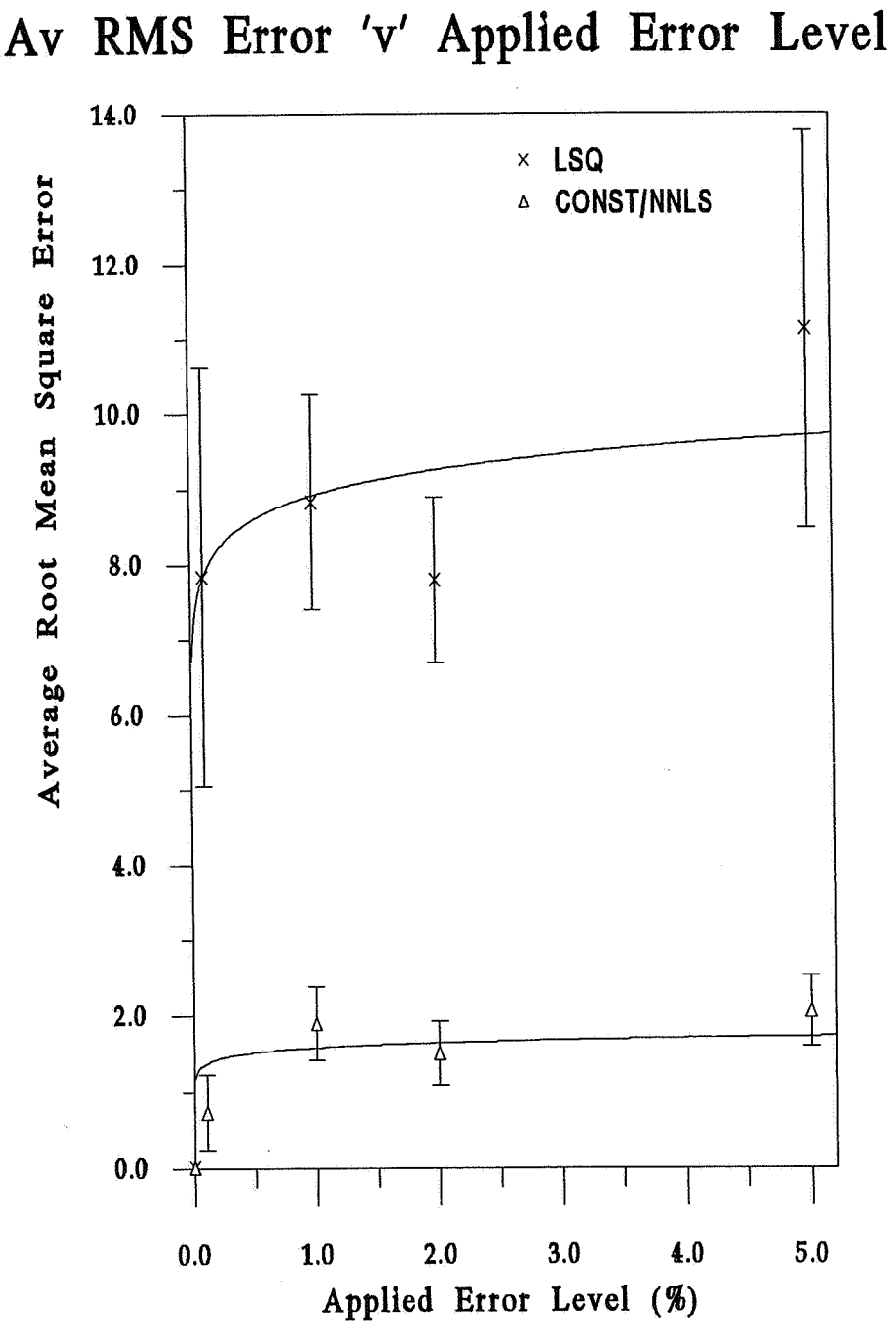

Figure 1. Average values of RMS Error plotted against Applied Error Level.

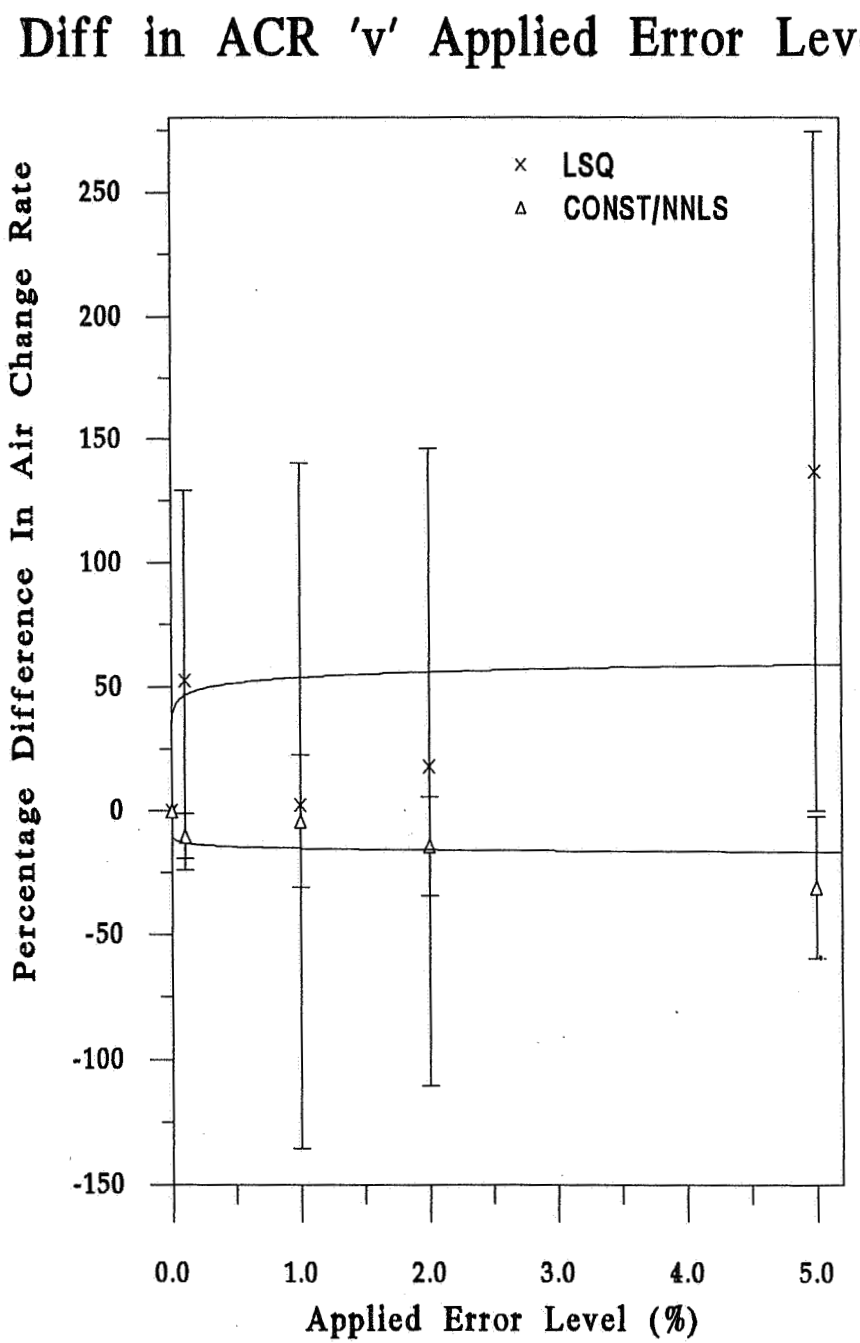

Figure 2. Percentage Difference in Air Change Rate plotted against Applied Error Level.

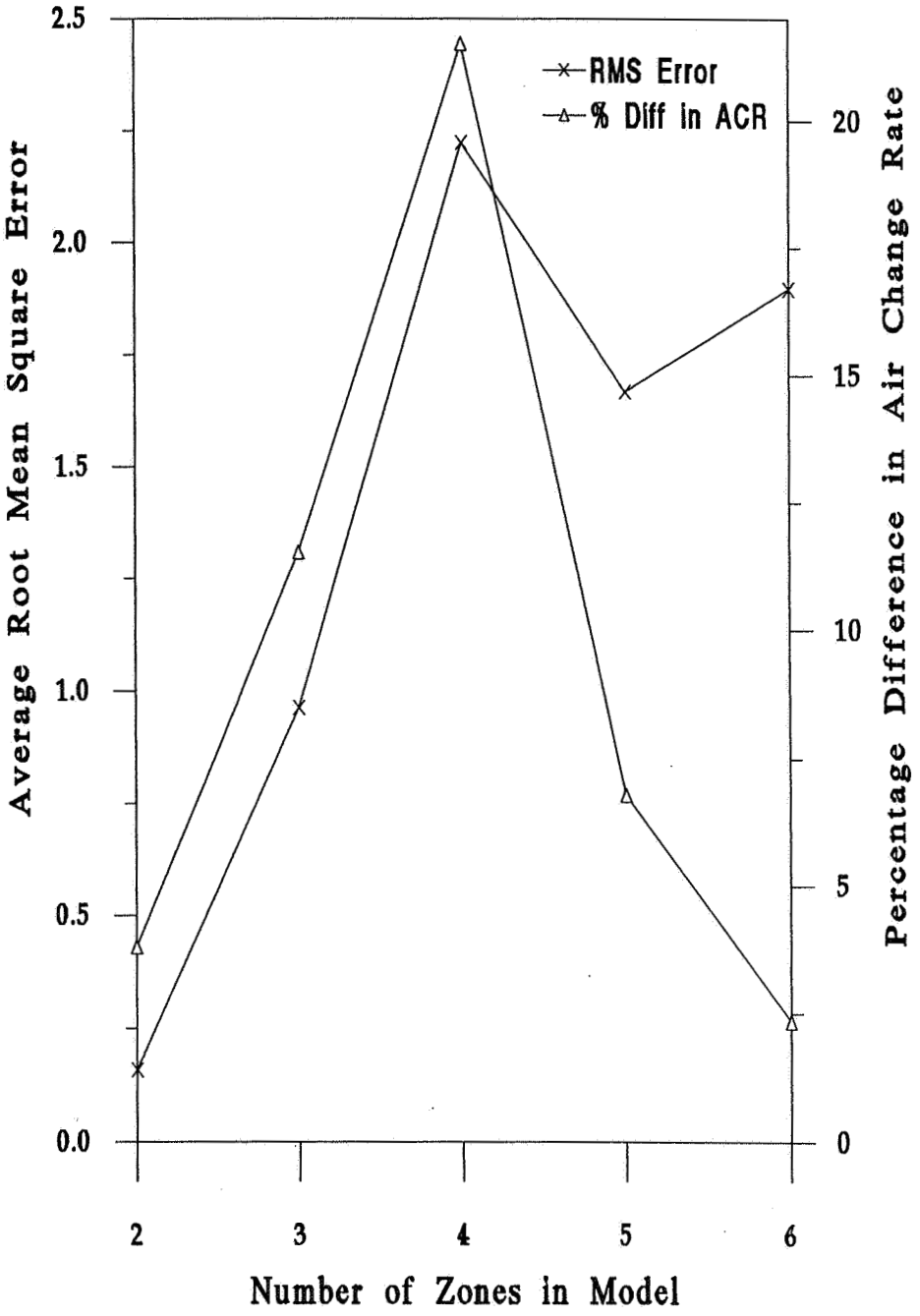

Figure 3. Average values of RMS Error and Percentage Difference in Air Change Rate for each model.

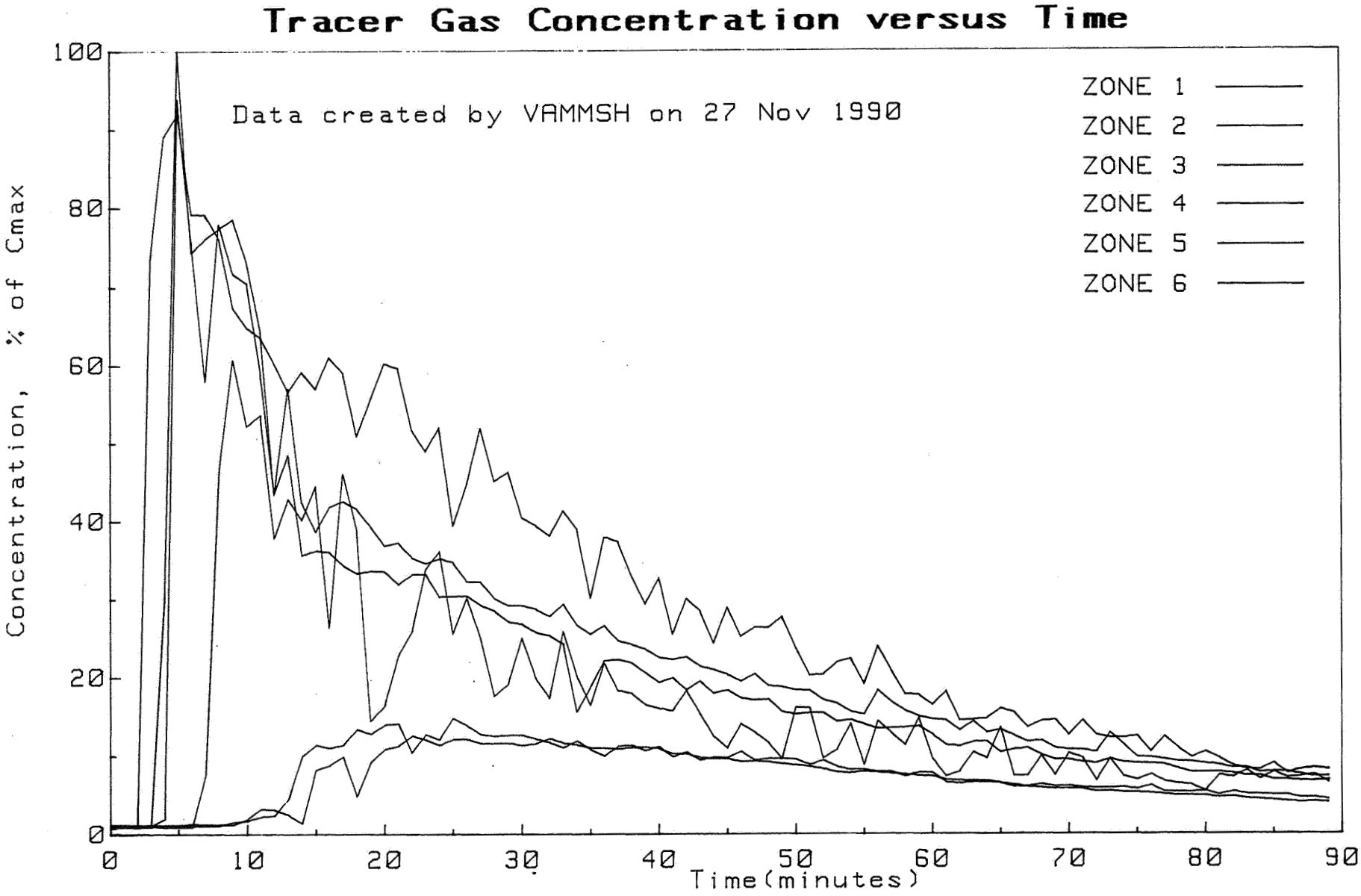

Figure 4 Typical set of decay curves for an industrial hall.

AIR MOVEMENT & VENTILATION CONTROL WITHIN BUILDINGS

12th AIVC Conference, Ottawa, Canada
24-27 September, 1991

PAPER 27

Application of Tracer Gas Analysis to Industrial Hygiene Investigations.

Richard A Grot* and Peter L Lagus**

* Lagus Applied Technology
Olney, MD 20832
USA

** Lagus Applied Technology
San Diego, CA 92121
USA

1 Introduction

This article discusses the application of tracer gas methods to industrial hygiene investigations. It introduces the basic concepts necessary to understand the application of tracer gas methods to particular airflow and contaminant movement measurements. It provides an overview of existing methods which can be used to obtain quantitative data on a variety of airflow and contaminant movement related questions which often are of interest to the industrial hygienist. A general description of each method is given, along with the pertinent equations used to extract quantitative information from the test results. Selected results from the use of each method are summarized. It will discuss the use of tracer methods to evaluate building and industrial ventilation systems and methods currently being developed to measure ventilation effectiveness. It will also discuss how to use ventilation measurement along with contaminant concentration measurements to infer contaminant source strengths. It will review the methods used to measure the performance of various systems designed to contain an airborne hazardous substance and assess the potential for spread of this substance into non-containment areas. The topics treated are the evaluation of fume hood re-circulation and re-entrainment, the evaluation of re-entrainment by building air intakes, the simulation of hazardous releases and the performance of secondary containment ventilated enclosures using tracer gases.

Tracer gas methods have been used for

- measuring building ventilation and air infiltration rates
- measuring airflow rates in ducts
- testing fume hoods for re-circulation and re-entrainment
- measuring exhaust re-circulation and re-entrainment
- estimating contaminant source strengths
- evaluating performance of ventilation systems and ventilation effectiveness
- characterizating hazardous substance releases
- evaluating temporary safe havens
- determining flow patterns and flow path tracing
- evaluating airborne hazardous substance containment
- validating models which predict airflow and contaminant levels.

Tracer gas methods have been used in office buildings, hospitals, schools, laboratories, chemical facilities, nuclear power plants, military facilities, semi-conductor fabrication facilities, pulp and paper mills, pharmaceutical facilities and petrochemical plants. In most applications, tracer gas methods are analytical tools which provide accurate means of determining airflow related parameters which are useful to industrial hygienists and in many situations are the only means of obtaining quantitative information. However, these methods are not yet widely known or used outside the research community.

1.1 Characteristics of a Desirable Tracer Gas

Though in principle any gaseous substance not normally found in the area being measured can be used as a tracer gas, the desirable properties of a substance used as a tracer in occupied buildings are that it be

- non-toxic and non-allergenic at the levels used
- chemically inert, odorless and tasteless
- non-flammable and non-explosive
- not naturally present in the building nor as a normal constituent of air
- easily transported and dispersed as an atmospheric gas
- easily and economically measured with high reliability
- measurable by established experimental techniques which preclude interference with air

- commercially available.

Historically, gases such as helium, hydrogen, methane, carbon dioxide, carbon monoxide, nitrous oxide and even radioactive gases have been used as tracers for ventilation and airflow studies. These gases obviously do not have all the properties of an ideal tracer.

1.2 Physical Properties of a Tracer Gas

Currently, the most commonly used tracers are sulfur hexafluoride, halogenated refrigerant compounds and perfluorocarbons. These gases are electronegative tracer gases which can be detected by electron capture gas chromatographs. They have most of the properties of an ideal tracer. They can be detected from the parts per million range to the parts per trillion range. There are several methods which can be used to measure tracer concentrations. These are listed in table 1. In selecting a tracer gas detector and designing one's measurement procedure several characteristics of the detector need to be considered including the range of detectable concentrations, the device's analysis time, the required airflow rate of the sampling device, and the need for expendable supplies such as compressed gas or other chemicals. Table 2 gives the relative costs for several tracer gases. As can be seen by examining the data in table 2, very large volumes can be measured at reasonable cost if gas detection equipment with measurement capabilities in the ppb or ppt range are used. Note that the column labelled "Detectable Concentration" should not be interpreted as "minimum detectable concentrations" as reported by some manufacturers but as the value at which accurate measurements (5% or less) can be made . The authors have successfully performed ventilation tests in buildings which have volumes over 10 million cubic feet. Table 3 lists the currently used tracer gases which can be used to measure airflows in large buildings at modest costs by using small quantities of tracer.

For tracer studies in commercial and industrial buildings, the ability to measure in the parts per billion range (and below) is very convenient: only small quantities of tracer need to be used, these levels are well above typical inside and outside backgrounds (with the exception of those halogenated compounds used as refrigerants), extreme care in handling of the gases is not required, and the levels are at least ten thousand times lower than accepted OSHA standard environmental levels for the respective gases.

2 The Evaluation of Ventilation Systems Using Tracer Gas Methods

This section will discuss the various tracer methods used to evaluate building ventilation systems and methods currently being developed to measure ventilation effectiveness. It will also discuss how to use ventilation measurement along with contaminant concentration measurements to infer contaminant source strengths.

In the evaluation of the performance of ventilation systems, tracer gas methods can be used for

- measuring building ventilation and air infiltration rates
- measuring airflow rates in ducts
- measuring the percentage of outdoor air supplied to the building
- measuring ability of a ventilation system to remove contaminants
- estimating contaminant source strengths
- evaluating ventilation effectiveness

The evaluation of ventilation systems in large buildings will be treated. A brief description on how to use tracer gases to measure airflows in ventilation systems, the assessment of ventilation effectiveness and the use of tracer gases in the estimation of contaminant source

strengths will be given. The inaccuracy of using CO_2 measurements for measuring ventilation rates will be discussed. Finally some examples of using multiple tracers gases for the assessment of complex airflows will be presented.

2.1 Measurement of Ventilation and Air Infiltration

Determination of the ventilation characteristics of residential, industrial and commercial structures has developed into a relatively well-known technology over the last fifteen years. Concerns of health, safety and energy conservation have largely been responsible for driving this development. Tracer gas characterization of ventilation systems has become widely accepted within the building engineering community. In fact ASTM Standard E-741 was promulgated to provide a standard method for measuring air-leakage (ventilation) rates within structures. Over ten years ago the International Energy Agency established a center for air infiltration and ventilation in the United Kingdom to which the United States is a member. This organization publishes a quarterly review of air infiltration and ventilation research and maintains a data base on air infiltration and ventilation research, publications and measurement techniques.

There are three principal techniques for quantifying the air leakage/ ventilation rates within a structure: the tracer decay method, the constant injection method and the constant concentration method. The fundamental principle underlying each of these techniques is the mass balance equation describing the release of a tracer gas in a building (see Appendix I). The critical assumption of these methods is that the tracer gas is uniformly mixed in each zone of the building and remains so during the period of measurements. The major difficulty in using the methods is usually the attainment of a state of uniform mixing. The greatest error resulting from the application of the techniques to ventilation measurements is the inability to ensure the existence of this condition by the person performing the test. However, in most practical situations, an experienced professional can achieve an adequately mixed space.

The Tracer Decay Method.
The simplest and most widely used tracer gas technique for measuring ventilation is the decay method in which a quantity of tracer is injected into the building, allowed to mix and then the decay of the tracer concentration with time is measured. The ventilation rate is in this case given by the equation

$$I = \frac{1}{t} \ln\left(\frac{C_o}{C_t}\right) \qquad (1)$$

where t is the time, C_o and C_t are the initial and final tracer concentrations respectively and I is the building air change rate. The air change or air exchange rate is the volume normalized ventilation or air leakage flow rate ($I = Q_L/V$, where Q_L is the ventilation or air leakage flow rate and V is the volume of the building or space being measured). This technique requires only the measurement of relative tracer gas concentrations after which the calculation required to determine I is straightforward. The measuring equipment can be located within the space or building. Alternately, building air samples containing tracer may be collected in suitable containers and analyzed off-site. Automated systems have been developed which can control the injection and sampling of tracer in multizone buildings and do real time analysis of the data. Figure 1 illustrates a schematic of the steps to be taken to perform an air change rate measurement using the tracer decay method. These steps are:

1. Inject tracer into the building
2. Wait for the tracer to mix

3. Collect at several samples at each location for a period of about two hours recording the time of each sample
4. Determine the concentration of each sample
5. Calculate the air change rate using equation 1.

From an industrial hygiene perspective, the significance of knowing I can be seen by recasting equation (1) into the following

$$C = C_0 \exp(-I \cdot t) \tag{2}$$

This form of the equation implies that within a room with an air change rate of 1, after one hour, an initial concentration will be diluted to 37% (e^{-1}) of its original value. In this example, if the air change rate were doubled or one waited two hours, the initial concentration would be diluted to 9% (e^{-2}) of the original value. Thus, knowledge of the actual air change rate allows an estimate to be made of the time which must elapse after a release of gas or vapor in an area before concentrations within the area are at a safe level.

Constant Injection Method

The second most common method employed to measure building ventilation rates is the constant injection method. In this method, tracer gas is injected into a test volume at a constant injection rate f while the resulting concentration is allowed to reach an equilibrium value C_∞. The ventilation or airflow rate into the test volume is determined from the relationship

$$Q = \frac{f}{C_\infty} \tag{3}$$

where Q is the airflow rate. Figure 3 shows an application of this method to the measurement of airflow in a duct. Note that this method provides a measure of the actual flow rate and not the air change rate. It does require that the measuring equipment be properly calibrated. The use of this method along with equation (3) requires that equilibrium be reached (under many situations this may take several hours for whole building measurements), and that the flows which are being measured remain constant over this period. These assumptions can be relaxed if more sophisticated data analysis and data collection methods are used. However, there are many situations under which the constant injection method has advantages over the decay method: in spaces which have high air change rates or in spaces in which the flow is directional and therefore it would be difficult to maintain the uniform mixing required in a decay test.

The results of a constant injection tracer test can be used directly to estimate the equilibrium level of a inert pollutant released by a constant source strength σ into the test volume

$$C_{pollutant} = \frac{\sigma}{Q} \tag{4}$$

where $C_{pollutant}$ is the resulting pollutant concentration.

Constant Concentration Method

The third method used for measuring building air infiltration rates is the constant concentration method. This method requires sophisticated computerized control algorithms. It is based on the principle that if the concentration of a tracer is maintained constant in a space while measuring the injection rate of tracer gas into this space required to maintain the constant concentration, then the flow of air into the space is given by the equation

$$Q_{in}(t) = \frac{f(t)}{C_{target}} \quad (5)$$

where $Q_{in}(t)$ is the airflow rate into the space from the exterior, C_{target} is the controlled level of tracer and f(t) is flow rate of tracer required to maintain the target concentration at the time t. This method has the advantage of being able to measure the amount of air entering a specific zone of a building from the outside.

2.2 Instrumentation Required

Figure 2 outlines the instrumentation required to perform a tracer gas test of a building ventilation system. The basic instrumentation and materials required to perform tracer gas evaluation of ventilation systems are 1.) suitable quantities of tracer gases, 2.) a tracer gas concentration measuring device, 3.) air sampling and sample collection system, 4.)tracer gas injection systems and 5.) a data acquisition and control system. The sophistication of the system depends on the application. It can be as simple as series of air sampling containers and syringes with all analysis done in a laboratory off-site or as complicated as automated micro-processor controlled injection, multi-point sampling, data analysis and recording system used to generated data unattended over long periods of time.

In general, the evaluation of building ventilation systems requires the measurement of tracer concentrations over time at several locations in the building. This requires an air sampling system or network. The complexity of this sampling network can vary from simple manual collection systems using syringes or air sample bags to complex permanently or semi-permanently installed network of tubing, sampling manifolds and sample pumps which bring air samples from remote locations to a central point. In mechanically ventilated buildings, the building air handling system can be used as a sampling network. The decision on which type of system to use depends on the goals, resources and accuracy required by the investigation and the complexity of building being evaluated. If one requires only a one-time evaluation of a system, manual collection of data is usually the most cost effective, though in complex facilities this procedure is labor intensive.

A method for the injection of tracer into a building is also required. In mechanically ventilated buildings the injection is usually accomplished using the building air handling systems. The tracer is injected into each air supply system. In complex, compartmentalized buildings individual injections into each zone of the building is often the only method which can be used for injection of tracer. It should be emphasized that the injection of tracer into the building must be planned carefully if uniform initial concentrations are to be obtained in a reasonable length of time. This is often overlooked in the technical literature where emphasis is usually given to mixing devices such as circulating fans. The steps in planning an injection strategy for an investigation are: calculate the volume of each separate zone of the building, determine which zones are served by which air handling systems, determine the target concentration desired and calculate the quantity of tracer needed to reach the target concentration. In manual injection, it is good practice to use partial injections of the tracer in many locations in the volume being studied in order to obtain uniform mixing quickly. When using the building ventilation system, inject the tracer over a period of at least 5 minutes unless one is performing pulse tests. Certain safety considerations should also be considered. The indoor air quality concentrations should not be exceeded for the tracer used. This means that one should keep the level of a tracer to less the 1/10th its TLV and it is good practice to keep it below 1/100th its TLV. If automated injection systems are used, a safe design requires that 1/10th the TLV not be exceeded even if all tracer in the container is released at once.

2.3 Measurements in Large Buildings

This section will discuss the application of tracer gas methods to the measurement of ventilation rates in large buildings. There are two general categories of large buildings: highly compartmentalized buildings with many individual zones each served by individual ventilation equipment and buildings, though large, that are served by only a few air handlers. Figure 3 shows a schematic of an elementary school (highly simplified, the actual school had over 30 individual rooms). Each classroom as well as the cafeteria, office, gym, music room and hall were served by a separate ventilation system. The purpose of the test was to determine if the minimum setting of the ventilation systems provide sufficient outdoor air for the students. The only practical way to test this building was to use manual injection and sampling. The procedure which the authors used was to calculate the volume of each "zone of the building" and then use this volume to calculate the quantity of tracer which should be injected into each zone to produce an initial concentration of 10 ppb - at the upper end of the linear range of the monitor used. The determined quantity of gas was injected by the authors and a custodian of the school over a period of a few minutes. A period of one half hour was allowed for the tracer gas to mix in the space. For the next two hours the tracer decay was monitored by collecting 60cc syringe samples in each room. The results of this test are shown in Figure 4. It was planned to collect 4 samples per decay; however the collection of samples was interrupted for a period of about hour due to changing of custodians and only three samples were collected in some rooms. With four data points, there was no problem accurately determining the air change rate in a room. With three data points, if they did not lie on a straight line as for classroom 105, a large error or uncertainty occurred in the measurement (the numbers in parentheses in Figure 4 are the errors in the air change rate). For the gym which also only had three data points, they all lay on a straight line and therefore an accurate measurement could be made.

Figure 5 shows a schematic of a typical office building HVAC system in which a few large air handlers provide air to large zones of the building. In such a building the air ducts can be used for the injection and sampling of tracer in the building. In such a system, tracer is injected into the supply air and sampling is done in the return air. Figure 5 shows typical injection and sampling point for such a test. Figure 6 showed the tracer concentrations in the space measured with an automated tracer monitoring system. The economizer cycle is in operation during the test. The ventilation rate during the day varied from approximately 1.3 to 2.0 air changes per hour. The air change of rate when the fans were off was approximately 0.3 changes for the previous night and 0.13 the next night.

It should be noted that the ventilation and infiltration rates can be highly weather dependent. The building ventilation and air infiltration rates for the above office building are shown in Figure 7 as a function of inside-outside temperature difference. Building ventilation rates (open diamonds) are between 0.4 to 2.2 air changes per hour during periods when the building is occupied with the most typical values being about 1.0 to 1.2 air changes per hour. The extreme of 0.4 occurs during extremely hot summer conditions or extremely cold winter conditions. For comparison, the new ASHRAE ventilation standard requires 20 cfm per person for office buildings. This is equivalent to 0.8 to 0.9 air changes per hour if the building is occupied at a density of one person per 135 $ft.^2$ and if the 20cfm requirement is to be satisfied.

The building air leakage (uncontrolled air exchange when the HVAC fans are off during unoccupied hours - solid squares) is between 0.2 and 0.4 air changes per hour. This is a building designed to be energy efficient and these values indicate that the exterior walls of the building are not tight by what we would consider typical of US office buildings. (Note: The surface to volume ratio of an office building is about 1/6 th that of a home. Therefore the walls of this building are equivalent to the walls of a house with an air leakage of about 1.2 to 2.4 air changes per hour - very loose).

A detailed examination of the data shows that the air handling system can easily control the amount of air required for the building. The outside air is well distributed and there is little or no evidence of short circuiting of the outside supply air or poor mixing due to the operation of the variable volume air handling system. In the summer and warmer periods of the fall and spring the typical operational mode of this air handling system runs the system at 100 percent outside air from early morning to a point in the day when the outside temperature reaches about 26 degrees C at which point the system is run at between 10 to 20 percent outside air. In the winter an economizer mode of operation is used in which the amount of outside air was determined by the cooling requirements of the building.

Figure 8 summarizes the results of the weather dependence of the building ventilation rate in eight federal office buildings. With the exception of the Federal Building in Springfield, MA , these buildings exhibit the phenomenon of low ventilation in hot summer conditions (the Anchorage building never reached those conditions) and cold winter conditions. In buildings with leaky exterior envelopes, in very extreme winter conditions, the exchange rate is dominated by natural infiltration and will increase with decreasing exterior temperature (see the paper by Grot and Persily [1985]).

2.4 Measurement of Airflows in Ventilation Systems

Tracer gas measurements can also be used to measure and characterize airflows in ventilation systems. The details of the procedure used depends on the building ventilation system. Figure 9 shows a schematic of a commonly encountered office ventilation system with recirculation. Since much of the building air is recirculated, typical air balancing procedures cannot be used to determine the amount of outside air supplied to the space. This can be done with a tracer gas using the procedure shown in Figure 10. Tracer is injected at a constant flow rate into the supply duct of the building. Tracer concentrations are measured upstream and downstream of the injection point in the supply duct, in the space of the building and in the return air. Using mass balance equations, one can determine the air supply flow rate, the percent of outside air supplied and the percent of building air infiltration. This method is more accurate then those typically used by air balancing technicians. The amount of exterior air reaching a zone can also be determined by measuring the concentration increase caused by an injection of a known amount of tracer in the building supply air.

2.5 Ventilation Effectiveness

There has been great interest in the ventilation research community over the concept of ventilation effectiveness and ASHRAE currently has a standards committee which is developing tracer gas test methods for assessing ventilation system effectiveness. The industrial hygienist should be aware that there is still considerable technical discussion of the concept of ventilation effectiveness and how it is to be measured. If one reviews the technical literature on the subject, there are probably over twenty different definitions of ventilation effectiveness. There are however two which seem to be used more frequency

than others: the concept of concentration or extraction efficiency and the local age of air definition of ventilation effectiveness. To measure the concentration or extraction efficiency, a constant injection test is performed with the tracer source in the occupied space. When equilibrium is obtained, the tracer concentrations are measured in the occupied space and in the exhaust air. The extraction or concentration efficiency ε_j at a location j is defined as

$$\varepsilon_j = \frac{C_{exhaust}}{C_j} \tag{6}$$

where $C_{exhaust}$ is the exhaust air tracer concentration and C_j is the tracer concentration at a location j in the space.

The age of air definition of ventilation effectiveness attempts to determine how long a package of air remains in a space. This is accomplished by creating an uniform concentration of tracer gas in the space by using a constant injection of tracer into the building supply air. The injection of tracer is turned off and the average concentration of the tracer during the decay at a given location is measured using a integral sampling technique. The local mean age of air is defined as

$$\tau_j = \frac{\int C_j(t)dt}{C_j(0)} \tag{7}$$

where $C_j(0)$ is the initial tracer concentration. The local ventilation efficiency is defined as

$$e_j = \frac{\tau_n}{\tau_j} \tag{8}$$

where τ_n is the inverse of the whole building air change rate.

2.6 Ventilation Performance from CO_2 Measurements

Many industrial hygienists have been using $C0_2$ measurements to estimate building ventilation rates. A detailed check of this procedure has been undertaken by the National Institute of Standards and Technology (Persily and Dols [1990]). They found that this technique is not reliable when the building is occupied. During periods when the building is unoccupied, the decay of CO_2 will yield an estimate of the building ventilation rate if sufficient CO_2 remains in the building. Figure 11 shows a typical weekly and daily profile of CO_2 levels in the Portland Federal Building. Note that steady state is never obtained. This non-attainment of equilibrium leads to a large over estimate of the ventilation rate occurring in the building.

Figure 12 shows the maximum daily CO_2 level as a function of air exchange rate. Carbon dioxide levels are seldom over 600 ppm on a building average and only a couple of times ever over 1000 ppm at any location in the building. (The new ASHRAE standard proposes a maximum level of 1000 ppm; complaints from building occupants begin to occur when levels exceed 600 ppm). A closer examination of the hourly CO_2 levels in the building shows that the measured levels are never at steady state and usually have two daily peaks - one around 11 am and the other around 3 pm. This is also shown by the values of the source strength constant of the fitted curve in Figure 12. The value of

source strength constant, 100 ppm per hour, is approximately 1/3 the value of the source strength constant derived from equilibrium theory based on the occupancy of the building.

Carbon dioxide levels can be used to indicate that a ventilation systems is not performing properly; however they cannot be used to give a accurate value for the building ventilation rate.

2.7 The Estimation of Contaminant Source Strengths

It is possible to use tracer gas measurements along with pollutant measurements to estimate contaminant source strengths. The contaminant source strength can be defined as

$$\sigma_{pollutant} = \frac{\Delta C_{pollutant}}{Q_{in}} \tag{9}$$

where $\Delta C_{pollutant}$ is the difference between the interior and exterior pollutant concentrations and Q_{in} is the total inflow rate measured by a tracer test for the space.

Figure 13 shows the effect of building ventilation rate on the total VOC concentration. Table 4 gives the effect of ventilation rates on the individual compounds detected in the building. The measurements were made on four different occasions over a period of 17 months (see Grot et al., 1987 and Hodgson et al., 1990). On each of these dates the building was being operated with four distinct air exchange rates (0.5, 1.36, 0.24 and 1.99 changes per hour) due to the prevailing exterior weather conditions. The curve in Figure 13 represents the predicted level of VOC's in the building using the source strengths estimated from the VOC levels and the air change rates. The source strength of total VOC was remarkably constant over the 17 month period between the first and last measurements. We have measured and identified 37 volatile organic compounds in the interior building space. These are given in Table 4. There were 5 oxygenated compounds, 6 halogenated compounds, 16 alkanes, 6 cycloalkanes and alkenes, and 5 aromatic hydrocarbons found in the building. All are at levels less than 1/1000 th of the OSHA standard environmental levels of industrial work spaces. (Note: The ASHRAE standard recommends that for indoor air quality the level be not more than 1/10 of OSHA SEL's.) The largest amount of the mass of the VOC's is concentrated in the alkane class (C_{10} to C_{12} branched decanes and undecanes). These are not particularly irritating compounds and there are no OSHA recommended levels for these substances. However very limited studies done in Denmark by Molhave [1983] indicated that many complaints will occur when the total levels of VOC's exceeds 5 mg/m^3 and it has been recommended by researchers (Tucker, 1988) at EPA Research Triangle Park that a prudent target level for total VOC's be 1 mg/m^3. All four measurements sets that were made in the building were greater than 1 mg/m^3 and the building exceeded 5 mg/m^3 when the ventilation rate was below 0.5 air changes per hour. Though operating the ventilation system at 100 percent outside air would keep the levels near the target of 1 mg/m^3, identification and limitation of the sources is a better strategy.

Figure 14 shows the short term variation in VOC source strengths over a period of four days, beginning at 6 am on Friday before the building was occupied, carrying over the weekend when only a few occupants were in the building and continuing till 6pm on Monday. It is clear from the data in Figure 14 that the source strengths were greatest during the occupied day and low in the evenings even when the HVAC was off and on the weekends when few people were in the building. Therefore the source of VOC's was

activity related and closer comparison of the chromatographs of samples in the building and those of the liquids used by the copiers in the building confirmed that the liquid copiers were the major source of VOC's.

2.8 Multi-Tracer Techniques

The above tracer gas measurement techniques generally employ a single zone model of a building. In some cases, a single zone is not adequate to model a building's infiltration characteristics, or one is interested in the airflows between various zones of a building. In these cases, multi-chamber building models and multiple tracer gas measurement techniques are used. The use of multiple tracer techniques for building airflow studies began in the middle seventies. A table of tracer gases that have been used in ventilation measurement applications has been provided in table 3. Multiple tracer measurements often involve the use of gas chromatographs designed to determine simultaneously the concentration of the different gases; however, separate continuous infrared analyzers have also been successfully used for simultaneous analysis of SF_6, CO_2 and N_20 (Perera et al. 1983).

An illustration of the simultaneous chromatographic separation of six refrigerants is provided in Figure 15. Note that the time for a single measurement of the six gases is on the order of ten minutes. A throughput time of this magnitude may preclude the use of a single gas chromatograph in a constant concentration measurement. If one desires analysis times on the order of minutes, it is necessary to have several gas chromatographs available.

Multiple tracer gas measuring systems have been developed using both decay and constant injection techniques. In decay measurements, a tracer or several tracers are released at various locations as pulses (see Axley and Persily, 1990), and their concentrations are monitored in the various zones over time. Several measurement systems employing the decay method have been developed, including those of Prior et al. (1983) and Irwin et al. (1984). Both systems employ electron capture detectors, to measure refrigerants in the first system and perfluorocarbon tracers in the latter. I'Anson et al. (1982) also employs a decay system involving refrigerant tracers. In Figure 16 we show representative data from their paper in which two tracers are used to study the airflow between the upper and lower levels of a building. The refrigerant $C_2Cl_2F_4$ is injected downstairs and CCl_2F_2 upstairs. The movement of tracer between the zones and the subsequent decay is evident in the data. Analysis of these data yields the airflow rates between the two zones and from each zone to the outside.

A constant injection technique has been employed by Dietz and Cole (1982) and Dietz et Al. (1984a) using several perfluorocarbon tracers and passive samplers. In these measurements a different tracer is released at a constant rate into each zone and the average concentration in all zones is determined over the measurement period. From the injection rates and the average concentrations, one determines the airflows of interest. An example of this technique was given in the first article. This technique is used for long term studies of air infiltration behavior, consequently it is not generally useful in industrial hygiene applications.

There have been other multiple tracer studies including those of Foord and Lidwell (1973 and 1975) studying ventilation rates and interzonal airflows in hospitals. Lagus (1977) suggested the use (shown in Figure 17) of multiple tracer gases in multistory buildings for evaluating simultaneously infiltration rates on individual floors and airflow rates between floors by injecting a different tracer on each of three adjacent floors. Figure 18 shows an example of a constant injection measurement of ventilation and interzonal airflows in two adjacent, negative pressure laboratory rooms (Lagus 1984). The two laboratories are

each under negative pressure, and a different tracer gas is injected into each laboratory at a constant rate. Using the equilibrium concentration values, along with the known injection rates for the tracers, it is possible to calculate ventilation rates using equation (I-9) given in the appendix. The equilibrium tracer concentrations are shown in Figure 19. The measured airflow rates agree well with the ventilation rates measured by tracer decay. In addition, note the flow of the refrigerant $CBrF_3$ into the lower laboratory. Since the ventilation rate is now known on the lower floor, the steady value of $CBrF_3$ concentration in the lower floor, coupled with the measured value of the concentration in the upper floor, allows one to calculate leakage flow from the upper floor to the lower floor. This evidence of undesired airflow between the laboratories led to the laboratory owner taking remedial action. Similar analyses can be extended to additional floors or zones using additional tracer gases. However, the experimental complexity of these measurements usually requires the supervision of an experienced investigator. Nevertheless, in those cases where multiple flow regimes need to be analyzed simultaneously, a multiple tracer technique is perhaps the only valid experimental approach. A detailed description of this method is beyond the scope of this article. Industrial hygienists should be aware that these interzonal airflow measurements can be made if required. However, in most situations, methods described below will provide more direct answers to contaminant transport or containment questions.

3 Airborne Hazardous Substance Assessment By Tracer Gas Methods

This section will present a description of several applications of tracer gas analysis to evaluate the performance of ventilation systems used for hazardous substance or contaminant containment and to investigate airflow patterns induced by these systems. Within this general area, tracer gas methods can be used to:

- Evaluate the performance of secondary ventilation systems used for hazardous containment.
- Delineate airflow patterns to allow proper placement of health and safety monitors.
- Document the existence of and provide quantitative estimates of potential hazardous gas or vapor leakage from one area to another.
- Evaluate areas within buildings for suitability as temporary safe havens.
- Document the existence and magnitude of exhaust gas re-circulation and re-entrainment within occupied buildings.

Each of these topics will be discussed below.

3.1 Fume Hood Re-Entrainment and Re-circulation Testing

Fume hood re-circulation studies are normally performed by injecting a known flow rate of tracer into a fume hood and then monitoring the room surrounding the fume hood for the presence or absence of tracer gas. Injection into the fume hood is performed by using a cylinder of diluted compressed tracer gas as a source. Figure 20 provides a schematic drawing of the tracer source cylinder within a fume hood. The flow rate of tracer is controlled by an orifice or an electronic mass flow controller. The fume hood duct concentration is

$$C_{duct} = \frac{C_{tracer} \times Q}{F_D} \qquad (10)$$

where

Q = Tracer injection rate
C_{duct} = Fume hood concentration
C_{tracer} = tracer injection concentration
F_D = Duct flow rate

To check for re-circulation, samples of laboratory air are obtained at a number of locations over a limited time period and are analyzed for the presence or absence of tracer. If a concentration of tracer , C_{lab}, is measured within the laboratory, this implies re-entrainment or re-circulation of fume hood exhaust. The ratio of the laboratory concentration to the duct concentration yields a measure of the dilution of the stack effluent

$$D = \frac{C_{lab}}{C_{duct}} \tag{11}$$

where D is the dilution ratio.

Knowledge of this dilution ratio allows assessment of the potential for hazard to laboratory personnel from a particular species being exhausted through the fume hood. This ratio is applicable to all non-reacting species. Thus a dilution ratio measured by the tracer technique can be used to estimate concentrations of hazardous gases and vapors which may be released in the fume hood being studied. The results of the test can be used to adjust the fume hood exhaust to an optimal level, ensuring the safety of the workers at a minimum expenditure of energy.

The evaluation of fume hood containment using a tracer gas was pioneered by Caplan and Knutson. The American Society of Heating, Refrigerating and Air-Conditioning Engineerings (ASHRAE) promulgated the standard ASHRAE 110 for evaluating fume hoods using the methods developed by Caplan and Knutson. In this test procedure, a mannikin is placed in front of the fume hood and sampling for the tracer is done in the region near the mannikin's face.

This technique has led to an increased understanding of the influence of the user and the local ventilation system on the performance of fume hoods. Unfortunately, this technique only addresses the problem of the adequacy of the fume hood to contain flow within it.

There is a second and potentially more important question which can be also addressed with a tracer technique, namely how much, if any, of the effluent being contained and exhausted by the fume hood is making its way back into the laboratory, laboratory building, or surrounding buildings?

The return of exhausted gas into the building or laboratory is known as re-circulation or re-entrainment. While the words are often used interchangeably, in this article, re-circulation will be taken to mean exhaust gas which enters the building (or laboratory) before it is expelled to the outside air. Re-entrainment will be taken to mean exhaust gas which has been expelled from the building through a vent or duct and subsequently reenters the building due to wind induced airflow patterns around the building.

A simple constant flow tracer test can be used to investigate and quantify potential re-circulation and re-entrainment of fume hood exhaust. Tracer is injected into the fume hood and the surrounding area is sampled for the presence of tracer gas. Injection can be either continuous or pulse as described in the first article. Sampling can be effected by either grab samples or time averaged bag samples.

Table 5 presents the results of tracer re-circulation tests performed for a research laboratory building. Data are presented as dilution ratios as described in the first article. A total of 32 fume hoods were evaluated. Of this total, 7 hoods evidenced measurable re-circulation. In order to eliminate the possibility of back streaming of tracer from the hood into the laboratory, tracer was injected directly into the exhaust slot at the top of the flume hood enclosure. The measured dilution factors ranged from roughly 700 to 7000. Note that re-circulation was measured not only in the rooms containing the hoods, but in 4 cases, measurable tracer was found in adjacent rooms. All of the hoods were of an older design in which a booster fan is located in the ductwork immediately above the false ceiling in the laboratory. The run of duct immediately downstream of this booster is therefore under positive pressure and is the most likely source of exhaust re-circulation. From these measured data one can calculate the potential hazard for any assumed release within the fume hood. For instance, for several of the hoods tested a release of bromine into the hood sufficient to result in an exhaust duct concentration of 1000 ppm would result in the re-circulation of approximately 1ppm of bromine into the lab rooms. This concentration could present a health hazard and as such would require remedial action.

3.2 Evaluation of Exhaust Re-Entrainment and Re-circulation

Figures 21 and 22 show two examples of exhaust re-entrainment and re-circulation in a building. Figure 21 shows the re-entrainment from an exterior contaminant source, while Figure 22 illustrates re-circulation caused by the re-entrainment of a building exhaust. Both situations can be tested using tracer methods which will provide quantitative information to assist in evaluating the potential hazard due to re-entrainment. There are two methods which can be used to evaluate this re-entrainment: the steady state method which consists of injecting tracer gas at a constant flow rate in the vicinity of the source being evaluated and the pulse technique in which a specific quantity of tracer gas is injected in a manner consistent with an anticipated occurrence of the spill or exhaust of contaminant at the source. The first method yields a worst case evaluation of re-entrainment; the second more closely mimics a spill or inadvertent release and yields an estimate of the resulting dosage to which a person would be subjected. In the steady state method, the concentration at various parts of the building and in various air intake ducts is measured. Several useful measures can be derived from these tests. In the case of an air intake duct, the percent of exhaust re-entrained can be calculated from the equation

$$\% = \frac{F_D \times C_D}{Q_s} \qquad (12)$$

where

F_D is the duct flow rate
C_D is the tracer concentration in the duct
Q_s is the source flow rate of tracer

In many buildings, the air intakes are not the only location of re-entrainment. Areas of the building under negative pressure such as return air plenums, elevator shafts, entrance ways and points of air infiltration can also cause contaminant re-entry into the building.

The second method of evaluating the potential for re-entrainment is to inject a pulse of tracer and measure the integral of the concentration over the period of time for which exposure is to be evaluated. This can be done either by using a continuous monitor at each location or by employing an integrated sampling method such as the filling of a sample bag with a constant flow pump at a given location. The specific dosage of tracer at a given location in the building is determined by

$$d = \frac{C_{bag} \times t}{m_{tr}} \tag{13}$$

where

d is the dosage
C_{bag} is the concentration in the bag
t is the length of the time interval
m_{tr} is the mass of tracer injected

The dosage caused by any spill of a hazardous substance of mass M_h is then given by

$$dosage = d \times M_h \tag{14}$$

One drawback to the pulse test is that the result of a single measurement is much more dependent on local wind conditions than for a steady state test.

Table 6 gives the results of a re-entrainment test performed in a school in such that were indoor air quality problems. Each classroom of the school was serviced by a combination ventilation and heating/cooling unit (see Figure 26.). The flue for the gas heater in the HVAC unit was located on the opposite side from the air intake. The flue gas was exhausted by a power blower downward toward the roof surface. Several of these units were located on the roof of the school in close proximity to each other and at times under a parapet with the exhausts and intakes of adjacent units near each other. The data in Table 6 show that about 0.1 to 0.2 % re-entrainment of the flue gas through the air intakes of units adjacent to the fired gas heater in unit C. After a half an hour, the concentration of tracer in each classroom resulting from flue re-entrainment was measured. If these data are used in a mass balance model, the amount of tracer entering each room is about five times greater than the quantity entering through the air intake (0.8% to 1.6% of the quantity of tracer released). There seems to be a hidden leakage under the unit into the return air plenum serving the classrooms which is being re-circulated to the interior of the classrooms.

An estimate of the level of pollutants in the classrooms generated by the gas heater due to re-entrainment of the flue gases can be derived using the data from re-entrainment tests and data from ventilation tests by considering typical emissions from a convective gas heater. The steady state level of the pollutant in the room can be determined from the equation:

$$C = \frac{G \cdot D}{ACH \cdot Vol} \tag{15}$$

where:

C is the pollutant concentration in mg/m^3
G is the pollutant generation rate in mg/hr
D is the measured dilution ratio
ACH is the air change rate in air changes per hour
Vol is the volume of the room in m^3

The worst case of re-entrainment in this school, 4.4%, was measured for classroom K. Table 7 gives the results of a typical use of measured dilution ratios and room air change rates to estimate the levels of CO_2, CO and NO_x which could result from the enter of flue gas into the classrooms.

3.3 Hazardous Substance Containment Testing

Tracer gas methods can be used to test the integrity of a hazardous substance containment system or a secondary containment ventilation system. Figure 23 shows a schematic of a test procedure for implementing a secondary containment ventilation system test using a tracer gas. Monitoring is implemented by injecting a constant flow of tracer into a hazardous containment area and monitoring the periphery for the presence or absence of the tracer. If no tracer is found within the non-hazardous periphery, no breach of containment has occurred. If tracer is detected within the non-hazardous area of the facility, this presents unambiguous evidence of a containment breach. The magnitude of the tracer concentration yields quantitative information on the magnitude of the integrity breach. If the ventilation rate of the non-hazardous area is known or measured, then an effective leakage rate of the breach can be calculated. The effective leakage rate can be defined as the fraction of total leakage from a containment area into a non-containment area. The effective leakage rate is given by

$$L_{eff} = \frac{C_p}{C_{con}} \times I_p \tag{16}$$

where

L_{eff} is the effective leakage rate
C_p is the tracer concentration in the non-hazardous area
C_{con} is the tracer concentration in the containment area
I_p is the ventilation flow rate in the non-hazardous area

If it is desired to know the probable concentration of a given airborne contaminant at a number of locations which are separated from the containment area, but for which there exist potential flow paths, tracer concentration measurements can be made at these locations and a dilution ratio calculated

$$D_{loc} = \frac{C_{loc}}{C_{con}} \tag{17}$$

where

D_{loc} is the dilution ratio
C_{loc} is the tracer concentration at the location of interest
C_{con} is the tracer concentration in the containment area

The dilution ratio at a given location can be used to assess the hazard to persons working at that location if the concentration of the hazardous substance in the containment area is known.

Figure 24 depicts the use of tracer to test for the leakage from a hazardous area into a control room. Release of a tracer at a constant flow rate in the hazardous area, coupled with measurements within the controlled area, can be used to evaluate the potential hazard to persons working in the control room and to assess the ability of the containment system to protect the control room personnel.

Figure 25 suggests a method for measuring and locating leaks in a fresh air supply duct to a control room. In many HVAC systems, especially in return air and fresh air supply ducts which are under negative pressure with respect to areas through which they pass, inadvertent and non-design leakage can be a problem if these ducts pass through hazardous areas. A constant injection of tracer into the duct, followed by subsequent measurements along the duct, affords both the measurement of the flow rate through the duct and the possibility of locating the major leakage points.

In many cases a room, such as a control room or a computer room in a process plant, is isolated in a ventilation sense from the remainder of the plant. Since duct work is seldom truly leak tight, it is possible for inleakage into the return portion of the control room ductwork to engender measurable concentrations of hazardous gases or vapors within the control room.

A tracer test can be used to measure the amount of unwanted inleakage into the control room. Knowledge of this inleakage, as well as any potential hazardous concentration in the area of the return ducting, allows calculation of actual hazardous concentrations (and hence exposures) within the control room.

A typical scenario is presented in figure 23. A uniform tracer concentration is established in the volume surrounding the return duct, and any resulting tracer concentration in the control room is measured. A schematic of the actual ventilation flows in a typical control room is presented in figure 27. Note that the makeup air is provided from outside the HVAC Equipment Room. For the test shown in figure 23, there was concern about potential contaminants within the HVAC Equipment Room migrating to the Control Room via return duct inleakage. A uniform tracer concentration was established within the HVAC Equipment Room and the resulting tracer concentration within the Control Room was measured. The fact that ANY tracer was measured in the Control Room established that Control Room inleakage via the return duct could result in contamination of the Control Room.

A simple mass balance, keyed to figure 27, yields the equation

$$Q_{\text{in}} = \frac{(C_s \cdot Q_s - C_r \cdot Q_r)}{C_{hvac}} \tag{18}$$

where

Q_{in}= Control Room inleakage rate

Q_s = Flow rate in Control Room Supply Duct

Q_r = Flow rate in Control Room Return Duct

C_s = Tracer Concentration in Control Room Supply Duct

C_r = Tracer Concentration in Control Room Return Duct

C_{hvac} = Tracer Concentration in HVAC Equipment Room

Measured data for this test are provided in Table 8. The inleakage shown was for a run of duct approximately 100 feet long. Though this example was for a control room, it could easily apply to inleakage of corrosive compounds into a control computer room in a chemical process plant.

3.4 Airflow Pattern Testing/Hazardous Substance Migration

Perhaps the simplest use of a tracer gas is to track the airflow patterns within a complex industrial environment. In Figure 28, we illustrate the use of a tracer to provide both qualitative and quantitative information about the flow patterns within a chemical process facility which was designed to destroy quantities of obsolete toxic material. In the facility shown, toxic materials enter through the Supply Conveyor Room. The toxic materials were utilized in small containers, a number of which were in turn stored in larger transportation casks. The material within the individual containers was in a liquid state, but its vapor was extremely toxic. Within the plant, incoming transportation casks were received and stored in the Supply Conveyor Room. The transportation casks were then transferred into a negative pressure glove box where they were opened. The smaller containers were taken out of each

cask inside this glove box. From here the containers were conveyed to a rotary kiln for destruction. The kiln was located in an adjacent building. Health and safety monitors were located at locations B and E in Figure 28. In order to assess the potential hazard that a leaking cask in storage could pose to unprotected personnel in the Disassembly Room, a test was performed in which a constant flow of sulfur hexafluoride tracer gas was injected into the Supply Conveyor Room to simulate a leaking cask. Grab samples were taken throughout the Disassembly Room and analyzed for the presence of tracer gas. Results are provided in Table 9. Note that the tracer concentration within the Supply Conveyor Room was not greatly diluted by flow into the Disassembly Room. Furthermore, the concentration at location B was lower than practically any where else in the room, even though this was the location of one of the two health and safety monitors. Additional tracer gas measurements showed that it took approximately 4 minutes for the concentration at location G and D to become substantial while it took roughly ten minutes for the concentration to rise to a comparable level at both locations E and B. Thus by means of a simple tracer test, it was possible to quantify the hazard within the Disassembly Room due to leakage of vapor within the supply conveyor room and to evaluate the appropriateness of the location of the health and safety monitors within the facility.

In industrial facilities health and safety monitors (chemical, hazardous vapor, or radiation) are often located for the convenience of installation and maintenance personnel in the absence of more compelling data such as the tracer data presented above.

The concept of using a tracer to examine flow patterns can be expanded to encompass the investigation of multiple flow paths simultaneously. All that is required is a distinct tracer gas for each flow path to be investigated. For the purposes of the test a flow path may be an identifiable path or it may be a single air handling unit within a complex building. Practically speaking, testing with more than three or four gases simultaneously is very tedious and time consuming. The data, however, can be extremely informative.

An example in which three flow paths were tracked simultaneously using three tracer gases (Halocarbon 13Bl, Halocarbon C-318, and Perfluorodimethylcyclobutane, PDCB) is provided in figure 2 (Lagus et. al, 1988). This shows one level of a seven storey auxiliary building within a plant complex. Tracer source locations are marked by large letter S's, while sampling locations are marked by X's. Source injections were performed continuously over a period of four hours during which time grab samples were taken throughout the building at distinct locations at selected timed intervals. These samples were then analyzed on-site for the presence of tracer gas.

The requirement for this testing arose due to the discovery of occasional episodes of higher than expected concentrations of hazardous gases at locations that should not experience such levels with the ventilation in its normal mode. The tracer source locations were chosen to correspond to locations which could act as sources for the gases. The ventilation system was designed to contain the hazardous gases in these areas. In Figures 29 and 30, the solid arrows denote the anticipated flow directions based on the design of the ventilation system. The dashed arrows show the actual flow directions as discerned by the tracer measurements. It is apparent that for some of the locations the ventilation system was not performing as designed. It should be emphasized that immediately prior to performing these tests, the entire building ventilation system had been balanced by a licensed test and balance (T&B) contractor, thus the flow directions actually observed are not due to the system being out of balance.

For several of the flow tests performed, tracer concentrations were measured on adjacent floors implying the existence of flow or migration between floors. Gas migration was also seen to occur up the stairwells. For some of these cases it was possible to quantify the amount of flow entering particular areas on the adjacent floor. An example of tracer data which can be used for this type of interpretation is shown in Figure 31. In one particular room of interest, an inleakage of 3 cfm was detected during this testing. Note that the transient build-up of concentration shown in figure 4 has gone to completion and that the resulting tracer concentrations are approximately steady state. Reference to the discussions surrounding equation (16) apply to these types of problems, and the mathematical analysis presented there, allows one to calculate leakage flow rates into selected rooms. This technique can be extremely useful when an estimate is required of the potential threat created by the accidental release of a hazardous gas or vapor within an area of a plant. It is important to realize that the simple interpretation described in the first article cannot be undertaken if the tracer concentrations are changing as a function of time.

Another useful assessment of the performance of this same auxiliary building ventilation system was made by placing the building ventilation system in its emergency mode. By design, in the emergency mode, the ventilation system splits the building into two zones separated at the fourth level. The idea is that in the event of a malfunction, the lower floors could become contaminated. Hence, any air in this region should not interact with air above the fourth level. It is passed to the outside through an elaborate filter system. The question naturally arose during the course of these measurements as to the degree of ventilation isolation. Accordingly, a massive tracer release was undertaken in the lower floors with subsequent sampling on the upper floors. No tracer was detected over an extended period. This lack of detectable tracer coupled with a knowledge of the tracer concentration in the lower floors could be used to place an upper bound on any potential leakage across the fourth floor boundary. Equation (16) can again be used where the concentration measured (or should we say not measured) corresponds to the detection limit for the particular tracer. For the building shown above, the ratio of tracer below and above the fourth floor was 50,000 to 1. This implies that any flow across the boundary was negligibly small.

3.5 Temporary Safe Havens

A safe haven is a room or a building that, by virtue of its specific design and construction, will afford full protection to a limited number of personnel for the expected duration of an exposure to a toxic release. Safe havens (typically control rooms required for the orderly shut down of a process) usually require special HVAC system features and/or supply clean breathing air for a designated number of personnel.

A temporary safe haven does not provide the same level of protection as a safe haven, but can provide valuable time at the onset of a crisis such as the accidental release of a hazardous or toxic gas. Like a safe haven, a temporary safe haven is a room or building that provides protection from toxic fumes, but the protection is for a limited time--possibly less than the duration of exposure to a toxic cloud.

Most toxic gas release incidents are of short duration or are controlled quickly. Therefore, occupancy of a temporary safe haven is preferable to immediate evacuation and, in most cases, affords full protection. Even for prolonged releases, a temporary safe haven provides additional time while the emergency is assessed and allows first respondents to organize an orderly evacuation if necessary. For the temporary safe haven concept to be useful in an emergency response function, it is important to know the minimum protection afforded by specific buildings so that protected assembly points can be selected. Many plant sites have hesitated to designate temporary safe havens because no quantitative method was available to ensure adequacy of candidate buildings or rooms.

A method based on the tracer concentration decay method (ASTM Standard E741) has been suggested as a means to evaluate buildings or rooms within buildings for suitability. By first measuring the air infiltration rate as described in the first and second articles, Jann (1989) provided a series of nomographs based on the measured air exchange rate in order to estimate the safe time within a temporary safe haven for several outside toxic challenges. These are reproduced in Figure 32. Since most toxic releases tend to be of rather short duration, nomographs such as these can be used to assess the degree of protection afforded by various potential temporary safe havens.

3.6 Secondary Ventilation System Testing

In many industries, especially in the semiconductor fabrication industry, process and fabrication equipment is often equipped with a secondary ventilation system to provide extra protection to plant personnel in the event of the release of chemicals (usually gases) used in the manufacture of semiconductors. In the event of a hazardous gas leak, the effectiveness of secondary exhausted enclosures becomes critical to prevent harmful exposure conditions. Reliance on gas detection for worker protection is ineffective in the absence of effective leak containment. By the time a large leak is detected harmful exposures could have already occurred. Detector cycle times and detector sensitivity limitations can lead to a considerable interval elapsing between introduction of a hazardous gas into the work area and any resulting emergency action.

Secondary enclosure exhaust ventilation and detection controls for hazardous gases used in the semiconductor industry are commonly installed according to equipment manufacturer specifications or theoretical design criteria. Before the advent of tracer techniques it was not possible to quantitatively test the working of these systems under actual operating conditions. A typical test setup is shown in figure 8. Tracer is injected into the enclosure at a known rate and the periphery of the enclosure is sampled for the presence of tracer (Tubby, 1991). It is possible to interpret the tracer resulting concentration in terms of concentration of process gases by means of ratio analysis as explained the discussion related to equation (17).

Typical data obtained from a test of a Chemical Vapor Deposition system are presented in table 9 (Orcutt, 1988). In this table, the dilution ratio normally measured has been converted to an equivalent concentration of process gas released within the enclosure. Note that for many of the gases used in semiconductor fabrication the equivalent leakage concentrations shown in this table are significantly in excess of allowable TLV values. There is now a SEMI Standard, S2-91, which mandates this type of testing for new semiconductor fabrication equipment.

Summary

This article has provided a summary of various tracer gas techniques which can be used in industrial hygiene investigations. It has discussed the three tracer gas methods used to measured building ventilation rates and building airflow rates. The testing of fume hoods for re-entrainment and re-circulation has been described. Methods using tracer gases for assessing the release of hazardous substance in a facility were outlined. The evaluation of computer models for predicting contaminant dispersal and air or contaminant movement using tracer gas testing was touched on. In future articles, each of these topics will be expanded upon to provide the reader more complete explanation of the use of tracer gas techniques for industrial hygiene investigations.

This article has presented the various tracer gas methods which can be used to assess the performance of building ventilation systems. Accurate measurements of total building ventilation and air leakage rate can be made in even large complex buildings at moderate expenditure of effort and cost. More complicated tests can be performed to measure airflows between zones of the building, to assess ventilation effectiveness and to aid in estimating contaminant source strengths.

This article discussed the use of tracer gas methods for the assessment of airborne hazardous substance releases. It showed examples of the use of tracer gas techniques for tracing air flow paths, evaluating fume hoods, measuring contaminant inleakage into air ducts and areas protected by secondary ventilation systems and measuring flue gas reentrainment. It gave examples of the quantitative use of tracer data for assessing the exposures and dangers which can be caused by the release of hazardous substances.

References

ASHRAE Standard 110-1895, "Method of Testing Performance of Laboratory Fume Hoods", Atlanta, GA: American Society of Heating, Refrigerating and Air-Conditioning Engineers

ASTM, 1983 ASTM E741-83, "Standard practice for measuring air leakage rates by the tracer dilution method", Philadelphia: American Society for Testing and Materials

Bhasin, D., Lagus, P.L. And Adams, W. 1989, "Noble Gas Migrations in Auxiliary Buildings, ASHRAE Transactions, American Society for Heating, Refrigeration and Air Conditioning Engineers, Atlanta, GA

Caplan, K.J. and Knutson, G.W., 1978, "Laboratory Fume Hoods: A Performance Test", ASHRAE Trans. V. 84

Diets, R.N. And Cole, E.A. 1982,"Air infiltration measurements in a home using a convenient perfluorocarbon tracer technique", Environmental International, Vol 8.

Dietz,R.N., Goodrich, R.W. ; Cote, E.A. And Wieser, R.F. 1986,"Detailed description and performance of a passive perfluorocarbon tracer system for building ventilation and air exchange measurements", in ASTM STP 904, Measured Air Leakage of Buildings, American Society for Testing and Materials, Philadelphia

Foord, N. And Lidwell, D.M. 1973, "A method for studying air movement in complex occupied buildings such as hospitals: halocarbons as gas tracers using gas chromatography", Bldg Services Eng., Vol. 41.

Grot, R.A. 1980 "A low-cost method for measuring air infiltration rates in a large sample of dwellings", in Building Air Change Rate and Infiltration Measurements, ASTM STP 719, American Society for Testing and Materials, Philadelphia

Grot, R.A. 1982, "The air infiltration and ventilation rates in two large commercial buildings" in proceedings of DOE/ASHRAE Conference, Thermal Performance of the Exterior Envelopes of Buildings II. Atlanta, GA ASHRAE SP 38.

Grot, R.A. et al. 1989,"Environmental Evaluation of the Portland East Federal Office Building - Preoccupancy and Early Occupancy Results, NISTIR 89-4066, NIST

Hampl, V., R.Niemela, S.Shulman, D.L. Bartley, "Use of Tracer Gas Technique for Industrial Exhaust Hood Efficiency Evaluation-- Where to Sample?" Am. Ind. Hyg. Assoc. J. 47(5):281-287 (1986)

Hampl, V., Evaluation of Industrial Local Exhaust Hood Efficiency by a Tracer Gas Technique" Am. Ind. Hyg. Assoc. J. 45(7)485- 490 (1984)

Hodgson, A.T. Et al. 1990,"Source Strengths and Sources of Volatile Organic Compounds in a New Office Building" Air and Waste Management Association, 82nd Annual Meeting, Paper 89-80.7, 1989 (also LBL-26950)

I'Anson, S.L., Irwin, C. And Howarth, A.T., 1982, "Air flow measurements using three tracer gases.", Building and Environment, Vol. 17.

Irwin, C., Edwards, R.E. And Howarth, A.T., 1984, "An improved multiple tracer gas technique for the calculation of air movement in buildings", Air Infil Rev. Vol. 5, No. 2.

Jann, P., "Evaluation of Temporary Safe Havens", J. Loss Prev. Process Ind. Vol 2,33-38 (1989)

Lagus, P.L. 1977. "Characterization of building infiltration by tracer dilution method.", Energy, Vol. 2.

Lagus, P.L., 1984, Unpulished study.

Lagus, P.L., Kluge, V., Woods, P. And Pearson, J. 1988a, "Tracer Gas Testing within the Palo Verde Nuclear Generating Station Unit 3 Auxiliary Building", Proceeding of the 20th NRC/COE Air Cleaning Conference, Boston, MA

Lagus, P.L., 1988b, "Tracer Gas Characterization of Fume Hood Re-entrainment and Recirculation", Technical Bulletin 88-2, S-Cubed Division, Maxwell Laboratories, La Jolla, CA

Lundin, L.I., 1986, "Air Leakage in Industrial Buildings - Description of Equipment", in ASTM STP 904, Measured Air Leakage of Buildings, American Society for Teating and Materials, Philadelphia

Orcutt, J.J., 1988, "Characterization of Hazardous-Gas Releases by Tracer-Gas Simulation", in Hazardous Assessment and Control Technology in Semi Conductor Manufacturing, ACGIH, Cincinnati, OH

Mohlave, L., 1984, "Volatile Organic Compounds as Indoor Pollutants" in Indoor Air and Human Health, P. Gammage and S, Kaze editors, Lewis, Publications.

Nazaroff, W.M. and Cass, G.R., 1988,"Mathematical Modeling of Indoor Aersol Dynamics", Environ. Sci. Technol, Vol 23 (no. 2)

Perera, M.D., Walker, R.R. And Oglesby, V.D., 1983, "Ventilation rates and intercell airflow rates in a naturally ventilated office building." in Air Infiltration Reduction in Existing Buildings, proceeding of the Fourth Air Infiltration Centre Conference, Elm, Switzerland.

Persily, A. And Axley, J. 1990, "Measuring Airflow Rates with Pulse Tracer Techniques", in Air Change Rate and Airtightness in Buildings, ASTM STP 1067, American Society for Testing and Materials, Philadelphia

Persily, A. And Dols, W.S. ,1990 "The Relation of CO_2 Concentration to Office Building Ventilation, ASTM STP 1067, American Society for Testing and Material, Philadephia

Prior, J., Litter, J. And Adlard, M., 1983, "Development of multi-tracer gas techniques for observing air movement in buildings", Air Infil. Rev., Vol. 4, No. 3.

Tubby, R.L. Tracer Gas testing of Secondary Exhaust Systems on Hazardous Gas Enclosures in press, Journal of the Semiconductor Safety Association (1991)

Tucker, G., 1988, "Factors influencing indoor air pollutants originating from surface materials' i preprint of conference "Healthy Buildings 88", Swedish Council for Building Research, Stockholm, Sweden

Table 1
Tracer Gases and Measurement Techniques

Technique	Gases
Thermal Conductivity Detector	Hydrogen Helium Carbon Dioxide
Electron Capture Gas Chromatograph	Sulfur Hexafluoride Halogenated Compounds Perfluorocarbons
Flame Ionization Gas Chromatograph	Ethane Methane
Infrared Absorption	Carbon Monoxide Carbon Dioxide Sulfur Hexafluoride Nitrous Oxide Ethane Methane

Table 2
Relative Tracer Gas Costs Taking Detectability into Account

Gas	Detectable Concentration (ppm)	Gas Volume Per Dollar		Maximum Measurable Volume Per Dollar	
	(ppm)	ft^3	(m^3)	ft^3	m^3
He	300	1.4	(0.13)	$4 \cdot 10^3$	$(4 \cdot 10^2)$
CO_2	1	7.0	(0.65)	$6 \cdot 10^4$	$(6 \cdot 10^5)$
N_2O	1	2.4	(0.22)	$2 \cdot 10^6$	$(2 \cdot 10^5)$
SF_6	$5 \cdot 10^{-6}$	0.13	$(1.2 \cdot 10^{-2})$	$2 \cdot 10^{10}$	$(2 \cdot 10^9)$
"	$5 \cdot 10^{-3}$	"	"	$2 \cdot 10^7$	$(2 \cdot 10^6)$
$CBrF_3$*	$5 \cdot 10^{-5}$	$3.7 \cdot 10^{-2}$	$(3.4 \cdot 10^{-3})$	$7 \cdot 10^8$	$(7 \cdot 10^7)$
PDCH**	$5 \cdot 10^{-5}$	$3.0 \cdot 10^{-3}$	$(2.8 \cdot 10^{-4})$	$6 \cdot 10^8$	$(6 \cdot 10^7)$

* bromotrifluoromethane (Freon 13B1)
** perfluorodimethylcyclohexane

Table 3. Electronegative Tracer Gases

Name	Symbol	Trade Name
Dibromodifluoromethane	CF_2Br_2	Freon 12B2
Trichlorofluoromethane	$CFCL_3$	Freon 11
1,1,1,-Ttrichlorotrifluoroethane	$C_2CL_3F_3$	Freon 113
Bromotrifluoromethane	CF_3Br	Freon 13B1
Qctafluorocyclobutane	C_4F_8	Freon C-318
Dichlorodifluoromethane	CCl_2F_2	Freon 12
1,2-Dichlorotetrafluoroethane	$C_2Cl_2F_4$	Freon 114
Chlorodifluoromethane	$CHClF_2$	Freon 22
Chloropentafluoroethane	$CClF_2CF_3$	Freon 115
Bromochlorodifluoromethane	$CBrClF_2$	Freon 12B1
Suflur Hexafluoride	SF_6	
Perfluorodimethylcyclohexane		PDCH
Perfluoromethylcyclohexane		PMCH
Perfluoromethylocyclopropane		PMCP
Perfluorodimethylcyclobutane		PDCB

Table 4.
Long-term variations in the concentrations and specific source strengths of individual VOC.

	CONCENTRATION (μg/m3)				SPECIFIC SOURCE STRENGTH (μg/m3-h)			
Date	8/4/87	10/14/87	1/13/88	10/28/88	8/4/87	10/14/87	1/13/88	10/28/88
Time	20:00	17-19:0 0	15-17:0 0	15-17:0 0	20:00	17-19:0 0	15-17:0 0	15-17:0 0
Vent. Rate	0.5	1.36	0.24	1.99	0.5	1.36	0.24	1.99
COMPOUND								
Oxygenated								
2-Propanol	14.8	20.2	137.2	26.5	5.8	21.9	31.6	52.6
2-Propanone	50.1	28.8	66.6	32.4	22.1	27.0	14.9	49.7
2-Butanone	40.9	6.2	15.3	5.7	19.0	2.5	2.0	7.6
Chlorinated								
Dichloromethane	32.4	2.6	13.4	2.7	15.9	1.3	2.7	5.4
1,1,1-Trichloroethane	13.5	13.8	119.7	17.1	5.4	13.6	27.5	27.0
Trichloroethene	16.4	7.2	58.2	14.8	8.2	9.7	11.0	27.6
Alkane + Cycloalkane								
2-Methylbutane	31.9	53.8	81.6	26.2	13.1	31.7	16.1	44.7
n-Hexane	11.3	10.0	24.0	9.2	5.7	6.7	3.7	14.6
Cyclohexane	5.7			2.7	2.4			4.2
n-Heptane	4.8	3.1	12.6	3.6	2.0	2.7	0.2	5.5
3-Methylhexane	6.0	4.0	14.7	3.5	2.4	3.1	0.0	5.2
Methylcyclohexane	5.1			1.7	2.4			2.5
2,2,4-Trimethylpentane	2.4	1.8	8.0	3.0	1.0	1.3	0.7	6.0
1,4-Dimethylcyclohexane	3.1				1.6			
n-Nonane	39.6	10.6	149.1	33.9	19.7	11.4	35.3	63.0
2,2,5-Trimethylhexane	2.4				1.2			
Isopar 2	147.0	82.5	638.7	95.4	72.8	104.2	151.7	179.7
n-Undecane	115.6	57.3	831.3	48.3	55.2	71.3	196.8	85.7
n-Dodecane	49.1	10.6	280.8	10.9	21.8	5.9	67.0	17.6
n-Tridecane		6.0	111.9	8.5		5.8	26.2	13.8
n-Tetradecane		36.1	245.3	27.0		43.0	57.9	49.5
Aromatic								
Toluene	60.4	81.3	91.0	33.1	22.7	80.9	13.7	50.2
Ethylbenzene	11.8	7.0	18.7	7.5	5.3	4.9	2.3	11.4
1,2-Dimethylbenzene	17.2	8.7	25.8	8.1	7.6	5.8	4.1	12.0
1,3-,1,4-Dimethylbenzene		18.1	54.5	18.3		11.7	8.8	26.6
1,3,5-Trimethylbenzene	4.1				1.6			
TOTALS								
Sum of Individual VOC	685	470	2998	440	315	466	674	762
Total Organic Carbon	5200	1900	11000	2300	2500	2400	2500	4300

Table 5. Flume Hood Dilution Factors

Date	Injection Room/Hood	Sample Room	Exhaust Duct Concentration	Average Concentration	Dilution Factor
2/28	652B	652	$20.6 \cdot 10^{-9}$	$21.5 \cdot 10^{-12}$	958
3/4	652B	652	$41.3 \cdot 10^{-9}$	$22 \cdot 10^{-12}$	1870
2/28	650B	650	$36.9 \cdot 10^{-9}$	$51 \cdot 10^{-12}$	724
3/4	650B	650	$37.1 \cdot 10^{-9}$	$40 \cdot 10^{-12}$	928
2/28	646A	646	$36.9 \cdot 10^{-9}$	$11 \cdot 10^{-12}$	3354
2/28	646A	644		$32 \cdot 10^{-12}$	1153
3/4	646A	646	$37.1 \cdot 10^{-9}$	$5 \cdot 10^{-12}$	7420
3/4	646A	644		$15 \cdot 10^{-12}$	2473
3/2	626A	626	$33.1 \cdot 10^{-9}$	$13 \cdot 10^{-12}$	2526
3/2	624A	624	$38.2 \cdot 10^{-9}$	$7 \cdot 10^{-12}$	5457
3/2	624A	622		$12 \cdot 10^{-12}$	3183
3/4	624B	624	$38.3 \cdot 10^{-9}$	$5 \cdot 10^{-12}$	7640
3/2	624B	626	$(32.6 \cdot 10^{-9})^{624B}$	$5 \cdot 10^{-12}$	6520
3/3	622A	622	$34.8 \cdot 10^{-9}$	$8 \cdot 10^{-12}$	4350
3/3	620B	624		$7 \cdot 10^{-12}$	4971
3/3	620B	620	$37.1 \cdot 10^{-9}$	$\leq 5 \cdot 10^{-12}$	7420?
3/3	620B	622		$27 \cdot 10^{-12}$	1374
3/4	620B	620	$37.1 \cdot 10^{-9}$	$5 \cdot 10^{-12}$	7420
3/4	620B	622		$15 \cdot 10^{-12}$	2473

Table 6. Results of Flue Gas Re-entrainment Test
Continuous Injection

Injection Rate 2.03 lpm of 1% SF_6
into Combustion Flue of Room 117
Flue Concentration of SF_6 = 57.0 ppm
Flue Flow Rate = 12.5 cfm

Room Air Intake Tracer Concentrations and Dilution Ratios

Intake Room #	Concentration (ppb)	Dilution Ratio
A	136.3	0.002
B	147.3	0.003
C	97.3	0.002
D	0.68	0.000
E	12.4	0.000
Music	2.1	0.000
Gym	104.8	0.002
Corridor	597.0	0.010

Resulting Tracer Concentrations in Rooms after 35 minutes

Room Number	Concentration (ppb)	Quantity of Tracer (cc)	Quantity Dilution Ratio
A	17.4	4.15	0.008
B	21.8	5.2	0.009
C	31.4	8.9	0.016
D	0.7	0.2	0.000
E	1.4	0.4	0.001
Music	1.8	1.0	0.002
Gym	3.4	1.9	0.003

Table 7. Estimate of the Pollutant Levels Caused by Flue Exhaust Re-entrainment

Typical Pollutant Generation Rates of Gas Convective Heaters
(50000 BTU per Hour)

Carbon Dioxide	2.690	kg/hr
Carbon Monoxide	4.374	g/hr
Nitrogen Dioxide	0.632	g/hr
Nitric Oxide	0.896	g/hr

Model Parameters Used to Estimate Re-entrainment

Room	Vol m^3	Dilution Ratio	ACH
K	162.67	0.044	0.63
I	162.67	0.002	0.58
gym	3095.26	0.055	0.41

Predicted Rise in Carbon Dioxide, Carbon Monoxide, Nitrogen Dioxide and Nitric Oxide Caused by Continuous Operation of Heating System 125.

Room	CO_2 mg/m^3	ppm	CO mg/m^3	ppm
K	1154	641	1.9	1.6
I	57	32	0.1	0.1
gym	116	65	0.2	0.2

Predicted Rise in Nitrogen Dioxide and Nitric Oxide Caused by Continuous Operation of Heating System 125.

Room	NO_2 mg/m^3	ppm	NO mg/m^3	ppm	NOx mg/m^3	ppm
K	0.27	0.15	0.38	0.31	0.66	0.36
I	0.01	0.01	0.02	0.02	0.03	0.02
gym	0.03	0.02	0.04	0.03	0.07	0.04

Table 8. HVAC Equipment Room PV Duct Inleakage

Supply = 10854 cfm
Return = 9074 cfm

A Train

Time	Room Concentration (ppb)	Supply Concentration (ppb)	Return Concentration (ppb)	Flow (cfm)
5	30.0	500	92	153
6	28.3	460	92	147
7	26.7	460	118	147
8	25.2	480	120	164

Table 9. Secondary-Containment Test for Chemical Vapor Deposition Process (Orcutt, 1988)

Time (sec)	Sample Location	Measured SF6 Concentration (ppb)	Equivalent Workroom Contamination (ppm)
30	North	0.335	0.7
360	North	10.33	2.8
30	South	0.480	0.11
360	South	9.90	2.7
30	East	5.76	1.5
360	East	50.0	13.4

Table 10. Dilution Ratios in Disassembly Room

Concentration in Supply Conveyor Room = $1.33 \cdot 10^{-8}$

Station	Dilution Ratio
B	0.12
D	0.47
E	0.32
G	0.14
H	0.34
I	0.12

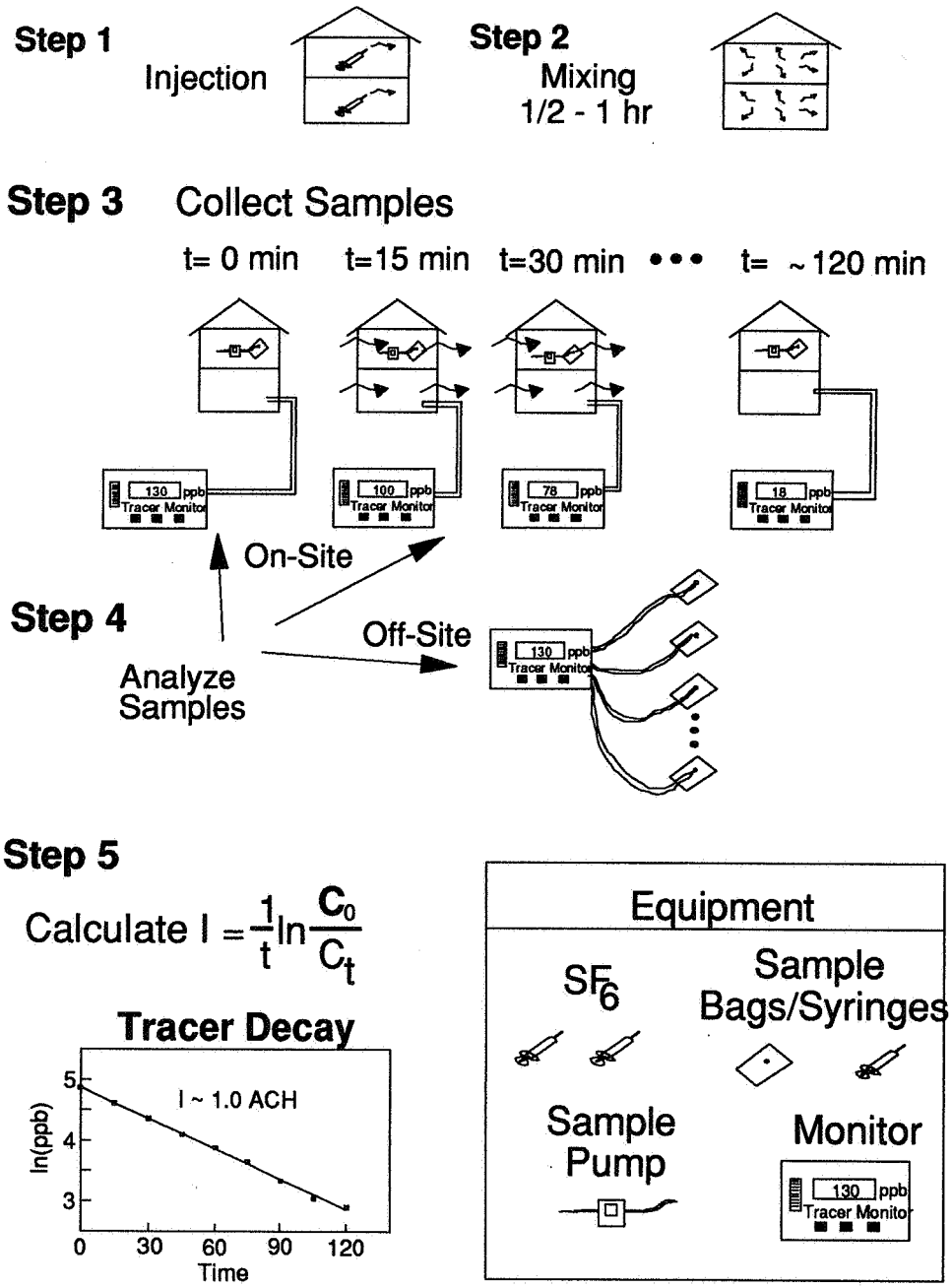

Figure 1. Schematic of Steps Required to Perform Ventilation Measurements Using the Tracer Decay Method

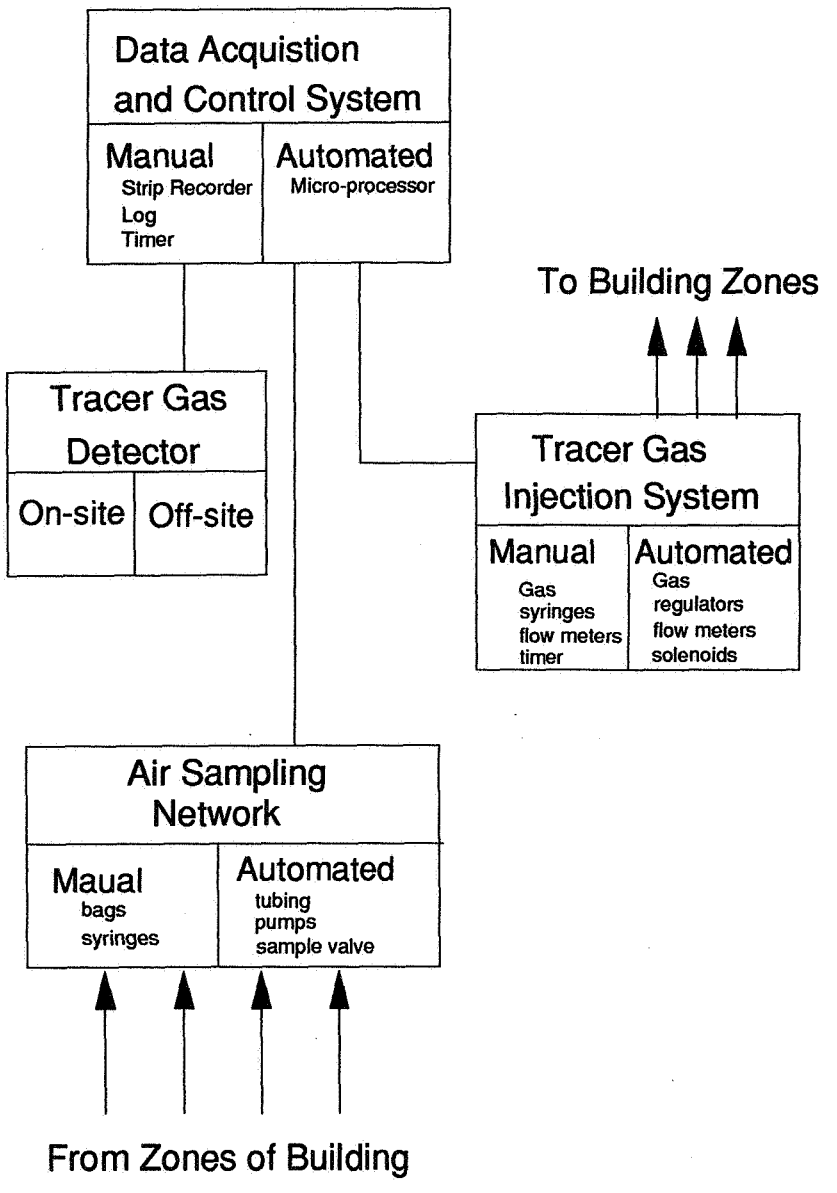

Figure 2. A Schematic of a General Tracer Gas System for Building Ventilation Studies

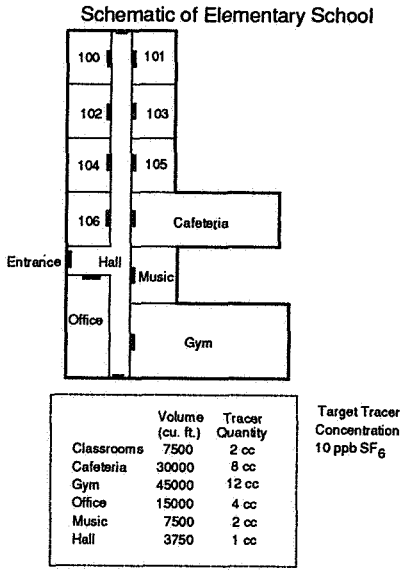

Figure 3. An Example of a Compartmentalized Building - An Elementary School

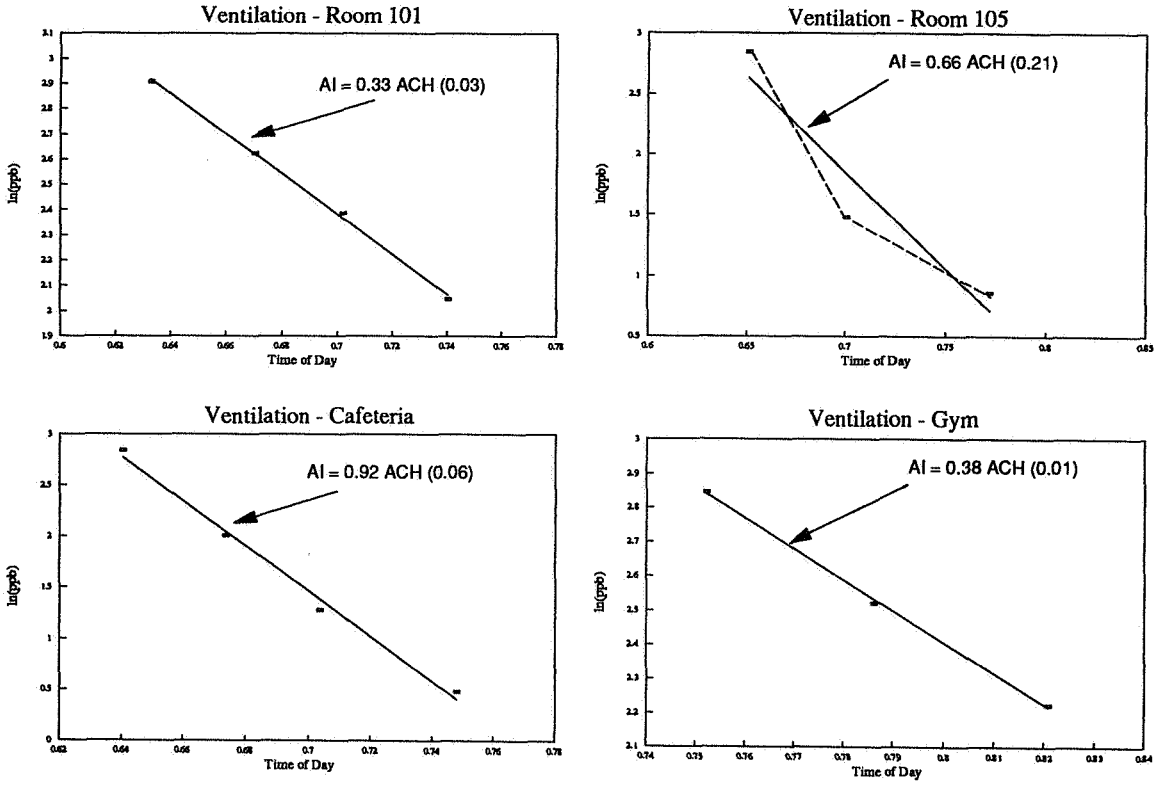

Figure 4. Results of a Tracer Decay Test in Four Rooms of an Elementary School

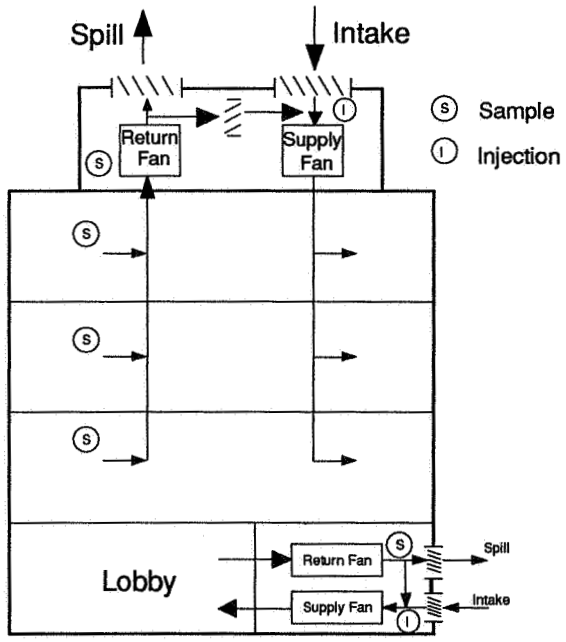

Figure 5. A Schematic of a HVAC System Used for Tracer Sampling and Injection in a Large Building

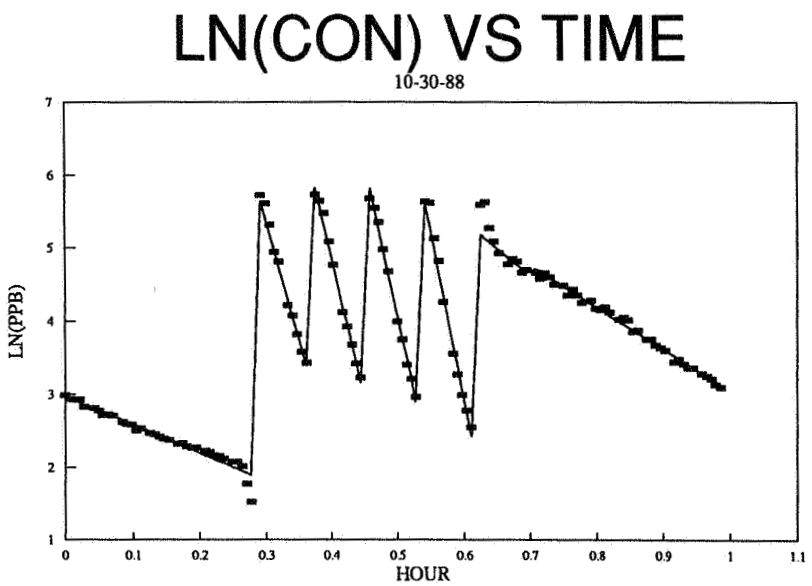

Figure 6. Results of a Tracer Decay Test Using an Automated Tracer Monitoring System

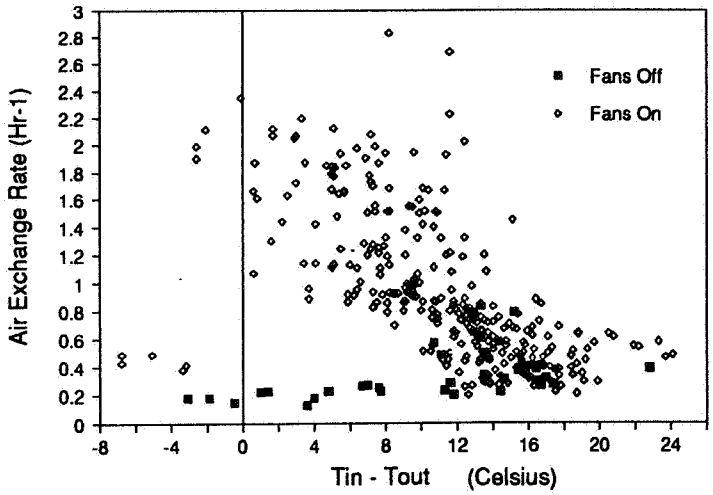

Figure 7. Air Exchange Rate versus Inside-Outside Temperature Difference

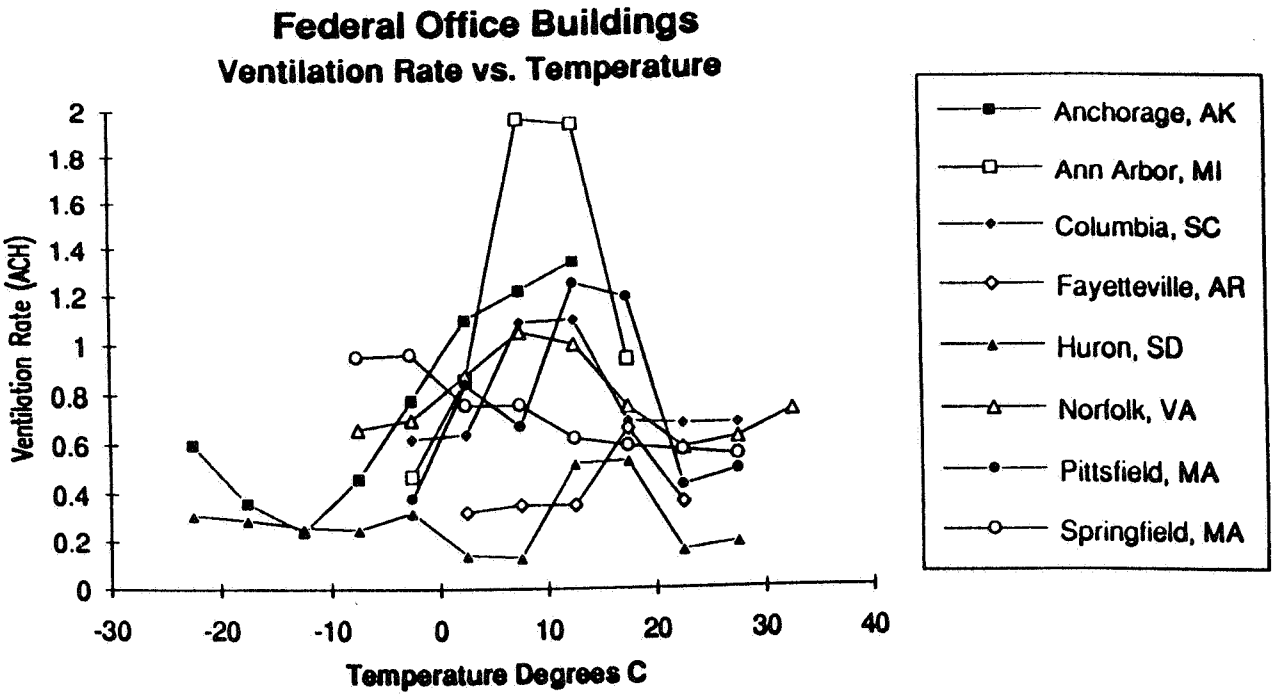

Figure 8. Example of Weather Dependence of Ventilation Rates in Eight Federal Office Buildings

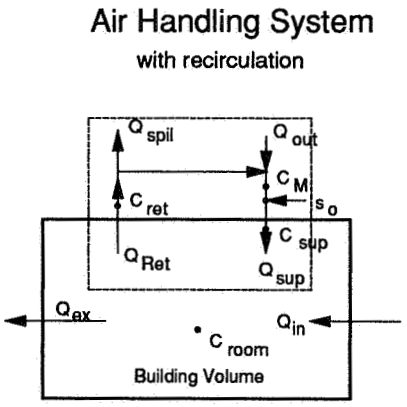

Equations

Percent Outside Air

$$\% = 1 - \frac{C_M}{C_{Ret}}$$

Air Infiltration

$$Q_{in} = Q_{sup}\left(\frac{C_{sup}}{C_{room}} - 1\right)$$

Supply Airflow

$$Q_{sup} = \frac{s_o}{C_{sup} - C_M}$$

Figure 9. Schematic of Measurement Locations for Evaluation of HVAC System

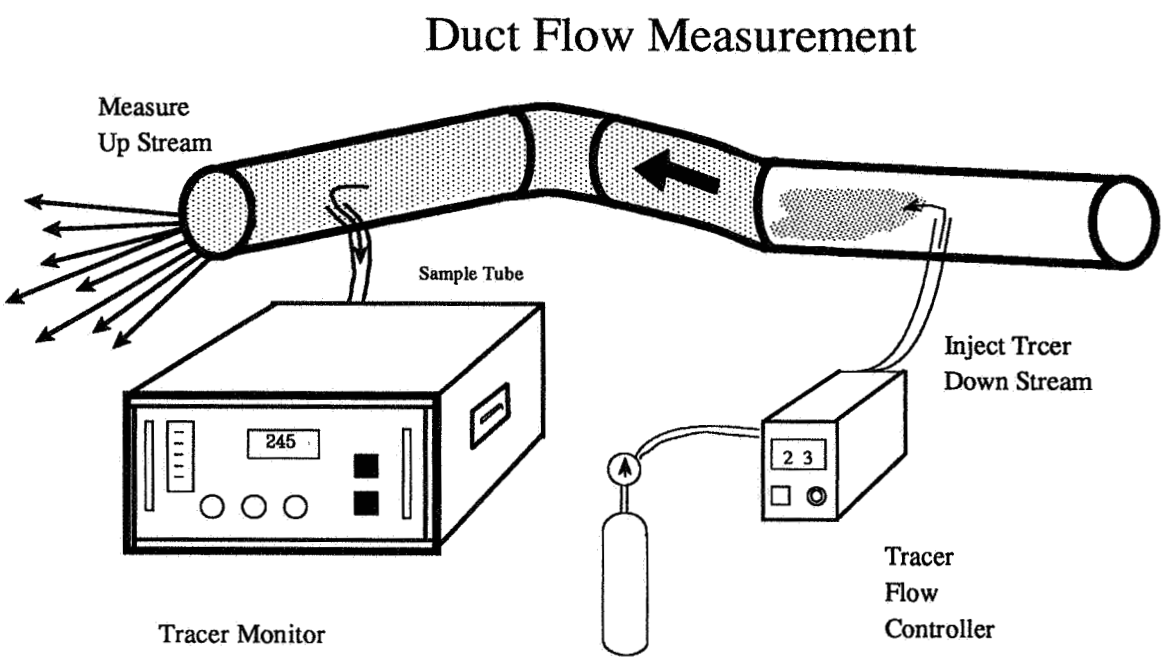

Figure 10. Use of the Constant Injection Method for Measuring Airflow in a Ventilation Duct

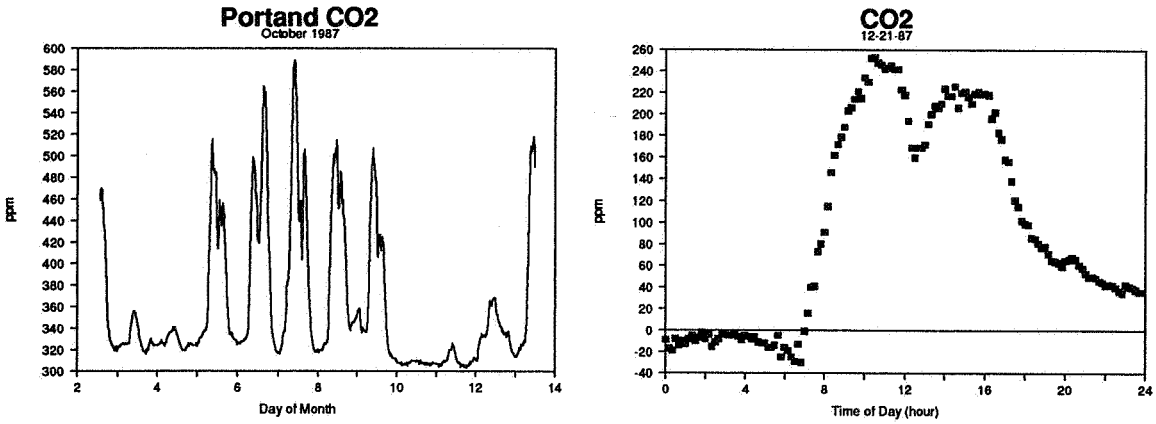

Figure 11. Daily Variation in Carbon Dioxide Levels in an Office Building

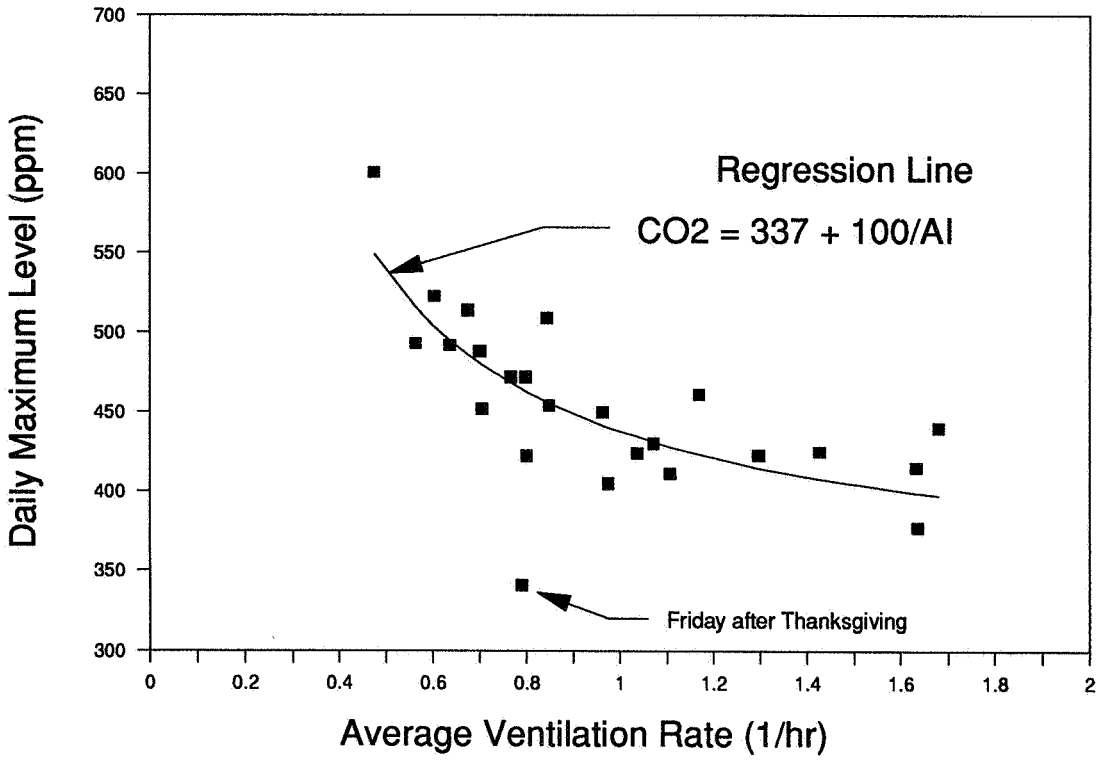

Figure 12. Carbon Dioxide Level versus Ventilation

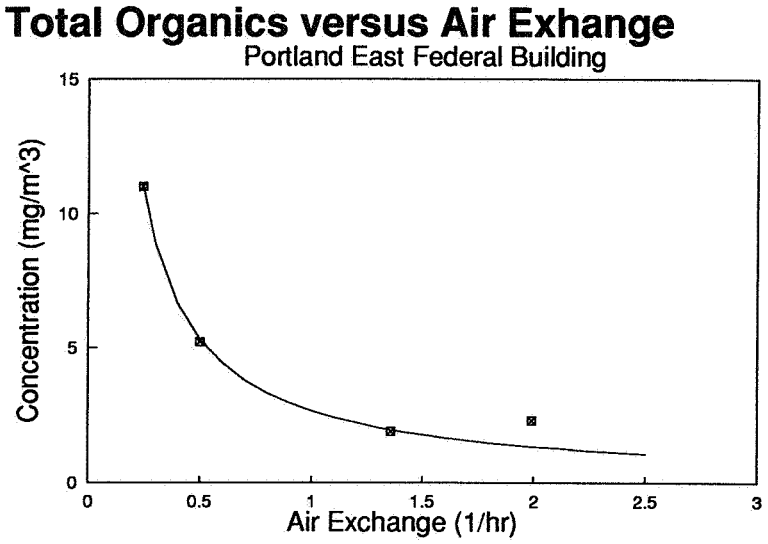

Figure 13. Total Volatile Organics versus Ventilation Rate

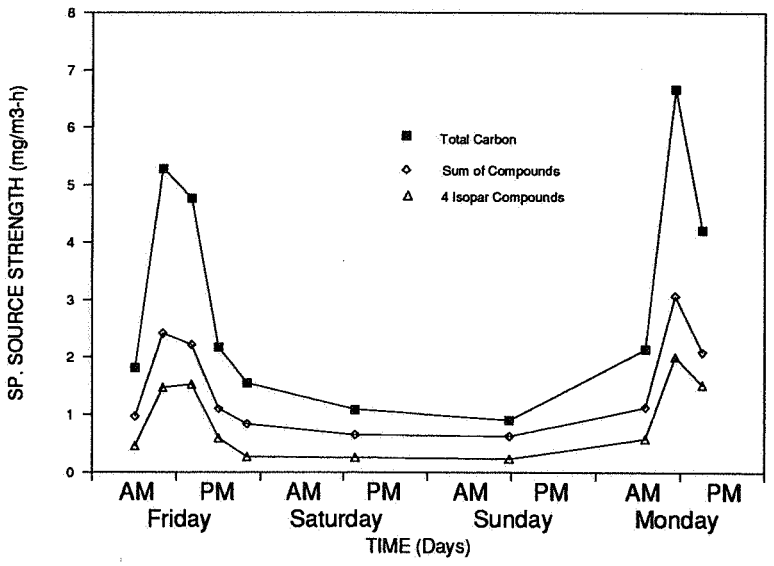

Figure 14. Variation in VOC Sources over a Four Day Period

MULTIPLE TRACER GAS CHROMATOGRAPH SEPARATION

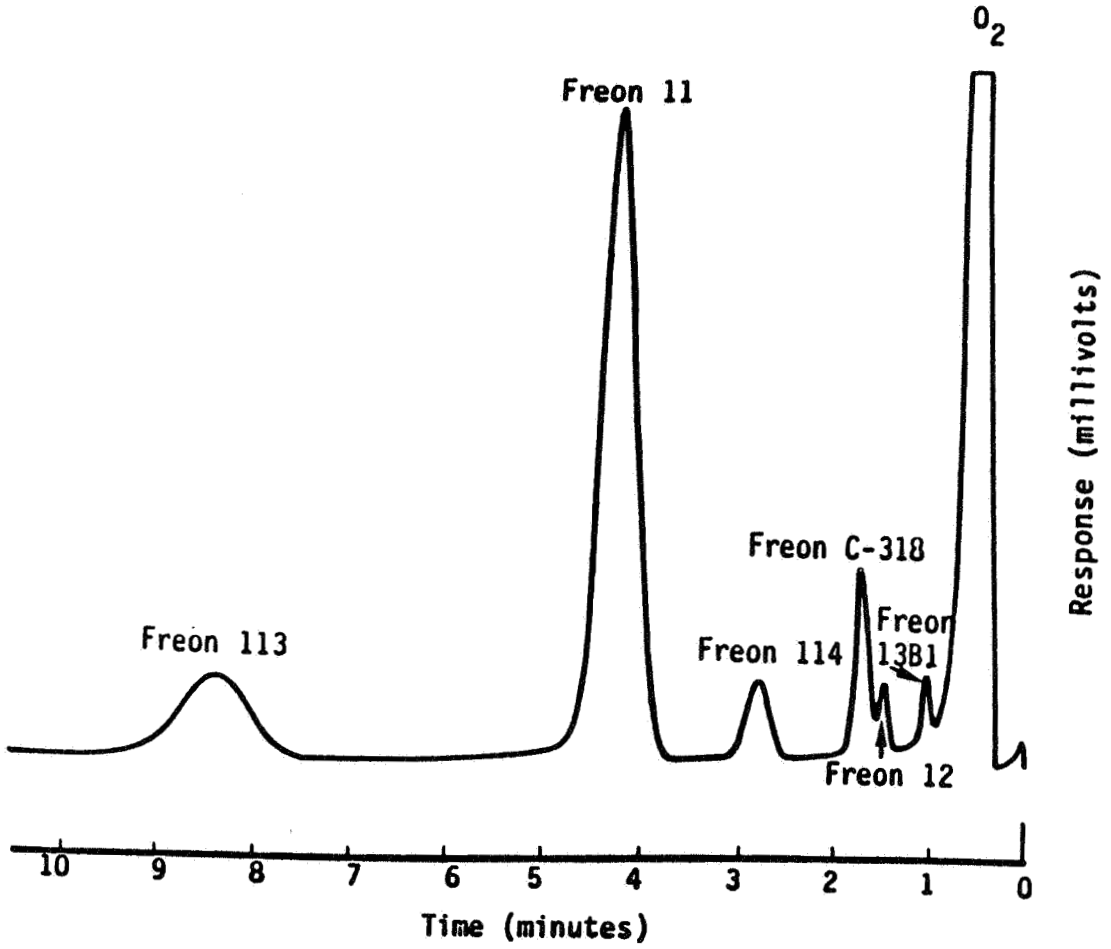

Figure 15. Separation of Multiple Tracers on a Gas Chromatograph

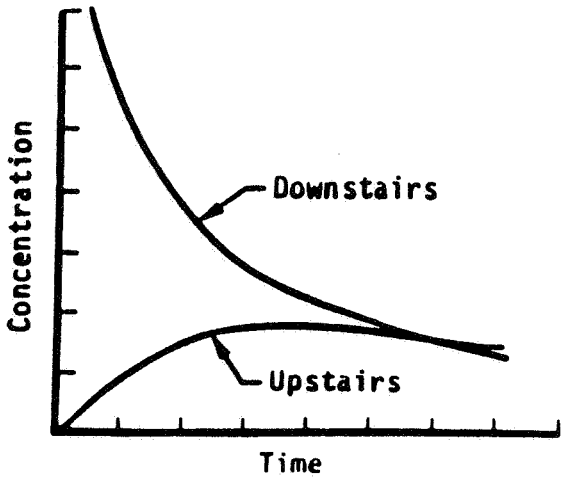

Concentration of Freon 114 against time, upstairs and downstairs.

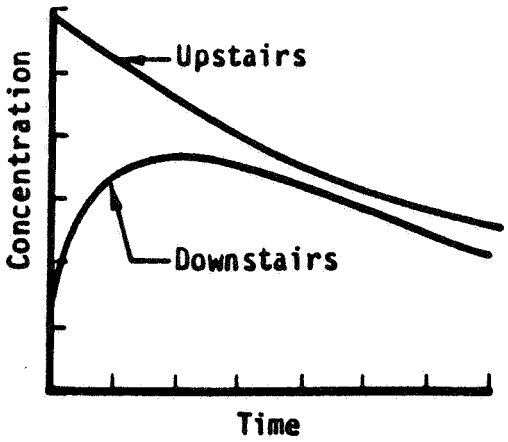

Concentration of Freon 12 against time, upstairs and downstairs.

Figure 16. Example of Two Tracer Decay Test

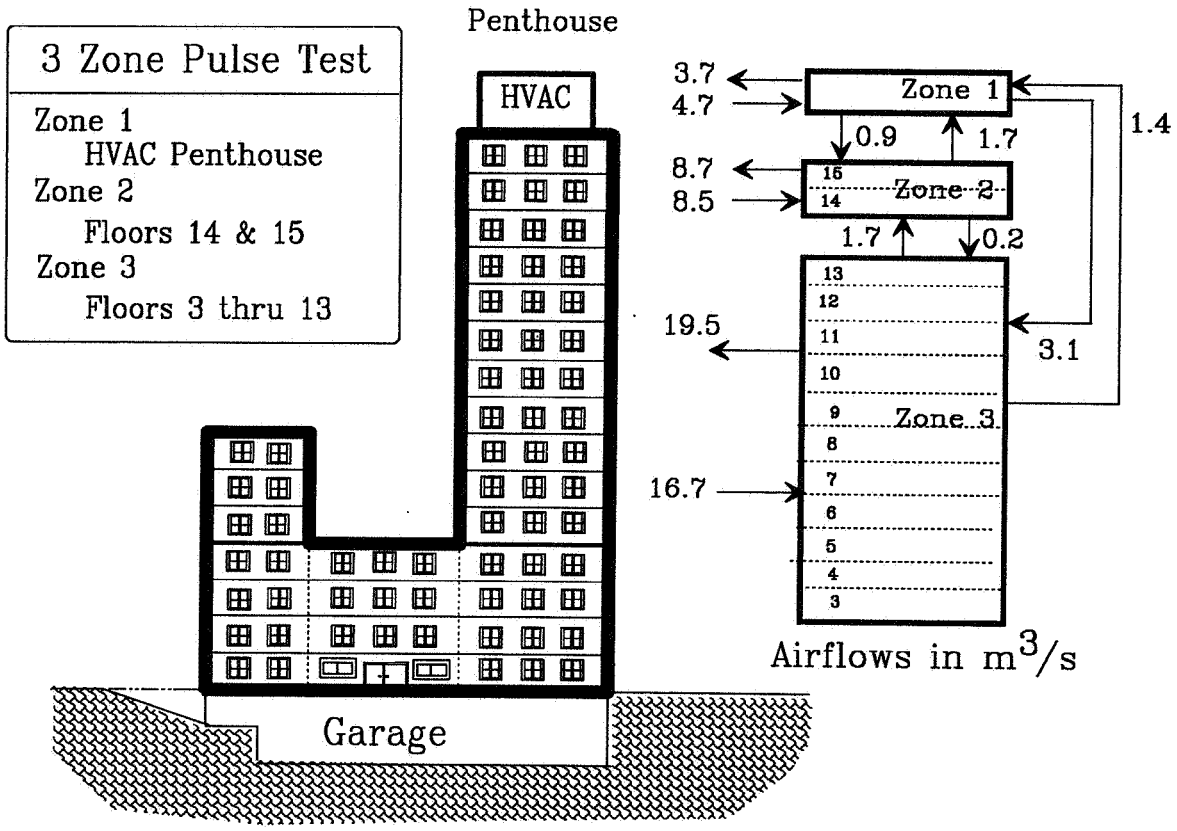

Figure 18. Use of Single Tracer to Determine Air Change of Sections of a Building

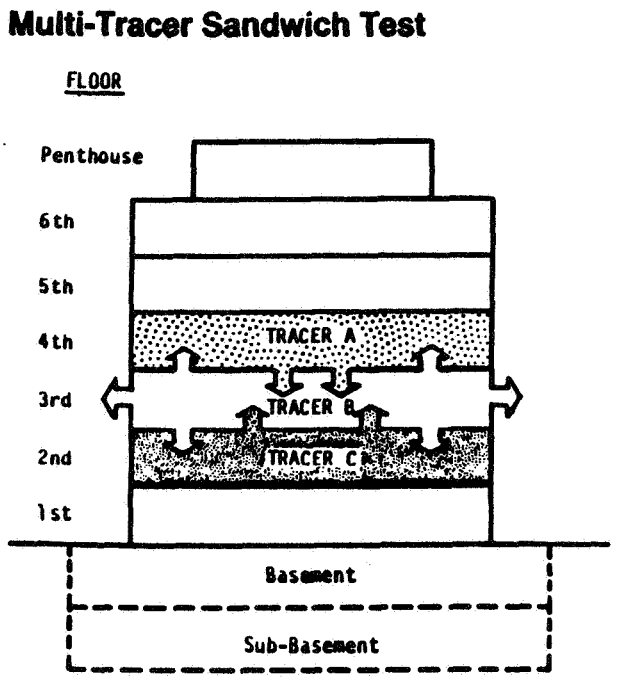

Figure 17. Use of Multiple Tracers to Measure the Ventilation Rate on a Floor of a Building

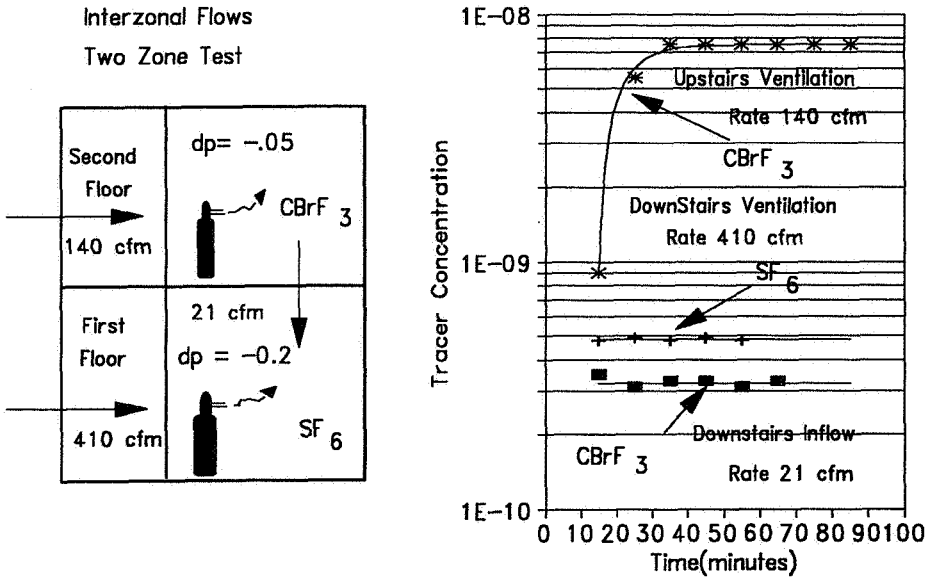

Figure 19. Two Tracer Test for Measuring Airflows from a Laboratory

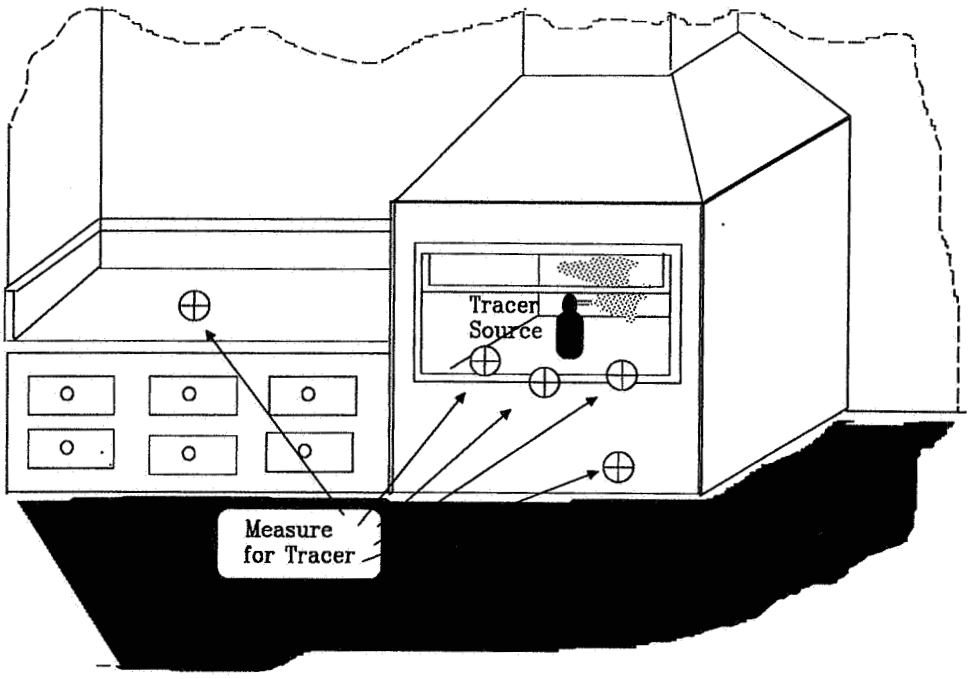

Figure 20. Schematic of Test Procedure for Evaluating Fume Hoods

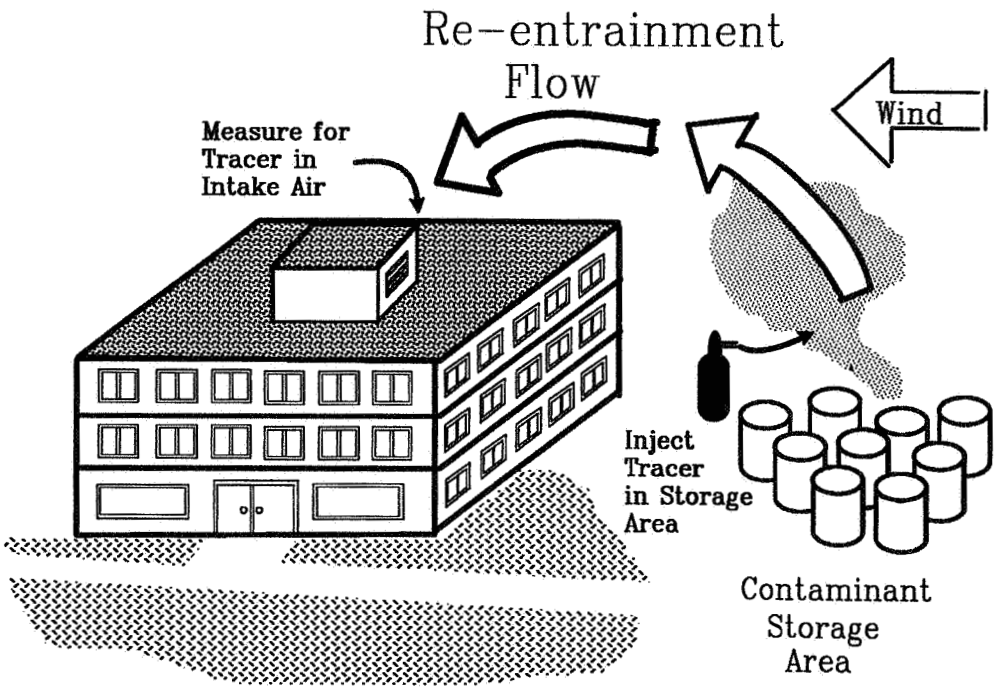

Figure 21. Schematic of Test for Measuring Re-entrainment and Re-circulation from an Exterior Contaminant Source

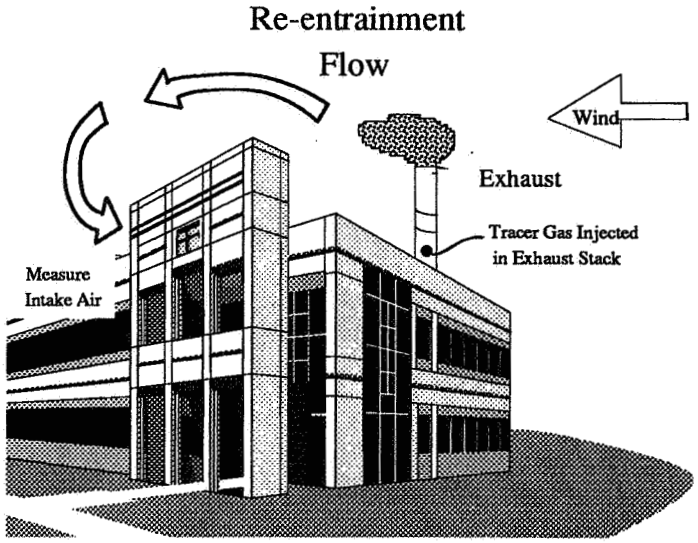

Figure 22. Schematic of Test for Measuring Re-entrainment and Re-circulation from a Building Exhaust

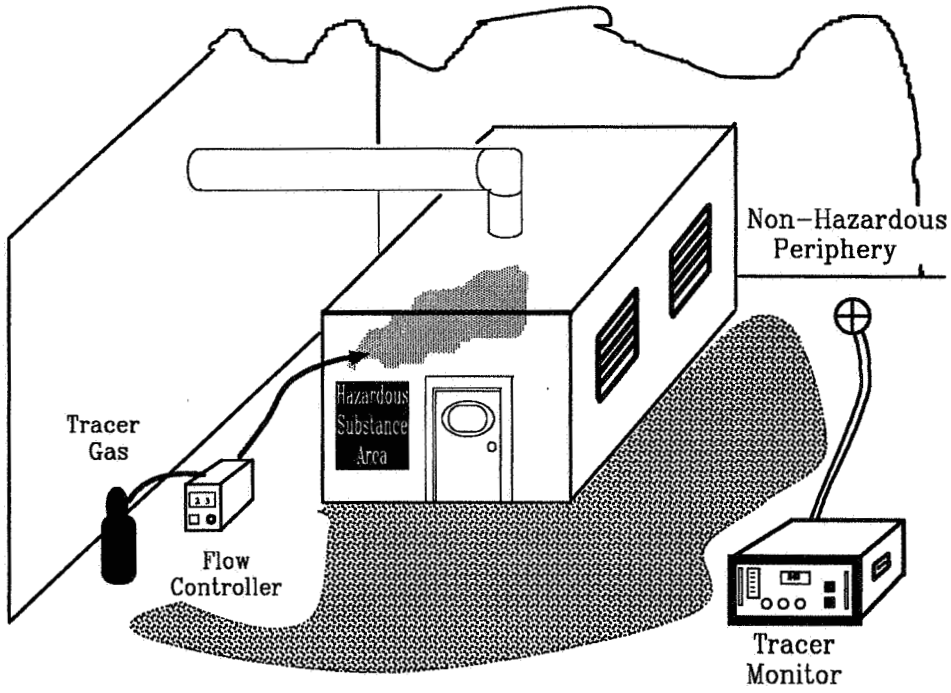

Figure 23. Integrity Breach Testing Using a Tracer Gas

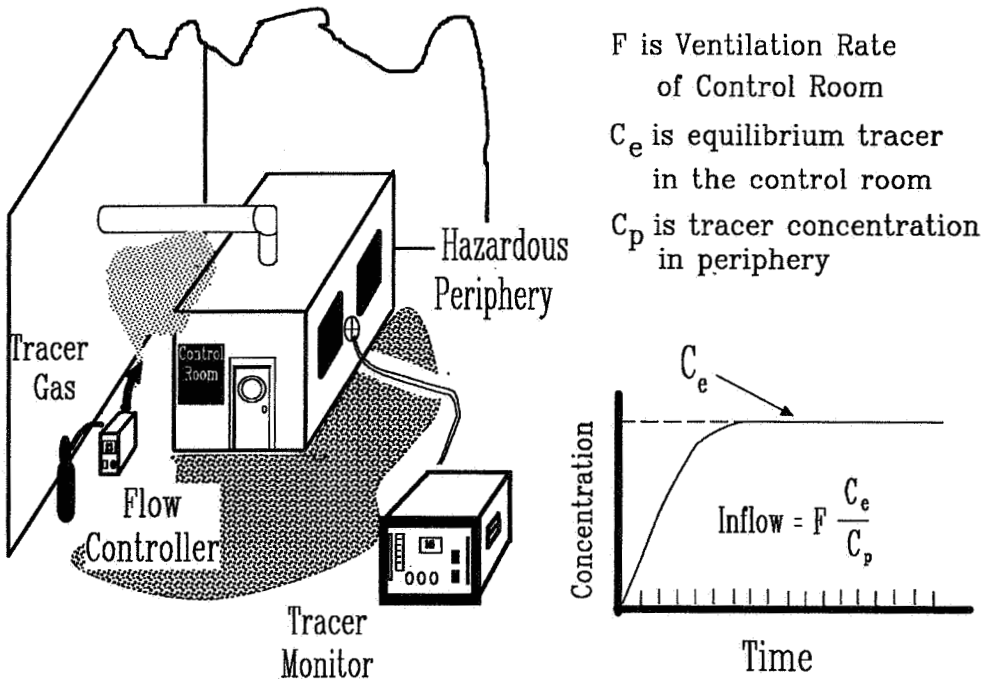

Figure 24. Testing for the Potential of Contaminant Leakage into a Control Room.

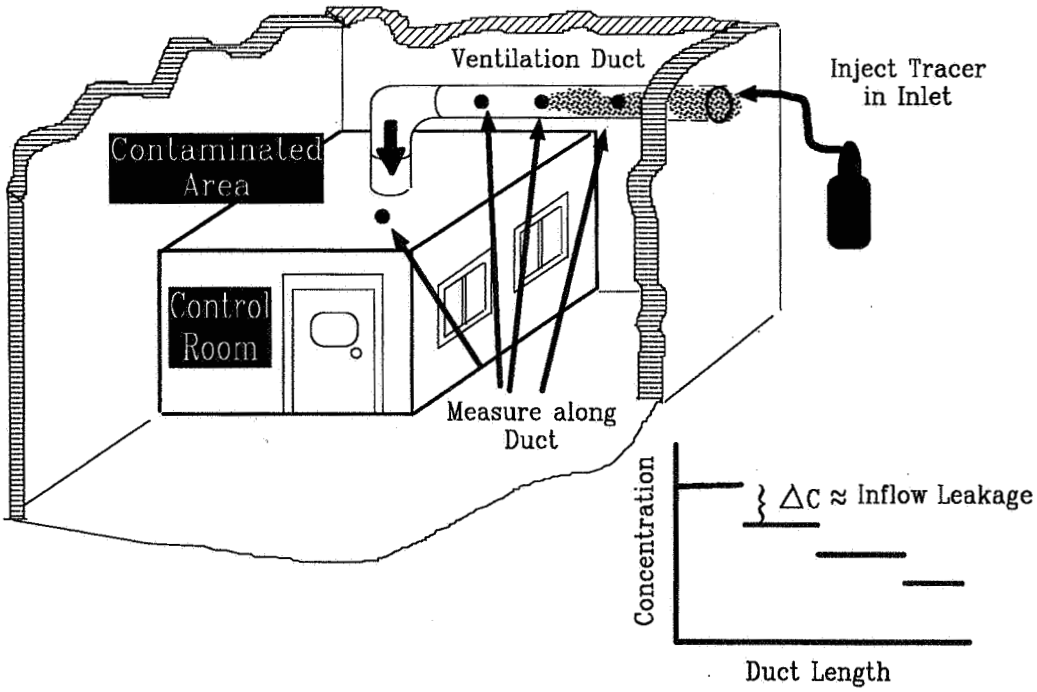

Figure 25. Measuring and Locating Leaks in Negative Pressure Supply Air Duct Passing through a Containment Area.

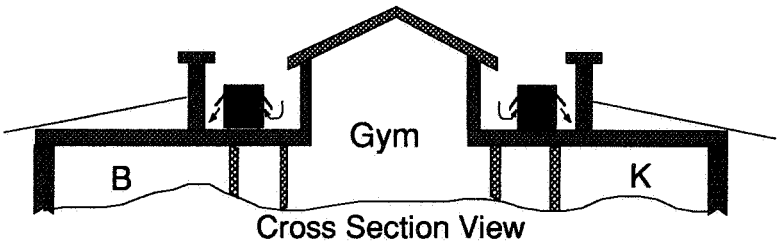

Cross Section View

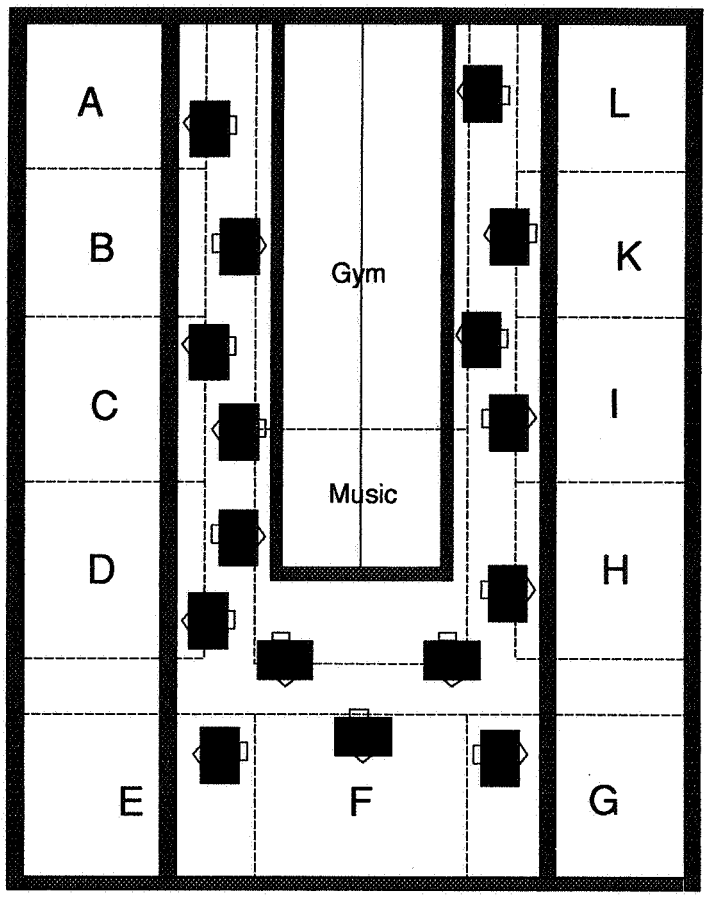

Top View of Roof

Flue Exhaust Re-entrainment

Figure 26. Schematic of Flue and Intake Locations for Tested Elementary School.

Figure 27. Schematic of Flows Used to Quantify Inleakage Data

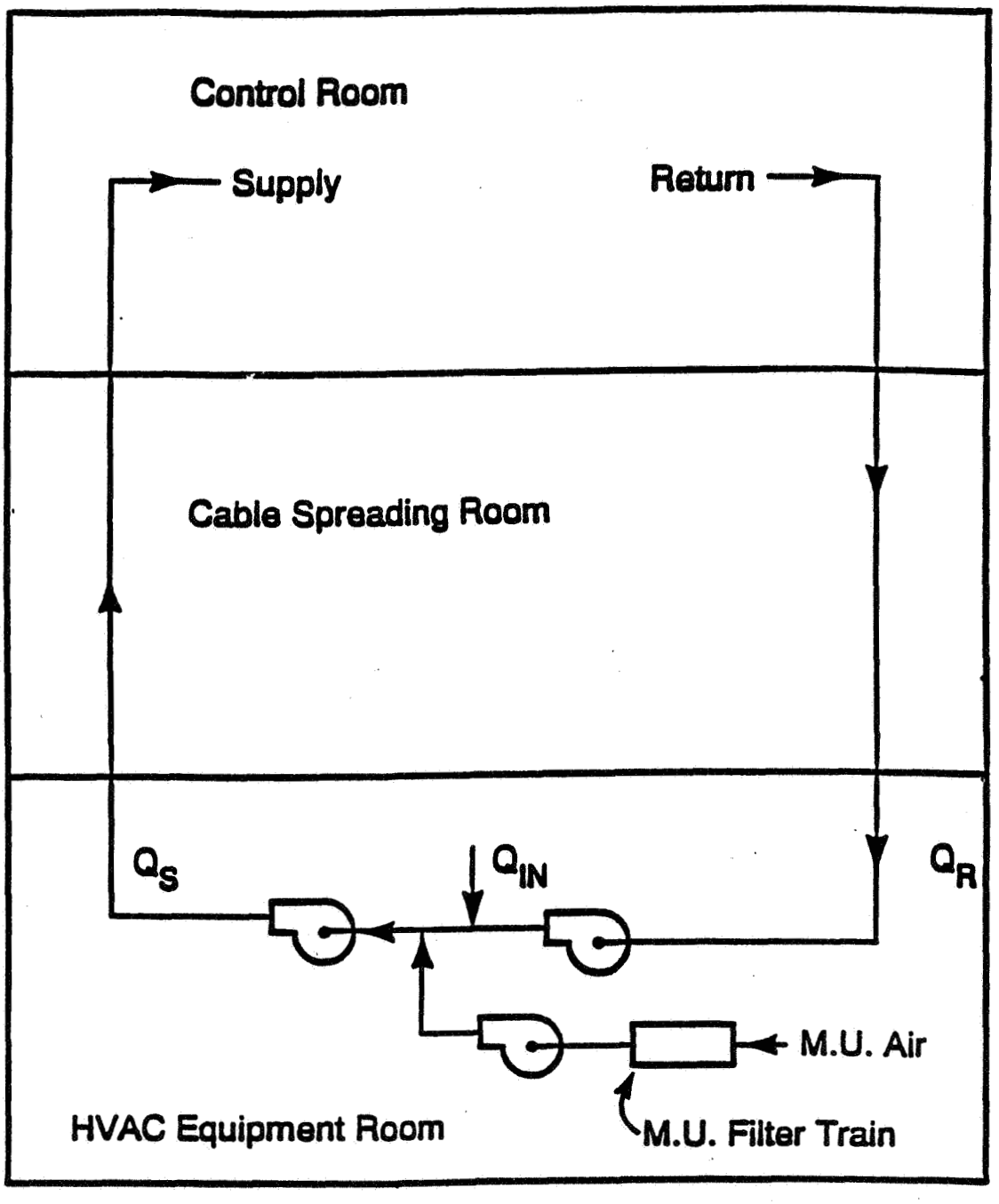

Figure 28. Plan View of Disassembly Room

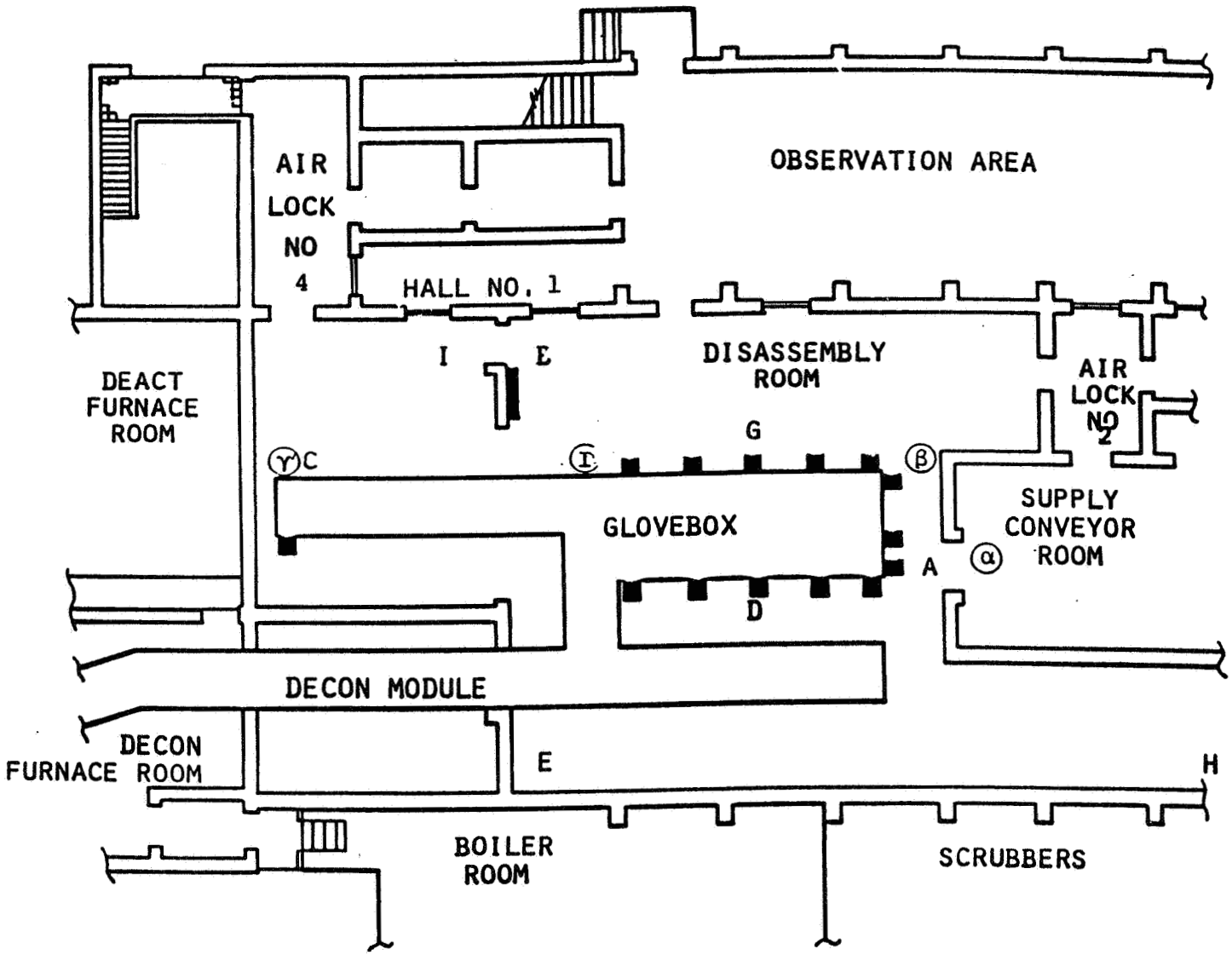

Figure 29. Schematic of Test Tracer Test in a Nuclear Facility.

Solid lines are design airflow paths, dashed lines are measured airflow paths.

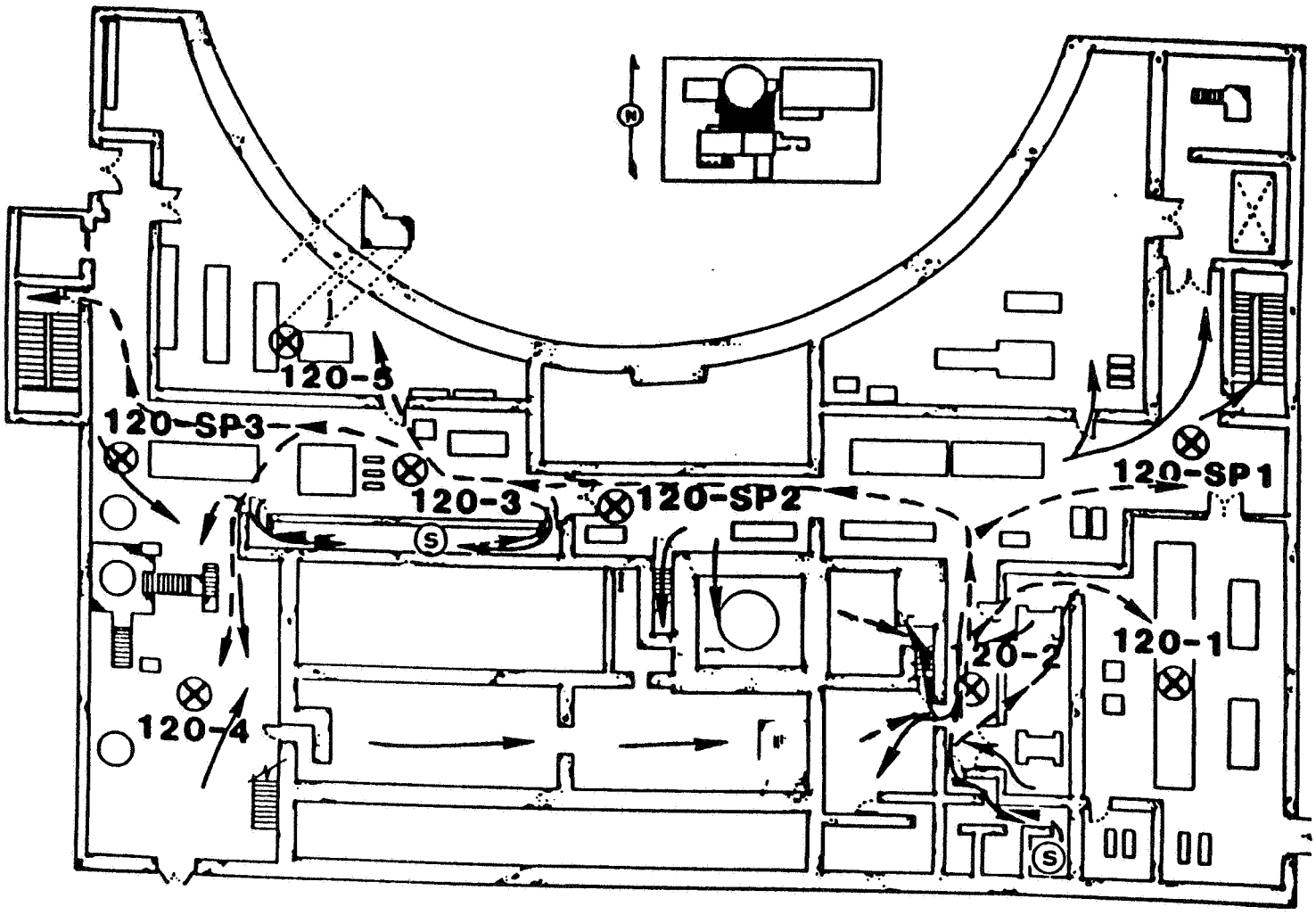

Figure 30. Expanded View of Design and Measured Airflow Paths in a Nuclear Facility. Solid lines are design airflows paths, dashed lines are measured airflow paths.

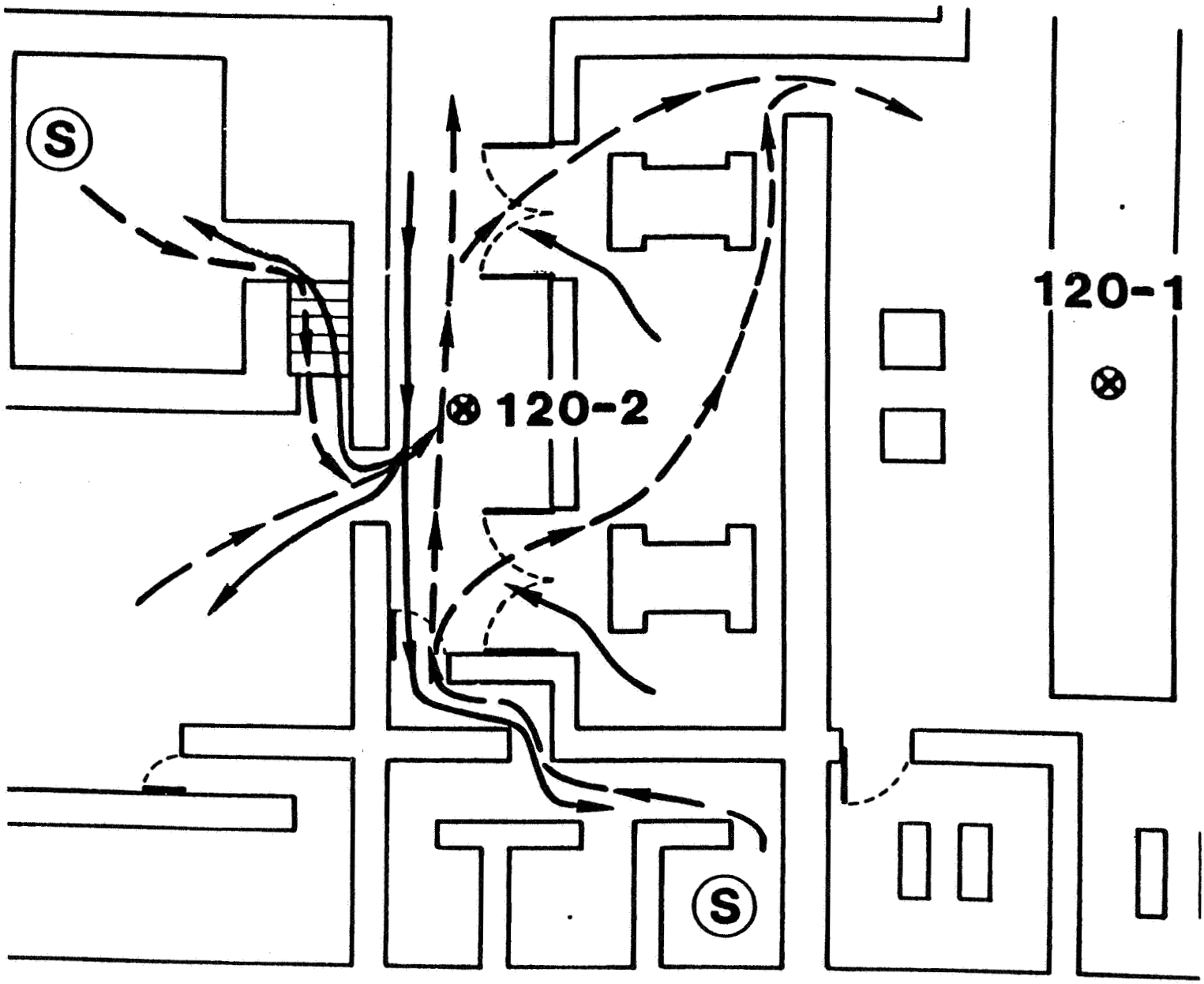

Figure 31. Example of Steady State Tracer Concentrations From Which Dilution Ratios Can be Calculated

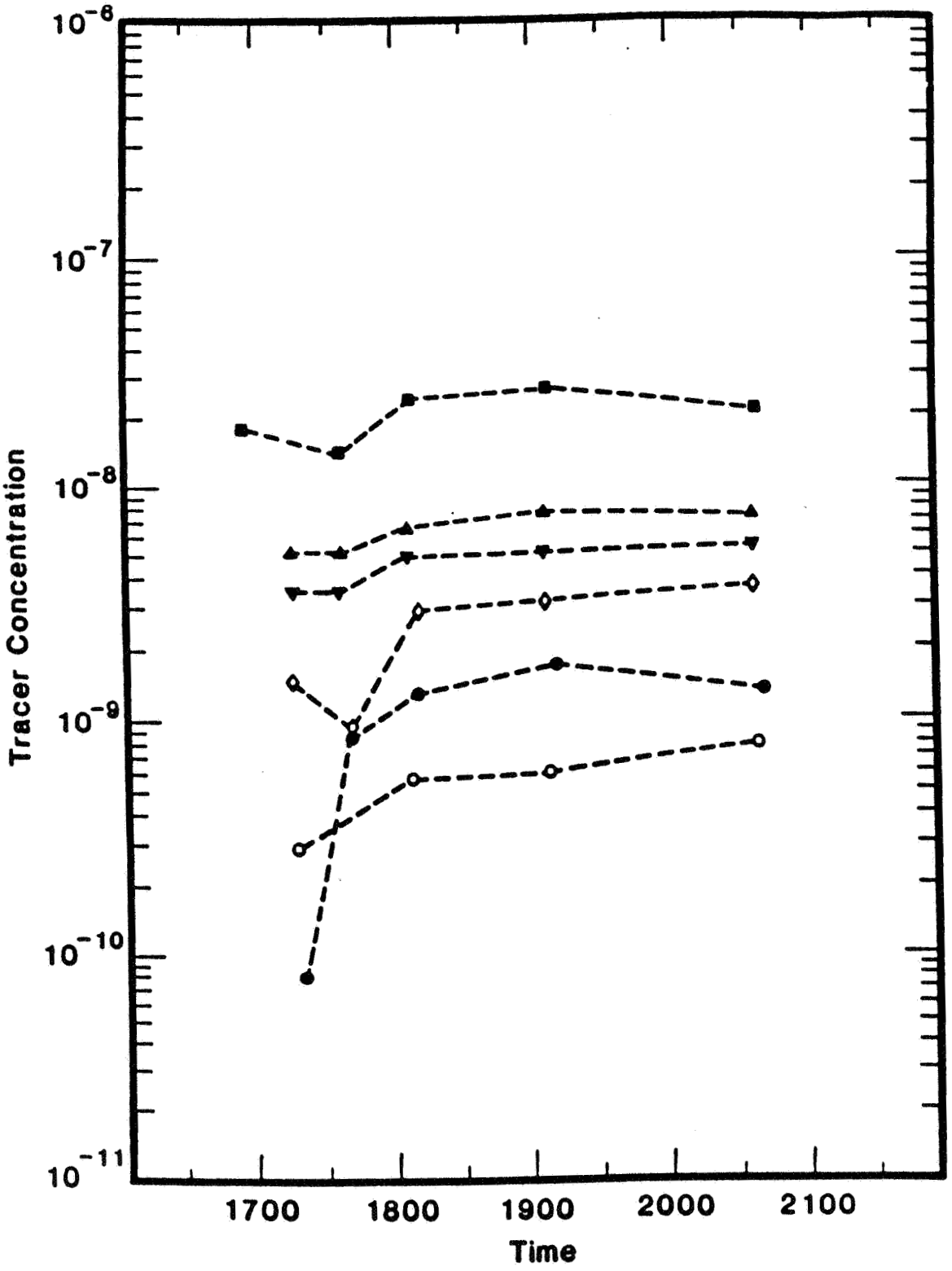

Figure 32. Nomographs Used to Determine Occupancy Time Versus Toxic Challenge for Temporary Safe Havens (Jann, 1989)

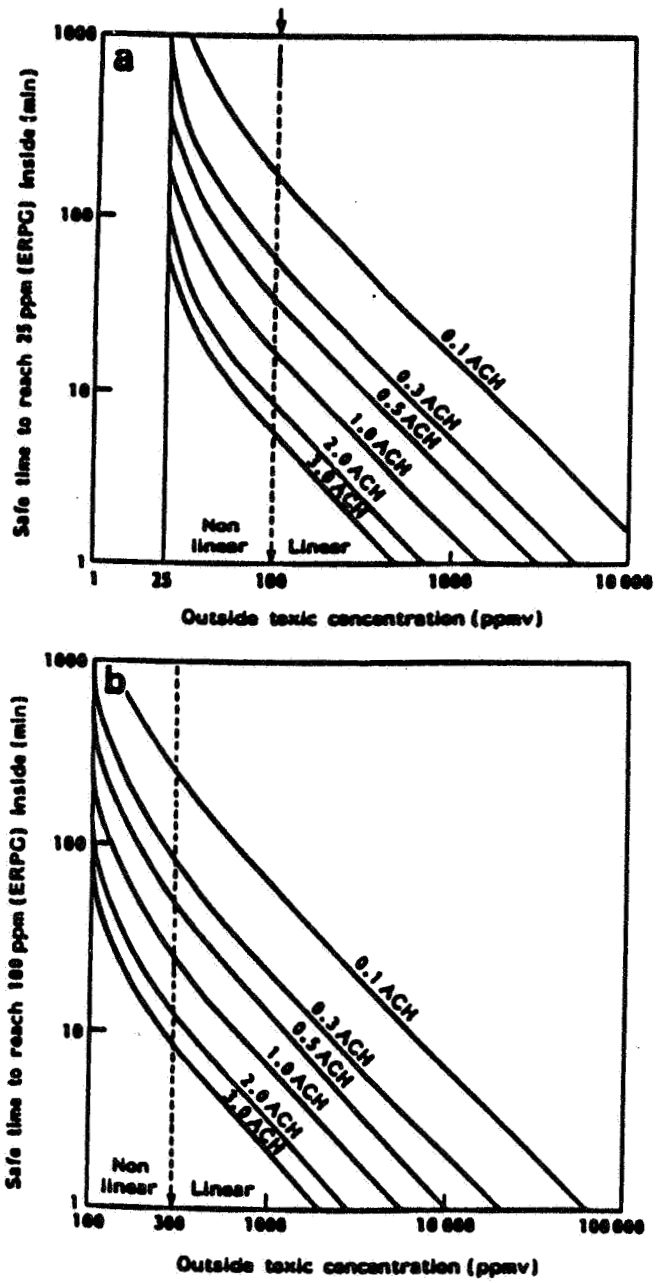

Appendix I
Theory of Tracer Gas Methods for Determining the Building Air Change Rate and the Building Airflow Rate

The theoretical assumptions which form the basis for tracer gas testing of single zone buildings can be explained by studying Figure 1. In this situation, there is one well mixed zone in which air is entering through known or unknown flow paths at a flow rate Q_{in} and exiting the space through know or unknown flow paths at a flow rate Q_{out}. If a tracer gas is introduced into the space, the basic equation for a tracer gas concentration C(t) in the zone is given by the conservation of mass of the tracer in the zone:

$$\frac{d}{dt}(\rho VC) = C_0 Q_{in} - C Q_{out} + s \qquad (1)$$

where

ρ is the density of air in the zone (moles of air per m^3)

V is the volume of the zone

C is the concentration of the tracer per unit mass of air (moles of tracer gas per mole of air)

C_0 is the concentration of tracer in the region exterior to the zone in the same units as C

Q_{in} is the mass flow rate of air into the zone from the exterior (moles of air per second)

Q_{out} is the mass flow rate of air out of the zone (moles of air per second)

s is the generation rate of tracer in the zone (moles of tracer per second)

V is the volume of the zone in m^3.

The basic assumptions leading to the derivation of equation (1) are:

- The tracer gas in the zone is well mixed and therefore can be represented by a concentration density independent of the spatial position in the room.

Note: This assumption can be relaxed somewhat to the assumption that the average concentration in the zone is the same as the average value of the tracer in the airflows out of the zone

- The air in the room is of uniform density which is independent of the spatial position in the room.

Note: To this point, no assumption has been make as to the temporal dependence of the quantities in equation (1). That is ρ, C, C_0, Q_{in}, Q_{out}, s and even V are arbitrary functions of time as long as the above two assumptions are satisfied. Useful and accurate information can be obtained from tracer gas experiments without restrictive assumptions on the temporal dependence of this quantities.

The second basic equation for analyzing tracer gas data is the equation for conservation of mass for air flowing into and out of the zone. Under the second assumption of equation (1), the conservation of mass for air flowing into and out of a zone is:

$$\frac{d}{dt}(\rho V) = Q_{in} - Q_{out} \qquad (2)$$

In the common situation of constant temperature, pressure and zone volume, equation 2 is nothing more than a statement that the flows into the zone are equal to the flows out of the zone. Equations (1) and (2) have been written in mass units: flow in mass per unit time and concentrations in mass of tracer per mass of air. This is the simplest form of the equations when temperature and pressure are not constant or when the exterior temperature is different from the interior temperature. It is also in the authors' opinion, the easiest way to make temperature and pressure corrections when such precision is required; however in most investigations little error is introduced by using volume flows rates (cfm) or volume concentrations. If the left hand side of equation (1) is differentiated by parts and equation (2) substitutes for $\frac{d}{dt}(\rho V)$, equation (1) reduces to

$$\rho V \frac{dC}{dt} = (C_0 - C)Q_{in} + s \tag{3}$$

Equation (3) is the fundamental equation of tracer gas test methods in a single well mixed zone..

There are several quantities of interest which can be determined by tracer gas experiments:

- The air change rate $\lambda(t)$ defined as

$$\lambda = \frac{Q_{in}}{\rho V}$$

- The air inflow rate $Q_{in}(t)$

Equation (3) can be put into several different forms depending on which quantity is to be measured and the type of tracer experiment (decay test, constant injection or constant concentration) to be performed.

Determination of the Air Change Rate λ

Equation (3) can be solved for λ to yield

$$\lambda(t) = -\frac{d}{dt}(\ln \hat{C}) + \frac{\hat{s}}{\rho V \hat{C}} \tag{4}$$

where

$$\hat{s} = s - \rho V \frac{dC_0}{dt}$$

$$\hat{C} = C - C_0$$

Though in principle, equation (4) can be used to estimate $\lambda(t)$, in practice accurate determination of the derivative of the concentration from experimental data is not possible. In practice one is also usually interested in the average air change rate over a period of time (t_1,t_2). Integrating equation (4) over the interval (t_1,t_2) leads to the equation:

$$\lambda_{av}(t_1,t_2) = \frac{1}{t_2 - t_1}\ln\left(\frac{\hat{C}(t_1)}{\hat{C}(t_2)}\right) + \frac{1}{t_2 - t_1}\int_{t_1}^{t_2} \frac{\hat{s}(\tau)d\tau}{\rho(\tau)V(\tau)\hat{C}(\tau)} \tag{5}$$

where

$$\lambda_{av}(t_1,t_2) \equiv \frac{1}{t_2-t_1}\int_{t_1}^{t_2} \lambda(\tau)d\tau$$

Equation (5) can be used to determine the building air exchange rate in all three tracer test methods. All quantities on the right hand side of equations (5) are measurable during a tracer test. However, each tracer test method is designed to simplify the form of equation (5) and it is the simplified forms which are usually used in the analysis of tracer data. Equation (5) is useful in assessing errors caused by the lack of fulfillment of the assumptions of each test procedure: the effect of small leaks of tracer in a tracer decay test, the error caused unsteady flows or lack of equilibrium in the constant injection test and the error caused by deviations in the zone concentration from the target concentration in the constant concentration method.

The Tracer Decay Method.
For the tracer decay method, after injection, the tracer injection rate s = 0. The exterior tracer concentration must also be constant (for a properly selected tracer, it is zero). In this case the equation (5) reduces to the following simple relationship for the building air change rate which occurred in the time period (t_1,t_2):

$$\lambda_{av}(t_1,t_2) = \frac{1}{t_2-t_1}\ln\left(\frac{\hat{C}(t_1)}{\hat{C}(t_2)}\right) \qquad (6)$$

In practice, tracer decay data are usually analyzed by plotting the logarithm of the concentration versus time (see Figure 6 for an example) and portions of the data for which the decay is linear are analyzed statistically by fitting a straight line to the data. That the resulting plot is a straight line requires the added assumption that the flow rates are constant. This is not required for the use of equation (6); however it is necessary to assure that the lack of a logarithmic decay, if it does occur, is not due to poor initial mixing or the invalidity of the single zone assumption.

Constant Injection Method
In the constant injection method, tracer gas is injected into a test volume at a constant injection rate s_0 and the tracer concentration is monitored until an equilibrium value C_∞ is reached. Equations (5) and (6) then reduce to the following simple expression for the ventilation or airflow rate into the test volume:

$$q_{in} = \frac{s_0}{(C_\infty - C_0)} \qquad (7)$$

Equation (7) is also used to determine ventilation flow rates in ducts, though the derivation in this case is different and requires the assumption the tracer concentration is uniform across a duct cross-section. It must be emphasized that equation (7) is valid only for steady flows. If fluctuations in the flow are observed (by noticing oscillations in the tracer concentration), equation (5) can be used to obtain the average flow rate during a period of time or to estimate the error caused by using equation (7).

Multi-Chamber Theory

In some investigations, a single zone model of a building is not adequate and a multi-chamber or multi-zone approach must be used. Figure 2 depicts the air and tracer gas fluxes for three interacting zones. The theory behind multi-chamber methods is complex and it is only outlined here. The mass balance for a tracer in the i^{th} zone is given by the equations:

$$\frac{d\rho_i V_i C_i}{dt} = -Q_i^{(out)} C_i + \sum_{i \neq j} Q_{ij} C_j + s_i \quad i = 1...N \tag{8}$$

where $Q^{(out)}_i$ is the sum of all flows out of the i^{th} zone and Q_{ij} is the flow to the i^{th} zone for the j^{th} zone. In the above equations, the exterior denoted by the subscript 0 and N is the number of zones.

Using the conservation of mass for the airflows, equations (8) can be written as

$$\rho_i V_i \frac{dC_i}{dt} = -Q_{i0}(C_i - C_0) + \sum_{\substack{i \neq j \\ j \neq 0}} Q_{ij}(C_j - C_i) + s_i \quad i = 1..N \tag{9}$$

Equation (9) is the basis for most multi-zone and multi-tracer methods. For multi-tracer methods, an equation of the form of (8) or (9) is formed for each tracer gas used in each zone. In principle, in a building with N zones, a properly designed experiment with N tracers can determine all interzonal airflows and the airflows to and from the exterior for each zones (that is, there are N^2 equations for N^2 unknowns). The simplest multi-tracer test is done by injecting a different tracer at a constant injection rate into each zone and waiting until equilibrium is reached. Therefore the derivatives on the left hand side of equation (9) are zero. In the case of strongly interacting zones, this interaction sometimes leads to poorly conditioned equations which are difficult to solve accurately.

To avoid ill-conditioned equations, the system of equations (9) is often integrated over a period of time (t_1,t_2), assuming that the airflows are constant, to produce

$$\rho_i V_i (C_i(t_2) - C_i(t_1)) = -Q_{i0} \int_{t_1}^{t_2} (C_i(t) - C_0(t))dt + \sum_{\substack{i \neq j \\ j \neq 0}} Q_{ij} \int_{t_1}^{t_2} (C_j(t) - C_i(t))dt + \int_{t_1}^{t_2} s_i(t)dt \tag{10}$$

Equations (10) are the bases of the so-called integral-pulse method (see Persily and Axley [1990]) in which pulses of tracer are injected into each zone. One advantage of this method is that all quantities appearing in equations (10) can be measured simply without resorting to the mathematical evaluation of the integrals. The integral of the concentrations are determined using standard integral sampling techniques such as filling air sample bags at a constant rate over the time period of the test. The integral of the injection source rate is the total quantity of tracer injected during the time of the test.

Constant Concentration Method

In a multi-chamber test, if a method can be found to keep the concentrations in all interior zones the same, the derivatives on the left hand side of equation (9) are zero as are the terms in the summation on the right hand side. Equations (9) then yield the following simple expression for the flow of exterior air into the zone:

$$Q_{i0}(t) = \frac{s_i(t)}{(C_{target} - C_0)} \tag{11}$$

where $Q_{i0}(t)$ is the airflow rate into the space from the exterior, C_{target} is the controlled level of tracer and $s_i(t)$ is flow rate of tracer required to maintain the target concentration at the time t. Sophisticated micro-processor controlled systems have been designed by various research laboratories to make constant concentration measurements.

Bounds for $\lambda_{av}(t_1,t_2)$

Thought equation (5) can be used to estimated the average air change for an arbitrary tracer experiment, usually simplified expressions are employed. Bounds on the accuracy of these estimates can be derived from equation (16) for arbitrary injection rate s(t) if either the exterior concentration C_0 is constant or a decreasing function of time.

If c_m is an arbitrary constant concentration and similarly for ρ_m, V_m then by it is straight forward to show from equation (5) and the definition of $s_{av}(t_1,t_2)$ that

$$\lambda_{av}(t_1,t_2)-\frac{1}{t_2-t_1}\ln\left(\frac{\hat{C}_1}{\hat{C}_2}\right)-\frac{1}{t_2-t_1}\frac{s_{av}(t_1,t_2)}{\rho_m V_m C_m}=\frac{1}{t_2-t_1}\int_{t_1}^{t_2} s(\tau)\left(\frac{1}{\rho(\tau)V(\tau)C(\tau)}-\frac{1}{\rho_m V_m C_m}\right)d\tau \quad (12)$$

Let V_{max} and c_{max} denote the maximum values of V and c in the interval (t_1,t_2) and V_{min} and c_{min} the corresponding minimum values of these quantities. Then setting V_m and c_m equal to V_{max} and c_{max} in equation (12), if the exterior concentration of tracer is constant or decreasing, the integral on the right hand side is greater than or equal to zero. Similarly setting V_m and c_m equal to V_{min} and c_{min} in equation (12), the integral on the right hand side of equation (12) is less than or equal to zero. Therefore $\lambda_{av}(t_1,t_2)$ can be bounded by:

$$\frac{s_{av}(t_1,t_2)}{\rho_{max}V_{max}C_{max}}\le\lambda_{av}(t_1,t_2)-\frac{1}{t_2-t_1}\ln\left(\frac{\hat{C}_1}{\hat{C}_2}\right)\le\frac{s_{av}(t_2,t_1)}{\rho_{min}V_{min}C_{min}} \quad (13)$$

Application to Constant Injection

For constant injection $s(t)=s_0$, a constant value if the exterior tracer concentration is constant. The general expression of equation (9) is valid with $s_{av}(t_1,t_2)=s_0$. In a constant injection experiment two situations are common: case 1 in which the increase in tracer concentration is monotonic and case 2 in which the tracer concentration is oscillates about some average value.

Case 1:

The monotonic increasing C(t), $C_{min} = C_1$ and equation (10) can be written as

$$\lambda_{av}(t_1,t_2)-\frac{s_0}{\rho_{min}V_{min}C_1}\le-\frac{1}{t_2-t_1}\ln(1+e_2)-\frac{s_0}{\rho_{min}V_{min}C_1}\frac{e_2}{1-e_2} \quad (14)$$

where $e_2 = (C_2 - C_1)/C_1$ is the relative increase in tracer concentration.

This expression allows one to estimate the error in the average air change rate when equilibrium have not been reached.

Case 2:

In the case of cyclic oscillations in the tracer concentration around some average value (This occurs when equilibrium has been reached, but the air change rate is not constant, but oscillates about some average value), one can choose t_2 such that $C_2 = C_1$ in which case

$$\frac{s_0}{\rho_{max}V_{max}C_{max}}\le\lambda_{av}(t_1,t_2)\le\frac{s_0}{\rho_{min}V_{min}C_{min}} \quad (15)$$

Application to Constant Concentration

For constant concentration, one attempts to control the injection of tracer such that a target concentration is obtained and held constant. In such an experiment one can in actuality maintain this target concentration only to within some tolerance. In practice the actual concentration in the zone oscillates about the target concentration and in this case one can choose t_2 such that $C_2 = C_1$. Equation (13) reduces to

$$\frac{s_{av}(t_1, t_2)}{\rho_{max} V_{max} C_{max}} \leq \lambda_{av}(t_1, t_2) \leq \frac{s_{av}(t_2, t_1)}{\rho_{min} V_{min} C_{min}} \tag{16}$$

Equation (13) can be used to bound the error in estimating the average air change rate if the control of the constant concentration system is not perfect.

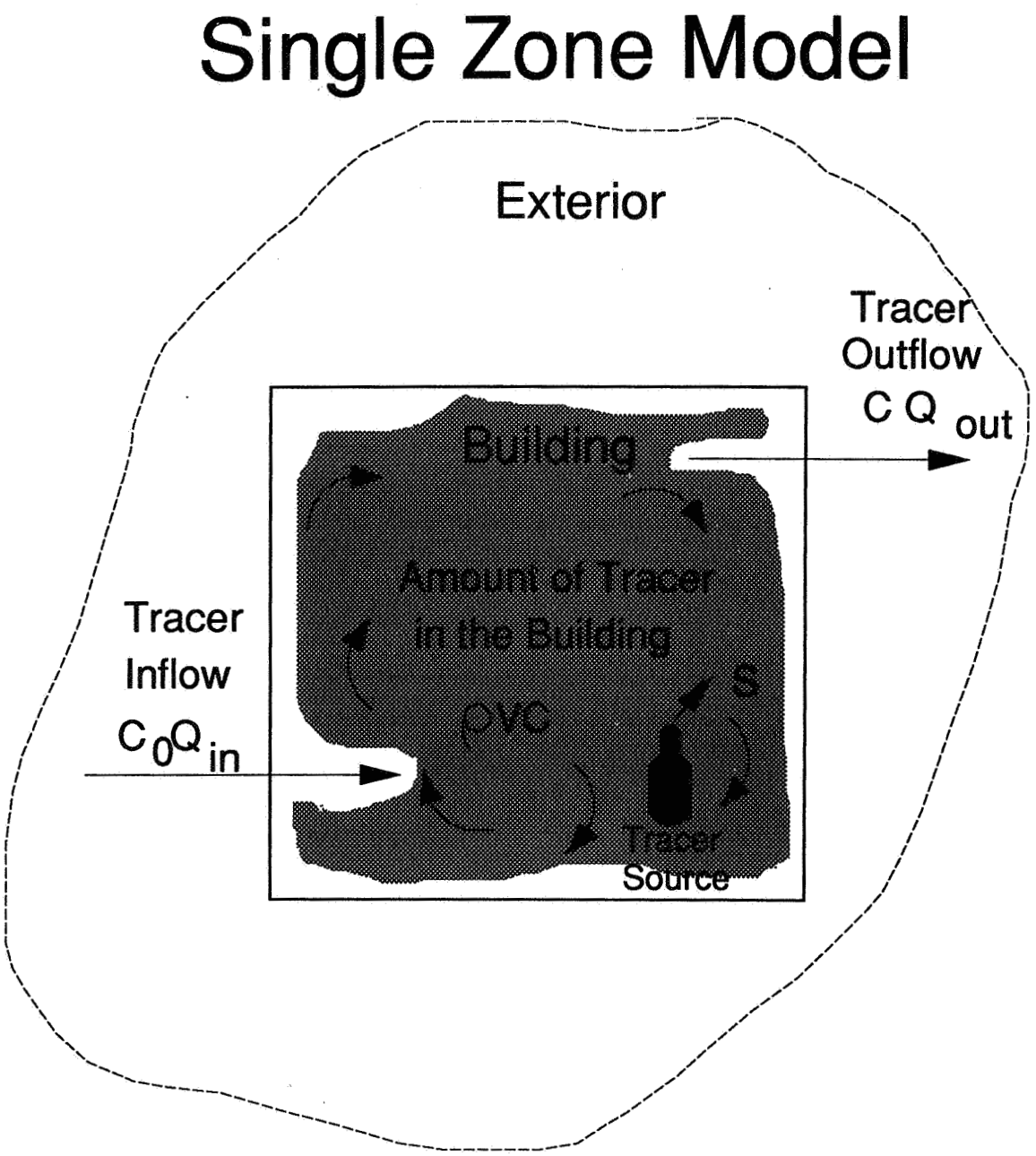

Figure I-1. Single Zone Model for Tracer Experiments

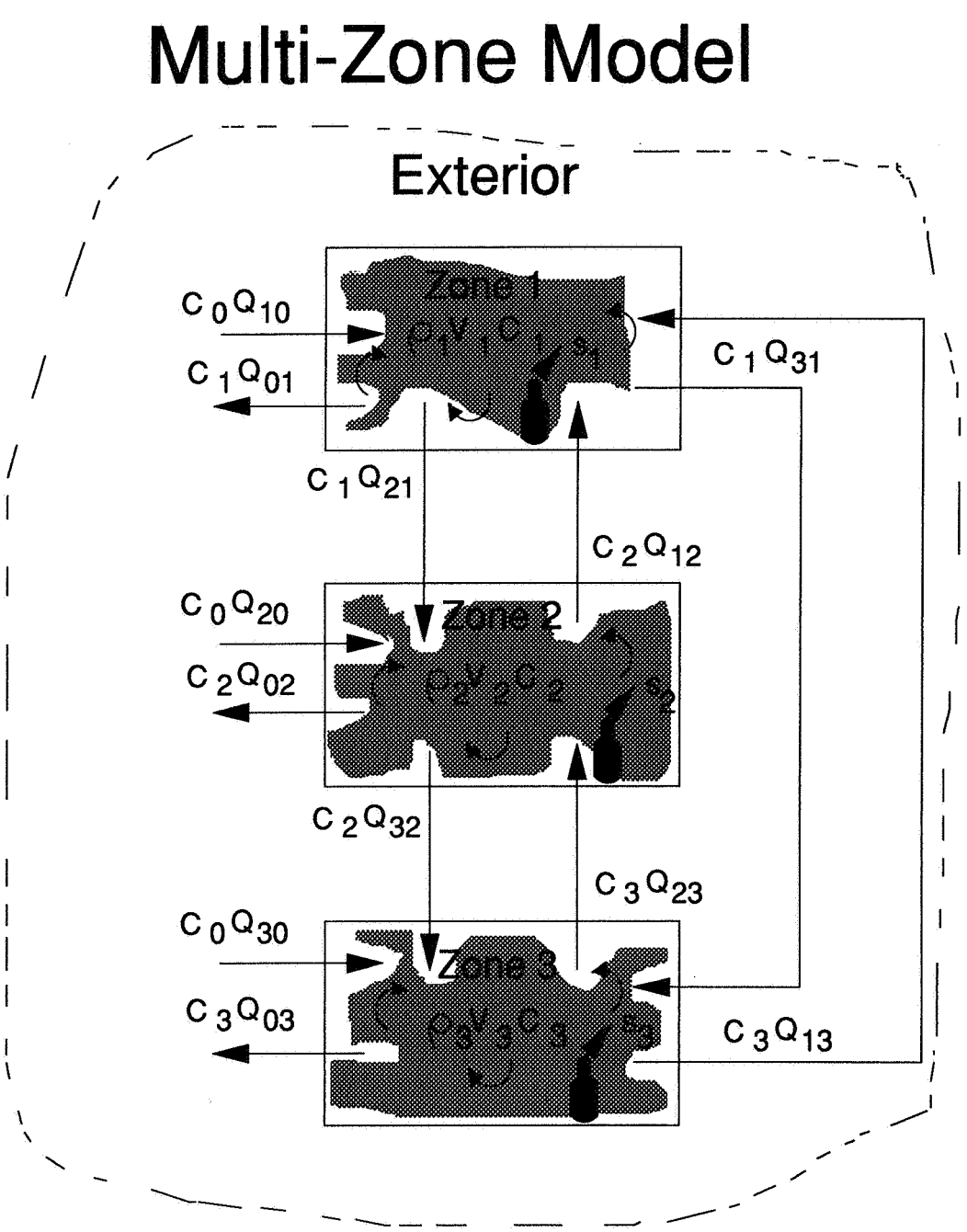

Figure I-2. Multi Zone Model for Multi-Chamber Test

AIR MOVEMENT & VENTILATION CONTROL WITHIN BUILDINGS

12th AIVC Conference, Ottawa, Canada
24-27 September, 1991

PAPER 28

Single-Sided Natural Ventilation - How Deep an Office?

M.K. White and R.R. Walker

Building Research Establishment
Garston, Watford WD2 7JR
England

SINGLE-SIDED NATURAL VENTILATION - HOW DEEP AN OFFICE?

White, M K and Walker, R R.
Building Research Establishment,
Garston, Watford, WD2 7JR.

Tel. 0923 664469
Fax. 0923 894010

Country: UK

ABSTRACT

Concern about the atmospheric greenhouse effect and depletion of the ozone layer has led to growing attention being paid to the gaseous emissions resulting from the use of building services. It is generally acknowledged that, in operation, air conditioned buildings consume more energy, producing more carbon dioxide, and potentially can lead to the release of ozone depleting gases (CFC's and HCFC's) from their refrigeration plant. In addition, the risk of health related problems such as sick building syndrome appear to be greater in air conditioned buildings. As a result, there is renewed interest being shown in designing for natural ventilation, thereby avoiding, or minimising, the need for air conditioning.

Traditional guidance recommends cross-ventilation, but this is often not practicable in many modern designs for office buildings. However, there is relatively little guidance on designing for offices with natural ventilation from one side only.

This report describes tracer gas measurements of the local mean age of air at different locations within an office room. These results are used to assess the distribution of fresh air at different depths, and to give guidance on the depth over which single-sided ventilation is effective.

THE AIR INFILTRATION AND VENTILATION CENTRE was inaugurated through the International Energy Agency and is funded by the following thirteen countries:

Belgium, Canada, Denmark, Germany, Finland, Italy, Netherlands, New Zealand, Norway, Sweden, Switzerland, United Kingdom and United States of America.

The Air Infiltration and Ventilation Centre provides technical support to those engaged in the study and prediction of air leakage and the consequential losses of energy in buildings. The aim is to promote the understanding of the complex air infiltration processes and to advance the effective application of energy saving measures in both the design of new buildings and the improvement of existing building stock.

Air Infiltration and Ventilation Centre

University of Warwick Science Park,
Barclays Venture Centre,
Sir William Lyons Road,
Coventry CV4 7EZ,
Great Britain.

Telephone: +44 (0) 203 692050
Fax: +44 (0) 203 416306

Operating Agent for International Energy Agency, The Oscar Faber Partnership, Upper Marlborough Road, St. Albans, UK

Printed by Information Press Ltd., Oxford, England.